General Disclaimer

One or more of the Following Statements may affect this Document

- This document has been reproduced from the best copy furnished by the organizational source. It is being released in the interest of making available as much information as possible.

- This document may contain data, which exceeds the sheet parameters. It was furnished in this condition by the organizational source and is the best copy available.

- This document may contain tone-on-tone or color graphs, charts and/or pictures, which have been reproduced in black and white.

- This document is paginated as submitted by the original source.

- Portions of this document are not fully legible due to the historical nature of some of the material. However, it is the best reproduction available from the original submission.

SECOND INTERIM REPORT

SPACE-BASED SOLAR POWER CONVERSION AND DELIVERY SYSTEMS STUDY

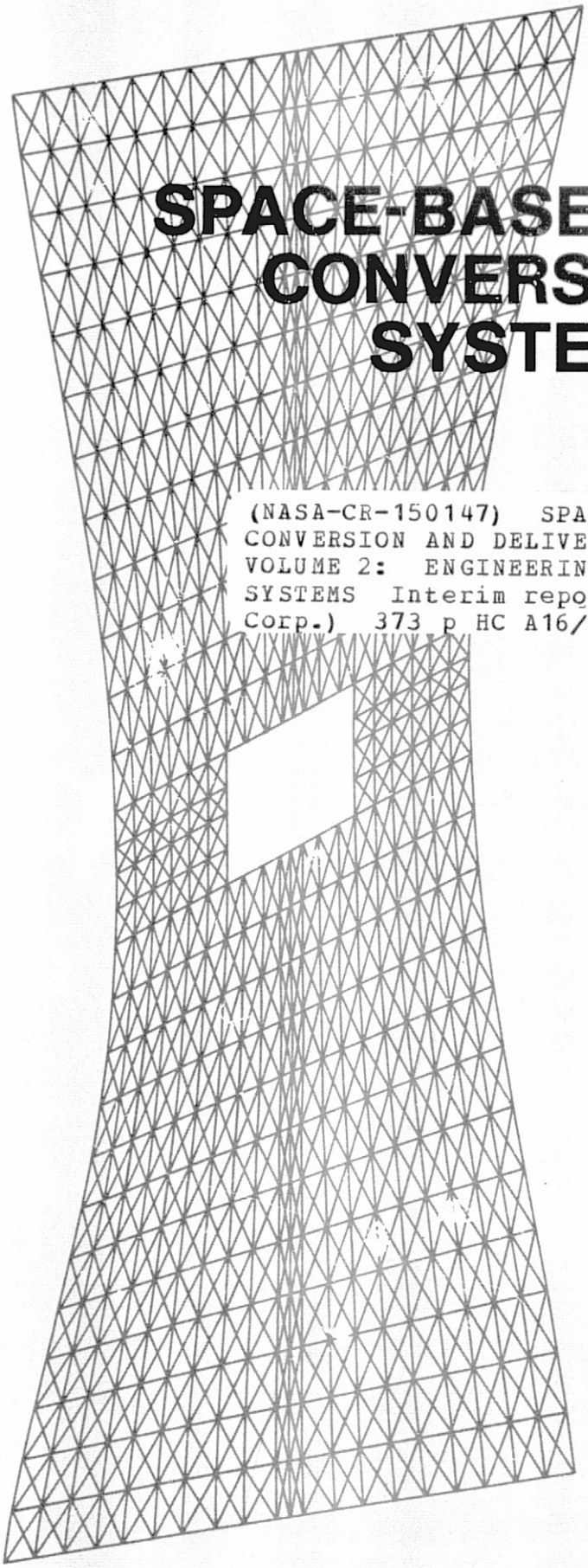

VOL II
ENGINEERING ANALYSIS OF ORBITAL SYSTEMS

GRUMMAN

SECOND INTERIM REPORT

SPACE-BASED SOLAR POWER CONVERSION AND DELIVERY SYSTEMS STUDY

VOL. II
ENGINEERING ANALYSIS OF ORBITAL SYSTEMS

30 JUNE 1976

Submitted to ECON Inc. in fulfillment of
ECON Agreement E-100 as part of Contract
NAS 8-31308 to NASA/MSFC.

Grumman Aerospace Corporation
Bethpage, N.Y. 11714

Report Output Sources

Report Paragraphs	Contract Phase I	Contract Phase II
2.1	√(G)	
2.1.1 → 2.1.3	√(G)	
2.1.4		√(G)
2.1.5	√(G)	
2.2	√	√
2.2.1		√(G)
2.2.1.1 → 2.2.1.8		√(G)
2.2.1.9	√(G)	
2.2.2	√(G)	
2.2.3.1	√	√
2.2.3.2 → 2.2.3.5	√	
2.3	√	√
2.3.1	√	
2.3.1.1 → 2.3.1.4	G	
2.3.2		√
2.3.3		√
2.3.3.1 → 2.3.3.3		√
2.3.3.4	√	√
2.3.4	√	
2.3.4.1		√
2.3.4.2 → 2.3.4.5	G	
2.3.4.6		√(G)
2.3.4.7 → 2.3.4.8		√
2.4	√(G)	
2.5	√	
2.6		√(G)
3.1 → 3.3	√(G)	
4.1 → 4.4	√(G)	
4.5	√(G)	√
4.6	√(G)	
Appendix	G	

Legend: √ - Contract effort
√(G) - Grumman In-house work updated during contract
G - Grumman In-house work used directly

CONTENTS

CONTENTS (Cont)

CONTENTS (Cont)

CONTENTS (Cont)

ILLUSTRATIONS

ILLUSTRATIONS (Cont)

ILLUSTRATIONS (Cont)

ILLUSTRATIONS (Cont)

ILLUSTRATIONS (Cont)

ILLUSTRATIONS (Cont)

TABLES

TABLES (Cont)

1 - Introduction and Summary

The principal objective of the overall ECON study was to achieve increased understanding of the economic and technical aspects of space based power generation and transmission systems. Grumman participation in this contract was directed to a systems analysis of synchronous orbit-based power generation and relay systems that could be operational in the 1990 time frame. The contract was conducted in two parts, an initial contract phase during the period of February through November 1975, and an extension contract phase during the period of February through June 1976.

In the initial contract phase, Grumman's objectives were to: identify systems requirements for the orbiting systems; provide estimates of cost data for the orbiting systems, fabrication and assembly equipments, and transportation systems; and to define near-term research activities required to assure feasibility and development, launch, and operational capabilities of such systems in the post-1990 time frame. In the contract extension phase, Grumman's objectives were to provide technical support on engineering issues which are critical to a viable initial economic assessment of the photovoltaic concept of the Satellite Solar Power System. These included analysis of structures, control, and station-keeping, and the formulation of program plans and costs for the economic risk assessment by ECON. Figure 1.1-1 shows the schedule of tasks for the initial and extension contract phases and the periods in which they were performed.

During the initial study phase, analyses were performed using several different "baseline" configurations because the design was in an evolutionary state and was continually being improved as the results of each study were reported. In most instances, the data presented herein have been updated to the current baseline configuration. Where this was not possible, the key parameters related to the configuration discussed are identified. The following discussion describes the current baseline configuration and the results of the analyses performed using this configuration.

1.1 Baseline Satellite Solar Power Station

A series of system trade studies were conducted to evolve a baseline SSPS configuration to serve as a starting point from which further studies could be directed to define overall system design requirements. Figure 1.1-2 depicts an overview of the baseline established. This SSPS configuration generates 5000 MW of power, measured at the end of 5 years into life, at the output of the receiving antenna. It has two large

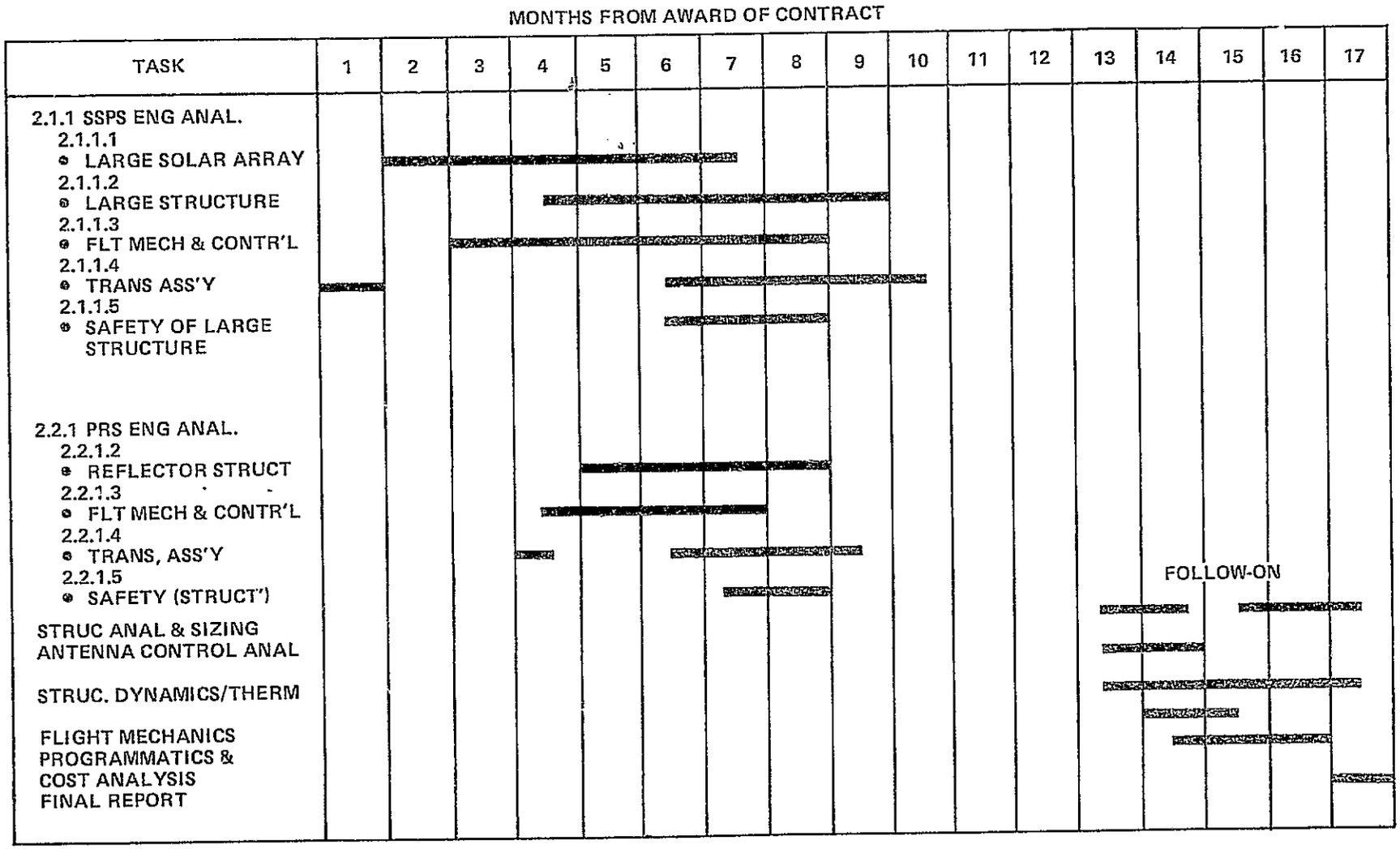

Figure 1.1-1 Space-Based Solar Power Conversion and Delivery Systems-Grumman Study

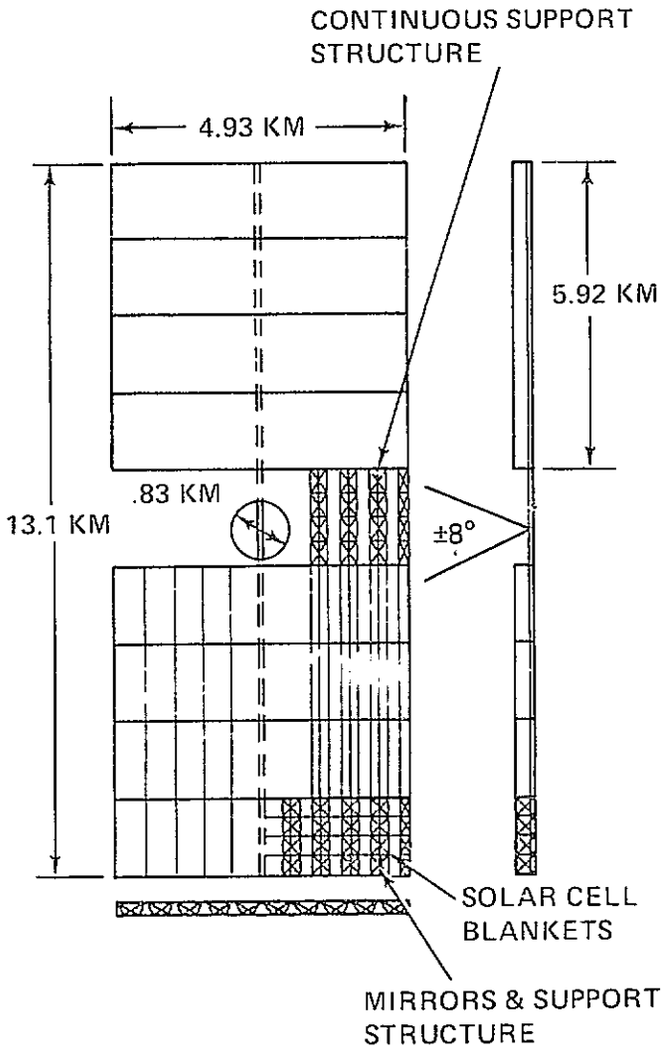

- CONCEPT DESCRIPTION

  COLLECTS SOLAR ENERGY USING PHOTOVOLTAIC CONVERTERS & TRANSMITS POWER TO EARTH AS MICROWAVE ENERGY. THE MICROWAVE ENERGY IS RECTIFIED TO DC POWER AT THE GROUND RECEIVING STATION

- CHARACTERISTICS

– POWER	5000 MW
– WEIGHT	18.1 X 10^6 KG
– SIZE	13.1 X 4.9 KM
– ORBIT	GEOSYNCHRONOUS
– LIFE	30 YR
– OPERATING FREQ	2.45 GHZ
– DC-TO-DC EFFIC	58%
– SOLAR ARRAY EFFIC	11.3%

- COSTS (1974 DOLLARS)

– IOC	1990-1995
– DDT&E	
· DIRECTLY RELATED	$20.4B
· SUPPORT PROGRAMS	$23.5B
– UNIT COSTS	$ 7.6B
– OPERATING COSTS	$218 M/YR (AT 50% CONFIDENCE LEVEL)

Figure 1.1-2 Satellite Solar Power Station

photovoltaic solar cell arrays, each approximately 6 by 5 km, interconnected by a carry-through structure of dielectric material. The 0.83 km diameter microwave antenna is located on the centerline between the two arrays and is supported by the central power transmission bus (mast) structure that extends the full length of the power station. The antenna is attached to the mast by a rotary joint system with unlimited freedom of rotation in azimuth (East-West) and ±8 degrees in elevation (North-South).

The solar cell blankets, which are positioned between channel concentrators, operate at an overall efficiency of 11.3% at the end of 5 years into life. The microwave subsystem operates at a frequency of 2.45 GHz and has a dc-to-dc efficiency of 58%.

Development cost for the satellite itself has been estimated at $20.4B (1974). Supporting programs that could be developed independently of SSPS (for example, transportation vehicles, space stations, etc.) have been estimated to cost $23.5B (1974). The unit cost for SSPS has been estimated at $7.6 B (1520 $/kw) (1974). Included in unit costs are the cost of the satellite subsystems, the cost of transportation, and the cost of assembly. Operating costs for the satellite and ground receiving antenna have been estimated at $218M/Yr. In arriving at this maintenance cost, it was assumed that a space station is fully manned at all times.

Figure 1.1-3 summarizes the SSPS mass properties at the start and conclusion of the initial study phase. The increase in mass from 11.5×10^6 kg is due to refined estimates of the microwave subsystem resulting from Raytheon's MPTS studies (NAS3-17835, see CR-134886). The largest increases are in the microwave tubes and waveguides. Refined estimates of the microwave efficiency chain are the dominant forces in the increase of the solar array mass from 9.6×10^6 kg to 12.3×10^6 kg. The array structure increased due to analysis that indicated that lateral support structure was needed to improve column stability of the main longitudinal beams.

For purposes of comparison, a 5000 MW and 10,000 MW system are presented. The power-to-mass ratios of the major subsystems are:

- Solar Array = 0.7 kw/kg (power measured at output of array)
- Transmitting Antenna = 0.9 kw/kg (power measured at output of ground rectenna)

The major element efficiencies used in sizing the baseline SSPS are summarized in Figure 1.1-4.

SUBSYS/COMP	SSPS MASS PROP. AT START OF STUDY		SSPS MASS PROPERTIES RESULTING FROM STUDY			
	5GW; 1 km DIAM ANTENNA		5GW; 0.83 km ANTENNA MASS		10GW; 1.18 km ANTENNA MASS	
	kg X 10^6	LBM X 10^6	kg X 10^6	LBM X 10^6	kg X 10^6	LBM X 10^6
SOLAR ARRAY	(9.57)	(21.1)	(12.30)	(27.29)	(23.98)	(52.8)
• BLANKETS	6.11	13.47	7.83	17.25	15.66	34.49
• CONCENTRATORS	0.93	2.05	1.23	2.71	2.46	5.42
• NON-CONDUCTING STRUCT	1.73	3.81	2.33	5.14	4.58	10.09
• BUSSES, SWITCHES	0.23	0.51	0.27	0.59	0.31	0.68
• MAST	0.57	1.26	0.64	1.37	0.97	2.12
MW ANTENNA	(1.89)	(4.16)	(5.55)	(12.22)	(10.74)	(23.66)
• MW TUBES	0.63	1.39	2.33	5.13	4.66	10.26
• POWER DIST	0.03	0.07	0.54	1.19	0.72	1.59
• PHASE CONTROL ELECT	0.28	0.61	0.13	0.29	0.28	0.62
• WAVEGUIDES	0.70	1.54	2.31	5.09	4.60	10.13
• STRUCTURE	0.25	0.55	0.14	0.31	0.28	0.62
• CONTOUR CONTROL	–	–	0.10	0.22	0.20	0.44
ROTARY JOINT			(0.17)	(0.37)	(0.20)	(0.43)
• MECHANISM	–	–	0.066	0.14	0.093	0.20
• STRUCTURE	–	–	0.106	0.23	0.106	0.23
CONTROL SYSTEM	(.02)	(.04)	(0.036)	(.079)	(0.055)	(0.121)
• ACTUATORS			0.012	0.026	0.015	0.033
• PROPELLANT/YR			0.024	0.053	0.040	0.088
TOTAL SYSTEM	11.48	25.30	18.06	39.75	34.38	77.01

- MAJOR CHANGES IN CONFIGURATION
  - REFINED ESTIMATE OF ANTENNA WGT FROM MPTS STUDIES NAS 3-17835
  - REFINED ESTIMATE OF MICROWAVE EFFIC CHAIN INCREASES POWER SOURCE SIZE

Figure 1.1-3 Mass Properties

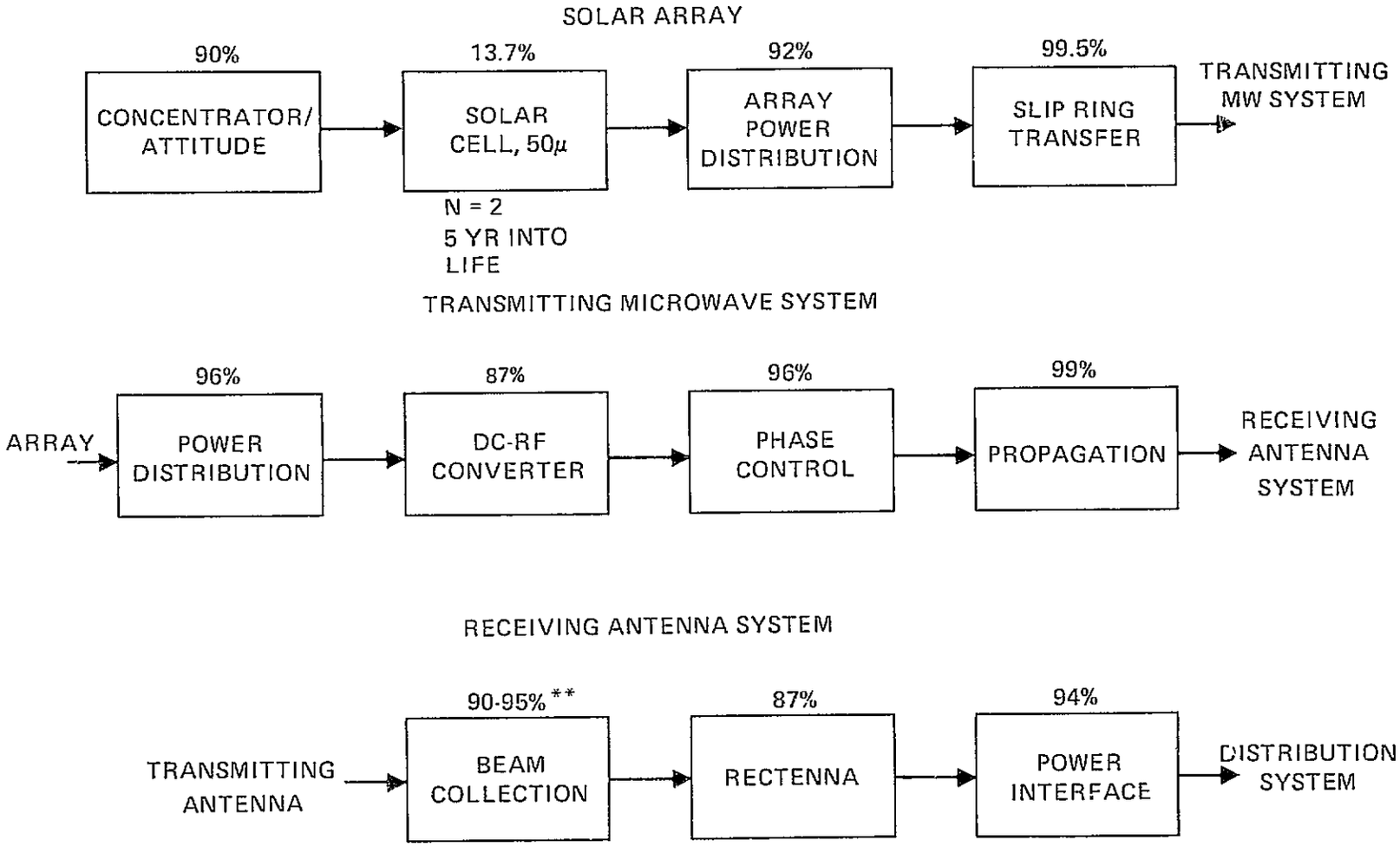

Figure 1.1-4 SSPS Nominal System Efficiency Chain

The total solar array efficiency is projected at 11.3%. The system is sized to generate 5000 MW of ground output power during the summer and winter months, accounting for the cosine losses that result from fixing the array normal to the equatorial plane. The nominal solar cell efficiency is 13.7% (5 years into life) at a concentration ratio of 2. The total degradation due to radiation damage over 30 years is 20 percent. The power distribution efficiency was selected through a mass tradeoff, which considered power bus system material, cross-section, and operating temperature.

The total microwave system efficiency, measured from the input bus to the transmitting antenna to the output bus of the ground rectenna, is 58%. An amplitron efficiency of 85% has been reached experimentally, adding confidence to our projection of achieving 87% over the next ten years. Beam collection efficiency was selected based on minimum cost of the product of the areas of the transmitting and receiving antennas.

Figure 1.1-5 shows the key inputs to this study from the Raytheon MPTS studies. Specific mass, specific cost, and efficiency trends with frequency are shown for the amplitron. These favor a selection near 2.45 GHz, which is in the center of the industrial microwave band. An output power level selection at 2.45 GHz should be near 5 KW for the individual tubes.

A critical factor in the selection of operating frequency and system power level is the ground power density. Also shown are peak ground power density as a function of frequency and power level. Reference values of power density are shown for sunlight (100 mW/cm^2), the USA standard for continuous exposure to microwave (10 mW/cm^2), and an estimate for onset of ionospheric modification (20 mW/cm^2). Based on these trends, the baseline system size was limited to 5000 MW, consistent with the biological standards and the impact of ionospheric changes.

Figure 1.1-6 summarizes the tradeoff used to select the basic solar array configuration. A comparison of a 2-mirror corrugated design and a 4-mirror "petal" design was made for various solar cell thicknesses and concentration ratios. System mass was shown to be minimum at a concentration ratio of approximately 2 for the options considered.

In an effort to simplify the mechanical devices used in the system, solar tracking was restricted to one axis. Solar tracking in the north-south direction was not adopted. The impact of this approach on system efficiency at the summer and winter solstices shows that the 2-mirror "corrugated" design is more forgiving than the 4-mirror system. The 2-mirror approach was baselined for this study.

Transportation costs were determined to be a large contributor to the total cost of the system. Figure 1.1-7 summarizes the tradeoffs used

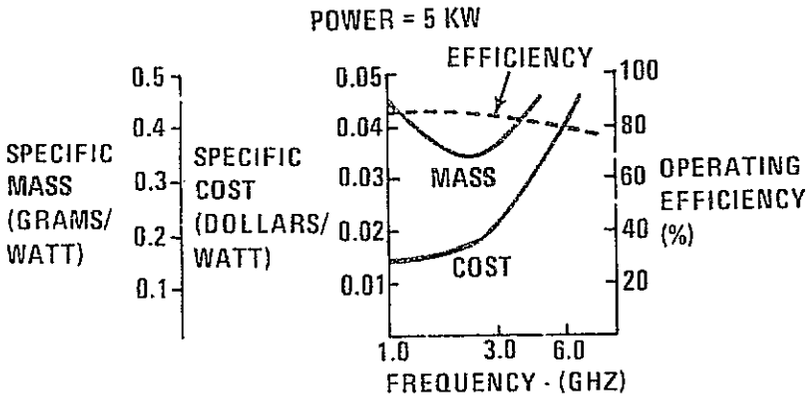

AMPLITRON MASS/COST/EFFICIENCY VS FREQUENCY

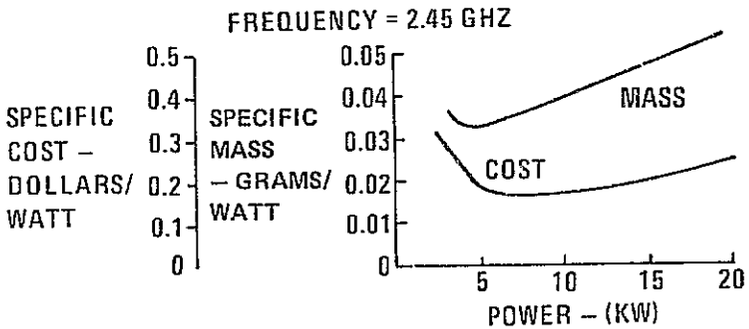

AMPLITRON MASS AND COST VS POWER

SYSTEM POWER LEVEL SELECTION

- SSPS OUTPUT POWER WAS SELECTED TO:
  - LIMIT PEAK POWER DENSITY ON GROUND TO BE NEAR USA STANDARD FOR CONTINUOUS EXPOSURE ($10 mW/cm^2$) AND
  - LIMIT POWER DENSITY AT THRESHOLD FOR CHANGES IN IONOSPHERE ($20 mW/cm^2$) FOR 2.45 GHZ AT 5000MW)
- 5000MW GROUND OUTPUT POWER LEVEL USED FOR INITIAL PLANNING PURPOSES BASED ON POTENTIAL TO MEET THESE CONSTRAINTS

MICROWAVE CONVERTER PARAMETER SELECTION

- SPECIFIC WEIGHT, SPECIFIC COST & EFFICIENCY TEND TO FAVOR:
  - SELECTION OF FREQ = 2.45 GHZ
  - POWER LEVEL = 5000W

FOR MICROWAVE CONVERTER

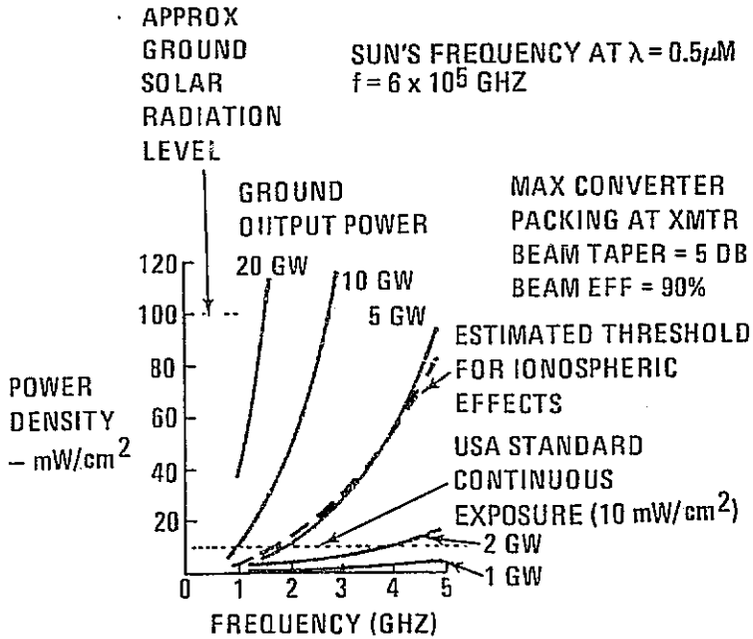

PEAK GROUND POWER DENSITY VS FREQUENCY

Figure 1.1-5 Microwave Configuration Tradeoffs (Ref: NAS3-17835)

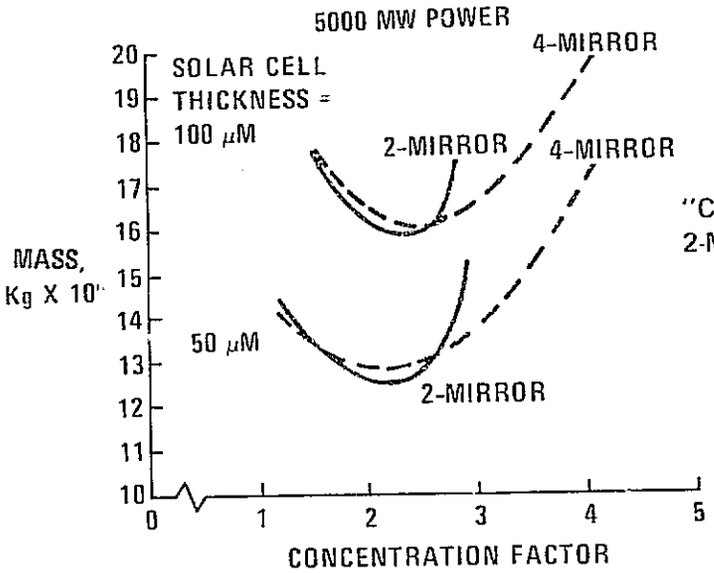

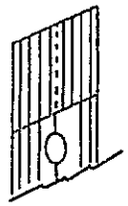

"CORRUGATED"
2-MIRROR SYSTEM

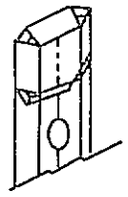

"PETAL"
4-MIRROR SYSTEM

STUDY ASSUMED

- ARRAY FIXED NORMAL TO EQUATORIAL PLANE
- PASSIVELY COOLED ARRAY
- SOLAR CELL EFFICIENCY DROPS WITH INCREASED CONCENTRATION RATIO DUE TO INCREASED TEMPERATURE

PRELIMINARY FINDING

- BOTH 2-MIRROR "CORRUGATED" DESIGN AND 4-MIRROR "PETAL" DESIGN TEND TO HAVE MIN. WGT AT A CONCENTRATION RATIO SLIGHTLY ABOVE 2
- THE 2-MIRROR SYSTEM IS SIGNIFICANTLY LESS AFFECTED BY ATTITUDE MISALIGNMENTS RELATIVE TO SUN LINE
- 2-MIRROR SYSTEM SELECTED FOR PRELIMINARY PLANNING PURPOSES

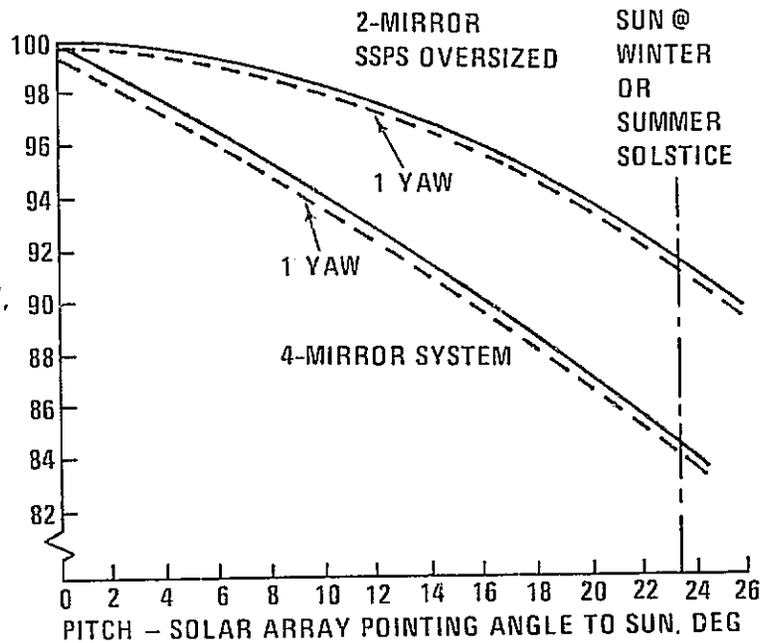

Figure 1.1-6 Solar Array Configuration Tradeoffs

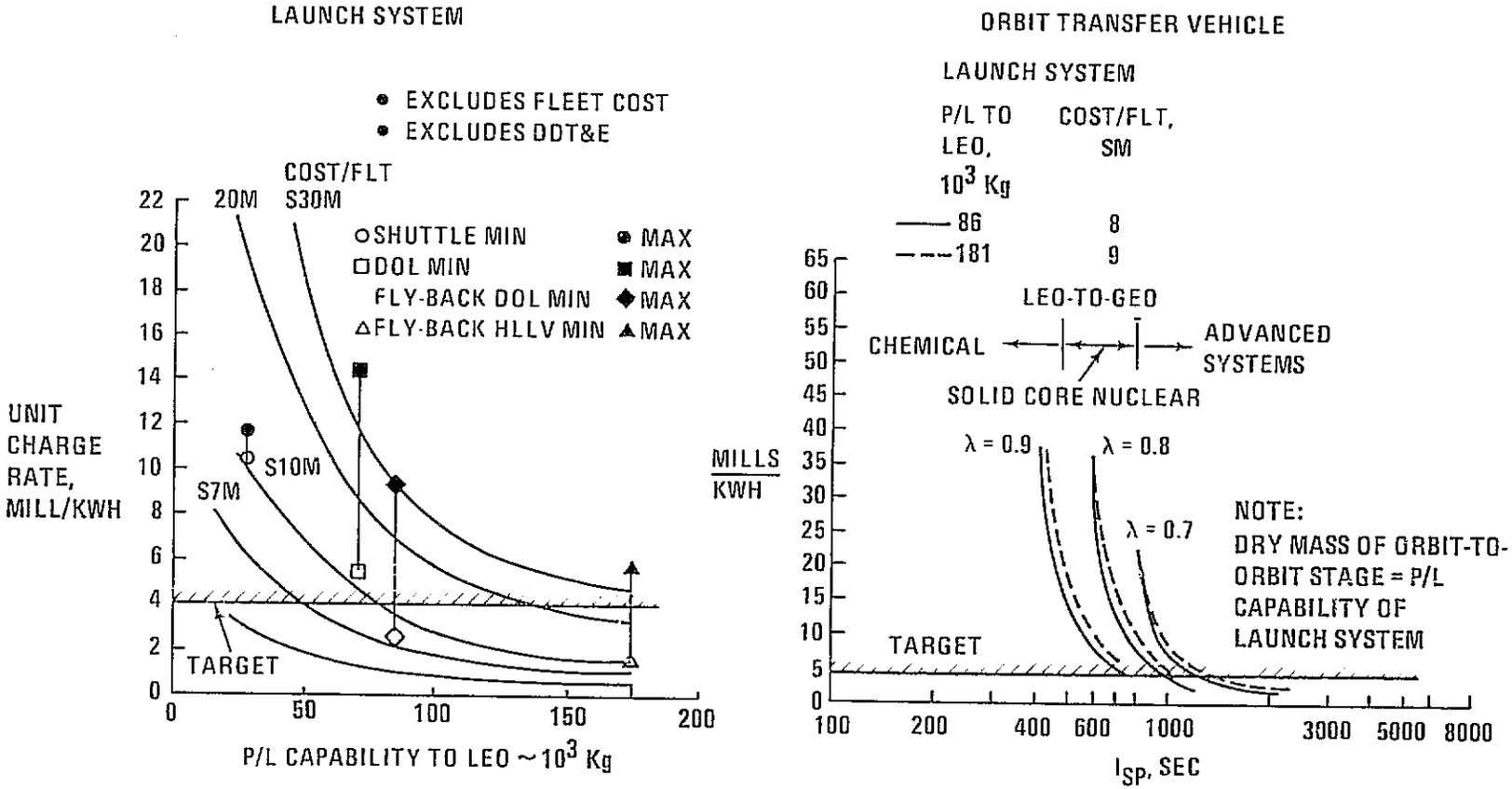

- LAUNCH SYSTEM PAYLOAD TO LEO GREATER THAN 181,000 KG OR LOW COST PER FLIGHT (FULLY RECOVERABLE SYSTEM) REQUIRED TO MEET SSPS COST TARGETS
- ADVANCED ORBIT TRANSFER VEHICLES (I_{SP} > 1000 SEC) NEEDED TO MEET COST TARGETS
- ASSUMPTIONS USED FOR COSTING & PLANNING
  - FULLY RECOVERABLE HLLV ($9M/FLT, $400M/UNIT)
  - 10N STG TRANSFERS ENTIRE SSPS TO G E O ($190M/UNIT)

Figure 1.1-7 Transportation Tradeoff

to identify transportation system characteristics needed to provide an economically viable SSPS. A cost target of 4 mills/KWH was established for the launch system and orbit transfer vehicle based on an overall SSPS competitive cost of 25 mills/KWH. To satisfy these goals, a launch system must have a high recoverability rate or heavy lift capability. A heavy lift launch vehicle with 181,000 kg payload to low earth orbit was baselined for these initial economic studies. An orbit-transfer-vehicle with a specific impulse in excess of 1000 sec desensitizes the effects of mass fraction on overall SSPS cost for transfer to geosynchronous altitude. An ion stage was baselined for this study.

1.1.1 Engineering Analyses and Major Findings

Using the mission scenario wherein the SSPS is assembled in low earth orbit (LEO) and transferred in its entirety to geosynchronous orbit (GEO), structural analyses were conducted to evaluate the major load effects resulting from LEO operations, the orbit transfer maneuver and operations at GEO altitude. The major loadings considered were aerodynamic drag and gravity gradient forces acting in LEO, the forces resulting from thruster application during orbit transfer, and the thruster forces resulting from attitude control and station-keeping maneuvering at GEO.

Aerodynamic and gravity gradient forces commensurate with those acting at an altitude of 370 km on the baseline SSPS with one half the solar blanket deployed were evaluated. This configuration was representative of the condition where a sufficient amount of the solar blanket was deployed in LEO for providing power to the ion thrusters used for orbit transfer. The results of this analysis, as shown in Figure 1.1-8a, reveals that the bending and torsion moments resulting from these forces are significantly lower than the allowable limits. Thus, it was established that aerodynamic and gravity gradient loads acting in LEO are not major factors in defining SSPS structural design requirements.

Loads imparted to the baseline structure from forces applied during low thrust orbit transfer maneuvering were analyzed for three thrust application techniques to determine orbit transfer trip times and their impact on structural design requirements. One technique, representative of ion thrust powered by the SSPS solar array, consisted of a concentrated thrust, located on the antenna rotary joint at the center of the satellite, gimballed to maintain the thrust force tangent to the orbit plane while the solar array is maintained inertially fixed toward the sun. Other techniques considered consisted of distributed thrust applied to the solar array, in one case applied to the upper and lower edges and in another uniformly distributed across the entire array. The results of this analysis are summarized in Figure 1.1-8b and show that the critical factor governing the magnitude of allowable thrust is the maximum allowable axial member load.

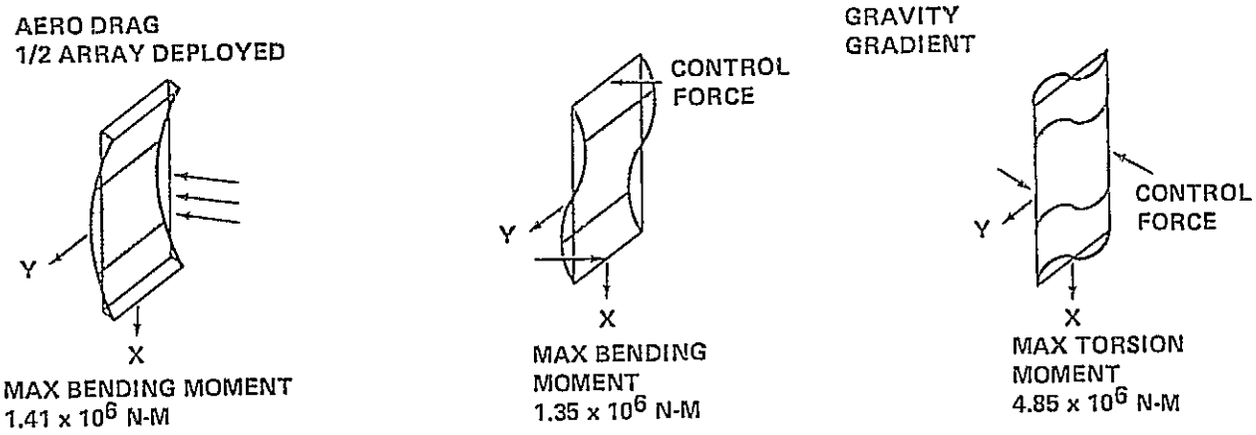

- TRIP TIMES TO 365 DAYS PERMISSIBLE
- ALLOWABLE BENDING MOMENT 12.7 x 10^6 N-M

a. LEO CONTROL EFFECTS

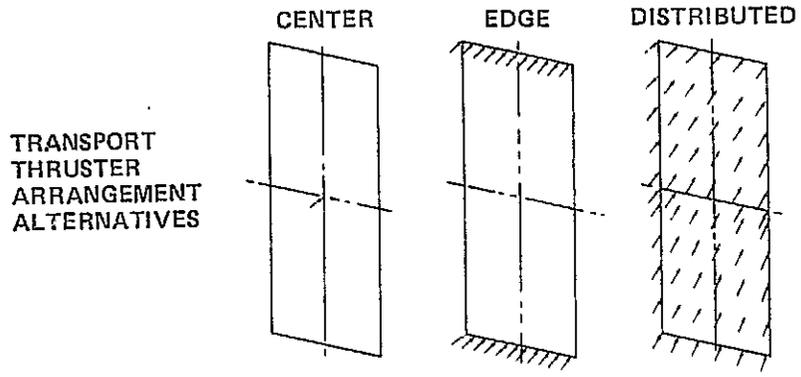

ALLOWABLE THRUST (N)	5793	2570	13,802
MAX AXIAL MEMB LOAD (N)	5431	5431	5431
MAX WIRE LOAD (N)	−422	−223	−651
MAST BEND MOMENT (N-M)	5,936,000	3,938,000	6,473,000
ANT. LOAD FACTOR	9.06×10^{-5}	6.18×10^{-5}	1.51×10^{-4}

PERMISSIBLE TRIP TIMES

300 DAYS

100 DAYS

b. TRANSPORT ALTERNATIVES (ENTIRE SSPS)

Figure 1.1-8 Structural Loads Sources

For the baseline analyzed, the maximum allowable axial member load, 5431 N, corresponds to permissable trip times of approximately 300 days for the concentrated thrust and 100 days for the uniformly distributed thrust. The 370 day trip time may be reduced to approximately 170 days by a gradual buildup of thrust over a period of one hour. Consequently, using the solar array for powering ion thrusters to transfer from LEO to GEO, trip times between 170 to 300 days are compatible with the baseline structure. Trip times as low as 100 days could be achieved by applying thrust uniformly across the entire array.

In performing the structural analysis, a structural model was developed by representing the structure as finite element bar members and concentrating the mass into node points (462 were utilized for half the structure). Modes and frequencies for this model were computed and utilized to analyze the structural loading resulting from attitude control system thruster excitation and stationkeeping maneuvering. The results of this analysis have shown that the on-orbit loads resulting from attitude and stationkeeping maneuvering at GEO are about an order of magnitude smaller than the allowable loads and, consequently, not a factor in establishing satellite structural design requirements.

An alternate mission scenario, wherein the satellite is transported to GEO in major subassembly units, was analyzed to determine the structural loadings resulting to these units as a function of trip time. Two such cases were investigated. One assumed the satellite was transported to GEO in three segments of equal mass, and another in three segments of equal area. In both cases, the results showed that higher thrust forces could be accommodated by these subassemblies resulting in trip times to GEO of from 25 to 80 days. An additional analysis considered the use of a single stage (LOX/LH_2) chemical Orbital Transfer Vehicle (OTV) for transporting subassembly modules to GEO. The baseline OTV used delivers a payload of 72,560 Kg (160,000 lbs) to geosynchronous altitude from low earth orbit. Because of this low payload capability only 8 bays of structure (each 493m x 493m) could be transported per trip. The loads resulting on these segments were approximately nine times greater than the allowable axial member loads making this scenario unfeasible for further consideration.

A thermal-structural analysis has been conducted to evaluate the structural loads imposed at GEO, both during sunlit and earth shadowing conditions. Average temperature profiles were estimated for major members of the baseline configuration during steady state sunlight conditions and during the 1.189 hours of maximum earth shadowing conditions. Uniform α/ϵ values were utilized. These temperature profiles were utilized with the structural model to determine the deflections and internal loads resulting during two specific conditions, in earth shadow with the mast

power off, and in sunlight with the mast power on. A summary of these results are presented in Figure 1.1-9 showing that in both cases, the longitudinal expansion of the central mast causes perpendicular deflections of the solar array with a maximum slope of 1.1 degrees (1 degree required) over a small section. Unacceptable compressive loads, more than 13 times the design value, occur in the cables directly attached to mast. That is, the cables require pre-tension loads 13 times the baseline value to prevent them from slackening under the thermal conditions assumed. It should be noted that the results indicated are highly correlated to the temperature differentials estimated between the structure and mast and should be further substantiated before redesign is initiated. If, however, these results are corroborated, potential corrections to be considered include strengthening the structure to prevent local deflection slopes greater than 1 degree and allowing the cables to go slack, strengthening the structure to permit higher cable preloading, or isolating the electrical transmission from the mast structure. Further design requirements and definition of the central mast are planned during follow-on study activities.

Attitude control analysis for on-orbit pointing requirements were conducted to evaluate the interaction between the roll control of the sun oriented solar array and the earth pointed antenna. Results of a simulation, which included models for structural compliance of the central mast and significant structural modes, are summarized in Figure 1.1-10. These results showed that the solar array limit cycle coupling has a significant impact on antenna control. By tightening the array limit cycle to approximately ±.5 deg (±1.0 deg is required), antenna pointing to ±1 arc min was achieved. It was also shown that a unidirectional slip ring drag torque results during steady state operations, thereby avoiding attitude disturbances from slip ring reversals. Further study is recommended to develop candidate rotary joint designs in more detail with subsequent dynamic analysis.

The effects of orbital perturbations on ground rectenna output power have been evaluated; the results indicate a significant impact on overall system performance. Figure 1.1-11 summarizes the results of the station-keeping analysis, defining the forces acting, the resulting satellite motions and the thrusting requirements needed to control satellite relative motion. Thruster maneuver corrections are identified, requiring thruster application every 57 days for solar radiation eccentricity and earth ellipticity effects. This duty cycle is based on controlling East-West satellite drift to within $\pm 2.5^{o}$. For closer control tolerances, the duty cycle must be increased. Inclination effects (North-South drift) requires corrections on a yearly basis whereas solar radiation forces effecting orbital period are nulled continuously. For thrust levels associated with ion thrusters (4.45N), a total of approximately 14,000 thrusters are required for three-axis translation with burn durations from 5 to 10 days.

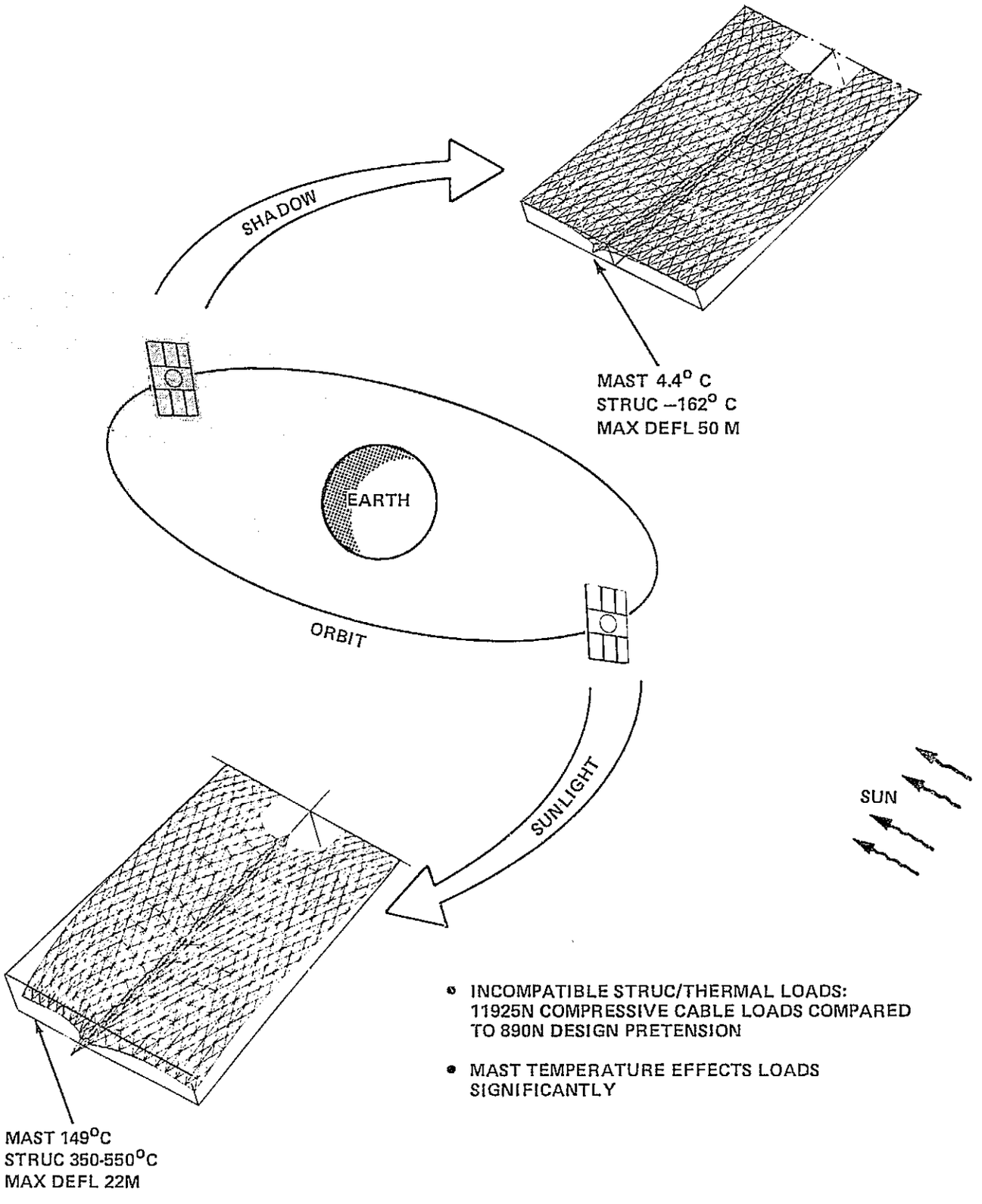

Figure 1.1-9 Structural/Thermal Analysis Results

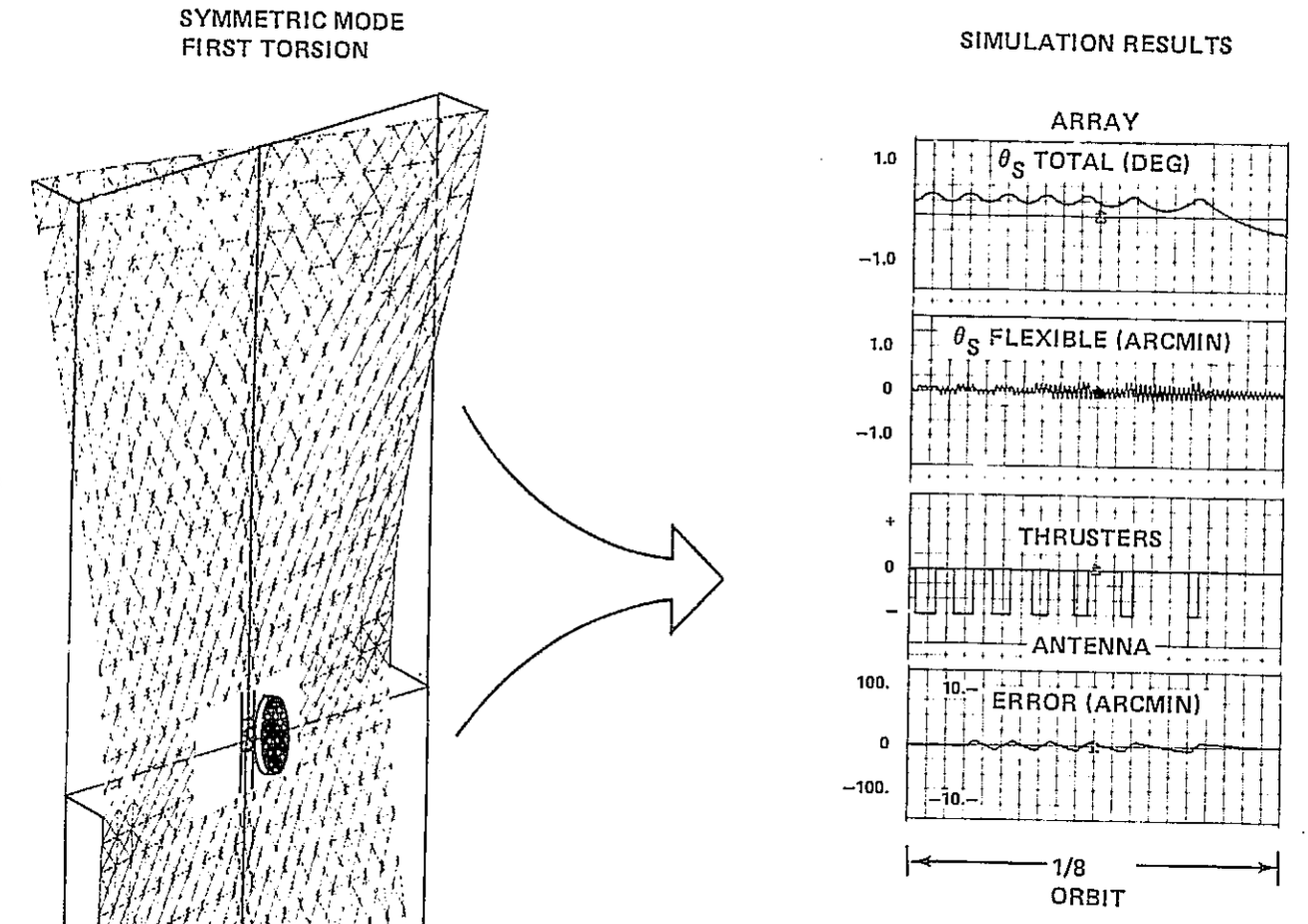

SIGNIFICANT PARAMETER		VALUE
SOLAR ARRAY INERTIA	–	2.44×10^{13} kg-M
ANTENNA INERTIA	–	2.44×10^{11} kg-M
MAST STRUC COMPLIANCE	–	5.02×10^{9} N-M/rad
SLIP RING DRAG TORQUE	–	1.36×10^{6} N-M
LOWEST STRUC MODE FREQ	–	14.14 C/HR

REQUIRED PERFORMANCE ACHIEVED

- LIMIT CYCLE ARRAY CONTROL – ±1 DEG
- ANTENNA POINTING – ±1 ARCMIN
- UNIDIRECTIONAL ANTENNA MOTION & SLIP RING DRAG
- 10/1 STRUC-TO-CONTROL FREQUENCY
- CONTROL THRUST NOT CRITICAL IN STRUC SIZING

Figure 1.1-10 Antenna/Solar Array Roll Control Interaction

STATIONKEEPING

- ORBITAL PERTURBATIONS OF SATELLITE IF UNCHECKED CAN RESULT IN A SIGNIFICANT POWER LOSS AT THE GROUND RECTENNA

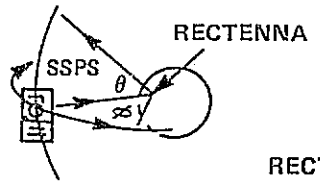

CAUSES (PERTURBATIONS)	EFFECTS	CORRECTION DUTY CYCLE (DAYS)
• GRAVITATIONAL POTENTIAL OF THE SUN & MOON	ORBITAL INCLINATION DRIFT	365
• SOLAR RADIATION PRESSURE	ORBITAL ECCENTRICITY VARIATION	57 DAYS
	ALTITUDE VARIATION	CONTINUOUS
• MICROWAVE RADIATION PRESSURE	SATELLITE ALTITUDE VARIATION	57 DAYS
• ELLIPTICITY OF EARTH EQUATORIAL PLANE	SATELLITE LONGITUDINAL DRIFT	57 DAYS

RECTENNA POWER OUTPUT SENSITIVITY TO BEAM ANGLE DEVIATION

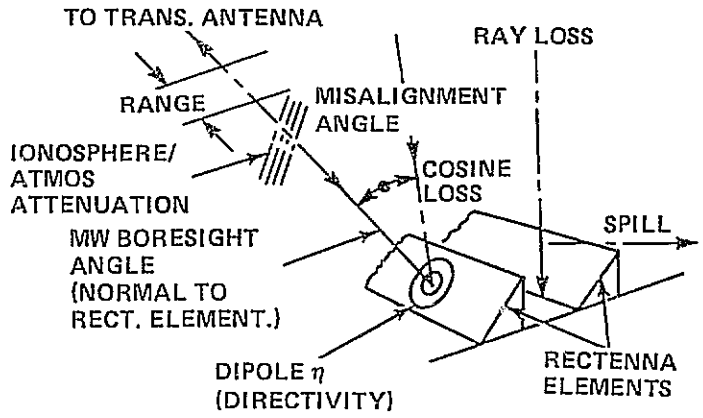

14,000 .445 N THRUSTERS REQUIRED FOR STATION-KEEPING

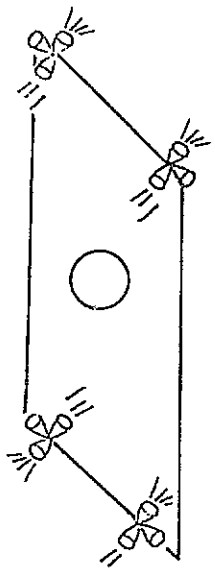

THRUSTER REQUIREMENTS
(BASED ON ± 2.5° ALLOWABLE LONGITUDINAL DRIFT)

CAUSES	ANNUAL ΔV REQTS, M/SEC	TOTAL THRUST REQTS, N
GRAVITATIONAL POTENTIAL OF SUN & MOON	45.7	602
SOLAR RADIATION PRESSURE	146 (ECC) 23 (ALT)	905.8 8.5
MICROWAVE RADIATION PRESSURE	9 (ECC) .6 (ALT)	8 .5
ELLIPTICITY OF EARTH EQUATORIAL PLANE	2	8.5

Figure 1.1-11 Orbital Mechanics Analysis Results

1.1.2 Program Plans and Costs

In support of the economic analysis of low earth orbit demonstration satellites and geosynchronous earth orbit pilot plants, program development options leading to the on-orbit operation of the first 5 GW satellite were formulated and ROM cost estimated. Three program options were considered:

- Program I - consisting of the direct development of an operational satellite.
- Program II - a two-step program consisting of a 500 MW pilot plant placed at geosynchronous altitude prior to the placement of the first 5 GW operational satellite.
- Program III - a three-step program consisting of a low earth orbit 15 MW demonstration satellite, followed by a 1 GW pilot plant at geosynchronous orbit prior to the placement of the first 5 GW operational satellite.

A summary of the major activities associated with each of these programs is shown in Figure 1.1-12. Also shown is the total ROM undiscounted overall program costs. These data were compiled using Program III DDT&E and unit production cost data, as generated during the initial contract phase, and projected to Programs I & II using the Koelle model. This projection is based on the percentage of new technology estimated in the development of the demonstration satellite, pilot plants and operational satellites of Programs I & II as compared with Program III. Assembly and operations costs, however, were newly generated for all three programs, using a format similar to that used in the initial study. The major differences used in arriving at these cost estimates were in the types of transportation systems assumed available and the accounting policies adopted in representing assembly equipment and transportation system purchase costs. In these estimates, equipment costs were amortized over their expected lifetime rather than applied totally to the cost of demonstration and pilot plant satellite programs.

In combination with these program cost estimates, projections were made of the advances in technology resulting from the accomplishment of each of the major program milestones. These projections were expressed as the percentage by which the uncertainties in each of the risk model input parameters are reduced. The values projected for the three program options described are presented in Vol. III, Appendix E. In this data, the percentage notation refers to the percentage of certainty to which that specific input parameter is known, 100% indicating that the parameter is accuractely known, the specific value being listed as "most likely". The combined sets of data, that is, program cost estimates and technology advancement projections, were used by ECON to evaluate the methodology and provide results for the economic assessment of demonstration and pilot plant satellites.

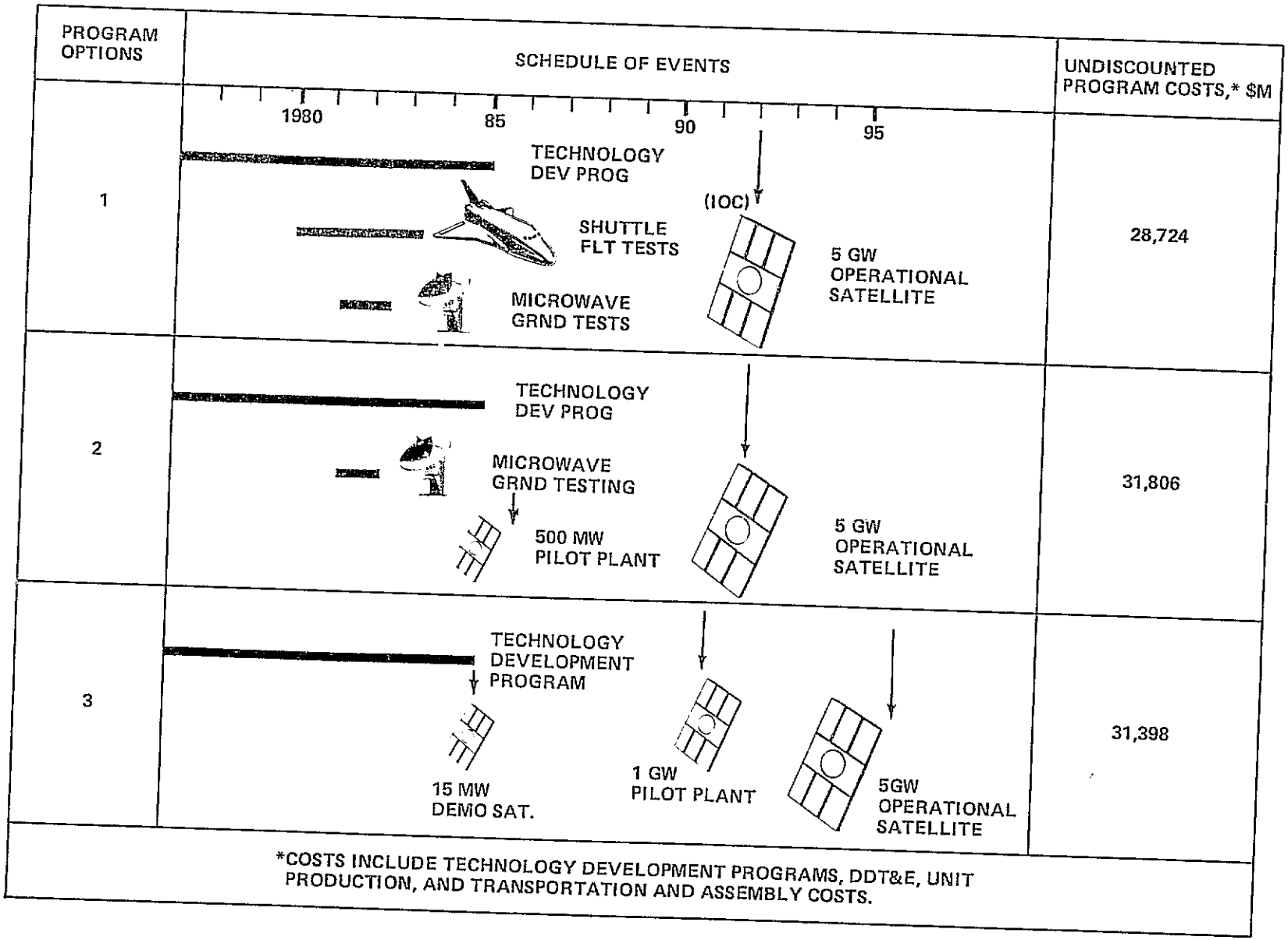

Figure 1.1-12 Program Options and Costs

A word of caution, regarding the use of the cost estimates and technology advancement projections for each of the program options described is warranted at this point. The data derived were based on extremely preliminary estimating techniques, assumptions and individual judgement, and were not intended for use in establishing quantitative conclusions. Rather, they were provided for use in developing a methodology by which an economic assessment could be made. Thus, the results established using this data should be interpreted accordingly.

1.2 Power Relay Satellite

The Power Relay Satellite (PRS) is an orbital-based power transmission system used for a concept comparison with terrestrial systems expected to be operational in the 1990 time frame. The PRS system transfers large amounts of power over great distances using a microwave transmitter from a ground-based, remotely located power generating plant. The microwave beam is reflected by the satellite in geosynchronous orbit to a ground-based receiving antenna located where the electrical power is needed (see Figure 1.2-1).

The characteristics of the PRS used in the economic comparison are also shown. A 10,000-mw system utilizing a 1-Km diameter reflector and 10-km diameter transmitter and receiving antenna on the ground was determined to be the best compromise of design variables.

The unit cost for the PRS is $8.6B for the system and $13.1B for supporting systems. An operating cost for maintaining the satellite, the transmitting antenna site, and the rectenna site was estimated at $106M/yr. As in the operating cost estimates for SSPS, a geosynchronous space station was assigned to each unit for purposes of housing maintenance crews, equipment, and spares.

Figure 1.2-2 summarizes the mass properties of the PRS reflector. The total system was estimated at 0.4×10^6 kg with the phase front control system electronics the major contributor. The structural arrangement used in this estimate is the same as that used for the SSPS transmitting antenna.

The PRS efficiency budget (prepared by Raytheon) in Table 1.2-1 reflects the additional efficiency losses relative to a SSPS receiving antenna. The SSPS requires transmission only from the satellite to the receiving ground station. A 95 percent beam collection was used for the up- and down-legs. Ionospheric loss of 2 percent for the two-way path is due to diurnal Faraday rotation effects using a linearly polarized rectenna. This could be eliminated with a dual polarized rectenna if shown to be economical. A 53 percent efficiency is taken to be the nominal PRS value.

Figure 1.2-3(a), prepared by Raytheon, illustrates how the transmitting antenna size (and reflector size) is determined by the power density of its center, aperture illumination taper, and total power transmitted. The latter depends upon receiving antenna output power and system efficiency. For the evaluation of environmental/biological effects, the key parameter is peak power density at the transmitting antenna. This is because the receiving antenna has the same diameter but lower power due to system efficiency losses. The beam taper of 10 dB is a good

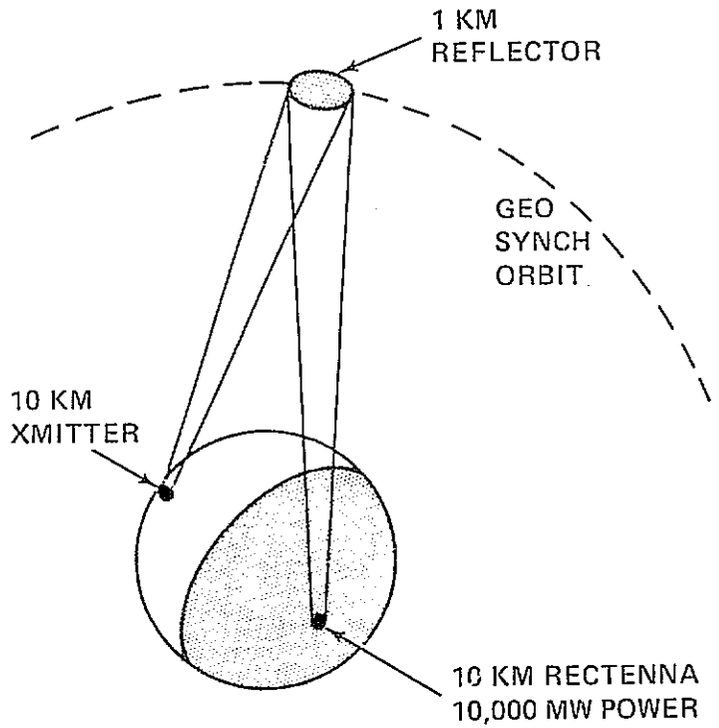

- CONCEPT DESCRIPTION

  TRANSFER LARGE AMOUNTS OF POWER OVER GREAT DISTANCES USING A MICROWAVE TRANSMITTER AT A GROUND BASED REMOTELY LOCATED POWER GENERATING PLANT AND REFLECTING MICROWAVE OFF OF A SATELLITE AT GEOSYNCHRONOUS ORBIT TO A GROUND BASED RECEIVING ANTENNA

- CHARACTERISTICS

– POWER	10,000 MW
– SATELLITE WEIGHT	0.42 X 10^6 KG
– SATELLITE SIZE	1 KM DIAMETER
– GROUND ANTENNA SIZE	
- XMITTER	10 KM DIAMETER
- RECEIVER	10 KM DIAMETER
– ORBIT	GEOSYNCHRONOUS
– LIFE	30 YR
– DC-TO-DC EFFIC	53%

- COSTS (1974 DOLLARS)

– IOC	1990 TO 1995
– DDT&E	
- DIRECTLY RELATED	$ 8.6B
- SUPPORT PROGRAMS	$13.1B
– UNIT COSTS	$ 8.2B
– OPERATING COSTS	$106M/YR

Figure 1.2-1 Power Relay Satellite

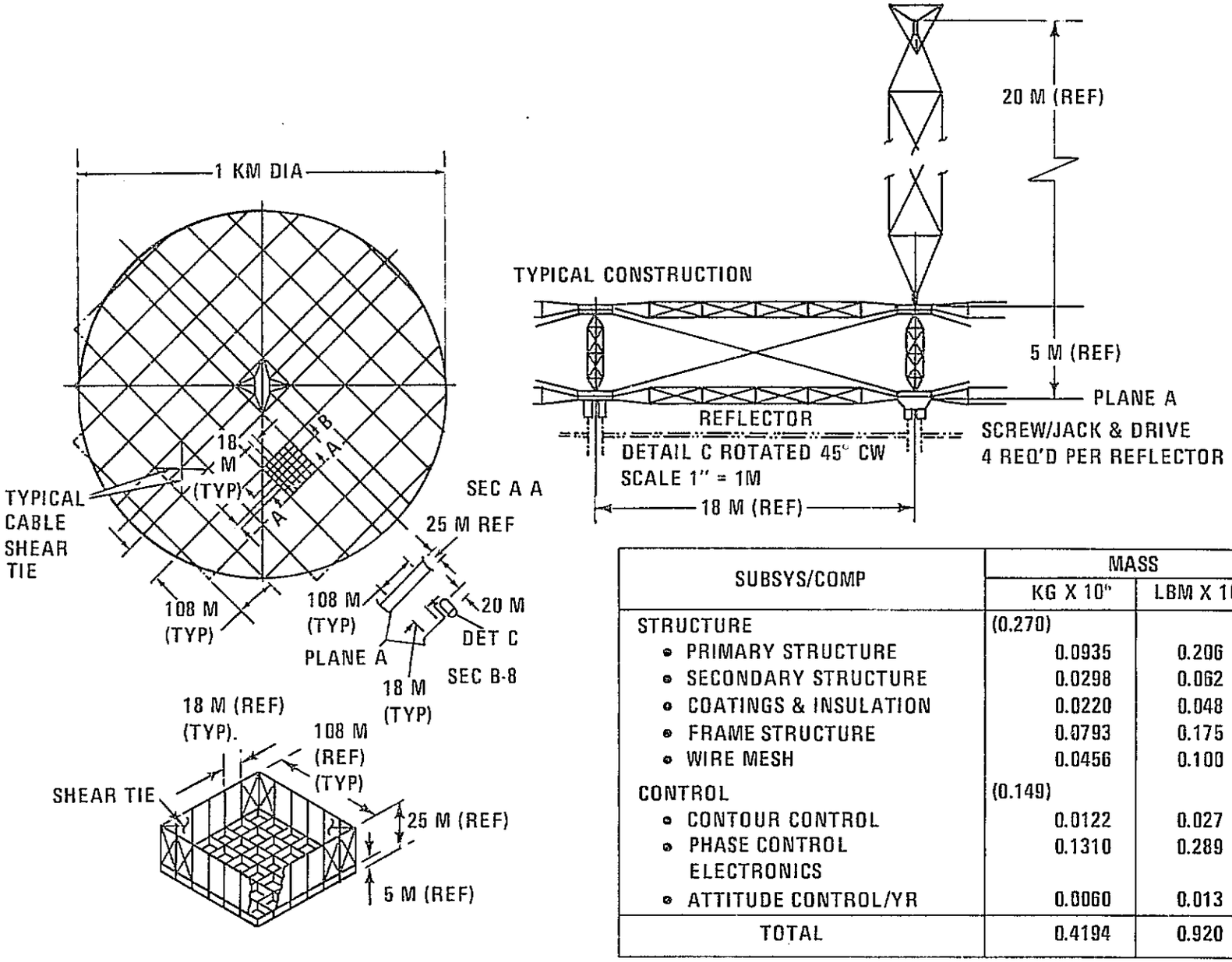

SUBSYS/COMP	MASS	
	KG X 10^6	LBM X 10^6
STRUCTURE	(0.270)	
• PRIMARY STRUCTURE	0.0935	0.206
• SECONDARY STRUCTURE	0.0298	0.062
• COATINGS & INSULATION	0.0220	0.048
• FRAME STRUCTURE	0.0793	0.175
• WIRE MESH	0.0456	0.100
CONTROL	(0.149)	
• CONTOUR CONTROL	0.0122	0.027
• PHASE CONTROL ELECTRONICS	0.1310	0.289
• ATTITUDE CONTROL/YR	0.0060	0.013
TOTAL	0.4194	0.920

Figure 1.2-2 PRS Mass Properties

Table 1.2-1 PRS Efficiency Train

TRANSMITTING ANTENNA	
• POWER INTERFACE	94
• DC-RF CONVERTER	87
• PHASE CONTROL	96
PROPAGATION	
• ATMOSPHERIC (2-WAY)	98
• IONOSPHERIC (2-WAY)	98
REFLECTOR	
• BEAM COLLECTION	95
• OHMIC LOSSES	99
• PHASE CONTROL	96
RECEIVING ANTENNA	
• BEAM COLLECTION	95
• RECTENNA	87
• POWER INTERFACE	94
	53

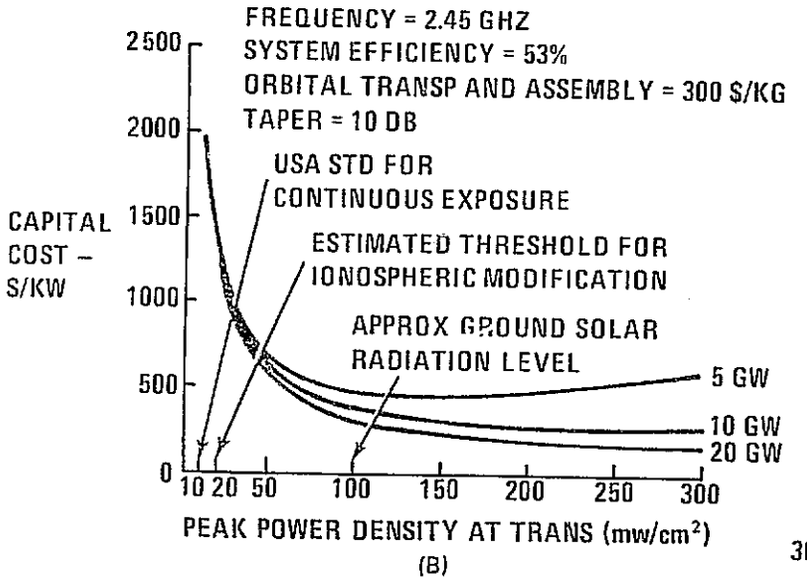

- PEAK POWER DENSITY AT XMITTER OF GREATER THAN 50 mW/cm^2 REQUIRED FOR REASONABLE COSTS. THIS LEVEL IS ABOVE U.S. STANDARD & MAY CAUSE CHANGES IN IONOSPHERE.
- COST SAVINGS ABOVE 10,000 MW NOT SIGNIFICANT

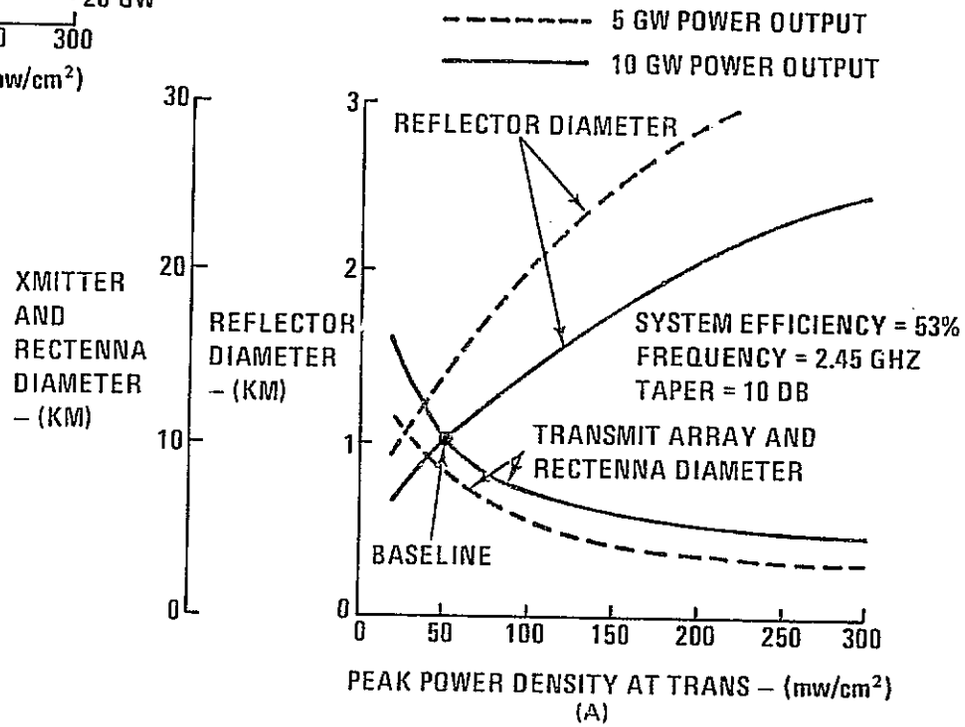

- 1 KM REFLECTOR USED FOR PLANNING AND COSTING

Figure 1.2-3 PRS Configuration Tradeoff

first choice for a 95 percent beam collection efficiency since it results in relatively small reflector dimensions.

The tradeoff between capital cost, system output power, and transmitting antenna peak power density is shown in Figure 1.2-3(b). Higher power densities than those assumed in the SSPS baseline can reduce costs, but there is greater risk of an environmental impact.

2- ENGINEERING ANALYSIS OF SPECIAL REQUIREMENTS FOR ORBITAL SYSTEMS, SATELLITE SOLAR POWER STATION

This section defines system requirements, alternate design concepts to satisfy these requirements, and reports analysis on key performance, cost, and development issues associated with each concept in the following major areas:

- Large solar arrays
- Large structure
- Flight mechanics and control
- Transportation, assembly and maintenance
- Microwave transmission.

Emphasis is placed on identifying operational and economic requirements for the orbiting systems, and defines near-term research activities which will be required to assure feasibility, development, launch and operational capabilities in the post-1990 time frame.

2.1 Large Solar Arrays

The solar array which comprises between 70 and 80% of the orbital system weight must be defined with care to avoid highly pessimistic or optimistic results. This study has considered a broad range of performance, mass and cost parameters.

The following summarizes the pertinent results:

- A passively cooled silicon blanket array tends to show minimum weight at a concentration ratio of:
  - Two to three for front-lighted design
  - Six to ten for a two dimensional back-lighted design
  - Above 100 for a three dimensional back-lighted design.
- A solar blanket cost range of $\$54/m^2$ to $\$150/m^2$ is reasonable. The lower number is in line with the ERDA goal for terrestrial arrays and the $\$150/m^2$

is consistent with todays space qualified blanket fabrication techniques for quantity production in excess of 20×10^6 m^2 of array.

A beginning of life silicon solar cell efficiency of between 18 to 20% (Concentration Ratio = 1) is a reasonable span for assessment of SSPS feasibility. The upper level of efficiency can be achieved with the following technology advances:

- Increase in collection efficiency (small effect)

- Decrease base resistivity to 0.01 ohm-cm

- Higher doping in p and n regions.

- Improvement in radiation damage resistance and annealing is key to SSPS feasibility. A problem with low resistivity cells is a tendancy to have lower minority carrier life times due to a higher density of recombination centers. However, this phenomenon is process dependent. A research effort into the nature and control of the formation of recombination center could lead to high minority carrier lifetimes in low resistivity cells along with high radiation damage resistance. Annealing methods using lithium doped cells or through optical/thermal techniques should be pursued.

Other photovoltaic materials and concepts should be evaluated in an overall study of concentration ratio selection. The work to date under this contract has looked only at the silicon cell potential. A brief study of Gallium Arsenide which can theoretically achieve higher efficiency than silicon and is reportedly more resistent to radiation and thermal degradation, has shown considerable promise. Though potentially more costly than silicon cells, the proper selection of concentration may provide a favorable cost picture. Cadmium Sulfide solar cells are lighter and less costly than silicon cells, but do not achieve the performance and stability of silicon. Multi-junction, edge-illuminated silicon cells have improved radiation tolerance relative to the conventional cell. These cells can operate at high concentration ratios and could offer some attractive configuration approaches. Multi-layer solar cell concepts, which combine the short-wave characteristics of one material and the longer wave characteristics of the silicon cell, have projected efficiencies as high as 30%. Such a device will likely be heavy, but proper selection of concentration may result in a favorable design.

2.1.1 Solar Array Configuration Evolution

The SSPS configuration evolution to date has considered the options shown in Figure 2.1-1. Starting at the top of the figure, the first two concepts represent configuration approaches using flat solar arrays. These approaches were characterized by their high gross weights and extreme flexibility of the solar array assemblies, which was indicative of attitude control problems. In the third concept, an attempt was made to achieve a much stiffer configuration, one which, would be less susceptible to gravity-gradient torques. In this "birdcage" approach, the solar blankets were distributed in vertical strips around the periphery of two drum-like structures. All strips were oriented normal to the sunline, those at the sides and rear of the drums viewing the sun through the gaps separating the sails on the sun side. Mass was high, however, due to the structural weight penalty and to the large solar cell area.

In the fourth concept, lightweight reflectors were used to concentrate the solar flux onto smaller-size solar arrays. In this, the "back-light" approach, the solar arrays faced away from the sun, with thin-film coated mirrors mounted on the booms used to reflect the sunlight back onto the working side of the solar cells. The mass of this concept was considerably less than the earlier approaches. The next two concepts are indicative of front-lighted designs with concentration and will be discussed in more detail later in this section.

A key systems issue to be addressed prior to selection of the solar array configuration is to delineate the preliminary analysis of concentration ratio shown in Figure 2.1-2. This preliminary analysis was performed to determine weight variations due to structural arrangement. It assumes that solar cell efficiency does not vary with increased concentration and does not consider the thermal control system weight to achieve constant efficiency.

Though the model used in this analysis is simplified, the results do indicate a trend. Back-lighted arrangements result in lower specific weight for concentration ratios above two. A two-dimensional, back-lighted design is lighter than a three-dimensional design, though the pointing requirements may prevent achieving concentration ratios above ten. The parabolic back-lit design is the most attractive mass for high concentration, though if the degradation in cell efficiency and increased weight for thermal control were added to the parametrics, the resulting design may not be lower in mass and cost than the low concentration concepts.

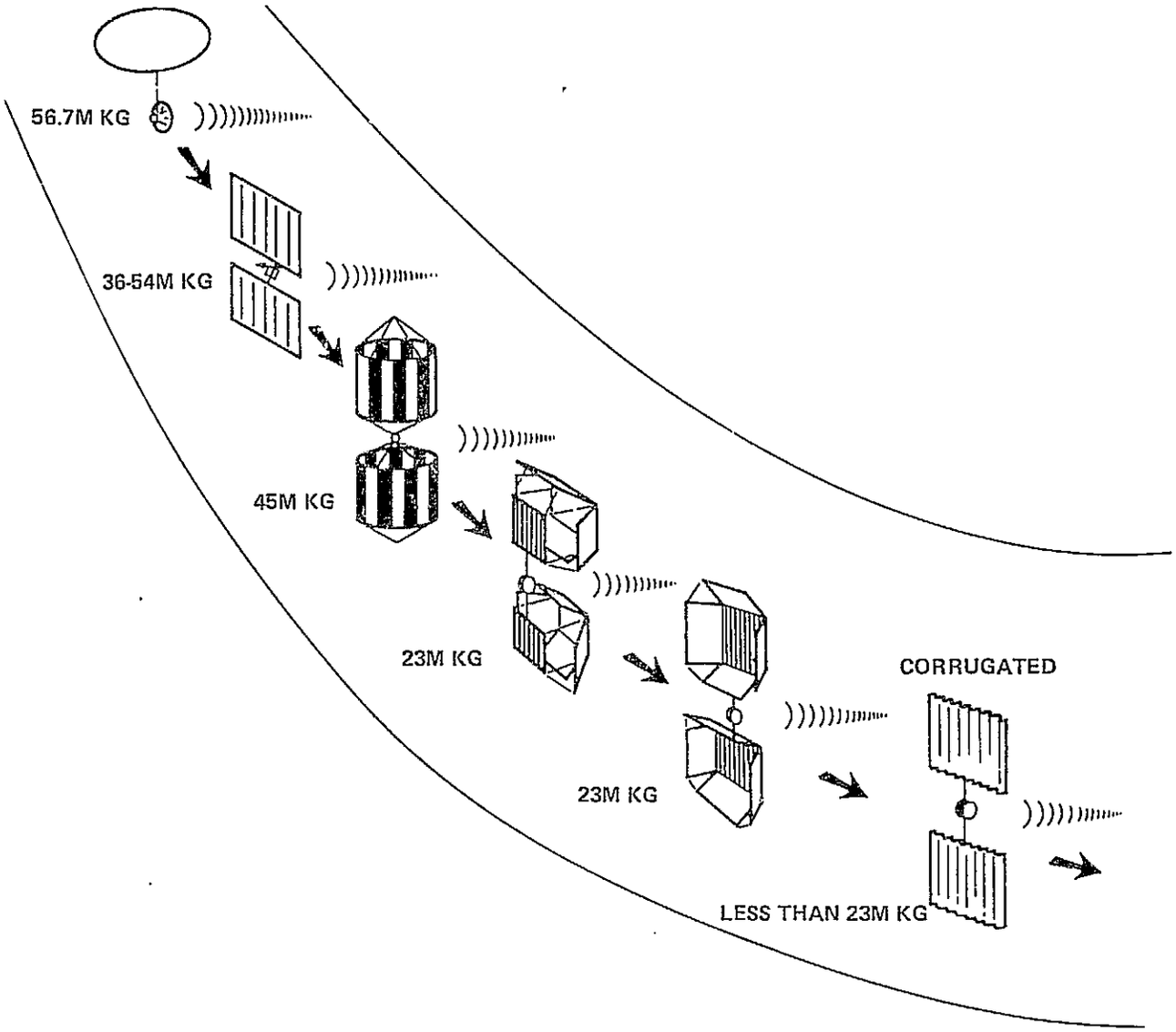

Figure 2.1-1 Configuration Evolution

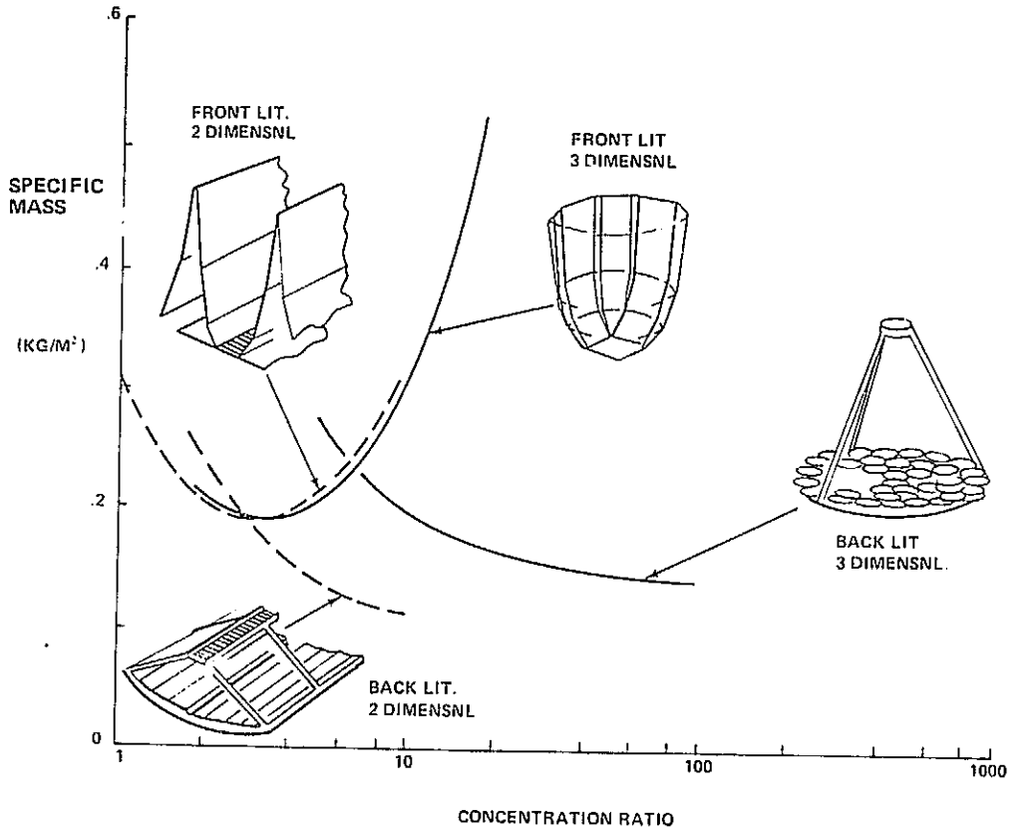

Figure 2.1-2 Specific Weight Variation With Concentration Ratio

An across-the-board design analysis is needed to fully consider:

- Concentration ratio
- Cell efficiency with increased temperature
- Thermal control
- Pointing control
- Transportation and assembly cost.

2.1.2 Silicon Array - Two vs Three Dimensional Front-Lit Configuration

This preliminary study has concentrated on the silicon solar cell's application to the SSPS. The solar cell data used in solar array configuration trade-offs is taken from extensive Spectrolab studies on SSPS feasibility reported in Ref. 2.1-1 and 2.1-2.

The solar cell blanket is a composite assembly of solar cells, interconnectors, radiation shielding and substrate. Present-day spacecraft solar arrays do not use the solar cell "blanket" concept but rather are mounted to a rigid substrate and coverglass for radiation shielding is bonded to the top of the solar cell. These concepts are relatively massive with a typical power to weight ratio of 22 W/kg.

Both NASA and DOD have extensively studied the "roll-out" blanket design. The conventional roll-out blanket bonds the interconnected solar cells to a plastic substrate and bonds silica or glass onto the solar cell as a radiation shield. Power-to-weight ratio of 160 W/kg (without deployment mechanism) are predicted. The current silicon solar blanket utilizes a 200 μm thick cell.

Spectrolab has proposed an ultra-light solar cell blanket with characteristics shown in Tables 2.1-1 and 2.1-2 using 100 μm and 50 μm thick solar cells. The major road blocks to achieving these thin solar cell arrangements is that of fabrication and handling. It is projected that fabrication technology improvements over the next 10 to 15 years will be able to overcome these road blocks.

Table 2.1-1 Mass of 50 μm Solar Cell Blanket (1985)

ELEMENT	MASS mg/cm^2	ACCUM MASS mg/cm^2	POWER TO MASS RATIO, W/kg
SOLAR CELL, 50 μm	16.8	16.8	1590
FEP COVER, 25 μm	5.5	22.3	1200
INTERCONNECT Ag MESH	1.4	23.7	1130
SUBSTRATE, KAPTON	1.8	25.5	1050
SUBSTRATE ADHESIVE FEP, 13 μm	2.7	28.2	950

CELL OUTPUT POWER = 26.7 mW/cm^2 AT 27°C. AM0
AT BEGINNING OF LIFE

Table 2.1-2 Mass of 100 μm Solar Cell Blanket (1985)

ELEMENT	MASS mg/cm^2	ACCUM MASS mg/cm^2	POWER TO MASS RATIO, W/kg
SOLAR CELL (100 μm)	28.6	28.6	930
FEP COVER (25 μm)	5.5	34.1	780
INTERCONNECT Ag. MESH	1.4	35.5	750
SUBSTRATE, KAPTON	1.8	37.3	715
SUBSTRATE ADHESIVE FEP (13 μm)	2.7	40.0	665

CELL OUTPUT POWER = 26.7 mW/cm^2 AT 27°C. AM0
AT BEGINNING OF LIFE

In the development of solar cell weights (Tables 2.1-1 and 2.1-2), no basic "scientific" discoveries were assumed; that is, exotic new materials and forms (such as thin film cells) were not assumed in evaluating SSPS feasibility, but only reasonably projected improvements for crystal silicon cells were included.

The ideal efficiency of a silicon solar cell has been postulated in Ref. 2.1-3 as between 19 and 22%. Papers, Ref. 2.1-3, have outlined approaches for raising the typical 10% solar cell efficiency to 20%. In fact, COMSAT, has already reported 15% efficiencies in laboratory tests. Assuming a nominal increase in collection efficiency and a voltage increase consistent with 0.01 ohm-cm material, the efficiencies given in Ref. 2-1-1 and 2.1-2 are below that predicted for an ideal semiconductor.

Spectrolab used a computer program to extensively study the affects of environment (e.g., temperature, radiation and microwave fields) on the performance of the solar cells shown in Tables 2.1-1 and 2.1-2. Primary emphasis was directed toward defining solar cell performance variation with parameters that influence configuration design. Therefore, the irradiance and temperature dependent variable were studied for mirror/filter configurations. Figure 2.1-3 presents the results of this computer analysis. The solar cell efficiency is plotted against concentration ratio for a cell in orbit for five years (a fluence of 10^{15}, electrons/cm^2 and a suitable damage coefficient selected from the NASA Radiation Effect Handbook). Under the assumed fluence and with one mill FEP teflon covering, it is projected that the non-annealable degradation of the solar cell will be 6% after five years.

2.1.2.1 Two and Four Mirror Concentrator Configuration

This effort has concentrated on analyzing the two most promising silicon cell solar array configurations studied over the past few years. The first is a two mirror system Figure 2.1-4, composed of corrugations of solar blankets and concentrators assembled on two panels and connected by a large diameter central mast. The second concept, Figure 2.1-5, is a four mirror system in a petal arrangement. The two panels of the petal concept are also connected by a large diameter central mast and stiffened with carrythrough structure running the length of the entire assembly.

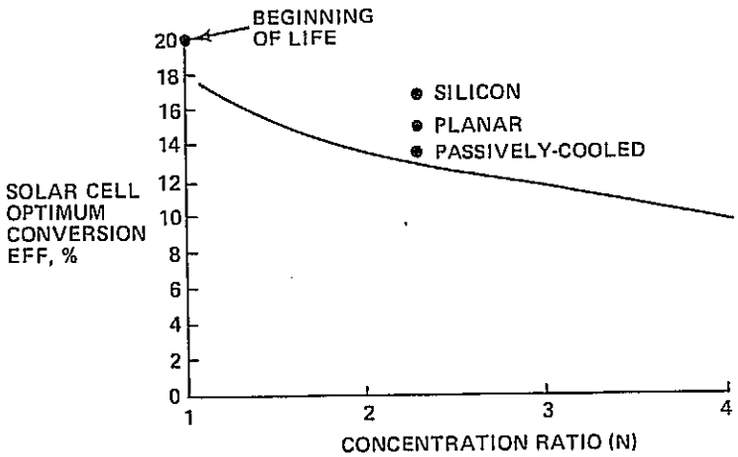

(NOTE:--CELL CONVERSION EFFICIENCY FOR INCIDENT IRRADIANCE VS CONCENTRATION RATIO, FILTER CONFIGURATION OPTIMIZED FOR EACH RATIO, SOLUTION GIVEN FOR OPERATING TEMPERATURE. FLUENCE = 10^{15} E/CM^2 (1 MEV)

REF: SPECTROLAB

Figure 2.1-3 Solar Cell Efficiency

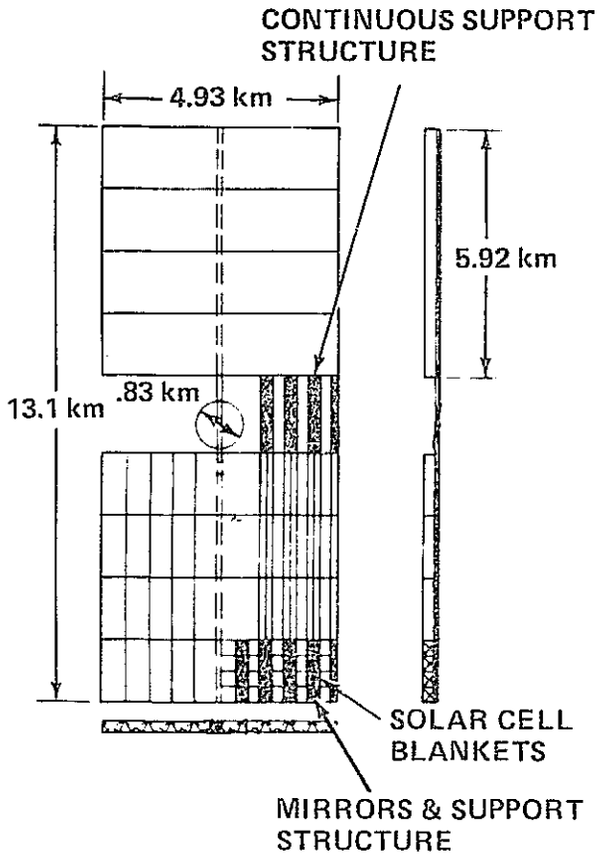

Figure 2.1-4 Typical 2-Mirror System, Concentration Ratio = 2

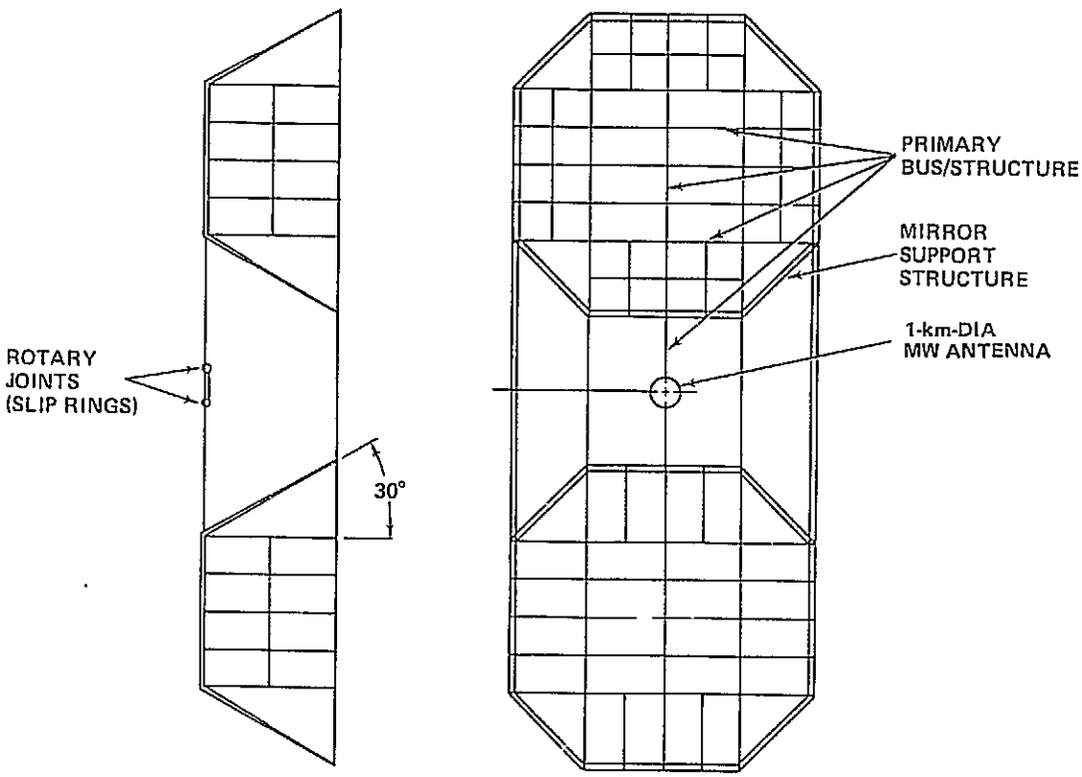

Figure 2.1-5 Typical 4-Mirror System, Concentration Ratio = 3

The groundrules and assumptions used in sizing the configurations are:

- Microwave efficiency = 58% measured from the input to the antenna bus system to the output of the rectenna
- Array distribution system efficiency = 92% measured from the output of the solar cell to the input of the antenna bus system
- Solar blanket weight
  - 100 μm thick cell = 400, 000 kg/km^2
  - 50 μm thick cell = 282,000 kg/km^2
- Concentrator blankets
  - 20,000 kg/km^2
- Central mast
  - 48,600 kg/km length
- Structure
  - 13,860 kg/km length.

The structural and central mast weights are normalized to the SSPS weight statement and structural arrangement presented in Ref. 2.1-4. The unit factor for structure and mast is in terms of total length of material used in the configuration. The solar blanket weights are consistent with Tables 2.1-1 and 2.1-2.

A computer sizing program was used to prepare the weight comparisons shown in Figure 2.1-6 for the 2 and 4 mirror systems. The 2 mirror corrugated design is slightly lighter in weight than the 4 mirror system for both the 50 μm and 100 μm solar cell concepts. Though the solar blanket area for the 4 mirror system could be driven to smaller levels than the corrugated design, the structural penalties and decrease in solar cell efficiency associated with increased concentration ratio in the petal concept, balances the potential area advantage. In fact, both configurations demonstrate a minimum weight at a concentration factor of slightly above two.

Mass sensitivity to variations in solar cell efficiency, microwave efficiency, solar blanket weight and system

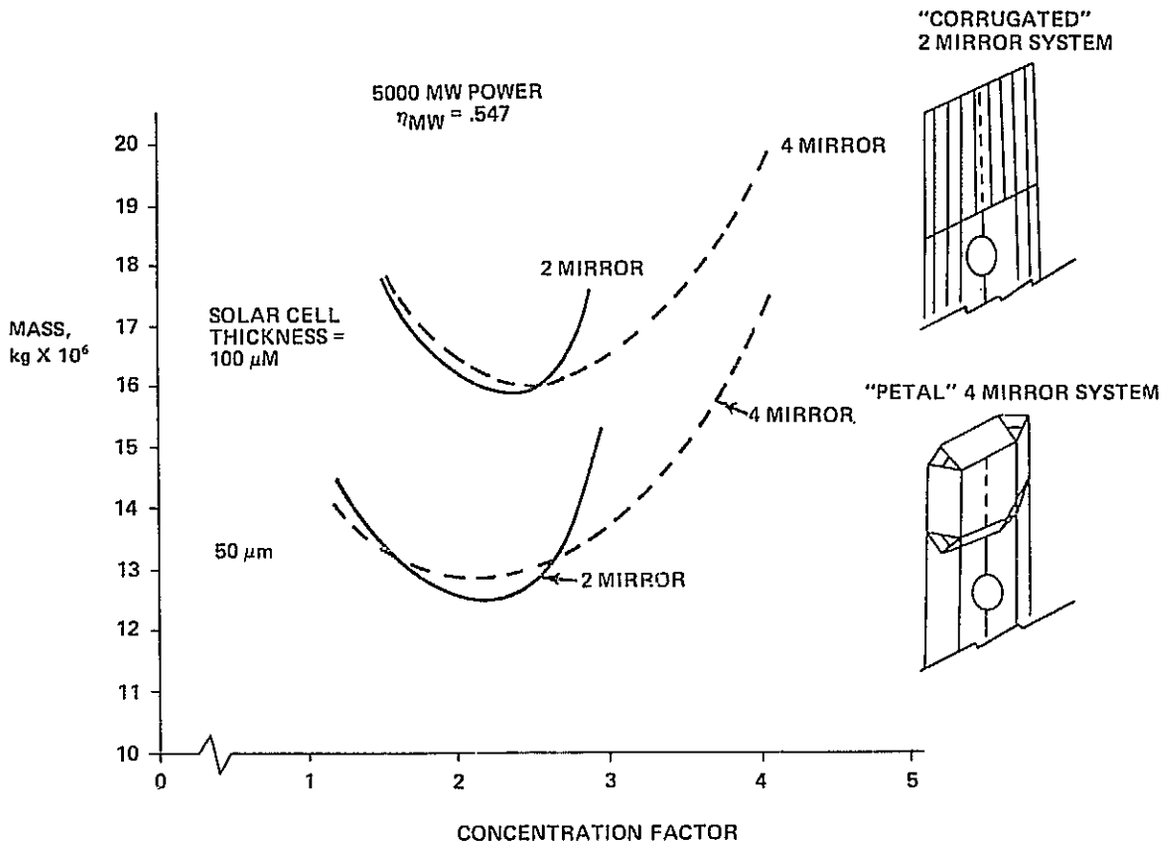

Figure 2.1-6 Solar Array Configuration Mass Comparison

ground output power are shown in Figure 2.1-7. A 10% variation in the efficiency will vary solar array weight 1.2 x 10^6 kg while a 10% variation in microwave efficiency varies solar array weight 1 x 10^6 kg. The 100 μm solar cell results in a solar array that is 3.7 x 10^6 kg heavier than its 50 μm counterpart.

2.1.2.2 Cost Comparison

2.1.2.2.1 Cost Factors - Three values for unit cost factors are given in Table 2.1-3 for the solar blanket, concentrators, structure, transportation and assembly. The low cost factor for solar blankets is consistent with the national goal of $0.50/W (peak) by 1985. A cost of $0.50/W represents a cost of 0.0054 $/cm^2 ($5/ft^2) of solar cell area at an average solar insulation of 1000 W/m^2 (Ref. 2.1-5). The middle value of 0.0068 $/cm^2 is an estimate of space qualified solar cells which utilize edge-defined film-fed growth (EFG) of silicon ribbons. A EFG ribbon cell cost analysis, reported in Ref. 2.1-6, indicated that the total cell cost is 0.38 cent per cm^2. This is added to the projected lamination cost of 0.3 cent per cm^2 to arrive at a total of 0.68 cent per cm^2. The total solar blanket costs established in Ref. 2.1-5 for the high cost approach is 1.5 cents per cm^2.

To check feasibility, the projected cost spread for the operational SSPS solar blanket was compared with historical data in Figure 2.1-8. A production learning curve was established using actual experience on the initial 2 x 2 cm cell, widely used on unmanned spacecraft, and the 2 x 6 cm cell produced for the Skylab program. This established a 75% learning curve for solar blanket costs using conventional fabrication techniques. The high cost estimate $150/m^2 for the operational SSPS falls directly on this trend line.

Technology improvements in fabrication techniques which can reduce the cost of today's blankets from $4000/m^2 to $1200/m^2 could be adequate to achieve the $54/m^2 goal for SSPS.

The p=0.75 estimate for concentrator mirror cost shown in Table 2.1-3 is based on information from Ref. 2.1-5 which places these costs at 0.07 cent per cm^2. More recent inquiries into the cost of aluminized Kapton place these costs at 0.01 cent per cm^2. The middle value shown in Table 2.1-3 is the average of the low and high estimate.

The p=0.75 estimate for structure, $134/kg. was reported in Ref. 2.1-7 and represents the cost of preparing aluminum

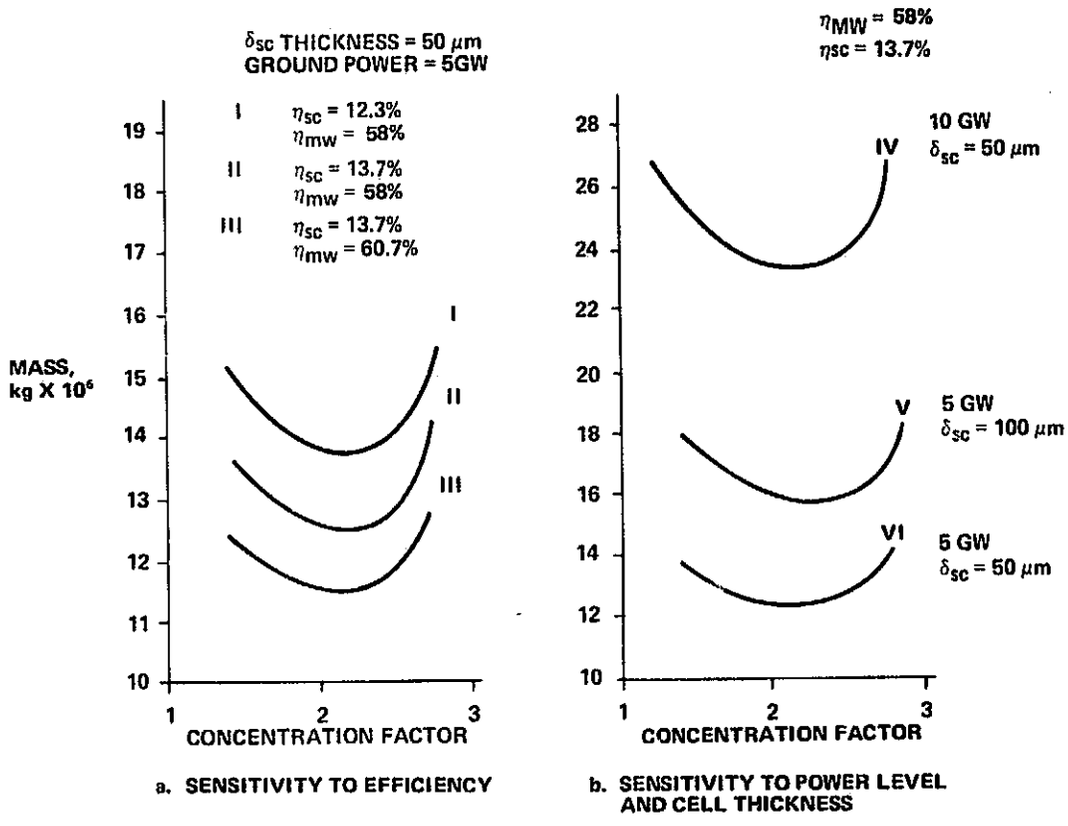

Figure 2.1-7 Solar Array Mass Sensitivity, 2-Mirror Corrugated Configuration

Table 2.1-3 Solar Array Cost Factors Estimate Uncertainty (P = Confidence Level)

ELEMENT		P = 0.25	P = 0.50	P = 0.75
SOLAR BLANKET;	$/km²	54 X 10⁶	68 X 10⁶	150 X 10⁶
CONCENTRATORS;	$/km²	1.1 X 10⁶	3.8 X 10⁶	6.5 X 10⁶
STRUCTURE;	$/kg	4.4	44	134
STRUCTURE FAB;	$/kg	59 } 63.4	88 } 132	106 } 270
TRANSPORTATION	$/kg	105	165	284
ASSEMBLY	$/kg	66 } 171	121 } 286	330 } 614

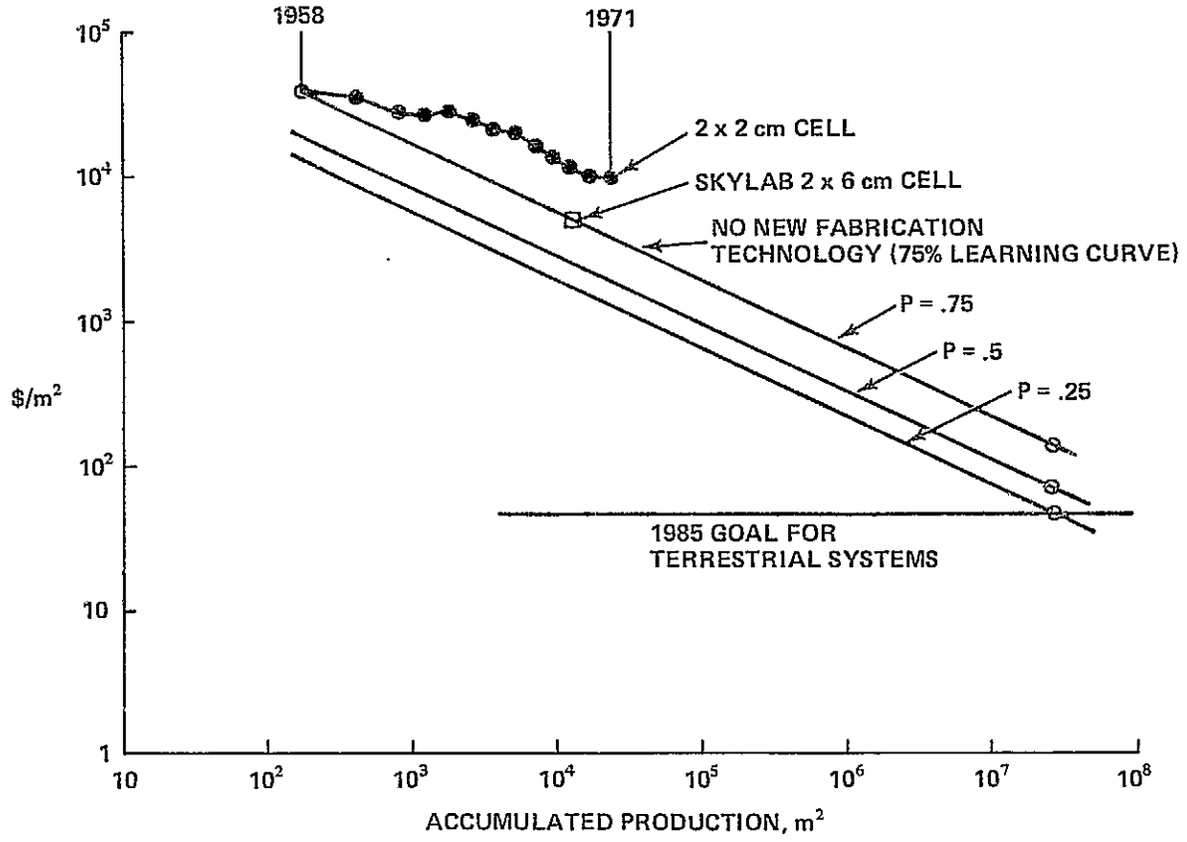

Figure 2.1-8 Projected Silicon Solar Cell Costs

flat stock for shipment to the SSPS assembly site. (The flat stock is fabricated into compression members at the on-orbit site). The prefabrication costs included in the $134/kg include cost of material, preforming, deburring, trimming, heat treating, anodizing and some degree of chem milling in an aerospace shop (mostly hand made). The middle value, $44/kg, is representative of the lowest cost aluminum sheet metal part made in an aerospace shop. The low value, $4.4/kg, is representative of the cost of mass producing the material to specification 25.4 cm wide, 10 to 15 mil thick, anodized 5056-0 condition aluminum) at the mill and by-passing all aerospace shop work. The rate of on-orbit fabrication of structural elements working from the preprocessed flat stock has been estimated at 191 kg/hr, Ref. 2.1-7. At this rate, the cost would run approximately $59/kg of structure. This estimate has been used under the p=0.25 list. The p=0.5 and p=0.75 estimates were arrived at by lowering the basic production rate.

The assumptions used to establish transportation and assembly costs are shown in Table 2.1-4. The p=0.25 estimate assumes the availability of the Heavy Lift Vehicle and an advanced electric propulsion stage. Assembly is assumed to be performed remotely at a rate of 4.5 kg/hr. Man's participation in the operation is restricted to monitoring and maintenance of assembly equipment. The p=0.5 and 0.75 values assume somewhat higher levels of transportation costs resulting from using derivatives of Shuttle rather than the development of a new launch system. The rate of assembly has been lowered from the 4.5 kg/hr at p=0.25 to 0.9 kg/hr at p=0.75 in a remote assembly operation (see paragraph 2.4).

2.1.2.2.2 Sensitivity Studies - A cost spread for three corrugated solar array configurations are shown in Figure 2.1-9. The concept utilizing a 50 μm thick solar cell at an efficiency of 13.7% has been considered the "strawman" for the SSPS over the past two years. Concept II indicates the cost sensitivity to solar cell thickness and concept III reflects the combined effect of increased solar cell weight and decreased efficiency.

The cost for the operational system solar array using the low cost estimates is $380/kW, and $812/kW including transportation and assembly. These totals represent a simple sum of the cost elements. Costs can run as high as $1250/kW using the mid-value cost estimates and as high as $2670/kW using the high-end costs. Clearly they must be brought down to at least the mid-value estimates.

Doubling the solar cell thickness increases capital cost 15% (Figure 2.1-9). The only contributor to this increase is the cost of transporting the heavier array. A combined increase in solar array weight and a 10% decrease in

Table 2.1-4 Transportation and Assembly Cost Assumptions

CONFIDENCE LEVEL	COST ELEMENT	VALUE, $/KG	COMMENT
P = 0.25 ESTIMATE (OPERATIONAL SYSTEM)	• TRANSPORT TO LEO • TRANSPORT TO GEO • ASSEMBLE • FAB OF STRUCT	79 26 66 60	• HLLV WITH 181,000 KG P/L • ADVANCED ION • REMOTE CONTROLLED ASSEMBLY AT 9.1 KG/HR • BEAM FABRICATION RATE = 191 KG/HR
P = 0.50 (PROTOTYPE PLANT)	• TRANSPORT TO LEO • TRANSPORT TO GEO • ASSEMBLE • FAB OF STRUCT	121 44 121 88	• FLY-BACK DOL WITH 88,500 KG P/L • 13.6 KG/KW ION STG • COMBINED REMOTE AT 2.3 KG/HR • BEAM FABRICATION RATE = 166 KG HR
P = 0.75 (DEMO PLANT)	• TRANSPORT TO LEO • TRANSPORT TO GEO • ASSEMBLE • FAB OF STRUCT	179 106 331 106	• DOL WITH 74,800 KG P/L • 2 STG CHEMICAL • REMOTE AT 0.9 KG/HR • BEAM FABRICATION RATE = 95.3 KG/HR

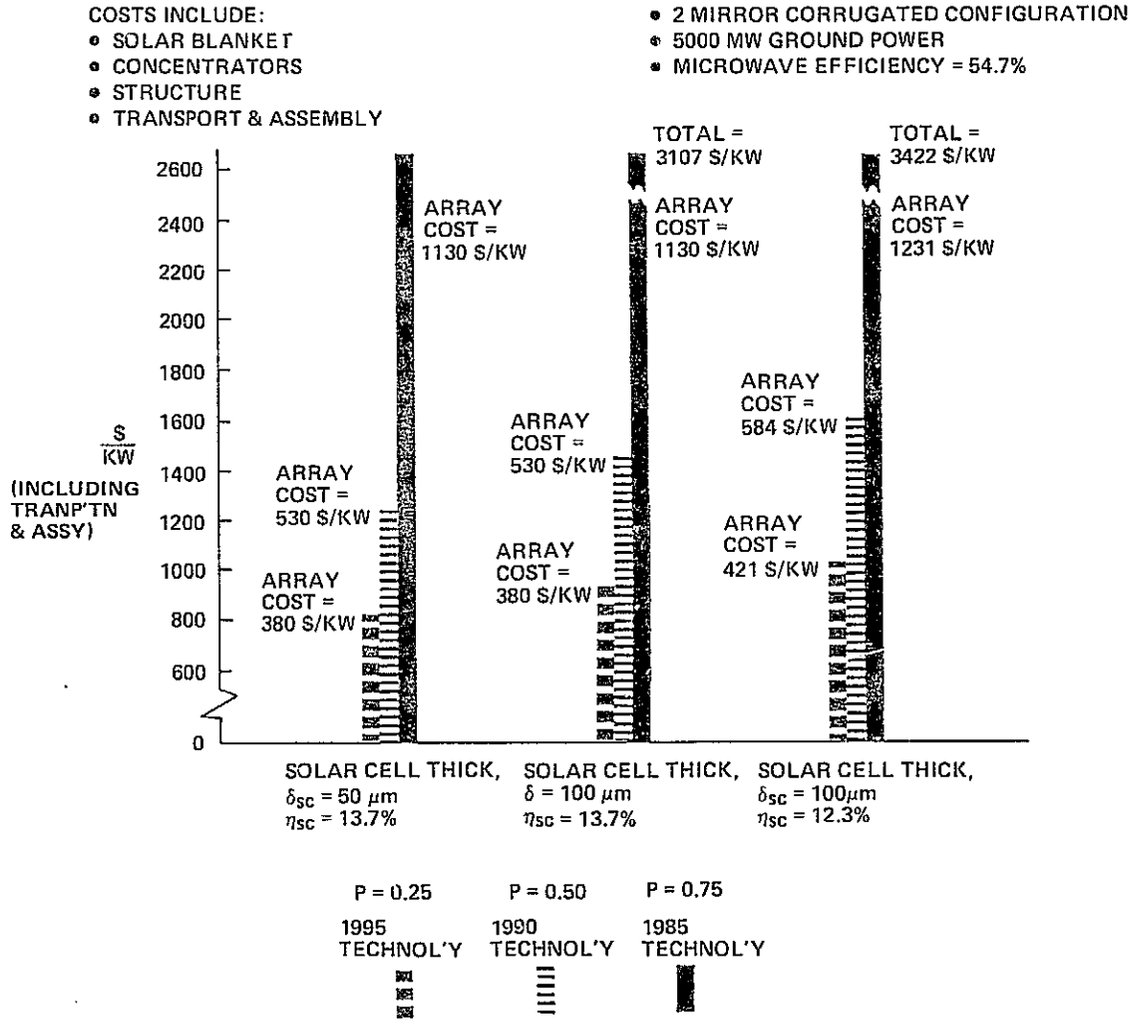

Figure 2.1-9 Solar Array Cost Comparison

efficiency, Concept III, increases capital costs 26% relative to the "strawman". This increase reflects the added cost for transportation and the increase in solar cell area.

Figure 2.1-10 presents a cost sensitivity to total power generated by the satellite. A 10 GW system which utilizes the 50 μm solar cell results in a net decrease of 6% relative to the strawman. This suggests that the selection of satellite power level will have a bearing on the cost competitiveness of the SSPS.

The 2-mirror strawman design is compared with 4-mirror designs in Figure 2.1-11. The strawman design is slightly less than a petal configuration with a concentration ratio of 3, and 21% less than a design with a concentration ratio of 4.

Figure 2.1-12 presents the trends in a more general solar array design/cost trade. Solar array costs ($/kW) are plotted against variations in solar blanket costs, solar blanket mass/efficiency and transportation/assembly costs. The solid line represents the SSPS goal for efficiency (13.7% @ N = 2), mass (0.282 kg/m^2) and transportation/assembly cost ($182/kg (see subsection 2.4). The dashed line shows the effect of an increase in transport/assembly costs to $1000/kg; while the dashed/dot line represents near-term technology solar blanket mass (0.525 kg/m^2) and efficiency of 9.7% @ N = 2 at a transport cost of $182/kg.

Significant improvements in solar cell performance and design as well as low-cost transportation are required to achieve a cost effective blanket in the region of $55/$m^2$, the national goal for solar blanket costs. A more in-depth assessment of these trade parameters should be undertaken including evaluation of the development costs required to achieve the desired goal. From an SSPS viewpoint, more dollars spent on low cost, ultra light, space qualified solar arrays may be a better investment than development of improved transportation systems. If the solar blanket technology programs cannot feasibly achieve the performance goals, development of low-cost assembly and transport systems would be the better investment.

2.1.3 Gallium Arsenide Array

The multilayer Al-GaAs/GaAs cell has been given more attention in the past few years, and recent lab data shows these cells to have high efficiency at concentration and to be less susceptible to radiation degradation. Thinner cells and potentially lighter weight is predicted. Costs are not apparently driven by materials availability according to Alcoa.

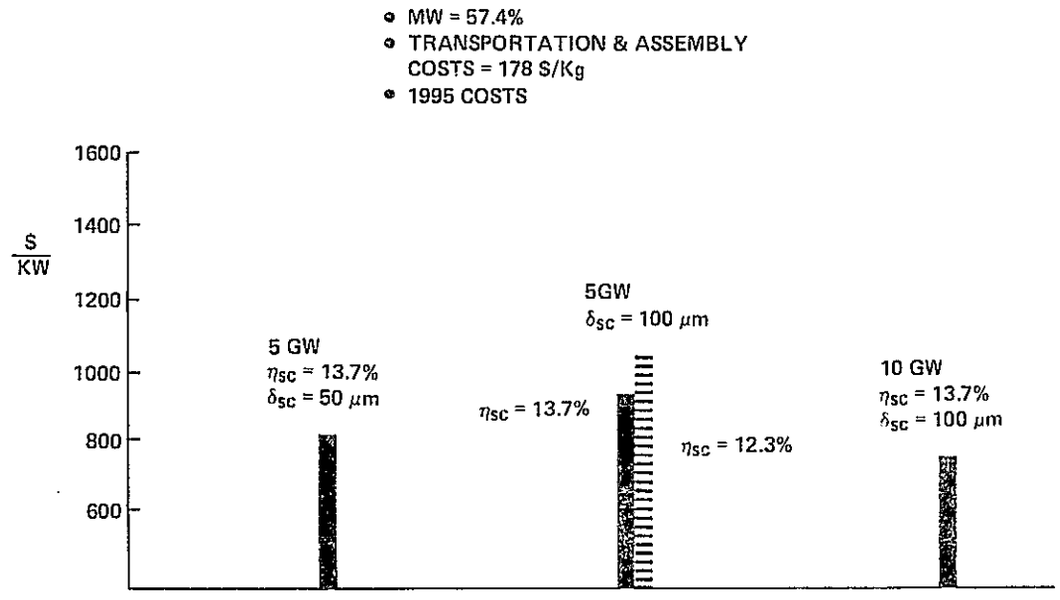

Figure 2.1-10 1995 Technology Cost Base

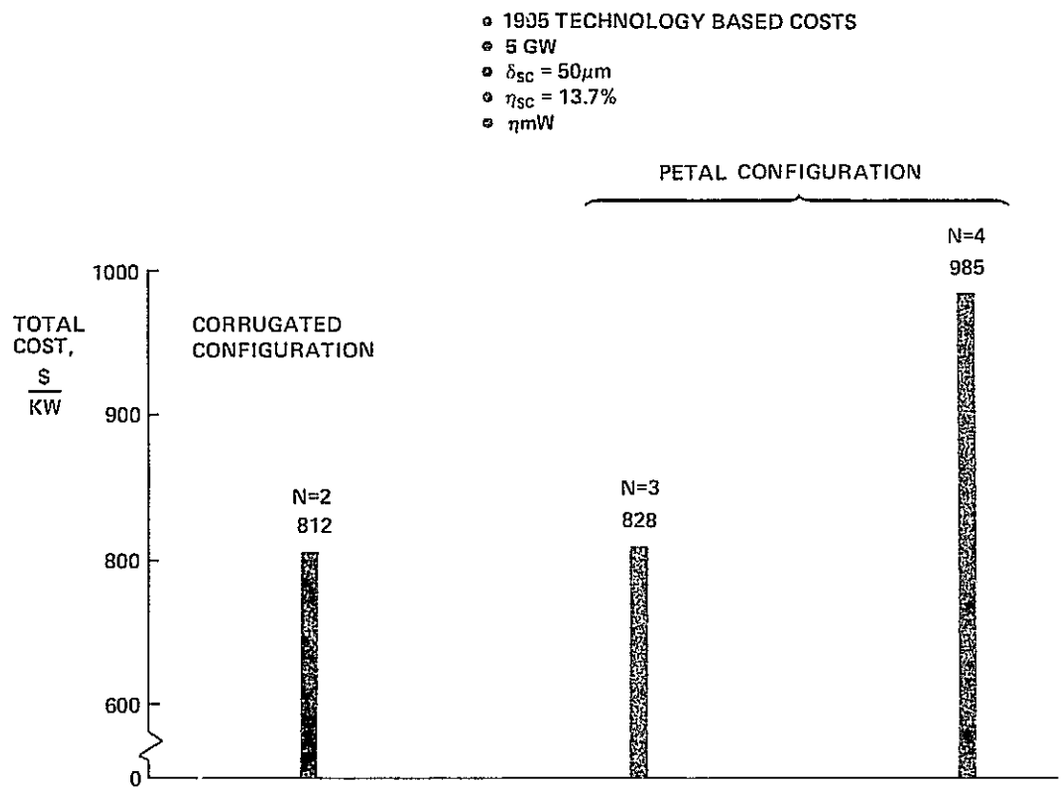

Figure 2.1-11 Configuration Cost Comparison

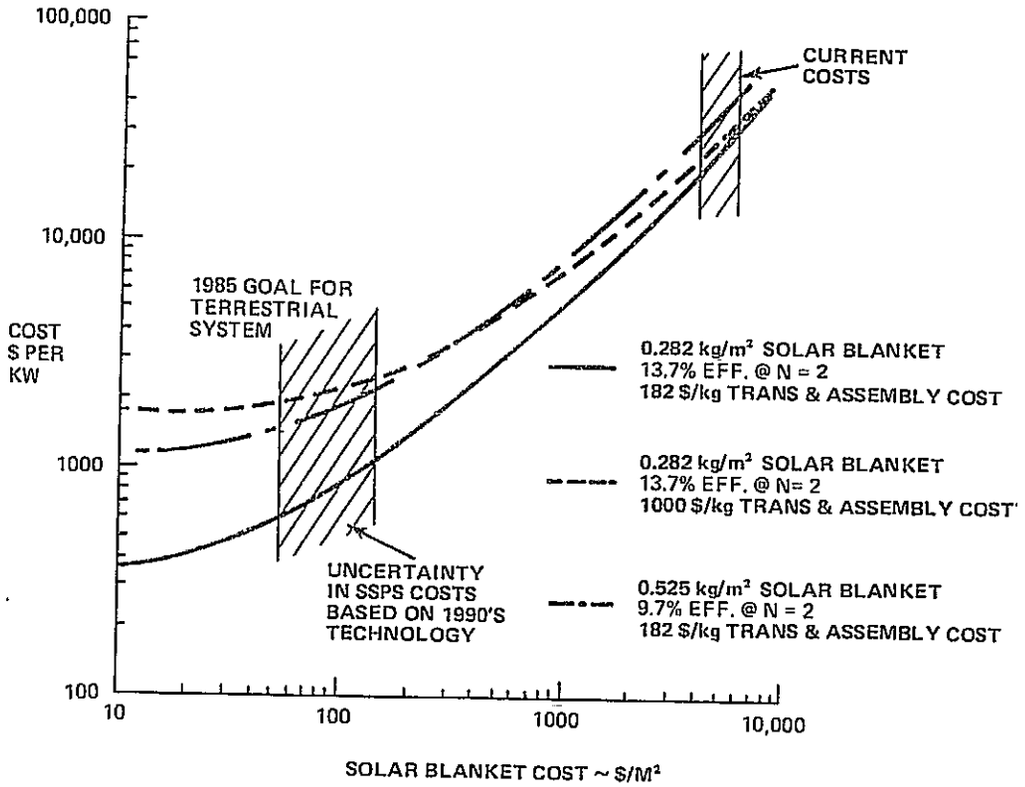

Figure 2.1-12 Solar Array Design Cost Trade

Gallium is a by-product of the aluminum industry. The technology required to reduce cost for this cell is similar to that for Silicon, namely, development of high productivity manufacture.

Estimates of Al GaAs/GaAs performance in air mass zero is shown in Figure 2.1-13. These trends were derived from test data provided by Varian Associates in Palo Alto, California. This data was obtained using an experimental 1/2-inch diameter cell operated at air mass 1.4 over a wide range of concentration and temperature ($1<N<312$; $30^{\circ}C<T<200^{\circ}C$). The I-V characteristics and spectral response at air mass zero (provided by Varian) was used to roughly estimate performance at AMO. The measured sensitivity of efficiency to operating temperature was used to adjust performance to the expected steady state temperature on a passively cooled SSPS solar blanket. A comparison with the expected Si performance is included in Figure 2.1-13. The data in this figure is considered a low estimate.

Figure 2.1-14 presents solar array weight variations with concentration. The Al-GaAs/GaAs configuration shows the potential to achieve lower weight than the projected Si blanket at concentrations of between six and ten. One major uncertainty in estimating the configuration weights shown is the structural weight variations with variations in concentration. The structural weight per unit area of solar blanket and mirror was extrapolated from the 2- and 4- mirror designs available at Grumman. These are front-lighted designs using flat mirror surfaces. At some higher concentration it would become advantageous to consider back-lighted designs (see paragraph 2.1.1). Therefore, a sensitivity to the assumed structural trends is also presented.

The mass sensitivity studies indicate that the Al-GaAs/GaAs solar array should be studied further.

2.1.4 Approaches For Improving Solar Cell Performance

A number of approaches for enhancing solar cell performance, primarily by increasing the concentration ratio, have been identified. The approaches include a heat pipe application, a passive conduction heat transfer scheme, and the use of heterojunction techniques. The first approach makes use of a heat pipe, made of mylar (or similar) film, in an inflatable "beach raft" configuration with discrete cylindrical cells. This "pipe" or vapor chamber could be used in conjunction with a number of local concentrator designs, such as, the concept shown in Figure 2.1-15a.

The passive conduction approach utilizes local concentrators, with the reflector made of a conductive material tied to the cell itself, Figure 2.1-15b. The reflector thus becomes an extended radiation fin which reduces temperature.

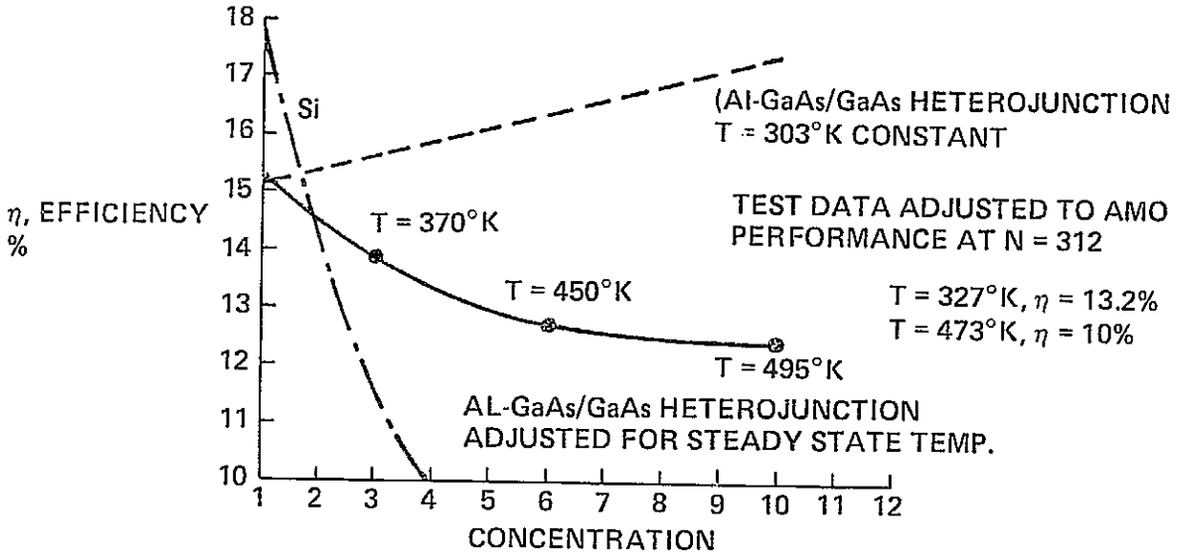

Figure 2.1-13 Estimated Al-GaAs/GaAs Performance (AMO)

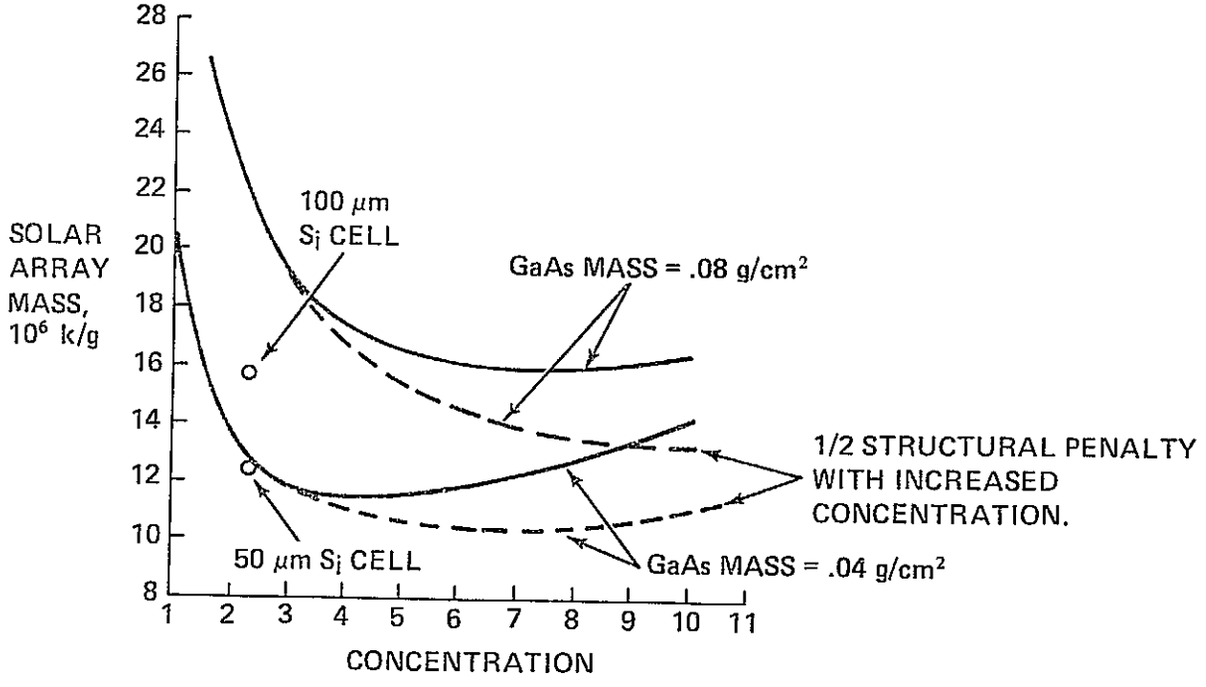

Figure 2.1-14 Estimated Solar Array Weight

Other concepts which have been identified for increasing solar cell efficiency utilize heterojunction techniques with III-V compound materials such as gallium arsenide (GaAs), indium phosphide (InP), gallium phosphide (GaP), and aluminum gallium arsenide (AlGaAs). For example, in 1969, a p-Si-n-GaAs heterojunction cell was claimed to have an efficiency of 28%, and a n-InP-p-GaAs was claimed to have an efficiency of 30%; the arrangement shown in Figure 2.1-15c (Honeywell) was said to have an efficiency of 30%.

Another heterojunction technique concept involves the utilization of multilayered cells in which the upper layer, with a high band gap (such as GaP), converts the higher energy photons (current flow) and passes the remaining photons to the next highest band-gap material (such as silicon or gallium arsenide) for further current generation. The lowest energy photons eventually are passed to low band gap material such as germanium. The advantage of the multilayered cell is that the total power per unit area (or efficiency) appears capable of reaching a theoretical maximum efficiency of 50% with further development. Such cells can be arranged in stacked modules as shown in Figure 2.1-16.

Still another arrangement consists of a combination of solar concentrator mirrors and various band-gap cells, Figure 2.1-17, in which mirrors reflect an optimized bandpass, such as 0.5 to 0.9 μm for the Si or GaAs cells, 0.2 to 0.5 μm for the GaP cells, and 0.9 to 2.5 μm for the Ge cells.

All of these systems, however, require further development, detailed optimization, and the performance of tradeoff studies. Several other solar cell systems also are presently being evaluated for the SSPS application.

2.1.5 Summary of Issues

A major uncertainty that precludes arriving at a clear cut statement of SSPS economic viability is the cost of the solar blanket. Methods and technical direction for potentially achieving low cost silicon solar blankets have been identified. What is needed is an active solar cell development program which concentrates on:

- Fabrication - Development of methods to fabricate low resistivity silicon materials:
  - Methods for continuous growth of single crystal ribbons
  - Methods for highly automated, high rate assembly of cells into integrated blankets

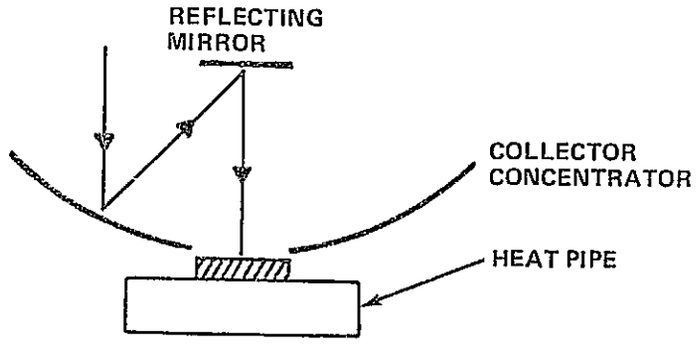

a. HEAT PIPE APPROACH

b. PASSIVE CONDUCTION APPROACH

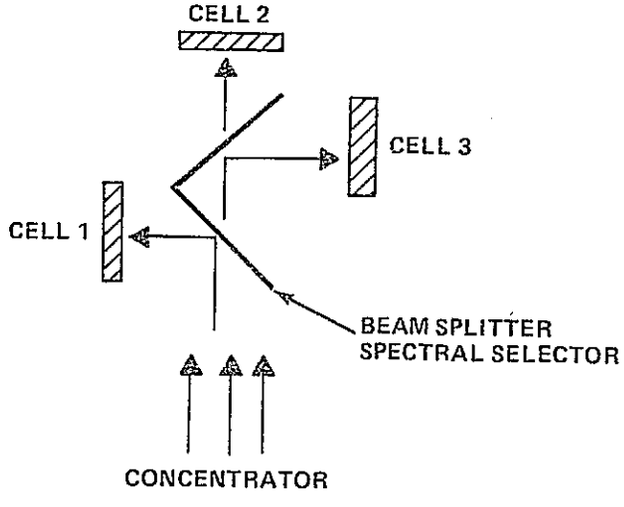

c. BEAM SPLITTER APPROACH

Figure 2.1-15 Solar Cell Improvement Concepts

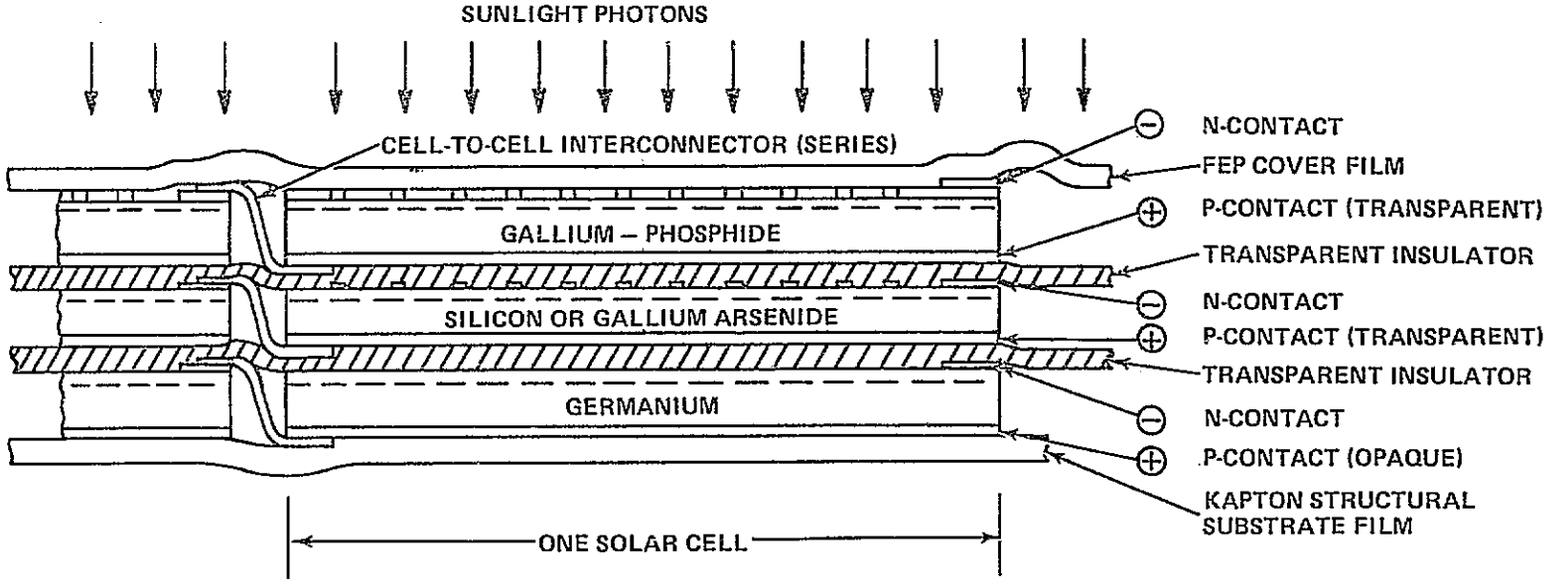

Figure 2.1-16 Multiple-Material Stacked Cell Concept

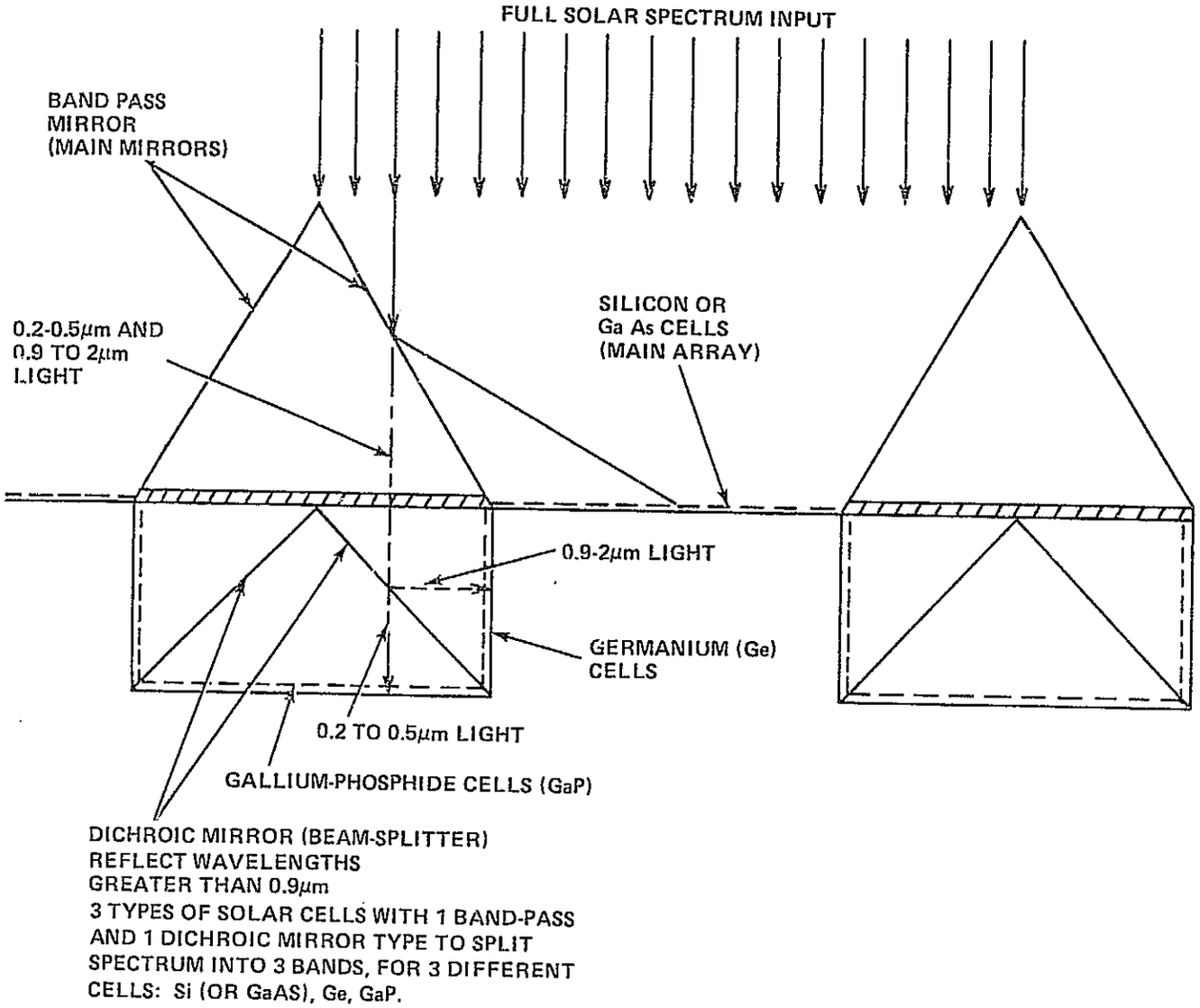

Figure 2.1-17 Multiple-Material Mirror Concept

- Improved Efficiency:
  - Processes for achieving low resistivity silicon solar cells
  - Improvements in collection efficiency
  - Improvement in doping methods to increase radiation resistance
  - Development of simple annealing methods to maintain high cell efficiency with time.

Investigations into methods to improve cell efficiency are important to meeting SSPS goals. The efficiency must increase from about 14% (N = 1) to 18% (N = 1) while reducing thickness of the device from 200 μm to 50 μm. These investigations should include experimental development of new conversion devices such as the heterojunction Ga AlAs/GaAs cell.

The need to reduce cell fabrication cost is critical to SSPS. Large quantity production will naturally help reduce cost but additional cost savings can be achieved with new crystal growth processes and new automated cell fabrication techniques.

Large solar arrays that can be effectively handled are a key to SSPS. Presently, solar arrays are made much like an art mosaic, where individual cells are fitted, interconnected, and bonded to substrate. Improvements can be achieved by developing light-weight blanket encapsulation techniques, lightweight structural weaving techniques, new thermal control coatings, improved radiation-resistant materials and better automated techniques for integrating and testing the blanket. Automated blanket fabrication techniques are needed to reduce cost.

Solar concentration is shown to reduce SSPS cost. Low mass mirror design concepts and their implementation are needed. New antireflective coatings will help improve solar cell life and performance. If high concentration is used, techniques for fabricating lightweight structure and contour control are needed.

The SSPS will generate high voltage power in a relatively stable thermal environment but must maintain performance during a 30-year exposure to ultraviolet radiation as well as trapped particle radiation. The objective is 6% degradation over five years. Improvements in environment resistance can be achieved by improved material, spectral wavelength matching, high-voltage-plasma interaction protection, meteorite hardening, and development of annealing techniques.

Multi-megawatt solar power generation requires switching protection at high voltage and current. Development of high voltage switches and control devices are needed. Circuit design must consider induced magnetic moments to reduce effects on the overall spacecraft control. The high voltage also could lead to corona formation that could reduce component life. A key trade is to determine the extent to which the conducting busses can also be used as structure. A tradeoff between ease of assembly, cost, mass, reliability, and electrical efficiency should be studied.

2.1.6 References

2.1-1 Spectrolab - 6011-03 Progress Report - "Feasibility Study of Satellite Solar Power Station," 1 October 1972.

2.1-2 Spectrolab - 6011-02 "Progress Report - Feasibility Study of Satellite Solar Power Station", 1 September 1972.

2.1-3 NAS, "Solar Cells - Outlook for Improved Efficiency", 1972.

2.1-4 NSS-MO-75-109, "SSPS Engineering Analysis of Special Requirements Transportation to Low Earth Orbit," 21 February 1975.

2.1-5 JPL, "Progress Report No. 2 - Comparative Assessment of Orbital and Terrestrial Central Power Station", August 1 to November 30, 1974.

2.1-6 NASA CR-2357, "Feasibility Study of a Satellite Solar Power Station," February 1975.

2.1-7 MPTS-R-002, "Task 2 Concept Definition, Microwave Power Transmission System Studies - Mechanical Systems & Flight Operations," 12 December 1974.

2.2 Large Structures

The large structures study had the following objectives:

- Re-evaluate the SSPS two-dimensional, front-lighted structural design
- Estimate member sizes based on design requirements for the operational environment and the compatibility of the design with fabrication
- Develop a structural model for use in loads, controls, and thermal response studies
- Establish estimates for the non-conductive and conductive structural mass for the array
- Establish structural mass estimates for the antenna
- Define key structural/materials issues.

Key results of the study can be summarized as follows:

- The baseline structural configuration appears to be incompatible with the thermally induced internal loads during both sunlight and earth shadow conditions. Longitudinal expansion of the central mast (estimated at 149°C from power conduction heating effects) relative to the solar array structure results in perpendicular deflections to the solar array. Maximum deflections of 50 meters were estimated for earth shadow conditions, and maximum deflections of 22.6 meters were estimated for sunlight. The maximum slope of 1.1 degrees which occurs for a small portion of the array, exceeds the established 1 degree requirement. As a result, compressive loads of 11925 N occur in cables directly attached to the central mast; this compares with a design load for cable pretension of 890 N.
- Analysis results are correlated to the temperature assumed for the central mast; a more refined estimate of the central mast temperature profile thus should be established, and further thermal-load analyses then should be performed.
- The assembled structure is compatible with the maximum aerodynamic and gravity gradient forces applied during low earth orbit operations.

- The assembled SSPS is capable of supporting loads applied from ion propulsion stages for transportation to geosynchronous orbit. When applying concentrated thrust forces at the rotary joint (to achieve thrust vector rotation) thrust magnitudes of not more than 5793 N (1302 lb) are allowed; this results in trip times of about 300 days. For a thrust application uniformly distributed across the solar array, a maximum thrust of 13,802 N (3103 lb) can be applied; this results in a trip time of approximately 100 days.

- Transporting major SSPS subassemblies to geosynchronous orbit using chemical propulsion systems is not feasible. Thrust/mass ratios of typical chemical propulsion system stages result in applied loads much greater than the subassemblies can accommodate. Lower thrust/mass chemical stages, commensurate with the allowable applied loads, provide inefficient performance.

- Attitude control thrust requirements are not critical in baseline structural sizing. Structural excitation by roll, pitch, and yaw thruster firings, with 14 symmetric modes considered (11 elastic plus 3 rigid body) indicate structural loads significantly smaller than allowable loads.

- Although control forces are low, significant reductions in array stiffness are not feasible if an adequate margin (factor of ten) is to be maintained between control and structural frequencies.

- Stationkeeping translational maneuver requirements are well within allowable thrust magnitudes. Thrust forces of approximately 934 N (210 lb) applied at the edges of the solar array compare favorably to the allowable 2570 N (578 lb).

2.2.1 Solar Array Structure

2.2.1.1 Configuration

Figures 2.2-1, 2.2-2, and 2.2-3 show the general structural arrangement of the SSPS vehicle. The main structural framework for each solar array consists of a large diameter (80 m) coaxial mast transmission bus, transverse DC power buses, and non-conductive struts. Shear loads are transmitted by tension-only wires. Structural continuity between the two solar arrays is supplied by the mast and non-conductive structure running outboard of the antenna. The baseline array is 13.1 km (8.14 miles) long and 4.93 km (2.91 miles) wide, with a .83 km (.52 miles) diameter microwave antenna located approximately at its center.

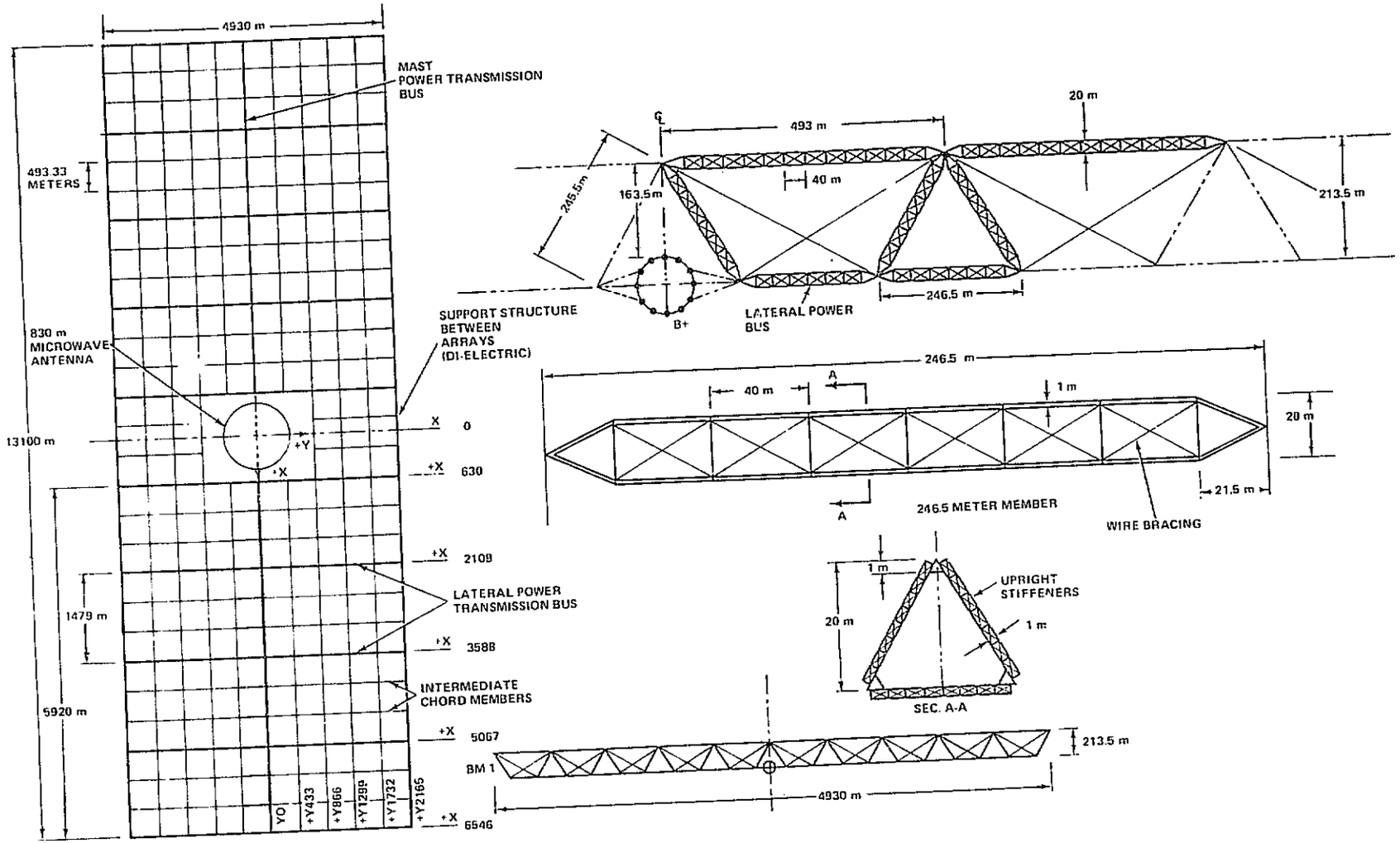

Figure 2.2-1 SSPS Structural Arrangement

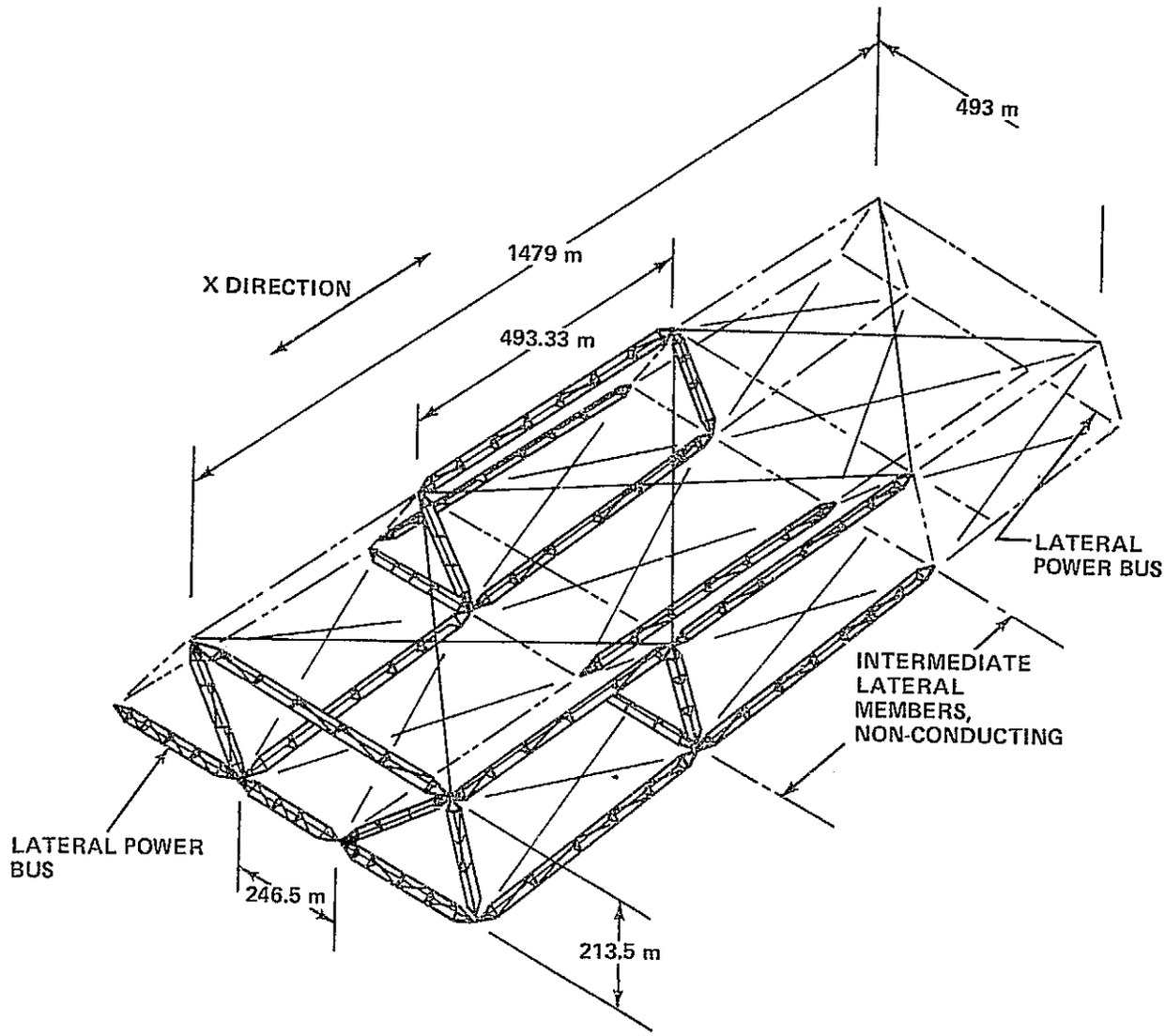

Figure 2.2-2 SSPS Structural Assembly of 1479 m Segment

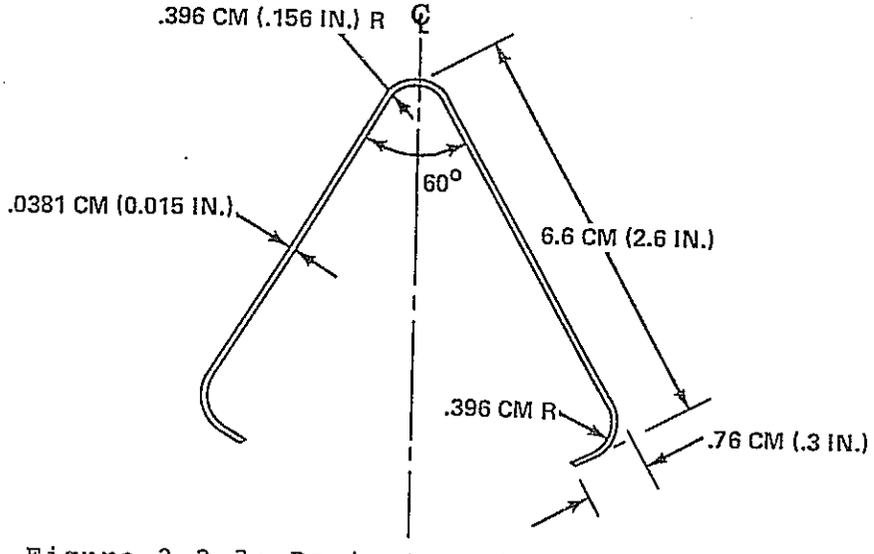

Figure 2.2-3 Basic Structural Cap Member

The total mass of the array in synchronous earth orbit is 18.06 x 10^6 kg (39.75 x 10^6 lb). With the exception of the carry-through structure surrounding the microwave antenna (X = - 630 to X = + 630m), the structure is constructed of aluminum alloy. The carry-through structure, which must have microwave transparency, is constructed of S-glass/epoxy with quartz wire tension braces.

The solar array structure consists of 20 longitudinal (X-direction) truss girders inclined 30 degrees off the Z axis. The truss girder consists of three 20 meter deep, 393 meter long cap members; shear stiffness is provided by cross bracing cables. The large diameter (80 m) coaxial mast transmission bus which carries power to the microwave antenna is located on the lower centerline (-Z213.5m). The mast member sizes are based on power transmission requirements. The mast is also considered part of the primary structure and is included in the analyses. The primary chordwise structural members are located at X630, X2109, X3588, X5067, and X6546. As shown in Figure 2.2-1, these members are made up of 246.5 x 20m and 493 x 20m girders. All the lower members (at -Z213.5m) of these chordwise trusses are conductors which carry electrical power to the main bus or mast. These members are also considered structurally effective. Located at each 493 meter interval within the 1479 meter bays, additional chordwise members reduce the column length of the longitudinal members. Analysis of the 1479m longitudinal members for combined compression loads and bending moments induced by blanket pre-tension loads imposed the requirement for additional supports.

Each primary member (20 m) consists of three 1-meter truss girder cap members stiffened by 1-meter truss girders spaced at 40 meters and cross bracing cables. The 1-meter truss girder is the basic structural member; it consists of three vee hat section caps braced every 3 meters. The basic structural element vee hat section .0381 cm (0.015 in.) thick, is shown in Figure 2.2.3. The material selected for the basic element in the study is 2219 aluminum in the T62 condition, and is roll-formed into the vee hat section. The 2219-T62 alloy has the following room temperature properities:

- F_{tu} = 54 ksi
- F_{ty} = 36 ksi
- E = 10.5 x 10^6 psi
- p = 0.102 lb per cubic in.

The vee hat section was selected for several basic reasons: the member will tend to have lower thermal gradients across the section, and components can be automatically fabricated from raw sheet stock using free flying modules, as shown in Figure 2.2-4; the vee hat section also has flat surfaces which facilitate attachment, whether by welding, bonding, or mechanical device.

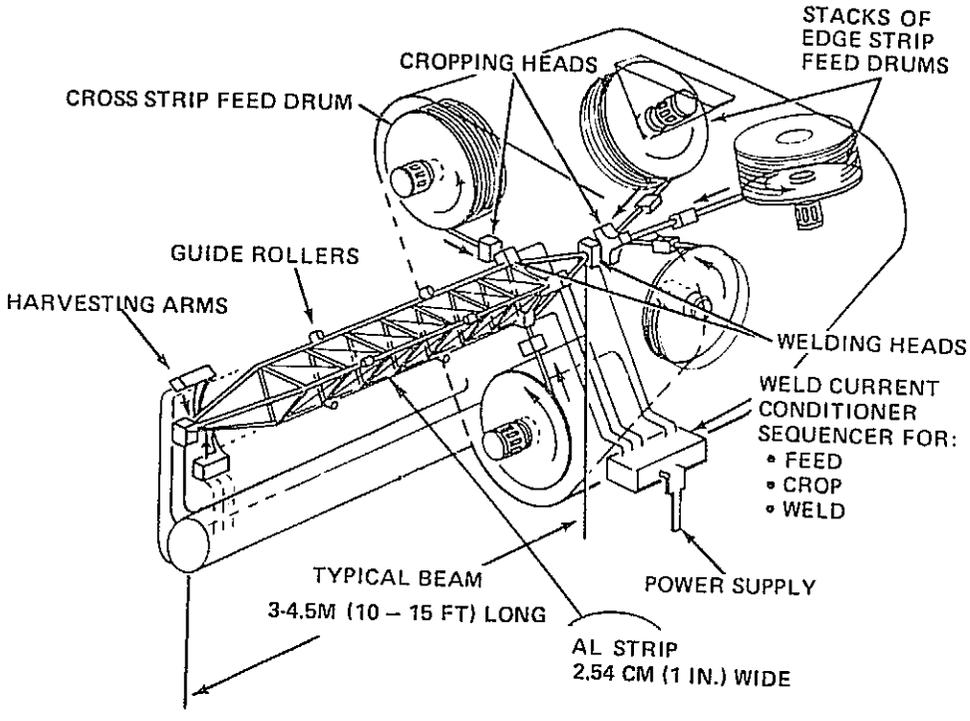

Figure 2.2-4 Fabrication of Compression Girders

2.2.1.2 Design Data

Reference 2.2-1 defines the control forces necessary to correct for orbital drift caused by disturbances,such as solar pressure of 3176N (714 lb) limit per side. Using beam theory, this load was used to obtain member loads and size the structure. The 3176N limit forces applied at each tip of the array produced a peak axial load of 7606N (1710 lb) for the 20m cap member. The 7606N load includes an ultimate factor of safety of 1.4. Since this member consists of 9 vee hat sections, the design load per hat section of 845N (190 lb), ultimate. The 7606N ultimate load is used in combination with the .7 N/m pretension load on the truss girder applied by the solar blanket.

Basic design temperatures have been estimated to be between 80 and 100°F, with proper coatings. Further studies are necessary to evaluate possible thermal stresses and distortions.

2.2.1.3 Basic Structural Element

The basic cap section of the one meter member section shown in Figure 2.2-3 was analyzed for column stability and the Euler column strength as shown in Figure 2.2-5, for various lengths. Using the ultimate design load of 845N, a spacing of 3 meters was selected for cross bracing. For the 20 meter member which is made up of three one meter members, an ultimate design load of 2535N (570 lb) was used. A 40 meter spacing for cross bracing was selected. The data shown in Figure 2.2-5 were derived as part of "Space Fabrication Techniques Study Program (NAS 8-31876)".

2.2.1.4 Mathematical Model and Natural Frequencies

A structural mathematical model was developed to determine SSPS response to the following factors:

- Transport and On-Orbit Loads
- Thermal Loads
- Control System Excitation

The baseline structure was idealized into a mathematical model by lumping masses into node points, and representing the structure by finite element bar members for the 20m deep element and bending elements for the mast. To reduce the number of degrees of freedom, the antenna was placed at the geometric center of the array and symmetry and antisymmetry was assumed. The assumptions used in deriving the model are given in Figure 2.2-6.

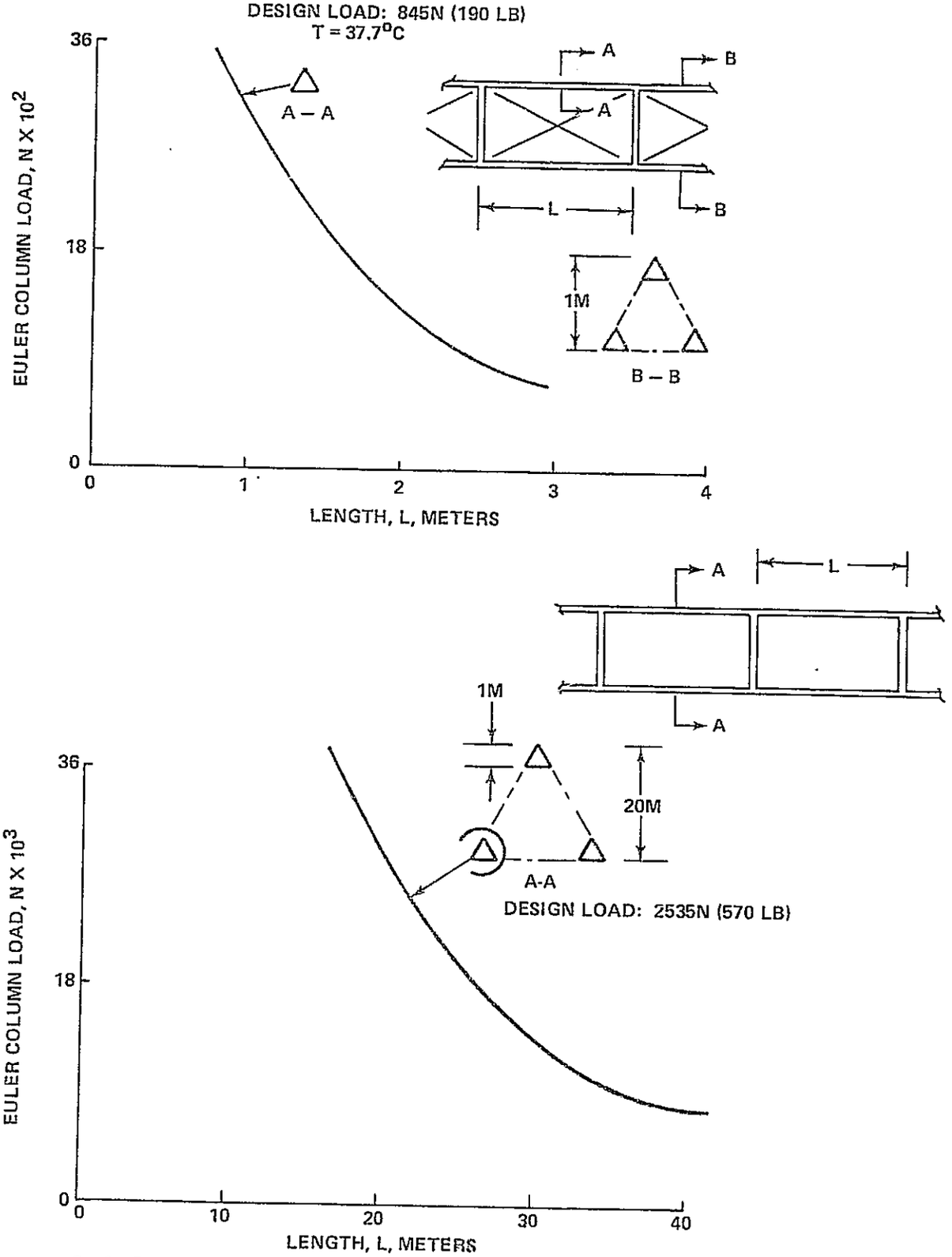

Figure 2.2-5 Space Fabrication Study (NAS 8-31876) Solar Array - Basic Structural Elements, Aluminum Alloy

- Structure is symmetrical about antenna centerlines perpendicular and parallel to mast.
- Analysis uses only half structure.
- Antenna is included as rigid body, rigidly attached to flexible mast, and lies at center of structure.
- Antenna has 6 degrees of freedom.
- Mast is idealized as consisting of multiple beams with bending stiffness and torsional capability.
- Mast moments of inertias are based on six current elements per polarity.
- All other support structure is idealized as axial loaded struts.
- Solar array elements lie in plane of blankets.
- Total cross section area of non-conductive struts is 3.69 cm^2 (.572 $in.^2$) for aluminum and 12.32 cm^2 (1.91 $in.^2$) for dielectric.
- Total cross section area of conductive struts is 10.80 cm^2 (1.674 $in.^2$) for + bus and 21.61 cm^2 (3.35 $in.^2$) for – bus.
- Tension-only wires are replaced by single tension/compression struts – cross section area is .079 cm^2 (.0123 $in.^2$) for aluminum and .079 cm^2 (.0123 $in.^2$) for quartz.
- Model representing half structure consists of 1127 members and 462 nodes.
- Satellite is distributed as lumped masses at node points.
- Dynamic math model is reduced from the structural math model using consistent (Guyen) mass reduction.

Figure 2.2-6 Structural Math Model Assumptions

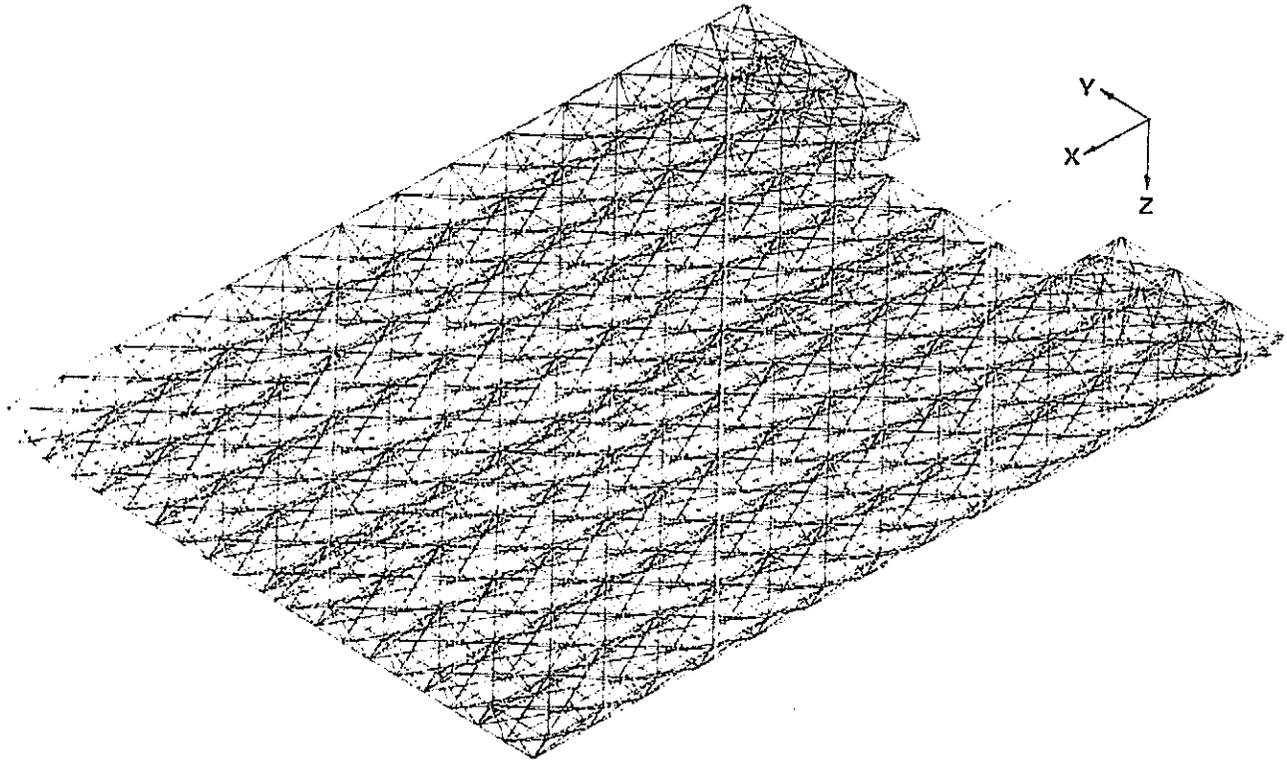

- HALF STRUCTURE CONSISTS OF 1127 MEMBERS AND 462 NODES
- SATELLITE MASS DISTRIBUTED AS LUMPED MASSES AT NODE POINTS
- TENSION–ONLY WIRES REPLACED BY TENSION/COMPRESSION STRUTS
- PROPERTIES (FULL STRUCTURE)

  MASS = 18.06×10^6 kg
  (39.74×10^6 LB)

  $X_{CG} = 0$

  $Y_{CG} = 0$

  $Z_{CG} = 261.6$M (858.3 FT)

  $I_X = 2.445 \times 10^{13}$ kg-m^2 (1.803×10^{13} SLUG-FT^2)

  $I_Y = 1.883 \times 10^{14}$ kg-m^2 (1.389×10^{14} SLUG-FT^2)

  $I_Z = 2.118 \times 10^{13}$ kg-m^2 (1.5652×10^{14} SLUG-FT^2)

Figure 2.2-7 Structural Model Representation

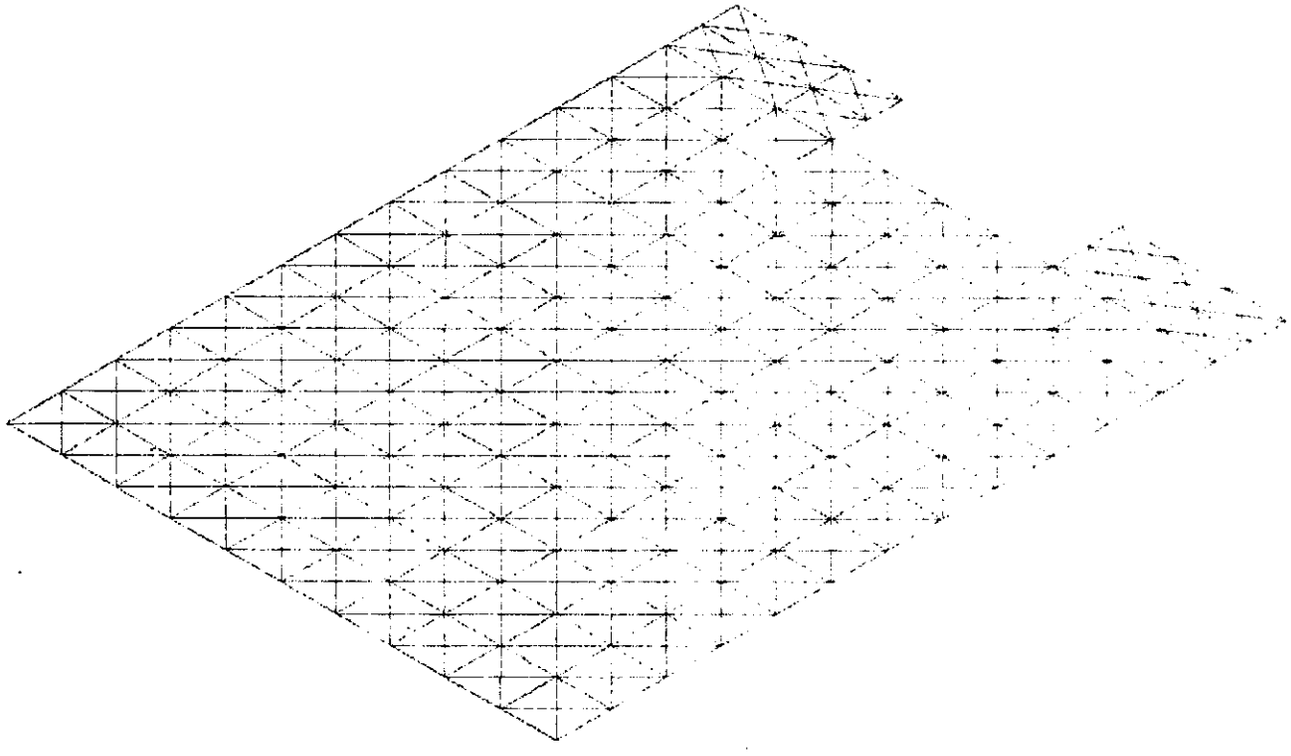

a. TOP DECK

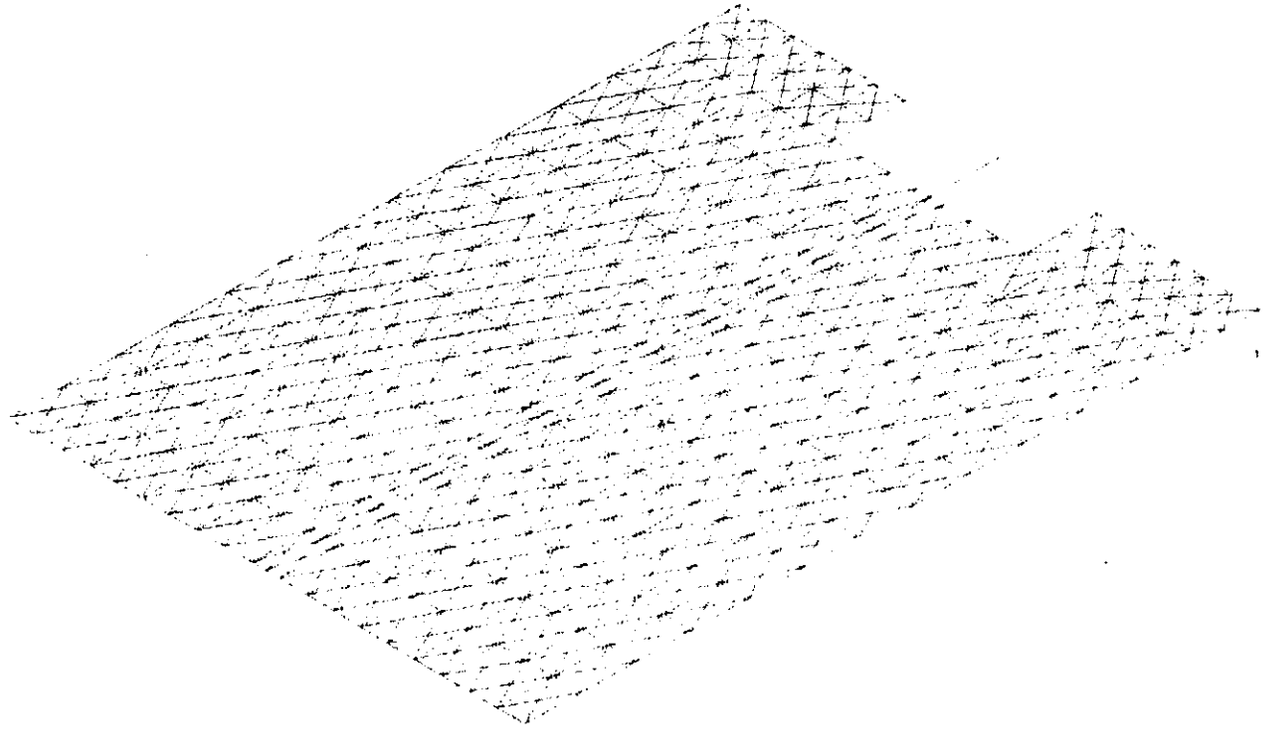

b. BOTTOM DECK

Figure 2.2-8 SSPS Structural Math Model, Sheet 1 of 2

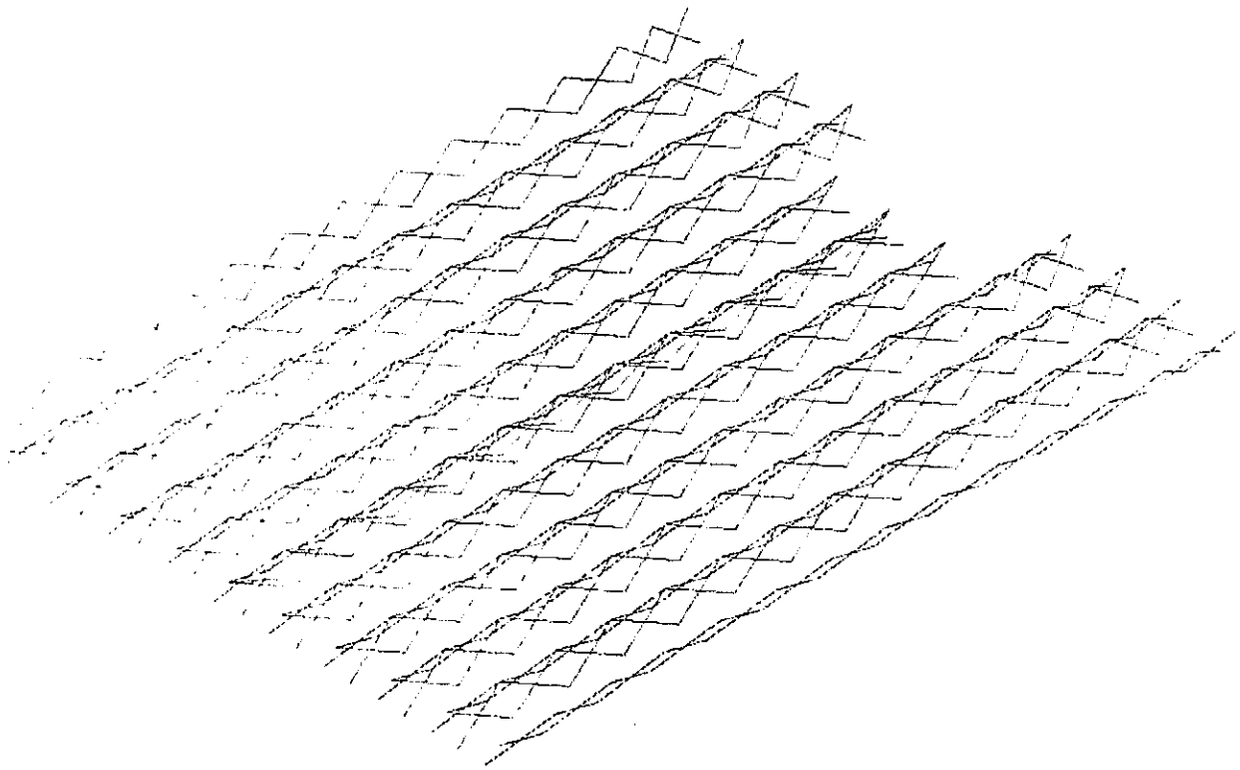

c. CONCENTRATOR WIRE BRACING

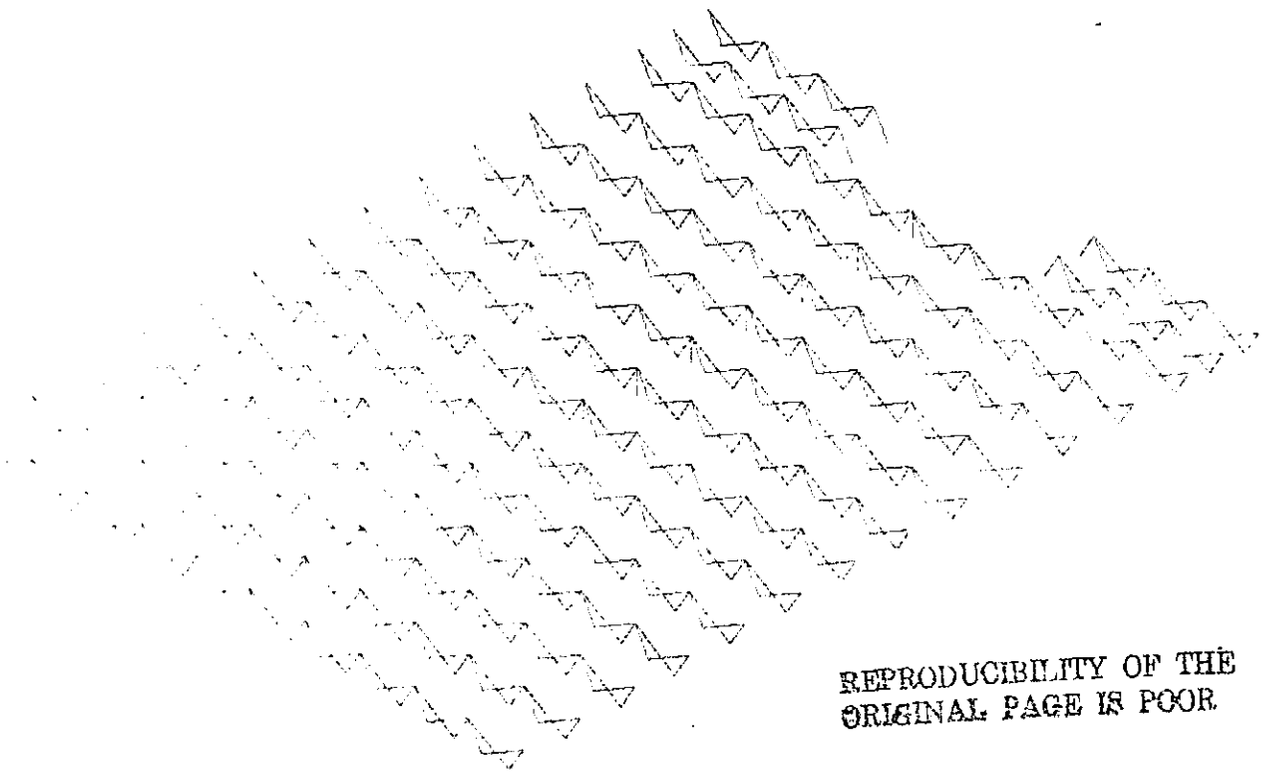

d. BETWEEN DECK BRACING

Figure 2.2-8 SSPS Structural Math Model, Sheet 2 of 2

Table 2.2-1 SSPS Symmetric Modes - Structural Model - 1364 Degrees of Freedom

MODE	FREQ C/HR	GEN MASS, KG X 10^{-6}	(LB X 10^{-6})	GEN STIFFNESS, N/M	(LB/IN.)	DESCRIPTION
1	0	2.014	(4.440)	0	(0)	RIGID ROTATION (θ_X)
2	0	9.013	(19.870)	0	(0)	RIGID TRANSLATION (Z)
3	0	9.013	(19.870)	0	(0)	RIGID TRANSLATION (Y)
4	5.26	1.970	(4.343)	166.29	(.948)	1ST VERT BEND. (Z)
5	14.14	0.6859	(1.512)	417.70	(2.381)	1ST TORSION (θ_X)
6	17.09	1.956	(4.311)	1740.68	(9.923)	1ST VERT BEND. ANT. OUT PHASE (Z)
7	18.91	3.570	(7.870)	3889.76	(22.175)	1ST LATERAL BEND (Y)
8	28.27	0.6080	(1.341)	1480.78	(8.442)	2ND VERT. BEND (Z)
9	28.78	0.8385	(1.849)	2115.83	(12.062)	2ND TORSION (θ_X)
10	32.21	1.037	(2.286)	3275.75	(18.675)	1ST CHORD BEND + 1ST VERT BEND (Z)
11	39.26	0.5898	(1.300)	2796.34	(15.942)	1ST CHORD BEND + 2ND VERT BEND (Z)
12	41.32	3.172	(6.994)	16500.19	(94.067)	2ND LAT BEND (Y)
13	45.24	0.7723	(1.703)	4814.34	(27.446)	3RD TORSION (θ_X)

NOTE: GEN MASS AND STIFFNESS IS FOR 1/2 SSPS

Table 2.2-2 SSPS Antisymmetric Modes - Structural Model - 1342 Degrees of Freedom

MODE	FREQ C/HR	GEN MASS KG X 10^{-6}	GEN MASS (LB X 10^{-6})	GEN STIFFNESS N/M	GEN STIFFNESS (LB/IN.)	DESCRIPTION
1	0	2.473	(5.453)	0	0	RIGID ROTATION (θ_Z)
2	0	2.195	(4.839)	0	0	RIGID ROTATION (θ_Y)
3	0	9.013	(19.870)	0	0	RIGID TRANSLATION (X)
4	9.36	0.8832	(1.947)	235.55	(1.343)	1ST TORSION (θ_X)
5	15.65	1.971	(4.345)	1470.79	(8.385)	1ST VERT BEND. (Z)
6	19.93	0.7238	(1.596)	875.68	(4.992)	2ND TORSION (θ_X)
7	29.30	5.382	(11.866)	14072.25	(80.226)	1ST LAT BEND. (Y)
8	30.83	1.231	(2.714)	3564.54	(20.321)	1ST CHORD BEND. + VERT BEND. (Z)
9	35.05	0.7767	(1.712)	2906.79	(16.572)	2ND VERT BEND. + CHORD BEND. (Z)
10	35.85	0.9206	(2.030)	3603.66	(20.544)	3RD TORSION (θ_X)
11	35.98	0.8570	(1.889)	3381.18	(19.276)	CHORD BEND + VERT BEND. (X)
12	41.72	5.713	(12.595)	32091.72	(182.958)	2ND LAT BEND. (Y)
13	43.02	1.478	(3.259)	8332.30	(47.502)	IN PLANE BEND. (Z) + VERT BEND. (Z)
14	52.42	0.8633	(1.903)	7175.85	(40.909)	3RD VERT BEND. + CHORD BEND (Z)

NOTE: GEN. MASS AND STIFFNESS IS FOR 1/2 SSPS

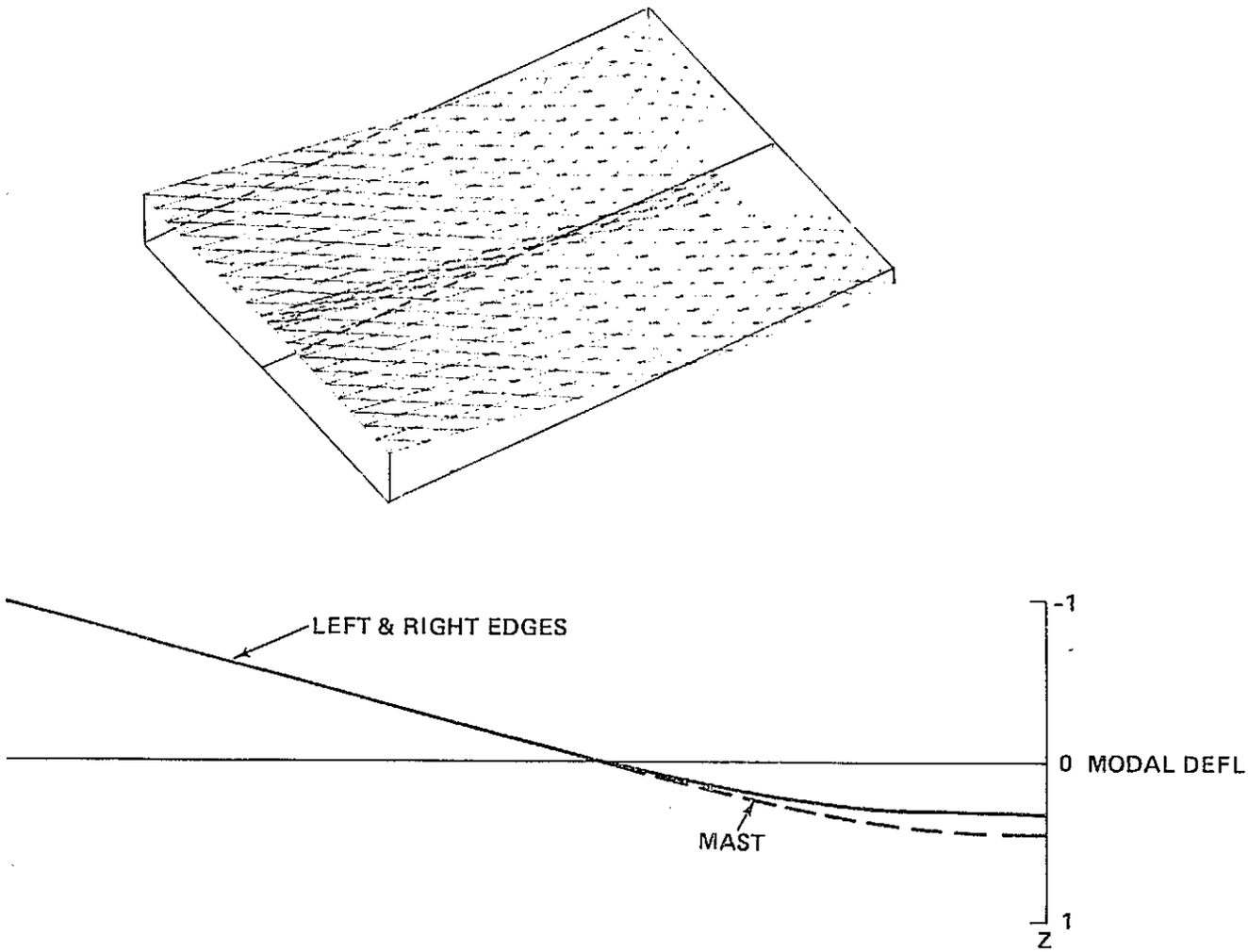

Figure 2.2-9 SSPS Symmetric Mode - First Bending
(Frequency = 5.26 C/Hr)

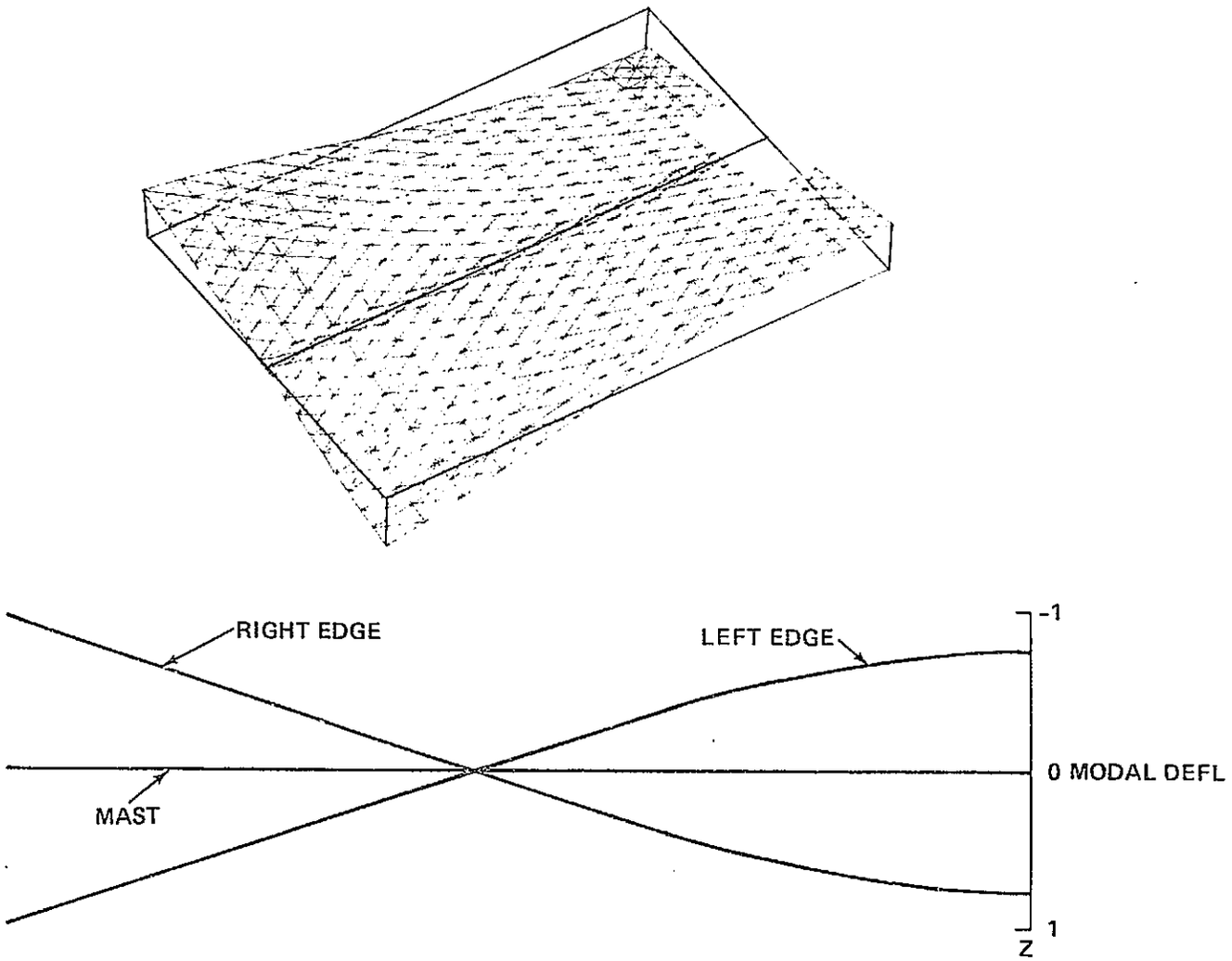

Figure 2.2-10 SSPS Symmetric Mode - First Torsion
(Frequency = 14.14 C/Hr)

An isometric view of the structural model is shown in Figure 2.2-7. The top deck, bottom deck, concentrator wire bracing, and structure between decks are shown in Figure 2.2-8. Each active mode has three translational degrees of freedom, node points on the mast have three additional rotational degrees of freedom. The symmetric model has 1364 degrees of freedom, and the antisymmetric model has 1342 degrees of freedom. Excluding the wire bracing, the half structure has 462 modes and 1127 members.

As part of the checkout of the structural model, modes and frequencies were calculated using NASTRAN. Thirteen symmetric modes (3 rigid + 10 elastic) and fourteen antisymmetric modes (3 rigid + 11 elastic) were determined. These modes are summarized in Tables 2.2-1 and 2.2-2. The lowest symmetric elastic mode occurs at 5.26 cycles/per hour, as shown in Figure 2.2-9. This bending mode will be excited by symmetric thruster forces, such as those used in transport from low earth orbit to geosynchronous orbit. The second symmetric elastic vibration mode occurs at 14.14 cycles/per hour, as shown in Figure 2.2-10. This torsion mode is the lowest mode that is excited by roll control thrusters in their present configuration. The lowest antisymmetric elastic mode is the torsion mode shown in Figure 2.2-11 (9.36 cycles/per hour). The second antisymmetric elastic vibration mode occurs at 15.65 cycles per hour as shown in Figure 2.2-12. This bending mode is the lowest mode that is excited by pitch control thruster firing.

The full size structural model data were used for the control analysis summarized in paragraph 2.3. The structural model was reduced to a dynamic model using the NASTRAN consistent (Guyan) reduction technique. The reduced models, with 174 degrees of freedom (symmetric) and 162 degrees of freedom (antisymmetric), were used to determine SSPS response to on-orbit and transportation thruster loads.

2.2.1.5 Transport Loads - LEO to GEO

Loads during transport from low earth orbit (200 n mi) to geosynchronous orbit were investigated for the total SSPS as well as for major segments. Although the thrust application is general in nature, an underlying assumption is that ion thrusters that are distributed or in clusters will be used for propulsion. The solar array itself will supply the power for these thrusters.

Thrust forces related to 90, 150, and 365 day transit times for the complete SSPS were established. Figure 2.2-13 shows preliminary static bending moments for these trip times that would be produced by thrusters mounted centrally on the rotary joint (so as to maintain the thrust tangential to the orbit plane). A comparison of bending moments with the allowable

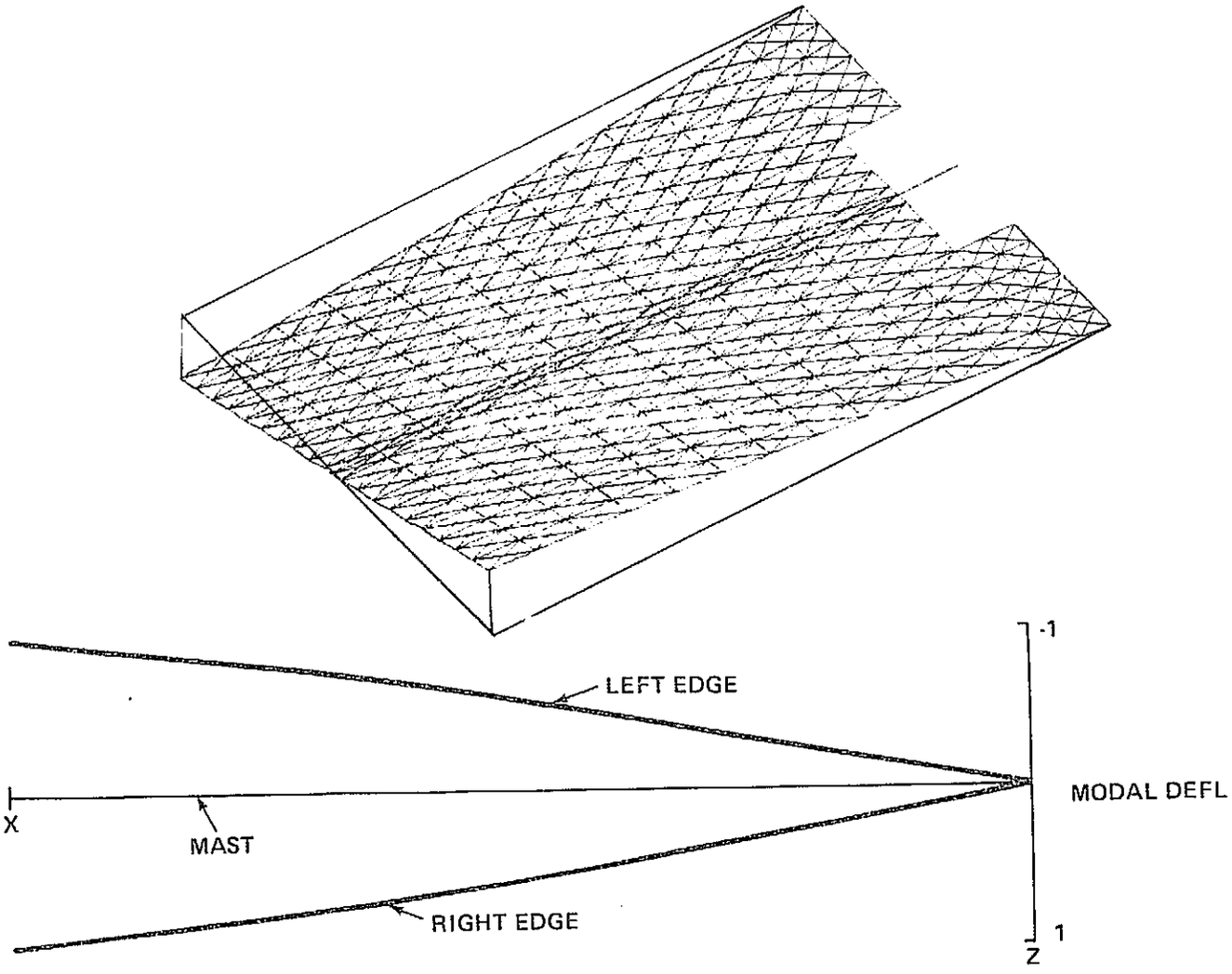

Figure 2.2-11 SSPS Antisymmetric Mode - First Torsion
(Frequency = 9.36 C/Hr)

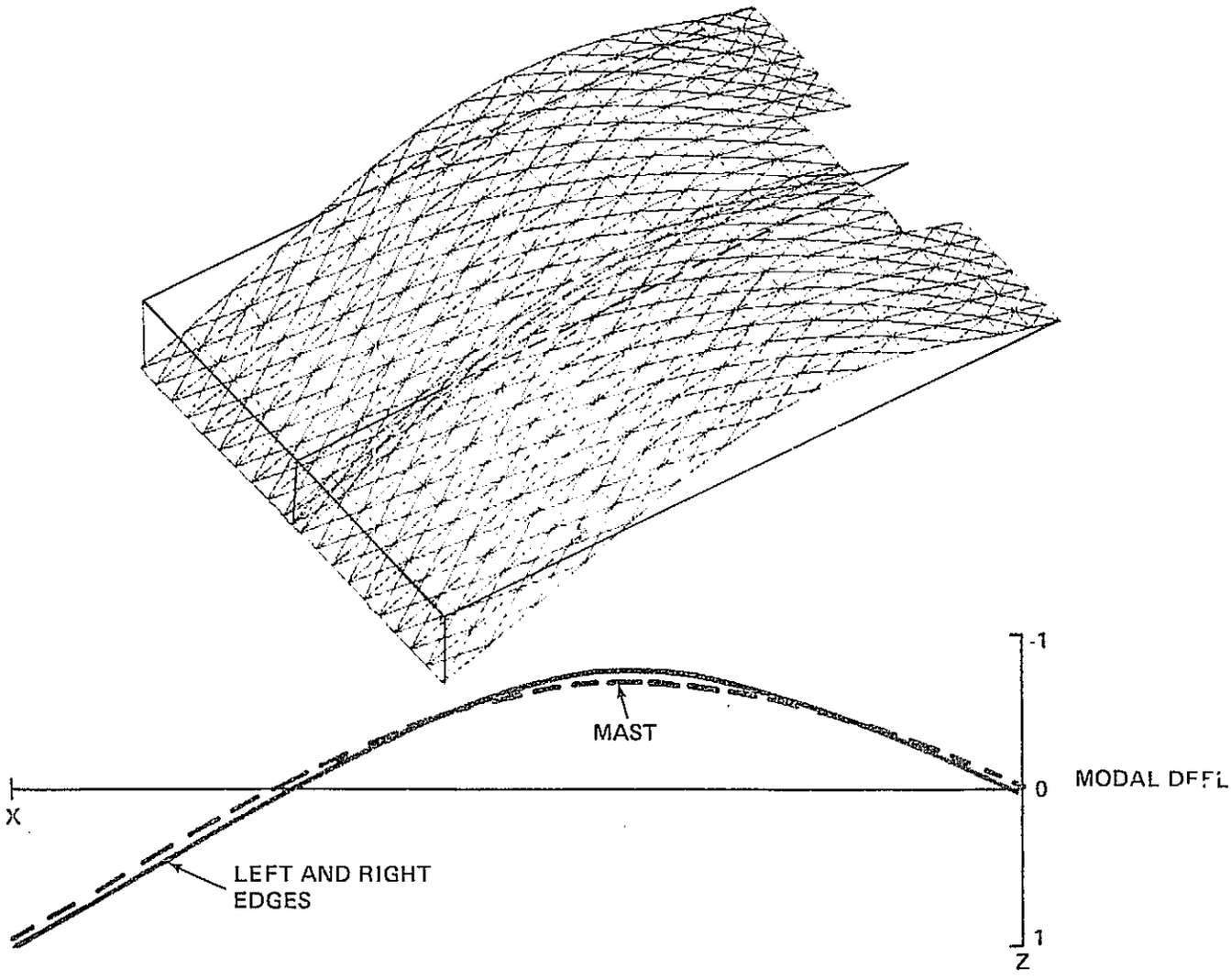

Figure 2.2-12 SSPS Antisymmetric Mode - First Bending
(Frequency = 15.65 C/Hr)

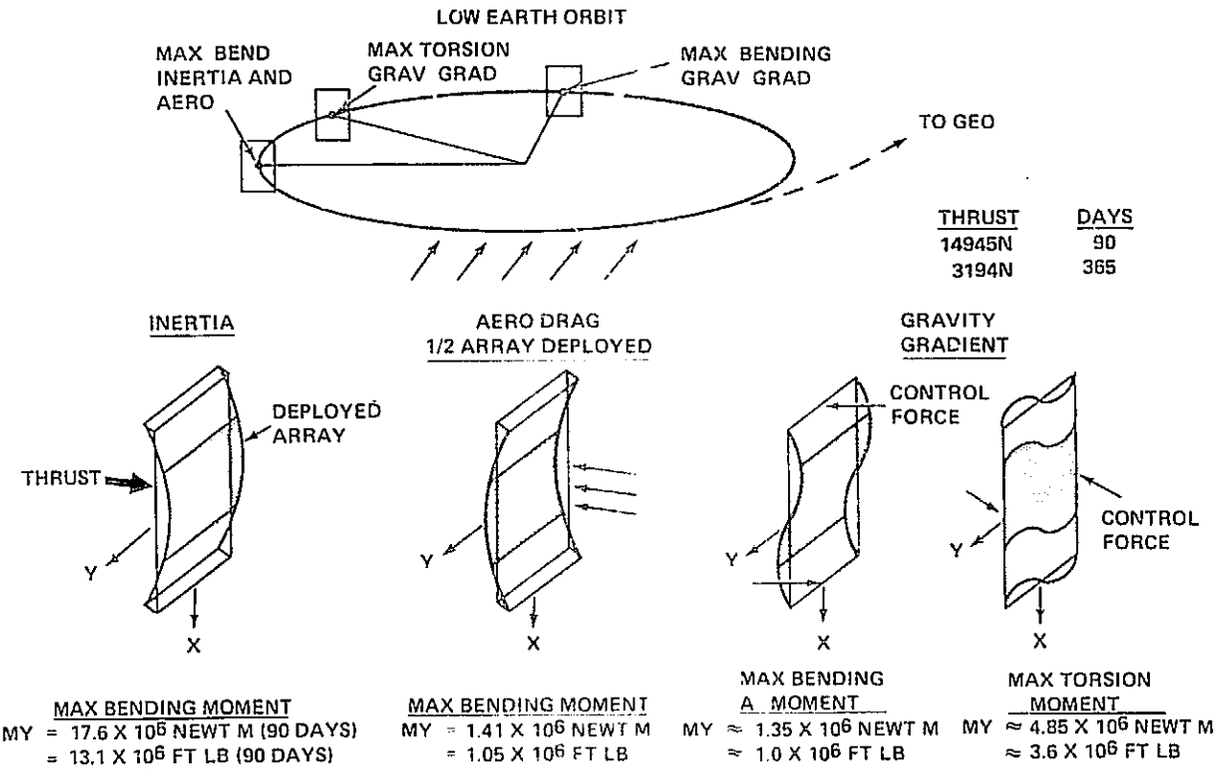

Figure 2.2-13 Transport Loads - SSPS Total

bending moment (12.7×10^6 N M) indicates that trip times of 365 days are acceptable. Also shown in Figure 2.2-13 are bending and torsion moments resulting from aerodynamic drag and gravity gradient forces in LEO. These loads, as shown are well below allowable limits. The inertia loads should be increased further (1.5 to 2.0) to allow for thruster startup transients. With a magnification factor of two, the allowable centrally applied thrust would be 5338 N (1200 lb); this corresponds approximately to a trip time of 315 days.

Distributing the thrust on the face of the SSPS would be a more efficient method of transport, from the point of view of loads. Moreover, a distribution of thrusters along the outboard edges of the array (X = ± 6546m) being considered for station-keeping would reduce plume impingement effects. Therefore, SSPS responses to a 1000N step force were calculated for the following cases:

- Center Load
- Edge Load
- Distributed Load

The reduced dynamic model previously discussed was used to determine the response of 183 critical member loads. The maximum response due to 1000N step load for various member types is summarized in Table 2.2.3. Using the maximum allowable limit load in an axial member (5431N = 1221 lb) as a criterion, the values of Table 2.2-3 were used to determine the allowable thrusts shown in Figure 2.2-14. For the center load, the allowable thrust would be 5793N (1302 lb), rather than the 5338N (1200 lb) obtained using static analysis and a magnification factor of two. For the edge load case, the allowable thrust would be reduced to 2570N (578 lb). As expected, distributing the thrust yields the highest allowable total thrust (13802N, or 3103 lb). Note that the maximum compressive load in the support wires varies from -220 to -650N for the three cases. The wires must be pretensioned to values greater than these levels to remain effective. In the mathematical model, the antenna is mounted with its plane perpendicular to the thrust; however, the resulting load factors are below the allowable antenna value ($Ny_{all} = 3.5 \times 10^{-4}$) in all cases.

If the SSPS were divided into three segments for purposes of transport, thrust levels could be increased. Two such cases were investigated, Figure 2.2-15:

- Case A - Segments of approximately equal mass
- Case B - Segments of approximately equal length

Table 2.2-3 SSPS - Summary of Internal Loads (N) and Moments (n-M) - 1000N Stepload

DESCRIPTION	NO.	CENTER MAX	NO.	CENTER MIN	NO.	EDGE MAX	NO.	EDGE MIN	NO.	DISTRIBUTED MAX	NO.	DISTRIBUTED MIN
AXIAL MEMBER												
UPPER DECK FRAME MEMBER LOAD	132	11.5	105	−477.5	105	634.9	105	−402.8	105	335.7	132	−5.01
LOWER DECK FRAME MEMBER LOAD	107	591.9	134	−7.06	107	432.5	107	−843.0	134	2.94	107	−393.5
DIAGONAL – FRAME MEMBER LOAD	54	53.7	125	−39.4	122	65.9	54	−78.5	125	25.7	123	−33.6
UPPER DECK LONG. MEMBER LOAD	68	34.2	140	−937.5	140	2113	141	−61.7	140	432.5	141	−54.5
LOWER DECK LONG. MEMBER LOAD	145	430.6	145	−25.5	145	48.2	145	−1036.3	145	47.2	145	−194.6
MAST SUPPORT VERTICAL LOAD	63	4.11	131	−.58	131	3.08	63	−5.92	131	.12	63	−2.14
CONCENTRATOR WIRE LOAD	75	32.4	76	−33.4	76	86.9	75	−83.9	76	15.52	75	−15.0
UPPER DECK WIRE BRACING LOAD	175	5.73	174	−15.9	176	30.7	175	−8.93	174	8.95	175	−2.37
LOWER DECK WIRE BRACING LOAD	98	10.2	97	−7.45	97	17.5	98	−20.9	97	3.43	98	−4.72
FRAME WIRE BRACING LOAD	60	69.8	127	−72.9	59	86.0	60	−86.5	127	49.9	128	−47.2
MAST SUPPORT WIRE BRACING LOAD	102	29.8	101	−30.6	101	86.1	102	−82.6	101	14.7	102	−14.4
BEAM MEMBER												
MAST SHEAR LOAD, V_X	91	732.1	85	−732.1	25	1713	31	−1713	85	345.3	91	−345.3
MAST SHEAR LOAD, V_Y		0		0		0		0	160	3.36	154	−3.36
MAST SHEAR LOAD, V_Z	153	629.0		−629.	92	773	86	−773	159	304.9	153	−304.9
MAST BENDING MOMENT M_X	28	.06	34	−.059	155	.235	161	−.235	34	12,840	28	−12,840
MAST BENDING MOMENT M_Y	163	1024600	57	−826,490	157	1323000	163	−1,532,200	157	372,920	163	−468,970
MAST BENDING MOMENT, M_Z	162	.016	162	−.017	162	.055	162	−.062	162	2008.6	162	−1174

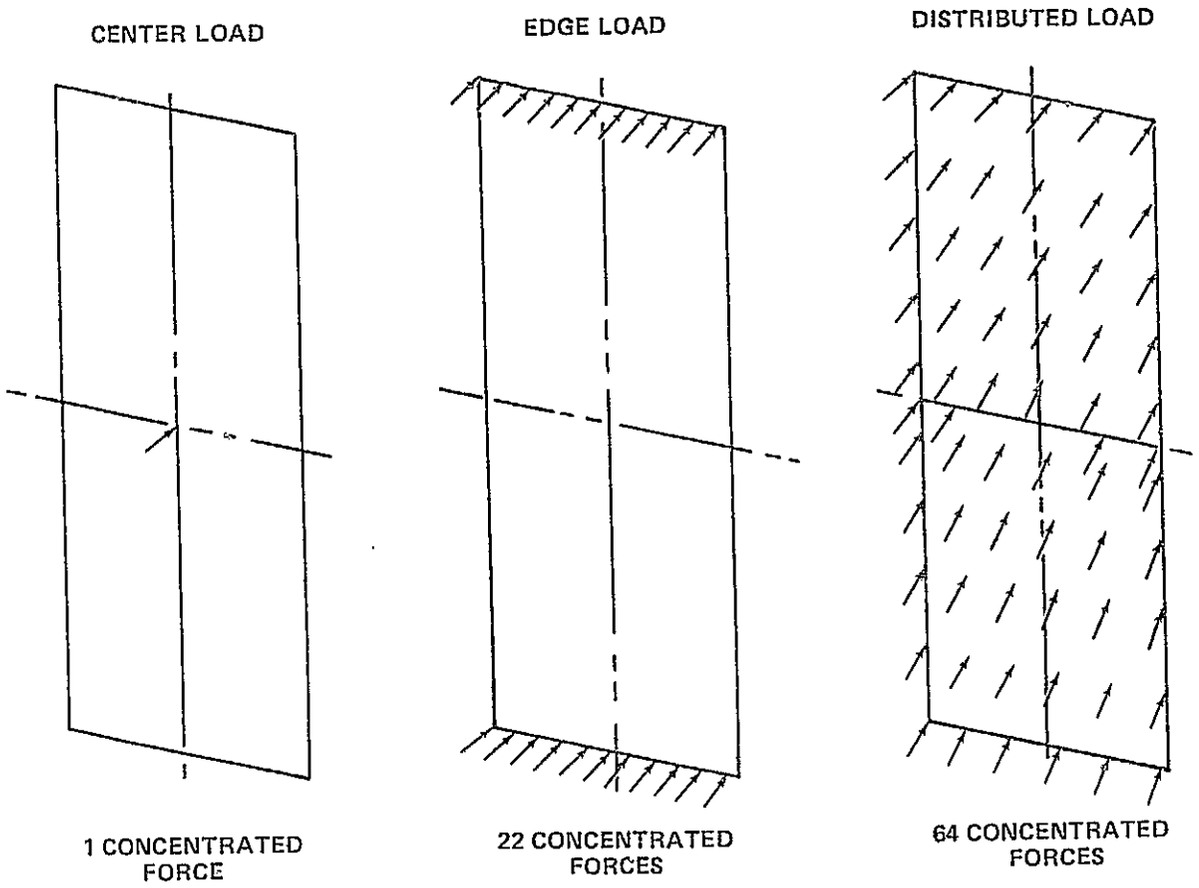

DESCRIPTION	CENTER	EDGE	DISTRIBUTED
ALLOWABLE TOTAL THRUST, N (LB)	5793 (1302)	2570 (578)	13,802 (3103)
MAX. AXIAL MEMBER LOAD, N (LB)	5431 (1221)	5431 (1221)	5431 (1221)
MAX. WIRE LOAD (COMP), N (LB)	–422 (–95)	–223 (–50.2)	–651 (–146)
MAST BENDING MOMENT, N-M (FT-LB)	5,936,000 (4,378,000)	3,938,000 (2,904,000)	6,473,000 (4,774,000)
ANTENNA LOAD FACTOR	9.06×10^{-5}	6.18×10^{-5}	1.51×10^{-4}

Figure 2.2-14 Comparison of Internal Loads and Moments for SSPS Transport (Step Thrust Input) - Limit

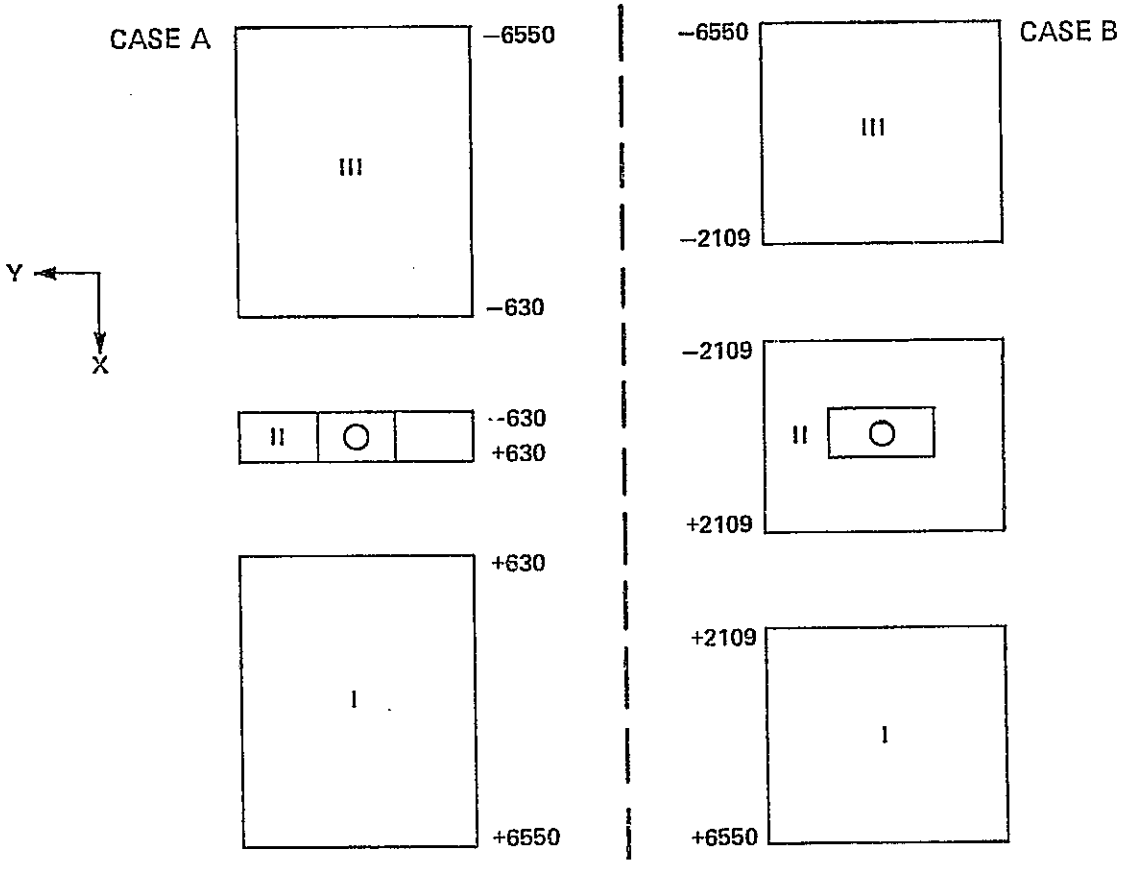

	CASE A		CASE B	
	SEG I & III	SEG II	SEG I & III	SEG II
MASS, KG (LB)	6.01×10^6 (13.25×10^6)	6.01×10^6 (13.24×10^6)	4.70×10^6 (10.37×10^6)	8.61×10^6 (18.99×10^6)
LENGTH, M (FT)	5920 (19,423)	1260 (4133)	4441 (14,570)	4218 (13,839)
WIDTH, M (FT)	4330 (14,206)	4330 (14,206)	4330 (14,206)	4330 (14,206)
$M_{X_{ALL}}$, M-N (FT-LB)	15.0×10^6 (11.06×10^6)	2.30×10^6 (1.70×10^6)	11.5×10^6 (8.5×10^6)	9.23×10^6 (6.81×10^6)
$M_{Y_{ALL}}$, M-N (FT-LB)	12.7×10^6 (9.33×10^6)	–	12.7×10^6 (9.33×10^6)	12.7×10^6 (9.33×10^6)
STATIC THRUST$_{ALL}$, N (LB)	17,148 (3855)	66,554 (14,962)	21,316 (4792)	41,840 (9406)
STEP THRUST$_{ALL}$, N (LB)	8576 (1928)	33,277 (7481)	10,658 (2396)	20,920 (4703)
N_Z	2.9×10^{-4}	1.13×10^{-3}	4.62×10^{-4}	4.93×10^{-4}

Figure 2.2-15 Significant Factors Concerning Inertia Loads and Moments Due to Orbital Transfer - Segments - Central Thrust

The structure in each case is segmented at a frame station, and the existing frame is assumed to remain with each segment to avoid dangling longitudinal members. Loads were calculated for a centrally applied thrust on each segment; results are summarized in the figure. For the Case A, in which each segment is of approximately equal mass, the allowable thrust for a suddenly applied thrust is 8576N (1928 lb) on the outer segment and 33277N (7481 lb) on the central segment. The antenna must rotate in a manner such that its plane is parallel to the direction of thrust, since the allowable load factor perpendicular to its face is exceeded. For Case B, in which each segment is approximately equal in length, the allowable thrust for the outer segments increases to 10658N (2396 lb), and the thrust for the center segment is 20920N (4703 lb). In this case, also, the antenna plane must be parallel to the thrust direction.

The use of a cryogenic OTV for transport was investigated. The OTV assumed had a payload capability of 711680N (160,000 lb) with a combined load factor which varied from .25 to .4. Because of the low payload capability relative to the total SSPS, only small segments can be transported. For example, 8 bays of structure, excluding concentrators and blankets, have a mass of 71,487 Kg (157,600 lb). One bay (493 x 493m) with concentrators and blankets, has a mass of 48,082 Kg (106,000 lb). The total force on this segment (189,134N) is well above the load that can be tolerated by the axial members (4 x 5431N = 21724N). This method of transport thus is not feasible for array segments.

Preliminary inertia loads and allowable thrust values for various forms of SSPS transport have been considered, since the thrust application methods investigated were general, specific means of achieving the required thrust must be investigated. For example, ion thrusters are capable of producing thrusts only of the order of .44N (.1 lb), thousands of these thrusters thus would have to be mounted in order to produce the required thrust levels. The following specific problem areas must be investigated:

- Number of thrusters required
- Methods of attachment
- Method of thrust vectoring
- Effects of plume impingement

For full SSPS transport, the centrally located thrust force has the advantage that it can be vectored by rotating it along with the movable mast. However, a distributed thrust allows a significantly greater total thrust to be used and must be considered.

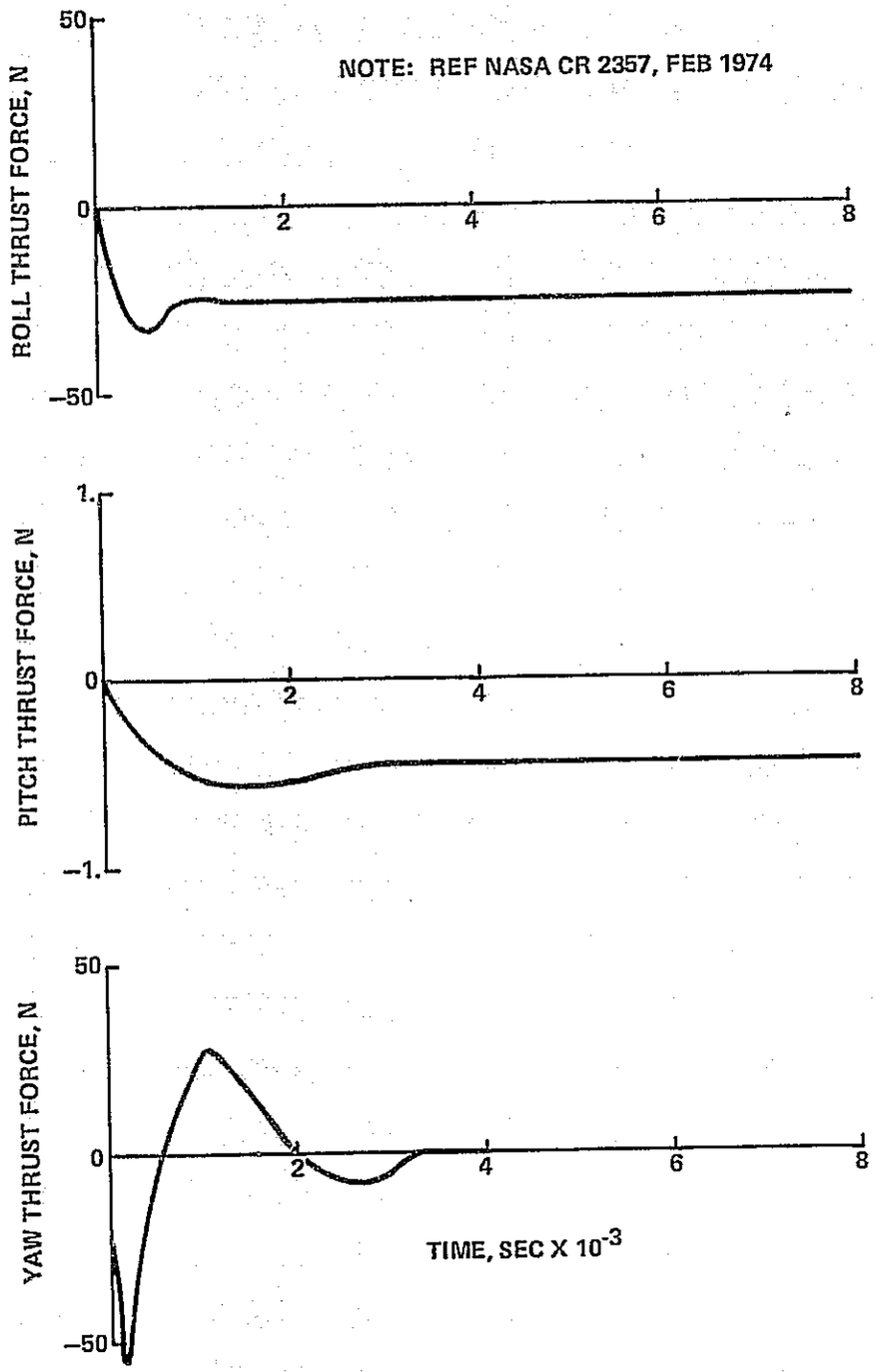

Figure 2.2-16 SSPS Flexible Body Control Force Time Histories

C-2

Segmenting the SSPS for transport provides greater thrust values (shorter transport times), but introduces the problem of rejoining at geosynchronous orbit. Since the two cases investigated are not necessarily optimum, the following areas should be investigated with respect to segmentation:

- Methods of rejoining segments for structural and electrical continuity
- Methods of docking segments at geosynchronous orbit.

Note that the allowable thrusts summarized herein include a magnification factor of 2 to account for suddenly applied loads. Allowable thrust can be increased if the thrust is applied slowly or increased in steps over a long period of time relative to the SSPS bending frequencies.

2.2.1.6 On Orbit Thruster Loads

A previous study (Reference 2.2-1) generated attitude control force-time histories for the SSPS in geosynchronous orbit. In both roll and pitch, the disturbance torque was assumed constant, and the control thrusters continuously exerted force in coupled pairs at the extremities of the array. In the nominal yaw orientation, the SSPS experiences zero disturbance torques, and the yaw response was calculated by assuming an initial yaw attitude of .001 radians. The thruster force time histories are shown in Figure 2.2-16. The maximum thruster force in roll is 33.8N (7.6 lb), in pitch is .58N (.13 lb), and in yaw is 55.3N (12.4 lb).

Modes and frequencies for the reduced dynamic model of the SSPS were used in conjunction with the applied forces described to obtain vehicle response. Maximum deflections, accelerations, and critical member loads (183) were obtained.

Roll response was calculated for 4000 seconds using 14 symmetric modes (11 elastic + 3 rigid body). The elastic modes ranged in frequency from 5 to 50 cycles/per hour. The maximum deflection (elastic) is directly under the thruster forces (coordinate 157) and is .079m (.29 in.). A plot of the deflection time history at coordinate 157 is shown in Figure 2.2-17. Note that after the initial transient (0 to 2000 sec), the response slowly decays at approximately 14 cycles/per hour. A structural damping value of $g = .01$ was assumed for all modes. A summary of the maximum internal loads is given in Figure 2.2-18. The maximum axial load in the monitored members is 78.2N (17.6 lb); the maximum load in a wire is only 3.93N (.88 lb). The maximum torsion on the mast is 34990 Nm (28772 in-lb). The distribution of internal load suggests that a large amount of the torsion is resisted by the mast.

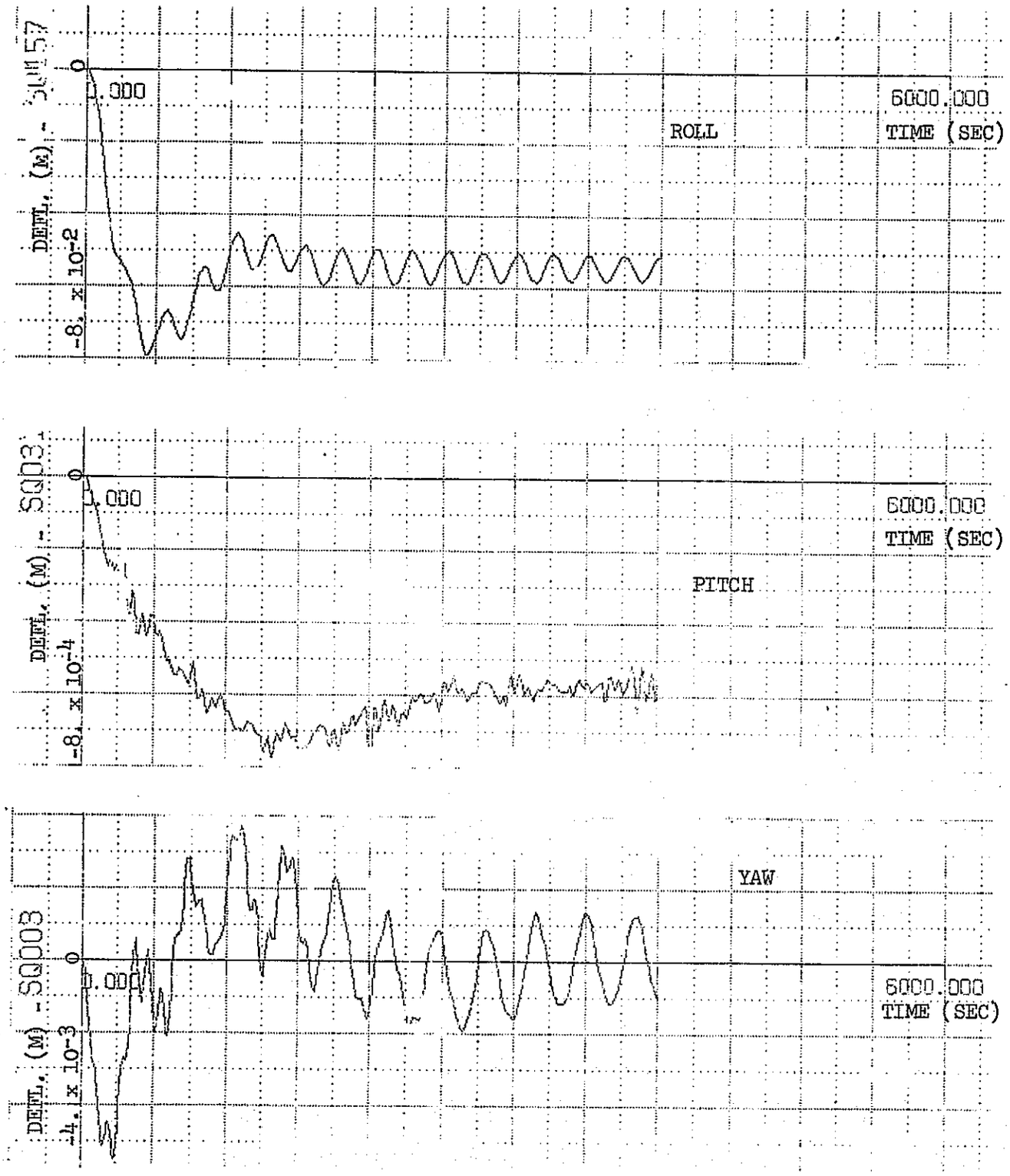

Figure 2.2-17 SSPS Maximum Deflection Response to Control Thruster Forces

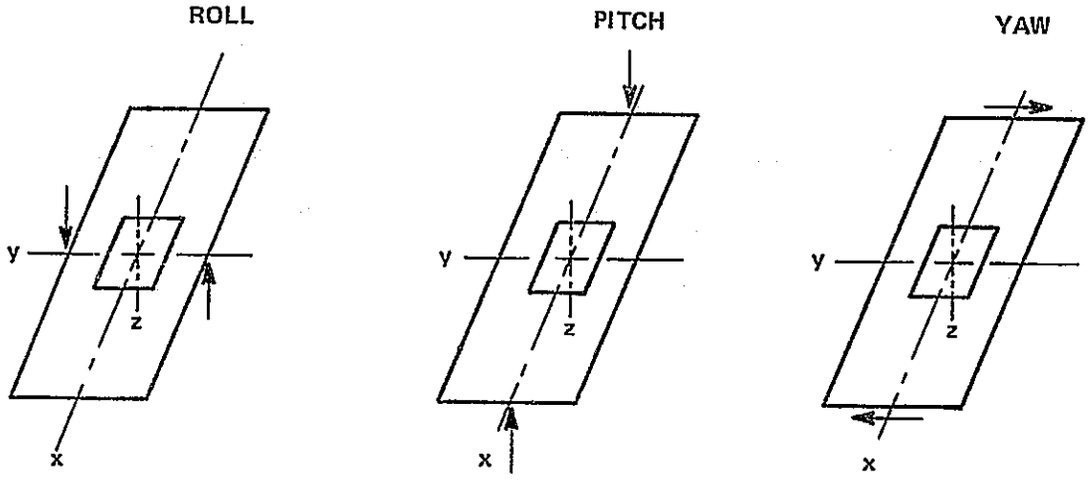

	ROLL	PITCH	YAW
MAXIMUM THRUSTER FORCE, N	33.8	.58	55.3
MAXIMUM AXIAL MEMBER LOAD, N	78.2	.13	3.57
MAXIMUM WIRE LOAD, N	3.93	.037	.968
MAXIMUM MAST BENDING MOMENT, M-N	34990	145.7	3777.7

Figure 2.2-18 SSPS - Summary of Maximum Internal Loads and Moments - Attitude Control Thruster Firing

Pitch response was calculated using 14 antisymmetric modes (11 elastic + 3 rigid body) with the elastic modes ranging in frequency from 10 to 57 cycles/per hour. Again, the response was determined for 4000 seconds, with g = .01 damping for all modes. The maximum deflection (elastic) is directly under the thruster force (coordinate 31), and is .00078m (.0029 in.). A plot of the deflection time history at coordinate 31 (mast tip) is shown in Figure 2.2-17. Maximum internal loads are summarized in Figure 2.2-18. The maximum axial load in a member is .13N (.029 lb), and the maximum wire load is .037N (.008 lb). The maximum pitch bending moment is 145.7 Nm (119.8 in.-lb).

Yaw response was determined using the same modes and damping as were used for calculating pitch response. Maximum deflection, which occurs at the outboard tips of the array (coordinate 3), is ±.00549m (.020 in.). The deflection response of coordinate 3 as shown in Figure 2.2-17, decays at approximately 10 cycles/per hour.

Maximum internal loads for yaw are summarized in Figure 2.2-18. The maximum axial load in a member is 3.57N (.80 lb), and the maximum wire load is .968N (.22 lb). The maximum mast yaw bending moment is 2990.5 M-N (2459 in.-lb), and is coupled with a maximum mast torsion of 3777.7M-N (3106 in.-lb).

The response due to attitude control thruster firing is small in comparison to the loads used to size the SSPS vehicle. The allowable member axial load (5431N) is two orders of magnitude greater than the loads calculated. Although present values of roll control force are greater than those used in this investigation (440 versus 33.8), (internal loads will probably still be an order of magnitude less than allowable. These loads must eventually be investigated for fatigue effects.

In addition to thruster firing for attitude control, thrusters also will be fired for stationkeeping. A total thrust of 2570N (578 lb) was given as the maximum allowable for edge mounted thrusters, Figure 2.2-14; the currently required total thrust of 912 to 934 N for stationkeeping (See paragraph 2.3) is below the allowable value.

2.2.1.7 Thermal Analysis

The transient temperature response of the SSPS structure during eclipse by the earth shadow was determined. The temperatures obtained were average temperatures for major members (246.5M and 493M), and are consistent with the level of approximation in the structural mathematical model. The assumptions used in generating these temperatures are given in Figure 2.2-19.

- THE BASIC STRUCTURAL BUILDING BLOCK IS AN OPEN "TRIANGLE," 5.08CM (2 IN.) ON A SIDE, .0381 CM (.015 IN.) THICK, AND IS MADE OF ALUMINUM.
- THE ALUMINUM MATERIAL HAS BEEN TREATED TO PROVIDE AN ALZAK SURFACE FINISH WITH α_S/ϵ = .2/.75.
- THE SOLAR CELLS OPERATE AT 380°K, HAVE A FRONT SURFACE EMISSIVITY OF .82, BACK SURFACE EMISSIVITY OF .9, A MASS PER UNIT AREA OF .282 kg/m^2, AND A SPECIFIC HEAT OF .2 CAL/gm°K.
- THE REFLECTOR IS MADE OF ALUMINIZED KAPTON, THE REFLECTOR (ALUMINIZED) SIDE IS .2/.05; THE BACK SIDE IS TREATED TO PROVIDE AN EMISSIVITY OF .9.
- THE REFLECTOR COVERS THE ENTIRE STRUT TO WHICH IT IS ATTACHED.
- THE SSPS IS IN GEOSTATIONARY ORBIT WITH ARRAY MAJOR AXIS PERPENDICULAR TO THE EQUATORIAL PLANE, AND MINOR AXIS PERPENDICULAR TO THE SOLAR VECTOR; THE TIME OF YEAR FOR WHICH THIS ANALYSIS IS PERFORMED IS THE EQUINOX.
- SSPS PASSES FROM FULL SUN TO FULL SHADOW INSTANTANEOUSLY, AND THE DURATION OF SHADOW IS 1.189 HOURS. EARTH IR IS 1.6 Btu/hr FT^2.

Figure 2.2-19 Assumptions Used in Determining Thermal Transients During Eclipse

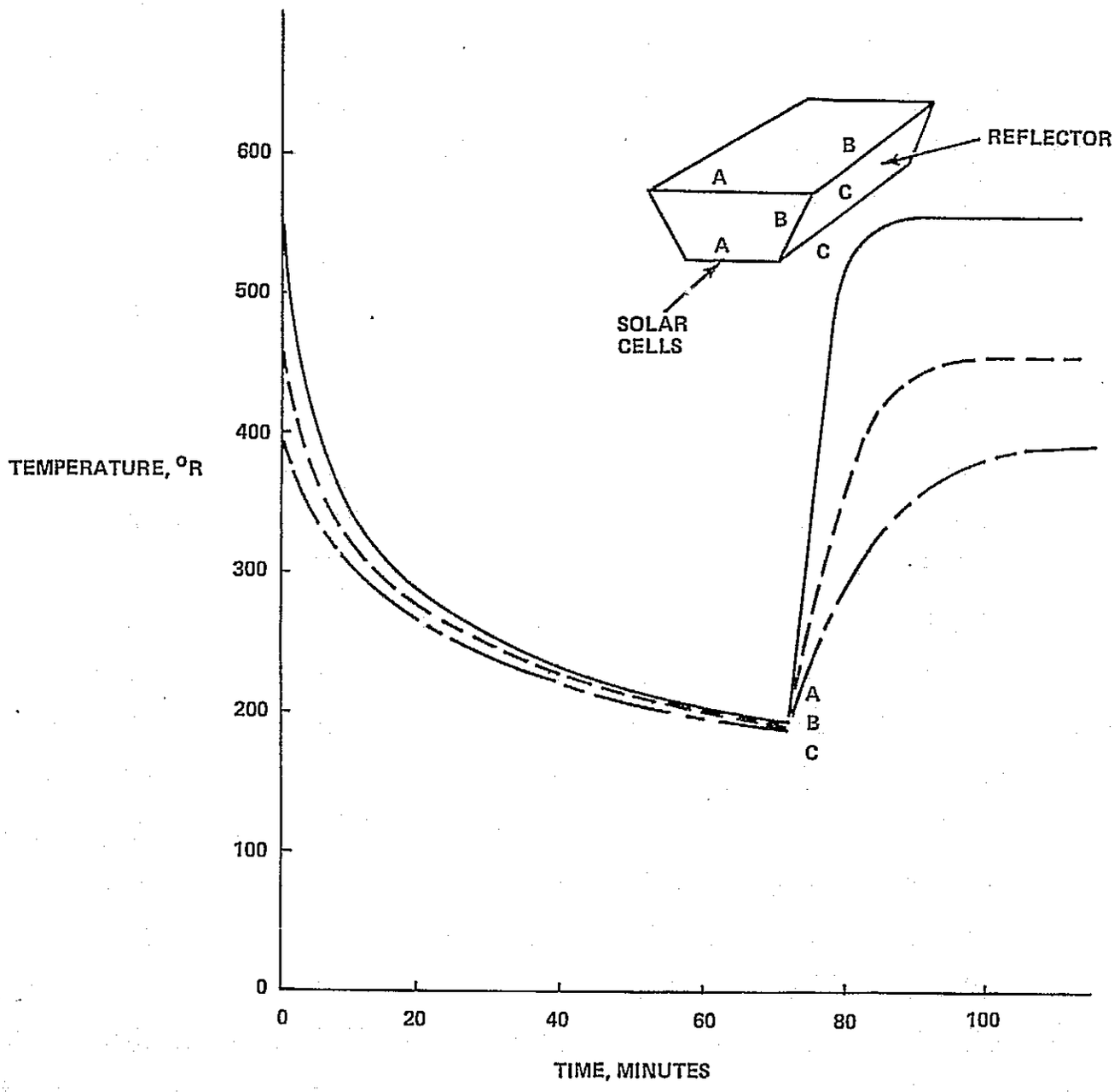

Figure 2.2-20 Average Temperature of Major Members Not in Proximity to Antenna During Eclipse

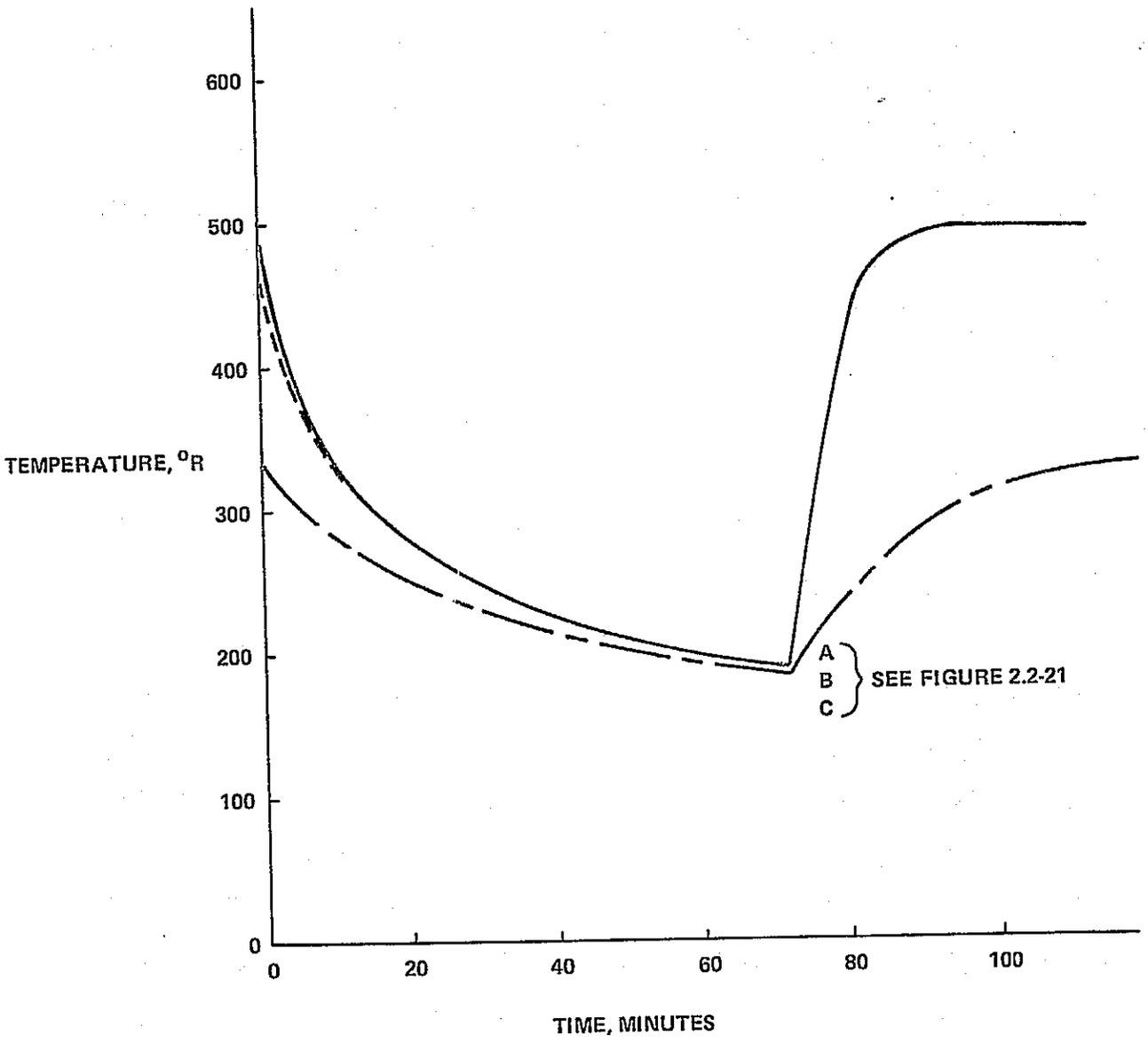

Figure 2.2-21 Average Temperature of Major Edge Members at Edge of Array During Eclipse

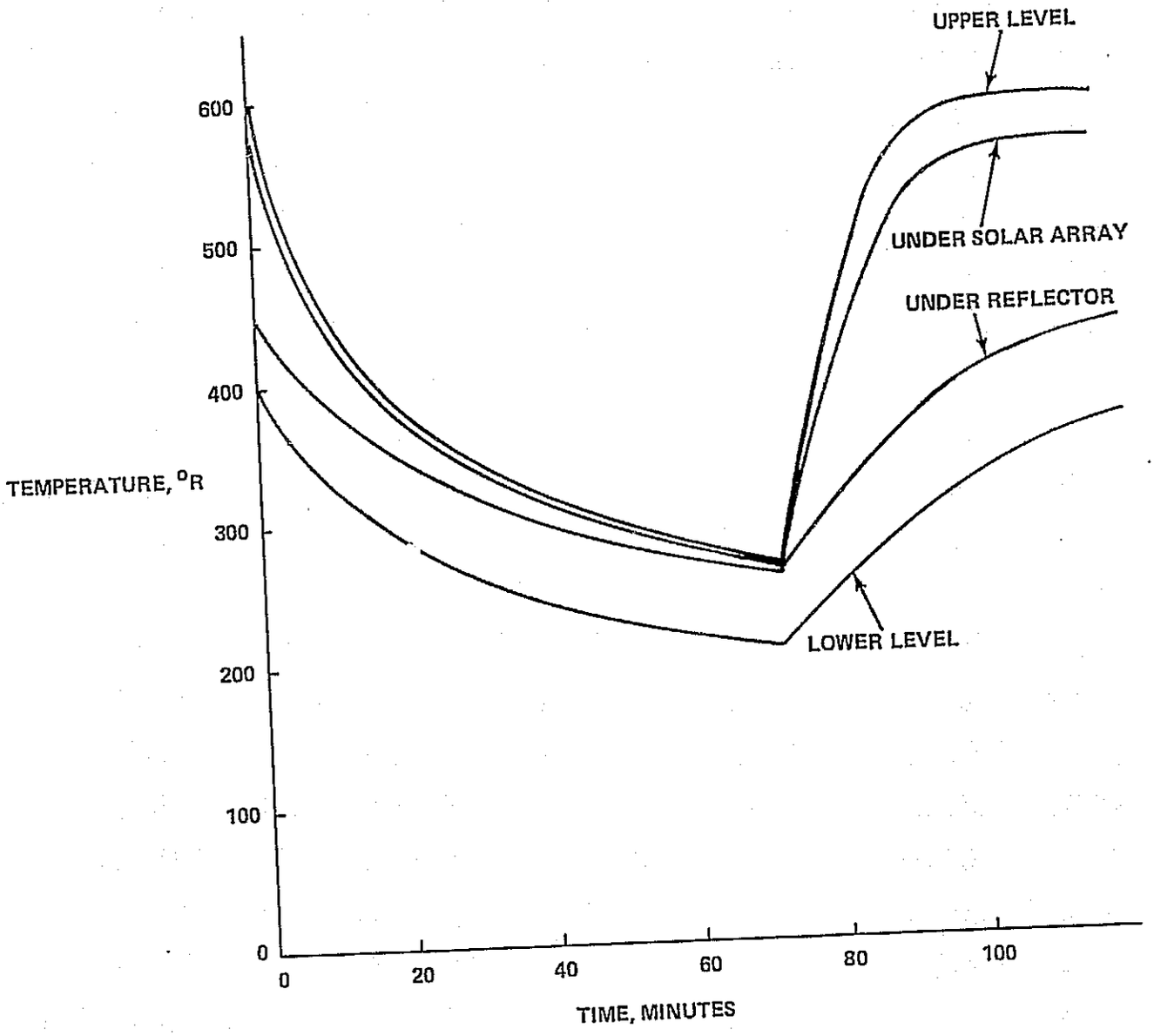

Figure 2.2-22 Temperature of Wire Braces During Eclipse (Aluminum Wire, 0.318 CM in Diameter)

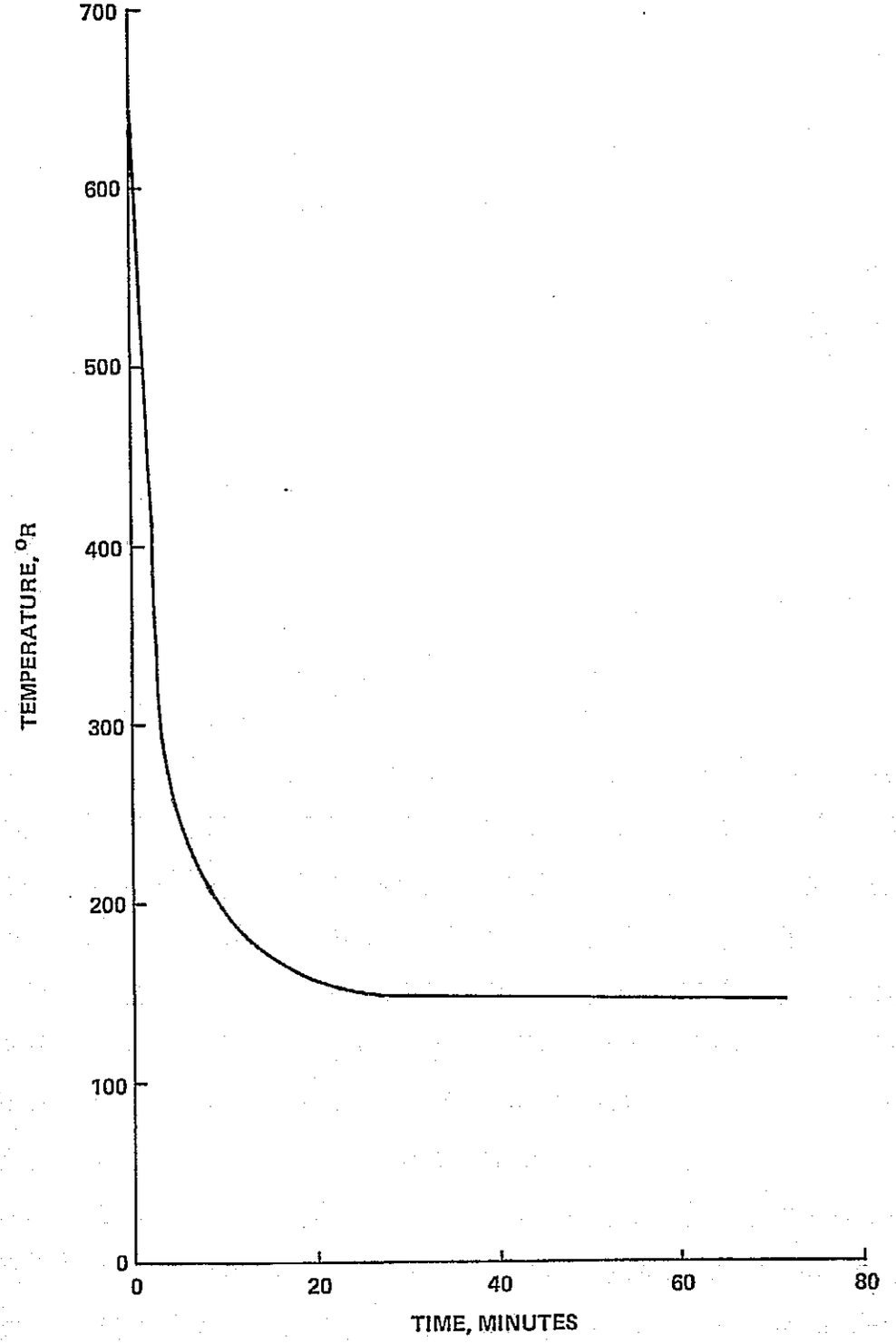

Figure 2.2-23 Solar Cell Temperature During Eclipse, 0.282 Kg/M^2 Cell

Temperature time histories for major members during eclipse (1.189 hours) are given in Figure 2.2-20 for members one bay in from the array edge, and not in the proximity of the antenna. Similar data for members at the edge of the array are given in Figure 2.2-21. The wire bracing, shown in Figure 2.2-22, changes temperature more slowly than the triangular sections, be cause of a lower surface-to-volume ratio. The steady state temperature of the concentrators is -5°C (483°R), and drops quickly to -220°C (96°R) when entering the shadow. Solar cell cooldown is also rapid, as shown by the response when entering the shadow given in Figure 2.2-23.

As previously stated, the temperatures given are averages consistent with the level of approximation required by the structural math model. The amount of structural material obtained within the boundaries defined by the truss is so small that conduction and radiation interchange, except at the basic "building block" level, is negligible. Temperatures within a given strut can vary by more than than 55°C (100°R). Gradients will also exist in the basic triangular element. These variations may be of more importance than the gross strut-to-strut variations considered here.

Temperatures were obtained for one uniform value of α_s/ε. The temperature variations can be minimized by selectively specifying coatings.

The SSPS is simultaneously exposed to solar heating (and cooling during eclipse) and to electrical heating in the transmission busses and mast. Based on the structural model previously defined, a static structural analysis was used to determine deflections and internal loads for the combined thermal conditions. The cables were assumed able to sustain compression so that the necessary preloads could be estimated. The following two conditions were investigated:

- SSPS in earth shadow with a mast power off
- SSPS in sunlight with mast power on

For both conditions, the mast temperature due to electrical heating was assumed to be 149°C (760°R); however, the heating in the lateral busses was not considered. With the SSPS in the earth's shadow, structure other than the mast was assumed to be at -18°C (459°R), Figure 2.2-24. With the SSPS in sunlight, the temperature distribution on the array was consistent with those shown in Figures 2.2-20 through 2.2-23 at time equal zero.

The deflections of the array for both conditions are shown isometrically in Figures 2.2-25 and 2.2-26 and in contour plots of Figures 2.2-27 and 2.2-28. The major effect is the longitudinal expansion of the mast.

SSPS IN EARTH SHADOW			SSPS IN SUNLIGHT		
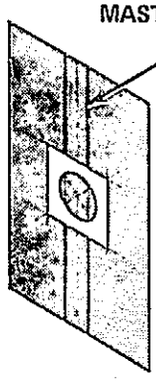			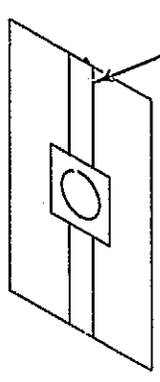		
MAST TEMP:	°C °F °R	4.4 40 500	MAST TEMP:	°C °F °R	149 300 760
STRUCTURAL TEMP:	°C °F °R	–162 –260 200	STRUCTURAL TEMP:	°C °F °R	SEE FIGURES 2.2-20 AND 2.2-24) AT t = 0
MAXIMUM DEFL:	m ft	50 164	MAXIMUM DEFL:	m ft	22.4 73.5
MAXIMUM CABLE LOAD (COMPRESSIVE):	N LB	–9678 –2176	MAXIMUM CABLE LOAD (COMPRESSIVE):	N LB	–11925 –2681

NOTE: DESIGN LOAD FOR CABLE PRETENSION OF 890N (200 LB) IS EXCEEDED IN SUPPORT CABLES DIRECTLY ATTACHED TO THE MAST.

Figure 2.2-24 SSPS Thermal Structural Analysis

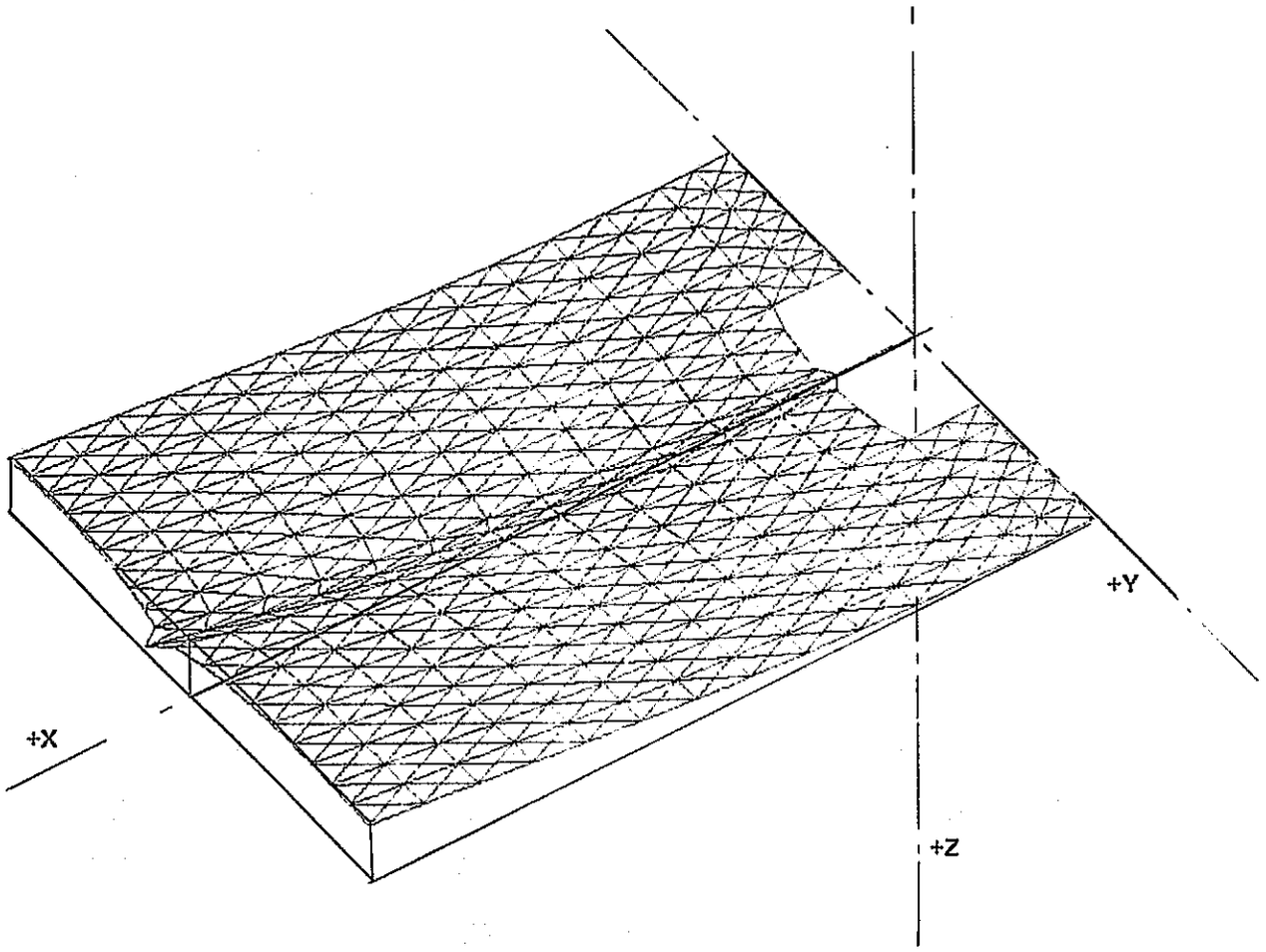

Figure 2.2-25 Deflection of SSPS in Earth Shadow

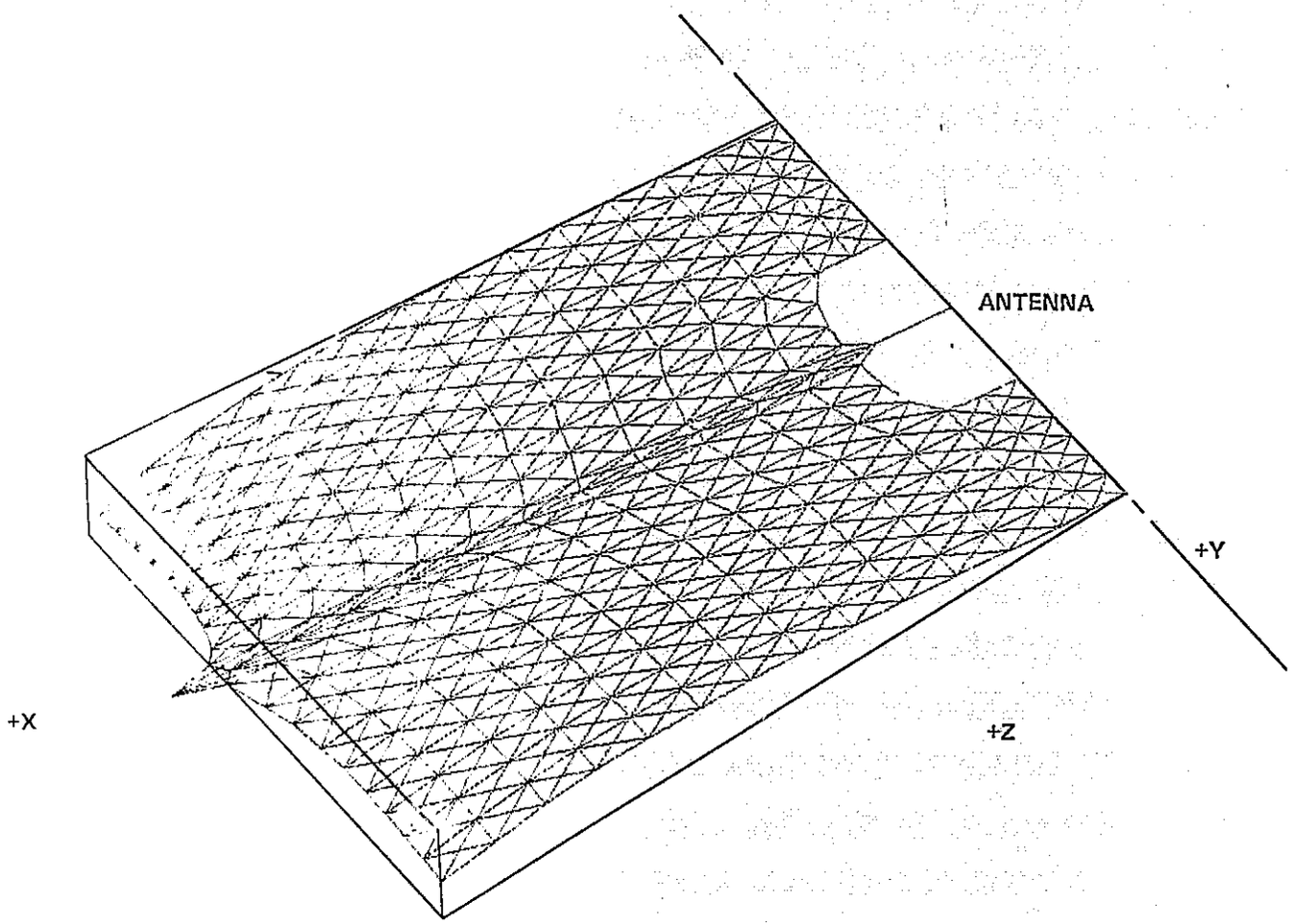

Figure 2.2-26 Deflection of SSPS in Sunlight

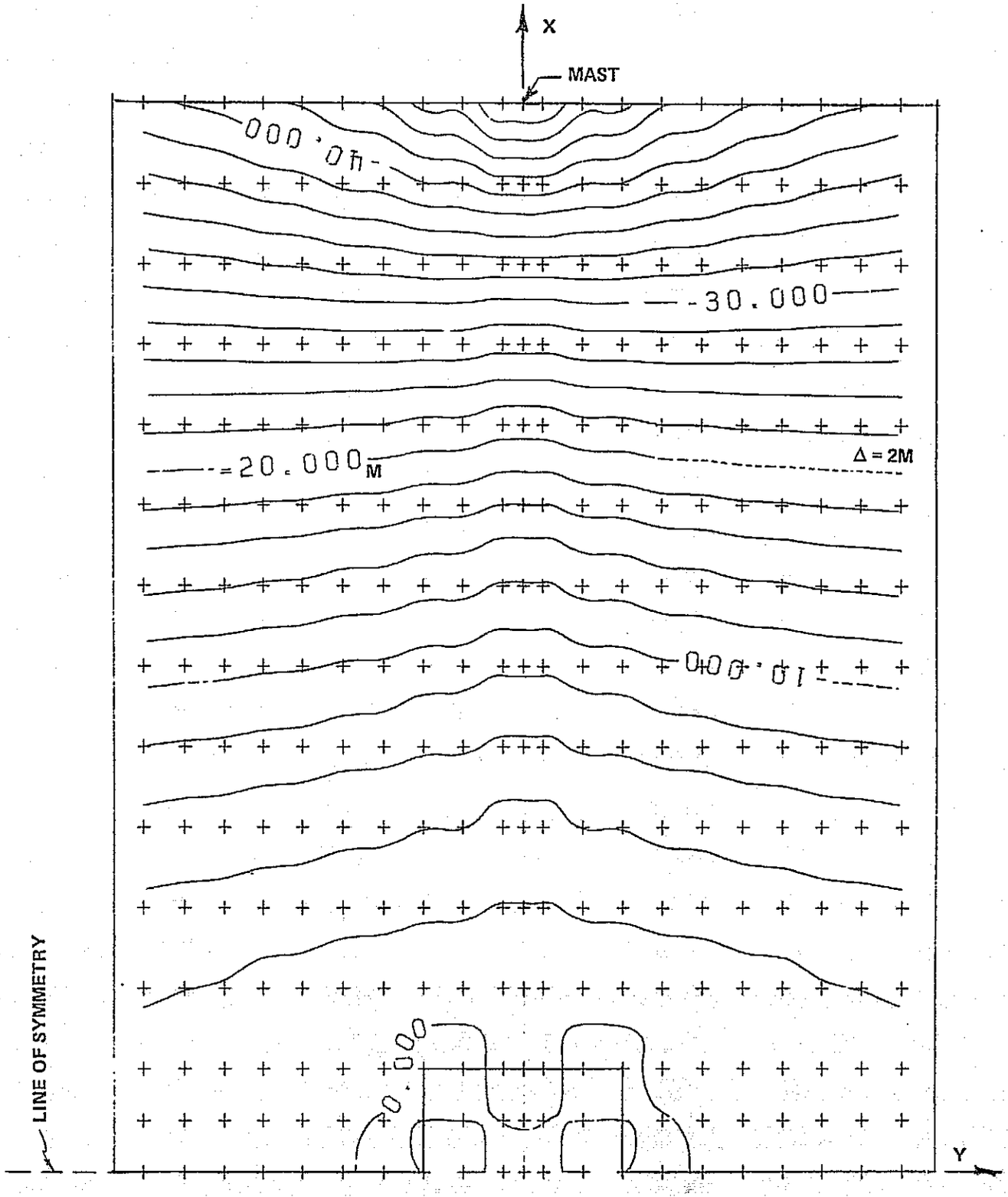

Figure 2.2-27 Contour Plot of Deflection of SSPS in Earth Shadow

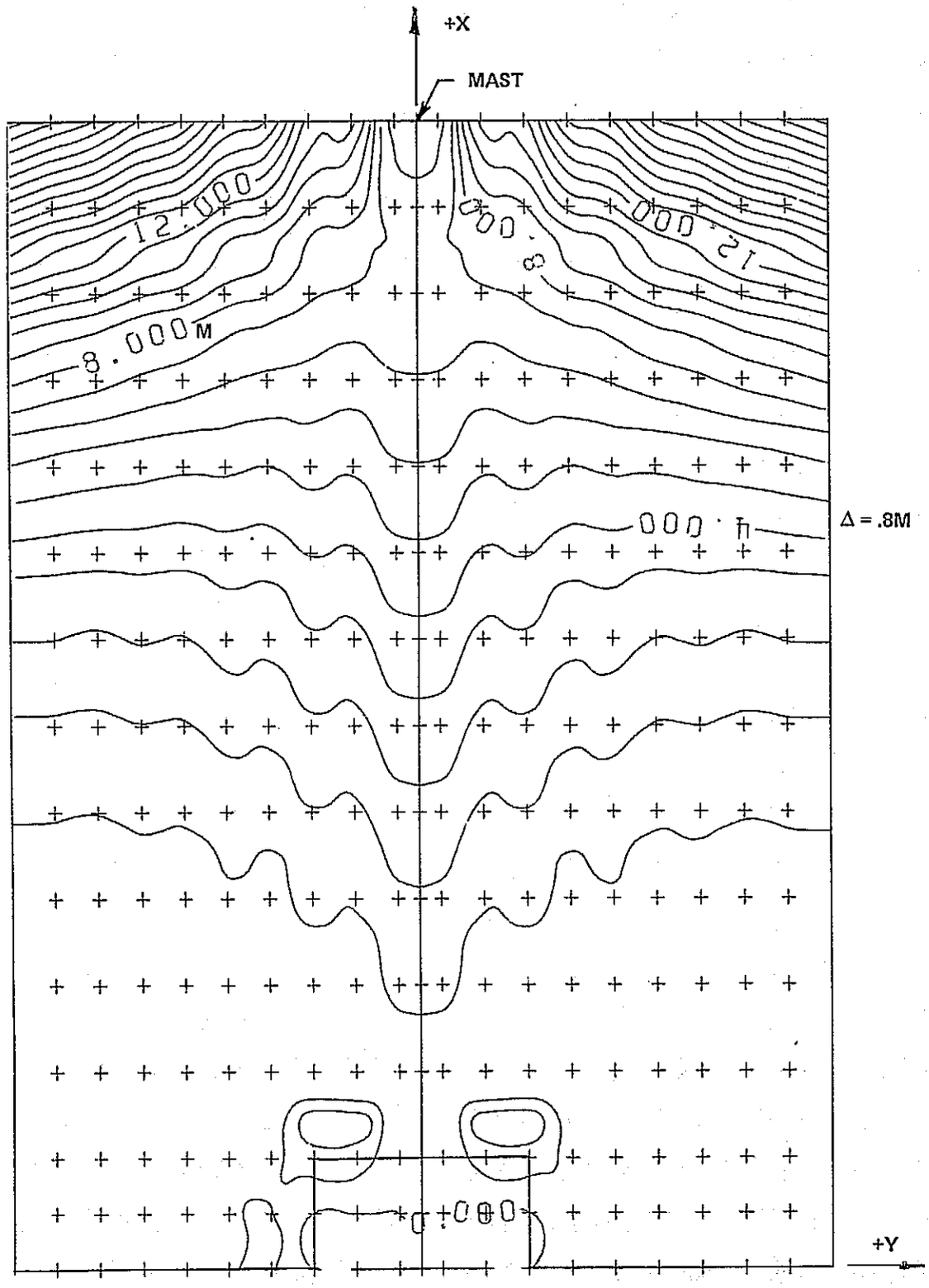

Figure 2.2-28 Contour Plot of Deflection of SSPS in Sunlight

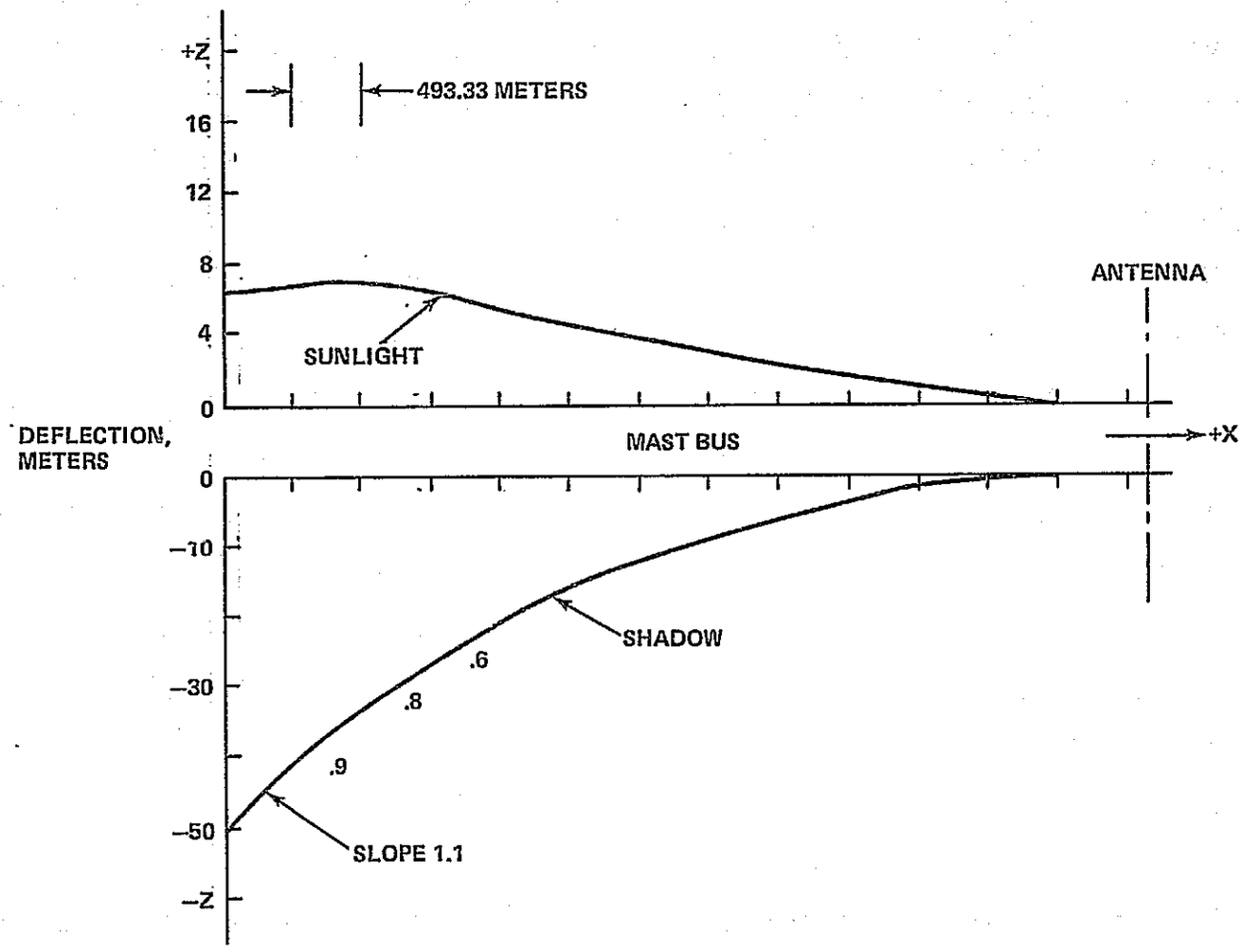

Figure 2.2-29 Mast Bus Deflection and Slope

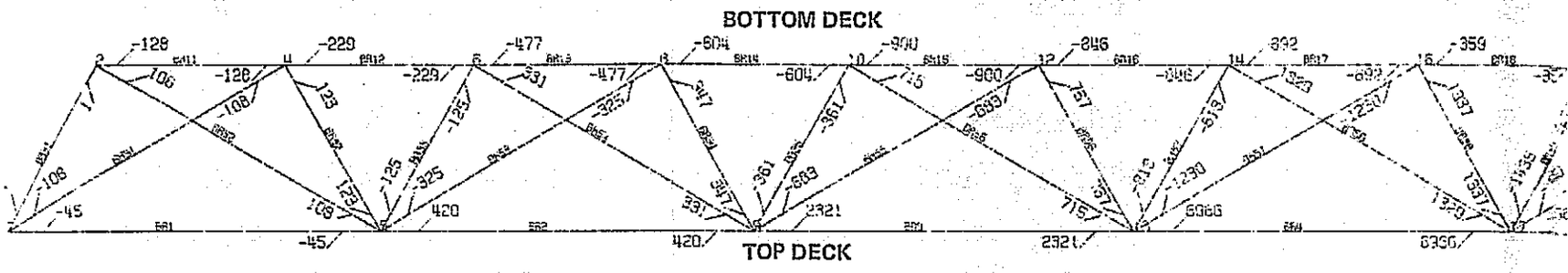

a. SHADOW

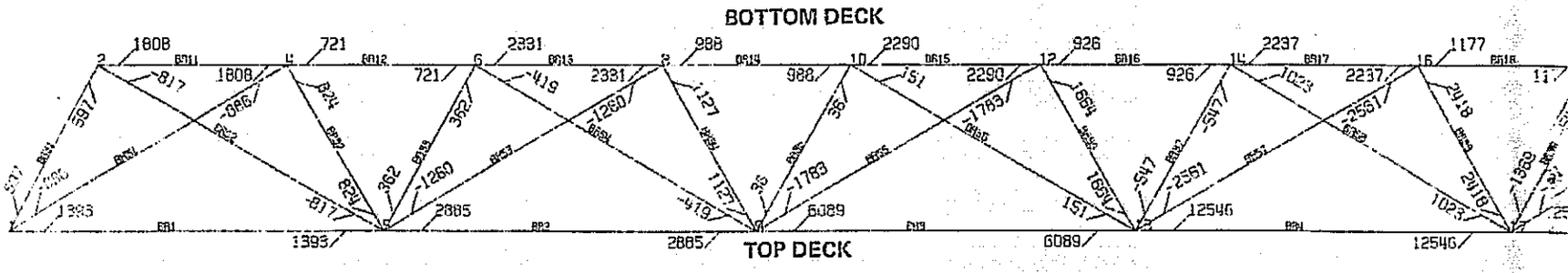

b. SUNLIGHT

FOLDOUT FRAME

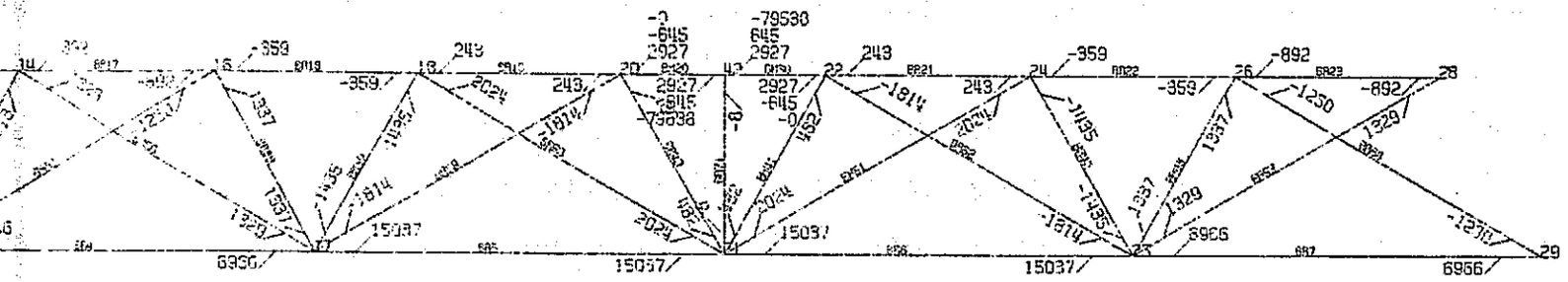

a. SHADOW

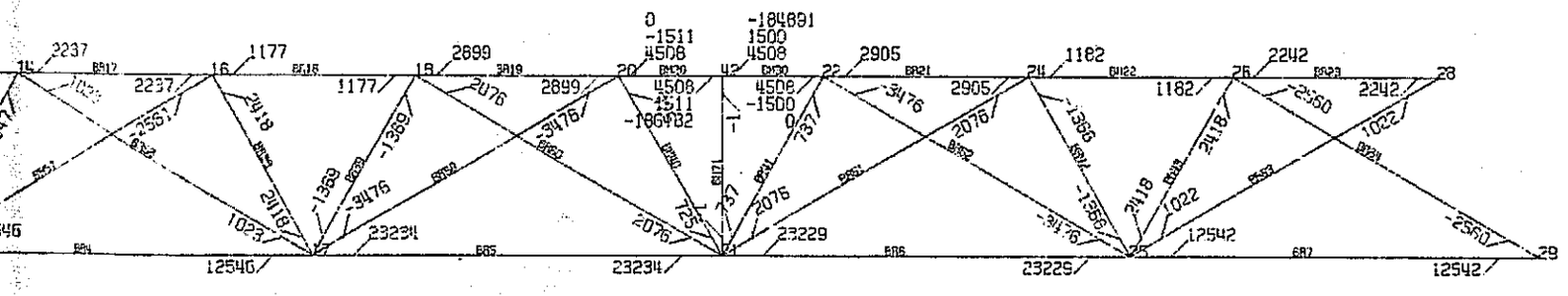

b. SUNLIGHT

Figure 2.2-30 Critical Frame Member Loads

FOLDOUT FRAME 2

The solar array structure attempts to retard the expansion and deflections perpendicular to the solar array plane are induced. The maximum deflection (Z) for the array in shadow is 50 meters at the tip of the mast; the maximum deflection at the corner of the array is 22.6 meters. Mast deflections are shown in Figure 2.2-29. The maximum slope (1.1°) occurs at the tip of the mast for the array in shadow. The 1° slope requirement for the array was exceeded by only a small portion of the array.

Array members are primarily in tension, with compressive loads induced by bending. For the members which were monitored, upper deck longitudinal member loads vary from +21562N to -5137N for the vehicle in shadow, and from +25601N to -6471N for the vehicle in sunlight. Lower deck longitudinal members are in tension, reaching maximum values of 36038N in shadow and 44851N in sunlight. A typical distribution of member loads for a critical frame is shown in Figure 2.2-30. The maximum loads in an upper deck lateral frame member vary from 15307N to -45N for the vehicle in shadow. For the vehicle in sunlight, the upper deck members are all in tension with a maximum load of 23234N. Similarly, for the lower deck, the laterial member loads vary from 2927N to -900N (shadow), and the maximum upper deck tension load is 4508N.

Cable loads are maximum in the cables that connect the mast to the SSPS structure. The maximum compressive load, which occurs with the array in sunlight, is -11925N. The maximum compressive cable load for the vehicle in shadow is -9678N. The loads are excessive for the existing structure (present design load = 890N). The values indicate the magnitude of preload required to keep the cables taut.

The cable preload requirement is strongly related to the operating mast temperature. Additional study is required to define mast temperatures accurately, so that the preload requirement can be determined. Furthermore, a realistic estimate of lateral bus electrical heating must be considered for follow-on thermal-structural analysis.

In the resizing of the existing structure, the following items should be considered:

- Preloading of the cables
- Allowing cables to go slack under compression loadings
- Isolation of the electrical transmission from the mast structure

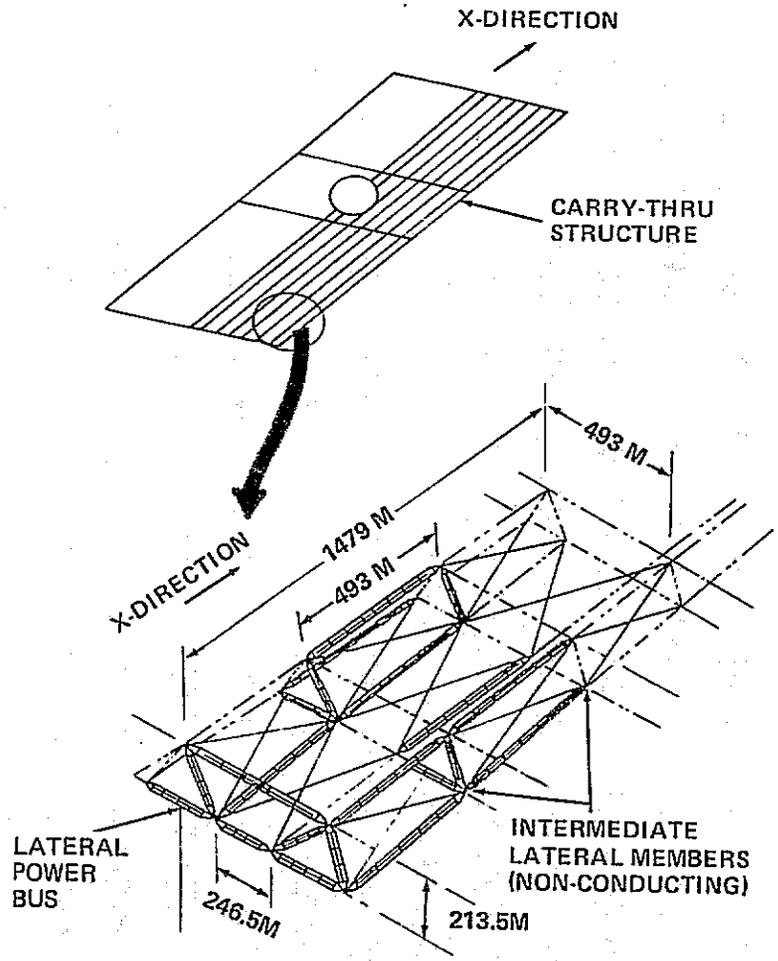

ARRAY

CHORDWISE MEMBERS (ALUMINUM) (1.499 X 10^6 LB)

MEMBER	NUMBER	WGT/MEMBER LB	WGT LB X 10^6	MASS 10^6 KG
246.5 M	520	1503	0.782	0.355
49.3 M	260	3009	0.782	0.355
213.5 M	52	1362	0.071	0.032
163.5 M	39	1042	0.041	0.019
LONGITUDINAL MEMBERS (ALUMINUM) (2.833 X 10^6 LB)				
493 M	792	3009	2.383	1.082
CARRY THROUGH STRUCTURE (GLASS) (0.33 X 10^6 LB)				
CHORDWISE MEMBERS				
246.5 M	24	1503	0.036	0.016
49.3 M	12	3009	0.036	0.016
213.5 M	8	1362	0.011	0.016
LONGITUDINALS				
493 M	72	3009	0.217	0.099
BRACING			0.043	0.020
SUBTOTAL			4.689	2.129
10% NON OPTIMUM FACTOR			0.465	0.211
TOTAL			5.154	2.340

Figure 2.2-31 Solar Array Non-Conducting Structure

- Thermal stress analysis of detailed structural components (i.e., joints, stiffeners, etc)

- Overall buckling stability and buckling stability of individual trusses.

Preliminary calculations indicate that thermally induced loads will be greater, when the vehicle reenters sunlight, than those shown.

2.2.1.8 Weights of Non-Conducting Structure

Figure 2.2-31 summarizes the solar array structural arrangement and weights. The primary structural element is a truss girder built up from roll formed modified vee hat sections with bent up stabilizing angles at the outstanding legs. The basic structural member was designed as a 1-meter deep truss girder.

The structural members were designed for a limit control force, at each array tip, of 3176N times a factor of safety of 1.4. A peak 845N ultimate compression load was used to size the aluminum vee hat section.

Pretension forces in the mirrors and solar blankets were combined with the axial compression loads to assess the beam column strength of the 493-meter longitudinals. The total mass of all non-conducting structure was calculated at 2.3×10^6 kg, including 10% non-optimum and contingency factors.

The preliminary stationkeeping load (3176N) which was to size the structure has since been superseded by a lower value (See paragraph 2.3). With the exception of thermal loading, however, the structure sized from this load has proved suitable for the design conditions investigated. The conditions included:

- Synchronous orbit transport loads

- On-orbit thruster firing loads

- Flexible neutral frequencies for control

- Thermal induced loads.

Transport loads to geosynchronous orbit are not critical, in themselves, since thrust forces can be adjusted to produce allowable loads. Because of the costs associated with longer transit times, a tradeoff between structural weight and transport costs must be performed. On-orbit loads due to repeated thruster firing are well below allowable levels, but must be evaluated for fatigue implications over a 30 year service life. The current control system produces a control frequency in roll of 1 to 2

cycles per hour. The lowest flexible mode affected by roll control is approximately 14 cycles per hour. Since a factor of 10 between control and structural frequencies is desirable, further reduction of present structural gages is limited because of the attendent reduction in stiffness. Thermal loads due to eclipse and power startup have produced requirements for structure resizing. The mast was sized to produce minimum weight for power heat dissipation. Since the operating temperature of 149°C (300°F) induces the critical local loads, further investigation of the mast design is required.

In addition to the cases investigated, an assessment of other loading conditions is required. The conditions include:

- Ground handling loads
- Launch loads
- Fabrication and assembly loads.

Fabrication and assembly loads in orbit are being investigated under a separate study contract, Space Fabrication Techniques Study Program (NAS8-31876).

2.2.1.9 Conducting Structure

Because of the large amount of conducting material required to collect the electrical power generated by the solar blankets and transmit it to the microwave antenna, the buss material has been integrated into the structure. Forces are generated in the buss/structure by the electric currents along the conductors. An effort was undertaken to size the power distribution system taking into account transmission efficiency, induced electromagnetic forces and system weight.

A weight optimization computer program was used to determine the preferred transmission efficiencies throughout the power distribution system. Figure 2.2-32 is a schematic of the electrical busses grid configuration and Figure 2.2-33 presents the electric current flow for a typical system. The optimum efficiency is 92% at an operating temperature of 38°C dropping to 91% at a temperature of 149°C. Electromagnetic forces between parallel mast buss elements are low due to the wide separation between members.

Table 2.2-4 summarizes the weight and cross section of the conducting structure.

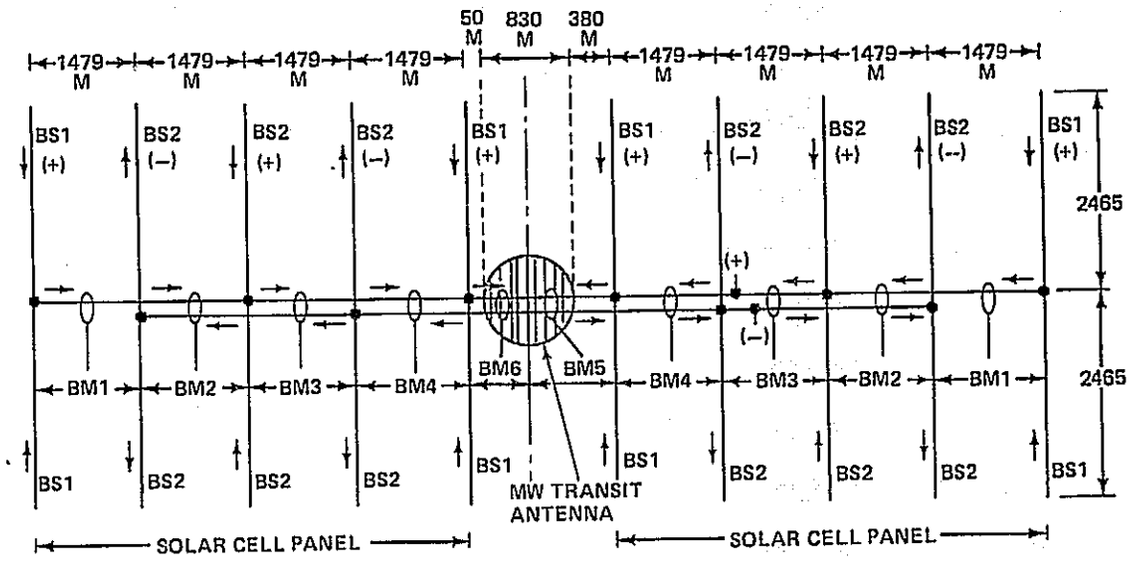

Figure 2.2-32 SSPS Conducting Structure Electrical Buses Grid Configuration

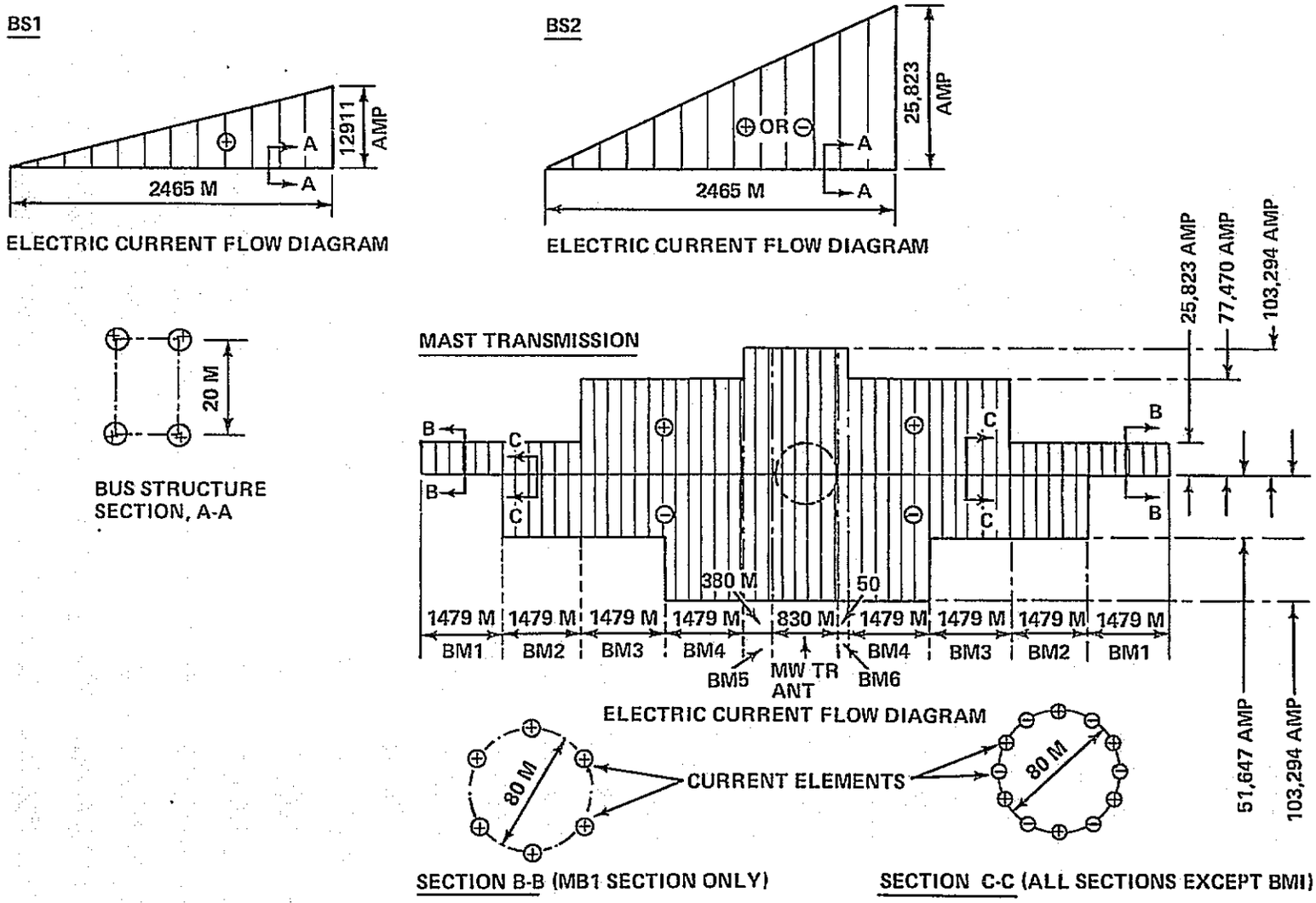

Figure 2.2-33 SSPS Conducting Structure - Solar Array and Mast Transmission Electric Buses Dimensions Electric Current Flow

Table 2.2-4 Conducting Structure Mass

MAST MASS			
MAST SEGMENT	LENGTH cm X 10^5	CROSS-SECTION cm^2	MASS. Kg. X 10^6
BM1	3.0	39.6	.033
BM2+	3.0	39.6	.033
BM2–	3.0	79.2	.066
BM3+	3.0	118.2	.098
BM3–	3.0	79.2	.066
BM4+	3.0	118.2	.098
BM4–	3.0	158.4	.132
BM5+	0.55	158.4	.024
BM5–	0.55	158.4	.024
BM6+	0.78	148.4	.034
BM6–	0.78	158.4	.034
		TOTAL	0.642

LATERAL BUS WEIGHT				
BUS MEMBER	LENGTH cm x 10^5	OPT CROSS-SECTION, cm^2	NO. OF MEMBERS	MASS, x 10^6
BS1	2465	10.8	8	.059
BS2	2465	21.6	12	.162
			TOTAL	.221

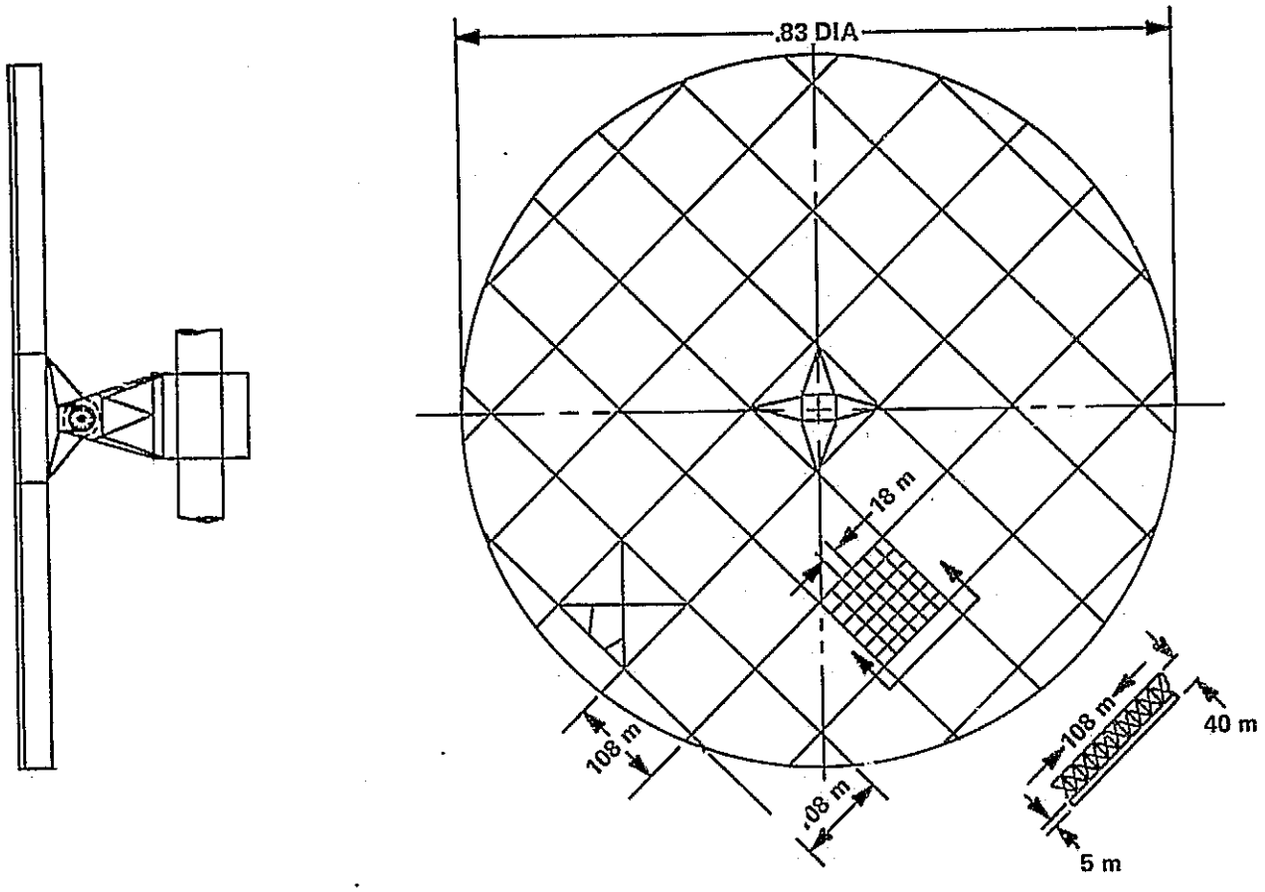

		ALUMINUM (2024-t6)
• TEMP, °K		450
• MODULES OF ELASTICITY, N/cm^2		6.2×10^6
• DENSITY, g/cm^3		2.80
• THICKNESS RANGE, cm		0.038 TO 0.102
• MASS	LB	KG
SUBARRAY PRI STRUCT	207	94
SUBARRAY SEC STRUCT	70	32
ANT. SUPPORT STRUCT	233	106
YOKE & MECHANISMS	146	66
COATINGS	31	14
AMPLITRON SUPPORT		
CONTOUR CONTROL ACTUATORS	185	84
AMPLITRON ATTACH STRUCT	35	16
TOTAL	907	412

Figure 2.2-34 Antenna Structural Arrangement

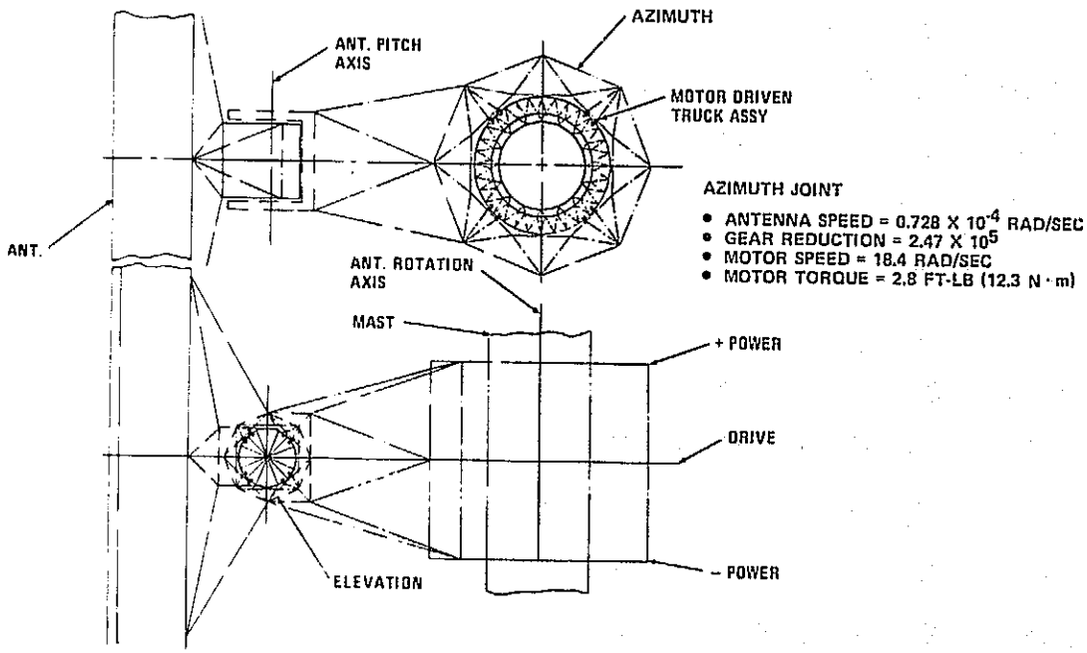

Figure 2.2-35 Rotary Joint

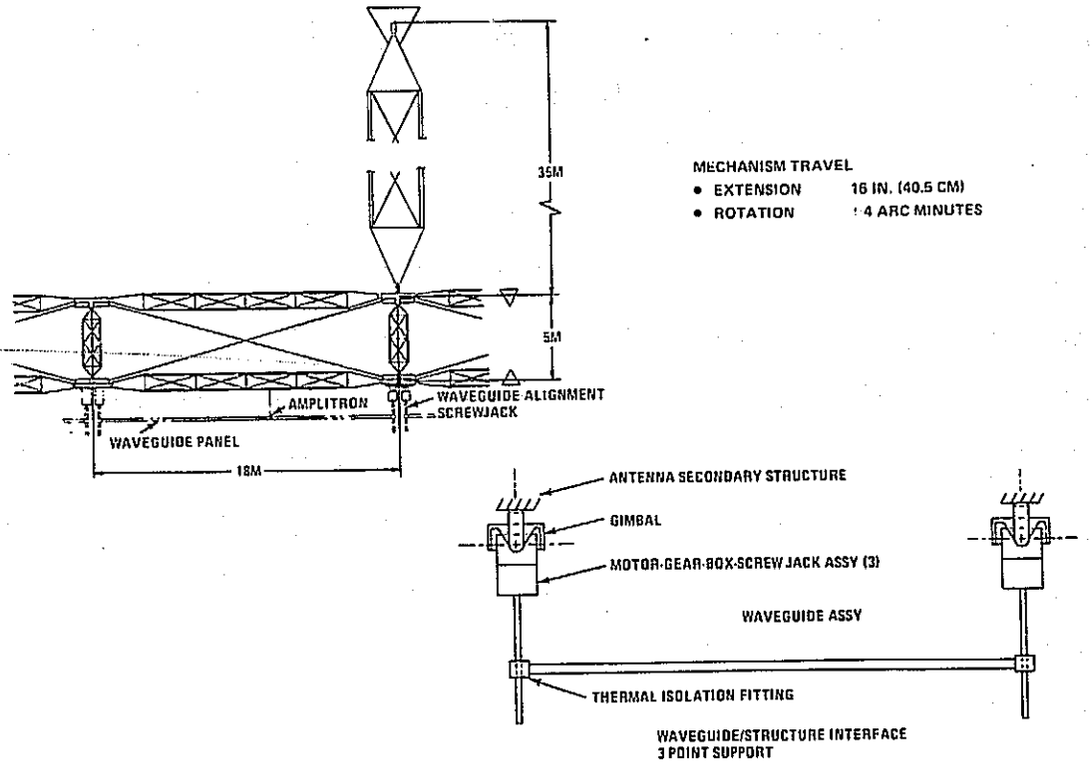

Figure 2.2-36 Structure/Waveguide Interface

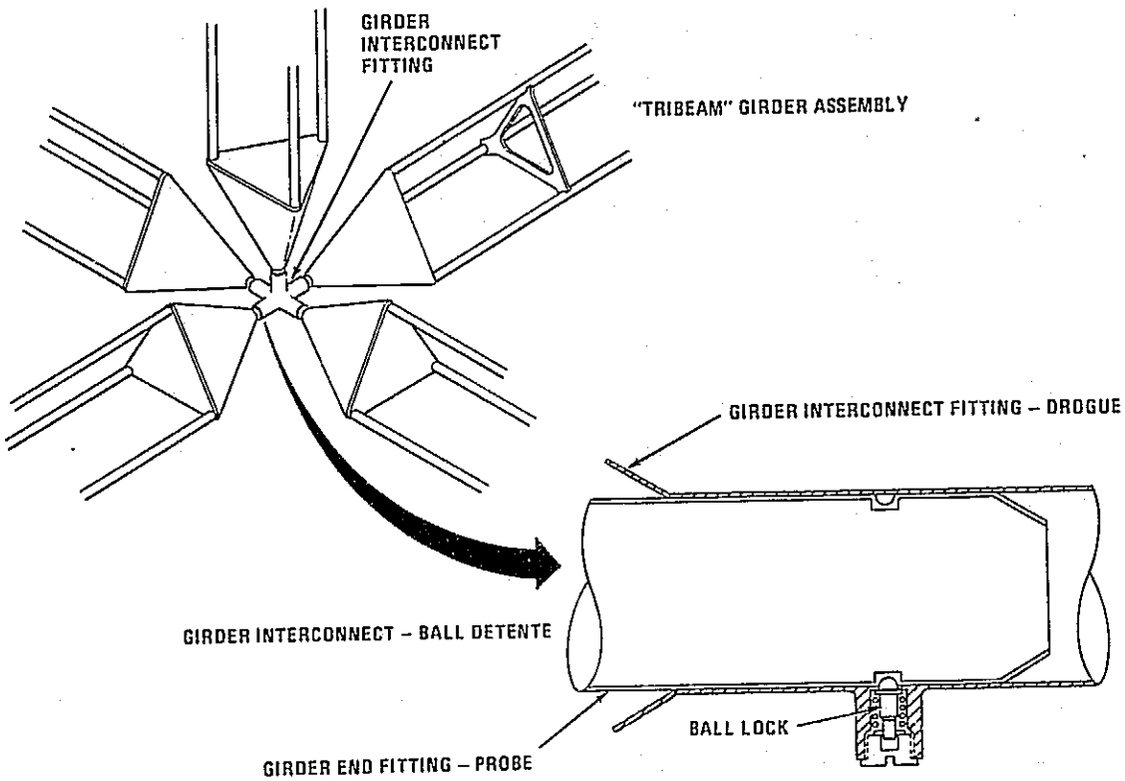

Figure 2.2-37 Structural Joints

2.2.2 Transmitting Antenna Structure

The microwave power transmission system (MPTS) is 0.83 km in diameter and 40m deep. The antenna is assembled in two rectangular grid structural layers. The primary structure is built-up in 108m x 108m x 35m bays, using triangular girder compression members 18m long x 3m deep. The secondary structure is used as a support point for the waveguide subarrays, and is built-up in 18m x 5m bays. The total antenna structure/mechanical system mass is 412,000 kg, Figure 2.2-34, using aluminum.

The antenna-to-spacecraft interface uses a 360° rotary joint for antenna motion perpendicular to the orbit plane (Azimuth joint) and a limited motion rotary joint, ±8°, for North-South pointing (elevation joint), Figure 2.2-35. Two slip ring assemblies (one for plus power and one for power return) are used for power transfer across the azimuth rotary joint and flex cable is used across the elevation joint. Both the azimuth and elevation joint drive assemblies utilize a geared rail about the diameter of the support structure and four DC brushless motor driven roller assemblies.

The structure to waveguide interface used three gimballed screw jack assemblies (Figure 2.2-36) to provide a mechanical tuning system for alignment of the waveguides after construction. Up to 40.5 cm of linear motion can be used to correct thermally induced antenna tip deflections and can also be used to correct a maximum expected 4 arc-min subarray misalignment.

Figure 2.2-37 is a typical conceptual design of a mechanical locking mechanism for structural joints. The girder interconnect fitting is similar to a docking drogue which utilizes a spring-loaded ball lock for fastening with the tri-beam end fitting.

A thermal analysis of the transmitting antenna yielded the following information:

- A triangular open section was best suited for the beam caps, resulting in the lowest temperature and temperature difference.
- The 35m long vertical members restrict the maximum waste heat power density at the center of the antenna to 3800 W/m^2 for aluminum construction and 8100 W/m^2 graphite/polyimide construction.
- The temperature difference between the upper and lower cap members (35m apart) is approximately 5 ± 1°K in the center and 13 ± 3°K at the edges.

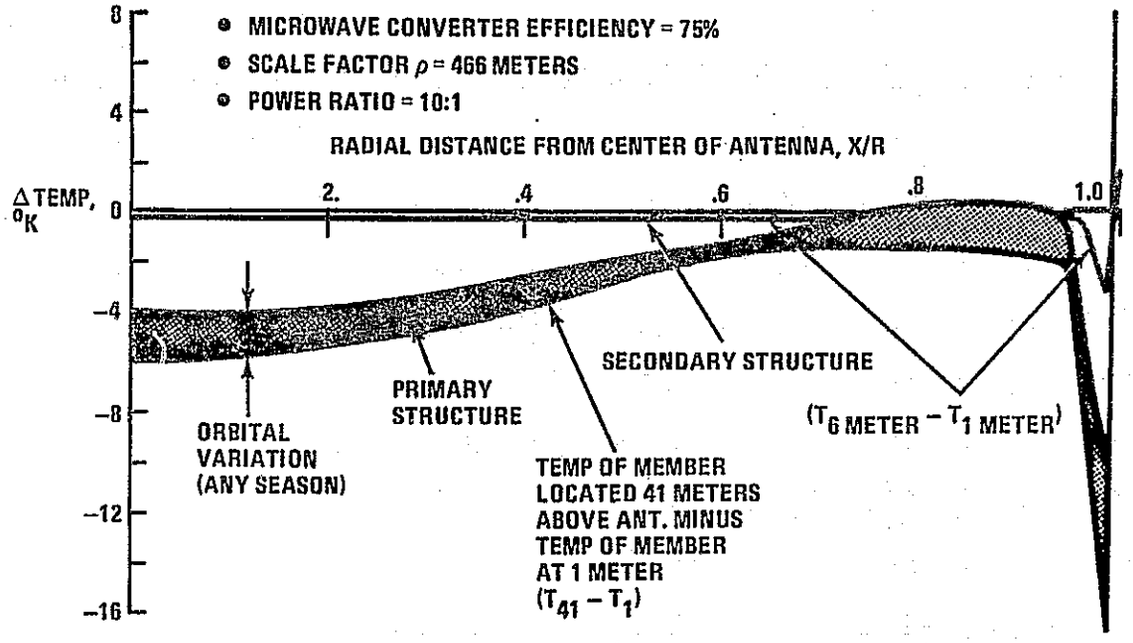

Figure 2.2-38 Temperature Difference Between Beam Cap Members Located Different Distances Above Antenna Surface

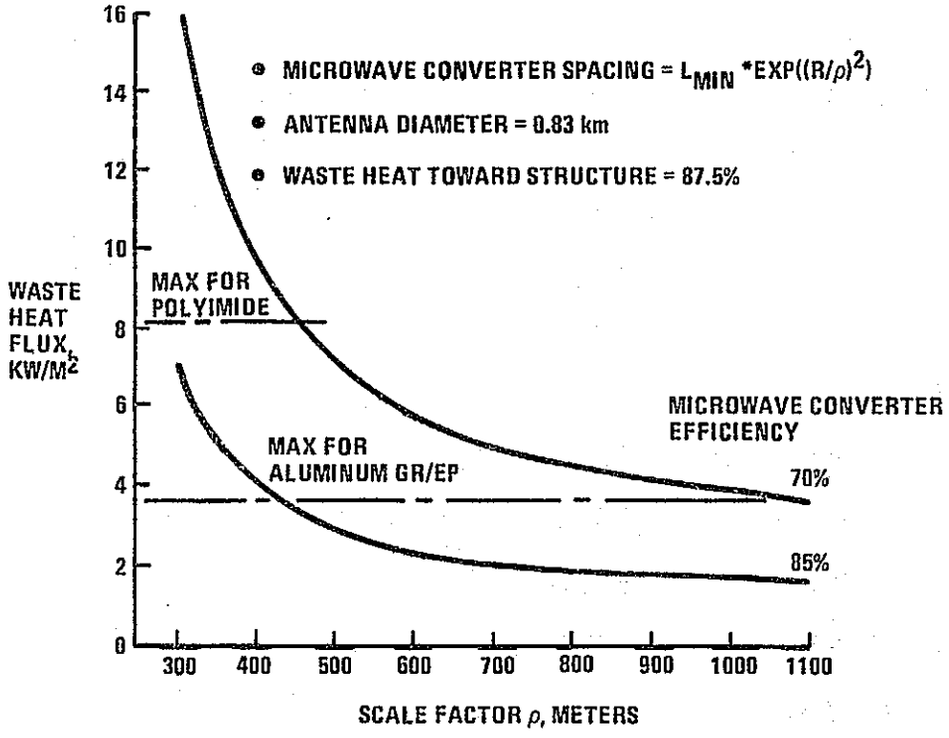

Figure 2.2-39 Waste Heat Flux at Center of Antenna as Function of Scale Factor

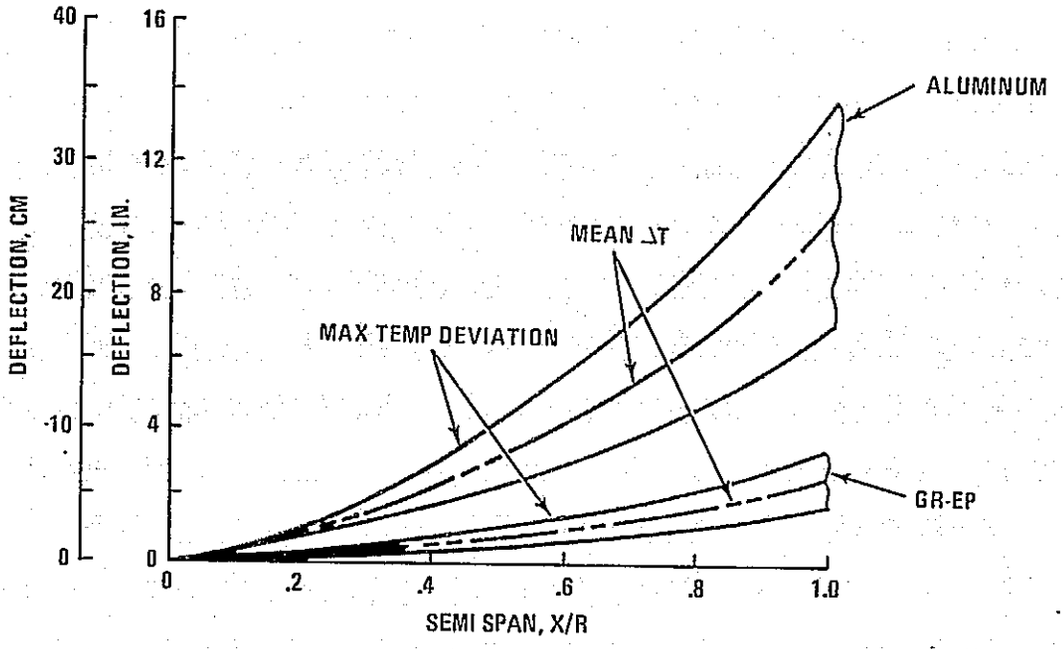

a. Typical Antenna Deflection Due to Thermal Gradients (40 Meter Beam Depth)

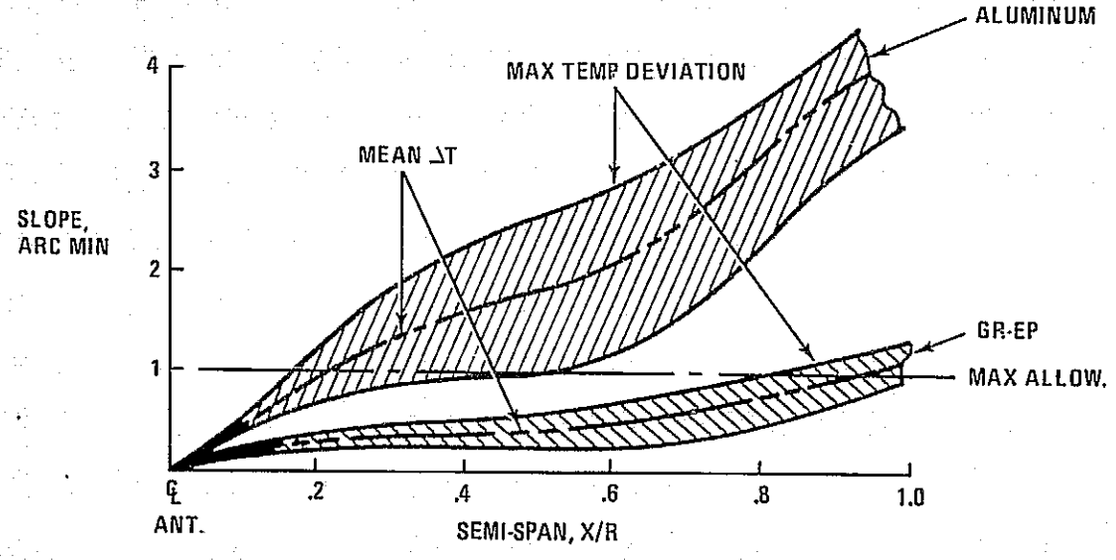

b. Typical Slopes of Structure Due to Thermal Gradients

Figure 2.2-40 Range of Thermally Induced Deflections and Local Slope

The temperature profiles along the horizontal structural triangular girder were evaluated for various orbital positions during the equinoxes and solstices. Figure 2.2-38 presents the expected variation in thermal gradients between primary and secondary structural caps. The average primary structure thermal gradient is approximately 5°K at the center of the antenna. The expected variation in this difference is ± 1°K.

The vertical columns of the structure have the same view of the antenna surface and space and consequently, cannot be easily configured with coatings, insulation or geometry selection to minimize peak temperatures of the material. Figure 2.2-39 shows the maximum waste heat flux that will be experienced by the vertical columns of a 1 km antenna for microwave converter efficiencies of 85 percent and 70 percent. Limitations as to the taper of the distribution (e.g., the db drop of power density at the antenna's center relative to its edge) must be imposed depending upon the structural material selected. A near uniform distribution must be used if the structure is aluminum or graphite/epoxy (70 percent converter efficiency). Because of the potential limitations that the structure could place on the layout of the microwave converters, the chosen material may be graphite, polyimide, steel or titanium. Selection of graphite/polyimide would be compatible with a desirable 5:1 db taper for the converter Gaussian distribution.

The range of thermally induced deflections and local slope are presented in Figure 2.2-40. Variations in slope with variations in orbital position exceeds 1 arc-min for an aluminum structure. The slope variations from a mean or average deformity is well within limits for graphite/epoxy. Assessment of secondary structure deformation shows that the worst deflections occur at the tips of the antenna, with maximum deflections not to exceed 10.5 mm over any one 18 x 18m subarray.

2.2.3 Summary of Issues

2.2.3.1 Static and Dynamic Structural Responses to Thermal and Load Environments

The SSPS design load environments which are of significant magnitude occur during the following mission phases:

- Launch conditions
- Manufacturing-in-space loads
- Assembly-in-orbit loads
- SSPS segment transfer loads from low earth orbit to geosynchronous orbit
- Orbital operational conditions.

Launch and manufacture loads are dependent on the method of fabrication of the SSPS; the assessment of these factors are being performed under contract NAS 8-31876. Orbital load conditions which contribute to the design of the structure include solar pressure, gravity gradient control torques, and orbital station keeping control forces. Though on-orbit control forces were shown to be low in relation to structural capability, they still must be evaluated with respect to repeated loadings over a thirty year life span. Geosynchronous orbit transport loads can be kept within allowable limits by accepting a penalty in transport time. Methods of effecting transport propulsion must be investigated in greater detail, and a cost tradeoff must be made between transport time and structural weight.

A significant thermal stress problem is caused by the thermal gradients that result from electrical power heating with the SSPS in sunlight or in earth shadow during eclipse. The following methods can be used to alleviate this problem:

- resizing
- allowing cables to go slack
- isolating mast electrical transmission from mast structure.

All of these methods require further evaluation because of the weight and stiffness penalties involved. In addition, the period of excitation during eclipse (0 to 72 minutes) may thermally excite a structural dynamic response. The effects of these oscillations on the overall system must be assessed.

As previously mentioned, the induced dynamic and thermal stress cycling must be evaluated with regard to service life. A tradeoff study must be performed to establish a rational scatter factor for life assessment. Whether the structure should be designed for a scatter factor of two times the 30 year required service life, or more, and the associated weight penalties, should be assessed. The thermal histories evolved from these studies should also be used to establish the preloading requirements on the solar blankets and mirrors. Again, the thermal/load time histories of these preloads, as they affect support structure, must be evaluated to establish the satellite integrity.

2.2.3.2 Analytic Tools and Techniques

2.2.3.2.1 Dynamic Response to Thermal Excitation - When the SSPS enters and leaves the earth's shadow, it undergoes severe temperature changes. The thermally induced deformations during this alternate cooling and heating may result in significant vibration of the SSPS. An investigation is recommended to determine the extent of this vibration.

The following three-phase analysis is a practical approximate approach to accomplish this study. In the first phase, the temperature time-history of the satellite would be predicted using existing computer programs such as NASTRAN or Grumman's Integrated Thermal Analysis Procedure. Next, the external loads which produce deformations that are equivalent to the thermal deformations would be generated. NASTRAN or Grumman's ASTRAL-COMAP computer program system could be used to accomplish this phase. In the third phase, three loads could be introduced into the new time-history program recommended in Item 2 in order to determine the dynamic behavior of the satellite.

2.2.3.2.2 Time-History Program with Accurate Evaluation of Gravity-Gradient Excitation - To study, in detail, the control of a flexible structure in a gravity-gradient field, it is necessary to accurately determine the difference between the gravity force and the orbital centrifugal force at each mass point. In many existing computer programs these effects are computed and then subtracted; however, the effects are nearly equal, and it is the small difference which is of consequence. This procedure is, therefore, considered too inaccurate to be of value. To significantly improve the procedure, the gravity and orbital centrifugal effects should be expanded in a series, analytically subtracted, and the result should be programmed in a general time-history structural program.

This computer program should be sufficiently general so that structures of any shape and mass distribution may be treated. In addition, to properly include gravity effects, it should have the capability of including a large variety of control systems as well as a general set of externally applied load. It should not rely on orthogonal functions such as modes for the reduction of coordinates, so that the above described expansion functions may be used. The resulting program would be a powerful tool for predicting the dynamic behavior of flexible structure in space.

2.2.3.2.3 Improved Method for Reduction of Number of Variables Used in Equations of Motion - It is likely that the attitude-control jets will excite a number of high-frequency vibration modes as well as the lower-frequency and rigid-body modes. These motions, in combination, may result in waves which emanate from each jet and damp out as they proceed through the structure. To accurately predict the dynamic behavior of the structure, it appears that an unusually large number of modes will be required; thus, the computer time and storage requirements would be excessive. For these reasons a study is recommended to determine more effective dynamic analysis methods for large flexible space structures. The improved techniques developed in this study will also provide increased confidence in the ability of the control system to achieve the required control.

In the recommended study, generalized coordinates such as components of wave functions would be considered as a substitute for higher order modes. Various sets of functions would be investigated, and the accuracy of the solutions obtained would be compared by substitutinn into the equations of motion. The study would proceed as follows:

- First treat simple structures such as beams and plates
- Study accuracy and compare with modal approach
- Based on the above results, develop methods to generate the desired functions for complex lumped mass structures such as the power station
- Study accuracy and compare with modal approach.

The end product would be a computer program which would automatically generate the required expansion functions.

2.2.3.3 Materials and Processes

The study summarized in this memorandum was based on the use of 2219 aluminum alloy T62 condition in sheet strip rolls which are carried aboard automatic manufacturing modules into orbit by the Space Shuttle or other large launch systems. The free flying modules roll form the basic structural elements which are assembled and welded into the progressively larger components. Investigations should be made to assess the use of other materials such as kevlar/polyimide composits, graphite/epoxy composites, beryllium alloys, titanium alloys and various other aluminum alloys. These materials evaluations should be coupled with the use of other structural shapes and configurations to obtain a more realistic trade study of weight, cost, and complexity. The various processes and techniques which could be considered are:

- Electron beam welding
- Spot welding
- Mechanical attachments
- Roll forming
- Composites layup
- Adhesive bonding
- Brazing
- Thermite welding

- Explosive welding
- Utilization of the space environment to enhance the processing of materials
- NDE evaluation
- Initial imperfection evaluation
- Quality Assurance

In evaluating materials applications the following should be considered:

- Strength and strength/weight ratio
- Modulus of elasticity and modulus/weight ratio
- Structural properties vs temp
- Fatigue properties vs temp
- Fatigue properties
- Coefficient of thermal expansion
- Thermal conductivity
- Creep, creep rupture
- Fracture toughness
- Stress corrosion susceptibility
- Formability/brittle behaviour
- Specific heat
- Meteoroid impact vulnerability
- Weldability
- Material density.

2.2.3.4 Manufacturing and Assembly Techniques

The capability to fabricate and assemble large structures in space is a key issue associated with the insertion of the SSPS into geosynchronous orbit. The design, fabrication, assembly and transportation of the large space structure present many significant problems requiring advances in the state-of-the-art

in the related structural, materials, manufacturing and assembly technologies. The manufacturing and assembly techniques proposed in this study is based on the use of free flying automatic fabrication modules. The module automatically fabricates and assembles from raw sheet stock the major structural components of the SSPS in low earth orbit. These members are assembled into modular sections and boosted into geosynchronous orbit for completion of assembly.

It is recommended that the above be studied in greater detail together with alternate methods of manufacture and assembly to establish the most cost effective and lightest configuration.

2.2.3.5 Structural Verification Techniques

It is recommended that investigations should be carried out to evolve methods for verifying the structural integrity of the SSPS vehicle. The application of ground test technique currently in use are obviously not feasible. It is proposed that ground test techniques for scale models which are structurally and dynamically similar be developed. This procedure will provide verification of analyses methods. A second phase of this study would be to design fabricate and flight test an instrumented model of reasonable scale for the same purposes as given above.

2.2.4 References

2.2-1 NASA CR-2357, "Feasibility Study of a Satellite Solar Power Station, "February 1974.

2.3 Flight Mechanics and Control

The objectives of the flight mechanics and control effort has been to establish engineering requirements for stationkeeping, positioning and attitude control for the SSPS. Stationkeeping requirements were established by analyzing orbit perturbations due to Earth oblateness, solar pressure, Sun-Moon gravity and electromagnetic forces. Attitude control requirements were established by assessing the effects of gravity gradient, solar pressure and microwave pressure disturbance torques.

Analysis of SSPS stationkeeping requirements has resulted in the following:

- SSPS stationkeeping propellant requirements are approximately 9072 Kg (20,000 lb) per year using ion propulsion (I_{sp} = 8000 sec)
- North-South drift has more impact on overall microwave transmission efficiency than longitudinal drift for the rectenna latitude considered (40°N)
- Solar pressure is the dominant orbit disturbance. Results show that this perturbation is most economically handled by continuously controlling orbit period and not correcting eccentricity. However, if the number of SSPS satellites goes above 12 units over the continental United States, the eccentricity drift should then be corrected. This will require an additional propellant consumption of 2132 Kg (47,000 lb) per year.
- Established a parametric rationale (based upon the maximum allowable deviation from assigned SSPS positions) which determined the thrust-time duty cycles which account for each orbital perturbation which would cause a change in position of a stationary satellite. For example, for a ±2.5° max allowable longitude drift, the governing drift is the eccentricity drift due to solar radiation pressure. The result is a 57 day duty cycle with 5 day orbit-keeping burns for drifts in eccentricity and longitude. For inclination drifts the duty cycle is 365 days with a 10 day ion-engine burn at a thrust level of 600N (135 lb); this requires 1350 thrusters, each with 0.45N (0.1 lb) thrust. A total of 14,000 0.1 lb thrusters are required to maintain allowable deviations.
- Developed a thruster analysis, establishing size, number of thrusters, and typical force (thrust) time histories nullifying each orbital drift (i.e. drift in eccentricity, period, inclination and longitude).

SSPS control system studies have found the following:

- The gravity gradient torques are the dominant disturbance to the spacecraft, requiring 8×10^9 Newton-meter-seconds momentum from the control system daily
- Transients from the antenna rotary joint control system used for antenna pointing, sizes the array roll thrusters (40 Newton engines mounted at the extremes of the array)
- CMG's are not applicable to the array control function. A control system for roll alone would weigh 20×10^6 kg using CMG's
- The SSPS configuration is sufficiently stiff to achieve better than 1° pointing accuracy
- Mechanical steering of the solar array to point toward the sun for the entire year, could result in a 10^6 kg decrease in system weight.
- The solar array roll control loop may be designed such that the slip ring drag torque will be unidirectional during steady state operation.
- The antenna azimuth control is not affected by the expected levels of structural compliance for the central mast.
- Array limit cycling amplitude reduction to alleviate effects on antenna control causes increased excitation of structural modes.
- Slip ring drag torque significantly affects antenna steady state pointing error.

Table 2.3-1 summarizes the yearly propellant expenditure for the SSPS. Two levels of expenditure have been listed. The lower level assumes that eccentricity drift due to solar pressure is not corrected. This is reasonable if the number of SSPS at geosynchronous orbit servicing the United States is less than 4. Beyond this number of satellites, eccentricity drift control is needed, increasing propellant consumption.

Table 2.3-1 SSPS Propellant Requirements, Isp = 8000 Sec

	LBM/YR	KG/YR
STATION KEEPING		
• LONGITUDE DRIFT	716	325
• INCLINATION DRIFT	14700	6673
• SOLAR PRESSURE		
– ALTITUDE DRIFT	5100	2315
– ELLIPTICITY DRIFT	0 (47040)*	0 (21343)*
• MICROWAVE PRESSURE	68	31
SUBTOTAL	20,092 (67132)*	9344 (30687)*
ALTITUDE CONTROL		
• GRAVITY GRADIENT	30,408	13,804
• ANTENNA CONTROL	162	7474
• SOLAR PRESSURE	870	394
• MICROWAVE PRESSURE	292	132
SUBTOTAL	31,732	14,404
TOTAL	51824 (98864)*	23748 (45091)*

*REQUIREMENT AFTER 4 SSPS ARE PLACED IN ORBIT TO SERVICE THE UNITED STATES.

2.3.1 Orbit Keeping

There are four major influences on the SSPS causing it to drift from its nominal orbital location. These are:

- Longitudinal Drift - The ellipticity of the earth causes the SSPS to seek out the earth's minor axes
- Inclination Drift - The interaction of the sun and moon's gravitation causes the orbit to regress so that its inclination changes with respect to the equator.
- Altitude and Eccentricity Drift - Solar pressure distorts the orbit from circular to elliptical and back again over a one year period. In addition, there is an effective altitude change which increases the orbital period and then restores it to nominal over the same elapsed time.
- Microwave Pressure - The electromagnetic fields at the aperture of the slotted array causes a "rebound" pressure on the antenna.

2.3.1.1 Longitudinal Drift

The earth's ellipticity causes a geosynchronous satellite to drift toward the minor axes of the earth's ellipsoid. These stable points are located at approximately 120°W and 60°E longitude. If uncontrolled, a satellite will drift as far past these stable nodes at its original longitudinal displacement, return, and then repeat the cycle. An SSPS, for example placed at 75°W longitude to optimally service the northeast, would drift past the western hemisphere stable point to a longitude of 165°W, or to a 90° longitude difference between the rectenna and satellite. At this longitude difference there is no line-of-sight, Figure 2.3-1. Therefore, some degree of longitudinal drift stationkeeping is required to ensure transmission. The longitudinal bounds within which the satellite must be maintained is a function of the effect variations in satellite drift have on overall system efficiency.

The stationkeeping propellant required to continuously correct longitudinal drift is shown in Figure 2.3-2 for 11.4 x 10^6 kg SSPS. The propellant quantities were calculated for variations in SSPS longitudinal position assuming the use of an ion propulsion engine with a specific impulse of 8000 sec. The worst case SSPS positions, 160°W, 75°W, 15°E and 105°E longitude, can be maintained with approximately 305 kg/yr of propellant.

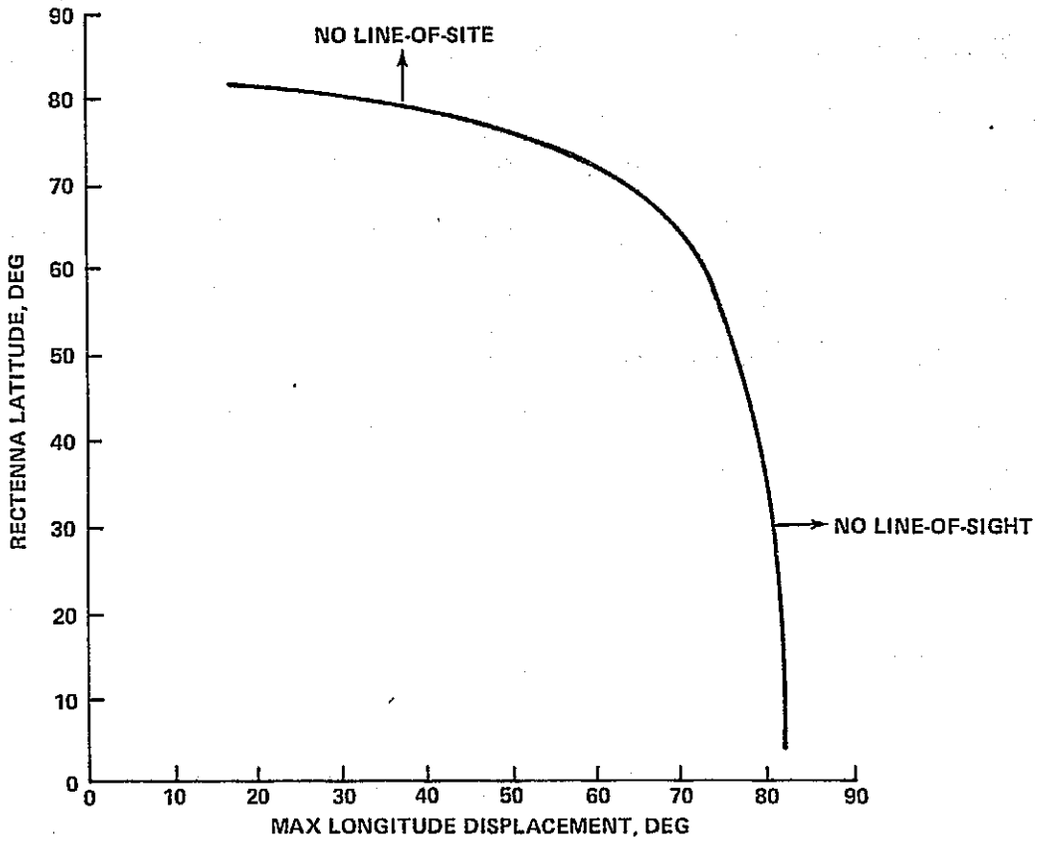

Figure 2.3-1 Maximum Longitude Displacement Between Rectenna and Satellite

The use of a cold gas system, Isp = 200 sec, would require closer to 12,200 kg/yr. The advantage of electric propulsion for the stationkeeping function is clear.

A continuous engine thrust level of approximately 2.2N would be required to maintain longitude. The feasibility of continuous ion thrust for 30 years is questionable. Current ion engines have demonstrated life of only 10,000 to 15,000 hr. A minimum of eighteen 2.2N engines would then be required over the life of the SSPS.

Alternate schemes to continuous thrusting should be investigated. If some drift from the nominal is tolerable, periodic two burn orbit adjustments could be used. Assuming a permissible burn period once a year of one hour, a 7565N engine would be required to make the adjustments. This thrust level could cause significant structural bending and overall spacecraft control problems. Therefore, some compromise between continuous thrusting and impulsive adjustment once a year is needed.

2.3.1.2 Inclination Drift

The gravitational influences of the sun and moon cause a gradual plane change in the SSPS orbit relative to the ecliptic. Because the desired SSPS orbit's equatorial plane is fixed relative to the ecliptic, the regression of this orbit takes on the form of an inclination drift relative to earth-centered coordinates. The total period of the regression from nominal to the maximum inclination of 15° is 53 years.

Figure 2.3-3 presents the time history of inclination for various initial orbit conditions. A unique set of orbit parameters with an inclination of -7.5° results in a stable orbit requiring no propellants for orbit maintenance. This orbit, however, would produce a figure eight around track. This ground track motion would cause a 16° variation in the rectenna to satellite line-of-sight for a rectenna located in the Northeast. Angular motions of this type have two effects when the satellite is in the southern half of its orbital swing:

- The path through the atmosphere is increased, decreasing efficiency

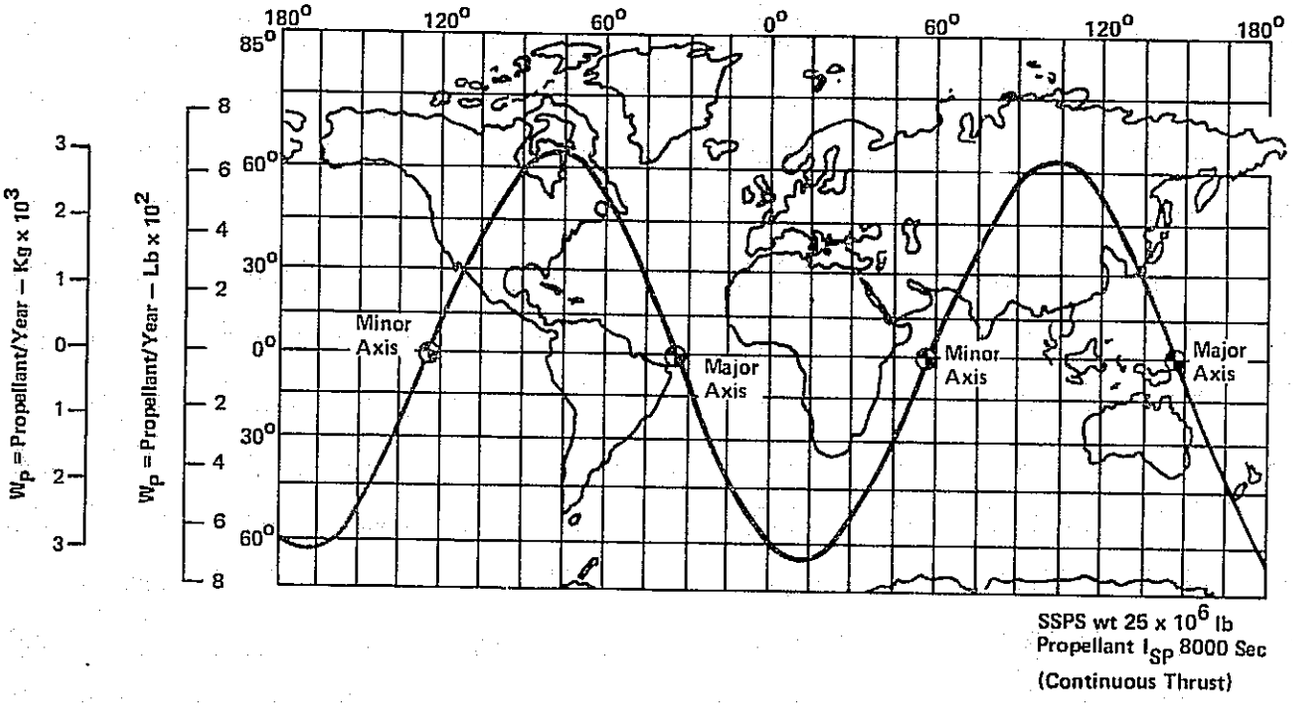

Figure 2.3-2 Longitudinal Drift Propellant Requirements/Year

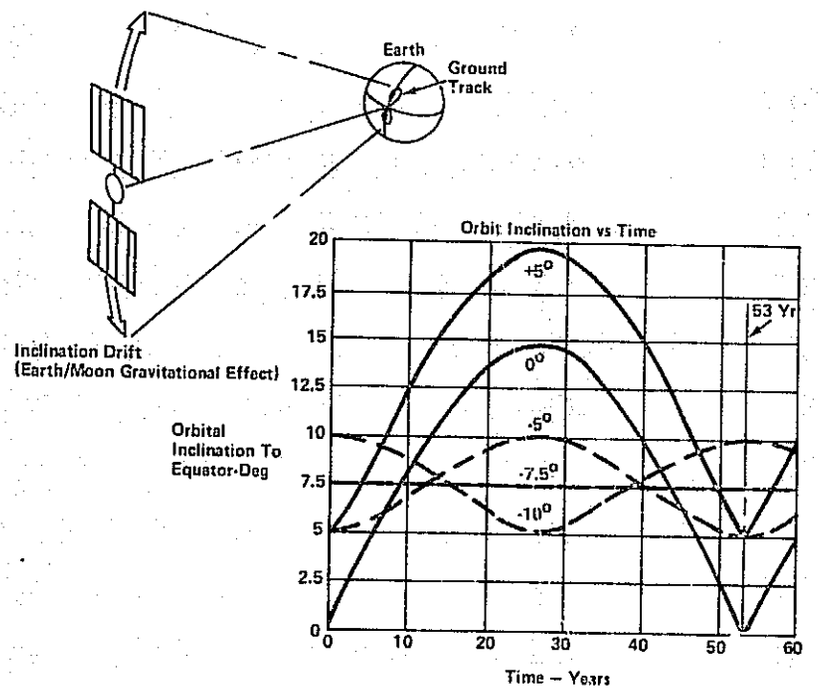

Figure 2.3-3 Inclination Drift Characteristics

- The ground pattern of the microwave beam elongates in the north-south direction requiring a larger rectenna to capture an equivalent amount of power. Figure 2.3-4 illustrates the impact of MW beam elongation on rectenna size requirements. The shaded area illustrates the beam ground pattern of the main lobe on a rectenna located at a latitude of 40°. This pattern is an ellipse with major and minor axes of 12 km and 8.5 km, respectively. An inclination drift of 20° would increase the north-south dimension of the rectenna from 12 km to 22 km. This equates into a 30% increase in required rectenna area for a 7.5° inclined orbit.

Figure 2.3-5 presents the SSPS propellant requirements for continuous correction of inclination drift. A propellant expenditure of about 6674 kg/yr is required to maintain an equatorial orbit using ion propulsion at a specific impulse of 8000 sec.

2.3.1.3 Altitude and Eccentricity Drift

Solar pressure has a considerable effect on the SSPS orbit because of the large area solar arrays. Figure 2.3-6 illustrates the effects of solar pressure on the SSPS orbital characteristics. Over a period of 170 days the circular orbit distorts to an ellipse with an eccentricity of 0.096. In addition the orbit period increases from 24 hrs to 24 hrs, 14 minutes. Both the orbit shape and period return to nominal after 340 days.

The solar radiation pressure at 1 AU is 4.65×10^{-5} dynes/cm^2 which produces a continuous force on the SSPS of from 50 to 70 LB (200 to 300 Newtons). The pressure due to solar wind proton flux is considerably lower than that caused by radiation and can be neglected (Ref. 2.3-1).

The effect of solar pressure as shown above is twofold. The first is a change in altitude and hence orbit period and the second a change in eccentricity. If the change in period goes unchecked, the SSPS will precess around the equator at a rate of approximately 3.5° per day. A propellant expenditure of 2315 kg/yr would be required to offset this highly undesirable satellite motion, Figure 2.3-7. The propellant required to correct the ellipticity has been calculated at 1.59×10^5 kg/yr Ref. 2.3-2. This propellant quantity assumes that an opposing force of 200 to 300N is continuously applied to offset the solar force. The effect of ellipticity on overall system performance, however, is not significant, provided the 24 hr orbit period is maintained. Ellipticity causes an apparent

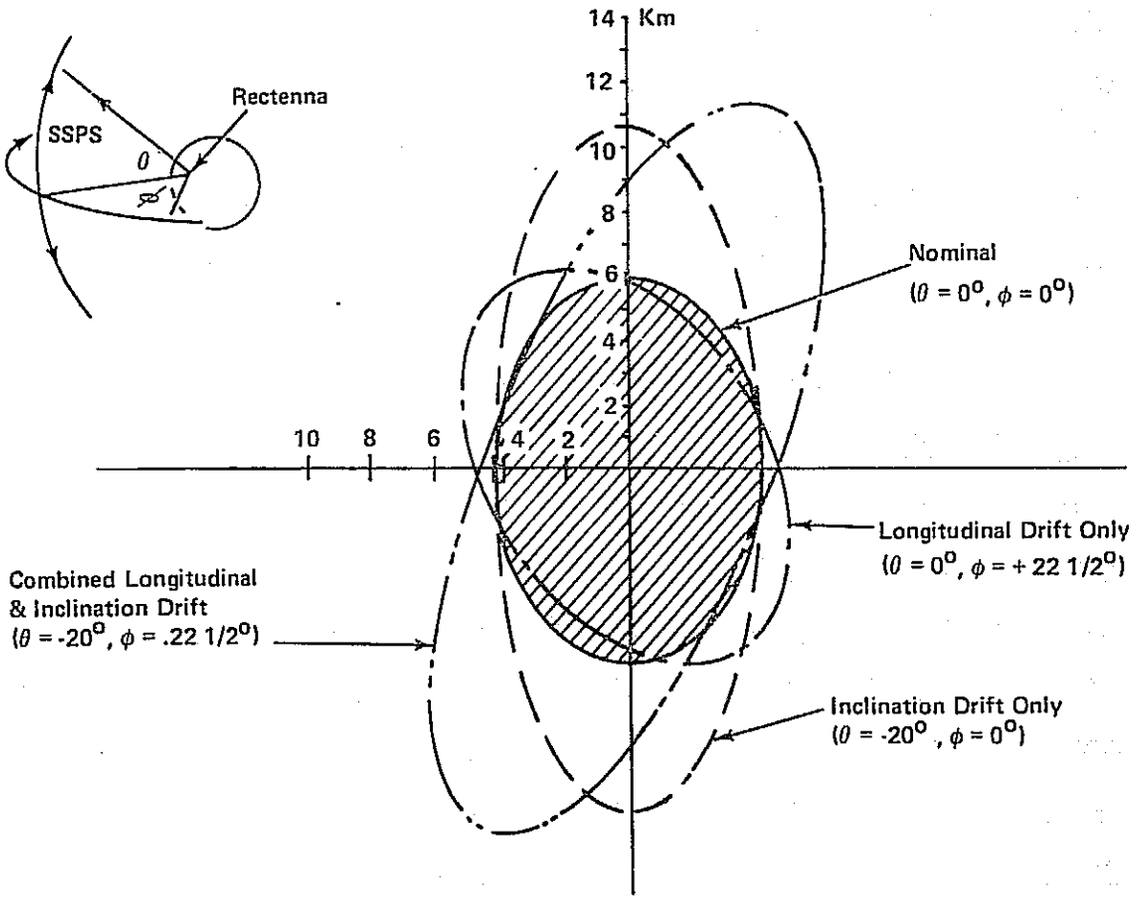

Figure 2.3-4 Main Lobe Ground Pattern Variations - 40° Latitude

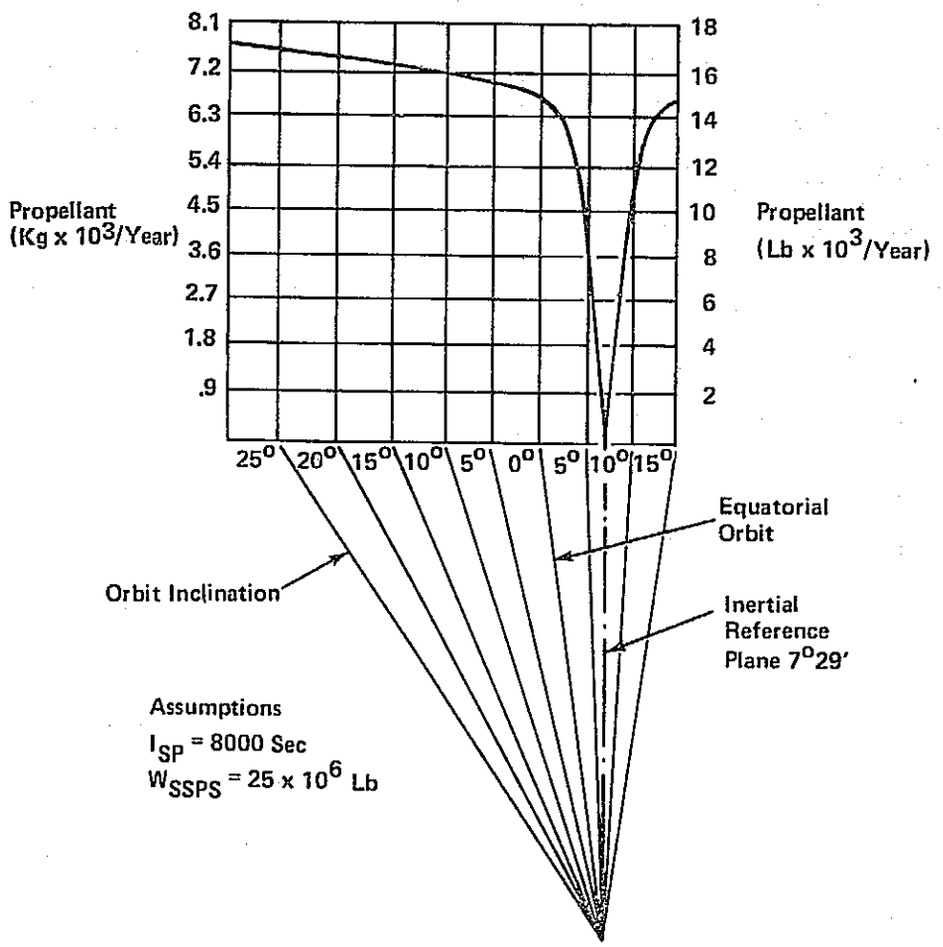

Figure 2.3-5 Typical Inclination Drift Propellant Requirements/Year

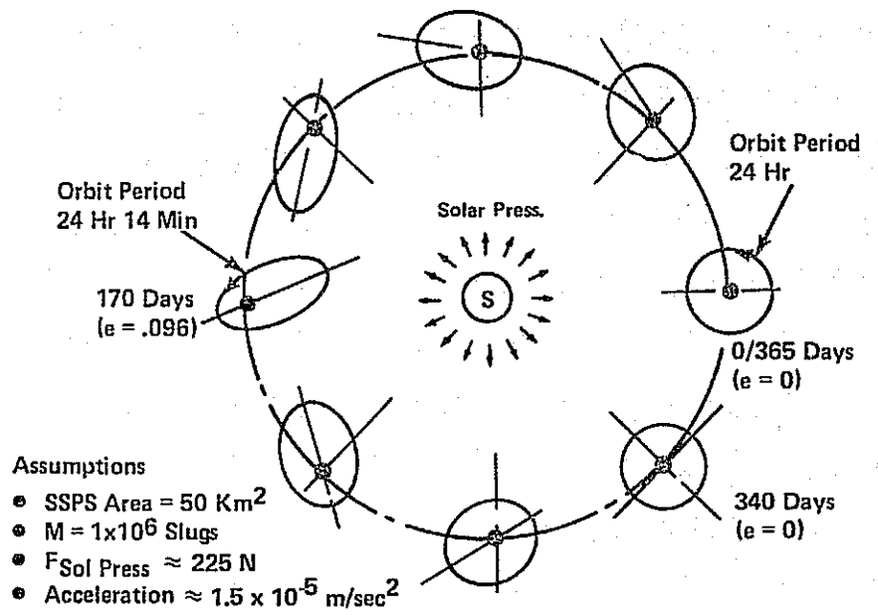

Figure 2.3-6 Altitude and Eccentricity Drift Characteristics – Solar Pressure

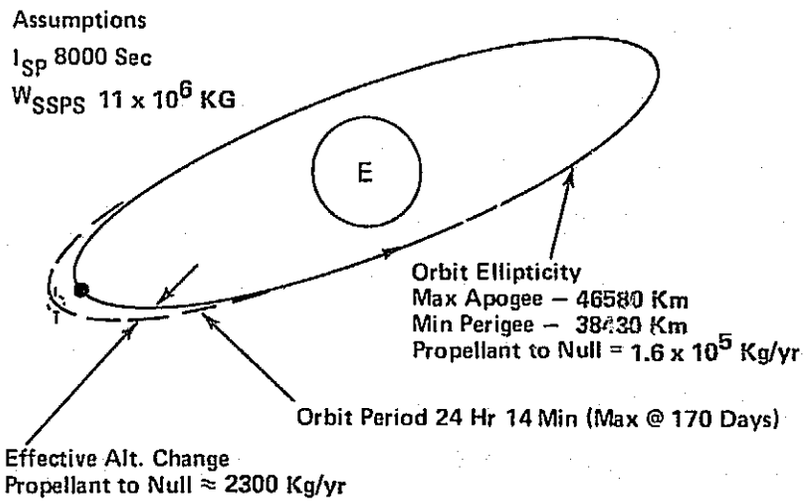

Figure 2.3-7 Eccentricity/Altitude Propellant Requirements

longitudinal drift to an observer on the ground. Characteristics of this drift is shown in Figure 2.3-8. The satellite will "lead" or "lag" the rectenna location by 11.0° during the course of one day. The effect of longitudinal drift on rectenna geometry is not as severe as the effect of inclination drift, Figure 2.3-4. The increased rectenna area needed to insure collection of microwave energy for a satellite that drifts 11.0° is 6%.

The amount of propellant required to control eccentricity drift and the apparent insensitivity of MW performance to the cyclic longitudinal motion of the satellite in an uncontrolled mode suggests that this perturbation be ignored. This is true if only one SSPS is in orbit. If a system of power satellites, used to meet a significant portion of future national energy requirements, is placed into operation, the effects of eccentricity drift could place a limit on the number of plants placed in orbit. Prime real estate at geosynchronous orbit lies between 30°W and 120°W longitude, or 66,228 KM of orbit arc length. The ±11.0° apparent longitudinal motion of the SSPS is equivalent to ±8090 Km of orbit arc. If each satellite is assigned 16190 Km to ensure no collision, a maximum of 4 SSPS can be placed in orbit. This limits system total output to 75 GW of power.

This undesirable limit to the total number of satellites in orbit strongly suggests that eccentricity drift should be corrected. An alternate approach to continuously thrusting to null solar pressure exits, precluding the requirement for an unacceptably high propellant consumption. Periodic posigrade/retrograde maneuvers performed at apogee and perigee of the eccentric orbit would economically maintain the orbit. The yearly propellant using this technique is 14,884 kg.

2.3.1.4 Microwave Pressure

A constant radial force of 17.8 Newton (4 lb) is exerted on the transmitting antenna. Reference 2.3-4 calculated this force assuming 10 GW of power into the microwave converters at a frequency of 3 GHz. A radial acceleration affects orbit eccentricity with only small perturbations to the orbit period. A force of 17.8N (4 lb) will cause ±1.8km (1 n mi) altitude perturbation over a period of 80 days. If this same force were applied along the velocity vector, the orbit altitude would vary 216 km (120 n mi).

The most economical approach to controlling this perturbation is to perform an apogee/perigee correction every two months rather than applying a continuous, opposing, radial thrust of 8.9N (2 lb). The yearly propellant requirement performing periodic horizontal thrust corrections would be 31 kg.

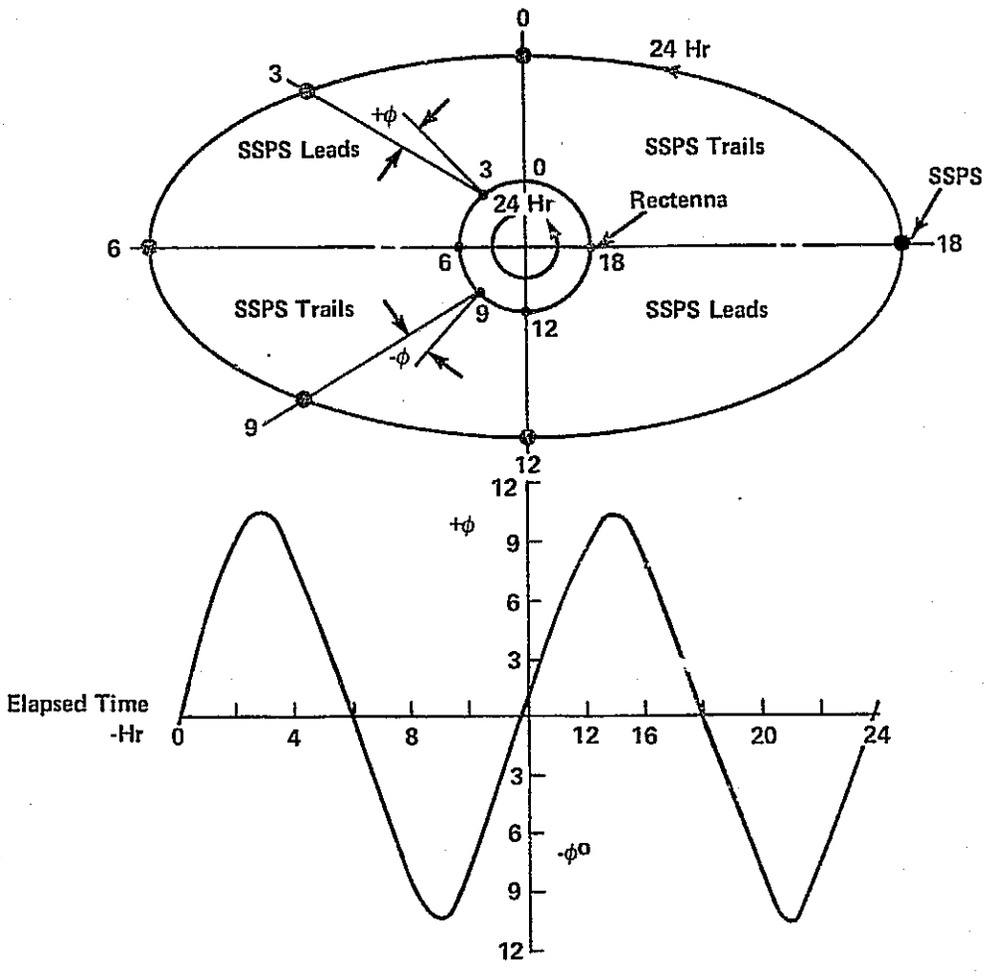

Figure 2.3-8 Apparent Longitudinal Drift vs Time

2.3.2 Effect of Stationkeeping Accuracy On Microwave Efficiency

Drifts and motion of the SSPS relative to the rectenna will result in MW beam misalignment from the nominal boresight. The rectified power output of the rectenna is sensitive to these beam angle deviations. The losses associated with orbit variations are shown in Figure 2.3-9. The rectenna power output efficiency variations are plotted against North-South (inclination drift) and East-West (longitudinal drift) boresight angle variations.

The major causes for the power loss are cosine loss, spillover and ray loss. When the SSPS drifts to the south, the effect is spillover; the beam spreads beyond the perimeter of the rectenna. When the satellite drifts to the north, the major effect is ray loss; microwave beams fall between rectenna elements, Figure 2.3-9.

The dipoles also have some directivity and there is an increasing penalty in power reception as the MW beam moves off the nominal boresight.

Ionsphere and atmosphere attenuation vary as a direct function of the beam insertion path length. As the satellite drifts the path through the atmosphere varies changing to some extent the system efficiency.

Figure 2.3-10 shows that rectenna performance is considerably more sensitive to vertical drift than to longitudinal. Losses due to longitudinal drift are primarily cosine effects while vertical misalignments causes ray loss and spill. The power loss due to the 3.5° longitudinal drift associated with uncorrected orbital ellipicity would be less than 1%. If the satellite were placed at an inclination of -7.5° to eliminate the need for north-south orbit keeping, the loss could be as great as 14.5%.

2.3.3 Parametric Rationale for Establishing a Thrust Time Duty Cycle

2.3.3.1 Thrust Level Analysis

The duty cycle for thruster operation depends on the maximum allowable longitude excursion from its assigned stationary longitude. Letting $2\Delta\lambda$ max be the total longitude drift (i.e., $\pm\Delta\lambda$ max), which is a function of eccentricity, earth's equatorial ellipticity, and altitude deviation from synchronous altitude. If the SSPS's are assumed to service 90° of CONUS longitude, then the total number (N) of servicing SSPS systems is given simply by

$$N = 90^\circ/2\Delta\lambda \text{ MAX}$$

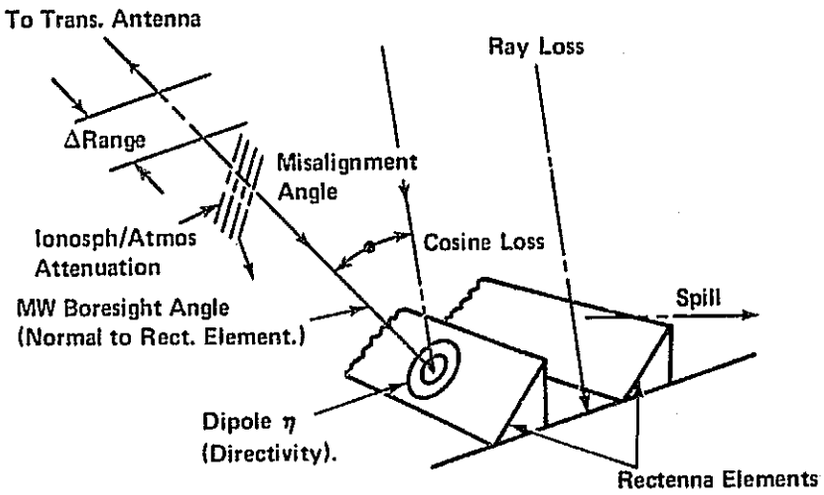

Figure 2.3-9 Rectenna Power Output Sensitivity to Beam Angle Deviation

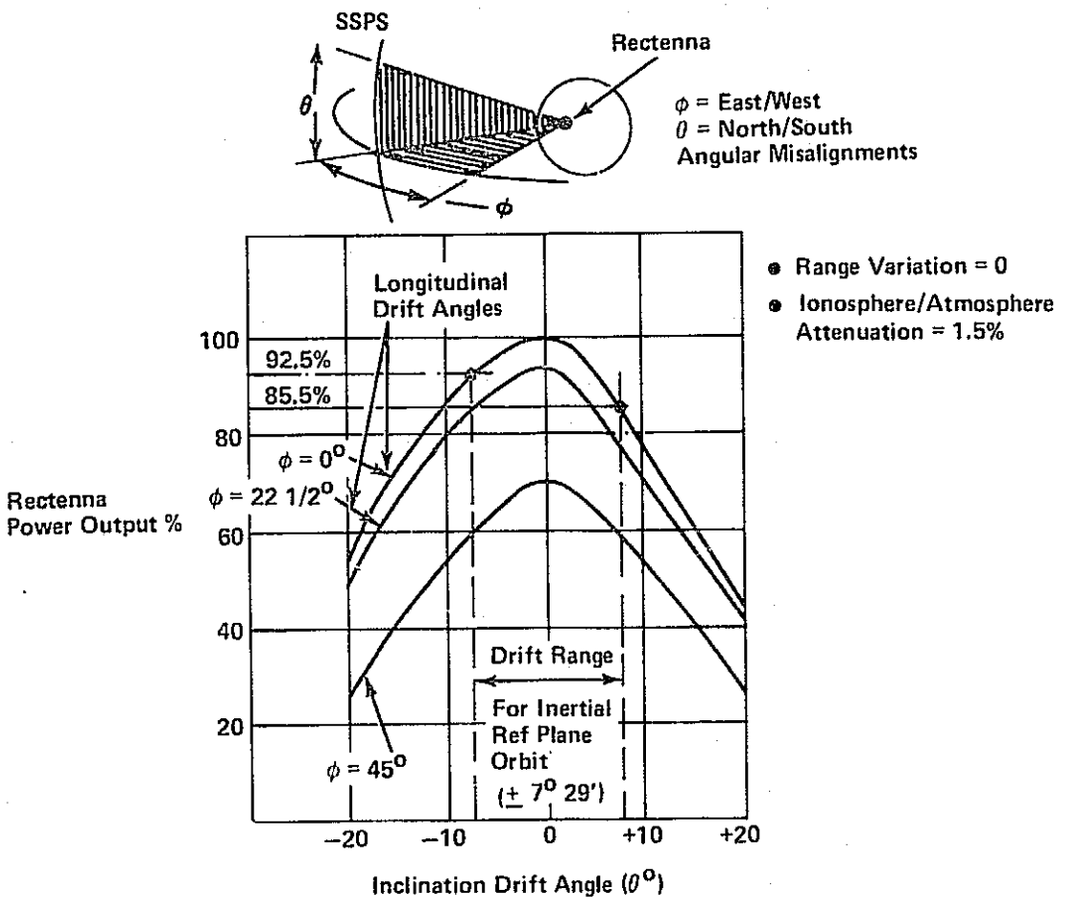

Figure 2.3-10 Inclination Drift Variations

From knowledge of the orbital mechanics of the perturbations, stationkeeping Δ V requirements are established. With knowledge of the engine Isp and the SSPS weight, the total force for the required stationkeeping maneuver may be computed. The required thrust level F is given by

$$F \doteq \frac{Wo\ \Delta V}{gt} \text{ if } \frac{\Delta V}{gIsp} \text{ is very small (i.e. less than 0.1).}$$

where

Wo = SSPS weight

and

t = stationkeeping thrust-on time.

For ion thrusters, the range of force, f , produced by each engine is

$$0.00445N\ (0.001\ lb) \leq f \leq 4.45N\ (1\ lb)$$

In 10 years the upper limit of the Isp will be of the order of 5000-15000 seconds, with a force upper limit of about 44.5N (10 lb). Assuming that f = 0.445N for each thruster,

$$N_{TH} = F/f$$

where N_{TH} is the minimum number of thrusters required for one-direction thrusting. However, the actual number of thrusters must be based on redundancy considerations to account for failures over the 30 year operational life of the SSPS:

- Redundancy, designated by ρ.
- Multiplicative factor, m, to account for the total MTBF to be 30 years, e.g. if MTBF if 15, then m = 2.

Therefore, the total number of thrusters (N_{TOT}) to be incorporated in the SSPS design is given by

$$N_{TOT} = \rho \; m \; N_{TH}$$

where

ρ = redundancy and m is a factor designed to yield a total MTBF of 30 years (e.g., if MTBF = 15, m = 2).

This establishes the number of thrusters required to produce a given total thrust level. The frequency and duration of the thrust application, which is essentially the definition of the duty cycle, is treated in paragraph 2.3.3.2.

2.3.3.2 Duty Cycle Determination for Each Unwanted Orbital Drift

2.3.3.2.1 Solar Radiation Pressure Effects on Eccentricity - The effect of solar radiation pressure on the SSPS is twofold. The first is to change the orbital eccentricity to a maximum of 0.096 from a circular, equatorial synchronous orbit; and the second is to raise the altitude by 274 Km or increase the equivalent synchronous period by 14 minutes. Both effects are cyclical, having a period of 340 days but achieving the maximum stated values at 170 days. Figure 2.3-11 shows

- the variation of eccentricity, ε, with time
- the maximum longitude excursion for each ε
- the resultant Δ V (2 Burn Hohmann) to nullify the eccentricity for each ε.

Figure 2.3-11 is used as follows: Assume that the maximum allowable longitude drift is +2.5°. Locate this point on the max $\Delta\lambda$ curve, and then draw a vertical (ordinate) line. This line, as shown in the example in the figure, gives a time of 57 days, ε of .0220, and required Δ V of 34.44 mps (113 fps).

Note that ion engine finite burn time Δ V is larger than the 2 burn Hohmann Δ V, although, for small Δ V, this difference is likewise small. For 30 year operation, however, this conclusion may have to be revised. Further investigation is required.

2.3.3.2.2 Solar Radiation Pressure Effects On Altitude (Period) - Any change in altitude results in an increased change in the period of the orbit, and thereby produces a westerly drift of the SSPS relative to its assigned location. If this perturbation were allowed to continue unchecked, it would result in 1.1°/day westward drift at the end of 57 days, and thus require an

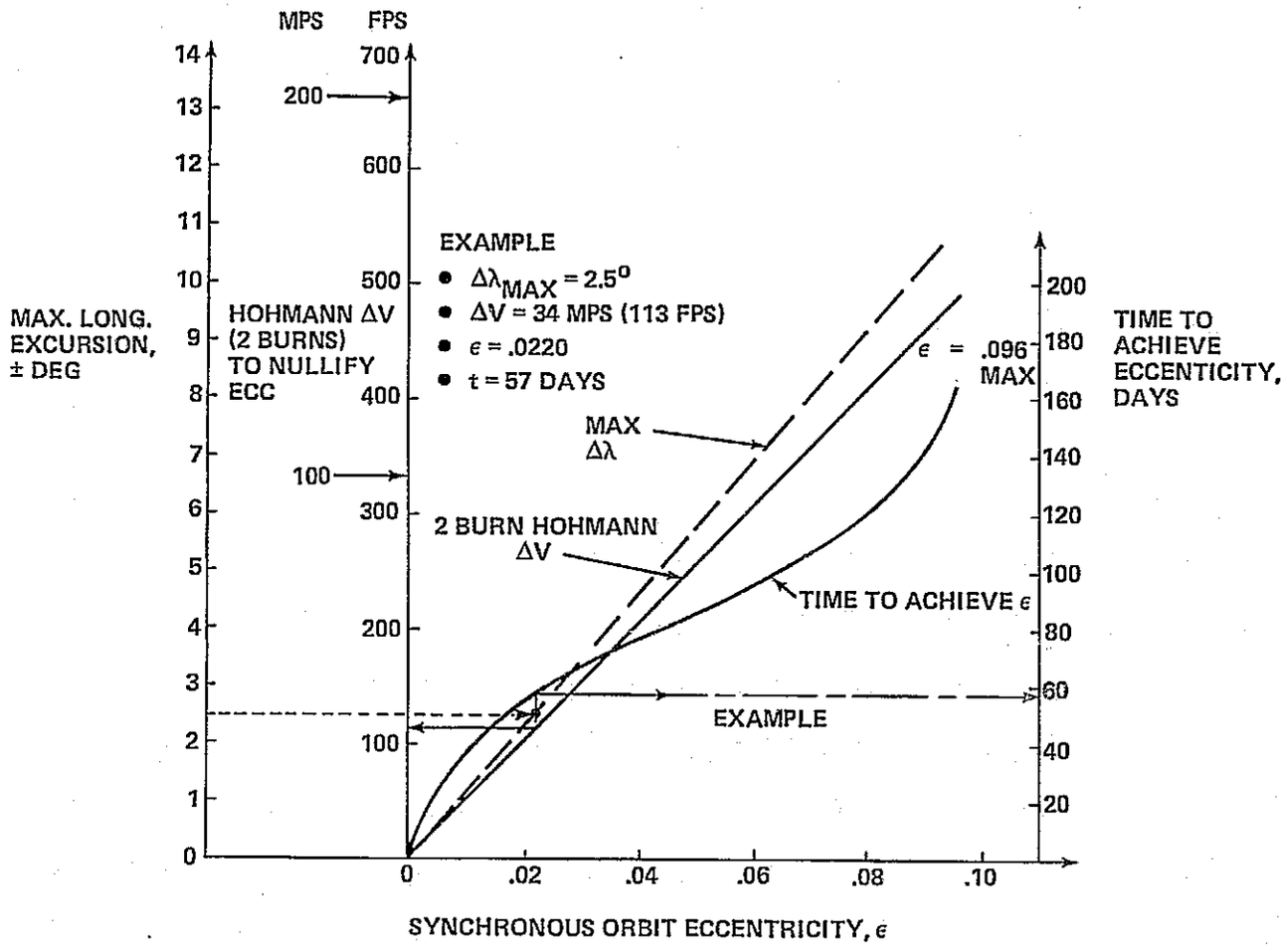

Figure 2.3-11 Solar Radiation Pressure Compensation

increased frequency in the application of the corrective station-keeping maneuvers. It is therefore desirable to remove this altitude drift on a continuous basis. A continuous force of 8.5N (1.9 lb) would yield a 3.66 mps (12 fps) Δ V at the end of 57 days. Thruster logic could be employed so that a series of jets would be alternately fired to produce the constant required thrust.

2.3.3.2.3 Microwave Radiation Pressure Effects - The perturbation resulting from a radial microwave radiation pressure force or the transmitting antenna is approximately 1/15 that of the solar radiation pressure. As an approximation, the Δ V effect and altitude are assumed to change in accordance with this approximation in perturbative force.

2.3.3.2.4 Earth's Equatorial Ellipticity Effects - The earth's equatorial ellipticity produces an E-W drift which becomes intolerable when the SSPS is located sufficiently far from one of the stable (minor) axes. Figure 2.3-12 shows the time to drift 5° as a function of relative longitude of the SSPS referenced to a stable axis. If $\pm 2.5^\circ$ about the assigned longitude is assumed to be the maximum allowable excursion, then 9 weeks are required between corrections for N-E servicing SSPS and 27 weeks for the SSPS servicing the S-W. The Δ V requirement per year may be determined from figure 2.3-13 (Reference 2.3-9). The annual Δ V requirements are 0.6 mps and 2.1 mps for the S-W and N-E satellites, respectively.

2.3.3.2.5 Luni-Solar Gravitational Effects - The sun and moon's gravitation fields are the predominant factors which affect the inclination drift. The relative geometry of these bodies and the earth relative to the ecliptic plane is critical for dealing with inclination drift. (See Figure 2.3-5.)

For stationary orbits, the annual inclination drift rate is 0.86°/yr. However, with inclination biasing (i.e., placing the SSPS in an orbit of -0.43° inclination) the inclination at

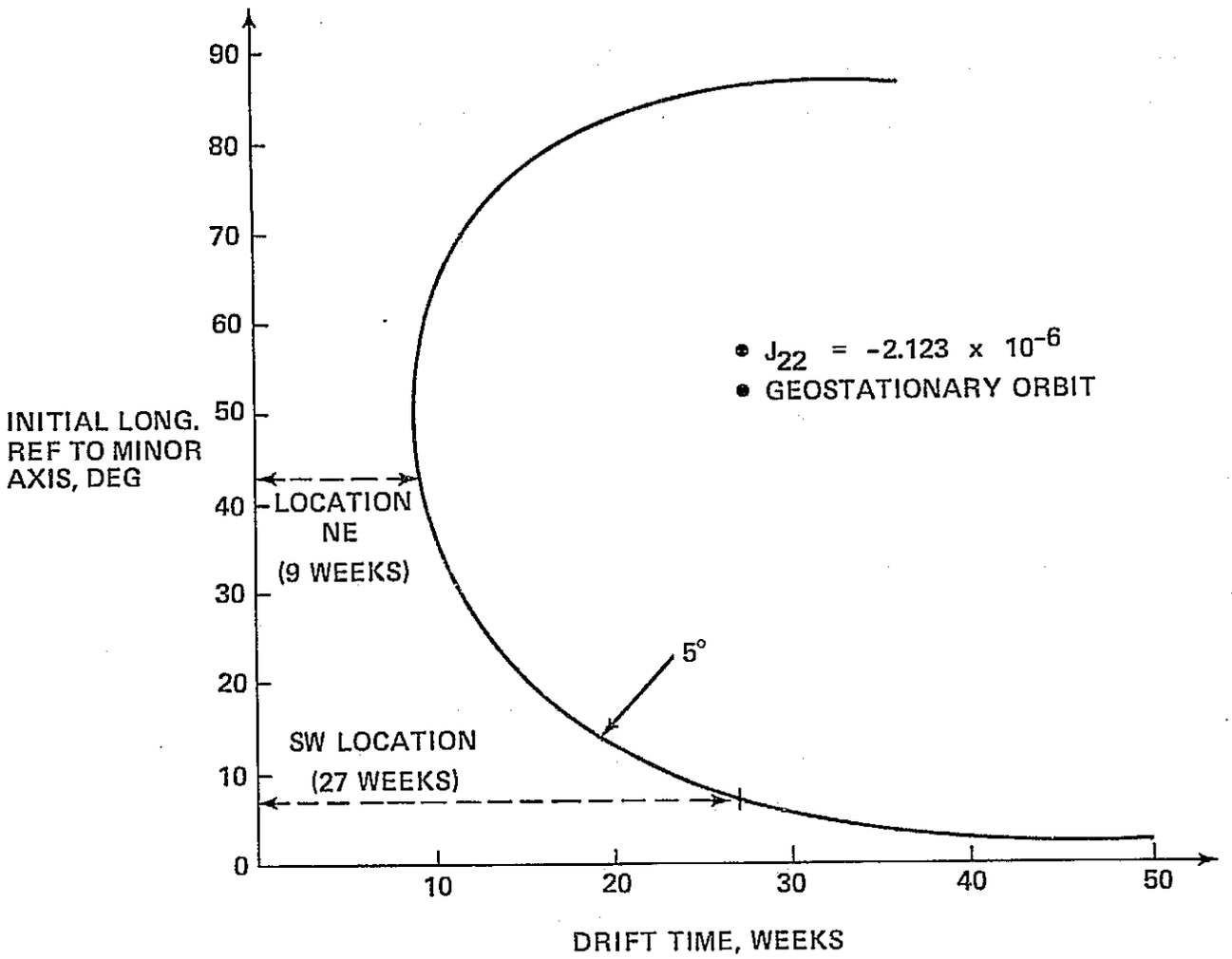

Figure 2.3-12 Time to Drift 5 Degrees

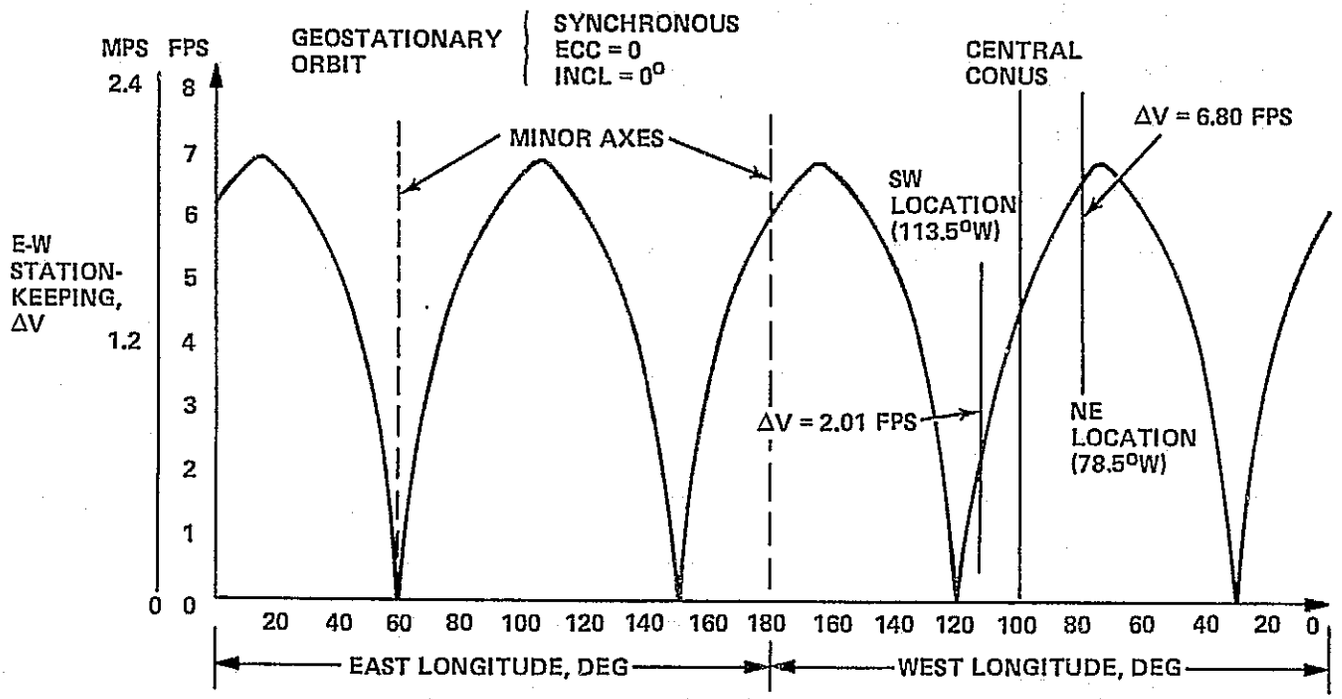

Figure 2.3-13 Stationkeeping ΔV Requirement Vs Longitude

the end of 1 year would be +0.43°. Assuming that a ±0.43° variation in inclination is tolerable, the duty cycle must compensate for inclination drift once per year, with a ΔV expenditure of 45 mps.

2.3.3.2.6 Typical Example of the Stationkeeping ΔV and Propulsion Requirements - Assuming that the maximum allowable longitude drift is ±2.5°, so that 5° maximum travel is allowed per SSPS, the number of satellites to service 90° of longitude real estate would 90°/5°/Sat or 18 SSPS satellites. The stationkeeping ΔV and propulsion requirements are summarized in table 2.3-2. The table shows that a 57 day cycle (i.e., stationkeeping maneuvers are performed every 57 days) yields the maximum cycle period. For purposes of a typical realistic example, the Isp for ion thrusters was assumed to be 5000 lbf-sec/lbm, and the burn time duration about 5 days for each maneuver. Though the cycle time will remain the same for the very low thrust requirements, the burn times will vary. On the basis of selecting 0.445 N ion thrusters, the number of thrusters and their location will be summarized in paragraph 2.3.3.2.8.

2.3.3.2.7 Thruster Time Histories - Based on the last column of table 2.3-2 for a 57 day cycle (except for inclination drift requiring a 1 year cycle), jet force time histories are established and summarized in Figure 2.3-14.

The following observations should be given due consideration in the deployment of thrusters, thruster sizing, cluster (of thrusters) arrangement and operational requirements in performing stationkeeping maneuvers:

- Not all the thrusting will be in the same direction.
  - Eccentricity, altitude, and E-W drifts require tangential burns for compensation.
  - Inclination drifts require burns normal to the orbital plane
    - o Inclination compensation should not be performed simultaneously with other drift compensations since the resultant force vector is skewed, thereby requiring more sophisticated guidance and control techniques.
    - o Most efficient inclination control results from burns normal to orbital plane in the vicinity of equatorial crossings (north or south).
    - o A 10 day cycle that does not conflict with other stationkeeping corrections should be selected.

Table 2.3-2 Summary of Stationkeeping Duty Cycle Inputs*

	PERTURBATION	TIME TO ± Δλ (5° TOTAL)	ΔV REQUIREMENT (57 DAY CYCLE)	ANNUAL ΔV REQUIREMENT	THRUST (57 DAY CYCLE)
	(UNITS)	DAYS	MPS (FPS)	MPS (FPS)	N (LB)
E-W DEVIATION	SOLAR RADIATION Δ ECC (.0220) Δ ALT (148 NM IN 170 DAYS)	 57 N/A**	 34.4 (113) USED ΔV ≐ 1.5 (5)	 146.3 (480) 9.8 (32)	 905.8 (203.3) 8.5 (1.9)
E-W DEVIATION	MICROWAVE RADIATION Δ ECC Δ ALT	 >>57 N/A**	 2 (7) USED ΔV = 0.09 (0.3)	 9.1 (30) 0.6 (2)	 8 (1.8) 0.5 (0.11)
E-W DEVIATION	E-W DRIFT (NE) (SW)	 63 189	 0.33 (1.1) 0.09 (0.31)	 2.0 (6.6) 0.6 (2.01)	 8.5 (1.9) 2.5 (0.56)
N-S DEVIATION	INCLINATION† DRIFT (.86°/YR)	365	7.2 (23.5) (OPTIONAL)	45.7 (150)	602 (135)

*I_{SP} = 5000 SEC, t = 5 DAY BURN PERIOD, GIVE ABOUT 10:1 QUIESCENT-TO-BURN TIME PERIOD
**CONTINUOUS THRUST SINCE ANY ALTITUDE VARIATION PRODUCES AN UNWANTED DRIFT
†I_{SP} = 5000 SEC, t = 10 DAY BURN PERIOD ONCE PER YEAR

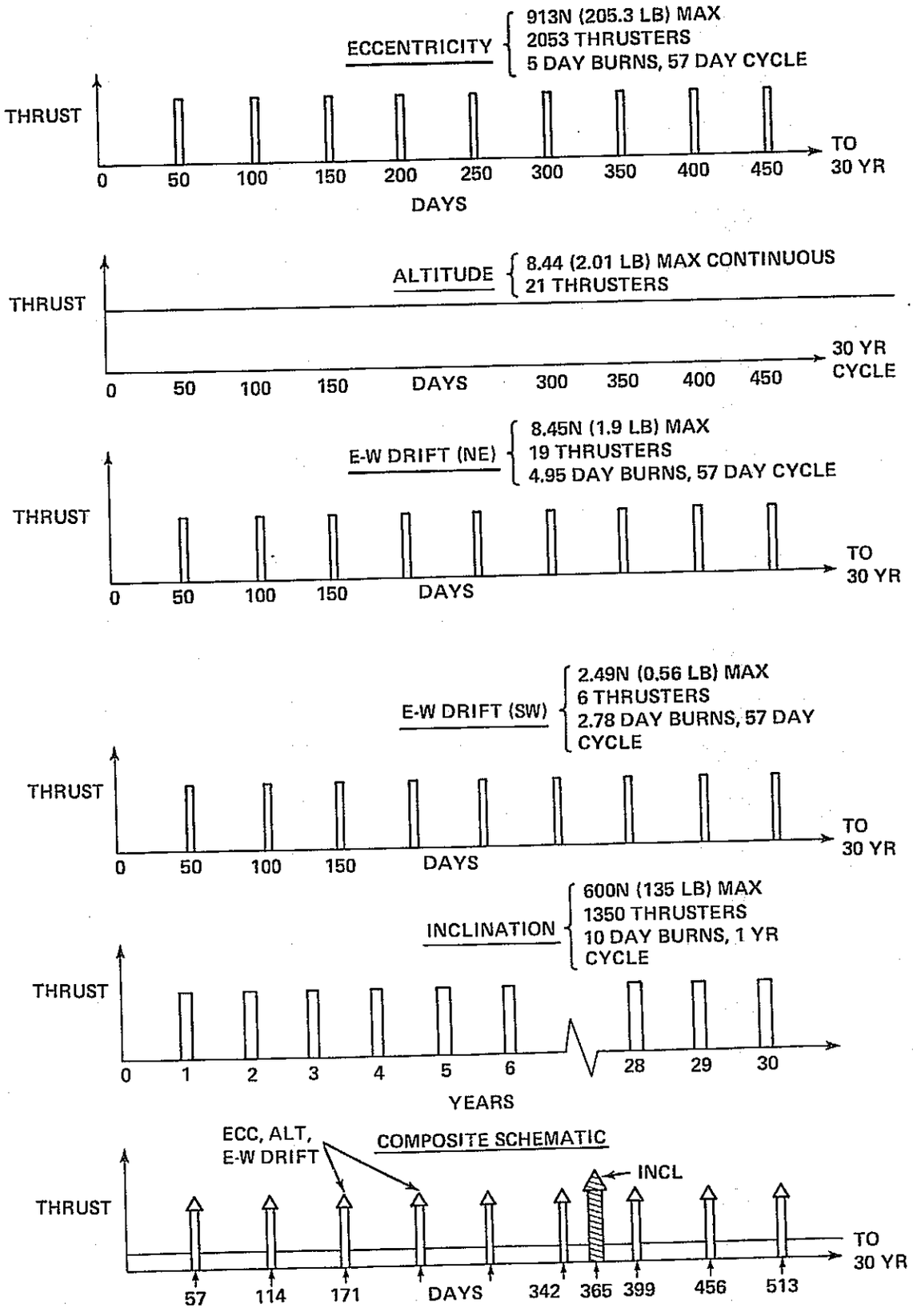

Figure 2.3-14 Thrust-Time Histories For Orbital Drift Compensation

- Thrusters should be considered as clusters of 4 thrusters - 2 more thrusters are needed for any radial compensation and for any induced unbalanced torques produced by the stationkeeping burns (See Figure 2.3-15 for cluster arrangements).

- For E-W stationkeeping maneuvers the burn should be made in such a manner that the correct velocity at the end of the burn brings the SSPS to -2.5° of the station's assigned position. See Figure 2.3-16 for a schematic representation of this rationale.

2.3.3.2.8 Number and Deployment of Thrusters - With the thrust level for each ion jet assumed to be 0.445 N, a minimum number of thrusters to perform the maneuvers may now be calculated (Table 2.3-3 presents a summary of the number of thrusters required).

N_{TH} = 6860 thrusters (N-E)

N_{TH} = 6886 thrusters (S-W)

m = MTBF factor (assumed to be 2 for space life of a thruster)

ρ = redundancy factor, assuming 1 in 50 thrusters will fail in 15 years

and

$$N_{TOT} = \rho\ m\ N_{TH}$$

$$= (1.0204)\ (2)\ (6886) = 14053 \text{ Thrusters (N-E)}$$

$$\text{or} = (1.0204)\ (2)\ (6860) = 14000 \text{ Thrusters (S-W)}$$

For 4.45 N thrusters, N_{TOT} would be approximately 1400.

2.3.3.2.9 Thruster Configuration Analysis - N_{TOT} thrusters, as given in paragraph 2.3.3.2.8, are to be deployed on each SSPS configuration. Each panel will have $N_{TOT}/2$ thrusters or $N_{TOT}/2x4$ clusters. Figure 2.3-17 schematically represents the cluster distribution about the outer edges of the SSPS. For very small thrust levels (i.e., E-W drift stationkeeping), the burn times may be trimmed so that continuous thrusting for 5 days minus Δ t, results.

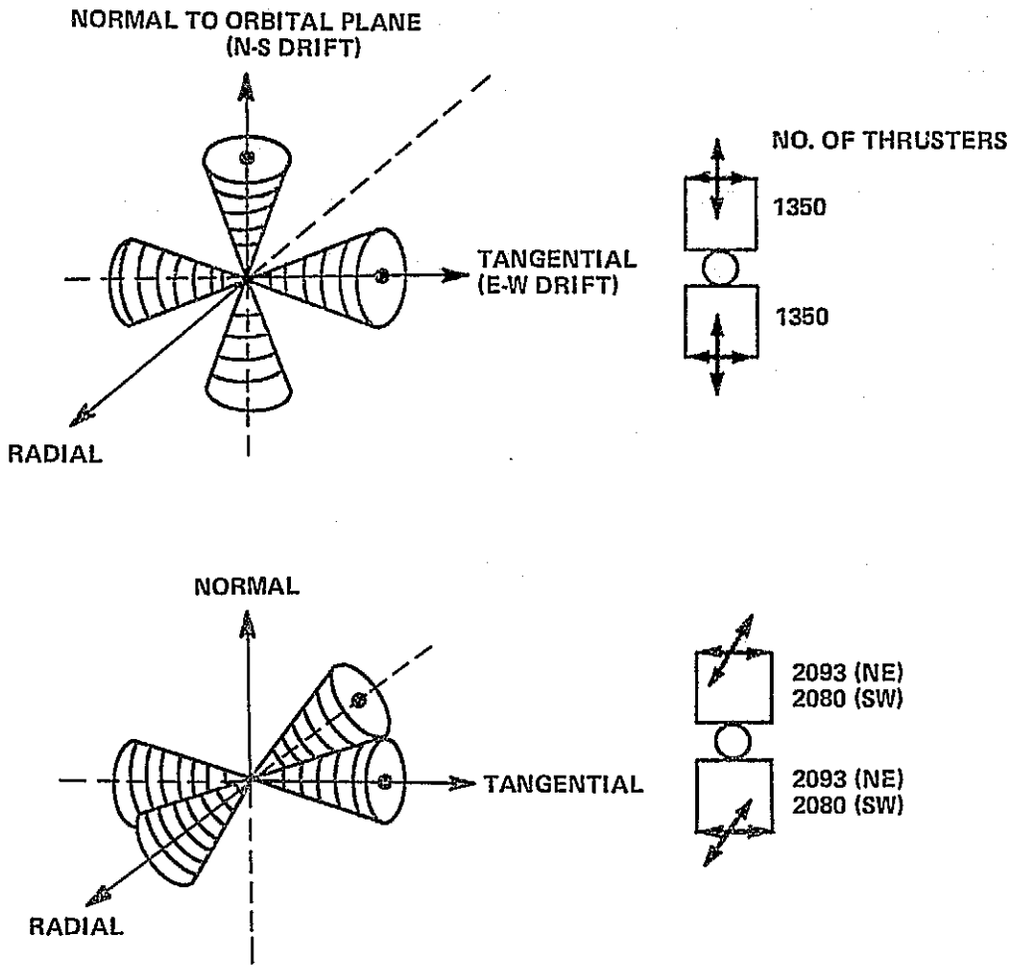

Figure 2.3-15 Thruster Arrangement and General Deployment on SSPS

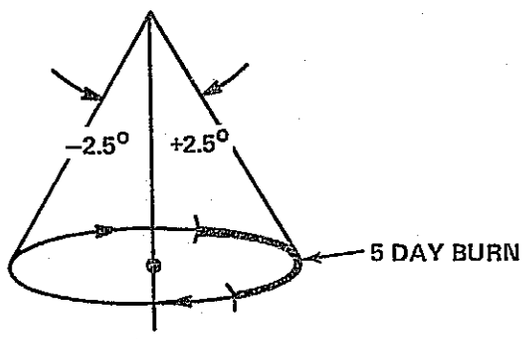

Figure 2.3-16 Duty Cycle for E-W Drift

Table 2.3-3 Thruster Analysis Summary

	MAX FORCE APPLIED, N (LB)	NO. OF THRUSTERS (0.1 THRUSTERS**)	DIRECTION OF THRUST
DRIFT (5 DAY BURNS)	913.2 (205.3)	2053.0	TANGENTIAL
ECCENTRICITY	8.94 (2.0)*	20.1	TANGENTIAL
ALTITUDE E-W			
(NE)	8.45 (1.9)	19.0	TANGENTIAL
(SW)	2.00 (.45)	5.6	TANGENTIAL
		TOTAL = 2080 (SW), 2093 (NE)	
INCLINATION (10 DAY BURNS)	600 (135)	1350	NORMAL TO ORBITAL PLANE

*CONTINUOUS THRUSTING
**USE OF 4.45N (1.0 LB) THRUSTERS WILL REDUCE THE NUMBER OF THRUSTERS BY A FACTOR OF 10.

NOTE THAT THE NUMBER OF THRUSTERS GIVEN IS THE MINIMUM, AND APPLIES TO ONE DIRECTION ONLY. FOR TANGENTIAL, OPPOSITE DIRECTION BURNS,

2X (2080 + 1350) = 6860 THRUSTERS WOULD BE REQUIRED (SW).
2X (2093) + 1350) = 6886 THRUSTERS WOULD BE REQUIRED (NE).

THIS ANALYSIS ASSUMES THAT THE BURNS OCCUR IN OVERLAPPING FASHION, EVERY 57 DAYS FOR TANGENTIAL BURN CORRECTIONS. A MORE COMPLEX DUTY CYCLE COULD BE CHOSEN IN WHICH ALTITUDE COMPENSATION, E-W DRIFT, AND ECCENTRICITY DRIFTS ALL SHARE THE SAME THRUSTERS WITH ALTERNATING BURN SEQUENCES. THIS MORE COMPLEX POLICY FOR MINIMIZING THE NUMBER OF THRUSTERS DOES NOT OFFER MUCH OF AN ADVANTAGE, SINCE THE ECCENTRICITY IS THE OVERRIDING FACTOR AND THE OTHER TANGENTIAL DRIFT EFFECTS (i.e., E-W, ALTITUDE) REQUIRE A MUCH SMALLER NUMBER OF THRUSTERS BY COMPARISON.

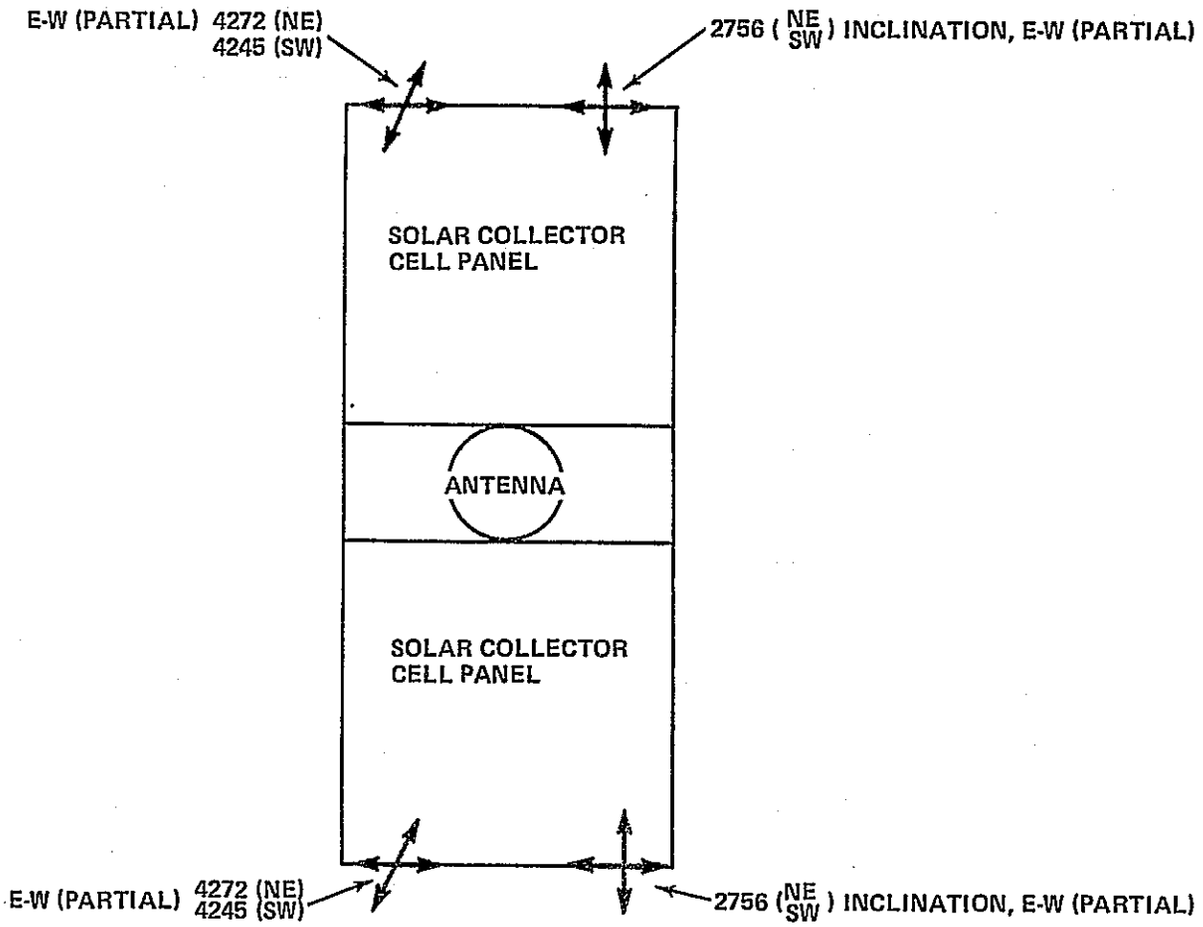

NOTE: ALL THRUSTERS ARE DEPLOYED IN SYMMETRICAL ARRANGEMENT

Figure 2.3-17 SSPS Thruster Distribution Schematic

2.3.3.3 Potential Areas for Further Study

Stationkeeping maneuvers can produce unbalanced or disturbance torques due to:

- Center of SSPS mass uncertainty
- Thruster mismatch (ablative and plume impingement differences cause force levels to vary slightly)
- Thruster misalignment
- Cluster nonsymmetry due to minor image-deployment mismatch
- Random failures of thrusters thereby producing unbalanced torques.

These considerations, to be most efficiently analyzed, should have an SSPS configuration simulation. The torsion, structural flexure, and bending effect on antenna pointing and power output efficiency may then be analyzed.

Due to the large area of SSPS, the following random, and hopefully non-catastrophic, environments impact the SSPS:

- Meteroids - Due to the huge panels (approximately 55 $km^2 \doteq 16\ nm^2$), the meteoroid environment in terms of steady state and sporadic meteoroid showers could cause orbital perturbations (not to mention SSPS damage). The 30 year operational life increases the probability of occurrence of these effects.
- Radiation (Solar Flares) - During certain phases of solar activity cycles (prior to and immediately after peak sunspot activity) high intensity solar flare activity often erupts. Huge clouds of high energy neutrons can impact the SSPS, causing orbital disturbances of sizes to be investigated. Solar flares, especially over 30 year life of SSPS, also impose requirements on construction of solar collector cells on the panels as well as maintenance and repair crew systems.
- Thermal - This environment may cause sufficient thermal bending and torsion, thereby changing the position of the cg and the locations of the thrusters, thus adding to the uncertainty in the precision of stationkeeping maneuvers (magnitude and direction).

2.3.3.4 Propellant Summary and Issues

Table 2.3-4 summarizes the yearly propellant requirements needed to maintain the SSPS orbit to within acceptable limits for overall favorable system efficiency. Two satellite locations are shown. The SSPS located at 113.5°W longitude is assumed to service the southwest. The second is located at 78.5° longitude for northeast service. Location 1 requires a total of 9116 kg/yr for stationkeeping and location 2, 9340 kg/yr.

The major issues of concern in performing the SSPS stationkeeping function are:

- Ion Engine Development - The size of the SSPS appears to preclude the use of more conventional cold gas propulsion packages. Ion propulsion is a natural control device because of the readily available power source. Little or no flight experience is available nor is any planned using ion engines. An alternate to ion propulsion is the resistojet with an I_{sp} = 850 sec using Hydrogen propellant. The same issues that were identified in Ref. 2.3-3 for the orbit-to-orbit transport stage apply to the on-orbit maneuver system. The selection of a propellant that will not contaminate the solar array and electronics is necessary. The uncertainty in Ion engine cost is a factor needing more analysis and definition. Efforts should be directed at increasing thruster life.

- Stationkeeping System/Structural Interaction - Continuous thrust levels on the order of 4 to 8 Newtons needed for stationkeeping are not expected to cause structural dynamic problems. However, if a control policy calling for continuous thrust cannot be achieved because of either orbital mechanics constraints or engine life limitations, high thrust engines and finite thrust guidance policies will be needed. Structural design criteria, using these systems will be different. An across the board study and simulation of these conditions is called for.

2.3.4 Spacecraft Attitude Control

Ground Rules and Assumptions:

- The SSPS is sized for a rectified ground power output of 5000 MW

- Equatorial synchronous orbit

- SSPS mass properties

Table 2.3-4 SSPS Stationkeeping Propellant Requirement

PERTURBATION	PROPELLANT (I_{SP} = 8000 SEC)	
	NOMINAL SOUTHWEST, LB/YR	NOMINAL NORTHEAST, LB/YR
• LONGITUDINAL DRIFT	224	716
• INCLINATION DRIFT	14700	14700
• SOLAR PRESSURE		
– ALTITUDE	5100	5100
– ELLIPTICITY	47,040	47,040
• MICROWAVE PRESSURE	68	68
TOTAL	20,092 (67,132)	20,584 (67,624)

SPACECRAFT WEIGHT = 25×10^6 LB

SOUTHWEST LOCATION = 113.5W LONG

NORTHEAST LOCATION = 78.5W LONG

*PROPELLANT REQUIREMENT AFTER 4TH SSPS

- The solar array vector normal is pointed to within ±1° of the projection of the sun vector on the equatorial plane.

Figure 2.3-18 defines the axis system used in calculating disturbance torques. The spacecraft longitudinal axis, x-axis, is normal to the orbit plane. The y and z axis lie in the orbit plane (Equatorial plane). The sun line is in the X-Z plane with a yearly oscillation about the y-axis of 23.5°.

2.3.4.1 Disturbance Torques

The external torques on the satellite result from the following sources:

- Aerodynamic
- Gravity gradient
- Solar pressure
- Magnetic
- Microwave pressure
- Rotary joint friction torques.

At an altitude of 35.8 x 10^6m, the atmospheric density is equivalent to the plasma proton density; 3.46 x 10^{-24} Kg/m^3 (3 x 10^{-22} slug/ft^3) Ref. 2.3-5 which results in a dynamic pressure of 7.3 x 10^{-14} Newton/m^2. The resulting aerodynamic force on the SSPS is only 22.4 x 10^{-6} Newtons, which produces an insignificantly small disturbance torque on the nearly symmetric SSPS shape.

Solar radiation pressures have a much larger effect. Ref. 2.3-5, appendix A, derived the solar radiation torques for the specific SSPS, corrugated solar array design, considered in this report. The c.g. to c.p. distance for y-axis induced torque is 25m due to the offset of the microwave antenna. The x-axis torque is induced by off-nominal steering angles which causes a slightly different force on the corrugated mirror system. One side of the concentrator channel will receive more direct sunlight than the other with variations in the sun vector from nominal. The resulting solar radiation disturbance torques are:

T_x = 136 newton meter/degree

T_y = 5550 newton meter/degree

T_z = 0.0

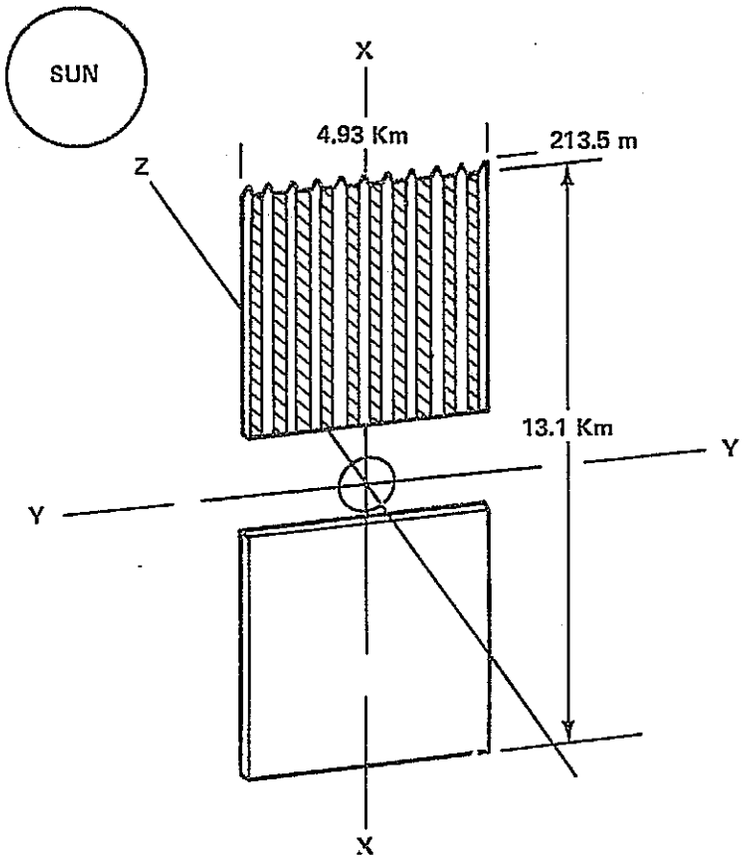

CENTERS OF GRAVITY

X arm = 0.1 km

Y,Z arms = ±0.026 km (85 ft) (Variation is due to the rotation of the MW Antenna)

MOMENTS OF INERTIA.

I_{xx} = 24.4×10^{12} kg-m^2 (18.00×10^{12} slug ft^2)
I_{yy} = 188.3×10^{12} kg-m^2 (138.9×10^{12} slug ft^2)
I_{zz} = 212.2×10^{12} kg-m^2 (156.6×10^{12} slug ft^2)

Figure 2.3-18 Axis System

Careful design of the solar blanket power distribution system will minimize the effects of magnetic induced torques. Figure 2.3-19 is a schematic of a proposed current flow pattern for one solar wing. Each unit magnetic field is adjacent to a field with opposite polarity. The net magnetic torque as calculated in Ref. 2.3-5, appendix B, is relatively small, i.e. 1.4×10^{-5} N-M. The prime magnetic torque contribution to an array with the loop design shown in Figure 2.3-19 is changes in the Earth's magnetic field with altitude and latitude. The SSPS is so large that examination of latitude and altitude difference between adjacent field loops results in a net torque.

An estimate of the force created by the radiation of electromagnetic energy from the microwave antenna has been computed assuming a total input power of 10^{10} watts and a transmitted frequency of 3 GHz, Ref. 2.3-4. The total force normal to the antenna is not expected to exceed 17.8 Newtons. This force produces a sinusoidal Y and Z axis torque with a peak amplitude of 2955 Newton-m at a period of 24 hr.

The gravity gradient torques acting on the SSPS will be at least an order of magnitude larger than the torques discussed above. For the moments of inertia shown in Figure 2.3-18, the torque magnitudes are:

T_y = 33,200 Newton-m/deg offset

T_z = 29,700 Newton-m/deg offset

$T_x = 1.89 \times 10^5 \sin (2 W_o t)$ N-m

W_o = orbital rate

t = time

Nominally, the x axis is perpendicular to the orbit plane resulting in no gravity gradient Torque about the Y and Z axis. However, spacecraft attitude will deviate up to the deadband and sensor accuracy of the control system. The twice orbital period and with a peak level of:

T_x (Peak) = 189,000 Newton-m

The rotary joint shown in Figure 2.3-20 is used to mechanically point the microwave antenna at the ground based rectenna. The antenna to array relative motion requires 360° travel each day. Slip rings are used to transfer power across the joint. Contact pressures between the brushes and rotary joint ring will vary between 27,550 N/m^2 and 68,940 N/m^2 (4 and 10 psi) for optimum power transfer, Ref. 2.3-8. At an assumed

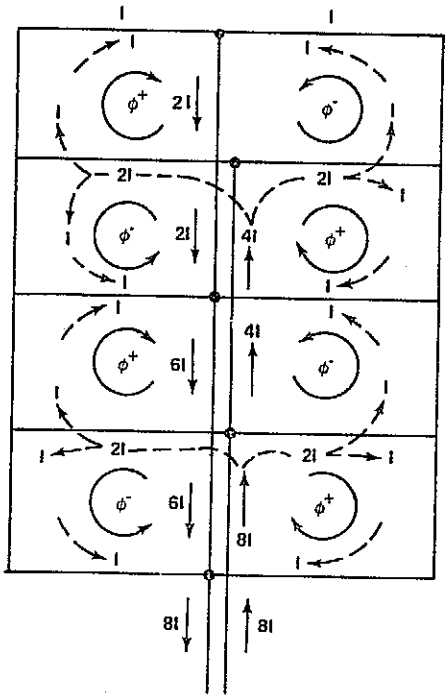

Figure 2.3-19 Solar Array Distribution System Layout

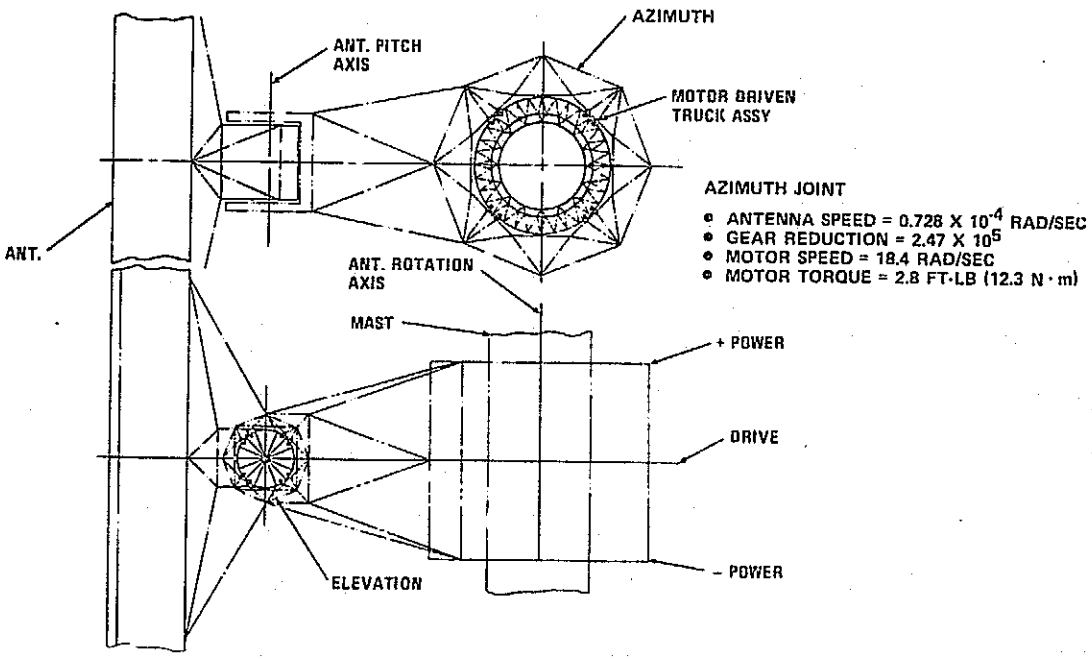

Figure 2.3-20 Rotary Joint

system voltage of 20 kv and a brush current rate of 7.75×10^4 A/m^2, 6.41 m^2 of brush area is required to transfer 10 GW of power. The total normal force of 4.45×10^5N is exerted on the slip ring. At a coefficient of rolling friction of 0.1 and a central mast diameter of 50 meters, 1.02×10^6 Newton-meters of torque is induced on the spacecraft.

A frictionless linear step motor, Figure 2.3-21, mounted about the perimeter of the central mast, is used to point the transmitting antenna and develops 1.02×10^6 Newton-meters t. to counterbalance the slip ring friction torque. During stea., state operations, no SSPS reaction control is needed to counter the slip ring torque. However, if there are reversals in the relative motion between the spacecraft and antenna, reaction control is required during these transient periods. The slip ring friction torque would then reverse sign and appear as a step input into the system.

Table 2.3-5 summarizes the disturbance torque discussed above. The largest torques are induced by the slip ring, antenna control system, and gravity gradients. All other induced torques are small and can be neglected.

2.3.4.2 Control Systems Options

Two system approaches for SSPS attitude control have been evaluated: (1) use of control moment gyros, which store momentum for part of the orbit (1/4 revolution) and dump momentum the next quarter orbit; (2) use of RCS or ion thrusters.

The SSPS x-axis momentum storage requirement to control gravity gradient torques alone amounts to 5.84×10^9 Newton-m-sec. State of the art CMG's, such as the Sperry single gimbal Model 1200, have a momentum-to-weight ratio of approximately 30 Newton-m-sec/kg. Assuming an order of magnitude improvement in CMG performance over the next 10 years, the total weight of the control system would be 19.3×10^6 kg, clearly unacceptable for SSPS application.

The reaction control force to exactly balance the gravity gradient torque about the x-axis is 40 Newton (9-lbf propulsion engines mounted at the extremes of the solar array each with a 2.47 km lever arm). The design weight goal for the 30 cm ion engine for use on SEPS is 7 kg for the engine and 16 kg for the power conditioner. This engine develops 0.134 Newton of thrust for an equivalent thrust-to-weight of 5.8×10^{-3} Newton/kg. Without considering reliability issues, a control system using ion engines would require eight engines for a total system weight of 6,896 kg for roll control alone.

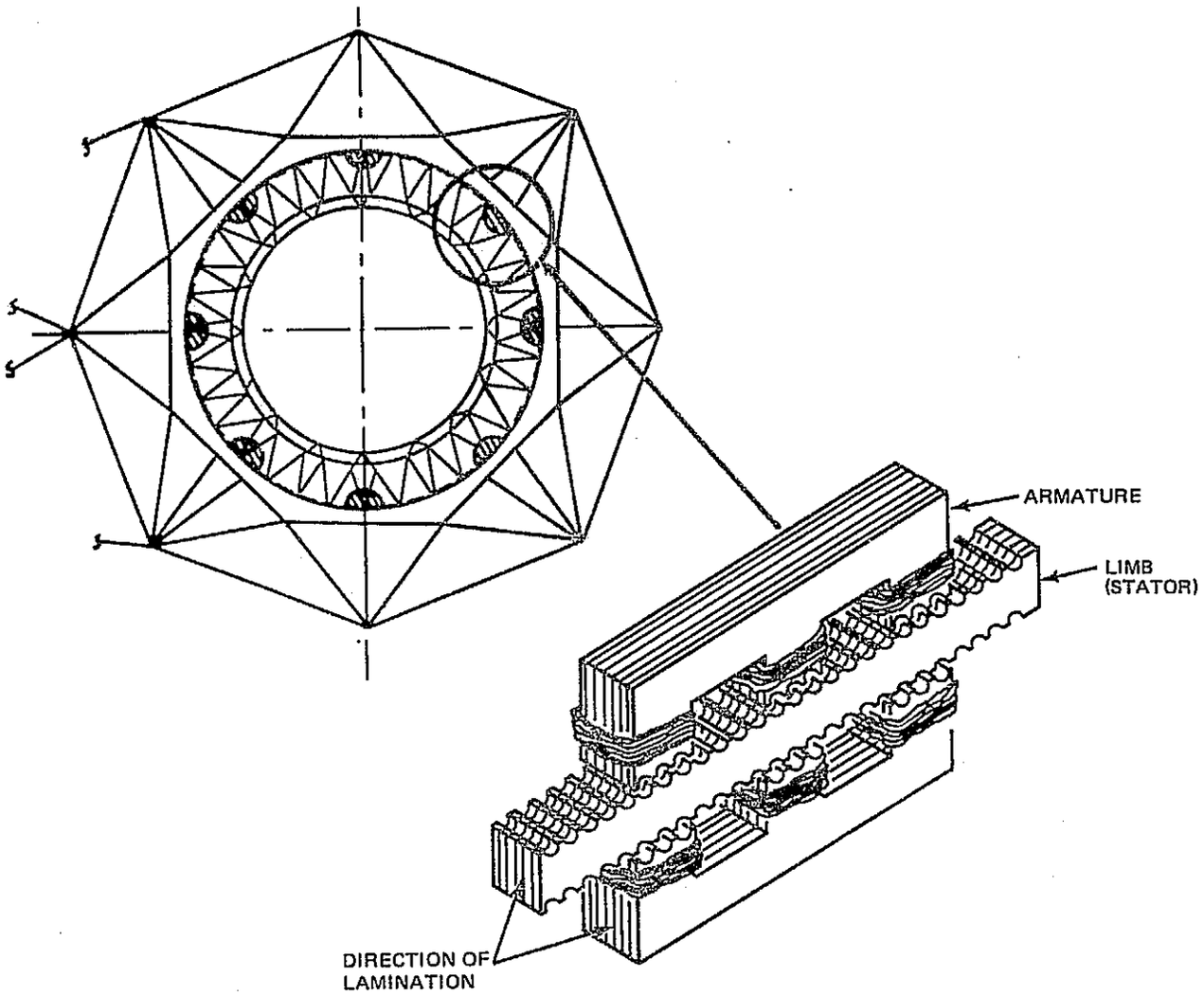

	WEIGHT	
	LB	Kg
LIMB (STATOR)	2214	1020
ARMATURE	432	196
	2642	1116

Figure 2.3-21 Linear Step Motor Drive Assembly

Table 2.3-5 Control System Performance

CONTROL SYSTEM CHARACTERISTICS
- DAMPING = 0.5
- FREQUENCY = STRUCT FREQ/10

TORQUE DISTURBANCE	AXIS TORQUE (N·m) (ROLL) X	(PITCH) Y	(YAW) Z
SOLAR PRESSURE (1 DEG ERROR)	136	5500	0
MW PRESSURE (PEAK)	0	2955	2955
GRAVITY GRADIENT	189,000	33,200	29,700
ANTENNA CONTROL	200,000	0	0
TOTAL	2,189,136	41,655	32,655
FLEX BODY ERROR SENSITIVITY RAD/N·m	3.09×10^{-9}	2.58×10^{-9}	1.22×10^{-9}
STEADY STATE ARRAY POINTING ERROR (RAD)	0.0068	0.00011	0.00004
BENDING MODE DATA – 1ST ANTI-SYMM MODE			
• FREQ (RAD/SEC)	0.0492	0.0178	0.025
• GENERALIZED MASS (SLUGS)	120,828	159,888	157,200
• NORMALIZED DISPL. (FT/FT)	1.0	1.0	0.992
• NORMALIZED SLOPE (RAD/FT)	0.413×10^{-3}	0.18×10^{-3}	0.214×10^{-3}

2.3.4.3 Propellant Requirements

Table 2.3-6 summarizes the SSPS propellant requirements using ion propulsion (Isp = 8000 sec) and chemical propulsion (Isp = 300 sec). A total yearly propellant use of 14870 kg of mercury results from an ion engine system and 397,188 kg of propellant with the chemical system. Electric propulsion, though heavier in inert weight, provides a more economical approach to attitude control.

2.3.4.4 Pointing Requirement

Solar Array output power decreases with deviations in attitude relative to the sun. Figure 2.3-22 shows system efficiency as a function of deviation angle for a two mirror and four mirror solar array. It can be seen that the four mirror system is more sensitive to steering angle errors than the 2 mirror system. Efficiency drops off at 3% per degree of attitude error for the 4 mirror configuration and at the rate of 1.7% per degree for the corrugated 2 mirror system.

The baseline corrugated design efficiency can be improved significantly by pivoting the solar panels so that the arrays can be kept normal to the sun vector throughout the year. The current design is fixed and, therefore, operates at 90% efficiency at the summer and winter solstice. What is meant by fixed is that the longitudinal axis is kept normal to the equatorial plane. The configurations presented in Ref. 2.3-6 assumed fixed solar arrays and were oversized to generate 5 GW ground power during the summer and winter months. This added 454×10^3 kg to the spacecraft weight and approximately \$75/KW to the system cost. A pivot system similar to the concept shown in Figure 2.3-23 could retrieve these losses. The dynamics, disturbance torque, etc. of this configuration is different than the concept analyzed. The pivot and solar array geometry must be selected in a manner that would maintain the principal axis of mass inertia along a line normal to the equatorial plane. The reliability and control of the pivot mechanism would also be an issue needing closer evaluation before this approach is accepted.

If the array attitude is allowed to deviate $\pm 1^\circ$ from nominal, the spacecraft design penalties are:

Weight = 19,237 kg

Cost = \$3/kw

Table 2.3-6 Attitude Control Propellant Consumption

	SPACECRAFT AXIS			
	X	Y	Z	
INERTIA (KG-KM^2)	14.24×10^6	123×10^6	137×10^6	
DAILY MOMENTUM STORAGE, N.M. SEC				
• GRAVITY GRADIENT	6.25×10^9	9.31×10^8	8.10×10^8	
• ANTENNA CONTROL	3.9×10^7	–	–	
• SOLAR PRESSURE	1.18×10^7	4.795×10^8	–	
• MICROWAVE PRESSURE	–	8.51×10^7	8.51×10^7	
TOTAL	6.30×10^9	2.26×10^9	1.661×10^9	
DAILY PROPELLANT CONSUMPTION, KG/DAY				
• I_{SP} = 8000 SEC	33.0	4.8	3.54	
• I_{SP} = 300 SEC	866	128	94	
YEARLY PROPELLANT CONSUMPTION, KG/YR				TOTAL KG
• I_{SP} = 8000 SEC.	11826	1752	1292	14870
• I_{SP} = 300 SEC.	316,090	46,720	34,378	397,188

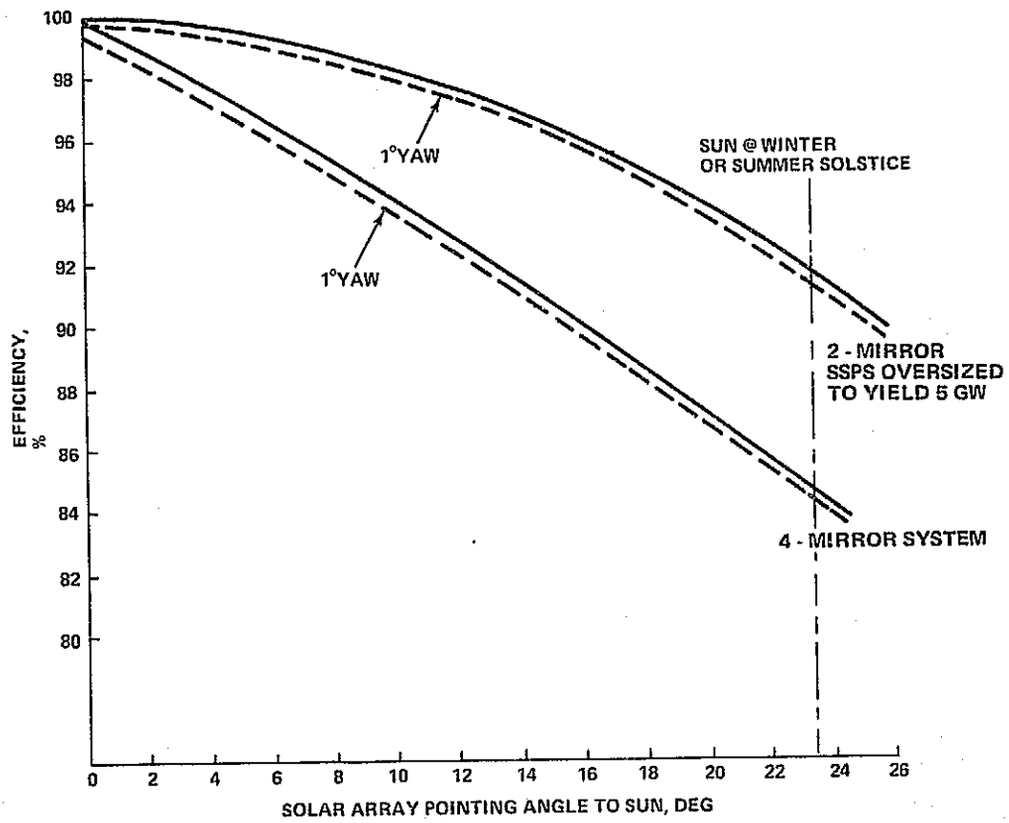

Figure 2.3-22 SSPS Efficiency vs Solar Array Pointing Accuracy

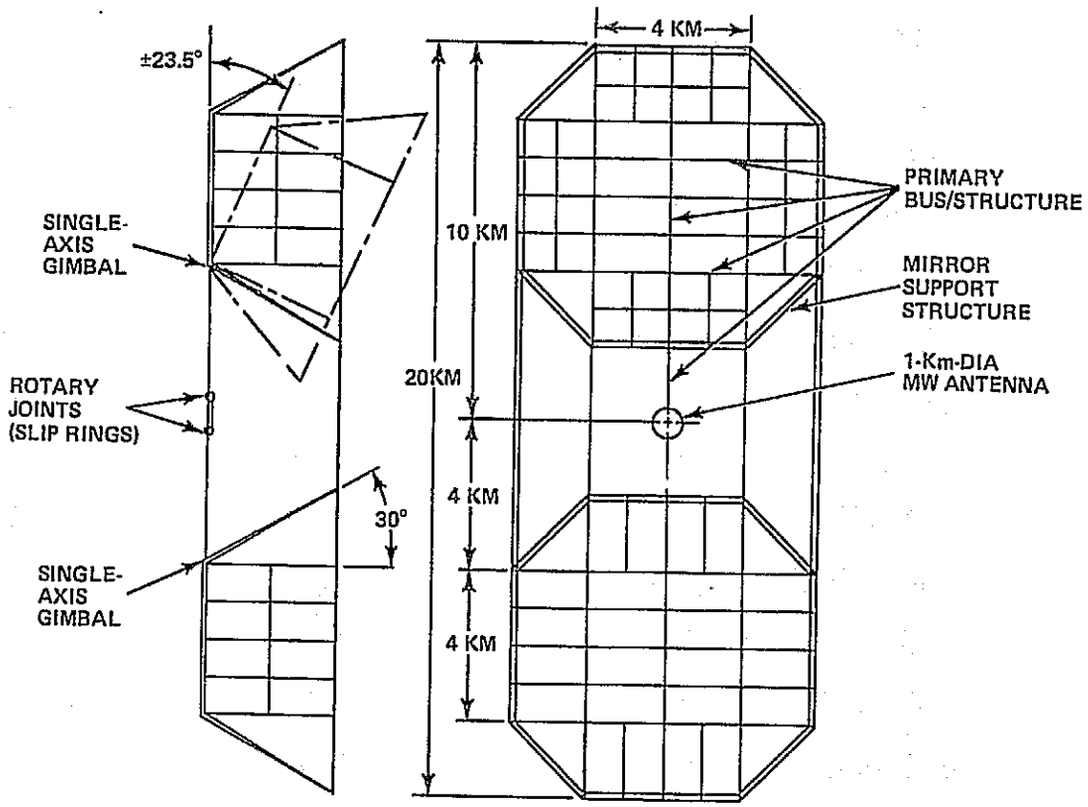

Figure 2.3-23 Typical Solar Array Pivot

2.3.4.5 Control System Performance

Table 2.3-5 summarizes the pertinent control analysis information. The peak disturbance torques and source are listed. The control system performance, and structural dynamic characteristics are presented. The normalized structural dynamics data is specifically for a control system jet geometry which locates these actuators at the corners of the SSPS.

The analysis of the roll (x) axis system is extended in paragraph 2.3.4.6.

2.3.4.6 Antenna Azimuth Control Analysis

The performance of the azimuth control system of the antenna was analyzed with two specific objectives:

- Evaluate the interaction of the antenna mechanical control system with the array central mast
- Establish antenna control system requirements and limitations which affect overall microwave system performance.

Of particular concern was the effect of structural compliance of the mast on meeting the one arc-minute pointing accuracy of the antenna required for high microwave transmission efficiency. The high level of slip ring drag torque and a modeling of solar array flexibility were also considered. The primary technique used to evaluate the system's performance was a single-axis analog computer simulation of the antenna/solar array system.

The physical configuration of the baseline SSPS and corresponding model are illustrated in Figure 2.3-24. The analysis was concerned with simultaneous control of the antenna and solar array about the X axis and the interaction of the two control systems. The solar array must be oriented such that its normal is within ± 1.0 deg of the sunline. The antenna, meanwhile, must be oriented to a point on the surface of the earth within ± 1.0 arc min such that it makes one revolution in azimuth every 24 hours (geosynchronous orbit) relative to the solar array. The simplified model used reflects the fact that the effective spring rate of the antenna drive and the antenna structural compliance term are much smaller than the mast compliance effects. (The reverse is likely true for the elevation control of the antenna.) The basic approach used was initially to develop the designs of the two control loops independently, in order to select gains and establish basic performance capabilities. The combined operation of the total system then was investigated to determine nominal performance and the effects of parameter variations.

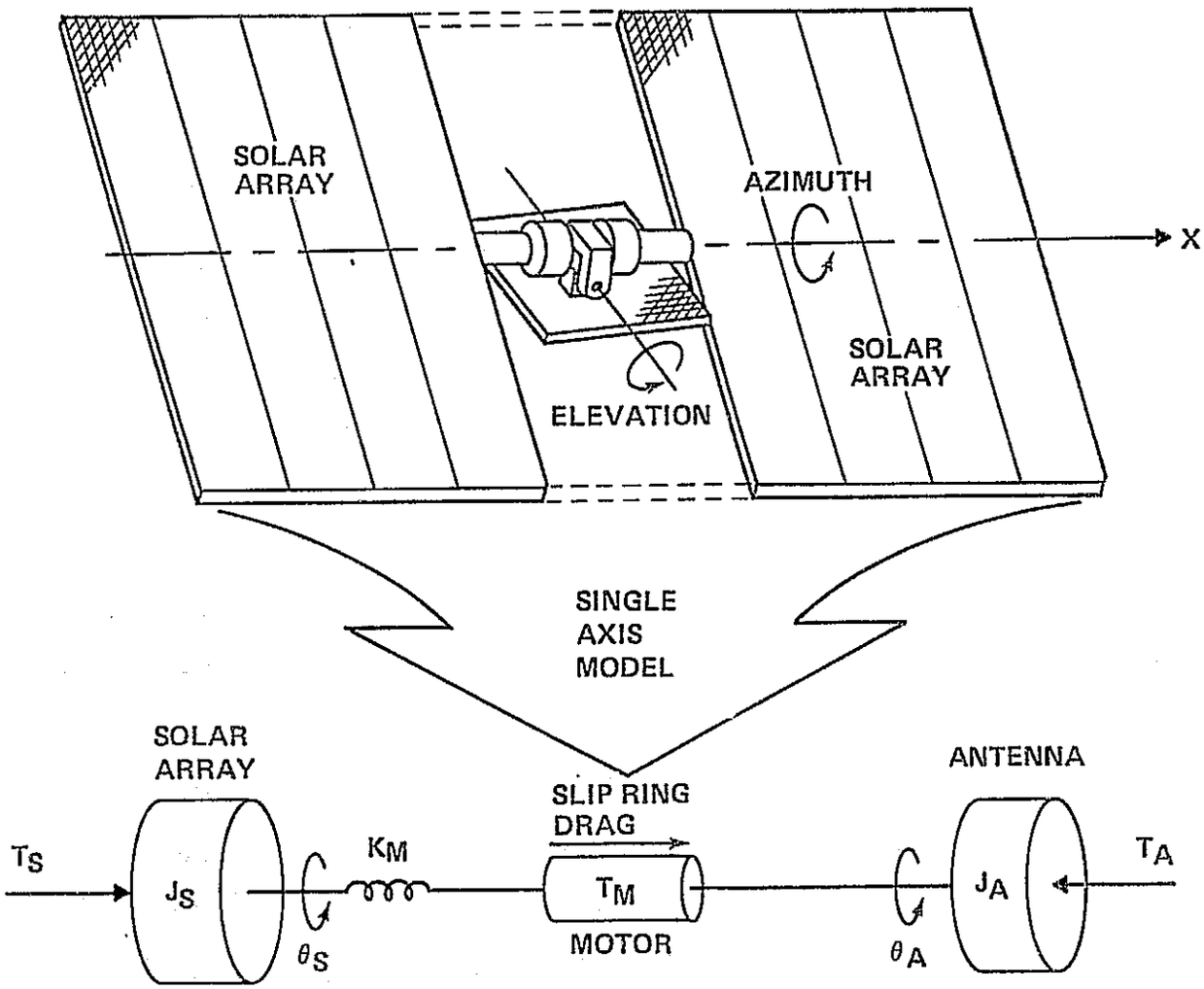

Figure 2.3-24 Antenna Azimuth Control

The block diagram of the combined solar array and antenna azimuth control system is shown in Figure 2.3-25. The solar array is initially modeled as a rigid body with inertia J_S. Control of the array is implemented with thrusters producing Tc torque driven by a control law of the form

$$\theta_S + K_R \dot{\theta}_S = \pm\theta_{DZ}$$

where θ_{DZ} is a dead zone with hysteresis producing limit cycle operation. The net torque on the array is composed of the control torque (T_C), an external disturbance torque T_{S_D} and a reactive torque from the mast compliance term. Flexible structure dynamics are eventually added to the rigid solar array model, as explained later. The array command angle (θ_{S_C}) is normally zero.

The antenna is modeled as a rigid body of inertia J_A. The position control loop forms an error signal by subtracting measured position from the command angle. This signal is a ramp function with a slope of, W_O, orbital rate. The error, combined with measured rate, forms the drive voltage to the torque motor. The motor back-emf gain (K_B) feeds back the differential rate ($\dot{\theta}_A - \dot{\alpha}$) between the motor shaft and the base of the motor. It is this same rate term which determines the sign of the slip ring drag torque (T_{MD}) which subtracts from the motor torque acting on the antenna.

The coupling between the antenna drive and solar array is represented by intermediate angle α, which is defined at the base of the motor. The equation developing α is a fairly complex function of the motor voltage, drag torque, and antenna rate, in addition to the mast compliance term (K_M) which generates a torque as a function of the differential angle ($\theta_S - \alpha$).

The nominal values of the parameters developed for the system are shown in Table 2.3-7. The designation "configuration" parameter applies to the first six items because they are determined by the overall SSPS design. Therefore, slip ring drag torque (T_{MD}) is so designated because conventional slip rings reflect the specified power transfer approach. The remaining items are "design" parameters, indicating that they are selected as a result of control system requirements.

The solar array inertia (J_S) is two orders of magnitude greater than the antenna inertia (J_A), with pointing requirements in a similar ratio of 60 to 1 (60 arc min vs 1 arc min). However, the slip ring drag torque is an order of magnitude greater than the external disturbance torque acting on the solar array (1.4×10^6 N-M vs 1.4×10^5 N-M). Therefore, a large motor torque, which is required for antenna control, becomes significant when coupled through the mast to the solar array.

Table 2.3-7 Nominal Parameter Values

PARAMETER	SYMBOL	VALUE
SOLAR ARRAY INERTIA	J_S	2.44×10^{13} Kg M^2 (1.8×10^{13} SLUG-FT^2)
ANTENNA INERTIA	J_A	2.44×10^{11} Kg M^2 (1.8×10^{11} SLUG-FT^2)
MAST STRCUTURAL COMPLIANCE	K_M	5.02×10^9 NM/rad (3.7×10^9 FT-LB/RAD)
SLIP RING DRAG TORQUE MAGNITUDE	T_{MD}	1.36×10^6 NM (10^6 ft-lb)
DISTURBANCE TORQUE ON ANTENNA	T_{AD}	2.71×10^3 NM ($2. \times 10^3$ FT-LB)
DISTURBANCE TORQUE ON SOLAR ARRAY	T_{SD}	1.36×10^5 (1 + SIN $2W_O t$) NM
ANTENNA SERVO AMP GAIN	K_1	1 VOLT/VOLT
ANTENNA ATTITUDE SENSOR GAIN	K_2	4.2 VOLT/RAD
ANTENNA RATE SENSOR GAIN	K_3	–800 VOLT/RPS
MOTOR TORQUE CONSTANT MOTOR RESISTANCE	K_T R_M	$K_T/R_M = 1.36 \times 10^7$ NM/VOLT = (10^7 FT-LB/VOLT)
MOTOR BACK EMF CONSTANT	K_B	10^3 VOLT/RPS
SOLAR ARRAY RATE GAIN	K_R	200 RAD/RPS
SOLAR ARRAY CONTROL TORQUE	T_C	5.09×10^5 NM (3.75×10^5 FT-LB)
THRUSTER-IN VALUE	I	0.8 DEG
THRUSTER-OUT VALVE	O	0.57 DEG

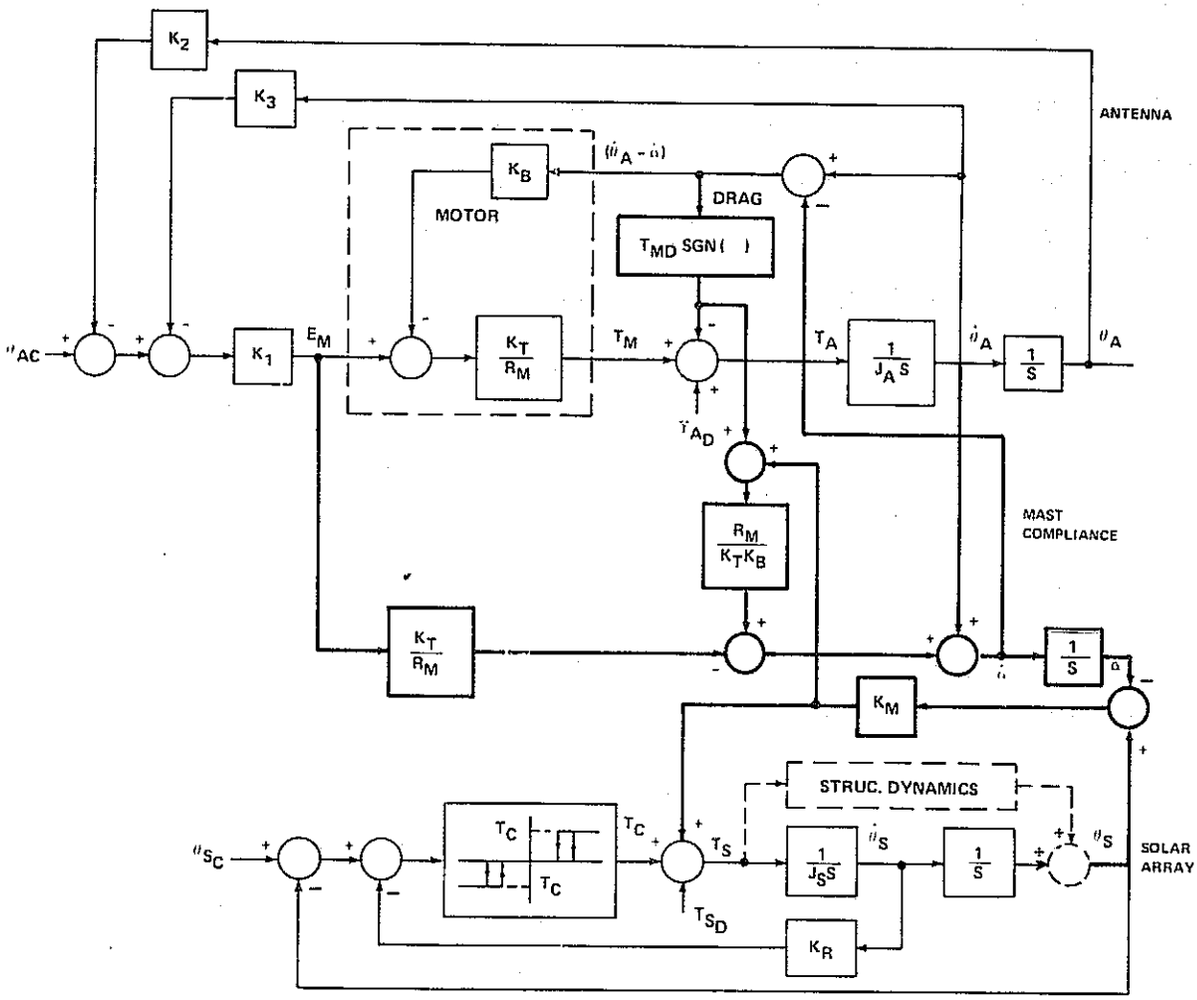

Figure 2.3-25 Azimuth Control Analysis Model

Although the initial loop designs for the antenna and solar array were developed independently, the initial scaling for the computer had to consider the combined operation. Difficulty was encountered in scaling because of the inertia differences which required that the motor back-EMF gain (K_B) be large. Stability analysis of the antenna loop reveals that stability is affected by the sum of K_B and K_3, the rate gain. Stability requires that $K_3 > -K_B$. Since K_B is always a positive quantity, any positive K_3 would satisfy this requirement. Too large a value for K_3 results in a highly damped response, which cannot satisfactorily follow the commanded antenna angle. Using a value of 1000 volts/rps for K_B resulted in a selection of -800 volts/rps for K_3 which provided satisfactory performance. Thus, positive rate feedback is used because of the large value of K_B.

The initial design of the solar array control loop is determined by the 1.0 degree control requirement and the nature of the disturbance torques. The solar array disturbance torque is composed of a constant term, due primarily to solar pressure and a sinusoidal term with a period of 12 hours due to gravity gradient. The magnitudes of both components are 1.36×10^5 N-M.

A general limit cycle phase plane is illustrated in Figure 2.3-26. The limit cycle rate (W_{LC}) is a function of the hysteresis value (I-O) and the rate gain K_R.

To minimize the impulse requirements, the phase plane trajectory in the dead zone, due to the disturbance torques, should traverse the width of the dead zone, coming just short of the boundary. Since the combination of equal constant and cyclical disturbance torque components does not permit this on a continuous basis (with fixed gains, etc), the design was made to minimize the impulse for the periods when the disturbance components are additive. The resultant operation is such that the trajectory hangs off on one side of the dead zone for a portion of the orbit, but eventually goes to an undisturbed, symmetrical response for the remainder of each orbit. The period of the limit cycle, therefore, changes during each orbit due to the cyclical torque.

The dead zone and control torque values were chosen to meet the ± 1.0 deg attitude requirements. Using the specified values of T_d and J_s and the selected value for T_c, $W_{LC} = 0.00091$ deg/sec. This is the optimized limit cycle rate in terms of the required attitude limit. It is significant that this rate is less than the nominal antenna rate of 0.0042 deg/sec. The relative rate between the antenna and solar array under steady state operation will, therefore, be of the same polarity (positive). As a result, the slip ring drag torque will not change polarity. This behavior is clearly demonstrated by the simulation results.

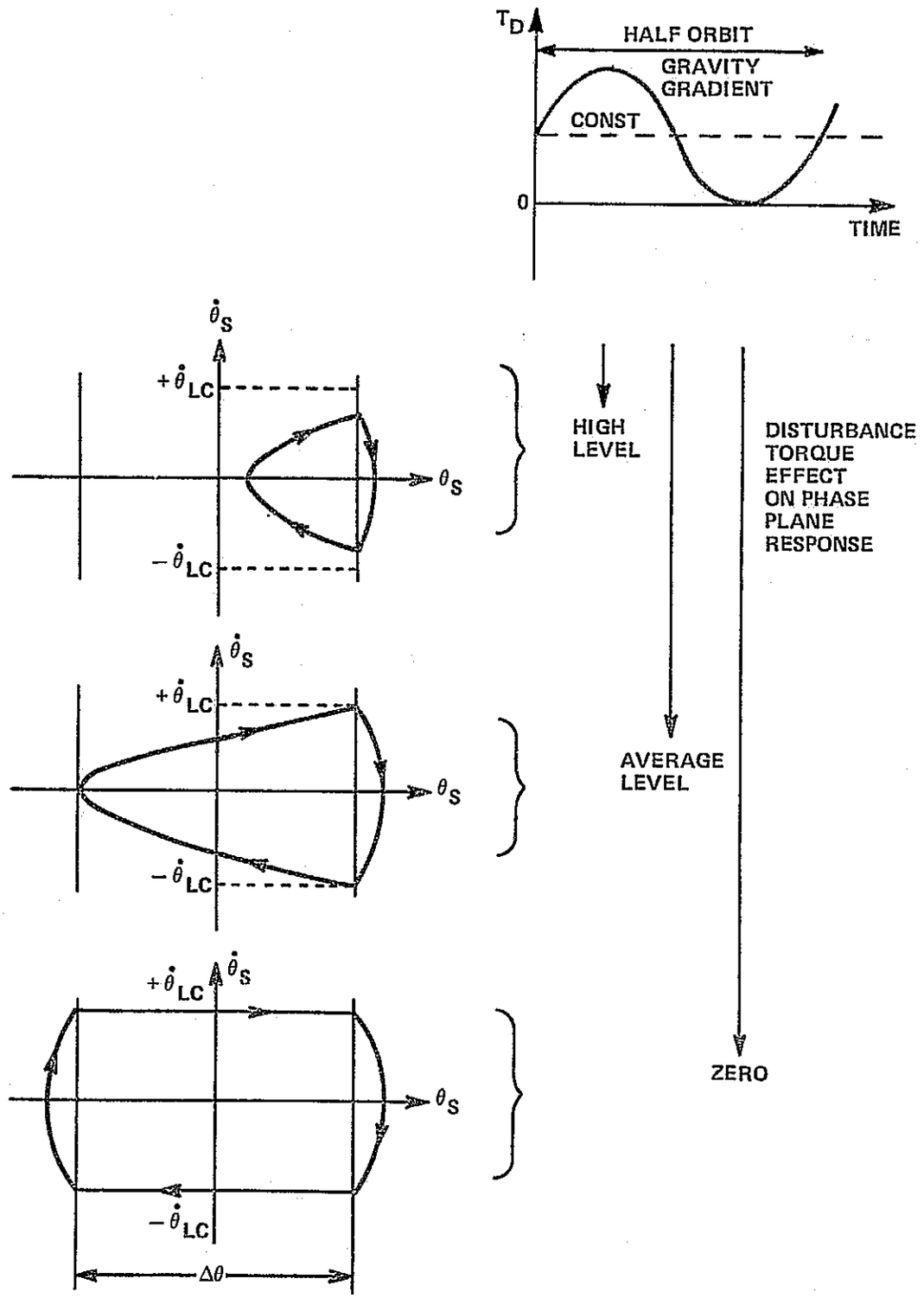

Figure 2.3-26 Typical Phase Plane Effects From Disturbance Torque Variations

The actual values of K_R, I, and O chosen for the initial design produce a limit cycle rate of 0.000575 deg/sec, or approximately 63% of the optimum value. This number corresponds to the limit cycle rate for the constant bias portion (1.36×10^5 N-M) of the disturbance torque.

The control loops for the antenna and solar array were combined, including the mast compliance term (K_m). The performance of the system for the initial parameter values indicated unsatisfactory antenna pointing with a large steady-state offset and a superimposed cyclic variation. Therefore, determining the sources of these effects and the development of techniques to improve the performance were emphasized as discussed in paragraphs 2.3.4.6.1 through 2.3.4.6.5.

2.3.4.6.1 Steady State Antenna Offset - The time history and phase plane response for the nominal conditions is shown in Figure 2.3-27. The solar array requirements are easily met, but the antenna pointing is clearly unsatifactory. The basic measure of antenna performance is $\varepsilon_A = (\theta_{AC} - \theta_A)$, the error between the antenna command angle, a ramp, and the actual antenna angle. The response exhibits a large steady state offset, ~ 95 arc minutes, and a cyclic variation of approximately 17 arc minutes peak-to-peak. This offset is characteristic of the ramp response of a type 1 servo. A simplified representation of the antenna loop is shown in Figure 2.3-28.

The steady state error to a ramp command with a slope W_O is plotted versus the position gain K_2 in Figure 2.3-29 for the nominal gains; simulation data points for the isolated antenna loop are indicated. The time history response for nominal parameter values with $T_{MD} = 0$ are presented in Figure 2.3-30. (The simulation data correctly duplicates the theoretical result.)

The steady state offset effect due to T_{MD} can be reduced by increasing the motor torque gain, K_T/R_M, but the offset cannot be reduced below the "No T_{MD}" value in Figure 2.3-30. In addition, the motor design requirements become even more stringent.

Two other approaches to the offset problem were investigated:

- integral control
- command bias

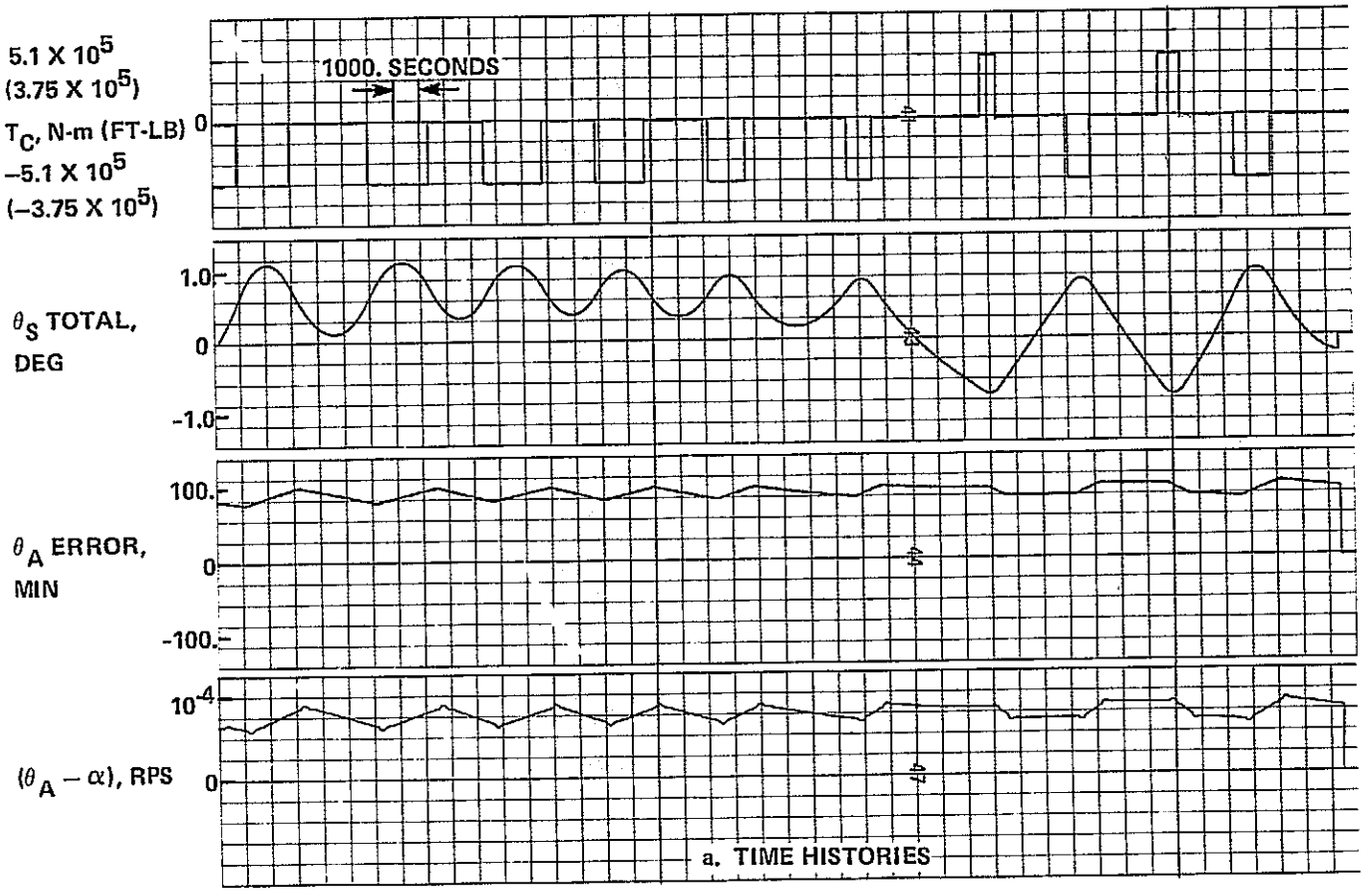

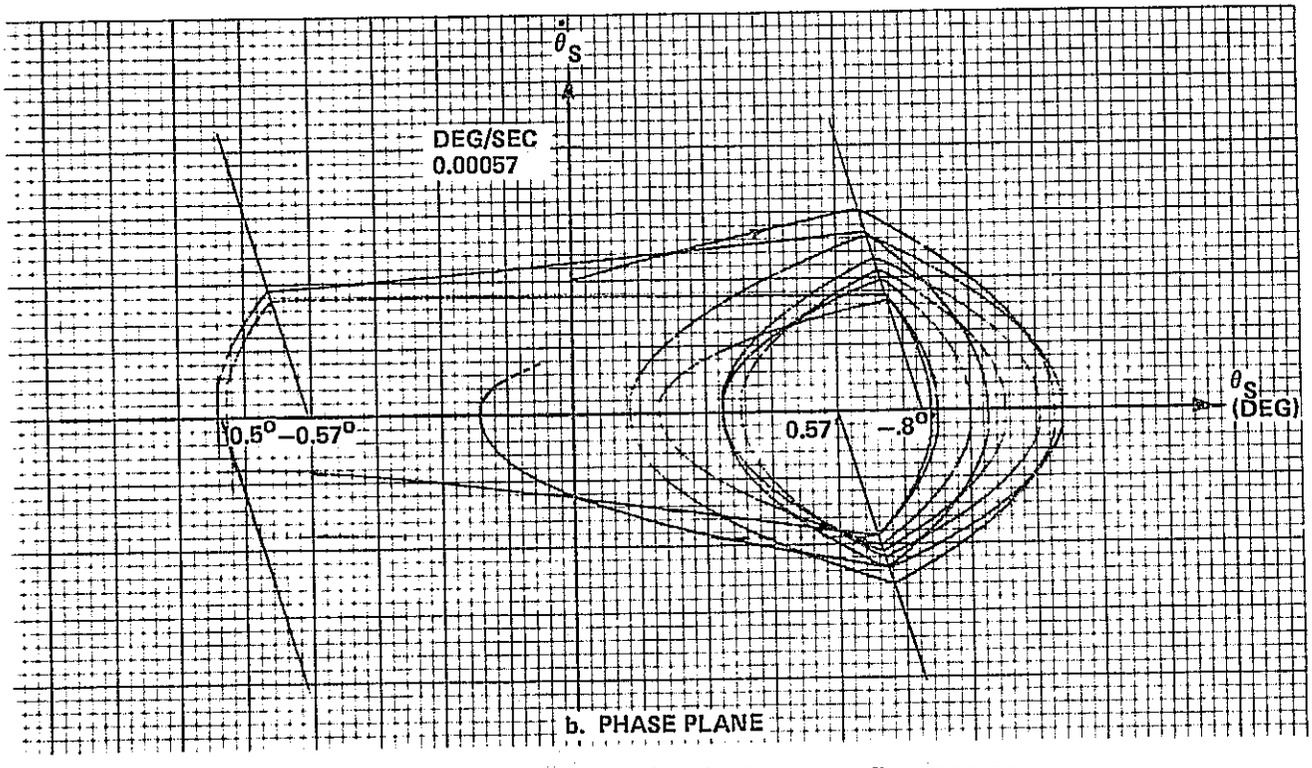

Figure 2.3-27 Nominal System Response

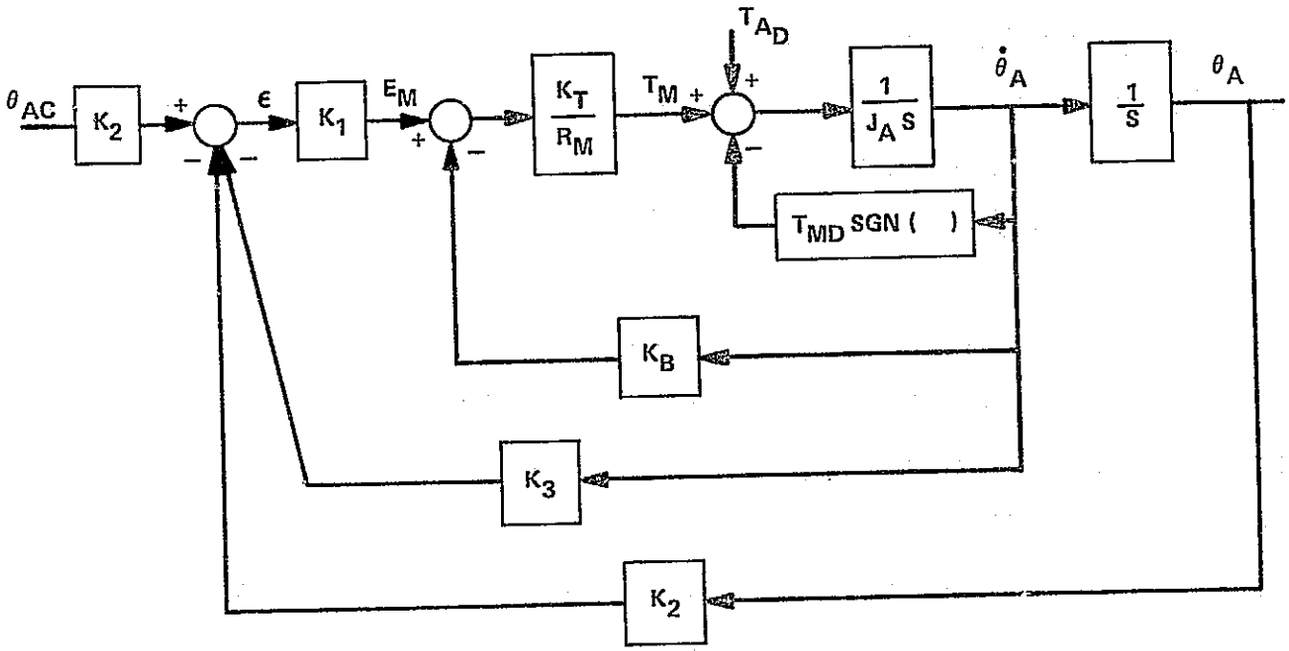

Figure 2.3-28 Simplified Antenna Block Diagram

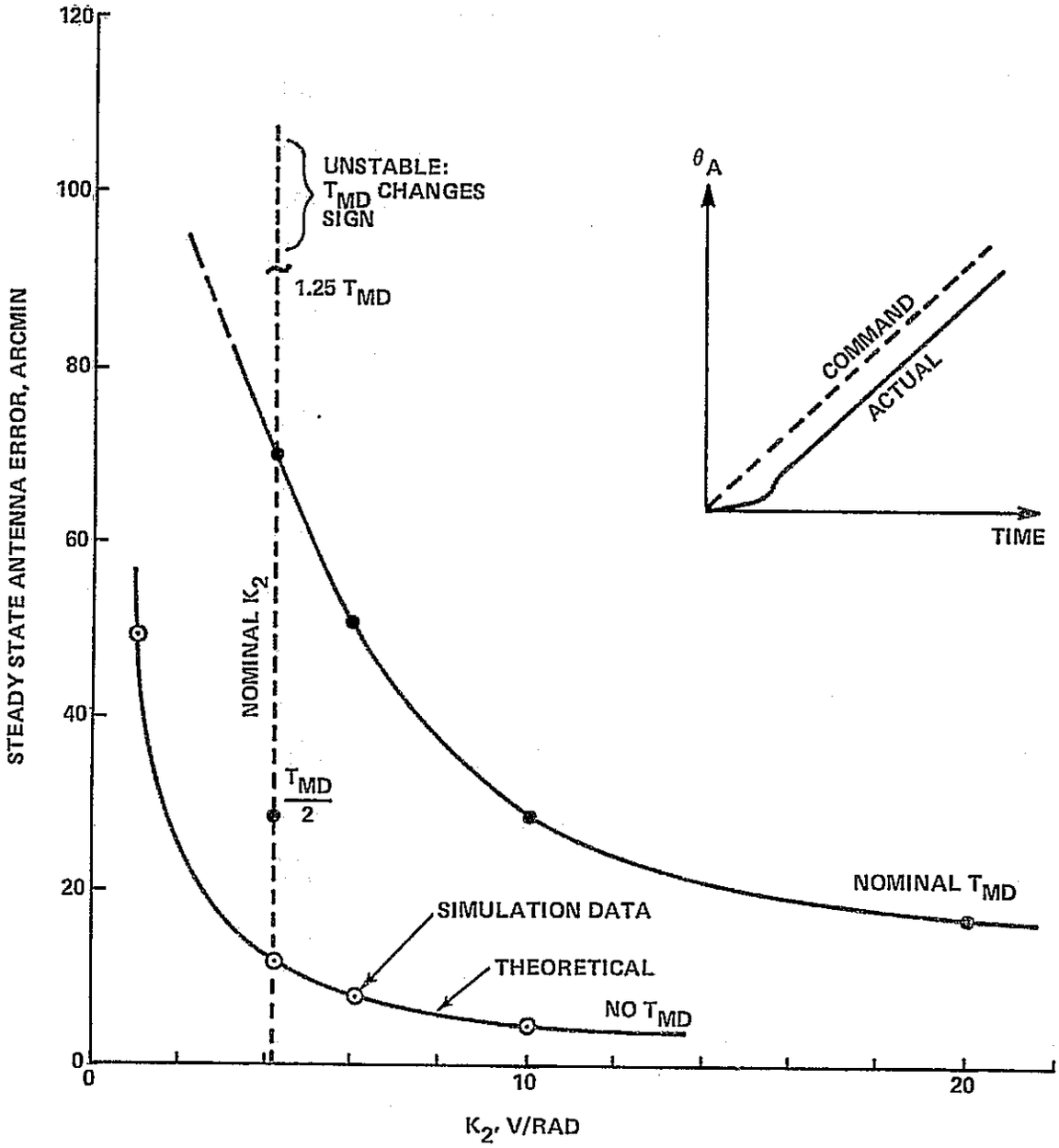

Figure 2.3-29 Antenna Steady State Offset Effect

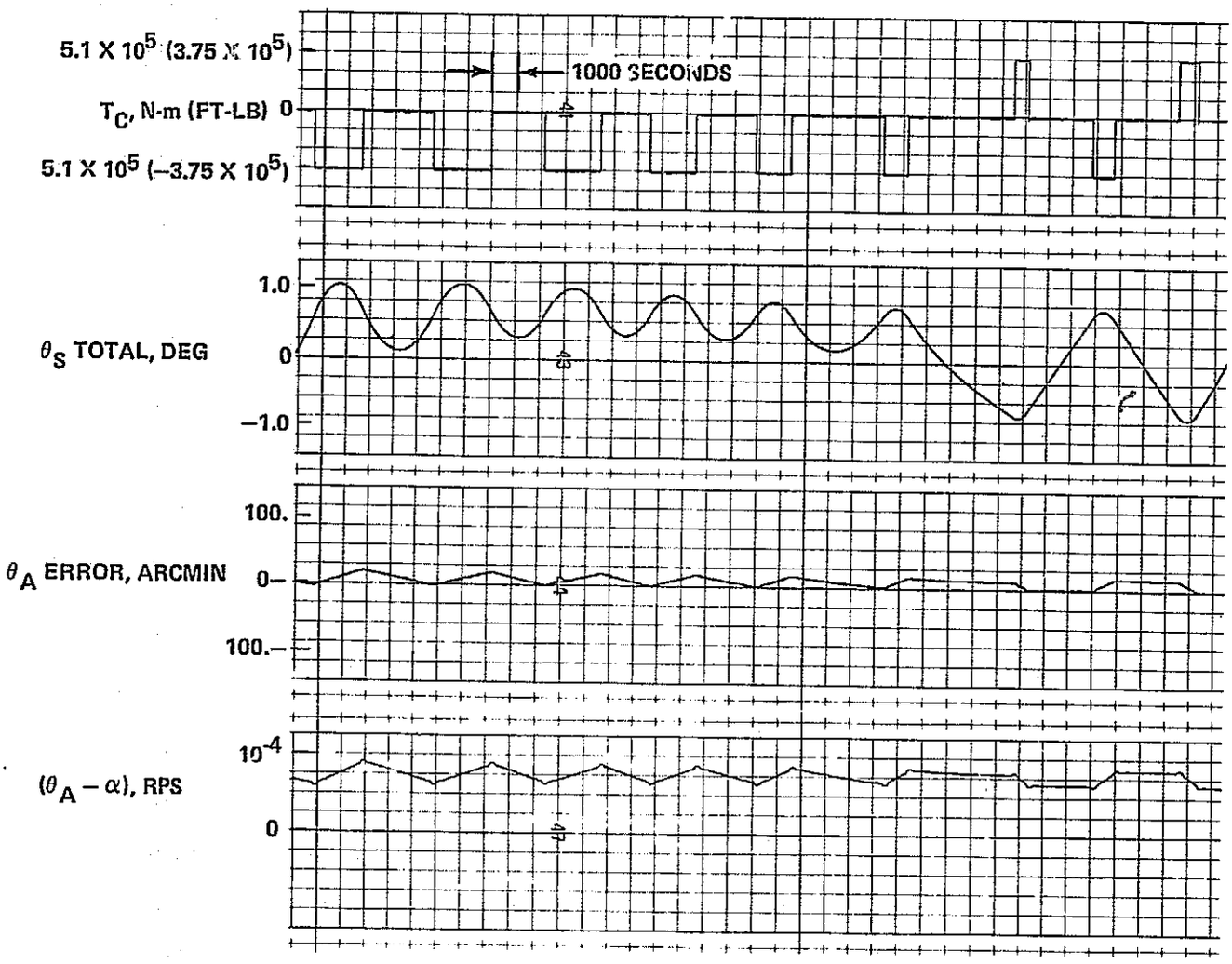

Figure 2.3-30 Nominal System Response With $T_{MD} = 0$

Integral control involves the addition of a K_4/S term in parallel with K_1 in Figure 2.3-28. With a small value of K_4, a steady state error produced by the primary K_1 loop is integrated to form a controlled θ_A response which reduces the error on a long term basis.

The second approach consists of using the measured steady state error to develop a command angle bias signal which shifts the θ_A response until the error is zero. This technique is really analogous to the integral control approach but, instead, uses the knowledge that the system is type 1 with a ramp input. The result of such an approach is effectively to remove the steady-state offset for a fixed value of drag (T_{MD}). However, changes in the value of T_{MD} as a function of time change the effectiveness of this approach; a better understanding of the nature of the drag torque thus is required before its effect can be fully understood and overcome.

The effect of the slip ring drag torque (T_{MD}), is shown by the Nominal T_{MD} curve in Figure 2.3-29. The steady state error is significantly increased by the drag term. The effects of increasing and decreasing T_{MD} are also shown by the discrete data points for the nominal value of K_2. For any value of drag torque, the steady state error may be reduced by increasing K_2. This approach, however, significantly degraded the transient response, to the extent that relative rate reversals caused T_{MD} to change sign. Potential instability problems arise when this occurs, especially if a variable T_{MD} and stiction are considered. To avoid these problems, the nominal value of K_2 was used, and alternate approaches to reduce the steady state error were pursued. Increasing T_{MD} above 1.7×10^6 N-M resulted in a similar instability problem, in which T_{MD} changes sign.

2.3.4.6.2 Cyclic Antenna Error - The cyclic variation of the antenna angular error is clearly related to the solar array limit cycle operation. The effect of varying the limit cycle amplitude and frequency was investigated by changing the thruster logic dead zone and hysteresis level. The result of this variation is shown in Figure 2.3-31 which plots peak-to-peak antenna error as a function of array limit cycle rate. The cyclic error is reduced, but not to the level required.

An alternate approach to controlling the antenna is to use the measured differential rate ($\dot{\theta}_A - \dot{\alpha}$) between the drive shaft and the motor base in the antenna loop, instead of just the $\dot{\theta}_A$ used in the initial configuration. This approach is referred to as the "K_3 MOD" case, indicating the input to rate gain K_3 has been modified. The effect of this change on the basic performance of the system is shown by comparing Figure 2.3-32 with Figure 2.3-27. The antenna error oscillation is reduced by a factor of about three. The effect is the same with or without

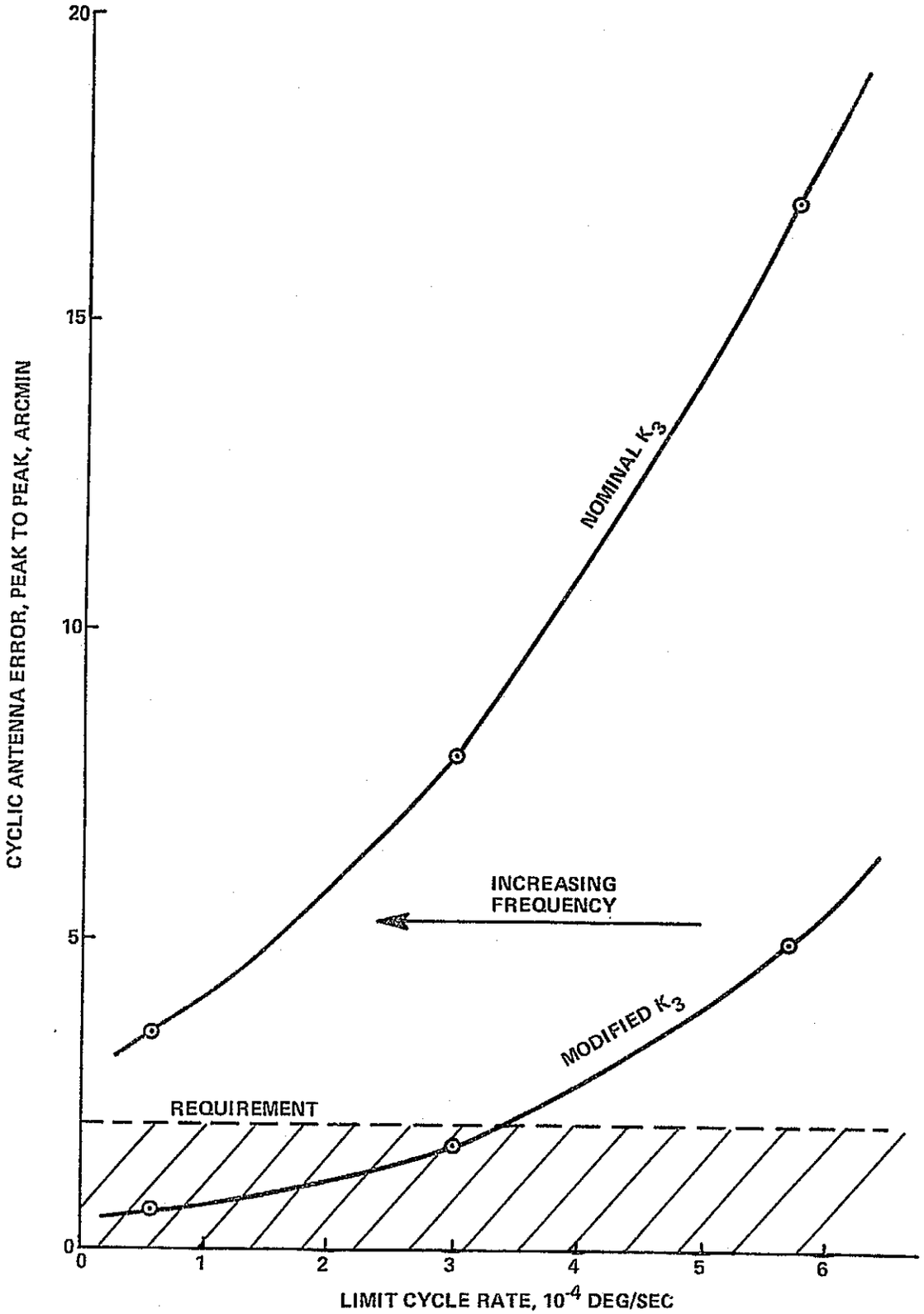

Figure 2.3-31 Antenna Cyclic Error Effect

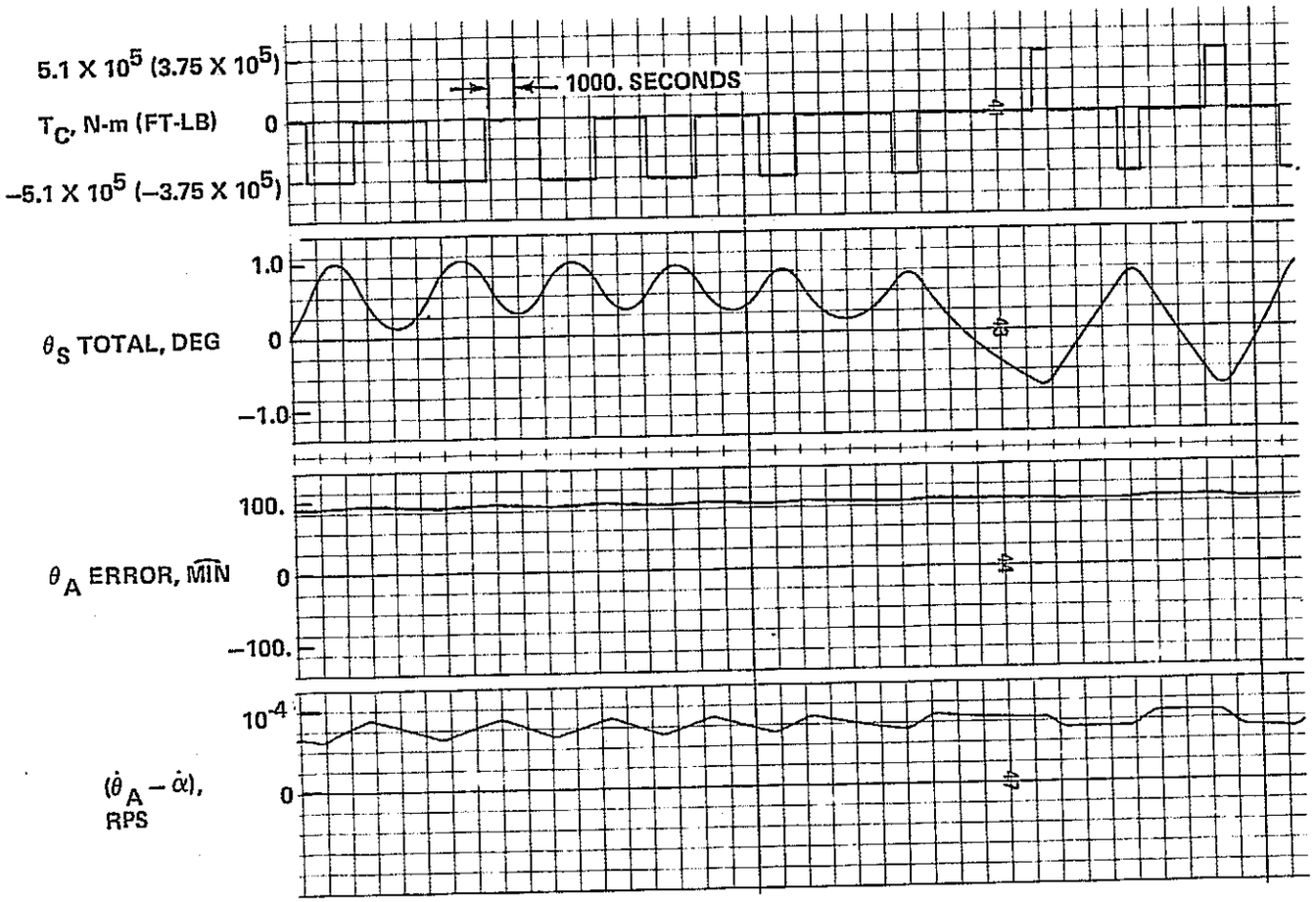

Figure 2.3-32 Modified K_3 Response (Nominal)

slip ring drag (T_{MD}). The combination of this modification with the changes to the array limit cycle considered results in the improvements indicated by the modified K3 curve in Figure 2.3-31.

2.3.4.6.3 Structural Flexibility Effects - At this point in the analysis, the relevant flexible modes of the solar array structure were introduced into the simulation. The structural model used is shown in Figure 2.3-33 along with the parameter values. Each mode is represented by a second order transfer function in parallel with the rigid body dynamics. A thruster firing is converted to a modal deflection at the thruster which operates on the corresponding generalized mass for the mode. The output is converted to a rotation at the mass center which adds to the angle from the rigid body model.

The effect of the structural modes was determined for the baseline system and for the system with the modified K_3 and tighter limit cycle control. The lightly damped (0.5%) structural modes, although well within the pointing requirements, are repeatedly excited at higher frequencies as the limit cycle rate is reduced. The response begins to border on instability at the lowest rate considered. The effect of increasing the thruster torque level has a similar effect.

2.3.4.6.4 Mast Compliance Effects - An investigation into the effect of varying the mast compliance term (K_M) showed that larger values (stiffer) than nominal did not appreciably change the magnitude of the antenna angle cyclic variation or steady state offset. However, for a reduction in K_M of about an order of magnitude, the antenna response became more lightly damped. For a value of $\sim 10^8$ N-M/Rad for K_M, the system became unstable. Qualitatively, this would appear to indicate that as the mast becomes less stiff (low K_M), the antenna drive mount lags the motion of the array to the extent that the antenna cannot be controlled for the case considered.

2.3.4.6.5 Final Configuration Results - The complete baseline configuration response with the antenna control loop reflecting the modified K_3 input and the added command angle bias, shown in Figure 2.3-34, is still short of the desired performance because of the antenna cyclic motion. The tighter limit cycle control of the array is the final change needed to meet the performance requirement as shown in Figure 2.3-35, although a higher level of excitation of the structural modes occurs.

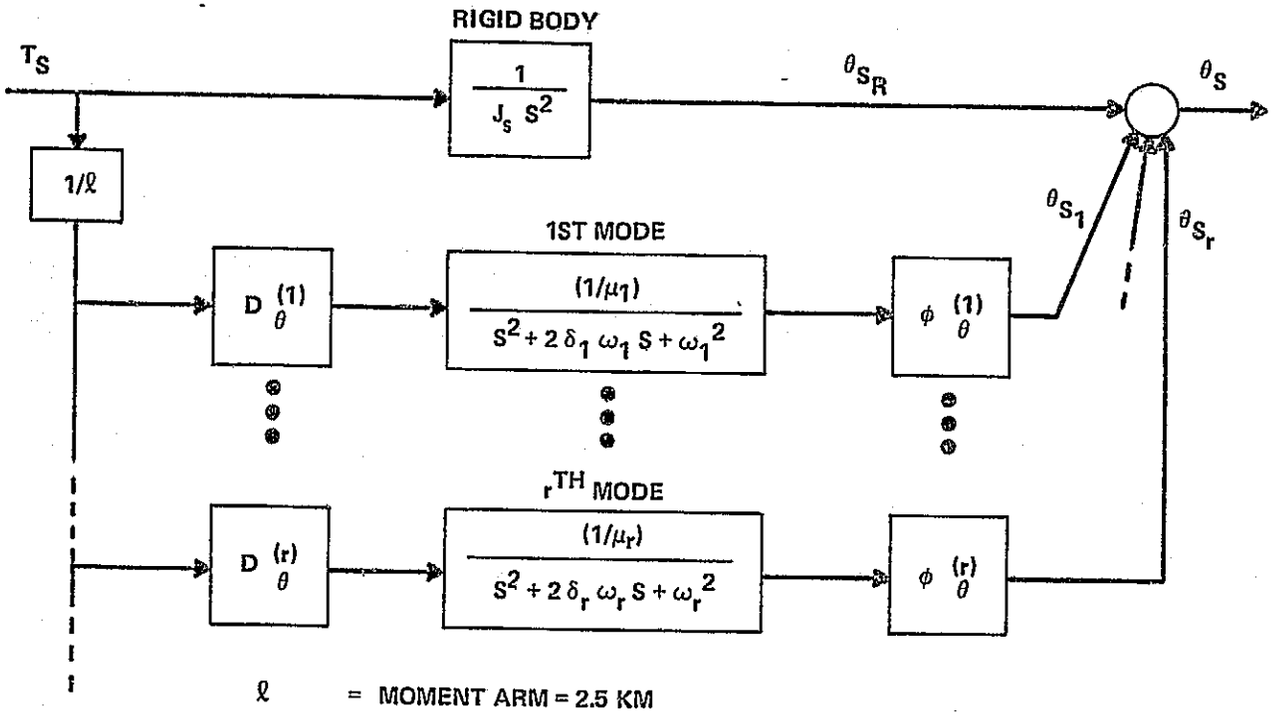

ℓ = MOMENT ARM = 2.5 KM

$D_\theta^{(i)}$ = MODAL DEFLECTION AT THRUSTER OF i^{th} MODE.

$\phi_\theta^{(i)}$ = MODAL ROTATION AT MASS CENTER OF i^{th} MODE.

μ_i = GENERALIZED MASS (i^{th} MODE)

ω_i = FREQUENCY OF i^{th} MODE

δ_i = STRUCTURAL DAMPING = 0.005

MODE	FREQUENCY, ω_i		GENERALIZED MASS, μ_i, KGM (SLUGS)	MODAL DEFLECTION, $D_\theta(i)$	MODAL ROTATION, ϕ_θ (i), RAD/M (RAD/FT)
	C/HR	RPS			
S5	14.14	2.465×10^{-2}	3.86×10^5 ($.0470 \times 10^6$)	−.768	5.09×10^{-5} (1.55×10^{-5})
S7	18.91	3.297×10^{-2}	3.57×10^6 ($.2446 \times 10^6$)	.290	1.04×10^{-4} ($.332 \times 10^{-4}$)
S9	28.78	5.017×10^{-2}	8.38×10^5 ($.05746 \times 10^6$)	.993	-5.45×10^{-5} (-1.66×10^{-5})
S12	41.32	7.204×10^{-2}	2.17×10^5 ($.2174 \times 10^6$)	−.0528	-1.70×10^{-3} (-5.18×10^{-4})
S13	45.24	7.887×10^{-2}	7.72×10^5 ($.05292 \times 10^6$)	−1.00	-1.95×10^{-6} ($-.594 \times 10^{-6}$)

Figure 2.3-33 Flexible Solar Array Model

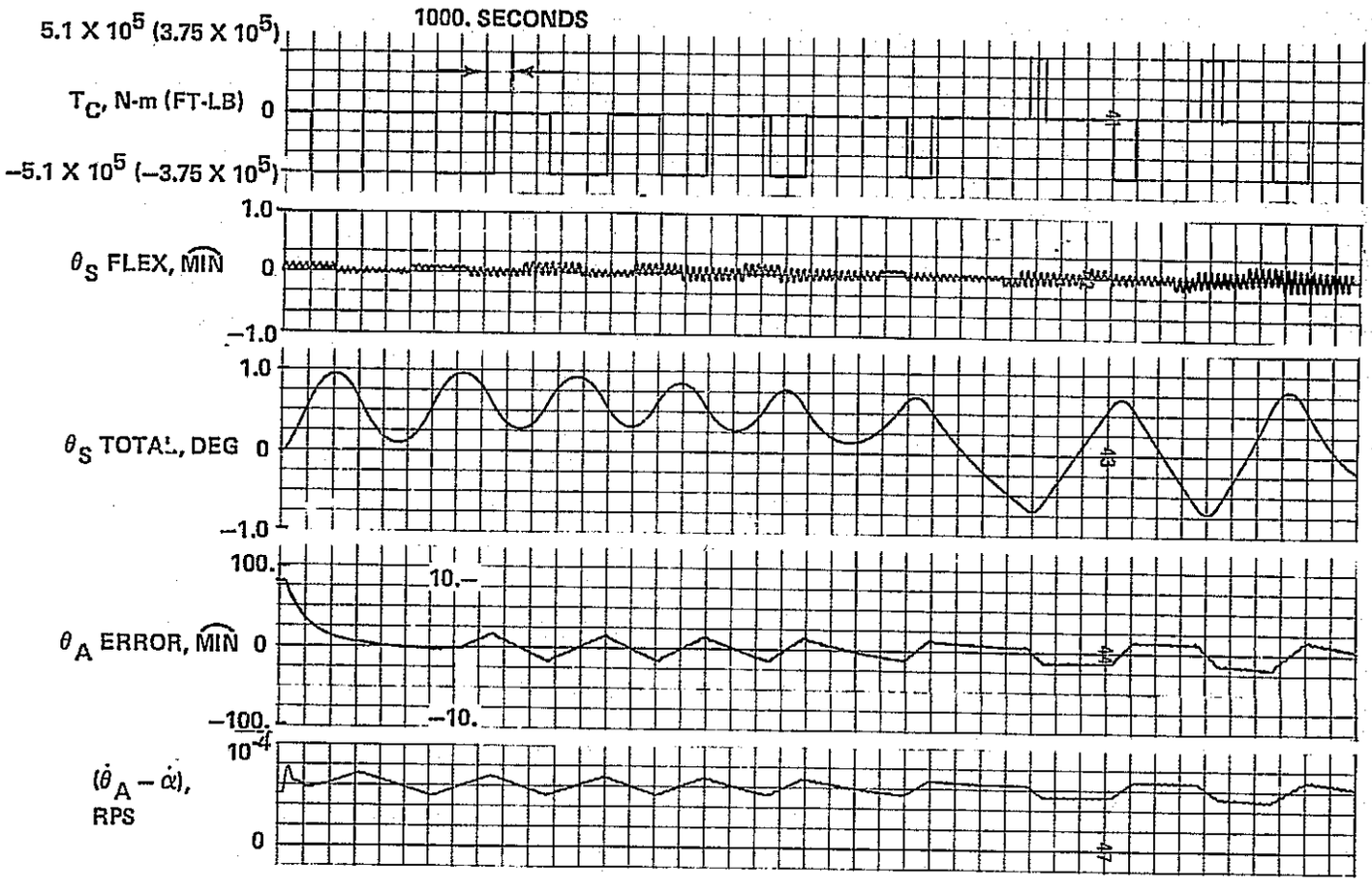

Figure 2.3-34 Modified K_3 Response (Nominal) With CMD Bias

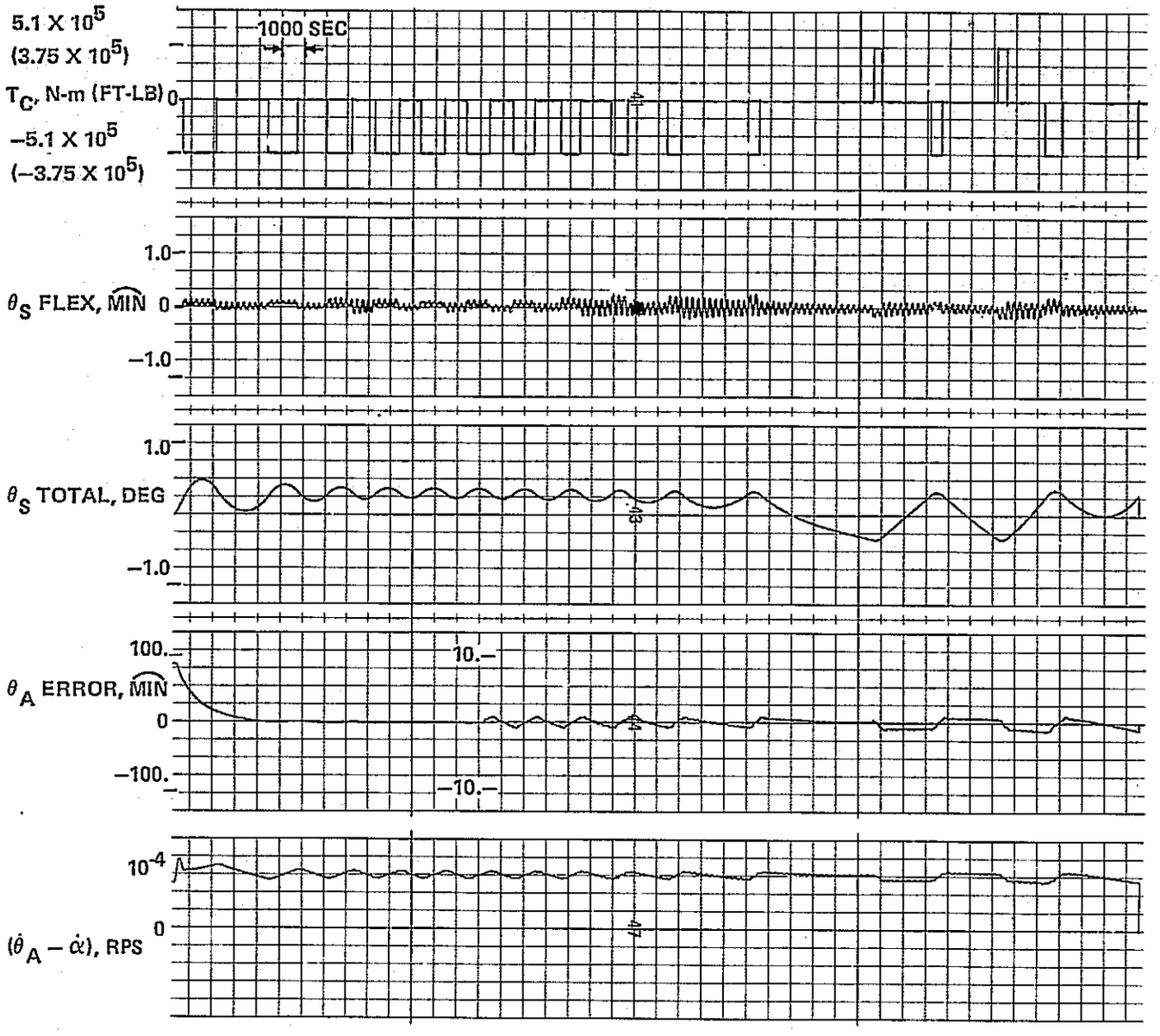

Figure 2.3-35 Modified K_3 Response (0.4 Degrees DZ) With CMD Bias

2.3.4.7 Key Conclusions

Analysis of SSPS attitude control has led to the following conclusions:

- The dominant disturbance torque is caused by gravity gradients. Approximately 14,000 kg/yr is required to compensate for satellite motion due to this disturbance
- Reaction control offers a lighter weight control system approach than momentum storage
- Solar array weight can be reduced if a pivot is used to point the panels at the sun during the winter and summer months
- Preliminary flexible body-control system studies show that the SSPS is sufficiently stiff to achieve ±1° solar array pointing accuracies
- A unidirectional slip ring drag torque during steady-state operation may be insured by proper design of the array control loop
- Array limit cycle coupling has a significant impact on antenna control
- Expected levels of structural compliance for the array mast have a minor effect on antenna control loop performance
- Tighter array control reduces the effect of limit cycling on antenna control but at the cost of higher excitation of structural modes
- Antenna control using the measured angular rate between the antenna and the base of the drive motor is desirable
- Significant increases in mast compliance effect system stability
- The steady state pointing error of the antenna is significantly effected by the slip ring drag.

2.3.4.8 Summary of Issues

The following issues have been identified:

- Effects of antenna flexibility on azimuth control performance

- Antenna elevation control including structural flexibility, flex-leads compliance, and cyclic disturbance torques
- Performance sensitivity to large variations of certain key configuration parameters, such as structural compliance of the mast
- Detailed design characteristics of a very high torque motor for the antenna drive
- Effects of high levels of drag torque and static friction on the antenna transient response during initial start-up of the earth acquisition and pointing operation
- Thruster life cycle effects and the implications relative to the array/antenna system design
- Control capabilities and requirements during SSPS buildup, and the relationship to the operational design
- Techniques for maintaining operational control of the antenna/array system through eclipse periods and the effect on the operational, non-eclipse design.

2.3.5 References

2.3-1 Grumman Report ASP 583-R-8, "Satellite Solar Power Station - Systems Engineering Report", November 1971.

2.3-2 Grumman Report ASP-583-R-11 "Satellite Solar Power Station - Technical Memoranda", June 1972.

2.3-3 Grumman Memo NSS-MO-75-111, "SSPS Engineering Analysis of Special Requirements - Orbit to Orbit Transportation", March 1975.

2.3-4 Grumman Memo ASP-611-M-1011 "Force Resulting From The Electromagnetic Radiation of Energy From the SSPS Antenna," September 1972.

2.3-5 Grumman Memo ASP-611-M-1004, "Sensitivity of Attitude Control Propellant Requirement to SSPS Deviation Angle Limits", August 1972.

2.3-6 Grumman Memo NSS-MO-75-118, "SSPS Engineering Analysis of Special Requirement - Large Solar Arrays", March 1975.

2.3-7 NASA CR-2357, "Feasibility Study of a Satellite Solar Power Station", February 1974.

2.3-8 Grumman/Raytheon, MPTS-R-002, "Microwave Power Transmission Systems Study - Task 2 Report," 12 December 1974.

2.3-9 Kaula, "Theory of Satellite Geodesy", 1966 Blarsdell Publishing Co., Waltham, Mass.

2.4 Transportation, Assembly and Maintenance

The cost of transportation, assembly and maintenance is the most significant variable in establishing the economic feasibility of the SSPS. The objective of this section is to outline approaches to the SSPS transportation and assembly, and to bound expected costs.

If SSPS electrical unit charge rates are to be kept low enough to be competitive with ground based power generation, the increment of the unit charge rate attributed to the transportation of materials to Low Earth Orbit (LEO) should not exceed 20 to 30% of the total, or approximately 4 to 5 Mills/kwh. Using 4 to 5 Mills/kwh as a cost target, the study has identified the following trends:

- Operating costs between $10M and $20M per flight are adequate to achieve cost competitive space-based power provided payload capability to LEO of greater than 182,000 Kg can be achieved in advanced launch systems

- Launch site operations may be a key issue in selecting launch system size. The larger the vehicle, the fewer launches per day along with a requirement for fewer launch opportunities.

Cost of transporting the SSPS from LEO to geosynchronous altitude is a strong driver in the selection of the assembly altitude. Candidate orbit-to-orbit transportation systems have been evaluated and indicate an incremental unit charge rate of 0.9 Mills/kwh ($26.5/Kg) can be achieved if major assemblies are fabricated in LEO and ion propulsion used to transport the assemblies (or major subassemblies) to geosynchronous orbit.

Assessment of assembly operations have indicated the following:

- Assembly using ground-based remote control trends to be lower in cost than manned space-based control of assembly operations.

- Assembly rates of better than 14 kg/hr, costs for space stations to accommodate assembly crews of less than $10M/man (ammortized over 5 SSPS units) and a low cost approach for resupply and recycling of crews is required if manned space based control of assembly is to be cost effective.

- Assembly at geosynchronous orbit using remote controlled techniques would be cost effective at assembly rates greater than 5 kg/hr.

Preliminary analysis of SSPS maintenance requirements have identified the following key issues:

- A detailed study, which trades off the cost of repair versus the loss of revenue if no repair is performed, is needed to establish reliability goals and maintenance support approaches.
- The major maintenance cost driver tends to be the control system (electric propulsion units).
- Proper layout of the solar blanket circuitry and microwave tube feed system could result in a near maintenance free design.
- A maintenance approach which shares man-rated equipments between many power stations is needed to reduce the impact of initial investment.

2.4.1 Transportation to Low Earth Orbit

2.4.1.1 SSPS Baseline Design and Launch Traffic Assumptions

The results of a detailed study of the SSPS, Ref. 2.3-1 and of the microwave antenna, Ref. 2.3-2, was used to compile a strawman definition of weights. The basic spacecraft generates 5 GW of power on the ground using two large photovoltaic solar arrays enhanced by concentrators, and transmits power to the ground with a slotted waveguide transmitting antenna. The basic factors of significance to this evaluation is the weight, 11.5×10^6 kg/SSPS and delivered power, 5 GW. This weight has been revised as a result of further study.

Estimates in power demand over the period 1990 through 2020 would require 5150 GW increase in electrical plant capacity if the traditional 6 to 7% growth continues. Figure 2.4-1 shows an illustrative launch model which must be transported per year to provide approximately 10% of the projected 6.4% growth. This model was used in this evaluation along with the assumption that one satellite can be assembled in one year.

2.4.1.2 Candidate Launch Systems

The matrix of potential launch systems are shown in Figure 2.4-2. These launch systems span a range of design approaches which vary from the use of the current Shuttle to the development of a fully reusable LOX/Hydrogen, Heavy Lift Launch Vehicle (HLLV) with a 182,000 Kg payload capability to LEO.

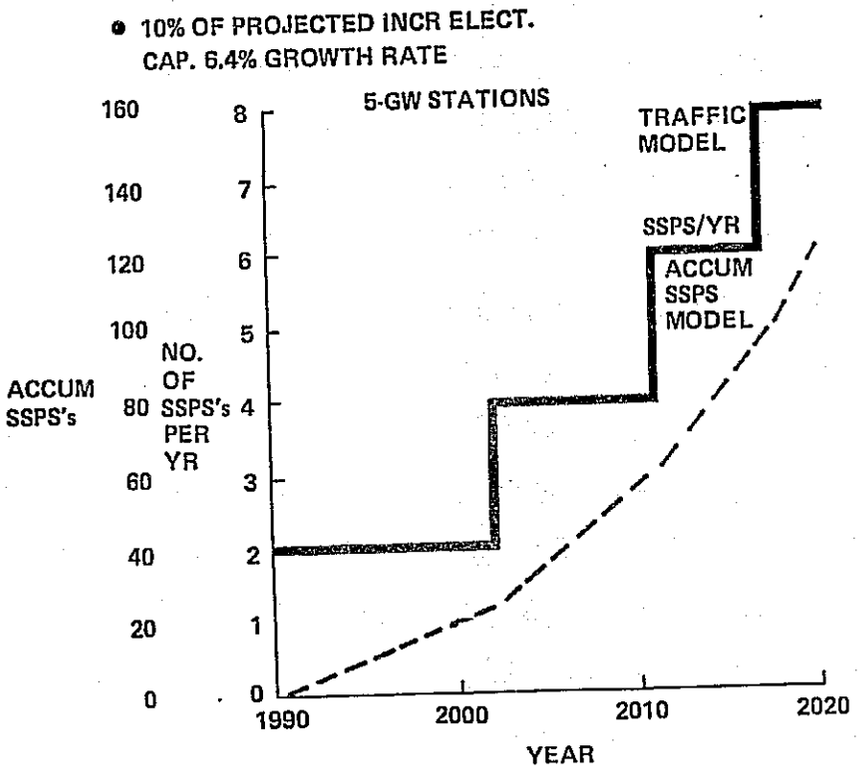

Figure 2.4-1 Traffic Model

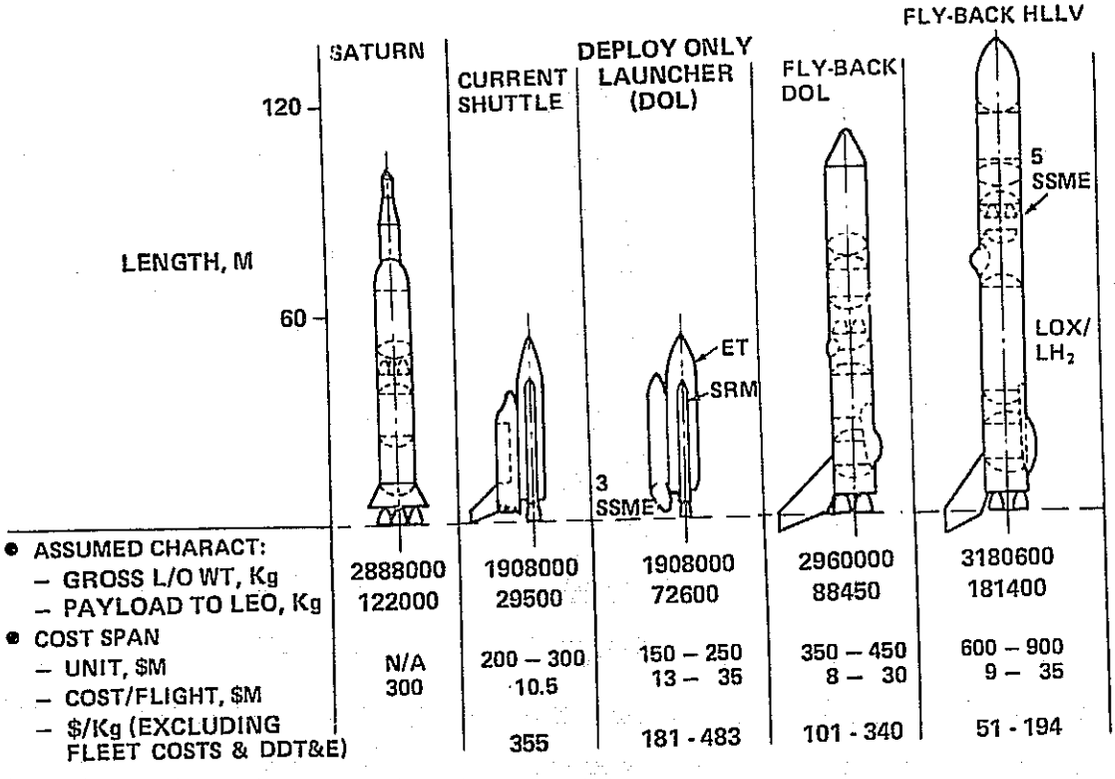

Figure 2.4-2 Typical Candidate Launch Systems

The candidate launch systems have been compared in terms of their contribution to the unit charge rate to power users following the methodology outlined by Aerospace in their BRAVO studies. A discount rate of 8.65% was used in this assessment. This rate is slightly higher than the 7.5% recommended by ECON. Costs include those required for operations, initial fleet purchase and fleet replacement. The discounted power demand for the mission model presented in Figure 2.4-1 is 1.15×10^{13} kwh assuming a 100% utilization factor. The user costs calculated here are inversely proportional to the utilization factor.

The effects of launch system cost and payload potential on unit charge rate are shown parametrically in Figure 2.4-3. Superimposed on the figure are four launch system options. Included is the span of operating costs which reflect the potential level of recoverability of the $110 million worth of hardware on the DOL, Flyback DOL and Flyback HLLV second stage. It becomes apparent that cost per flight, specifically the feasibility of second stage propulsion and avionics reuse, is as strong a cost driver as performance.

The combined effect of operations cost and fleet cost reflect the same trend, as shown in Figure 2.4-4. The uncertainty of reuse of second stage components could preclude achieving the highly desirable 40 to $100/kg launch system size for SSPS.

Figure 2.4-5 is an example of the worksheet used in the comparative economic assessment of launch systems. Use of the Shuttle would require close to 800 flights per year in the early phases of SSPS operation and would reach over 3000 flights in the 2020's. This latter figure represents approximately eight launches per day and the facility to recycle 120 Orbiters. The HLLV, however, would require only one to two launches per day and the refurbish facility to handle 20 vehicles. It may be the impact on launch facility, rather than the benefits of heavy lift payload capability on the SSPS user costs that will drive the selection of a HLLV second generation launch system size for SSPS.

These preliminary tradeoffs of launch systems for SSPS have shown:

- Recovery and low cost reuse of launch system second stage hardware is key to achieving competitive SSPS user costs.
- The impact of high density launch rate on launch facility operations should be closely evaluated to determine the booster approach for SSPS.

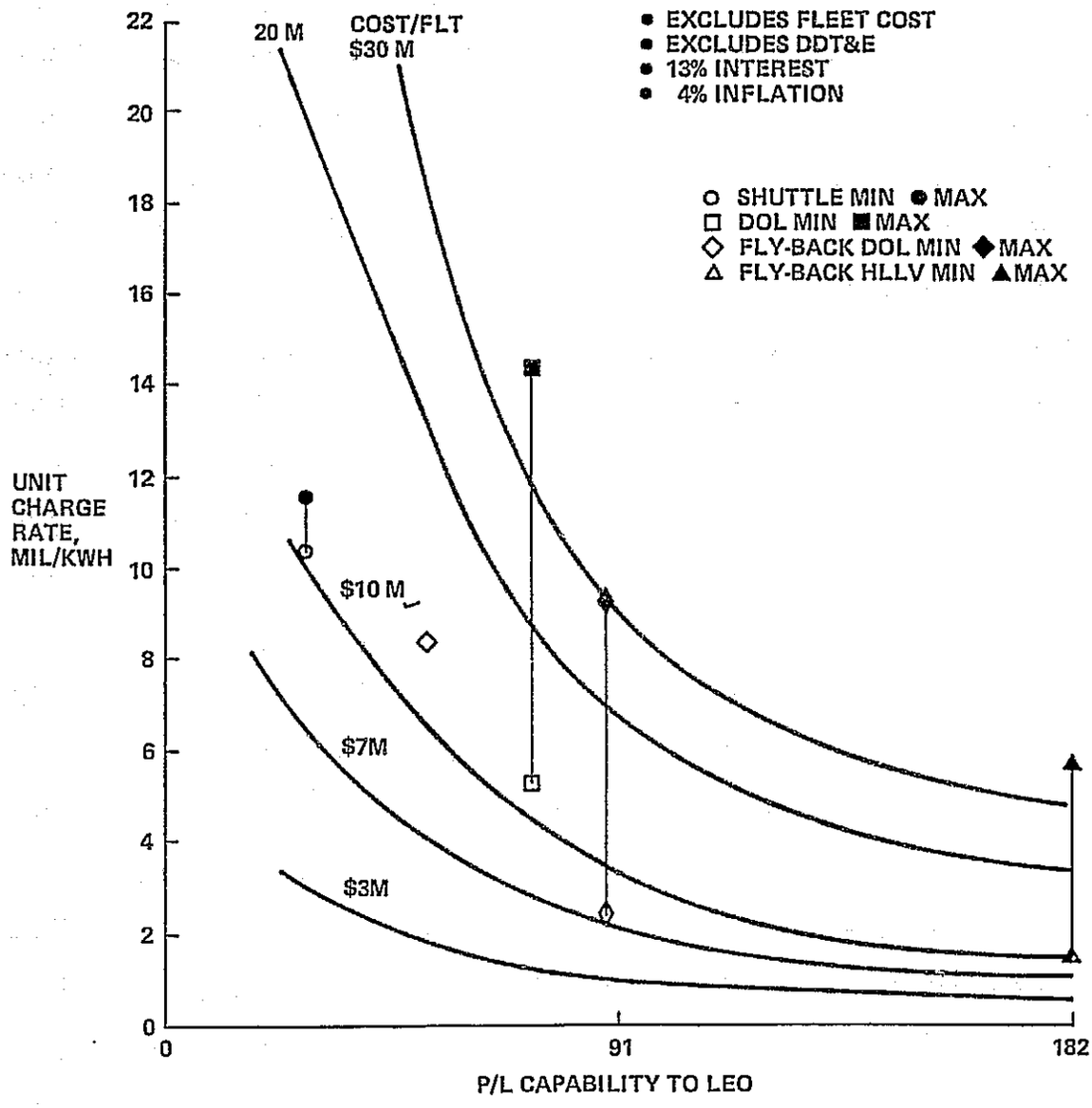

Figure 2.4-3 User Cost for Transportation to Leo

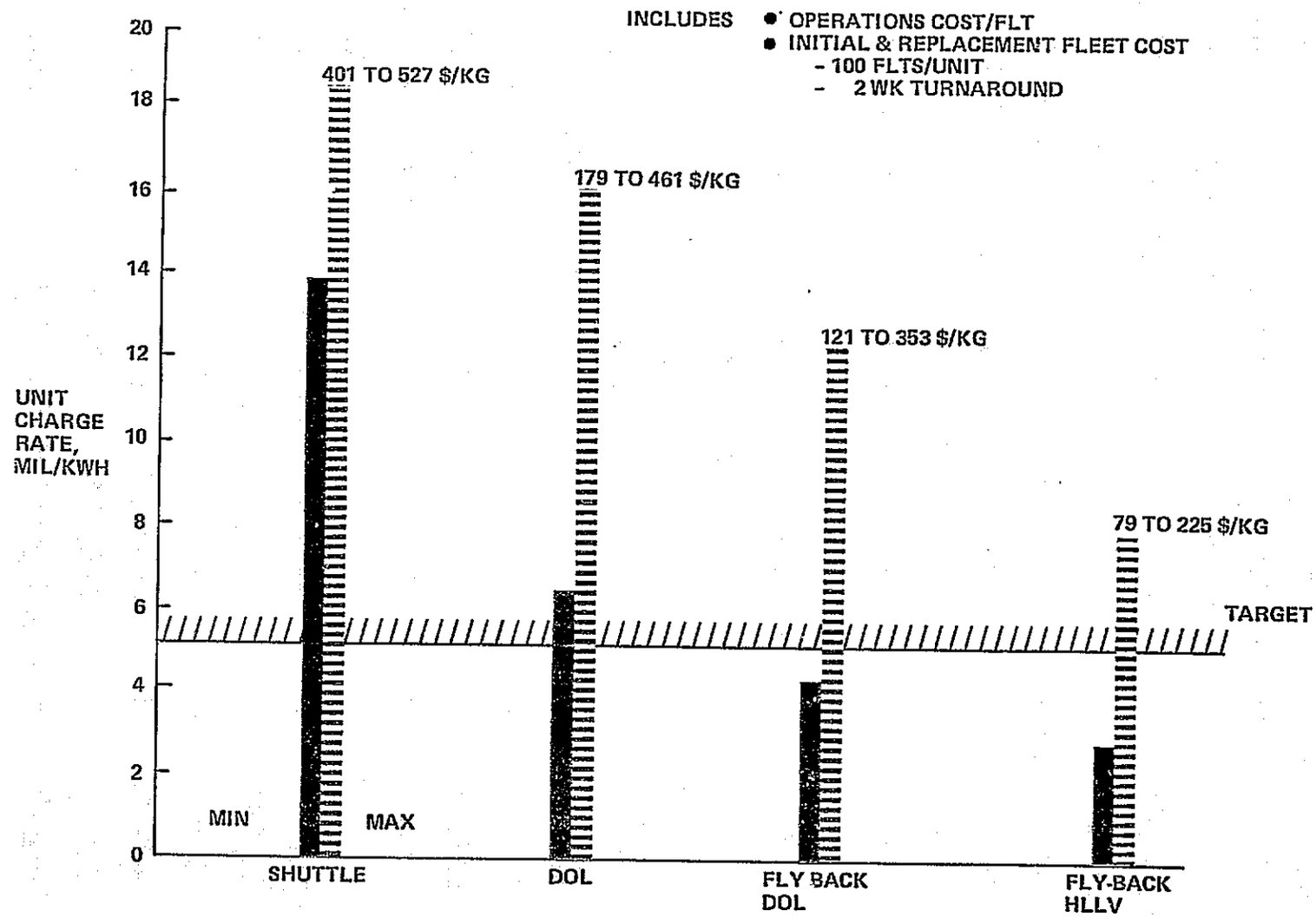

Figure 2.4-4 Launch System Comparisen

(1) TRANSPORT SSPS MATERIAL, 11.5 X 10^6 KG/SSPS
(2) LIFT-OFF-TO LEO

SHUTTLE

- LAUNCH VEHICLE LIFE = 100 FLTS
- TURNAROUND TIME = 2 WKS
- TRAFFIC = 10% OF POWER GROWTH

YR

COST ELEMENT	1990 1 2 3 4 5 6 7 8 9 2000 1 2	3. 4 5 6 7 8 9 10 11	12 13 14 15 16 17	18 19 20
POWER ADDED/YR GW	10 →	20 →	30 →	40 →
SSPS WGT/YR 10^6 KG	22.9 →	45.9 →	68.8 →	91.8 →
LAUNCHES/YR	778 →	1556 →	2334 →	3114 →
FLEET BUYS	30 0 0 0 30 0 0 0 30 0 0 0 30	30 0 0 30 30 0 0 30 30	30 0 30 30 30 0	60 30 30
AVG BUY/YR	9.24 →	16.68 →	20 →	39.9 →

CASH STREAM

OPERATIONS				
MIN x$10^6	8558 →	17116 →	25674 →	34232 →
MAX X$10^6	10892 →	21784 →	32676 →	43568 →
PRODUCTION				
MIN X$10^6	1848 →	3696 →	5544 →	7392 →
MAX X$10^6	2772 →	5544 →	8316 →	11088 →

ECONOMIC FACTORS

- DISCOUNT RATE = 8.65%
- DISCOUNTED DEMAND = 1.15 X 10^{13} KWH
- 100% UTILIZATION

UNIT CHARGE RATE~MIL/KWH

- MIN = 13.89
- MAX = 18.23

Figure 2.4-5 Transportation Evaluation Worksheet

2.4.2 Orbit-to-Orbit Transportation

The cost of transporting the SSPS from LEO to geosynchronous altitude is a strong driver in the selection of the assembly altitude. This section addresses candidate orbit-to-orbit transportation system approaches assuming that assembly is performed at the following altitudes:

- Low earth orbit, 463 Km (250 n mi)
- 12970 Km (7000 n mi)
- Geosynchronous orbit

The assessment of these options indicate that an incremental charge rate of 0.9 Mills/kwh (13% interest, 4% inflation) can be achieved if assembly is performed in LEO and ion propulsion (solar or nuclear) is used to transport the assembled SSPS to geosynchronous orbit. This corresponds to a $26/kg initial investment for orbit-to-orbit transportation. If assembly is performed at 12970 Km using large chemical stages to transport material from LEO and ion propulsion to transport the assembled SSPS to geosynchronous altitude, the orbit-to-orbit transportation cost would run $246/kg. The use of a large nuclear stage to transport materials from LEO to a geosynchronous assembly site would result in a cost of $280/kg.

2.4.2.1 Low Altitude Assembly Site

Figure 2.4-6 presents the characteristics of a typical ion propulsion stage which was used to evaluate the orbit-to-orbit transportation cost. This stage has been sized to transport the entire 11.4×10^6 kg assembled SSPS to geosynchronous orbit using a stage specific weight of 13.6 kg/kw. A launch system cost per flight of $8 million and a payload capability to LEO of 90,800 kg was used to determine costs to transport ion stages and propellants to orbit.

Figure 2.4-7 is a compilation of assumptions, yearly flight rates and fleet purchases used to establish the cash streams presented in Figure 2.4-8. A life per SEPS of 5 flights is assumed. The current 30 cm thruster program has demonstrated 10,000 to 15,000 hour life, Ref. 2.3-1. This would accommodate only two 1 year trip missions. It is felt a two to three fold improvement in thruster life over the next 15 years would be a reasonable assumption. It is also assumed that the SEPS solar array would be refurbished after each flight. The major concern being the degradation of the solar cells during the 160 days travelling through the Van Allen Belts.

PARAMETER	LOW TO GEOSYNCH		7000 n mi TO GEOSYNCH
	OPT 1	OPT 2	
SYS EFFIC, η	.7	.7	.7
– PROP. USE η_u	.9	.9	.9
– PWR EFFIC, η_u	.78	.78	.7
SPECIFIC WT, ,KG/KW	6.8	13.6	6.8
SPECIFIC IMPULSE, SEC	7964	5557	4631
THRUST, N	61.3	62.4	54.5
ELECT PWR, MW	107	78	57
PROP. WT (Hg), KG x 10^6	.77	1.2	0.4
STAGE WT, KG x 10^6	1.5	2.2	.77

Figure 2.4-6 SEPS Characteristics

(1) TRANSPORT ASSEMBLED SSPS TO GEOSYNCH ~ 11.5 MKG/SSPS
(2) ORBIT-TO-ORBIT VEHICLE, SEPS

- SPECIFIC WT = 14 KG/KW
- SPECIFIC IMPULSE = 5178 SEC
- THRUST = 2007N
- POWER = 66 MW
- PROP = 1.23 MKG MERCURY
- STG WGT = 2.2 MKG
- LIFE = 5 FLTS
- SOLAR ARRAY REPLACED AFTER EACH FLT
- LAUNCH SYSTEM PAYLOAD = 86.2 KKG

COST ELEMENT	YR 1990 1 2 3 4 5 6 7 8 9 2000 1 2	3 4 5 6 7 8 9 10 11	12 13 14 15 16 17	18 19 20
POWER ADDED/YR, GW	10 →	20 →	30 →	40 →
SSPS WGT/YR, MKG	23.0 →	45.90 →	68.86 →	91.81 →
SEPS FLTS/YR	2 →	4 →	6 →	8 →
AVG SEPS REPLACED/YR	0.4 →	0.8 →	1.2 →	1.6 →
AVG SEPS REFURB/YR	1.6 →	3.2 →	4.8 →	6.4 →
FLYBACK DOL FLT/YR FOR FUEL	27 →	54 →	81 →	108 →
FLYBACK DOL FLT/YR TO REPLACE SEPS	5 →	10 →	15 →	20 →
FLYBACK DOL FLT/YR TO REFURB SOLAR ARRAY	1 →	2 →	3 →	4 →
TOTAL FLYBACK DOL FLT/YR	33 →	66 →	99 →	132 →
FLYBACK DOL FLEET	2 0 0 0 2 0 0 0 0 0 0 2 0	2 0 0 0 2 2 0 0 0	2 4 0 0 0 2	2 2 0
AVG BUY/YR	0.46 →	0.67 →	1.33 →	1.33 →

Figure 2.4-7 Transportation Evaluation Worksheet

(1) TRANSPORT ASSEMBLED SSPS TO GEOSYNCH USING SEPS

- STAGE COST = $140M
- SEP SOLAR ARRAY COST = $500/KW
- OPERATIONS/FLT
  - GROUND = $1M/FLT.
  - PROPELLANT = $10/LB
- LAUNCH SYSTEM OPS COST = $10M/FLT.
- LAUNCH SYSTEM UNIT COST = $350M

COST ELEMENT 1974$	YR 1990 1 2 3 4 5 6 7 8 9 2000 1 2	3 4 5 6 7 8 9 10 11	12 13 14 15 16 17	18 19 20
SEPS OPS COST/YR, $	57.2×10^6 →	114.4×10^6 →	171.6×10^6 →	228.8×10^6
SEPS REPLACE COST/YR, $	56×10^6 →	112×10^6 →	168×10^6 →	224×10^6
SEPS REFURB COST/YR, $	52.8×10^6 →	105.6×10^6 →	158.4×10^6 →	211.2×10^6
SUBTOTAL $	166×10^6 →	332×10^6 →	830×10^6 →	1494×10^6
FLYBACK DOL OPS COST/YR, $	330×10^6 →	660×10^6 →	990×10^6 →	1320×10^6
FLYBACK FLEET COST/YR, $	161×10^6 →	234.5×10^6 →	465.5×10^6 →	465.5×10^6
SUBTOTAL, $/YR	491×10^6 →	894.5×10^6 →	1455.5×10^6 →	1785.5×10^6
TOTAL, $/YR	657×10^6 →	1226.5×10^6 →	2285.5×10^6 →	3279×10^6

INCREMENTAL UNIT CHARGE RATE = 0.88 MILLS/KWH

Figure 2.4-8 Transportation Cost Worksheet

The cash stream shown in Figure 2.4-8 results in an incremental user charge rates of 0.9 Mills/kWh. This rate is for an SSPS buildup which provides 10% of the added electrical capacity between 1990 and 2020 for a 6-7% growth rate. This charge rate corresponds to a cost-per-weight ratio of $26/kg.

2.4.2.2 12970 Km Altitude Assembly Site

The parametric data shown on Figure 2.4-9 strongly suggests that a high thrust Tug for transportation of material from LEO to a 12970 Km assembly site should have a specific impulse greater than 1000 sec to be cost competitive with the low altitude assembly option. The mass fractions (propellant weight/inert plus propellant weight) plotted on Figure 2.4-9 span a range of stages which represent chemical, (LOX/LH_2) nuclear, ($N\text{-}LH_2$) and advanced nuclear ($N\text{-}LH_2$). The stage labeled "nuclear" assumes use of a solid core nuclear engine similar to the small "alpha" or "gamma" engine from the Los Alamos Scientific Laboratory development program and used in the Nuclear Stage System Definition Study (NAS 8-27051). These stages typically have a mass fraction between 0.7 and 0.8 and specific impulses between 750 and 850 sec. The stage labelled "advanced nuclear" uses a gas core reactor and can potentially reach a specific impulse in excess of 2500 sec at a stage mass fraction of 0.7. The chemical stages can achieve mass fractions in the 0.9 range at specific impulses of as high as 470 sec.

The assembly at 129 70Km would require the development of two potentially high risk stages, the advanced nuclear and large ion stage. Therefore, a detailed assessment of the transportation cost for assembly at 12970 Km assumed the use of a large reusable interorbit chemical vehicle for transport of materials from LEO to 12970 Km, and a solar electric propulsion for transport of the assembled SSPS from 12970 Km to geosynchronous altitude.

Figure 2.4-10 lists the stage characteristics, flight schedule and fleet purchases required to meet the assumed electrical demand for SSPS power. As many as 350 launch vehicle flights per year (approximately one per day) is required in the first year alone to transport propellants and orbit-to-orbit stages to LEO. Eighty-nine RIV flights are required in the first year (approximately two per week) resulting in a significant on-orbit refueling operation.

The cost assumptions and cash streams used to establish unit charge rates for this option are shown in Figure 2.4-11. The incremental unit charge rate is 7.8 Mills/kwh which represents $247/kg.

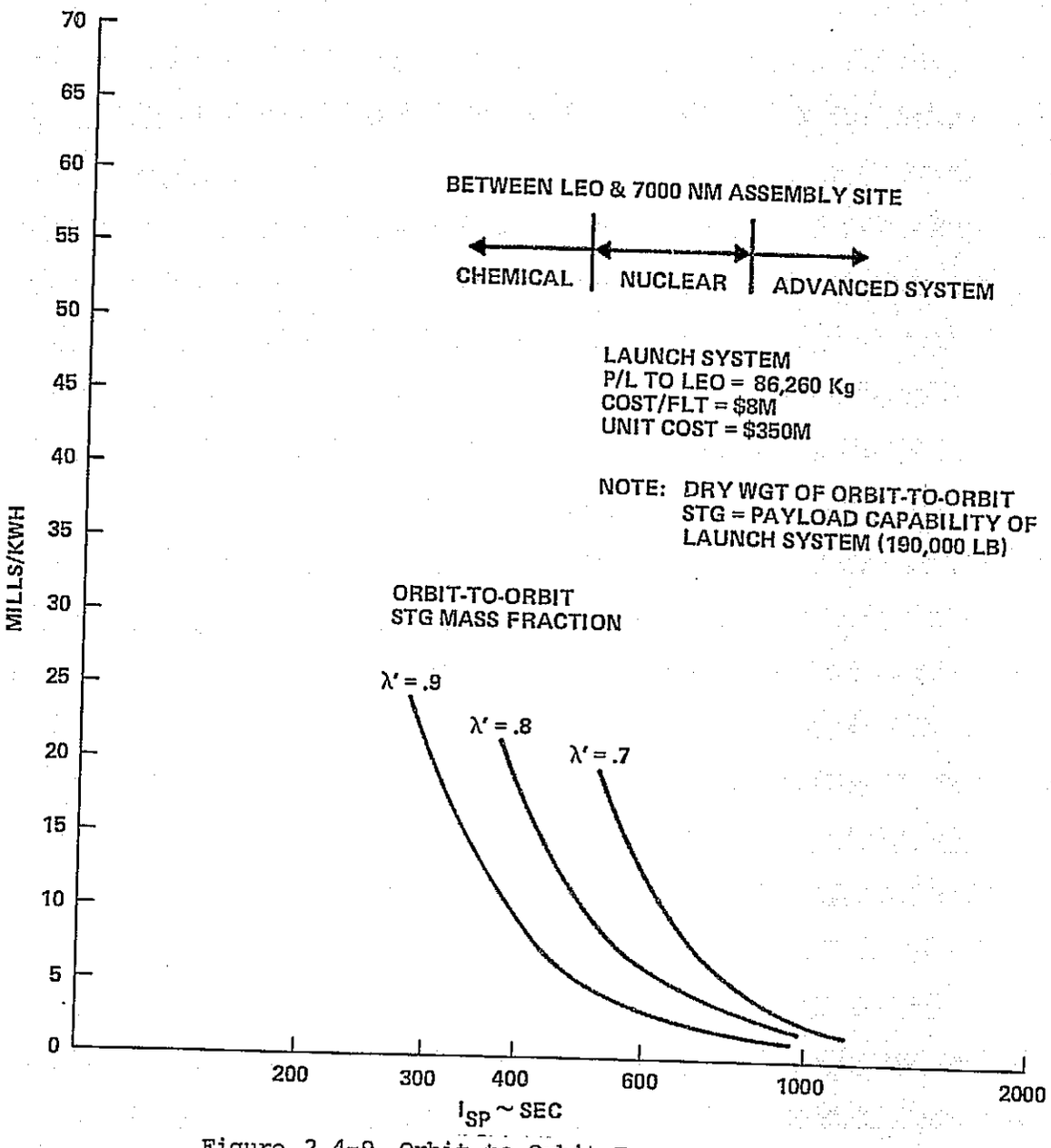

Figure 2.4-9 Orbit-to-Orbit Transport Cost

(1) TRANSPORT MATERIAL FROM LEO TO 12970 KM USING RIV
(2) TRANSPORT ASSEMBLED SSPS FROM 12970 KM TO GEOSYNCH

RIV CHARACTERISTICS/ASSUMPTIONS

- STG WGT = 363 KKG
- $\lambda = 0.9$
- I_{SP} = 465 SEC
- LIFE = 25 FLTS
- P/L FROM LEO TO 12970 KM= 259 KKG
- 2 WK TURNAROUND

LAUNCH SYSTEM

- P/L TO LEO = 86.2 KKG
- TURNAROUND TIME = 2 WKS
- LIFE = 100 FLTS

SEPS CHARACTERISTICS/ASSUMPTIONS

- SPECIFIC WT = 14 KG/KW
- SPECIFIC IMPULSE = 3252 SEC
- THRUST = 55.6 N
- POWER = 41 MW
- PROP = 0.59 MKG
- STG WGT = 0.54 MKG
- LIFE = 5 FLTS
- SOLAR ARRAY REPLACED AFTER EACH FLT
- P/L FROM 12970 TO GEO = 11.5 MKG

COST ELEMENT	YR 1990 1 2 3 4 5 6 7 8 9 2000 1 2	3 4 5 6 7 8 9 10 11	12 13 14 15 16 17	18 19 20
POWER ADDED/YR, GW	10	20	30	40
SSPS WGT/YR, MKG	23.0	45.90	68.86	91.81
SEPS FLTS/YR	2	4	6	8
AVG SEPS REPLACED/YR	.4	.8	1.2	1.6
AVG SEPS REFURB/YR	1.6	3.2	4.8	6.4
RIV FLT/YR FOR SEP FUEL	4	8	12	16
RIV FLT/YR TO REPLACE SEP	1	2	3	4
RIV FLT/YR TO REFURB SOLAR ARRAY	1	2	3	4
RIV FLT/YR FOR SSPS	89	178	267	356
TOTAL RIV FLT/YR	95	190	285	380
AVE RIV PURCHASES/YR	4	8	12	16
LAUNCHES/YR FOR SEP FUEL	11	22	33	44
LAUNCHES/YR TO REPLACE SEP	2	4	6	8
LAUNCHES/YR TO REFURB SEP SOLAR ARRAY	1	2	3	4
LAUNCHES/YR FOR RIV FUEL	338	667	1014	1352
LAUNCHES/YR TO PLACE RIV	1	2	3	4
TOTAL LAUNCHES/YR	353	706	1059	1412
LAUNCH FLEET	14 14 14 14 14	14 14 14 14 14 14 14	28 14 28 14	42 14
AVG PURCHASE/YR	5.4	9.3	14	18.7

Figure 2.4-10 Transportation Evaluation Worksheet

(1) TRANSPORT MATERIAL FROM LEO TO 12970 KM USING RIV
(2) TRANSPORT ASSEMBLED SSPS FROM 12970 KM TO GEOSYNCH

RIV
- OPS = $1M/FLT.
- UNIT = $36M

LAUNCH SYSTEM
- OPS = $10M/FLT
- UNIT = $350M

SEPS ASSUMPTIONS
- PROPULSION COST = $125M
- SOLAR ARRAY COST = $500/KW
- OPERATIONS/FLT
  - GROUND = $1M/FLT
  - PROPELLANT = $22/KG

(1974 $)

COST ELEMENT	1990 1 2 3 4 5 6 7 8 9 2000 1 2 YR	3 4 5 6 7 8 9 10 11 YR	12 13 14 15 16 17 YR	18 19 20 YR
SEPS OPS COST/YR, $	22.6×10^6 →	45.2×10^6 →	67.8×10^6 →	90.4×10^6
SEPS REPLACE COST/YR, $	50×10^6 →	100×10^6 →	150×10^6 →	200×10^6
SEPS REFURB COST/YR, $	32.8×10^6 →	65.6×10^6 →	98.4×10^6 →	131.2×10^6
SUBTOTAL, $/YR	105.4×10^6 →	210.8×10^6 →	316.2×10^6 →	421.6×10^6
RIV OPS COST/YR, $	95×10^6 →	190×10^6 →	285×10^6 →	380×10^6
RIV FLEET COST/YR, $	120×10^6 →	240×10^6 →	360×10^6 →	480×10^6
SUBTOTAL, $	215×10^6 →	430×10^6 →	645×10^6 →	860×10^6
LAUNCH OPS COST/YR, $	353×10^6 →	7060×10^6 →	1059×10^6 →	14120×10^6
LAUNCH FLEET COST/YR, $	1890×10^6 →	3255×10^6 →	4900×10^6 →	6545×10^6
SUBTOTAL, $/YR	5420×10^6 →	10315×10^6 →	15490×10^6 →	20665×10^6
TOTAL, $/YR	5740.4×10^6 →	10955×10^6 →	16451×10^6 →	21946×10^6

NPV = 8.812×10^{10}

INCREMENTAL UNIT CHARGE RATE = 7.662 MIL/KWH

Figure 2.4-11 Transportation Cost Worksheet

2.4.2.3 Geosynchronous Altitude Assembly Site

Figure 2.4-12 parametrically shows the relationship between orbit-to-orbit stage characteristics, launch system performance, and incremental unit charge rate. As in the case of the 12970 Km assembly site case, a high performance gas core reactor or ion stage would be required for this option to be cost competitive with the low altitude assembly plan. The alternate to using large transfer stages would be to use a medium sized ion stage to transport subassemblies to the geosynchronous site. The sensitivity to launch system payload to LEO is relatively small.

Figure 2.4-13 is a listing of Solid Core Nuclear stage characteristics, yearly flight rates and fleet requirements used in the cost streams shown in Figure 2.4-14. The incremental charge rate for this option is 8.7 Mills/kwh. This equates to $280/kg.

It is apparent that assembly at geosynchronous is not cost competitive with the low altitude assembly option if the nuclear high thrust vehicle is used. If smaller solar electric stages are used with a payload to geosynchronous altitude of approximately 200,000 kg, the incremental cost for orbit-to-orbit transport would be 1 Mill/kwh, approximately the same as for the low altitude assembly approach. The major difference between using only one large ion stage to transport the entire assembly versus perhaps 25 smaller ion stages would be an increase in mission control costs.

2.4.2.4 Supporting Data

Figures 2.4-15 through 2.4-17 list the characteristics and cost assumptions used in the comparison of the ion, chemical and nuclear tug. Ref. 2.3-3 was used to establish Cost Estimating Relationships (CER's) for application to these stage concepts. Ref. 2.3-3 quoted costs in 1970 dollars. An average inflation rate of 6.5% per year was used to establish costs in 1974 dollars.

The cost estimates for the electric stage, Figure 2.4-15, is considered optimistic. This data was extrapolated from information presented in ref. 2.3-3 for two solar electric stages with 20 kw and 40 kw power sources and two nuclear electric stages with 120 kw and 240 kw power sources. The ion stages being considered in this study require between 40 and 70 mw, several orders of magnitude higher than the available data base. Conversations with NASA LeRC personnel indicate that the current 30 cm (133 millinewton of thrust) engine costs $60,000 in lots of six. This equates to $4.4M/Kg or thrust. Cost data on the power conditioners is very sketchy at best due primarily to the status of technology at this time. LeRC

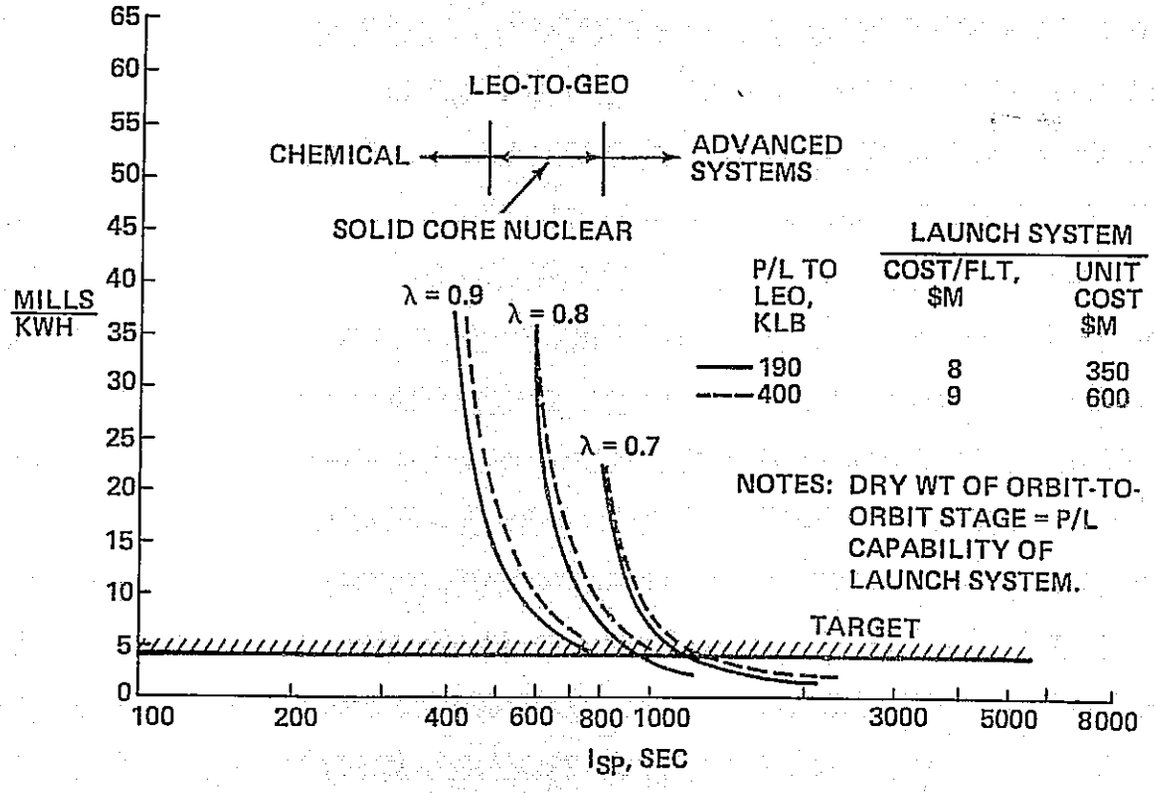

Figure 2.4-12 Orbit-to-Orbit Transport Cost

(1) TRANSPORT MATERIAL FROM LEO TO GEOSYNCH & ASSEMBLE.

LAUNCH VEHICLE

- P/L TO LEO = 86.2 KKG
- TURNAROUND = 2 WKS
- LIFE = 100 FLTS

NUCLEAR STG CHARACTERISTICS, SOLID CORE REALTOR

- STG WGT = 363 KKG
- $\lambda = 0.8$
- I_{SP} = 800 SEC
- P/L TO GEOSYNCH = 205 KKG
- LIFE = 25 FLTS
- TURNAROUND = 2 WKS

COST ELEMENT	1990 1 2 3 4 5 6 7 8 9 2000 1 2	3 4 5 6 7 8 9 10 11	12 13 14 15 16 17	18 19 20
POWER ADDED/YR~ GW	10 →	20 →	30 →	40 →
SSPS WGT/YR~ MKG	23.0 →	45.90 →	68.86 →	91.81 →
NUC FLTS/YR	112 →	224 →	336 →	448 →
NUC PURCHASED/YR	4 →	8 →	12 →	16 →
LAUNCH/YR FOR PROPELLANT	378 →	756 →	1134 →	1512 →
LAUNCH/YR TO REPLACE STAGE	4 →	8 →	12 →	16 →
TOTAL UPPER STG FLTS/YR	382 →	764 →	1146 →	1528 →
LAUNCH SYSTEM PURCH	11 0 0 11 0 0 11 0 0 11 0 0 11	11 0 11 11 0 11 11 0 11	22 0 11 22 0 11	33 0 11
AVG BUY/YR	4.2 →	7.3 →	11 →	14.6 →

Figure 2.4-13 Transportation Evaluation Worksheet

(1) TRANSPORT MATERIAL FROM LEO TO GEOSYNCH & ASSEMBLE

LAUNCH SYSTEM

- OPS = $10M/FLT
- UNIT = $350M

NUCLEAR TUG

- OPS = $1M/FLT
- UNIT = $600M

(1974 $)

COST ELEMENT	1990 1 2 3 4 5 6 7 8 9 2000 1 2	3 4 5 6 7 8 9 10 11	12 13 14 15 16 17	18 19 20
NUCL. TUG OPS $/YR	112×10^6 →	224×10^6 →	336×10^6 →	448×10^6
TUG FLEET COST $/YR	240×10^6 →	450×10^6 →	720×10^6 →	960×10^6
SUBTOTAL, $/YR	352×10^6 →	704×10^6 →	1056×10^6 →	1408×10^6
LAUNCH OPS $/YR	3820×10^6 →	764×10^6 →	11460×10^6 →	15280×10^6
LAUNCH FLEET COST $/YR	1470×10^6 →	2555×10^6 →	3850×10^6 →	5110×10^6
SUBTOTAL, $/YR	5290×10^6 →	10195×10^6 →	15310×10^6 →	20390×10^6
TOTAL, $/YR	5642×10^6 →	10899×10^6 →	16366×10^6 →	21798×10^6

INCREMENTAL UNIT CHARGE RATE = 8.73 MILLS/KWH

Figure 2.4-14 Transportation Cost Worksheet

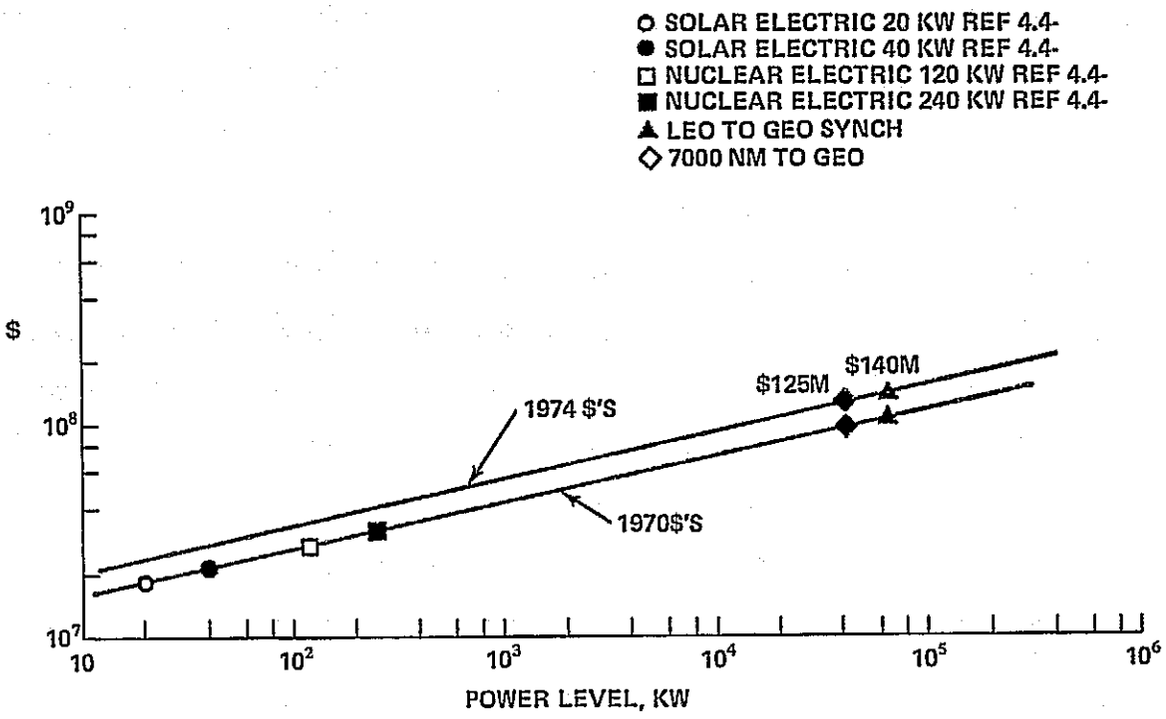

Figure 2.4-15 Unit Cost, Electric Propulsion

STAGE WEIGHT		363 KKG	
PROPELLANT WEIGHT		327 KKG	
I_{SP}		465 SEC	
LIFE		25 FLTS	
P/L TO 12970 KM		259 KKG	
	UNIT COST		
	$M	(1974 $)	
STRUCTURE	3.2		(SHUTTLE EXTERNAL TANK)
PROPULSION	4.0		(SSME)
ASTRIONICS	9.0		
THERMAL CONTROL	.6		
ASSEMBLY $ C/O*	16		
SUBTOTAL	32.7		
10% FOR MANAGEMENT	3.3		
TOTAL	36.0		
*INCLUDES SPARES & TOOLING			
OPERATION COST			
ACTIVITY LEVEL DEPENDENT COST/FLT	= .16		
ACTIVITY LEVEL INDEPENDENT COST/YR	= 9.77		

Figure 2.4-16 Supporting Data, Chemical Reusable Interorbit Vehicle

STAGEWEIGHT	363 KKG	
PROPELLANT WEIGHT	290 KKG	
I_{SP}	800 SEC	
LIFE	25 FLTS	
P/L TO GEO	205 KKG	
	UNIT COST $M (1974$)	
STRUCTURE	3.2	(SHUTTLE EXTERNAL TANK)
PROPULSION	8.2	(GAMMA ENGINE)
AUXILIARY PROPULSION	2.5	
ASTRIONICS	9.0	
ENVIRONMENT PROTECTION	.8	
ASSEMBLY & C/O*	32.5	
10% FOR MANAGEMENT	5.4	
TOTAL	61.6	

Fig 2.4-17 Supporting Data, Nuclear Reusable Interorbit Vehicle

would guess the cost of the power conditioner at $300,000 per thruster or the equivalent of $22M/Kg of thrust. This is based primarily on the cost of lab breadboard/brassboard models.

The ion propulsion stage is still the concept of choice even with a very conservative cost factor of $26.5 M/Kg of thrust. A repeat of the cost analysis using these high costs results in an incremental unit charge rate of only 3.5 Mills/kwh or an equivalent cost of $106/kg. The insensitivity of cost to very large variations in ion stage unit cost, performance and specific weight strongly suggests that this approach offers the least economic risk of all the orbit to orbit transportation options.

The cost estimates for the chemical, Figure 2.4-16, and the nuclear tug, Figure 2.4-17, were based on Ref. 2.3-3 and other source information on engine and tank costs.

2.4.2.5 Concept Comparison

Figure 2.4-18 summarizes a comparison of orbit-to-orbit transportation options. The lowest cost approaches involve use of ion propulsion. Assembly can be performed either in low earth orbit or at geosynchronous orbit and still result in approximately the same transportation cost. Those options using either a chemical or nuclear Tug result in unacceptably high costs. It is recommended that the large Tug not be considered as a prime mode for transport of material, though these type stages may have a place in the assembly and maintenance schemes as a personnel transporter.

The ion propulsion appears to offer the lowest cost approach for orbit-to-orbit transport of material. Many technology issues must be addressed before this approach can come to fruition. The following is a list of the more significant issues:

1. Development of large diameter thruster - Current engine development (LeRC) has concentrated on a 30 cm thruster. An extension of the ion thruster diameter to 1 meter seems within technical feasibility. The grid material of the engine will be the limit to the size of these devices. As the thruster operates, the grids distort thermally varying the spacing between the grids. Current grid material is columbium (Cb). For the next generation thruster, efforts are leaning to dished grids which will compensate for thermal growth and maintain constant grid spacing.

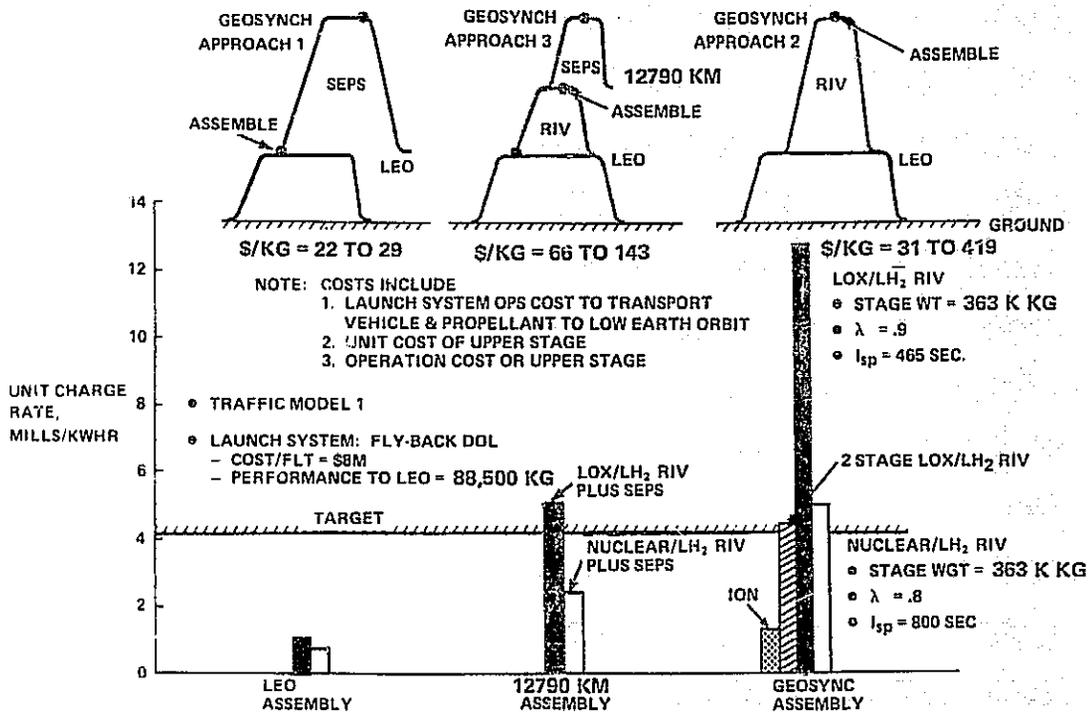

Figure 2.4-18 Concept Comparison, Orbit-to-Orbit Transportation

2. Selection and development of the power source. The major concern here is that to achieve the cost benefits offered by ion propulsion, the stage must transport materials through the Van Allen Belts. The silicon photovoltaic power source used as a baseline in these tradeoff study may not be the best approach when performance degradation of the cell due to radiation while in the Belts is more precisely taken into account. Alternates to this approach could be the use of Gallium Arsenide solar cells. The GaAs-cell appears to have a high degree of radiation resistance.

   Other power sources, such as nuclear or solar thermal, could readily get around the radiation problem but would introduce other technology problems. What is needed is an across the board system studies of all options to better identify the more attractive approaches and better define the technology issues.

3. Selection of the propellant. To date most technology development and systems study activity has concentrated on mercury as the propellant. Use of this material on as large a basis as is needed for the SSPS may not be acceptable to environmentalist; nor will it be acceptable in terms of the potential contamination to SSPS sensitive devices as the microwave converters and solar cells.

   Cesium has been considered as an alternate to mercury, however, no high voltage isolator material is available for use with Cesium. As in the case with selection of the power source, an across the board systems study of the propellant options is needed to better identify technology requirements.

2.4.3 Assembly

2.4.3.1 Fabrication and Packaging

A key tradeoff for obtaining cost competitive space-generated power is to determine the level of ground prefabrication versus the corresponding level of orbital assembly for each major component of the SSPS. The SSPS has a density of 1.0×10^{-3} Kg/M^3 while the launch vehicle has a density of 1 to 96 Kg/M^3. The method of packaging and assembling the spacecraft low density components will have a significant impact on transportation costs in terms of the launch system load factor (% of usable payload) that can be achieved on each flight.

Figure 2.4-19 outlines three approaches for part fabrication. Approach I assumes manufacture of articulated lattice tri-beams on the ground. These beam members can be compressed to 1/30 of their deployed length for packaging in the launch vehicle. Approach II assumes prefabrication on the ground of the longerons and intercostal elements of a structural tri-beam. Assembly of the beam is then performed in a manned space station using jigs and fixtures. Approach III assumes ground personnel prepare flat stock with appropriate coatings for installation into an automatic manufacturing module in space.

Figure 2.4-20 summarizes the pertinent characteristics of these approaches. Approach I, with the articulated lattice beam, could have a low packaging density. As many as 3582 additional flights of a launch system with 9.07×10^4 Kg payload capability and a packaging density of 48 Kg/M^3 would be required to deliver the volume represented by 1940 1.94×10^6 Kg of solar array and antenna structure. This increases overall system cost significantly.

Transport of the basic elements (Approach II) improves packaging density, but may require a large crew in orbit to perform parts assembly. At an assembly rate of 2.7 Kg/manhour, 22 12-man space stations are required to complete assembly in one year. The cost of space stations, the cost to transport and resupply the space stations add up to a significant contribution to overall system cost.

Complete fabrication and parts assembly in orbit (Approach III) can achieve 100% launch system load factors by transporting flat stock to an automated fabrication spacecraft. This concept requires a free flying or space station supported factory. It increases productivity greatly and reduces overall cost to manageable levels.

Fig. 2.4-21 is a conceptual drawing of a possible space fabrication unit. In this example, six drums of aluminum edge stripping are fed to forming rollers. A series of welding heads and cutters are used to fabricate the structural member from the formed stripping. An operations analysis of this automated process has estimated a rate of fabrication at 420 lb/hr. At this rate, two units would be required to produce the structural elements of the SSPS in one year.

Many issues need to be addressed to assess the feasibility of these machines. Some of these problems are:

- The need for heat treatment of the finished product
- Welding at zero-g

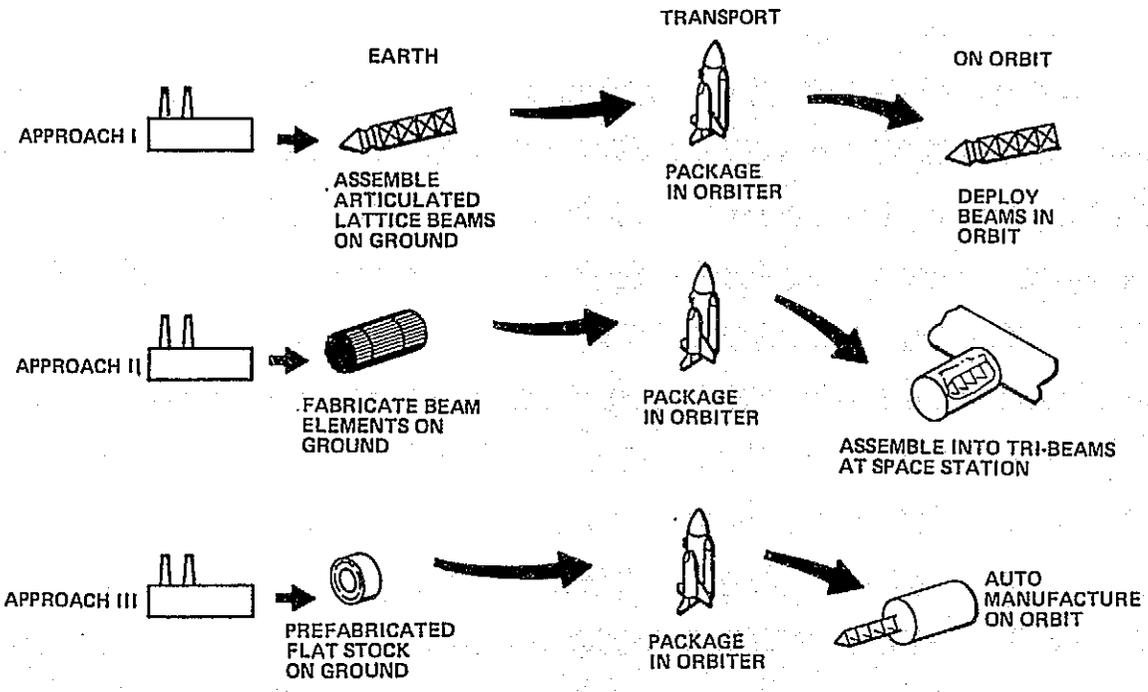

Figure 2.4-19 Structural Detail Parts Assembly Options

	APPROACH I	APPROACH II	APPROACH III
• CONDITION			
– GROUND	ASSEMBLE ARTICULATED BEAMS	FORM LONGERONS & CROSS MEMBERS	PREPROCESS FLAT STOCK
– IN-ORBIT	DEPLOY	ASSEMBLE	MANUFACTURE
• PKG DENSITY	1.6 TO 48 KG/M^3	14 TO 1200 KG/M^3	1600 KG/M^3
• SUPT EQUIP.	DEPL CANNISTER	22 SPACE STA	MANUFACTURE MODULES
• NO. F/B DOL FLTS TO DEPLOY STRUCT	3604 TO 120	352	22

Figure 2.4-20 Fabrication Option Comparison

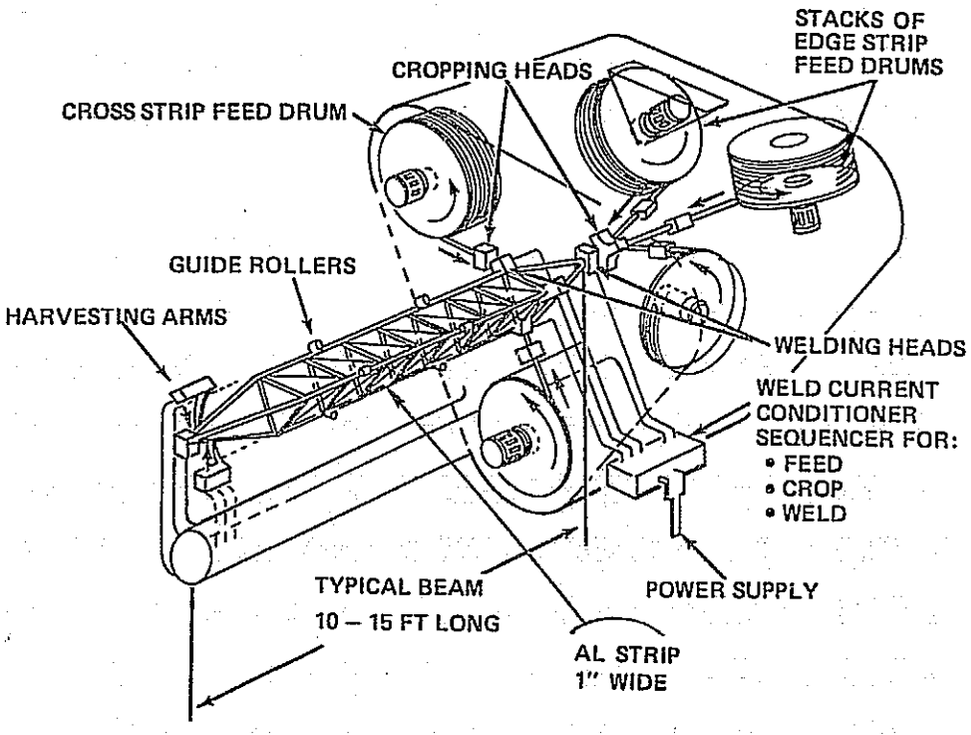

Figure 2.4-21 Fabrication of Compression Girders

- Application of coatings
- Rigging of the tension cable
- Internal stress levels introduced by the process
- Alignment.

2.4.3.2 Method of Assembly

The major issue to be answered, before cost effective SSPS assembly can be achieved, involves determining the degree of on-orbit manned participation in the assembly operation. In an effort to bound the problem, the following two extremes in basic approach to assembly have been considered:

- Remote assembly using teleoperators controlled from the ground
- EVA assembly.

2.4.3.2.1 Structural Assembly - The first requirement in this assessment is to establish an estimate for production rate. The assembly of a common component of the antenna structure, following the remote controlled functions shown in Figure 2.4-22, was assessed in Ref. 2.3-1. The time line analysis of these functions are shown in Fig. 2.4-23. Structural assembly of the antenna structure was estimated to be assembled at a rate of between 3 and 6 Kg/hr using teleoperators. A similar assessment of assembly using men in an EVA mode was assessed using the functions and estimated times shown in Figure 2.4-24. Structural assembly rates using the EVA approach was estimated to be somewhat higher, lying between 8 and 11 Kg/m-hr.

Recent studies performed by Martin (NAS 9-14319) established a rate of assembly for the antenna structure of between 300 and 400 kg/hr. Martin estimated that 2.3×10^6 kg of antenna structure could be assembled in nine months with teleoperators working 24 hours a day.

By way of comparison, a crew of six steel workers can raise the frame of a major building at the rate of 68 kg/m-hr (Means Building Guide). Aircraft final assembly, which includes not only the assembly of major structural elements, but

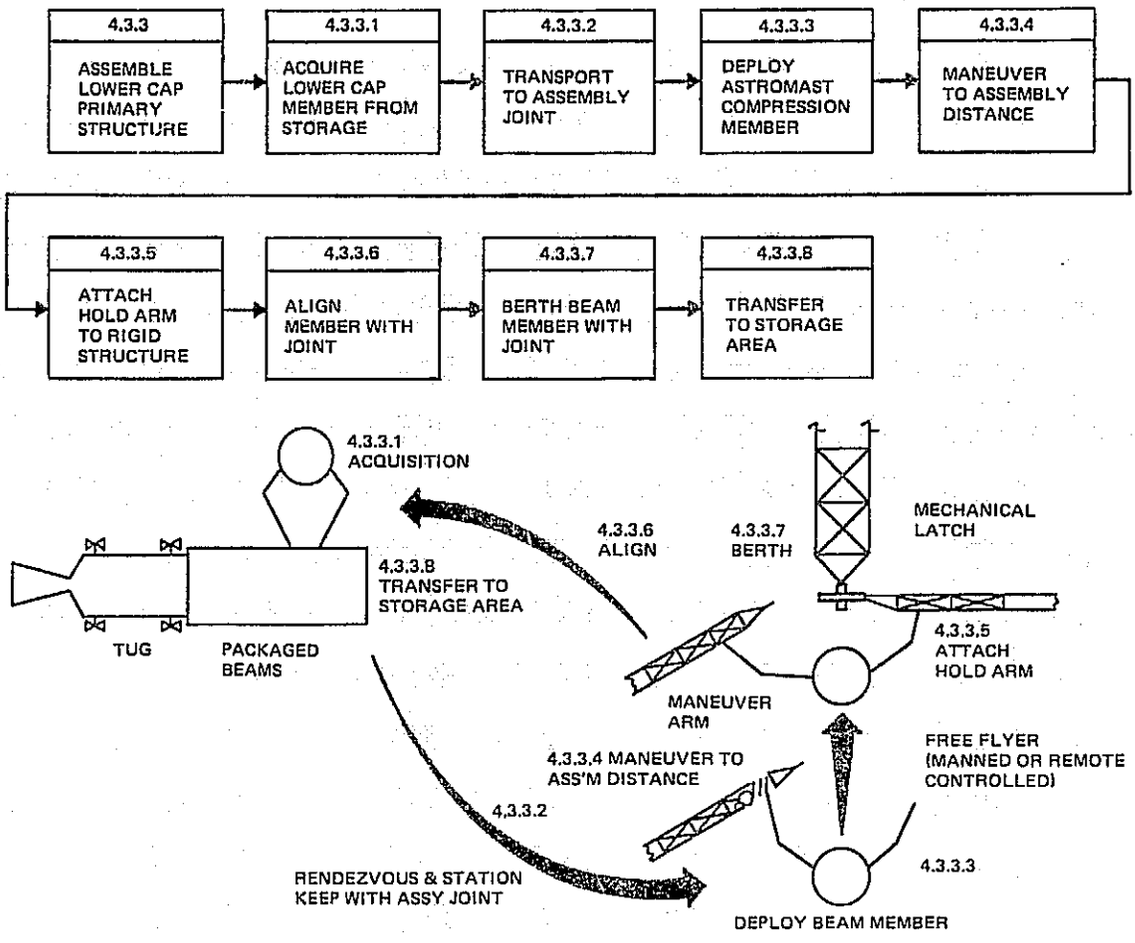

Figure 2.4-22 Remote Assembly of Structure, Typical Sequence

EVENT		TIME, MIN.				CONSUMABLES, KG			
		MINIMUM		MAXIMUM		PROPELLANT		ECS	
		ΔT	T	ΔT	T	MIN	MAX	MIN	MAX
4.3.3.1	ACQUIRE LOWER CAP FROM STORAGE	3.0	3.0	10.5	10.5	0.13	0.544	0.621	1.0
4.3.3.2	TRANSPORT TO ASSEMBLY JOINT	6.0	9.0	6.0	16.5	2.14	2.14		
4.3.3.3	DEPLOY ASTROMAST	2.0	11.0	2.0	18.5	0.11	0.11		
4.3.3.4	MANEUVER TO ASSEMBLY DISTANCE	0.5	11.5	0.5	19.0	1.4	1.4		
4.3.3.5	ATTACH HOLD ARM	3.0	14.5	10.5	29.5	0.16	0.54		
4.3.3.6	ALIGN MEMBER WITH ATTACH JOINT	3.0	17.5	10.5	40.0	0.16	1.2		
4.3.3.7	BERTH BEAM MEMBER WITH JOINT	1.0	18.5	1.0	41.0	0.05	0.05		
4.3.3.8	TRANSFER TO STORAGE AREA	5.0	23.5	5.0	46.0	2.14	2.14		
					TOTAL Kg	6.29	7.43	0.53	1.04

Figure 2.4-23 Remote Assembly Timeline

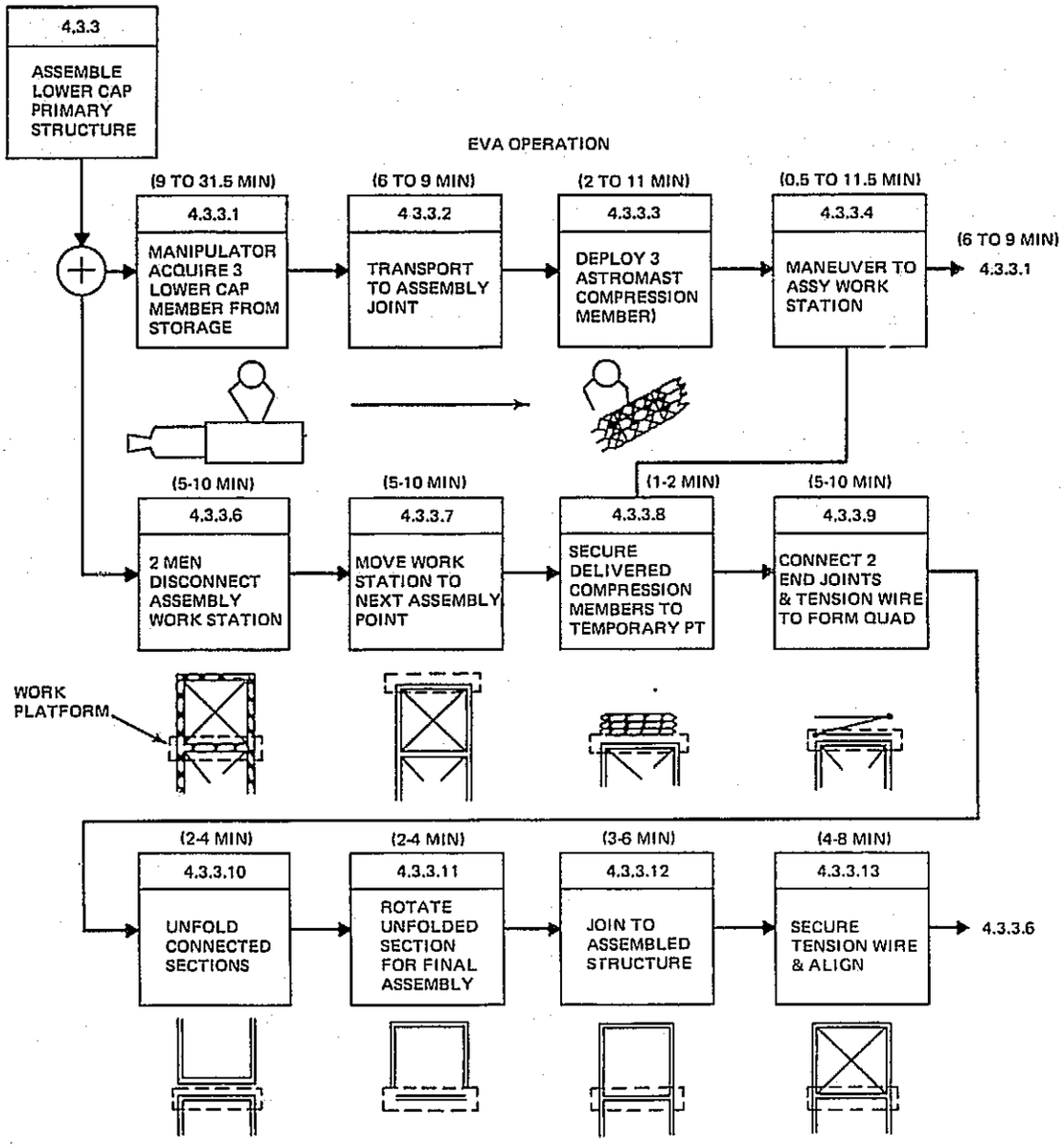

Figure 2.4-24 EVA Assemble Lower Cap; Primary Structure

also includes installation of hydraulics and electronics, is performed at the rate of 0.1 to 0.9 Kg/m-hr. It is anticipated that assembly of the SSPS will be somewhere between these extremes.

A cash flow analysis, which considers the cost of supporting space stations, launch costs to place the space station in orbit, and launch costs to resupply and recycle crews on 60 day centers was performed. At a structural assembly rate of 11 kg/m-hr, 117 crew members would be required to complete construction of one SSPS structure in one year. Ten 12 man modular space stations, or the equivalent, would be required to support the crew, and 58 Shuttle flights/year (six men per launch) would be required to resupply and recycle crews. The incremental unit charge rate for assembling the structure amounts to 2.6 Mills/kwh or approximately $66/kg for the 2 to 3 x 10^6 kg of SSPS structure.

If teleoperators are used and controlled remotely, 35 units are required to complete assembly of the structure in one year at a rate of 6 kg/hr. Elements included in the cost assessment are:

- Cost to transport teleoperators to the assembly site
- Cost to transport teleoperator propellants (0.1 Kg of propellant per kilogram of structure assembled)
- Cost to transport a six-man monitor crew to the assembly site every 30 days
- Cost for two TDRS systems for TV relay to earth
- Cost for ground crews to operate the teleoperators
- Unit costs of teloperators and launch system fleet replacement.

The remote controlled structural assembly approach results in an incremental increase in unit charge rate of only 0.2 Mills/khw or $8.8/kg. Figures 2.4-25 and 2.4-26 are the work sheets used in the cash flow analysis of assembly operations of the structure. All assumptions used in the analysis are indicated.

2.4.3.2.2 Assembly of Entire SSPS at Low Altitude - The above discussion addressed only the structural assembly. Assessment of the entire SSPS assembly would require significantly more depth of definition of each satellite component in order to

COST ELEMENT	1990 1 2 3 4 5 6 7 8 9 2000 1 2	3 4 5 6 7 8 9 10 11	12 13 14 15 16 17	18 19 20
STRUCTURAL WT/YR, MKG	3.88 →	7.766 →	11.64 →	15.53
MANHOURS/YR	3.45×10^5 →	6.9×10^5 →	10.4×10^5 →	13.8×10^5
MEN IN ORBIT	117 →	234 →	351 →	468
12 MAN SPACE STATIONS	11 →	22 →	33 →	44
AVG S/S REPLACE/YR	1.68 →	2.44 →	3.66 →	3.66
TRANSPORTATION				
AVG FLYBACK DOL FLTS/YR TO LAUNCH S/S	2.0 →	4.36 →	10.5 →	21.8
SHUTTLE SLTS/YR TO ROTATE CREW	58 →	116 →	174 →	232
AVG SHUTTLE FLEET REPLACEMENT/YR	0.67 →	1.2 →	1.45	2.89
• SPACE STATION COST, $/YR	1.275×10^9 →	1.856×10^9 →	2.778×10^9	2.778×10^9
• MANPOWER COST, $/YR	14.04×10^6 →	28.08×10^6 →	42.12×10^6	56.16×10^6
• SHUTTLE OPS COST, $/YR	0.638×10^9 →	1.276×10^9 →	1.914×10^9	2.552×10^9
• SHUTTLE FLEET COST, $/YR	0.134×10^9 →	0.240×10^9 →	0.290×10^9	5.78×10^9
• FLYBACK DOL OPS, $/YR	16×10^6 →	34.88×10^6 →	84×10^6	174.4×10^6
TOTAL	2.077×10^9 →	3.1349×10^9 →	5.108×10^9	11.34×10^9

MILLS/KWH = 2.77

SPACE STATION

- WT = 101,910 KG
- LIFE = 10 YR

ASSEMBLY MODE: EVA, 56 HR WK, LEO ASSEMBLY
ASSEMBLY RATE: 11 KG/M-HR
ASSEMBLY PERIOD: 1 YEAR/SSPS

- 3 CREWS $40,000/MYR
- SPACE STATION = $759M/UNIT
- FLYBACK DOL COST/FLT = $8M
- SHUTTLE COST/FLT = $11M
- SHUTTLE UNIT COST = $200 M

Figure 2.4-25 Assembly Evaluation Worksheet - EVA Operations (SSPS Structure)

COST ELEMENT	1990 1 2 3 4 5 6 7 8 9 2000 1 2	3 4 5 6 7 8 9 10 11	12 13 14 15 16 17	18 19 20
	YR			
STRUCTURAL WT/YR, MKG	3.88 →	7.766 →	11.64 →	15.53 →
MACHINE HR/YR, HR	$.658 \times 10^6$ →	1.317×10^6 →	1.975×10^6 →	2.633×10^6
MACHINES IN ORBIT	75 →	150 →	225 →	300 →
AVG MACHINE BUY/YR	23.1 →	41.7 →	50 →	23 →
MACHINE CONSUM./YR, KG	3.88×10^6 →	$.7766 \times 10^6$ →	1.164×10^6 →	1.55×10^6
TRANSPORTATION				
• FLYBACK DOL FLT/YR	4.6 →	9.1 →	13.6 →	18 →
• SHUTTLE FLT/YR (MONITORING)	24 →	48 →	72 →	96 →
NO. TDRS SYSTEMS	4 →	8 →	12 →	16 →
AVG BUY/YR	.62 →	.89 →	1.33 →	1.33 →
• MACHINE BUY/YR, $	23.1×10^6 →	41.7×10^6 →	50×10^6 →	23×10^6 →
• FLYBACK DOL OPS/YR, $	36.8×10^6 →	72.8×10^6 →	108.8×10^6 →	144×10^6 →
• SHUTTLE OPS/YR, $	312×10^6 →	624×10^6 →	936×10^6 →	1248×10^6
• TDRS BUYS/YR, $	18.6×10^6 →	26.7×10^6 →	39.9×10^6 →	39.9×10^6
• MANPOWER (GRD)	9×10^6 →	18×10^6 →	27×10^6 →	36×10^6 →

MILLS/KWH = 0.5

TELEOPERATOR

- WT = 181 KG
- CONSUMABLES = 0.1 LB/LB STRUCTURE
- LIFE = 5 YRS

SHUTTLE OPS = $13M/FLT
(INCLUDE SUPPORT MODULES)

FLYBACK DOL = $8M/FLT

ON-ORBIT MONITOR & SERVICE:

1 SHUTTLE/MONTH/SSPS

TDRS: 2 SYSTEMS/SSPS (10 YR LIFE)

TDRS
– $30M/SYSTEM

ASSEMBLY MODE: REMOTE
LEO ASSEMBLY

RATE = 5.9 KG/HR
WORK WK = 168 HRS

TELEOPERATORS:
UNIT = $1M

MANPOWER:

– 3 MEM/TELEOPERATOR
– $40,000/YR

Figure 2.4-26 Assembly Evaluation Worksheet - Remote Control OPS (SSPS Structure)

detail assembly flows and operations. Therefore, a parametric analysis has been performed varying what has been found to be the driver elements in the two basis assembly approaches.

The major cost drivers for remote controlled assembly shown in Figure 2.4-27, are assembly rate, teleoperator consumables rate and the number of manned maintenance/monitor facilities required. The manned facility assumed in generating Figure 2.4-27 is the Shuttle with a crew of six and an on-orbit operation time of 30 days per flight. A remote controlled assembly approach can achieve acceptable costs (2 to 4 Mills/kwh) at a production rate of 2 kg/hr if consumables usage is kept low.

The key technology issues with the remote controlled approach are communications and the overall complexity of mission planning required to safely perform assembly with many teleoperators in operation simultaneously.

Figure 2.4-28 relates the major cost driver for a space-based manned controlled assembly operations to the contribution final assembly makes to the unit charge rate (Mills/kwh) and cost per pound for assembly. The major drivers are assembly rate in terms of Kg/man-hour, the cost of space stations (assumes 10 year life) and the cost to recycle crews. No assumptions are made as to the level of automation achieved in the operation.

To achieve reasonable cost levels, i.e. 4 Mills/kwh, production rates in excess of 11 Kg/hr. are required along with low cost space stations ($16M/man) and transport modes that can recycle large numbers of crew members in one flight.

Figure 2.4-29 presents a comparison of cost between assembly at low altitude and at geosynchronous altitude for a remote controlled approach. The Shuttle, used as the manned maintenance/monitor facility at low orbit, is replaced by a six-man geosynchronous orbit space station. The appropriate manned Tug was added to the geosynchronous assembly site scenario.

Assembly at geosynchronous orbit tends to double assembly cost, though at assembly rates greater than 10 lb/hr, acceptable cost can be achieved. It is not possible to clearly select a preferred assembly site based on this data.

2.4.3.2.3 Summary of Issues - The top level assessment of assembly requirements has led to some general conclusions. The first is that manned participation in the assembly

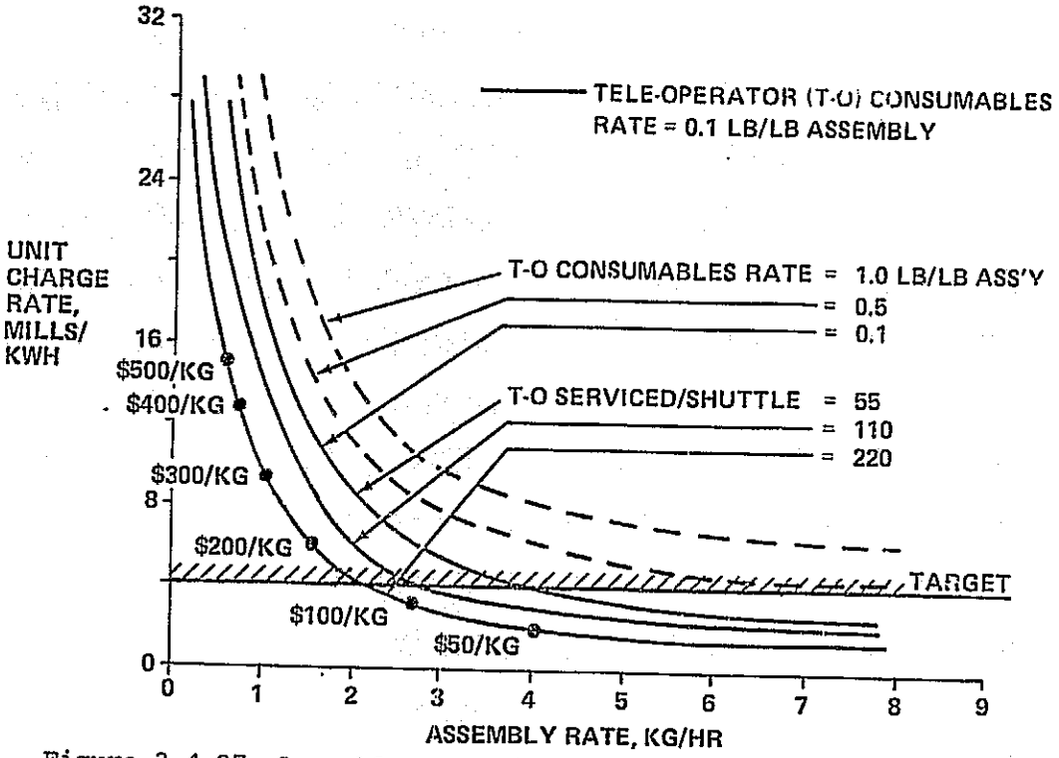

Figure 2.4-27 Assembly Cost, Remote Control From Ground (Low Altitude Assembly Site)

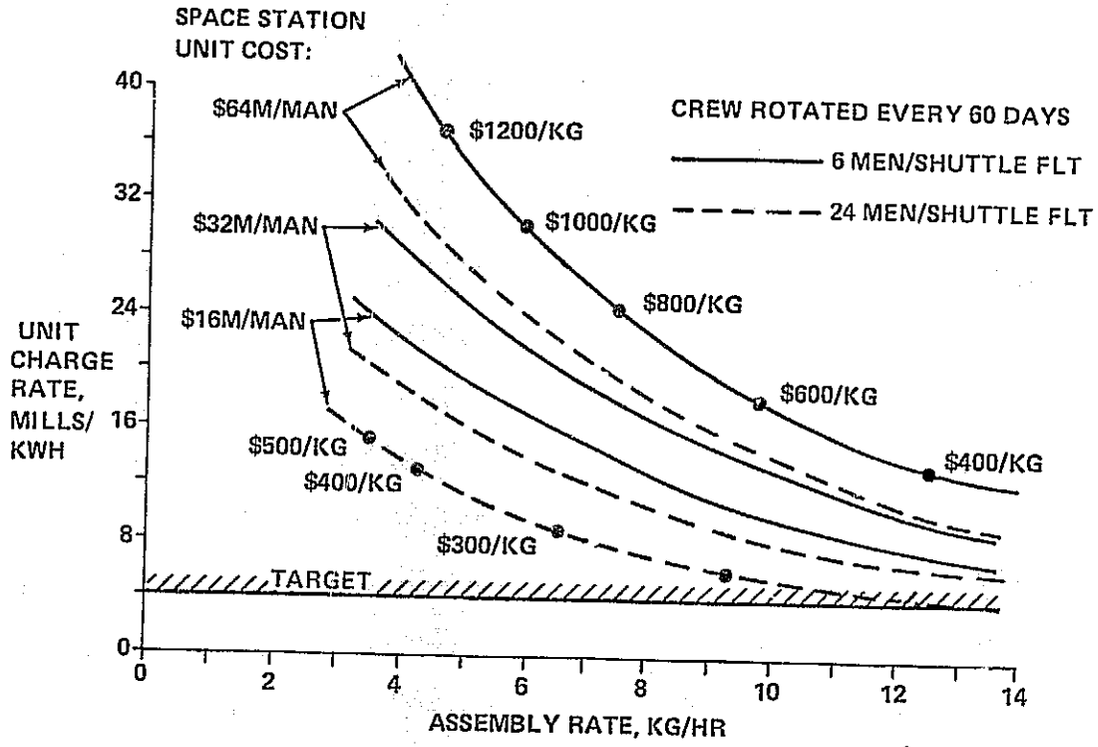

Figure 2.4-28 Assembly Cost, Manned Operations in Orbit (Low Altitude Assembly Site)

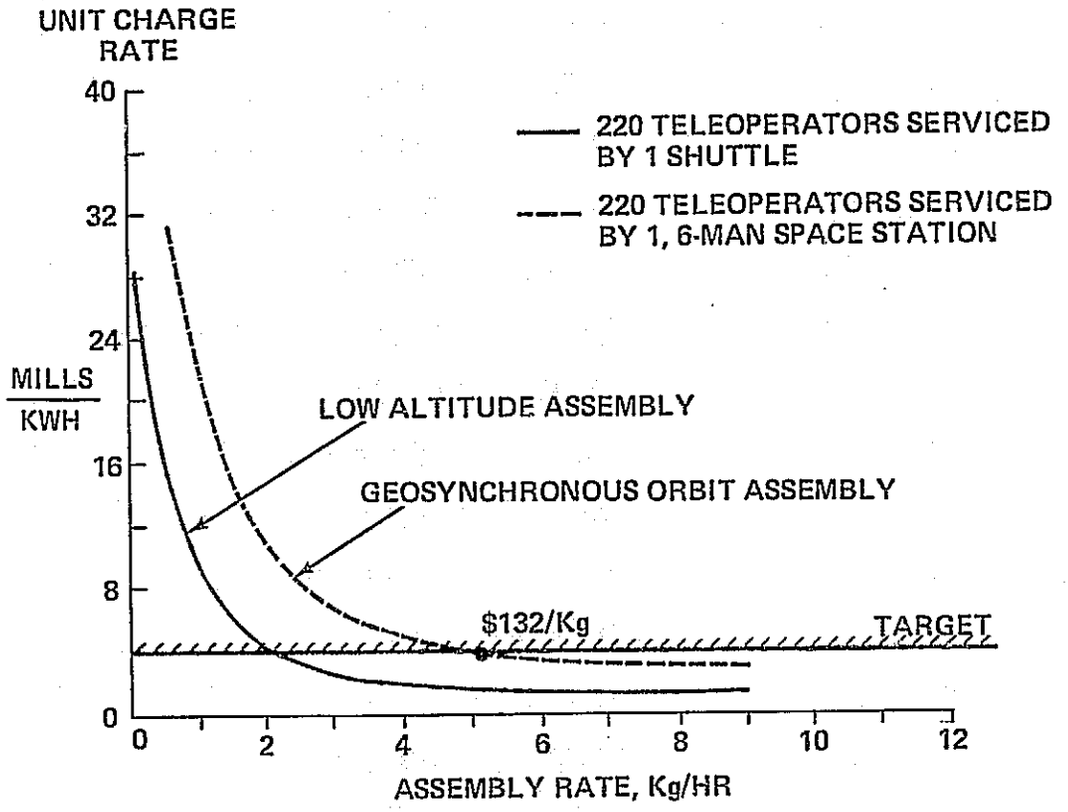

Figure 2.4-29 Assembly Cost, Remote Controlled Assembly

must be minimized to keep costs of supporting space stations down. Remote control of the assembly from the ground offers cost advantages, but much more technical work involving simulation is required to assess the feasibility of such an approach. Assembly with manned participation at a low altitude site could be cost competitive provided space station costs are reduced by a factor of four, and the Shuttle is provided a manned transportation payload module that can accommodate better than 24 men per flight.

Future systems study efforts should address the following:

- Low cost space stations with no scientific accommodations
- Conceptual designs for teleoperator vehicles for each unique element of the satellite
- Simulation data to determine man's productivity in a space environment.

The results of the above systems studies would identify the near term technology development efforts.

2.4.4 Maintenance

An assessment of the SSPS was performed to determine the need for maintenance and to identify the subsystems requiring major technology efforts to enhance reliability. The strawman SSPS used in the maintenance studies is an update of the configuration used in the transportation and assembly study. An SSPS weight of 17.84×10^6 kg including 24,000 kg of propellant for attitude control and stationkeeping was used.

The cost estimates established for transportation and assembly of the spacecraft have been modified for purposes of studying maintenance requirements. Figure 2.4-30 lists these cost estimates for an advanced technology base (1995). The cost to assemble has been doubled to establish a cost level for maintenance. This represents the cost of the added operation of disassembling the failed units using remote controlled manipulators.

2.4.4.1 SSPS Recurring Costs

Tables 2.4-1 through 2.4-3 lists the definition of the Lowest Replaceable Unit (LRU) for the solar array, the microwave antenna, the rotary joint and the array control system.

	COST ELEMENT	VALUE, $/KG	COMMENT
OPERATIONAL SYSTEM 1995 TECHNOLOGY	• TRANSPORT TO LEO	79	• HLLV WITH 181 KKg
	• TRANSPORT TO GEO	26	• ADVANCED ION
	• DISASSEMBLE & REASSEMBLE	132	• REMOTE CONTROLLED ASSEMBLY AT 9 Kg/HR
	• FAB OF STRUCT	60	• BEAM FABRICATION RATE = 191 Kg/HR

Figure 2.4-30 Transportation and Maintenance Cost Assumptions

Table 2.4-1 Solar Array Maintenance Cost

ELEMENT	LRU DESCRIPTION	LRU WT, Kg	LRU FAILURES OVER 30 YRS	COST OVER 30 YRS, $M	AVG PER YR, $M
1. BLANKET	80-1670 x 207m MODULES	97,484	1	41.90	1.40
2. CONCENTRATOR	160-1670 x 207m MODULES	768	1	0 .23	0.01
3. NON CONDUCT STRUCT	TO DESIGN	—	—	—	—
4. BUSSES	400m	26,000	1	8.29	0.28
5. SWITCHES	59 BLOCKING D10 DES/BLANKET LRU	97,484	1	41.90	1.40
6. MAST	6(+), 6(-) BUSSES/PANEL	85,000	1	27.12	0.9
			TOTAL MILLS/KWH =		$3.99M 9.1/YR

ASSMUPTIONS:

1. BLANKET – CELL OPEN CIRCUIT FAILURE = 2.6×10^{-4}/YR. THE PROBABILITY OF 5.6% LRU POWER LOSS OVER 30 YRS IS LESS THAN 10^{-99}. ONE LRU REPLACEMENT ASSUMED OVER 30 YRS.
2. CONCENTRATOR – MIRROR FAILURE LESS LIKELY THAN BLANKET FAILURE. ONE LRU REPLACEMENT ASSUMED OVER 30 YRS.
3. NON CONDUCTING STRUCTURE – ASSUMED NOT TO FAIL.
4. BUSSES – BUSS/CONNECTOR FAILURE RATE (OAO) = 10^{-9} F/YR. ONE LRU REPLACEMENT ASSUMED OVER 30 YRS.
5. SWITCHES – BLOCKING DIODE FAILURE RATE (OAO) = 10^{-7} F/YR. ASSUMES ONE BLANKET LRU REPLACED BECAUSE OF DIODE FAILURE.
6. MAST – SAME AS FOR BUSSES.

Table 2.4-2 Microwave Antenna Maintenance Cost

ELEMENT	LRU DESCRIPTION	LRU KG	LRU FAILURES OVER 30 YRS.	COST OVER 30 YRS, $M	AVG PER YR, $M
1 MW TUBE	1670 – 18 x 18m SUBARRAY	3017	4	5.73	0.19
2 POWER DIST	18 x 18m SUBARRAY	3017	1	1.43	0.05
3 COMMAND ELECTRONICS	1670 UNITS	467	3%	20.56	0.69
4 TRANS. ANTENNA (EXCLUDE TUBES)	1670 – 18 x 18m SUBARRAY	3107	1	1.43	0.05
5 STRUCTURE	TO DESIGN	–	–	–	–
6 CONTOUR CONTROL	6680 UNITS	22	1404	0.35	0.01
				TOTALS MILLS/KWH	0.99 0.02/YR

ASSUMPTIONS:

1. MW TUBE – MTBF = 1.14×10^{-6} HRS PROJECTED (NO MOVING PARTS, NO SEALS & LOW TEMPERATURE CATHODE).
2. POWER DIST – HIGHLY REDUNDANT SYSTEM EXPECTED TO MEET 30 YR LIFE REQ MT. ONE SUBARRAY FAILURE ASSUMED.
3. COMMAND ELECTRONICS – 30 YR LIFE ACHIEVED WITH HIGH LEVEL OF REDUNDANCY 3% FAILURE ASSUMED.
4. TRANS ANTENNA – WAVEGUIDES CONSIDERED STRUCTURE WITH LOW FAILURE RATE. ONE SUBARRAY FAILURE ASSUMED.
5. STRUCTURE – ASSUMED NOT TO FAIL.
6. CONTOUR CONTROL – FAILURE RATE = 0.8 F/10^{-6} (1% DUTY FACTOR) FOR BRUSHLESS DC MOTOR OPERATING AT 500°K.

Table 2.4-3 Rotary Joint and Array Control System

ELEMENT	LRU DESCRIPTION	LRU KG	LRU FAILURES OVER 30 YRS.	COST OVER 30 YRS, $M	AVG COST YR, $M
ROTARY JOINT					
• SLIP RING	24 BRUSHES, 4 SLIP RINGS				
– BRUSH		10	72	0.24	0.01
– SLIP RING		63	12	0.26	0.01
• DRIVE	8 BRUSHLESS MOTORS/GEAR TRAIN UNITS (4 ACTIVE, 4 STANDBY)				
– MOTOR/GEARS		1367	24	11.0	0.37
– LIM		1086	–	–	–
CONTROL SYSTEM					
• ACTUATORS	64 ELECTRIC ENGINES	203	640	1010	33
• PROPELLANT	24,000 Kg/YR	–	–	–	5.7
				TOTAL MILLS/KWH	39.09 0.9/YR

ASSUMPTIONS

1. 1. SLIP RING – PREVIOUS SPACE STATION STUDIES INDICATE MTBF = 10 YRS WITHIN REACH.
2. DRIVE – SAME AS SLIP RING.
3. ACTUATORS – CURRENT ESTIMATES PLACE ION ENGINE FAILURE RATE AT 3800 F/10^6 HR. ASSUME ORDER MAGNITUDE IMPROVEMENT AND A 10% DUTY FACTOR. COST ASSUMES $7500/KG. FOR ENGINE & POWER CONDITIONING.

Included are estimates of the failure rates and the corresponding number of LRU's replaced over the power station 30 year life. The recurring maintenance cost for the array is estimated at $3.99M/YR, while the cost to maintain the antenna is $0.99M/yr. The control systems, mainly the ion engines for pointing of the array and antenna rotary joint requires the most maintenance, $39.10 M/yr.

The series-parallel circuit design of solar blankets results in a highly reliable system. The blanket performance will degrade gracefully rather than exhibit abrupt power losses. Figure 2.4-31 is a tentative layout of 1/4 of the SSPS solar array. Each individual cell generates 1.5 watts, V_{mp} = 0.6V and I_{mp} = 2.472A. A string of cells 1670m long is set up in a series-parallel circuit arrangement to produce the 20 kv operating voltage. The LRU is a 1670 x 270m blanket, which lies between concentrators. Each LRU produces 117,000 KW. Five LRU panels connected in parallel form a sector, and eight sectors form one wing of the array.

A criteria has been tentatively established for determining when a blanket is replaced. This criteria is replace the LRU when the revenue lost over 30 yrs. is more than the cost to replace the LRU. At an assumed rate of 25 Mills/kwh for revenue and a transportation and maintenance cost of $238/kg, the LRU should be replaced after a degradation of 5.6% due to failures. (Radiation degradation is handled in the original design).

Analysis of the OAO solar arrays (Ref. 2.3-2) established the probability of an open-circuit failure of an individual solar cell at 2.63×10^{-4}/yr. At this rate, 621,732 cells per LRU will fail in 30 years. To produce a 5.6% degradation, 4.4×10^{6}/LRU cells must fail. The probability of losing 5.6% of the LRU power due to failures is extremely small. For all practical purposes the solar blanket is maintenance free.

A similar assessment of the concentrators and power distribution system show high reliability, particularly if high levels of redundancy are included in the original power distribution system design. The resulting maintenance costs are a fraction of the user charge rate, 0.1 Mills/kwh.

Analysis of the transmitting antenna (Table 2.4-2) using the 5.6% power loss per LRU criteria, shows that the replacement rate of the microwave components is also very low. Raytheon's rough estimate of the amplitron MTBF is based on the absence of tube components that usually cause failure, namely no moving parts, low temperature cathode and no seals. The antenna element requiring the most maintenance is predicted to be the contour control actuators. The high temperature

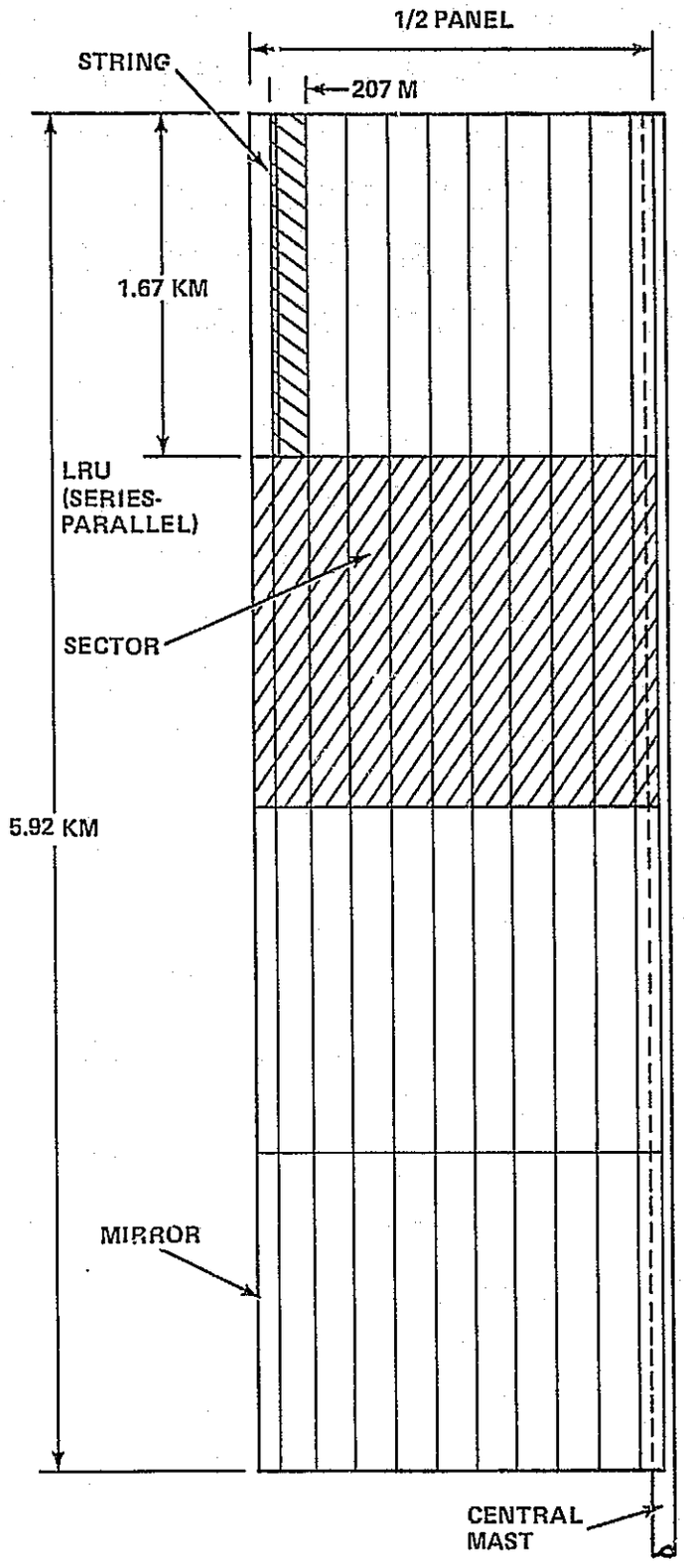

SOLAR CELL 5 CM X 8 CM
V_{MP} = 0.6 V
I_{MP} = 2.472 AMP
P = 1.484 WATT

STRING = 1670 M X 8 CM
NO. CELLS = 33,333
V = 20 KV
P = 49.47 KW
I = 2.472 AMP

LRU = 1670 M X 207 M
91% PACKAGING FACTOR
NO. PARALLEL STRINGS = 2364
V = 20 KV
P = 116,983 KW
I = 5849 AMP

SECTOR = 5 PARALLEL LRU
V = 20 KV
P = 584 MW
I = 29,200 AMP

PANEL = 8 PARALLEL SECTORS
V = 20 KV
P = 4679 MW
I = 233950

ARRAY = 2 PANELS
V = 20 KV
P = 9359 MW

POWER DISTRIBUTION EFF = .92

POWER TO ANTENNA AT
BEGINNING OF LIFE = 8610 MW

Figure 2.4-31 Solar Blanket Layout

environment could cause a high failure rate though the duty factor for this component for the SSPS is very low, less than 1%.

The SSPS subsystem that would require the most maintenance appears to be the array control systems, Table 2.4-3. Assuming an order of magnitude improvement in electric propulsion reliability indicated by Hughe's (Ref. 2.3-3), and a 10% duty factor, an average of 21 0.7-newton engines per year would require replacement.

2.4.4.2 Maintenance Support Costs

The non recurring (excluding development costs) and the recurring costs for maintenance support has been analyzed assuming the following scenario:

- A six-man space station is required for monitoring the satellite and for use as a repair shop and garage for maintenance teleoperators
- Maintenance is performed using ground controlled teleoperators
- Space Station crews are rotated four times per year using Shuttle and a chemical Tug
- An HLLV/ION stage (Payload = 181,000 Kg to LEO) is used to initially place the space station and to resupply the station once per year.

Table 2.4-4 summarizes the cost impact of using the assumed maintenance support scenario. The cost of a space station ($490M) was extracted from the Phase A space station studines for a Shuttle compatible modular design. Manipulator modules weight were taken from Ref. 2.3-4 and assumed to cost $44/kg. The cost of a mission control center was established using a cost factor presented in Ref. 2.3-3 for a ground based photovoltaic system.

The recurring cost for maintenance support are driven by the assumed rate of crew rotation and resupply. The staff requirements for mission control assumes 10 major console positions each requiring 4 men for around the clock monitoring. For each primary position (40) 3 additional positions for mission support, planning and software maintenance was assumed. A third tier of personnel, four positions per primary position was assumed for maintenance of the facility and operation of the equipments. A cost per man of $45,000 per year was used to establish yearly personnel costs.

Table 2.4-4 Maintenance Support Cost

NON RECURRING (EXCLUDES DEVELOPMENT)		
⊕ SPACE BASE		
– HARDWARE	$490M	(6 MAN SPACE STATION)
– TRANSPORT	$8M	(76, 700 KG AT $119/KG)
⊕ MANIPULATOR MODULES		
– 50 UNITS AT	$400M	(182 KG/UNIT AT $44 K/KG)
– TRANSPORT	$1M	(182 KG/UNIT AT $119/KG)
⊕ MISSION CONTROL FACILITY	$20M	(4 $/KW)
	$919M	
RECURRING/YR		
⊕ CREW ROTATION (4 FLTS)		
– SHUTTLE FLTS	$42M	
– SHUTTLE AMORTIZATION	$1.8M	(100 FLT LIFE)
– TUG FLTS	$4.0M	
– TUG AMORITIZATION	$0.6M	(20 FLT LIFE)
– CREW TRANSPORT MODULE	$4.M	
– CREW TRANSPORT MODULE AMORT.	$0.7M	(100 FLT LIFE)
⊕ RESUPPLY CREW & MANIPULATOR CONSUM.		
– HLLV (1/YR)	$9.M	
– AMORITIZATION	$6M	(100 FLT LIFE)
– ION STAGE	$1M	
– AMORITIZATION	$4.6M	(5 FLT LIFE)
⊕ MISSION CONTROL		
– PERSONNEL (320)	$14M/YR	
	$87.7M	(1.89 MILLS/KWH)

The initial investment for maintenance support equipment appears to be excessive for the amount of maintenance predicted. Modifications to the maintenance scenario assumed in the review should be evaluated. Perhaps the space base and teleoperators assigned to each SSPS could be used to service several satellites, thus reducing cost to each unit considerably. A second option would eliminate the use of multiple manned space stations. An on-orbit maintenance "Depot" facility would house spares and teleoperators and the manned transport vehicle would be of sufficient size to allow maintenance of support equipments and other functions requiring manned participation. In this manner, the costs for the man rated equipments can be shared by many power stations.

2.4.4.3 Sensitivity to Assumptions

The failure rates assumed in the assessment are soft at best. The failure rate for solar cells is based on OAO where careful selection of high quality components was the rule. On SSPS, mass production of solar blankets may preclude achieving as high a reliability. If the open-circuit failure rate for an individual solar cell increases an order of magnitude (2.63×10^{-3}/yr), 7.8% of the blanket LRU will fail in 30 years, requiring at least one replacement of the entire array ($112 M/yr) over the life of the satellite. The same trend can be demonstrated for the microwave components.

The 5.6% power degradation level before LRU replacement is driven by the assumed cost to repair (238 $/kg). If transportation and maintenance cost double, the point where cost of repair equals expected loss in revenue will also double. A study that more precisely evaluates the tradeoff between loss in revenue versus the cost to repair is needed for each major satellite component. Amortization of support equipment costs for various approaches to maintenance should be included in the optimization.

2.4.5 Maintenance Cost

Figure 2.4-32 summarizes the maintenance cost for the 1995 SSPS. This is consistent with the data presented in paragraph 2.4.3. No maintenance is assumed for the 1985 and 1990 systems though technology work to develop maintenance techniques would be part of these programs. It is difficult, however, to establish an estimate of these technology oriented efforts.

ELEMENT	LRU DESCRIPTION	LRU WGT Kg	LRU FAIL OVER 30 YRS	AVE $/YR $M	COMMENTS (LRU REPLACED AFTER 5.6% POWER REDUCTION DUE TO FAILURE)
SOLAR ARRAY					
• BLANKET	80–1670 X 207 M MODULES	97,900	1	1.4	2.6×10^{-4} /YR OPEN CIRCUIT FAILURE RATE (OAO)
• CONCENTRATOR	160–1670 X 207 M MODULES	7,687	1	0.01	MIRROR FAILURE LESS LIKELY THAN BLANKET
• NON COND STRUCT	TO DESIGN	–	–	–	STRUCTURE ASSUMED NOT TO FAIL
• COND STRUCT					
– BUSSES	400 M LONG	26,000	1	0.28	10^{-9} F/YR (OAO)
– SWITCHES	59 BLOCK DIODES/BLANKET LRU	97,484	1	1.40	10^{-7} F/YR (OAO)
○ MAST	6 (+), 6(–) BUSSES/PANEL	85,000	1	0.9	SAME AS CONDUCTING STRUCTURE
MW ANTENNA					
○ TUBES	1670–18 X 18 M SUBARRAYS	3,017 Kg	4	0.19	MTBF = 1.14×10^{-6} HRS PROJECTED
○ POWER DIST	18 X 18 M SUBARRAY	3,017 Kg	1	0.05	HIGHLY REDUNDANT SYSTEM
○ ELECT	1670 UNITS	467 Kg	3%	0.69	HIGHLY REDUNDANT SYSTEM
○ TRANS ANTENNA	1670 UNITS	3,017 Kg	1	0.05	WAVEGUIDE CONSIDERED STRUCT-NO FAILURES
⊗ STRUCTURE	TO DESIGN	–	–	–	ASSUMED NOT TO FAIL
⊗ CONTOUR CONT	6680 UNITS	220 Kg	1404	0.01	$0.8F/10^{-6}$ (1% DUTY FACTOR)
ROTARY JOINT					
⊗ SLIP RING	4 UNITS	10 Kg	72	0.01	MTBF = 10 YRS (SPACE STATION STUDIES)
• BRUSH	24 UNITS	63 Kg	12	0.01	MTBF = 10 YRS (SPACE STATION STUDIES)
⊗ DRIVE	8 BRUSHLESS DC MOTORS	1,367 Kg	24	0.37	MTBF = 10 YRS (SPACE STATION STUDIES)
REACTION CONTROL	64 ELECTRIC ENGINES	203 Kg	640	33.0	$3800F/10^{6}$ HR (ORDER MAGNITUDE IMPROVEMENT + 10% DUTY FACTOR)
PROPELLANT		24,000 Kg		5.7	YEARLY CONSUMPTION
					• SUBTOTAL 44.1
					• SO CREW ROTATION 73.0
					• MISSION CONTROL 14.0
					TOTAL 131.1 (3 MILLS/KWH)

Figure 2.4-32 Maintenance Cost - SSPS Spacecraft

2.5 Safety of Large Structures

A safety analysis has been performed for 15 identifiable mission and task phases associated with constructing and servicing the SSPS. Phases range from earth launch to the final salvage efforts at the termination of expected service life. Potentially hazardous situations were identified in virtually all phases. Of the approximately 30 natural and induced hazards which can conceivably influence project success, eight were examined to a depth commensurate with a preliminary analysis. Of major significance, design of the existing astronaut pressure suit may seriously limit his external activities unless design changes are considered.

This analysis was performed assuming assembly operations are Shuttle based. Future studies should include assessment of the impact of Space Station and the HLLV. Further studies are required to resolve questions which evolved during the course of this analysis as well as those natural and induced hazards which were not examined. Tables 2.5-1 through 2.5-3 provide an overview of astronaut participation in each of the 15 mission/task phases.

This section was prepared to identify potentially hazardous situations associated with the SSPS. In view of the limited actual experience data base available in the assembly and maintenance of large spaceborne structures under zero-g conditions, a large portion of the analysis relies on engineering judegment.

The analysis investigates astronaut involvement in the fabrication, assembly, preoperational checkout and maintenance events that are conceivable in the support of the station. The analysis utilizes material presented in the Task 2 Concept Definition Report, Number MPTS-R-002, dated 12 December 1974. This report is subject to refinement following resolution and disposition of design and fabrication options as well as the emergence of design details.

The examination was limited to the following natural and induced hazards: temperature, sunlight/darkness, collision with structural members, electrical shock, rotating machinery, structural failure, pressure suit design and fragmentation of pressure vessels.

2.5.1 Task/Malfunction Selection and General Assumptions

Representative tasks as well as typical malfunctions which can be experienced on manual or automatically operated

Table 2.5-1 Overview of Manned Participation

SPACE BASED SOLAR POWER						
PHASE	FUNCTION	CREW INVOLVEMENT	POTENTIAL SAFETY HAZARDS	SIM REQD	SUPPORT EQUIP. REQD	SPECIAL PCDR's REQD
LAUNCH	RESTRAIN SUPPORT MONITOR	NONE NONE MONITOR	PACKAGING FAILURES CAUSES COMPONENT DAM'G DOUBLE FAIL: COMM LOSS & SYS FAIL			
ORBITAL C/O	P/L DOORS OPEN RMS DEPLOY REMOVE PROTECT SHELL/DEPLOY	INITIATE OPERATE OPERATE	JAMMED DOOR NONE TIGHT SPACE DURING REMOVAL FROM P/L BAY SHROUD - HIGH DAMAGE POTENTIAL			X X
P/L ORBITAL RETRIEVAL	INSTALL/RETURN ITEMS P/L DOORS CLOSED	MONITOR/ VERIFY INITIATE	EVA COLLISION JAMMED DOOR	X		X X
SEGMENT ASSEMBLY (EARTH MFR'D.)	UNFOLD RIGIDIZE STABILIZE FREE	INITIATE NONE INITIATE INITIATE	CONTACT SHUTTLE/SHROUD FAILED JET(S), FUEL LOSS, TUMBLING, CON-TACT VEHICLE EVA		 X	 X X
ORBITAL FABRI-CATION	STOCK LOAD FABRICATE REMOVE ASSY STRUCT. TEST STOCK UNLOAD	MONITOR MONITOR OPERATE MONITOR MONITOR	PACKAGING FAILURE CAUSES EQUIP. DAMAGE/ EVA CONTACT MATERIAL BREAKAGE/EVA CONTACT JAMMED MANIPULATOR NONE NONE	X X X	X X X	X X X X X

Table 2.5-2 Overview of Manned Participation

SPACE BASED SOLAR POWER						
PHASE	FUNCTION	CREW INVOLVEMENT	POTENTIAL SAFETY HAZARDS	SIM REQD	SUPPORT EQUIP. REQD	SPECIAL PCDR's REQD
ASSEMBLY STORAGE	RMS DEPLOY	OPERATE/EVA	COLLISION/HIGH DAMAGE POTENTIAL = JET(S) FAIL TO CUT OFF	X	X	
	RMS REMOVE	OPERATE/EVA	EVA CONTACT	X		X
STORAGE RETRIEVAL	RMS INSTALL/ FREE/ STABILIZE	OPERATE/EVA	EVA CONTACT HIGH DAMAGE POTENTIAL	X	X	X
			FAILED JET(S), FUEL LOSS AND SYSTEM FAILURE			X
			SUNLIGHT/DARKNESS ERRORS			X
TRANSPORT SEGMENTS	STABILIZE THRUST	NONE	FAILED JET(S), FUEL LOSS			X
		INITIATE	THRUST EARLY/LATE			X
			CONTACT OTHER VEHICLE			X
ROTARY JOINT ASSEMBLY	ORIENT SECURE	OPERATE/EVA	EVA/STRUCTURE COLLISION - HIGH DAMAGE POTENTIAL	X	X	X
	OPERATE	INITIATE	EVA IRRADIATION EVA TETHER BREAKS	X	X	X
ANTENNA SEGMENT TO SEGMENT ASSEMBLY	STABILIZE	NONE	FAILED JET(S), FUEL LOSS			
	ORIENT	OPERATE/EVA	EVA TETHER BREAKS	X	X	X
	DOCK	OPERATE/EVA	EVA CRUSHED BETWEEN SEGMENTS	X	X	X
	LATCH	AUTO/VERIFY	PREMATURE LATCH & NEED FOR REDOCK SUNLIGHT/DARKNESS EXTREMES	X	X	X
	RIGGING	MONITOR	CABLE OVERLOAD		X	X

Table 2.5-3 Overview of Manned Participation

SPACE BASED SOLAR POWER (Cont.)						
PHASE	FUNCTION	CREW INVOLVEMENT	POTENTIAL SAFETY HAZARDS	SIM REQD	SUPPORT EQUIP. REQD	SPECIAL PCDR's REQD
ACTIVATE ASSEMBLIES INDIVIDUALLY	CHECKOUT INITIATE OPERATE	NONE NONE INITIATE	 EVA IRRADIATION	 X	 X	 X
PRE-OPERATION	FINAL ALIGNMENT CLEAR EQUIP.	MONITOR AUTO/VERIFY AUTO/VERIFY	EVA COLLISION COMM. LOSS EVA COLLISION	X	X	X
ACTIVATE ANTENNA	CHECKOUT OPERATE	MONITOR INITITAE	ELECTRICAL SHORTS MICRO WAVE LEAKAGE			X X
SCHEDULED MAINTENANCE CYCLE	R/R ARRAY COMPONENTS ORBITAL DECAY CORRECTION	OPERATE/EVA	EVA TETHER BREAKS ELECTRICAL SHORTS TEMPERATURE, SUNLIGHT/ DARKNESS EXTREMES			X X X
UNSCHEDULED MAINTENANCE	R/R ARRAY COMPONENTS R/R DAMAGED GIRDER(S)	EVA EVA	STRUCTURAL FAILURE MICROWAVE LEAKAGE ELECTRICAL SHORTS ELECTRICAL SHORTS SUNLIGHT/DARKNESS EXTREMES	X	X X	X X X X

equipment in a one-g environment were applied where they had a potential impact. In assessing and relating these inputs to the zero-g environment, the analysis assumes three basic improvements over their earth counterparts. These are:

1. Astronaut skills are at supervisory level and they are highly motivated

2. Equipment used to fabricate structural members and a majority of other station elements are automatic; can operate in a vacuum; are programmable and require minimal astronaut attendance in their operation

3. Space-peculiar equipment will be subjected to the same rigid design criteria established for the design of sophisticated spacecraft.

The first phase of the investigative effort was an examination of potential crew involvement during each mission phase. This was done to gain an overview of astronaut participation and to establish the man-machine-structure relationships which could be expected. Gross potential safety hazards were then identified as were requirements for simulator training, support equipment needs, and special procedural instructions. This information is presented in Tables 2.5-1 through 2.5-3.

The second phase is an extension of the overview, wherein potential tasks and malfunctions are identified to a depth commensurate with a preliminary analysis. The hazards associated with each of these is explored. In conducting this phase, it was found necessary to establish certain assumptions to provide a more rigid design information base. Should any of these assumptions be negated during subsequent design envolvement, the analysis must be restructured. This information is presented on Table 2.5-4 through 2.5-7.

2.5.2 Problem Overviews by Subject and Phase

Astronaut Pressure Suit Hazards (All Orbit Activities)

Several potential pressure suit problem areas have been identified. These areas will require further examination and evaluation.

1. Metallic components used in suit construction may jeopardize the astronaut when working in close proximity to electrical devices, harness, connectors, etc.

Table 2.5-4 Top Level Hazards

APPLICABLE HAZARDS	SPECIAL SAFETY REQUIREMENTS	REMARKS/COMMENTS/QUESTIONS
CANNISTER JAMS IN ITS RECEPTACLE DURING LOADING OPERATION.	PROVIDE MULTIPLE SCREW JACKS OR SIMILAR DEVICES TO ASSURE PRECISE ALIGNMENT LOADING CONTROL.	CREW TASK PROCEDURES WILL BE REQUIRED, OUTLINING JAM REMOVAL.
MATERIAL JAMS AND BREAKS IN FIXTURE.	PROVIDE A RAPID ACTING BRAKE AND LOAD SENSING DEVICE TO PRECLUDE EVENT.	REPAIR PROCEDURES ARE REQUIRED. DETERMINE NEED FOR MODULARIZING DAMAGE/WEAR PRONE EQUIPMENT ELEMENTS.
CANNISTER RATIONAL SPEED CONTROL ISSUES SPURIOUS SIGNAL, INTERRUPTING MATERIAL FEED.	PROVIDE A SPEED CONTROL INTERLOCK DEVICE AND FILTERS IN MOTOR CONTROL CIRCUIT.	A. INTERRUPTION OF FEED MAY APPLY SHEAR LOADS IN EXCESS OF ALLOWABLES. B. CONTINUED UNLOADING RESULTS IN JAMMED EQUIPMENT. C. HOW IS STRUCTURAL INTEGRITY VERIFIED?
IMPROPERLY SPLICED GIRDER LONGERON FAILS	PROVIDE ASSURANCE THAT LONGERONS REPAIRED DURING FABRICATION ARE SUITABLY IDENTIFIED.	RECOMMEND GIRDERS HAVING REPAIRED LONGERONS BE INSTALLED AT ANTENNA PERIPHERY ONLY. ESTABLISH REPAIR PROCEDURES.
ADHESIVE MATERIAL WHICH JOINS ABUTTING MEMBERS FAILS DURING ANTENNA ASSEMBLY.	A. IF A TWO PART EPOXY IS USED, — PROVIDE PRECISE MEASURING AND MIXING CONTROLS TO ASSURE PROPER MIX. B. PROVIDE CLEANLINESS CONDITION DETECTORS.	A. RECOMMEND PERFORMING A STUDY TO DETERMINE IF EPOXY EJECTION NOZZLE REQUIRES A SHUTTER TO PRECLUDE PREMATURE AGING. B. DETERMINE IF THIS WOULD BE CONSIDERED A SINGLE POINT FAILURE.
INCORRECT MATERIAL GAGE USED FOR LONGERONS AND/OR TRUSS	A. DESIGN CANNISTERS TO ACCEPT ONLY ONE MATERIAL GAUGE. B. EMPLOY NON-INTERCHANGEABLE CANNISTERS FOR VARYING GAUGE MATERIALS.	A. DETERMINE QA METHODS USED TO ASSURE THIS HAS NOT OCCURRED. B. DETERMINE THE IMPACT ON ANTENNA INTEGRITY IF THIS SHOULD OCCUR.

Table 2.5-5 Top Level Hazards

APPLICABLE HAZARDS	SPECIAL SAFETY REQUIREMENTS	REMARKS/COMMENTS/QUESTIONS
A. BURRS ON MATERIAL GOUGE INTERFACING MEMBERS DURING ASSEMBLY, JEOPARDIZING STRUCTURAL INTEGRITY. B. BURRS ON MATERIAL TEAR ASTROTECH SUITING DURING ANTENNA ASSEMBLY.	A. AND B. PROVIDE DEBURRING AND WIPING FIXTURE ON MATERIAL-TO-CANNISTER LOADING EQUIPMENT. PERFORM 100% INSPECTION.	A. REQUIRES AN AUTOMATIC INSPECT/REJECT CAPABILITY. B. DETERMINE CHARACTERISTICS TO LOOK FOR.
MECHANICAL FASTENER FIXTURE EJECTS MANDRELS. RESULTS IN: A. JAMMING OF ASSEMBLY FIXTURE MECHANISMS B. INJURES ASTROTECH C. DAMAGES STRUCTURE	PROVIDE PROTECTIVE SCREEN	
ASTROTECH CONTACT WITH LASER BORESIGHT BEAM.	PROVIDE PROTECTIVE SHIELDS TO PRECLUDE DIRECT VIEWING.	DETERMINE FEASIBILITY OF PROVIDING LASER PROTECTION ON CREW HELMET.
ELECTRICAL CIRCUIT PROTECTIVE DEVICES FAIL CLOSED.	PROVIDE REDUNDANT CB's FOR LOADS IN EXCESS OF *xx* AMPS	
PREMATURE RUNOUT OF MATERIAL	PROVIDE A "MATERIAL" REMAINING INDICATOR.	EVALUATE THE METHODS OF RESTOCKING MATERIAL.
PREMATURE LATCHING OF FIXTURE ARM LOCKING DEVICE	PROVIDE AN EMERGENCY MANUAL RELEASE.	
INADVERTENT ACTUATION OF MATERIAL CUT-OFF SHEARS DURING BLADE REPLACEMENT.	A. PROVIDE SWING OUT FEATURES FOR BLADE REPLACEMENT. B. PROVIDE AN ELECTRICAL INTERLOCK CIRCUIT TO PRECLUDE ITS OPERATION DURING MAINTENANCE. C. PROVIDE SUITABLE PROTECTIVE SHIELDS.	PROVIDE A LOCAL OVERRIDE CAPABILITY.

Table 2.5-6 Top Level Hazards

APPLICABLE HAZARDS	SPECIAL SAFETY REQUIREMENTS	REMARKS/COMMENTS/QUESTIONS
RUNAWAY STROKE ON EPOXY EJECTOR.	A. PROVIDE REDUNDANT CIRCUIT TRIP MECHANISMS B. SAID MECHANISM TO ACTIVATE WASTE DISPENSER AT EJECTOR NOZZLE.	
BUILD-UP OF EJECTOR TOOL HYDROSTATIC PRESSURE DUE TO CLOGGED ORIFICE.	A. PROVIDE A CONTAINMENT SHIELD AROUND EJECTOR BODY. B. INCORPORATE A RELIEF VALVE AND A WASTE DISPENSER.	WILL REQUIRE A HIGH PRESSURE WARNING DEVICE.
CONTACT WITH EPOXY CLEANING AGENTS MAY DETERIORATE ASTROTECH SUIT MATERIAL.	CONDUCT TESTS UNDER SPACE ENVIRONMENT CONDITIONS TO ENSURE COMPATABILITY.	
TEMPERATURE DELTA BETWEEN INTERFACING MEMBERS DURING JOINING PROCESS PLACES ABNORMAL LOAD ON JUNCTION.	PROVIDE A MEANS TO STABILIZE TEMPERATURE OF ADJOINING MEMBERS.	TEMPERATURE SENSING INDICATORS ARE RECOMMENDED.
ELECTRICAL SHORTS DURING MAINTENANCE STARTLES ASTROTECH (NO SHOCK HAZARD PRESENT). SHORT COULD RESULT IN: A. INJURIES DUE TO PHYSICAL REACTIONS. B. TEMPORARY BLINDNESS. C. TOOL DROPPED INTO MECHANISM(S). D. TOOL FUSED TO FIXTURE.	A. PROVIDE CIRCUIT INTERLOCKS TO CUT ALL POWER TO THE AUTOMATIC FIXTURE. B. MAINTENANCE BY-PASS CIRCUITS WILL NOT BE INCORPORATED.	SUIT MATERIAL IS CONSIDERED AN ADEQUATE BARRIER AGAINST GROUNDING. (EXCEPT AS NOTED ON PAGE 8, PARAGRAPH 1).

Table 2.5-7 Top Level Hazards

APPLICABLE HAZARDS	SPECIAL SAFETY REQUIREMENTS	REMARKS/COMMENTS/QUESTIONS
PREMATURE OPERATION OF PRESSURE CLAMP (AT EPOXIED JUNCTIONS)	PROVIDE A MECHANICAL LINEAGE OVER-RIDE (OR BACKUP) SYSTEM.	
OVERTRAVEL OF PRESSURE CLAMP	PROVIDE A VISUAL INDICATOR TO SHOW PRESSURE CLAMP STROKE	UNDETECTABLE STRUCTURAL DAMAGE COULD RESULT IN EARLY FAILURE.
UNDERTRAVEL OF PRESSURE CLAMP	SAME AS ABOVE	A. CONDITION DUE TO BACKING OFF OF ADJUSTMENT DEVICES. B. MAY RESULT IN WEAKENED JOINT AND RESULT IN EARLY FAILURE.
INTEGRITY OF ASSEMBLED STRUCTURE UNINOWN	PROVIDE FOR SAMPLE LOAD TESTING. EXAMPLES: A. SUBJECT NEW LOTS OF EPOXY TO TBD ON-SITE INTEGRITY TESTS B. SUBJECT NEW LOTS OF STRUCTURAL MATERIAL TO TBD ON-SITE INTEG-RITY TESTS. C. SUBJECT ASSEMBLED GIRDERS TO ON-SITE INTEGRITY TESTS. LOT NUMBER TBD.	PROGRAM AUTOMATIC FABRICATOR TO INTERRUPT NORMAL FABRICATION CYCLE TO PRODUCE SHORT TEST SECTIONS.

(a) Cuff reinforcements

(b) Umbilical connectors

(c) Zippers

(d) Visor hardware

2. Conventional back-pack to suit interconnect hoses routed on the suit exterior may be damaged or snagged by projecting hardware.

3. The externally mounted sun-shield (or its pivotal hardware) may be damaged or snagged by projecting hardware.

4. If unable to check body momentum, collision with the guy wires/cables serving as structural member stabilizers may result in localized friction which may burn through the pressure suit.

5. (a) The gap which exists between the existing back pack design and the astronauts helmet may be a detriment, in that it can serve to snag the guy wires noted in 4 above.

(b) Forces required to separate the pack from the suit will require further examination.

6. If a super oxide system for the generation of oxygen is to be considered, a literature search must be undertaken to determine its adequacy for extended EVA activity. The following must be critically examined:

(a) Method of attachment.

(b) Location of spare modules on the astronauts person

(c) Methods available for cartridge ignition.

(d) Hazards associated with igniting spare cartridges with a prepressurized system.

Launch Phase

Crew involvement is limited to assuring proper equipment tiedown and confirming that cargo manipulators have been checked and properly stowed. Failure to accomplish these tasks

can: (1) cause vehicle loss, (2) damage components, (3) prevent unloading of cargo, (4) result in excessive payload landing weight. At orbit rendezvous, a collision potential with previously placed components/work station exists.

Orbiter Checkout

The payload crew is responsible for releasing the cargo if they are jammed. Because a jamming potential exists, an emergency manual hinge pin release capability is recommended. Because of damage potential, which could preclude reentry, in-orbit storage of payload deployment devices spares is recommended.

Cargo removal may be damage critical because of limited maneuvering space. If solenoid equipped tie-down shackles are to be employed, test circuits should be provided to ensure proper sequencing prior to actual cargo deployment to preclude abnormal loads. Manual release overrides should also be provided.

Following deployment, thrust will initially be applied in limited bursts to assure proper trajectory. A high collision potential with a space station could exist.

Orbital Retrieval of Components Requiring Shuttle Return

Disposition of failed or expended life components is not known. Assuming their probable return, stowage may be critical in that payload center of gravity (CG) may not be within limits or they may shift or break loose during reentry. Either can cause payload loss.

Precise maneuvering of retrieved cargo within the cargo bay is not considered potentially hazardous. This assumes that packaging density is not as severe as it is during the earth loading phase. To assure proper cg placement, all cannisters or similar equipments will require suitable empty weight and cg location markings.

A jammed payload door or its locking mechanism are considered potentially hazardous because of EVA participation in freeing them. Because of damage potential, in-orbit spares for prime manipulator segments and payload doors are recommended.

Segment Assembly (Earth Manufacture)

Prefabricated segments are assumed to be folded within the payload cargo bay. Its extraction from the cargo bay is

considered a critical operation because of potential contact with payload shrouds. The greatest hazards are considered to be failure of individual propulsion units resulting in an erratic trajectory, loss of propellent resulting in a detonation and uncontrollable tumbling in transit to the final assembly site.

Orbital Fabrication

a. Assumptions

1. Winding of flat stock on dispensing cannisters will not result in stored energy capable of ejecting material when replacing depleted cannisters.

   Rationale: (a) Pressure hull shop area may be pierced/explosive decompression

   (b) Injury to Astrotech

2. Fabrication is accomplished in an unpressurized area.

   Rationale: If a pressurized area, transfer of a completed assembly to an exterior storage area would require evacuation of shop atmosphere. This results in:

   (a) An extensive number of depressurize/pressurize cycles of the hull

   (b) Potential loss of consumables (oxygen/nitrogen)

   (c) Increased power requirements

   (d) Increased weight for pumps, etc.

3. Cannisters are designed with an enlarged lip on one side to preclude improper fixture receptacle entry.

4. Loading orientation of material on cannister is positive to preclude opposite winding potential.

b. Analysis

Applicable hazards, special safety requirements and remarks/comments/questions are entered in Tables 2.5-4 through 2.5-7.

Antenna Segment To Segment Assembly

This activity is considered hazardous in view of the precise coordination which must be exercised to maintain identical closure speeds at both ends of the girder being installed. See also, Table 2.5-2 for additional hazards. To preclude occurrence of these hazards, the employment of a completely automated system should be investigated.

The conceptual multiple probe-drogue interconnect fitting depicted in report MPTS-R-002, should be modified to permit the installation and removal of individual girders. The method of securing abutting girders has not been resolved as yet, however, the following concepts should be evaluated: band clamps which engage abutting shoulders; tapered tongue and groove fittings; butt welded seams, etc.

Activate Assemblies Individually

The sole hazard which appears of consequence during this phase involves localized UV radiation during extended work periods. This assumes: (1) the astronaut will be required to initiate solar exposed circuit interconnect junctions at scattered locations on the antenna and Solar Array; (2) the task could be a highly specialized one and work is shared by a limited number of men, thus requiring extended duty periods. The term localized, as used herein, means that only small, scattered areas of the astronauts body are exposed to direct solar rays. Handling of solar blankets may be hazardous requiring that the blankets be oriented edgewide relative to the sun to preclude voltage buildup.

Pre-Operation

As in the preceding phase, UV radiation appears to be the solar hazard. It is assumed that a remotely activated and operated laser bore sighting device will be used during final alignment checks of the structure and wave guides and that there will be minimum astronaut involvement. Replacement of a failed waveguide alignment drive motor during this Phase will probably be done by the astronaut, exposing him to electrical shock only in the event of a control circuit failure in the "Power-On" mode.

It is assumed that good housekeeping practices will have been observed during the entire construction period. However, it is considered judicious to perform a visual check of the entire antenna/array surface and structural support area for debris. In lieu of direct astronaut involvement in the examination of the sunward array surface, the use of a remotely piloted vehicle equipped with television camera(s) and debris retrieval mechanisms should be investigated. To simplify the task of readily detecting construction support equipment, the use of contrasting paint applications or the attachment of direction finding equipment should also be investigated. Maintaining accurate inventory status control records should materially reduce debris which is potentially hazardous.

During this phase, it is assumed that devices have been installed on the antenna which will assure alignment with the ground based receiver. It is further assumed that alignment checks will be performed over an extended time period, with minimal power applied initially and then expanding to maximum power levels. During this period, all emergency shut-down systems should be activated.

Activation

It is assumed that during this phase, astronaut involvement will be terminated immediately following assurance that all systems are operating satisfactorily. The absence of power control details and their locations precludes performing other than a cursory assessment of the hazards involved following activation. These are considered minimal because of the preoperative checks which will have been performed before initiation of this phase. Therefore, potential hazards associated with electrical shorts, e.g., arcs and electrical shock, and that of microwave leakage would be expected to occur only following component failure or micrometeorite collision. Monitoring devices should detect these conditions and power in the affected area would be turned off prior to any action by a repair team. (See, also, unscheduled maintenance.)

Scheduled Maintenance Cycle

It is assumed that components subject to deterioration may require replacement at specified planned intervals to maintain operational efficiency. Further studies are required in order to: (1) determine the extent of hazard associated with isolated replacements versus that of block replacements or modifications; (2) determine the most cost-effective approach for scheduled component replacement. Special safety requirements can then be developed to fit the selected approach.

Because the orbital decay rate is constant and is readily plotted, its correction is considered a scheduled event. To reduce astronaut exposure to repeatable potential hazards, therefore, the planned replacement of components should be coordinated with orbital corrections.

Geosynchronous altitudes are considered prime real estate for future space activities. Because of this status, consideration must be given for its ultimate disposal. The development of salvage concepts will therefore be required in order to assess potential teardown hazards as they relate to: (1) the astronaut; (2) stations/equipments orbiting below the power station orbit; (3) inhabited areas on the surface of the earth.

Assembly Storage

Movement of completed assemblies to a storage area by a man-machine combination is assumed. Collision with previously stored components because of depth perception difficulties, extreme lighting contrasts, looking into the sun, misjudgments in speed and distance, erratic behavior of thrusters, or a fail-to-cut-off-power situation presents potential damage risks to stored items and/or injury to the astronaut. Experimentation prior to commencement of such activities appears desirable, particularly if this is not accomplished frequently. To preclude EVA/structure collisions resulting from thruster malfunctions, the employment of proximity cut-off switch circuits or other automatic cut-off devices should be investigated.

Storage Retrieval

The potential safety hazards and recommendations specified for the storage of assemblies are also applicable to their retrieval. A single exception might be the degree of hazard, i.e., a failure to cut power could result in extensive damage to previously erected antenna structure.

Transport of Segments

The identification of applicable transport hazards are entered in Tables 2.5-8 and 2.5-9. The analysis is applicable to the movement of all structural members.

Rotary Joint Assembly

(Applicable to azimuth and elevation yoke and the yoke support)

Table 2.5-8 Top Level Hazards

APPLICABLE HAZARDS	SPECIAL SAFETY REQUIREMENTS	REMARKS/COMMENTS
TRANSPORT MODE (MANIPULATOR) HIGH DAMAGE POTENTIAL SERVO DRIVE UNIT FAILS TO OPERATE.	PROVIDE INTERLOCKS BETWEEN VARIOUS DRIVE UNITS TO INHIBIT SYSTEM UPON FAILURE OF ANY ONE DRIVE UNIT.	• SIGNAL LAG TO BE INVESTIGATED
SERVO DRIVE LINKAGE JAMS DUE TO BREAKAGE, LOSS OF ATTACHING HARDWARE OR OVERCENTER CONDITION.	A. SPECIAL PROCEDURES REQUIRED. B. MINIMIZE NUMBER OF ADJUSTMENTS THAT ARE PERMITTED.	
SERVO DRIVE UNIT FAILS "ON"	PROVIDE REDUNDANT SWITCHING CIRCUITS.	
LOSS OF INCOMING SIGNAL	PROVIDE AN EMERGENCY BACKUP CIRCUIT	DETERMINE AVERAGE SIGNAL DURATION PERIOD. COUPLE WITH AUTOMATIC SHUTDOWN OF ALL SYSTEMS.
POWER SUPPLY DEGRADED	PROVIDE INSTRUMENTATION TO MONITOR POWER LEVEL CONDITION	INVESTIGATE NEED FOR PROVIDING A RESERVE POWER PACK.
DEBRIS JAMS FLEXIBLE JOINTS OR IS DEPOSITED ON CLAMPING SURFACE.	A. PROVIDE SHIELDS TO PROTECT JOINTS. B. SPECIAL PROCEDURES REQUIRED. CALLING FOR INSPECTION OF CLAMP SURFACE PRIOR TO LATCH ON	
OPERATOR OVERTORQUES CLAMP GRIP WHEN SECURING TO GIRDER BEING TRANSPORTED.	PROVIDE A TORQUE SENSING/LIMITING DEVICE	

Table 2.5-9 Top Level Hazards

APPLICABLE HAZARDS	SPECIAL SAFETY REQUIREMENTS	REMARKS/COMPONENTS
TRANSPORT MODE (PROPULSION PACK) HIGH DAMAGE POTENTIAL PROPULSION PACK SHIFTS ON STRUCTURE DURING "POWER ON".	PROVIDE BACKUP LOCKING DEVICE.	ASSUMING A CLAMP-ON DEVICE, INVESTIGATE IF STRUCTURE SHOULD INCORPORATE BUILT-IN STOPS TO PRECLUDE PACK SLIPPAGE.
VARIANCE IN THRUST BETWEEN NOZZLES.	A. PROVIDE A MANUAL METHOD OF CORRECTING ALTERED TRAJECTORY. B. PROVIDE COUNTER THRUST JETS INTEGRAL WITH THE POWER PACK.	
POWER DOES NOT TERMINATE UPON SIGNAL.	PROVIDE REDUNDANT CUT-OFF CIRCUITS.	DIRECT WIRE AS A BACKUP CONTROL SHOULD BE INVESTIGATED.
INTERMITTENT POWER PULSES	PROVIDE ACCELEROMETER OR SIMILAR DEVICE TO SENSE ERRATIC BEHAVIOR. SAID DEVICE TO INITIATE PROPULSION PACK SHUT DOWN.	1. LOW FUEL/OXIDIZER 2. CLOGGED FEED LINES 3. FAULTY PRESSURE REGULATOR
PRESSURIZED VESSEL(S) RUPTURE	A. ENCLOSE WITHIN PROTECTIVE FRAGMENTATION SHIELD WHEN NOT IN USE. B. PROVIDE THRUST NEUTRALIZING VENTS IN PRIMARY PACK SHIELD	• DETERMINE MAXIMUM NUMBER OF PRESSURE CYCLES. • DETERMINE POTENTIAL DAMGAE EXTENT TO STRUCTURAL MEMBERS.
OXIDIZER LEAKAGE	A. MINIMIZE NUMBER OF REMOVABLE CONNECTORS. B. PROVIDE REDUNDANT TANDEM SHUT-OFF VALVES.	• DETERMINE EFFECTS OF SPILLAGE ON ASTROTECHS SUIT, VISOR AND BACK PACK.

a. General Assumptions

1. Alignment of interlocking segments will not require special alignment tools.

2. Guides will be incorporated to feed modular sections into proper position and will not require precise positioning by the: a) remote manipulator; or b) the EVA team.

3. Astronaut involvement will be restricted to fine adjustments (mechanical) following complete placement of the yoke support on the mast.

4. Prior to assembly of the azimuth yoke support to the azimuth yoke, the yoke will be functionally checked to ensure proper structural alignment, freedom of rotation and control unit circuit integrity. Strap on power packs will be used for this check.

5. Solar array power is isolated from the yoke to mast work area.

6. All rotary drive and gear rack adjustments will be made prior to installation of the yoke support.

b. Analysis

The identification of applicable assembly hazards is entered in Table 2.5-10.

Future Safety Efforts

Analysis effort was limited to establishing those study efforts which would be required to identify potential hazards. Recommended future studies include:

(1) Assessments of the impact of critical operational failures, utilizing Failure Mode and Effect Analyses (FMEA) data.

(2) Evaluation of degradation which can be tolerated.

(3) Analysis to determine the probable effects from local structural failures.

(4) Explorations of hardware/component attachment options

Table 2.5-10 Top Level Hazards

APPLICABLE HAZARDS	SPECIAL SAFETY REQUIREMENTS	REMARKS/COMMENTS/QUESTIONS
ASTRONAUT CRUSHED BETWEEN SEGMENTS FOLLOWING JURY STRUT REMOVAL	PROVIDE A LOAD MEASURING DEVICE IN/ON JURY STRUTS TO INDICATE PRESSURE OF LOAD PRIOR TO ITS REMOVAL	DETERMINE FEASIBILITY OF INCORPORATING AN ELECTRICALLY ACTIVATED SCREW JACK TO RETRACT STRUTS AND TO POSITION YOKE ON CABLE SEGMENTED GEAR RACK.
ABRUPT START OR HALT OF YOKE DURING FUNCTIONAL CHECKOUT IMPARTS BREAKAWAY FORCE TO ASTRONAUT	PROVIDE A POWER GOVERNING DEVICE IN THE TEST POWER PACK CIRCUIT TO COMPENSATE FOR LOWER TORQUE DEMANDS	DETERMINE FEASIBILITY OF EMPLOYING LOW HORSEPOWER TEST MOTORS FOR THIS CHECK.
ELECTRICAL GROUNDING	SEE SUIT HAZARD ENTRY, PAGE 8.	
EVA TETHER BREAKS OR IS SEVERED	A. SPECIAL PROCEDURES SPECIFYING LOAD TESTING AND OPTICAL INSPECTION OF TETHERS. B. PROVIDE A WIPING OR SIMILAR DEVICE AT ALL ROTATING CONTACT SURFACES TO EXPEL OR PUSH ASIDE FOREIGN OBJECTS.	A. SHELF LIFE OF SPARES MAY BE CRITICAL. TIMING OF PURCHASING REPLACEMENT MAY BE CRITICAL.
YOKE TRAVEL LIMIT SWITCHES OUT OF ADJUSTMENT CAUSING ASTROTECH INJURY OR YOKE/SUPPORT DAMAGE.	A. SPECIAL PROCEDURES FOR ADJUSTING STOPS. B. AN INCHING SWITCH CAPABILITY IS RECOMMENDED TO PERMIT PRECISE CONTROL ON YOKE MOVEMENT.	

(5) Evaluation of near term and long term biological effects associated with microwave radiation at power levels generated by the system.

(6) Evaluation of the effects of microwave radiation on pressure suit metallic components.

2.6 Program Plans and Cost

During the initial contract phase, a strawman program was developed and used to establish total program costs through the development and operation of the first SSPS System. The program consisted of a three step development program that included construction and assembly of a low earth orbit demonstration facility (Demo Satellite) and a geosynchronous earth orbit plant as a precursor to the construction and operation of the first full scale SSPS. The definition of the work breakdown structure (WBS) and the associated program element costs evolved for that program are summarized in the Appendix A. These data served as a point of reference in developing cost data for alternative plans.

In the contract extension phase, three program plans evolved (one being an update of the strawman program) and cost-estimated for use in a preliminary assessment of the economic value of a LEO demonstration facility and a geosynchronous orbit pilot plant. The three plans consist of an update of the strawman program, omission of the Demo Satellite, and omission of the demo and the pilot plant, respectively. Program ROM costs were established for the design, development, test and engineering (DDT&E) phases; the unit production cost; and the transportation, fabrication, and assembly operations.

The results of the economic assessment of the demonstration and pilot plant satellites are presented in Vol III. These ROM cost estimates together with data projecting the advancement in technology resulting from the accomplishment of each of the major program milestones were used to evaluate the methodology and provide results for that economic assessment. These data are presented in Appendix E of Vol III. As is readily observed, the data derived are based on preliminary point estimating techniques and individual judgement, and were not intended for use in establishing quantitative conclusions. Thus, the results established using these data should be interpreted accordingly. However, qualitative conclusions established from these ROM cost estimates are as follows:

- The cost of transportation and assembly operations for the operational satellite is sensitive to the number of personnel required in orbit for manned assembly. Figure 2.6-1 shows the sensitivity of transportation and assembly costs in $/Kg, as a function at the percentage of assembly performed remotely.
- The development of HLLV launch system reduces transportation and assembly costs by a factor of more than 2, in comparison to DOL launch system.
- Although program costs appear to be less for the direct development to an operational satellite (i.e. no Demo satellite and no pilot plant), further studies should be performed to identify the cost of the sustaining engineering and development activities supporting the maturation of the SSPS configuration during the subsequent satellite builds.

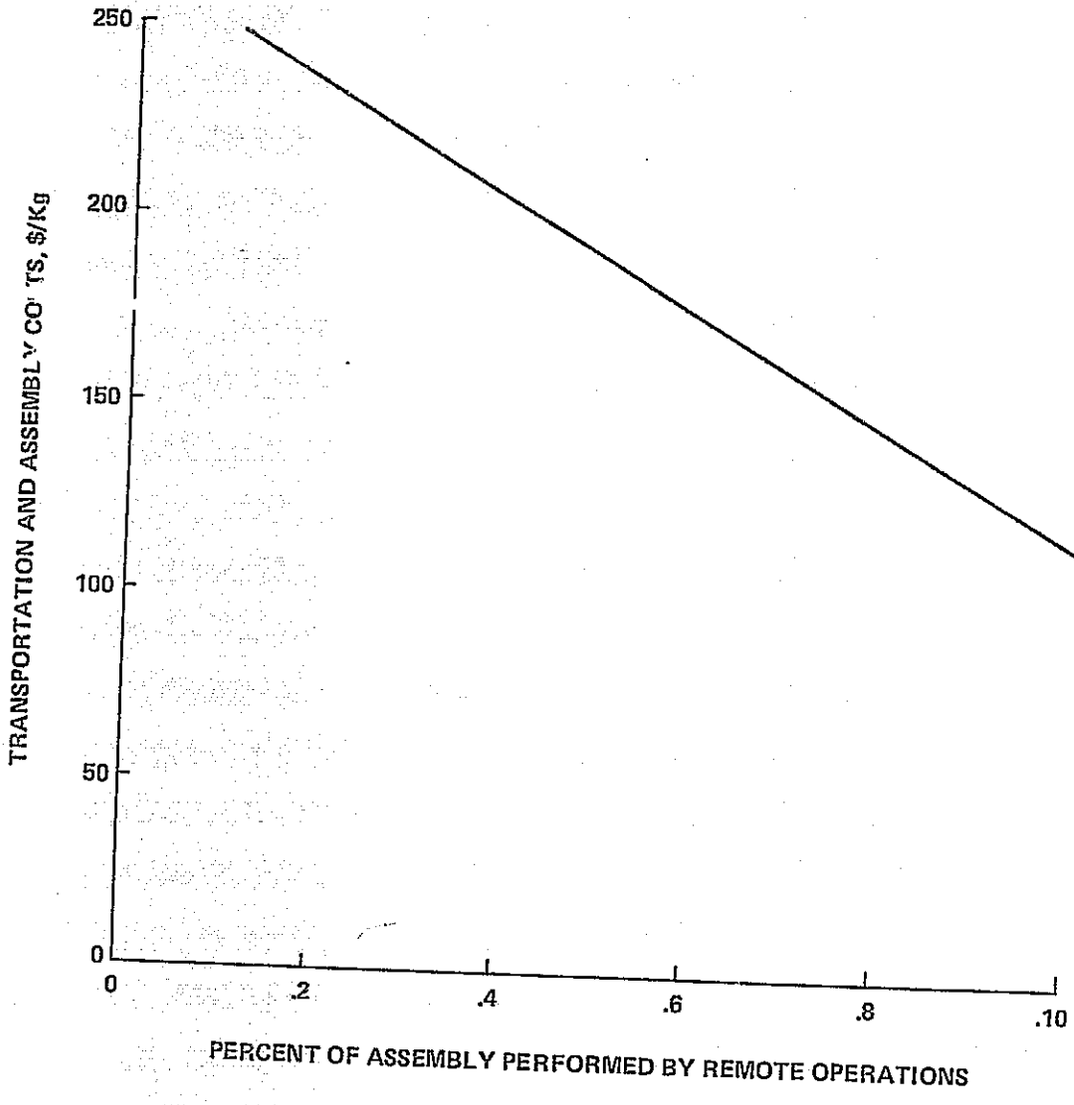

Figure 2.6-1 Transportation and Assembly Costs For Operational SSPS

Paragraphs 2.6.1 through 2.6.4 describe the three program options developed and their associated ROM costs. The updated strawman program is discussed first for overall continuity.

2.6.1 Program 3 - Demo Lab, Pilot Plant, Operational System Program

Figure 2.6-2 depicts the updated overall three-step program development leading to the placement of the first operational satellite at the end of 1995. This program is based on the development of a LEO 15 MW demonstration laboratory, to be operational at the end of 1985, and a 1 GW pilot plant satellite, to be operational at the end of 1991. Shown, also, is the time phasing of the critical technology development programs that are necessary to advance the state of technology to be utilized in the Demo Lab and pilot plant DDT&E phases. Associated transportation system development programs are indicated on Figure 2.6-2 by two time-phased development programs; for HLLV and the Advanced Ion OTV. The two schedules are based on their availability for either the pilot plant transportation to LEO and transfer to geosynchronous orbit or first availability for the operational system. Program costs were estimated based on HLLV and advanced Ion OTV availability for use with the pilot plant operations.

Development of associated assembly equipment, including fabrication modules, manipulators, and teleoperators, is scheduled for completion for the fabrication and assembly of the demonstration facility. The LEO space station, with a scheduled IOC during 1984, would serve as the habitat for the construction of the Demo Lab. Operational Status of a GEO space station is scheduled for the time of pilot plant operations at geosynchronous orbit.

2.6.1.1 Supporting Technology Program

Figure 2.6-3 defines the supporting technology program required for the orbital system elements. Specific technology objectives for the large solar arrays, the microwave transmission system, and the large structure and assembly have been identified, and are summarized in Section 4. Major solar-array technology improvements include solar cell conversion efficiency for lightweight solar cell blankets, blanket fabrication processing for large production quantities at economically viable costs, and solar cell thermal and radiation resistance improvements for long life compatibility. The microwave transmission system technology development relates to efficiency of DC to RF conversion, phase front control for beam pointing and focusing, and waveguide manufacturing with emphasis on fabrication and assembly. Antenna mechanical pointing technology development is concerned with actuator development, power transfer characteristics across

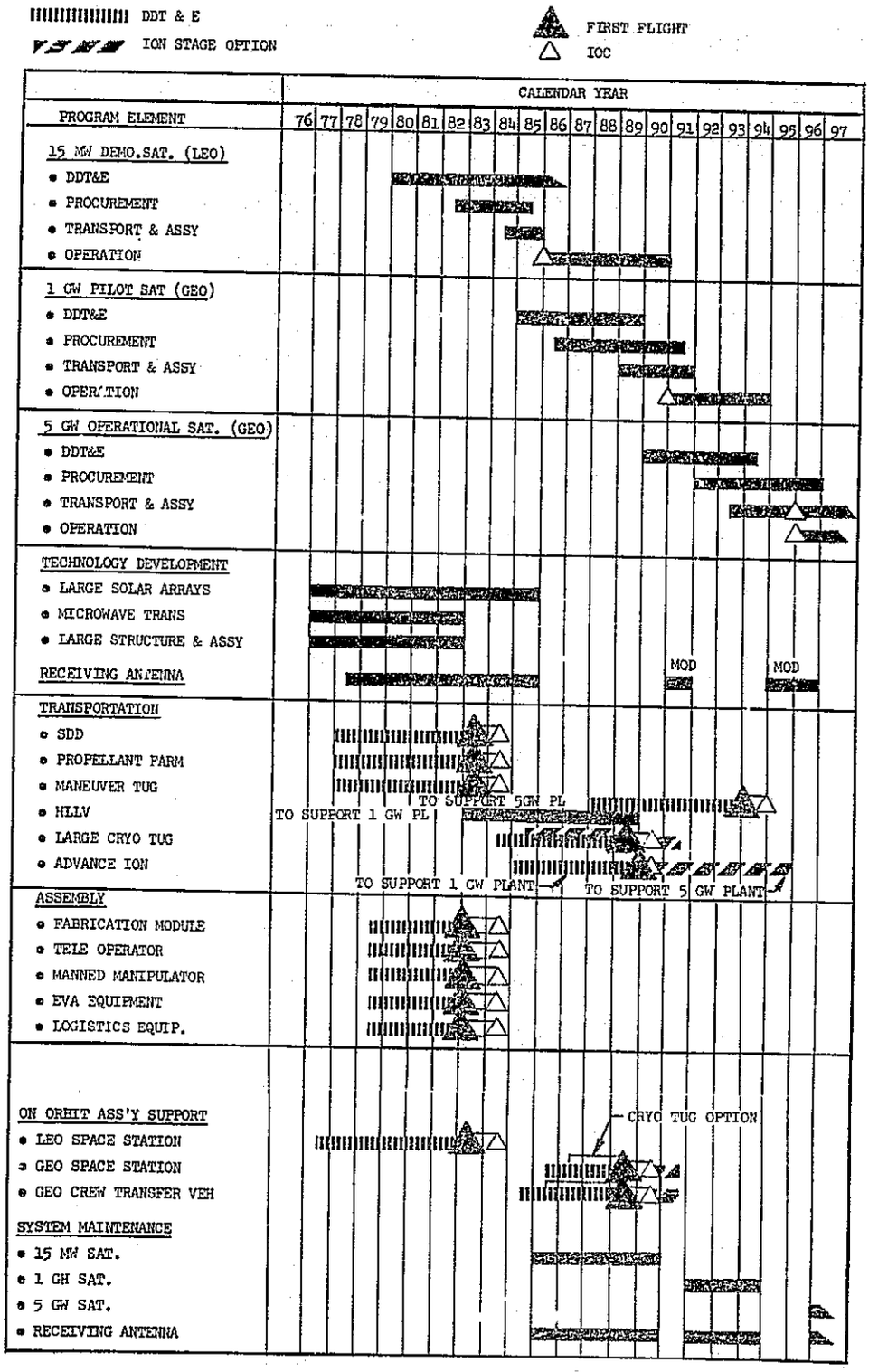

Figure 2.6-2 SSPS Program 3

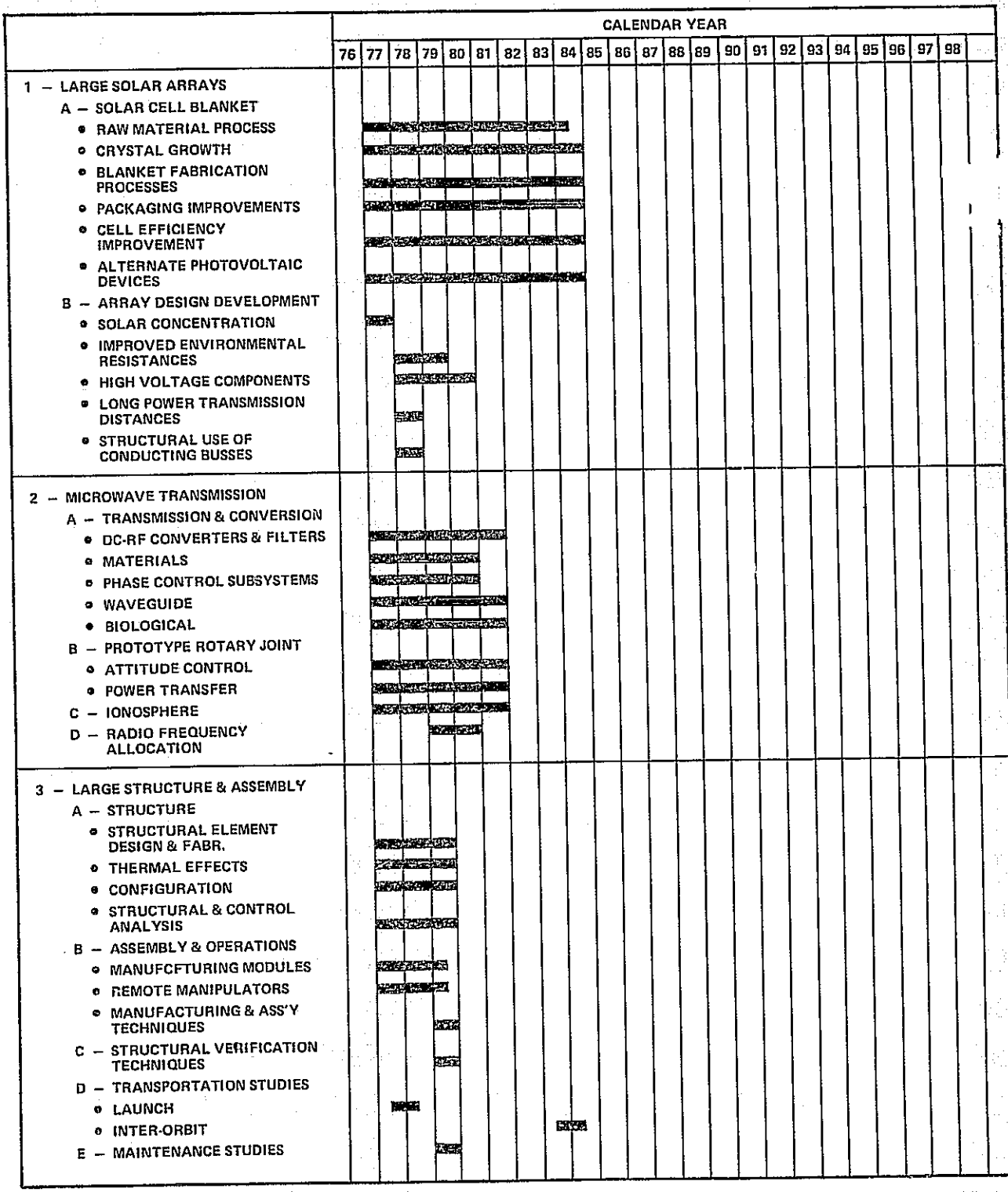

Figure 2.6-3 Supporting Technology Development, SSPS Program 3

flexible joints and conductors. Microwave beam effects on the ionsphere will stress evaluation of power density levels as a function of operating frequency. Further technology development of large structures will be directed to structural element design using thin wall aluminum and composites compatible with the applied loads, the thermal environment, and on-orbit manufacturing and assembly techniques. Emphasis also will be placed on the development of manufacturing modules and equipment used in the space-based fabrication and assembly of the SSPS.

2.6.1.2 Program Support Equipment Costs

Table 2.6-1 lists the ROM costs for support equipments that are directly and indirectly related to the SSPS. Those equipments listed as indirect were identified as having wide use in other programs, and a high potential of being developed independently of the SSPS program. Costs for these equipment were estimated using the Koelle cost estimating relationships (CER) shown in Figures 2.6-4 and 2.6-5. These data were presented at the "2nd Symposium on Cost Reduction in Space Operations" at the International Academy of Astronautics, 14 October 1972, by Dr. D.E. Koelle. The Koelle cost model was used because data are compiled at a "Systems" level. (Since the Aerospace model would require definition to the subsystem level, its use would require the resources not available for this study.)

Figure 2.6-4 presents the CER's used to establish ROM development and fabrication costs for the transportation systems. Figure 2.6-5 presents the CER's used to estimate the ROM development and fabrication costs for manned and unmanned assembly support equipments.

Note that Table 2.6-1 presents the CER number used, the weight used in the estimate, the percent of new technology assumed, and the number of units used to establish production costs on an 85 percent learning curve.

2.6.1.3 15 MW Demonstration Satellite

Figure 2.6-[illegible] is a conceptual design for a 15 MW (antenna output power) demonstration and test satellite. The solar array is designed with a concentration ratio of two. The silicon solar blanket efficiency was established using the projected efficiency for the SEPS array (12 percent), with efficiency degraded for the operating temperature at a concentration ratio of two. A power distribution system efficiency of 92 percent was assumed, and the projected microwave conversion efficiency of 82 percent was utilized to compute the array output power requirement.

Table 2.6-1 ROM Costs - Transportation/Assembly/Maintenance Equipment

ELEMENT	CER # USED	WGT USED IN CER Kg	% NEW TECH	ROM DDT&E $M	UNIT PRODUCTION COST $M	IOC	COMMENTS	NO. OF PROD UNITS ON 85% LEARNING CURVE
DIRECTLY CHARGEABLE TO SSPS:								
• ASSEMBLY EQUIP								300
– TELEOPERATORS	3	180	35	19	2.5	1985		50
– MAN. MANIPULATORS	4	1,940	75	365	11	1985		300
– EVA EQUIPMENT	4	90	75	26	1.5	1985		–
• LOGISTICS EQUIP.	3	–	0	44	–	1985	MODS TO ASSEMBLY EQ'P	–
• MAINTENANCE EQUIP.	3	–	0	44	–	1990	MODS TO ASSEMBLY EQ'D	100
• FABRICATION MOD.	3	4,540	50	271	12	1985	3 TYPES DEVEL'D	
SUBTOTAL				769				
INDIRECT CHARGES:								
• LEO TRANSPORT				N/A	200	1980		–
– SHUTTLE	–			380	150	1990	NO ENGINE DEVEL'MT	–
– DEPLOY ONLY LAUNCHER	2	286,000	30	6540	400	1995	ENG WGT = 63,600 Kg/ENG	
– HLLV	1&2	477,000	75				(H_2/O_2 = TURBOPUMP)	–
• SO TRANSPORT				166	15	1990	DERIVATIVE OF ET/SSME	–
– LARGE CRYO TUG	2	36,000	30	3847		1995		100
– ADVANCED ION	1&2	726,000	75	223	27	1990		300
– PROPELLANT DEPOT	3	30,000	30	215	2.6	1990		100
– TUG FOR DEPOT	2	1,300	30	190	23	1990		50
• SO CREW TRN MODULE	4	11,640	20	2225	62	1990		–
• LEO SPACE ST	4	76,450	50	224	62	1990		
• SO SPACE ST	4	76,450	0					
SUBTOTAL				14,010				

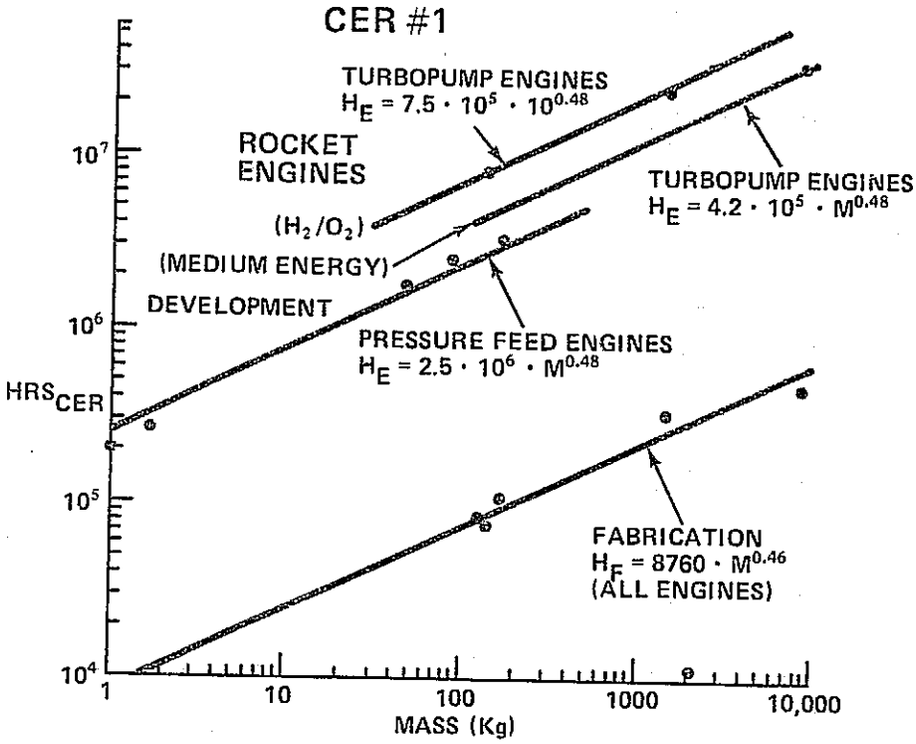

DEVELOPMENT AND FABRICATION EFFORT FOR LIQUID PROPELLANT ROCKET ENGINES

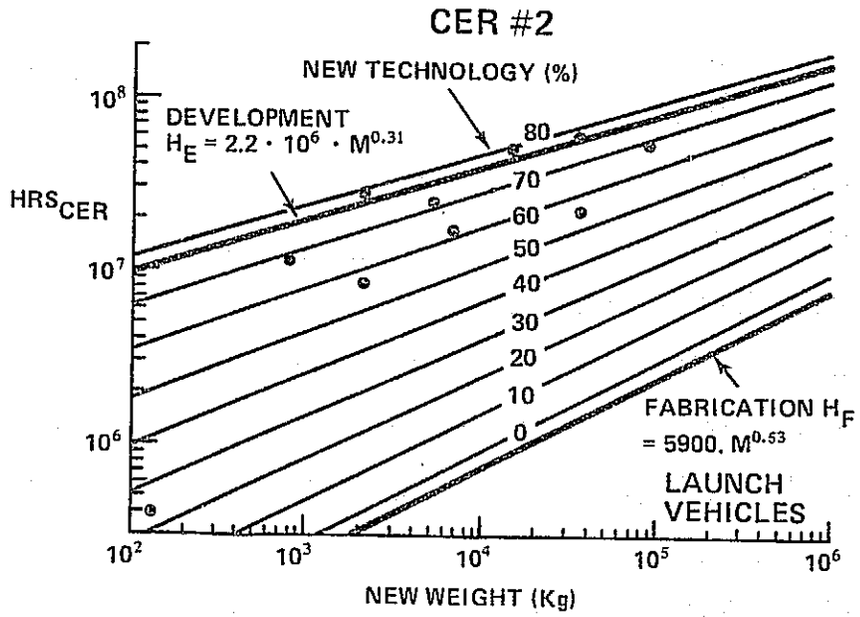

DEVELOPMENT AND FABRICATION EFFORT FOR LAUNCH VEHICLE STAGES VS. NET WEIGHT WITHOUT PROPELLANTS (EXCLUDING ENGINES'; INCLUDING ADAPTERS)

Figure 2.6-4 Cost Estimating Relationships

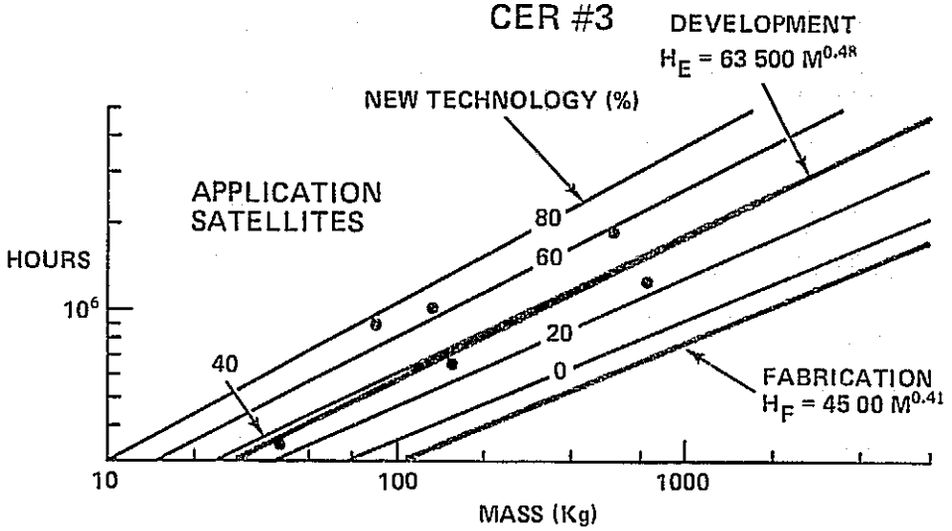

DEVELOPMENT AND FABRICATION EFFORT FOR APPLICATION SATELLITES

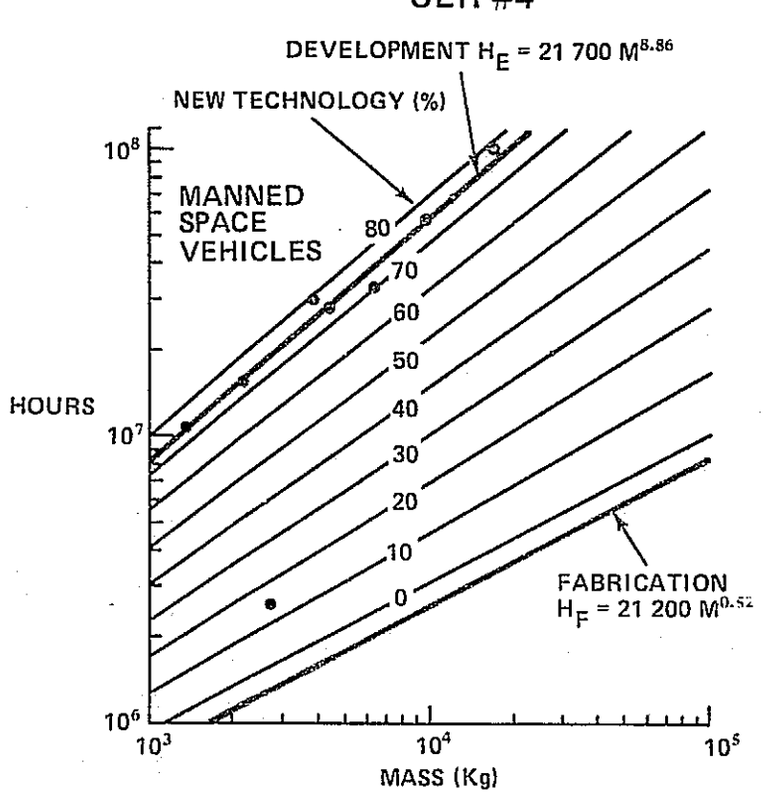

DEVELOPMENT AND FABRICATION EFFOR FOR MANNED SPACE VEHICLES VS. MASS (EXCLUDING PROPELLANTS)

Figure 2.6-5 Cost Estimating Relationships

15 MW OUTPUT POWER

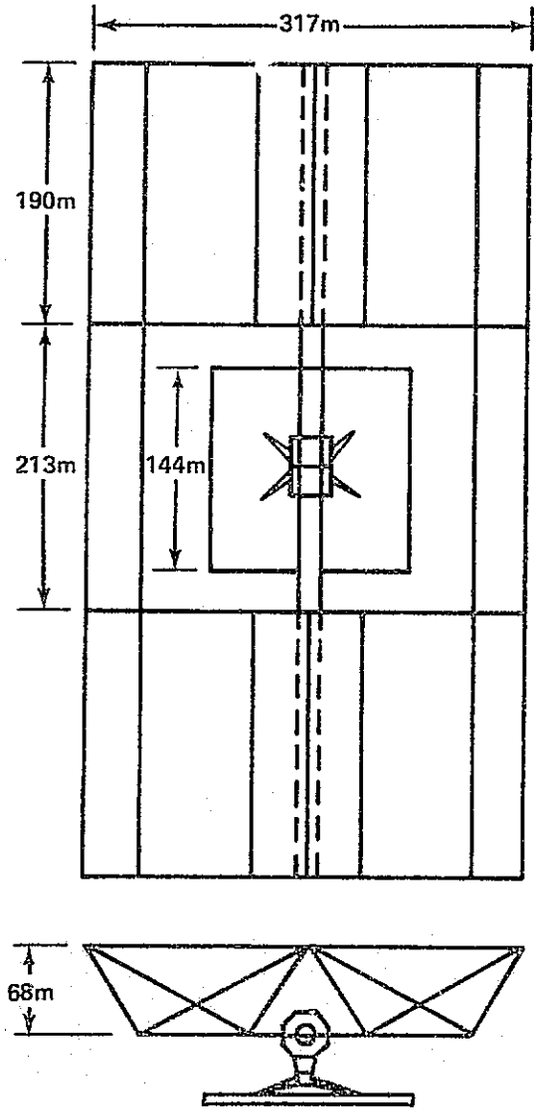

CHARACTERISTICS

- SOLAR BLANKET
  - CONCENTRATION RATIO = 2
  - CELL EFFICIENCY = 9.7%
  - POWER DISTRIBUTION EFF. = 92%
- MICROWAVE CONVERSION EFF = 82%

WEIGHTS (228,343 KG)

ARRAY

• BLANKET =	= 39,571 KG (0.525 KG/M^2)
• CONCENTRATOR	= 3014 KG (0.02 KG/M^2)
• NON CONDUCT. STRUCT.	= 16,692 KG (2.76 KG/M LENGTH)
• CONDUCT. STRUCT	= 2633 KG (2.76 KG/M LENGTH)
• MAST	= 1049 KG (2.76 KG/M LENGTH)
SUBTOTAL	= 62959 KG

ROTARY JOINT = 12,670 KG (1/10 WT OPS SYST)

ANTENNA

• STRUCTURE	= 9083 KG (.43 kg/m^2)
• CONTOUR CONTROL	= 3648 KG (.38 kg/m^2)
• POWER DIST	= 10648 KG (RAYTHEON EST)
• CONTROL ELECT	= 5632 KG (RAYTHEON EST)
• TUBES	= 2848 KG (RAYTHEON EST)
• WAVEGUIDE	= 95,296 KG (RAYTHEON EST)
SUBTOTAL	= 127,155 KG

Figure 2.6-6 Demonstration and Test Satellite

The array weight estimates were based on projected SEPS solar blanket weights (0.525 kg/m^2) and the projected use of 0.5 mil aluminized Kapton in the 1995 mirror system. The weight-per-unit-length of structure for the 1995 satellite was also used as the basis of establishing the non-conducting structural weights. The column lengths for this design are approximately the same as the 1995 system. The weight of the conducting structure and central mast are sized by electrical requirements of the operational system and structural requirements of this system. The rotary joint is scaled down (1/10 size) from the 1995 system. The total weight of the satellite should be 228,343 kg (503,148 lb).

Two options were considered for placing the 1985 Demo Satellite into low earth orbit. The first considered shuttle utilization exclusively, using a series of shuttle flights to transport materials and equipment to orbit and assembling in orbit. Figure 2.6-7 shows a mission schedule utilizing 53 flights. Mission 1 is a series of 24 flights that fabricates and assembles the complete antenna assembly. Missions 2 and 3 assemble the rotary joint and its interface with the antenna. Mission 4 assembles the central mast, and joins it to the rotary joint. Mission 5 assemblies the solar array and installs the microwave antenna to complete the assembly of the Demo Satellite. Mission 6 transfers the assembled satellite to its operational orbit.

The second option, illustrated by Figure 2.6-8, is the placement of a Space Station in low earth orbit, from which the Demo Satellite would be fabricated, assembled, and serviced. Materials and equipment would be delivered to the Space Station using the DOL launch system; a crew of six would fabricate and assemble the Demo Satellite over a period of 18 months. Table 2.6-2 summarizes the equipment needed in orbit and the number of DOL and shuttle flights required for material and crew transport. A total of 16 flights have been defined, of which nine are shuttle flights for crew rotation at 60 day intervals. Total program costs summarized in paragraph 2.6.1.5, were based on this option.

2.6.1.4 1GW Pilot Plant

A conceptual design of the 1 GW Pilot Plant placed at geosynchronous orbit and scheduled for operation at the end of 1991, together with the assumptions used in sizing the configuration is shown in Figure 2.6-9. Total system weight is 8.33 x 10^6 Kg. The transmitting antenna and rotary joint are assumed to be the same as in the operational configuration.

MISSION	81	82	83	84	85	COMMENT
			YR			
1 – COMPLETE ANTENNA ASSEMBLY				24 FLTS		
2 – ROTARY JOINT ASSEMBLY				4 FLTS		ADD S/C MODULE & LEAVE IN ORBIT
3 – ROTARY JOINT TO ANTENNA					3 FLTS	LEAVE IN ORBIT
4 – CENTRAL MAST & INTEGRATION TEST					2 FLTS	ADD TO ASSEMBLY IN ORBIT
DEMO SATELLITE:						
5 – SOLAR ARRAY ASSEMBLY					18 FLTS	ADD ANTENNA TO COMPLETE DEMO SAT.
6 – ASSEMBLY TRANSFER					2 FLTS	
TOTALS						53 FLTS

Figure 2.6-7 Mission Schedule Using Shuttle

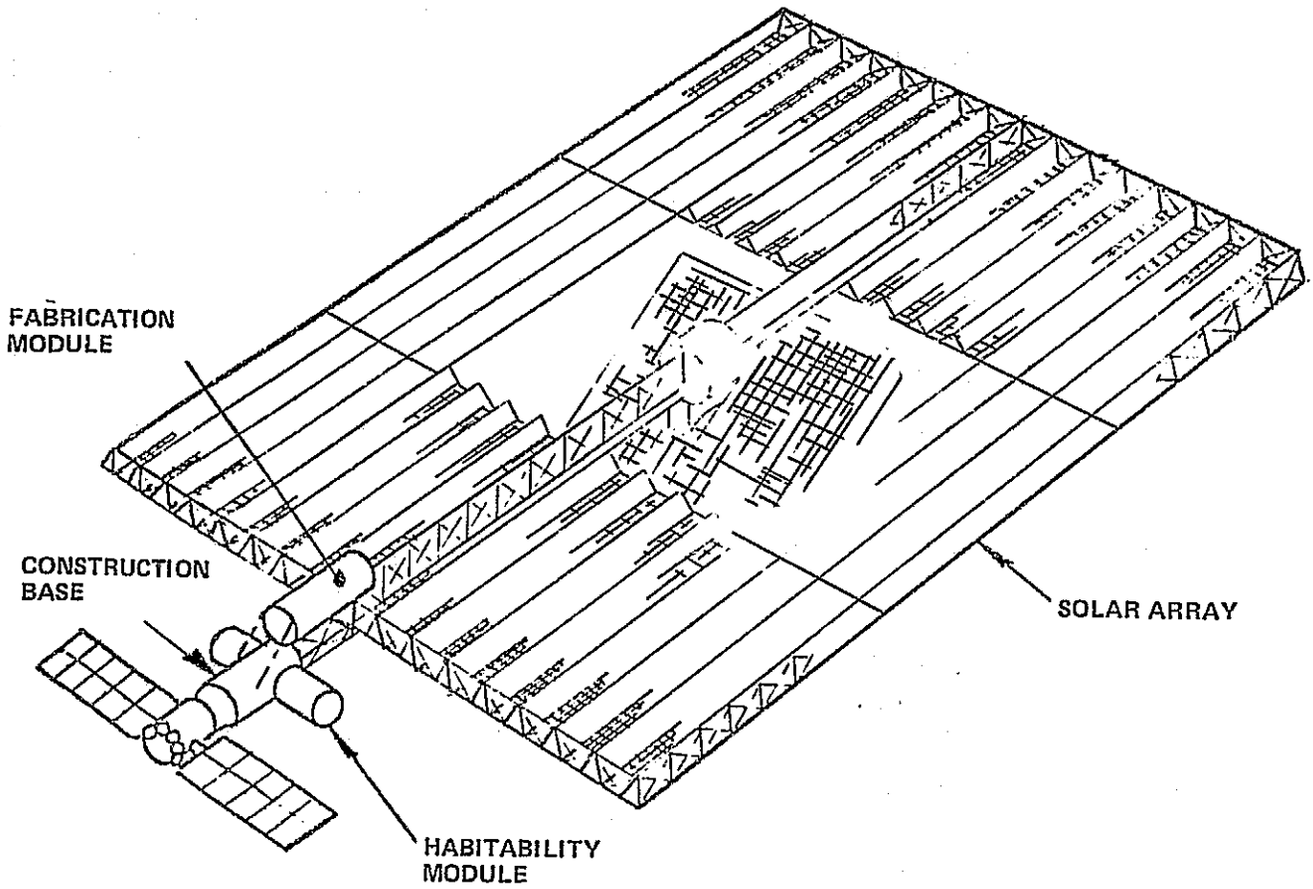

Figure 2.6-8 Space Station Construction of Demo Satellite

Table 2.6-2 Transport Flights to LEO for DEMO Satellite Construction Using Space Station

ELEMENT	WEIGHT TO LEO, 10^3 Kg	NO. OF DOL FLIGHTS	NO. OF SHUTTLE FLIGHTS
• SPACE STATION			
– 6 MAN HAB. MOD.	80	2	
– CONSTRUCTION BASE	10		
– FABRICATION MOD	5		
• ASSEMBLY EQUIP			
– MANNED MANIPULATOR	4	1	
– EVA EQUIPMENT	0.5		
• SUPPLIES			
-- SPACE STATION EQUIPT SUPPLIES	20		
– MISCELLANEOUS	3.5		
• MATERIAL TRANSPORT	229	4	
• CREW TRANSPORT			9
TOTAL	352	7	9

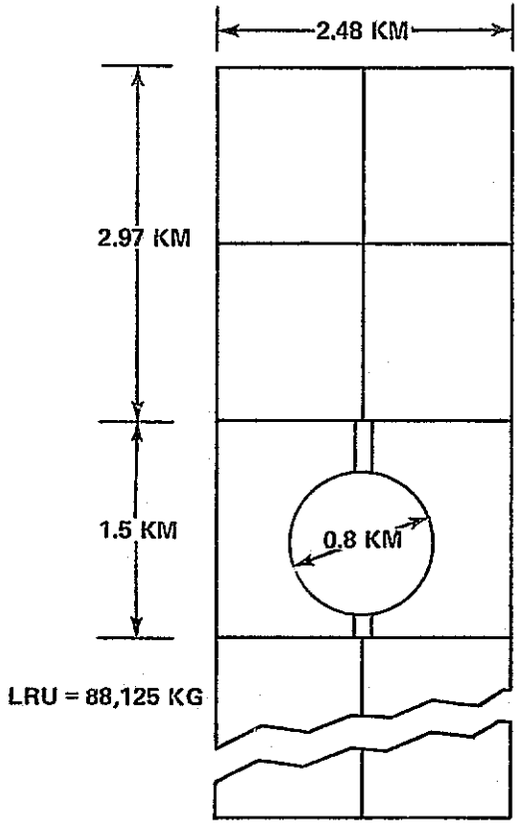

CHARACTERISTICS

- SOLAR BLANKET
  - CONCENTRATION RATIO = 2
  - CELL EFFICIENCY = 11%
  - POWER DISTRIBUTION EFF = 92%
- MICROWAVE CONVERSION EFF = 57% RECTIFIED AT GROUND

ARRAY	WEIGHTS KG X 10^6	COMMENT
• BLANKET =	2.82	(7.04 KM^2) (0.4 KG/M⊕)
• CONCENTRATOR =	0.31	(15.4 KM^2) (0.2 KG/M^2)
• NON CONDUCT STRUCT =	0.61	(18.5 KM^2) (0.033 KG/M^2)
• CONDUCTING STRUCT =	0.07	(18.5 KM^2) (0.004 KG/M^2)
• MAST =	0.38	(7.4 KM) (0.052 KG/KM)
	4.19	
ROTARY JOINT	0.20	(SAME AS 1995 SYSTEM)
MW ANTENNA	3.94	(SAME AS 1995 SYSTEM (WITH REDUCE # OF TUBES)
TOTAL	8.33	(18.3 X 10^6 LB)

Figure 2.6-9 Pilot Plant (1990) 1 GW Ground Power

The satellite is fabricated and assembled in LEO using Space Station modules, and transported to geosynchronous orbit by a series of large cryo OTV flights. The program plan also shows an option for the early development of an Advanced Ion Propulsion Stage for transfer of the pilot plant to geosynchronous orbit. This option, however, was not utilized to establish program costs; an advanced OTV was assumed available for transportation of the first operational satellite.

Table 2.6-3 summarizes the total equipment and supplies to be brought to LEO for the fabrication and assembly of the 1 GW pilot plant. Fourteen 6-man space station habitats are needed to support an assembly crew of 80 men over a 24 month period. The crew size was estimated by assuming that 50% of the fabrication and assembly is performdd by ground-controlled teleoperators, operating approximately 20 hours per day. The remaining assembly is performed by on-orbit crew operations. A 6 man GEO space station is deployed to support the on-orbit and maintenance operations.

The number of flights required to transport the equipment and supplies were evaluated for two transportation system options: Option 1 was based on the utilization of the DOL launch system; option 2 was based on the utilization of the HLLV launch system (starting in 1988). The total number of flights required for each of these launch systems are summarized in Table 2.6-3. Shuttle flights for crew personnel transport using the large passenger transport version also are shown.

2.6.1.5 Program 3 Total Costs

Using the data in the Appendix A as a reference, total program costs were established for the updated strawman program. Table 2.6-4 is a summary tabulation. DDT&E and unit production costs for the Demo Satellite. the Pilot Plant, and the Operational Satellite were used to establish costs for those elements of the program. The data was formulated during the phase I contract effort using a similar program development schedule and is considered directly applicable. Transportation and assembly costs for each of the mission elements were regenerated based on the several transportation and assembly options discussed previously.

Table 2.6-5 summarizes the mission costs for transporting and assembling the Demo Satellite by means of the series of shuttle flights described in paragraph 2.6.1.3. A 15% cost factor has been added to account for auxiliary equipment such as space platforms, power modules, etc.; an additional 10% is included to account for modifications to the shuttle support equipments, ground facilities, etc. The total Demo Satellite assembly program using shuttle is estimated at $962 M. Although these costs were not utilized in the overall program costing results, they are presented here for reference.

Table 2.6-3 Transport Flights to LEO and GEO for Pilot Plant

ELEMENT	NO. OF UNITS	WGT TO LEO 10^6 KG	OPTION 1 NO. OF DOL FLTS	OPTION 1 NO. OF SHUTTLE FLTS	OPTION 2 NO. OF HLLV FLTS	OPTION 2 NO. OF SHUTTLE FLTS
EQUIPMENT						
• LEO SPACE STATION (6 MAN/UNIT)	14	1.07	15		6	
• GEO SPACE STATION	1	.076	1		1	
• ASSEMBLY EQUIPMENT						
– MANNED MANIPULATORS	14	.0271	1		2	
– TELEOPERATORS	80	.0147				
– EVA EQUIPMENT	260	.021	1			
• FABRICATION MODULES	2	.002	1			
• LARGE CRYO OTV	3	.10				
• SUPPORT TUGS	10	.013				
• PROPELLANT STORAGE TANKS	6	.19	3			
• ORBIT MAINT MODULE	1	.002	1		2	
• CREW MODULE	1	.012				
SUPPLIES						
• CRYO PROPELLANTS		15.04	208		77	
• SPACE STA EQUIP & SUPPLIES			8		5	
• CREW ROTATION				16		16
MATERIALS TRANSPORT		8.33	115		46	
TOTALS			354	16	139	16

Table 2.6-4 Program 3 Total Costs

	COST $M	EXPENDITURE PERIOD		
SUPPORTING RESEARCH & TECH. PROG. • SOLAR ARRAY • MICROWAVE • STRUCTURAL TOTAL	358.9 60.4 39.3 458.6	1977 – 1985		
	DDT&E $M	UNIT PROD $M	ASSMEBLY OPERATION	EXPENDITURE PERIOD
LEO DEMO SATELLITE • SOLAR ARRAY • ANTENNA INTERFACE • TRANSMITTING ANTNENA • RECEIVING ANTENNA SUBTOTAL MANAGEMENT, S&I (40%) UNCERTAINTIES (20%) TOTAL	 1108 383 610 59 2160 864 432 3456	$7616/KW 114.2 45.7 22.8 182.7	1388 $/KG 317 317	1980–1985
PILOT PLANT • SOLAR ARRAY • ANTENNA INTERFACE • TRANSMITTING ANTENNA • RECEIVING ANTENNA SUBTOTAL MANAGEMENT, S&I (40%) UNCERTAINTIES (20%) TOTAL	 3104 446 320 1218 5088 2035 1017 8140	 765 105 144 392 1406 562 281 2249	$322/KG (HLLV) LAUNCH SYS $697/KG (DOL LAUNCH SYS) 2682 (5806) 2682	1985–1991
OPERATIONAL PLANT • SOLAR ARRAY • ANTENNA INTERFACE • TRANSMITTING ANTENNA • RECEIVING ANTENNA SUBTOTAL MANAGEMENT, S&I (40%) UNCERTAINTIES, (20%) TOTAL	 1024 149 260 403 1836 734 367 2937	 1828 156 861 2340 5185 2074 1037 8296	$148/KG 2679 2679	1990-1995
GRAND TOTALS	14992	10728	5678	$31,398 M

Table 2.6-5 Shuttle Utilization Flight Test Cost Summary

MISSION	SHUTTLE FLTS	SHUTTLE COSTS	YR	MISSION COST $M*
1	24	312	1983-1984	312
2	4	52	1983-1984	66.5
3	3	39	1984	41.5
4	2	26	1984-1985	29.6
5	18	234	1984-1985	254.7
6	2	26	1985	56.0
SUBTOTAL	53	689		760.3
15% for Shuttle Auxiliary Equipment				114.1
SUBTOTAL				874.4
10% for Shuttle Support System Mods				87.5
TOTAL				961.9

*Excludes cost of microwave components

Table 2.6-6 summarizes the Demo Satellite transportation and assembly costs based on the utilization of a LEO space station and the DOL launch system. The data were derived using the equipment cost summarized in the WBS of the appendix, with the LEO space station and launch vehicle fleet purchase costs amortized. The total Demo Satellite assembly costs were estimated at $317M ($1,388/Kg); this cost compares favorably to the corresponding assembly and operations cost shown in the Appendix. The data were utilized in establishing the overall program costs.

Table 2.6-7 summarizes the 1 GW Pilot Plant transportation and assembly costs with the DOL launch system option. These costs, as shown are estimated at $5804M ($697/Kg). Differences between this estimate and that shown in Appendix A are due primarily to the accounting policies adopted, since major equipment and launch vehicle purchase costs were amortized; the previous data were based on unamortized equipment costs.

Table 2.6-8 summarizes the 1 GW pilot plant transportation and assembly costs with the HLLV launch system option. As shown in the table, this option significantly reduces the costs of transportation and assembly.

Transportation and assembly costs for the operational 5 GW SSPS baseline configuration is summarized in Table 2.6-9. This cost estimate assumes that 80% of the assembly operations are performed by ground-controlled teleoperators, and that the remaining 20% require man-tended functions. A need for a synchronous orbit space station is assumed for final assembly, checkout, and maintenance functions. Total costs are estimated at $2666M ($148/Kg). Differences between these data and the data shown in the appendix are due principally to the costs assumed for crew rotation. This estimate assumed that a large passenger transport shuttle is developed, and available, in the 1990 time frame.

2.6.2 Program 1 - Direct Development of Operational Satellite

Figure 2.6-10 presents the overall program schedule for the direct development of an operational satellite with an IOC scheduled at the end of 1991. The DDT&E phase is assumed to commence in 1984, and is extended over a seven year period. The fabrication, assembly, and transport to GEO is performed over a three year period. The satellite on-orbit construction is supported by a LEO Space Station, and the assembled SSPS is transported to GEO using an advanced Ion propulsion stage. The GEO Space Station is used to support final assembly, checkout, and maintenance operations at geosynchronous orbit. The development schedule for the transportation systems, assembly equipment, and on-orbit support equipments are also shown.

Table 2.6-6 Transportation and Assembly Costs For LEO Demonstration Lab

ELEMENT	NO. OF UNITS	EQUIP. COST, $M	WGT. TO LEO, 10^3 KG	NO. OF DOL FLIGHTS	NO. OF SHUTTLE FLIGHTS	COST, $M	ASSUMPTIONS
EQUIPMENT:							(1) LEO SPACE STATION AMORTIZED OVER FIVE CONSTRUCTION PERIODS
• LEO SPACE STATION	1	47(1)	80	2		65	
• ASSEMBLY EQUIPMENT							
— MANNED MANIPULATOR	2	22	4			22	
— EVA EQUIPMENT	6	9	0.5			9	
• FABRICATION MODULE	1	12	5			12	
• CONST BASE FACILITY	1	30	10	1		39	
SUPPLY:							
• SPACE STA EQUIP AND RESUPPLIES			20			1	
• MISCELLANEOUS			3.5				
CREW ROTATION					9	108	
MATERIAL TRANSPORT			229	4		36	
SUBTOTALS			350	7	9	292	
• PERSONNEL						1	
• AMORTIZED L/V COSTS						24	
TOTAL						317	
TRANSPORTATION & ASSEMBLY COSTS, $/Kg						$1388	

NOTES:
1. LAB WGT = 228,343 KG
2. 100 PERCENT MANNED ASSEMBLY OVER 18 MONTH PERIOD

Table 2.6-7 Transportation and Assembly Costs for 1 GW Pilot Plant DOL Launch System

ELEMENT	NO. OF UNITS	EQUIP COST, $M	WGT TO LEO, 10^3 KG	NO. OF DOL FLIGHTS	NO. OF SHUTTLE FLIGHTS	COST, $M	ASSUMPTIONS
EQUIPMENT:							(1) LEO SPACE STATION AMORTIZED OVER FIVE CONSTRUCTION PERIODS
• LEO SPACE STATION (6 MEN/ UNIT)	14	268.8(1)	1.07	15		463.8	
• GEO SPACE STATION (6 MEN/ UNIT)	1	20(1)	0.076	1		33	
• ASSEMBLY EQUIP							
– MANNED MANIPULATORS	14	31(1)	0.0271			31	
– TELEOPERATORS	80	40(1)	0.0147	1		53	
– EVA EQUIPMENT	260	78(1)	0.021	1		91	
• FABRICATION MODULES	2	24	0.002			24	
• LARGE CRYO TUG	3	9(1)	0.10	1		22	
• SUPPORT (MANEUVER) TUGS	10	26	0.013			26	
• PROPELLANT STORAGE TANKS	6	33(1)	0.19	3		72	
• ORBIT MAINT. MODULE	1	3.2	0.002	}		3.2	
• CREW MODULE	1	23	0.012	} 1		36	
SUPPLY:							
• CRYO PROPELLANTS			15.04	208		2704	
• S/S & EQUIP RESUPPLY				8		104	
• CREW ROTATION					16	192	
MATERIALS TRANSPORT			8.33	115		1495	
SUBTOTAL				354		5350	
• PERSONNEL	804					36	
• AMORTIZED L/V COST						600	
TOTAL						5986	
TRANSP AND ASSEMBLY COST, $/KG						719	

NOTES:
1. PILOT PLANT WGT = 8.33×10^6 KG
2. 50 PERCENT MANNED ASSEMBLY, 50 PERCENT REMOTE ASSEMBLY

Table 2.6-8 Transportation and Assembly Costs for 1 GW Pilot Plant - HLLV Launch System

ELEMENT	NO. OF UNITS	EQUIP COSTS, $M	WGT TO LEO, 10^6 Kg	NO. OF HLLV FLTS (3)	NO. OF SHUTTLE FLTS (2)	COST, $M
EQUIPMENT:						
• LEO SPACE STATION	14(6)	268.8(1)	1.07	6		322.8
• GEO SPACE STATION	1	20(1)	0.076	1		29
• ASSEMBLY EQUIP						
— MANNED MANIPULATORS	14	31(1)	0.0271			31
— TELEOPERATORS	80(7)	40(1)	0.0147			40
— EVA EQUIPMENT	260	78(1)	0.021	2		78
• FABRICATION MODULES	2	24	0.002			42
• LARGE CRYO TUG	3	9(1)	0.10			9
• SUPPORT (MANEUVER) TUGS	10	26	0.013			26
• PROPELLANT STORAGE TANKS	6	33(1)	0.19			33
• ORBIT MAINT MODULE	1	3.2	0.002	2		21.2
• CREW MODULE	1	23	0.012			23
SUPPLY						
• CRYO PROPELLANTS			15.04	77		747
• S/S & EQUIP RESUPPLY				5		45
• CREW ROTATION (5)					12	144
MATERIALS TRANSPORT			8.33	46		414
• SUBTOTAL				139	12	2005
• PERSONNEL	804					36
• AMORTIZED L/V COST (4)						648.0
TOTAL						2689
TRANSP AND ASSEMBLY COST, $/KG						$323

ASSUMPTIONS

(1) COSTS AMORTIZED OVER 5 SATELLITE CONSTRUCTION PERIODS

(2) PASSENGER VERSION OF SHUTTLE-45 PASSENGERS TO LEO AT $9M/FLT

(3) HLLV CLASS 4 — 181.3 x 10^3 KG TO LEO

(4) L/V AMORTIZED BY TOTAL NO. OF FLIGHTS VS DESIGN LIFE

(5) CREW CYCLED EVERY 60 DAYS

(6) 9 KG/HR ASSEMBLY RATE, 56 HR WORK WEEK PER MAN

(7) 4.5 KG/HR ASSEMBLY RATE, 20 HR/DAY

NOTES:
1. PILOT PLANT WGT = 8.33 X 10^6 KG
2. 50 PERCENT MANNED ASSEMBLY, 50 PERCENT REMOTE ASSEMBLY

Table 2.6-9 Transportation and Assembly Costs - 5 GW Operational Satellite - 20 Percent Manual Assembly, 80 Percent Remote Assembly

ELEMENT	NO. OF UNITS	EQUIP COST, $M(1)	WGT TO LEO, Kg x 10^6	NO. OF HLLV FLTS(3)	NO. OF SHUTTLE FLTS	COST, $M
EQUIPMENT:						
• LEO SPACE STATION	12(6)	230	0.912	5	3	275
• GEO SPACE STATION	1	192	0.076	1		32.2
• ASSEMBLY EQUIPMENT						
– MANNED MANIPULATORS	12	26.4	0.023			
– TELEOPERATORS	225(7)	112.5	0.040		3	205.9
– EVA EQUIPMENT	100	30.0	0.009			
• FABRICATION MODULES	3	10	0.016			
• LARGE CRYO TUG	2	6	0.072	1		8
• MANEUVER TUG	11	5.7	0.013		1	10
• CREW MODULE	1	5	0.012		1	10
• PROPELLANT STORAGE TANKS	26	140	0.780	5		185
• ORBIT MAINT. MOD.	1	3.2	0.002			3.2
• ADVANCED ION STAGE	1	38	0.726	4		74
SUPPLY:						
• CRYO PROPELLANTS			0.981	6		54
• ION PROPELLANTS			0.772	5		45
• S/S & EQUIP. RESUPPLY			0.772	5		45
• CREW ROTATION(5)					24(2)	216
MATERIAL TRANSPORT			18.06	100		900
SUBTOTAL				132	29	2063
• PERSONNEL	663					29.8
• AMORTIZE L/V COST				528(4)	58(4)	586
TOTAL						2678.8
TRANS FABRICATION AND ASSEMBLY COST, $/KG						148

ASSUMPTIONS

(1) COSTS ARE AMORITZED OVER A 5 SATELLITE CONSTRUCTION PERIOD.

(2) PASSENGER VERSION OF SHUTTLE – 45 PASSENGERS TO LEO AT $9M/FLT

(3) HLLV CLASS 4 – 181.4 x 10^3 Kg TO LEO

(4) L/V AMORTIZED BY TOTAL NO. OF FLIGHTS VS DESIGN LIFE

(5) CREW CYCLED EVERY 60 DAYS

(6) 9 Kg/Hr ASSEMBLY RATE, 56 HR WORK WEEK PER MAN

(7) 4.6 Kg/Hr ASSEMBLY RATE, 20 HRS/DAY

NOTES:
1. SSPS WGT = 18.06 X 10^6 Kg
2. 2 YEAR ASSEMBLY PERIOD

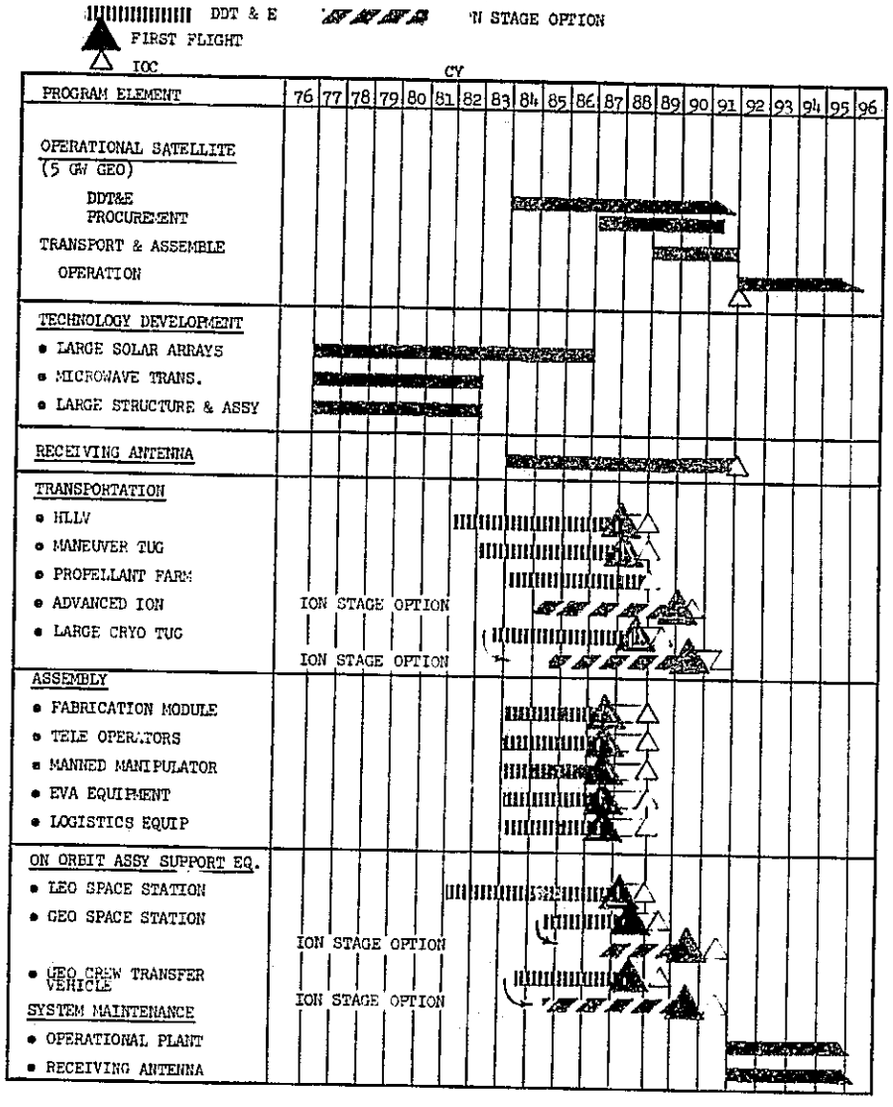

Figure 2.6-10 Overall Program Schedule - Program 1

2.6.2.1 Supporting Resear and Technology Program

An expanded Supporting Research and Technology Program necessary for the direct development of the SSPS is shown in Figure 2.6-11. The program contains much of the same technology development areas described for Program 3, but also includes participation in satellite and shuttle sortie mission flights. High voltage components are evaluated through payloads deployed using GEO high voltage satellite missions scheduled to commence in 1981. Shuttle sortie missions are used to support critical technology development in several areas. Figure 2.6-12 defines a series of flight test missions that also commence in 1981. Missions 2 and 3 evaluate methods for deploying and fabricating structural elements. Mission 4 addresses waveguide deployment and fabrication. Microwave components and electronics integration are demonstrated and evaluated in Mission 5. Mission 6 continued to evaluate manufacturing and assembly techniques by building and integrating subassembly-to-subassembly configurations. These shuttle sortie mission scenarios are considered essential for the direct development to an operational satellite.

Ground tests using ground antenna systems such as the Goldstone or Arricebo facilities are also included in this program for evaluating the interaction of microwave radiation with the ionosphere.

2.6.2.2 Program 1 Total Costs

Total program costs for the direct development to an operational satellite is summarized in Table 2.6-10. The supporting research and Technology Program includes the cost of the shuttle sortie flight test missions. Table 2.6-11 shows the costs associated with these scenarios.

DDT&E and unit production costs were estimated by projecting the data shown in the appendix using the Koelle Model. CER #3 as shown in Figure 2.6-5 for application satellites, relates manhours for development and fabrication as a function of the percentage of new technology estimated in its development. The cost data for the Operational Satellite in the three step development program is considered representative of a 20% new-technology build under the rationale that the Demo Satellite and Pilot Plant contribute significantly in its development; cost data were projected for the direct program by assuming it is representative of an 80% new-technology build.

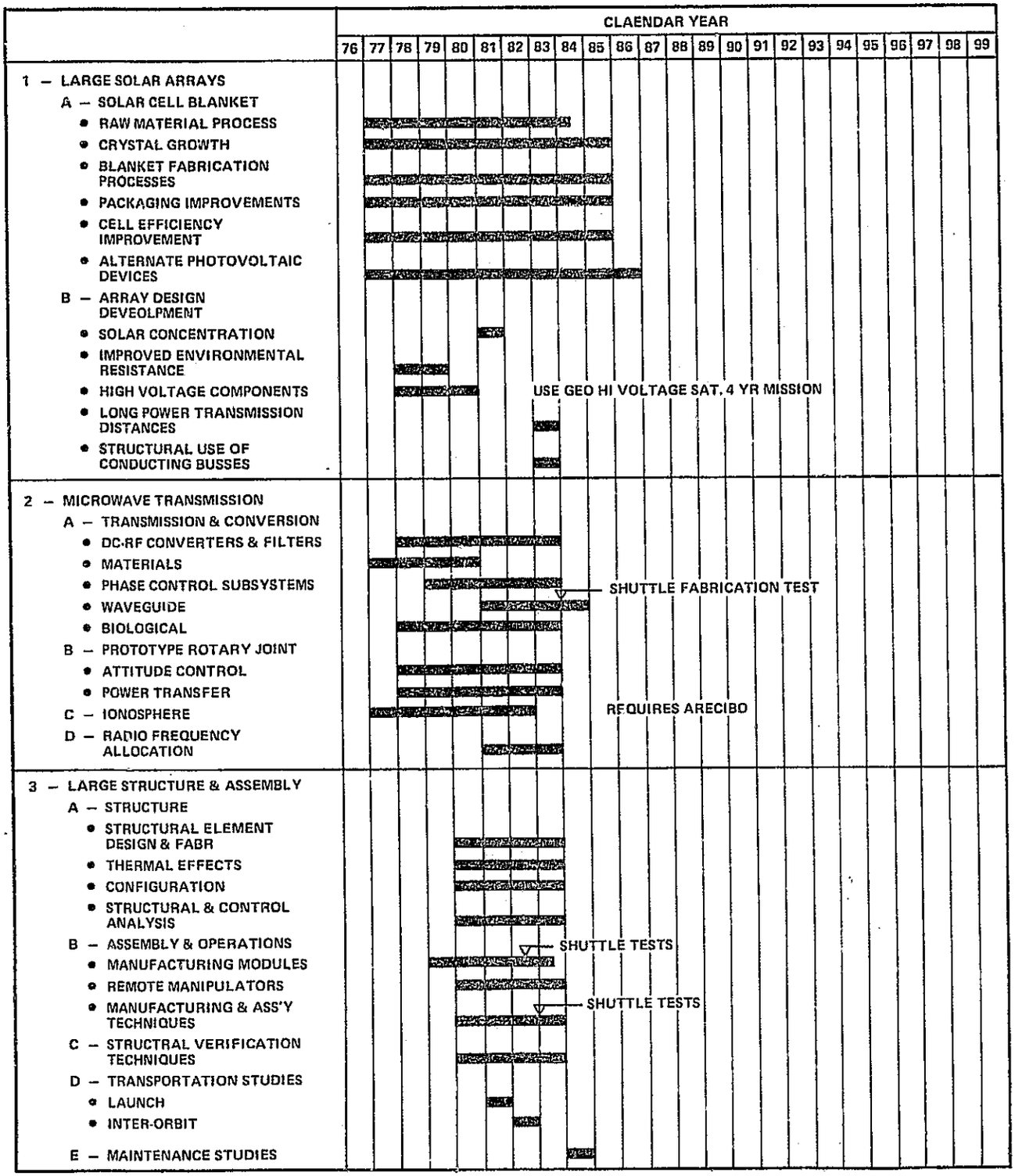

Figure 2.6-11 Supporting Technology Development, SSPS Program 1

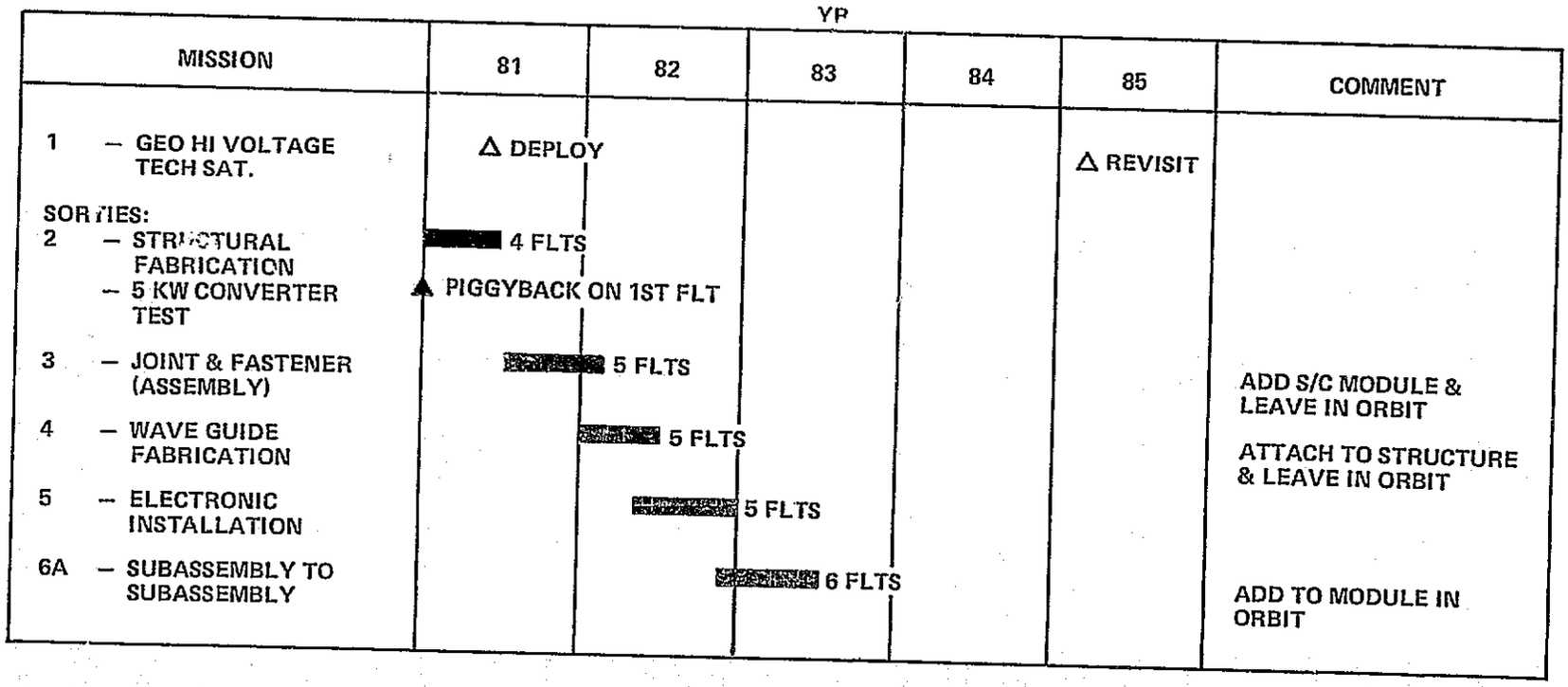

Figure 2.6-12 Program 1 - Supporting Technology Flight Tests

Table 2.6-10 Program 1 Total Costs

	COSTS, $M	EXPENDITURE PERIOD		
SUPPORTING RESEARCH & TECHNOLOGY PROG		1977–1985		
• SOLAR ARRAY	358.9			
• MICROWAVE	60.4			
• STRUCTURAL	39.3			
• SHUTTLE SORTIE MISSIONS	598.9			
TOTAL	1,057.6			
	DDT&E $M	UNIT PRODUCTION $M	ASSEMBLY OPERATIONS	EXPENDITURE PERIOD
OPERATIONAL PLANT			$233/KG	
• SOLAR ARRAY	4,687	1,973		
• ANTENNA INTERFACE	669	170		
• TRANSMITTING ANTENNA	915	1,250		1984-1991
• RECEIVING ANTENNA	1,583	3,140		
SUBTOTAL	7,854	6,803	4217	
MANAGEMENT, S&I (40%)	3,142	2,721		
UNCERTAINTIES (20%)	1,570	1,360		
TOTAL	12,566	10,884	4217	
GRAND TOTALS	13,624	10,844	4217	$28,724 M

Table 2.6-11 Supporting Technology Flight Test Cost Summary

MISSION	SHUTTLE FLTS	SHUTTLE COSTS	YR	MISSION COST $M*
1	1	13	1981	55.3
2	4	52	1981	79.5
3	5	65	1981-1982	59.5
4	5	65	1982	93.2
5	5	65	1982	73.0
6A	6	78	1983	78.6
SUBTOTAL	26	338		479.1
15% for Shuttle Auxiliary Equipment				71.9
10% for Shuttle Support System Mods				47.9
TOTAL				598.9

*EXCLUDES COST OF MICROWAVE COMPONENTS

Assembly and operations cost was developed for this program using a format similar to that shown in Program 3. The major difference assumed was that 80% of the fabrication and assembly phases would be performed by on-orbit manned operations, and that 20% would be performed using ground-controlled remote teleoperators. This representation was based on the lack of assembly expertise that is otherwise assumed to be gained during pilot plant operations. Table 2.6-12 summarizes the total-operations costs resulting.

2.6.3 Program 2 - Pilot Plant/Operational Satellite

A two step program based on the deployment of a 500 MW pilot plant as the first step to deployment an operational 5 GW satellite, to be activated at the end of 1991, is presented in Figure 2.6-13. This program was developed to assess the impact of including a pilot plant only as the development cycle to operational status. A 500 MW pilot plant was selected for establishing relative data on pilot plant sizing.

The overall program schedule contains all of the common assembly equipment, transportation systems, and on-orbit support equipment shown in programs 1 and 3, but time phases are slightly adjusted for their scheduled utilization. The most significant difference in schedules, as compared with the pilot plant schedule of Program 3, is the planned IOC date of the HLLV launch system. This program assumes HLLV availability for the operational satellite, and consequently is not operational to support the pilot plant operations. LEO and GEO space stations are brought to operational status to support the low orbit fabrication and assembly and geosynchronous orbit operations and maintenance.

2.6.3.1 Supporting Technology Program

Figure 2.6-14 summarizes the research and technology program development. Differences in this program relative to program Program 3 are small, in that the inclusion of a GEO high voltage satellite for high voltage component evaluation and ground antenna microwave beam-ionospheric evaluations are included.

2.6.3.2 500 MW Pilot Plant

Figure 2.6-15 depicts a conceptual design for a 500 MW pilot plant to be placed at geosynchronous orbit for operation by the end of 1985. The assumptions used in sizing the configuration are the same as those used as in Program 3. The total satellite weight is estimated at 5.59×10^6 Kg. The satellite is fabricated and assembled in LEO using a space station, and transported to geosynchronous orbit using a series of large cryo OTV flights. Launch operations to low earth orbit utilize the DOL launch system. Table 2.6-13 summarizes the equipment to be brought to low-altitude orbit and the number of DOL flights required. Also shown is the number of shuttle flights required for crew rotation.

Table 2.6-12 Transportation and Assembly Costs - 5 GW Operational Satellite

ELEMENT	NO. OF UNITS	EQUIP COST, $M[1]	WGT TO LEO, Kg x 10^6	NO. OF HLLV FLTS[3]	NO. OF SHUTTLE FLTS	COST, $M
EQUIPMENT:						
• LEO SPACE STATION (6 MAN)	47[6]	902.4	3.58	20		1082.4
• GEO SPACE STATION	1	19.2	0.076	1		32.2
• ASSEMBLY EQUIPMENT						
— MANNED MANIPULATORS	47	103.4	0.090			
— TELEOPERATORS	56[7]	28	0.010			
— EVA EQUIPMENT	300	90	0.027		6	283.4
• FABRICATION MODULES	3	8	0.016			
• LARGE CRYO TUG	2	6	0.072	1		8.8
• SUPPORT TUGS	40	20.8	0.052	1		23.8
• CREW MODULE	1	5	0.012		1	6.0
• PROPELLANT STORAGE TANKS	26	140	0.780	5		185.
• ORBIT MAINTENANCE MODULE	1	3.2	0.002			3.2
• ADVANCED ION	1	38	0.726	4		74
SUPPLY:						
• CRYO PROPELLANTS			0.981	6		54
• ION PROPELLANTS			0.772	5		45
• S/S & EQUIP. RESUPPLY			0.772	5		45
• CREW ROTATION[5]					75[2]	675
MATERIAL TRANSPORT			18.06	100		900
SUBTOTAL				148	81	3417
• PERSONNEL	895					40.3
• AMORTIZE L/V COST				592[4]	162	754
TOTAL						4212.1
TRANSP AND ASSEMBLY COST, $/Kg						233

ASSUMPTIONS

(1) COSTS ARE AMORTIZED OVER A 5 SATELLITE CONSTRUCTION PERIOD.

(2) PASSENGER VERSION AT SHUTTLE —45 PASSENGERS TO LEO AT $9M/FLT

(3) HLLV CLASS 4 — 181.4 x 10^3 Kg TO LEO

(4) L/V AMORTIZED BY TOTAL NO. OF FLIGHTS VS DESIGN LIFE

(5) CREW CYCLED EVERY 60 DAYS

(6) 9 Kg/Hr ASSEMBLY RATE, 56 HR WORK WEEK PER MAN

(7) 4.5 Kg/Hr ASSEMBLY RATE, 20 HRS/DAY

NOTES:
1. SSPS WGT = 18.06 X 10^6 Kg
2. 2 YEAR ASSEMBLY PERIOD

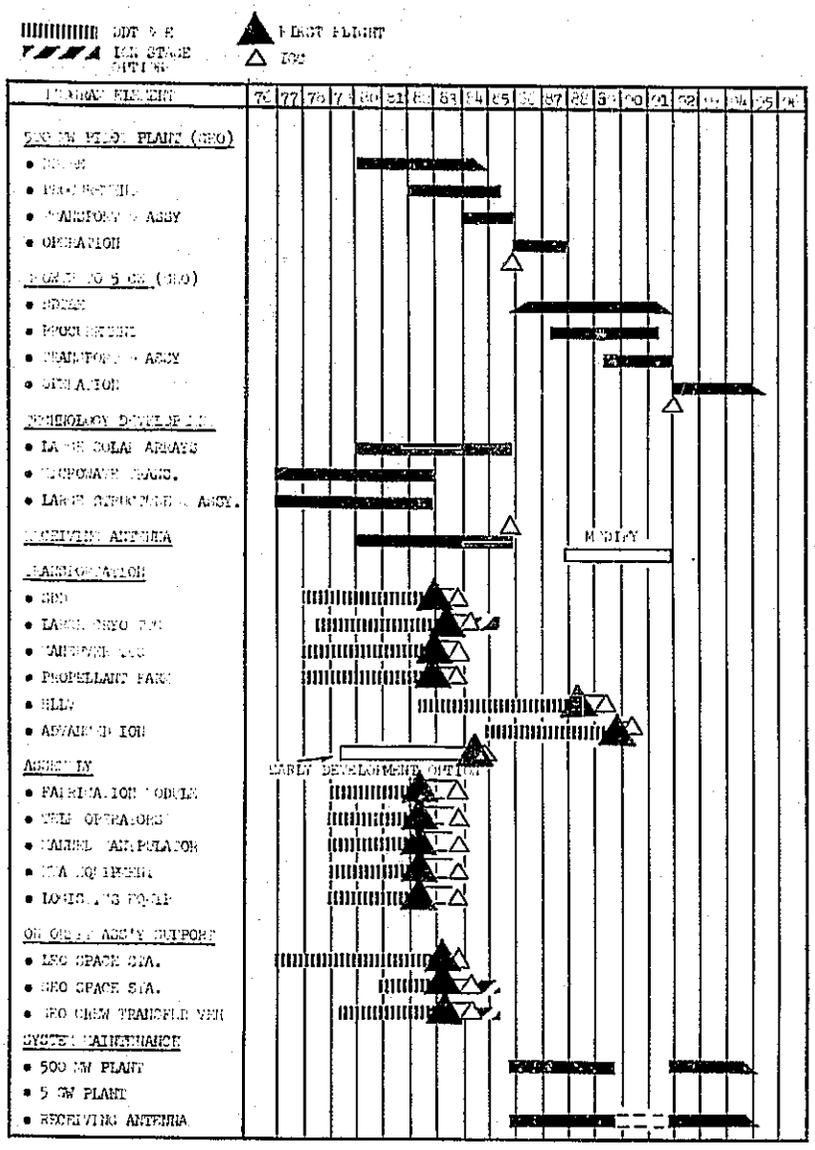

Figure 2.6-13 Overall Program Schedule, Program 2

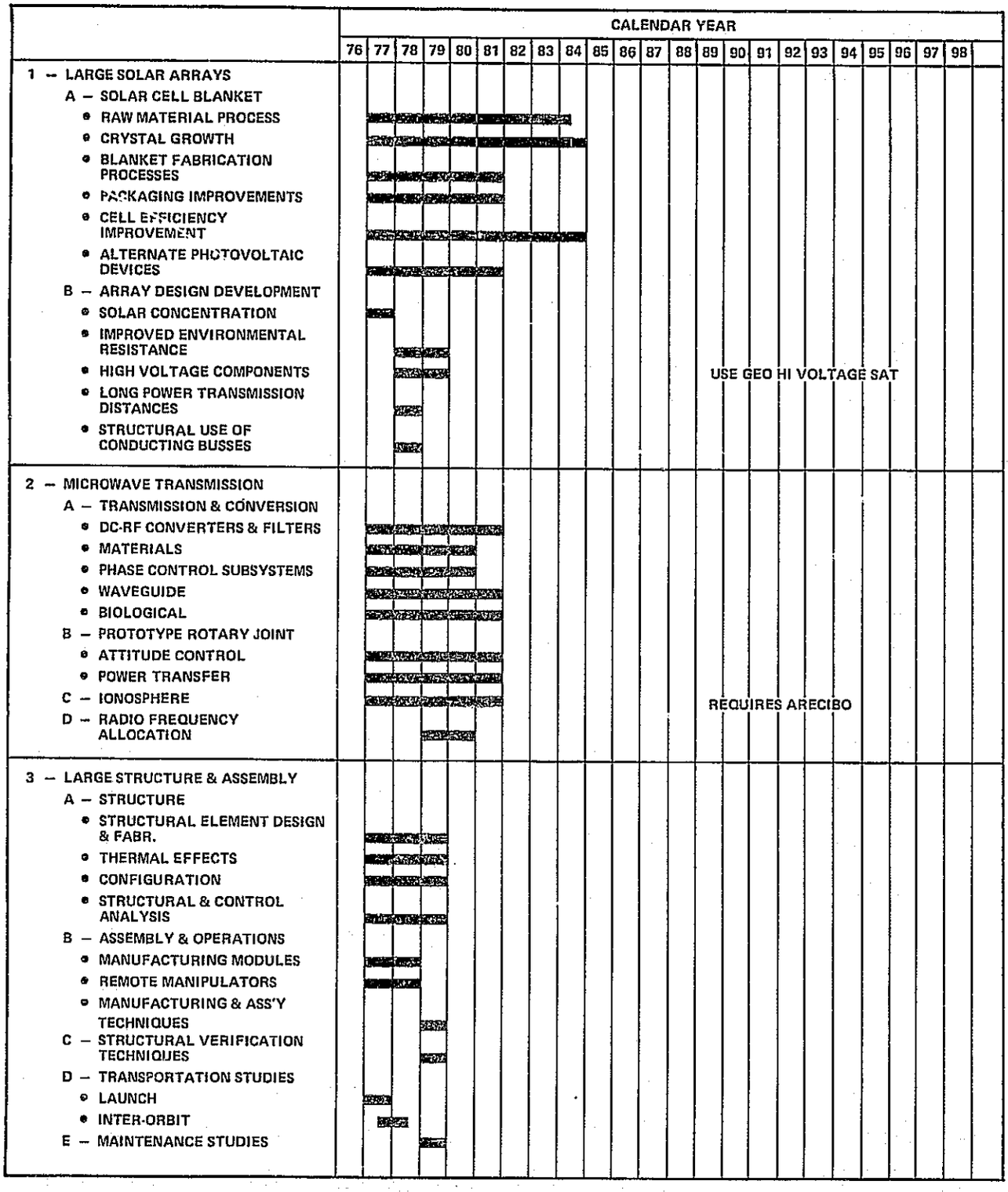

Figure 2.6-14 Supporting Technology Development, SSPS Program 2

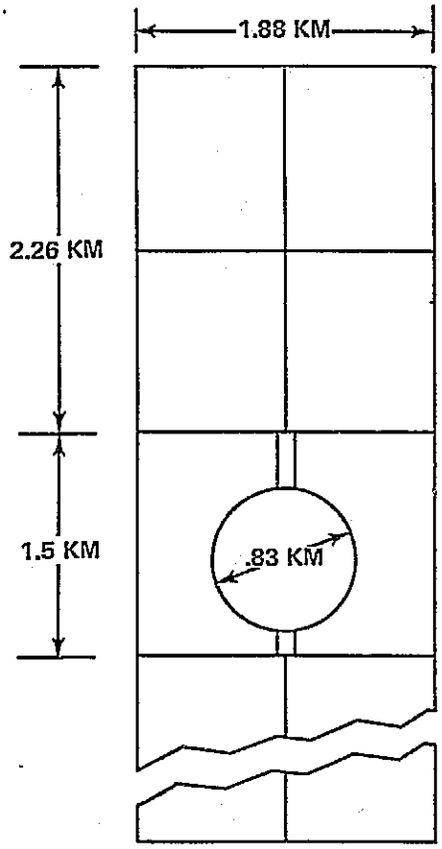

CHARACTERISTICS

- SOLAR BLANKET
  - CONCENTRATION RATIO = 2
  - CELL EFFICIENCY = 11%
  - POWER DISTRIBUTION EFF = 92%
- MICROWAVE CONVERSION EFF = 57% RECTIFIED AT GROUND

	WEIGHTS KG X 10^6
ARRAY	
• BLANKET =	1.71
• CONCENTRATOR =	.171
• NON CONDUCT STRUCT =	.28
• CONDUCTING STRUCT =	.034
• MAST =	.37
	4.19
ROTARY JOINT	.17
MW ANTENNA	2.85
TOTAL	5.59

Figure 2.6-15 Pilot Plant (1985) 500 MW Ground Power

Table 2.6-13 Transportation Flights to LEO For 500 MW Pilot Plant

ELEMENT	NO. OF UNITS	WGT TO LEO, 10^6 KG	DOL FLIGHTS	SHUTTLE FLTS
EQUIPMENT				
• LEO SPACE STATION	9	.675	10	
• GEO SPACE STATION	1	.076	1	
• ASSEMBLY EQUIPMENTS				
-- MANNED MANIPULATORS	9	.017	} 1	
– TELEOPERATORS	43	.008		
– EVA EQUIPMENT	100	.010		
• FABRICATION MODULES	2	.013	1	
• LARGE CRYO TUG	1	.072	1	
• SUPPORT TUGS	7	.009	1	
• PROPELLANT STORAGE TANKS	4	.127	} 2	
• ORBIT MAINT MODULE	1	.002	} 1	
• CREW MODULE	1	.012		
SUPPLIES				
• CRYO PROPELLANTS		12.	165	
• S/S & EQUIP RESUPPLY		.43	6	
• CREW ROTATION				8
MATERIALS		5.6	77	
TOTALS			266	8

2.6.3.3 Program 2 Total Costs

Program costs for the pilot plant/operational satellite program are summarized in Table 2.6-14. As used in estimating Program 1 costs, Appendix A data were projected using the Koelle Model. Both pilot and operational satellite DDT&E; unit production data were estimated by assigning new technology percentages to both sets of data. In estimating the pilot plant costs, for example, the reference data were assumed to reflect a 60% new technology build. This judgement was based on an estimate of the technology advanced from a 15 MW Demo Satellite construction and operation program. On that basis, a 70% new technology build was assumed for this program's costs. Similarly for the operational satellite cost projections, the reference costs were assumed to reflect a 20% new technology build, and the corresponding program costs for this program were based on a 25% new technology build. These results are shown in the summary costs.

Table 2.6-15 presents the cost of transportation, assembly and operations of the pilot plant. These transportation costs are significantly higher than for the Program 3 pilot plant primarily because of the unavilability of the HLLV launch system.

Presented in Table 2.6-16 are the transportation costs for the operational satellite. These costs are somewhat higher than the operational program costs in that a higher percentage of on-orbit manned assembly was assumed.

Table 2.6-14 Program 2 Total Cost

	COSTS, $M
SUPPORTING RESEARCH & TECHNOLOGY PROG.	
• SOLAR ARRAY	358.9
• MICROWAVE	60.4
• STRUCTURAL	39.3
• GEO SATELLITE	55.
TOTAL	513

	DDT&E $M	UNIT PRODUCTION COSTS, $M	ASSEMBLY OPERATIONS	
PILOT PLANT			$844/KG	
• SOLAR ARRAY	4035	380		
• ANTENNA INTERFACE	579	52		
• TRANSMITTING ANTENNA	793	77		
• RECEIVING ANTENNA	1218	200		
SUBTOTAL	6625	709	4718	
MANAGEMENT, S&I (40%)	2650	284		
UNCERTAINTIES (20%)	1325	141		
TOTAL	10,600	1134	4718	
OPERATIONAL PLANT			$191/KG	
• SOLAR ARRAY	1118	1828		
• ANTENNA INTERFACE	149	156		
• TRANSMITTING ANTENNA	260	861		
• RECEIVING ANTENNA	403	2340		
SUBTOTAL	1930	5185	$3457M	
MANAGEMENT, S&I (40%)	772	2074		
UNCERTAINTIES (20%)	386	1037		
TOTALS	3088	8296	$3457M	
GRAND TOTALS	14,201	9430	8175	($31,806M)

Table 2.6-15 Transportation and Assembly Costs For 500 MW Pilot Plant

ELEMENT	NO. OF UNITS	EQUIP COSTS, $M	WGT TO LEO, 10^6 KG	NO. OF DOL FLTS[3]	NO. OF SHUTTLE FLTS[2]	COST, $M
EQUIPMENT:						
• LEO SPACE STATION	9[6]	172.8[1]	.165	10		302.8
• GEO SPACE STATION	1	20[1]	.076	1		33.
• ASSEMBLY EQUIP						
— MANNED MANIP	9	20[1]	.0174	} 1		20
— TELEOPERATORS	43[7]	21.5[1]	.0082			34.5
— EVA EQUIPMENT	200	60[1]	.016			60
• FABRICATION MODULES	2	24	.013	1		37
• LARGE CRYO TUG	1	15	.072	1		28
• SUPPORT TUGS	7	18	.0091	1		31
• PROPELLANT STORAGE TANKS	4	21.5[1]	.1266	2		59.5
• ORBIT MAINT. MODULE	1	3.2[1]	.002	} 1		
• CREW MODULE	1	23	.012			36
SUPPLY:						
• CYRO PROPELLANTS			12.	165		2145
• S/S 1 EQUIP RESUPPLY			.43	6		78
• CREW ROTATION (5)					8	104
MATERIALS TRANSPORT			5.6	77		1001.
SUBTOTAL:				266	8	39678
• PERSONNEL	290					13
• AMORTIZED L/V (4)						756.0
TOTAL						4736.8
TRANS AND ASSEMBLY COST, $/KG						846

ASSUMPTIONS

(1) COSTS AMORTIZED OVER 5 SATELLITE CONSTRUCTION PERIODS

(2) PASSENGER VERSION OF SHUTTLE – 45 PASSENGERS TO LEO AT $9M/FLT

(3) DOL LAUNCH VEHICLE – 72,500 KG TO LEO AT $13M/FLT

(4) L/V AMORTIZED BY TOTAL NO. OF FLIGHTS VS DESIGN LIFE

(5) CREW CYCLED EVERY 60 DAYS

(6) 9KG/HR ASSEMBLY RATE, 56 HR WORK WEEK PER MAN

(7) 4.5 KG/HR ASSEMBLY RATE, 20 HR/DAY

NOTES:
1. PILOT PLANT WGT = 5.59 X 10^6 KG
2. 50 PERCENT MANNED ASSEMBLY, 50 PERCENT REMOTE ASSEMBLY

Table 2.6-16 Transportation and Assembly Costs - 5 GW Operational Satellite, 50 Percent Manned Assembly, 50 Percent Remote Assembly

ELEMENT	NO. OF UNITS	EQUIP COST, $M (1)	WGT TO LEO, Kg x 10^6	NO. OF HLLV FLTS (3)	NO. OF SHUTTLE FLTS	COST, $M	ASSUMPTIONS
EQUIPMENT:							(1) COSTS ARE AMORTIZED OVER A 5 SATELLITE CONSTRUCTION PERIOD
• LEO SPACE STATION	30(6)	576	2.29	13		693	
• GEO SPACE STATION	1	19.2		1		32.2	
• ASSEMBLY EQUIPMENT							
— MANNED MANIPULATORS	30	66	0.058		5	249.5	(2) PASSENGER VERSION OF SHUTTLE — 45 PASSENGERS TO LEO AT $9M/FLT
— TELEOPERATORS	141(7)	70.5	0.025				
— EVA EQUIPMENT	200	60	0.018				
• FABRICATION MODULES	3	8	0.014			15	
• LARGE CRYO TUG	2	6	0.072	1		22	(3) HLLV CLASS 4 — 181.4 x 10^3 Kg TO LEO
• SUPPORT TUG	25	13	0.033	1		5	
• CREW MODULE	1	5	0.012			85	
• PROPELLANT STORAGE TANKS	26	140	0.78	1		32	(4) L/V AMORTIZED BY TOTAL NO. OF FLIGHTS VS DESIGN LIFE
• ORBIT MAINTNEANCE MODULE	1	3.2	0.002			74	
• ADVANCE ION STAGE	1	38	.726	4			
SUPPLY:						54	(5) CREW CYCLED EVERY 60 DAYS
• CRYO PROPELLANTS			0.981	6		45	
• ION PROPELLANTS			0.772	5		45	
• S/S & EQUIP RESUPPLY			0.772	5		423	(6) 9 Kg/Hr ASSEMBLY RATE, 56 HR WORK WEEK PER MAN
• CREW ROTATION(5)					47(2)		
MATERIAL TRANSPORT				100		900	(7) 4.5 Kg/Hr ASSEMBLY RATE, 20 HR DAY
• SUBTOTALS	880			137	52	2457.7	
• PERSONNEL						39.6	
• AMORTIZE L/V COSTS				564(4)	106(4)	670	
TOTAL						3455.3	
TRANSP AND ASSEMBLY COST, $/KG						191	

NOTES:
1. SSPS WGT = 18.06 X 10^6 KG
2. 2 YEAR ASSEMBLY PERIOD

2.7 Cost and Risk Analysis Support

In support of the economic studies performed by ECON, Grumman provided data for two specific analyses; the cost and risk analysis and the economic analysis of demonstration and pilot plant satellites.

For the cost and risk analysis, a model was formulated in terms of a series of technical and cost input parameters, to estimate the size, mass, and cost of a unit production satellite and the cost of the associated equipment required for fabrication, assembly, and transportation. This model is described in Appendix A of Volume III. Input parameters for use in exercising this model were estimated in three categories: the best value, the most likely value, and the worst value. The ground rules utilized in estimating these parameters are based on the most likely value being the expected value for that parameter in the 1990 time frame. The best and worst values represent the absolute limits of the parameter as projected today for the 1990 time frame. These estimates are summarized in Appendix C of Volume III. Needless to say, these data are considered extremely "soft" at best; consequently, the results generated using these data should be interpreted accordingly.

3- ENGINEERING ANALYSIS OF SPECIAL REQUIREMENTS FOR ORBITAL SYSTEMS, POWER RELAY SATELLITE

3.1 Reflector Structure

This subsection summarizes the structural studies carried out on the Power Relay Satellite (PRS) orbiting system. Figure 3.1-1 lists the structural weights by subsystem. Excluded from the weights are the control electronics.

The following technical observations have been made:

1. Reflector surface roughness can be maintained to within 1/20 of a wavelength for each individual 18 by 18m reflector subarray. Over 3000 of there subarrays are used to form the 1 Km^2 reflector surface.

2. A mechanical screw jack system mounted at the corners of 18x18m reflector subarrays densensitizes reflector flatness to the static distortions of the supporting structure.

3. The wire mesh reflector surface can tolerate the sudden temperature variation during periods of occultation provided the reflector surface is mounted to the subarray support structure using pretensioned springs.

4. The material of choice is a hybrid composite graphite/epoxy, boron epoxy. The selection was made based on the desire for a material with high modulus and low thermal coefficient of expansion.

The key technical issue requiring detail study before concept feasibility can be verified is an assessment of the dynamics interaction of the contour control system of each 18 x 18m subarray with the support structure and the overall spacecraft attitude control system.

3.1.1 Structural Arrangement

The PRS configuration shown in Figure 3.1-2 consists of a primary structure with 25 meter deep truss girders spaced at 108 meters. Each 108 meter module is spanned by an 18 meter grid of 5 meter depth girders as shown. At the corners of the 18 meter modules are located electrically driven screw jacks to which are mounted the reflectors at the four corners. The primary structure is built up of 108 m x 108m x 20m deep bays; the upper cap consists of a triangular truss girder 108m long by 3m deep. The material used is a graphite epoxy composite. The secondary structure, which forms the lower cap of the primary bending structure, is 5m deep with bays of 18m x 18m as shown in the Figure 3.1-2. This 18 meter square

SUBSYS/COMP.	WEIGHT	
	Kg X 10^6	LBM X 10^6
• PRIMARY STRUCT	0.119	0.262
• SECONDARY STRUCT	0.038	0.084
• COATINGS & INSULATION	0.028	0.062
• FRAME STRUCTURE	0.101	0.222
• WIRE MESH	0.058	0.127
• CONTOUR CONTROL	0.155	0.341
• ATTITUDE CONTROL	0.006	0.013
TOTAL	0.505	1.112

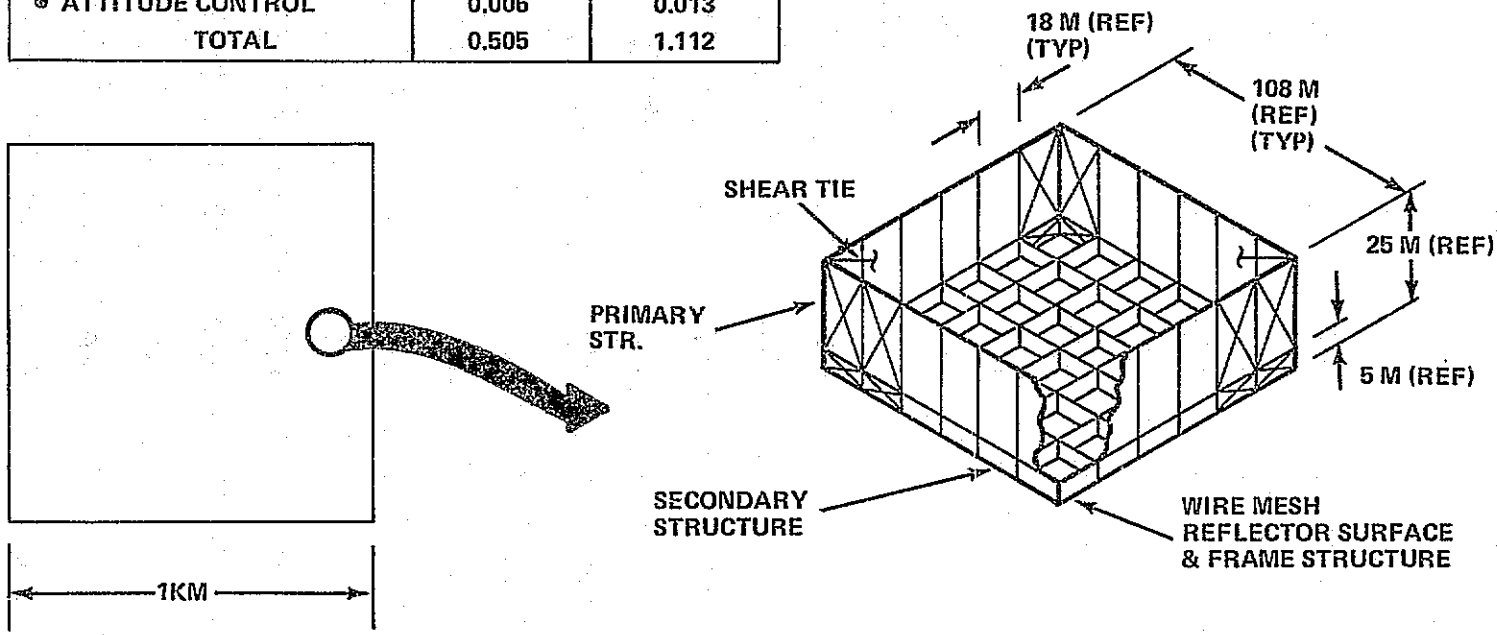

Figure 3.1-1 PRS Mass Properties

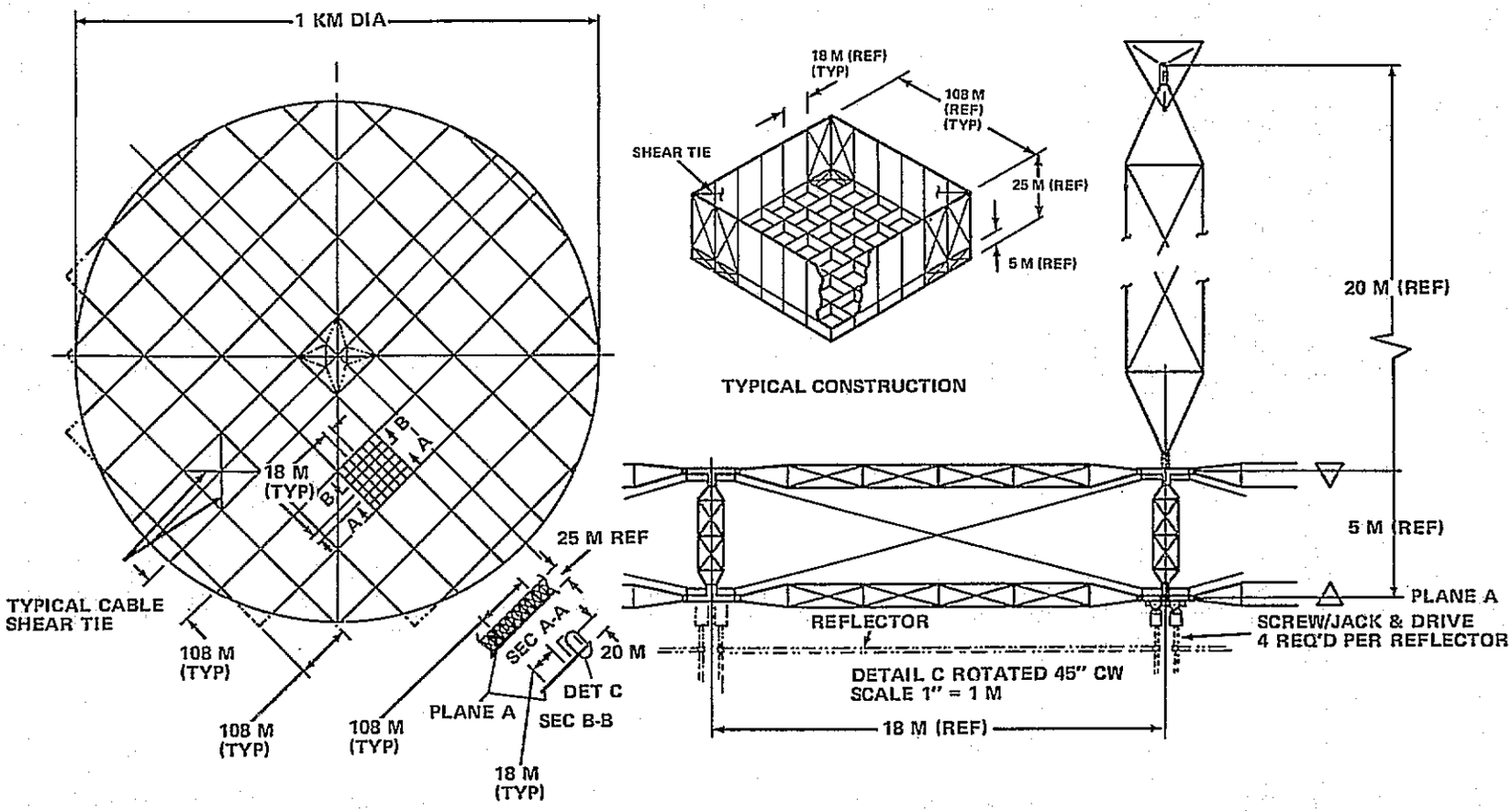

Figure 3.1-2 Configuration of a 1 Kilometer Diameter Power Relay Station

substructure spans the 108 meter bays and provides supports for the microwave reflector system. The secondary structure is also fabricated in the form of interconnected truss girders out of graphite/epoxy.

3.1.2 Design Data

3.1.2.1 Structural criteria and requirements - The requirement for surface smoothness used in this analysis of the reflector was $\lambda/80$ for λ = 10 cm, where λ is the wavelength. This is equal to approximately 1.2 mm for λ = 10 cm. Later information indicates that one twentieth of the wavelength surface smoothness is acceptable; this corresponds to a value of 5 mm. The effect of the relaxation on permissible deflection is to reduce the preload in the reflector.

The service usage life requirement is 30 years; the effect of this requirement is difficult to evaluate from a fatigue and/or creep viewpoint since time did not permit an evaluation of the loading spectra and the number of thermal cycles. Further study in this area is required. The factor of safety used for the evaluation is 1.50 for ultimate design loads.

3.1.2.2 Design Loads and Temperatures - The design loads for the PRS reflector support primary structure result from solar radiation pressure, microwave radiation pressure, gravitational forces and induced mechanical forces caused by thermal conditions. Insofar as the primary structure shown in Figure 3.1-2 was concerned, the member sizes for the SSPS microwave antenna were used unchanged for weight estimation. This procedure is not as conservative as may be assumed since the thicknesses in composite are minimum in either case.

The above mention design loads are used for sizing the reflector modules and are discussed further. The reflector selected is an aluminum woven wire mesh with wire strands equal to 0.15 mm diameter spaced at 2 mm and an overall dimension of 1000 m by 1000 m. The reflecting area of this surface is 15% of the total area of 10^6 square meters or 0.15 $km^2/km2$. The solar radiation pressure is $p = \frac{2}{3} I$ kp/km^2 where I is the solar constant and is equal to 1350 $W/_m2$. $p = 0.9$ $kp/_m2$; since the reflecting area is 0.15 $km^2/_{km}2$ the maximum solar radiation pressure is 0.135 $kp/_{km}2$. The microwave power radiation pressure is given by $P_r = \frac{2}{3}$ Is

where $I_s = \dfrac{\eta P_t^2}{I_t (3.26\ \lambda\ R)^2}$

$I_t = 0.1\ G\omega/km^2$

$\eta = 0.846$

$\lambda = 10^{-4}$

$R = 3.67 \times 10^4$ km

for the design condition P_t = 13 gigawatts

$P_r = 5.65\ kp/km^2$

This value is the critical loading condition for the reflector.

The estimated temperature ranges for the mesh and its support structure is as follows:

(1) Mesh:	Sunlight	$366^\circ K$	
	Eclipse	$116^\circ K$	$\Delta T = 250^\circ K$
(2) Structure:	Sunlight	$366^\circ K$	
	Eclipse	$-200^\circ K$	$\Delta T = 166^\circ K$

3.1.2.3 Material Property Data - The material selected for the overall reflector structural design shown in Figure 3.1-3 in the study is the hybrid composite graphite/epoxy, boron epoxy. The property data are taken from Grumman tests and the pertinent curves are reproduced in Figures 3.1-4 and 3.1-5. The laminate thicknesses are 2½ mils; in the following laminate is used throughout; its selection is based on the requirement for using a material with a high modulus and a low coefficient of thermal expansion.

The hybrid composite material lay-up of plies selected for application to the wire mesh reflector support structure consists of boron-epoxy 0° layers and graphite - epoxy for the $\pm 45^\circ$ and 90° layers. The selected laminate is $[0_2/\pm 45_2]$. The layup consists of two layers at zero degrees and two layers each at $\pm 45^\circ$ for a total of six plies of 2½ mils each. The total thickness is 3.8×10^{-4} m. Since no data was available in the $366^\circ K$ to $394^\circ K$ temperature range, the analysis is based on $450^\circ K$ property data.

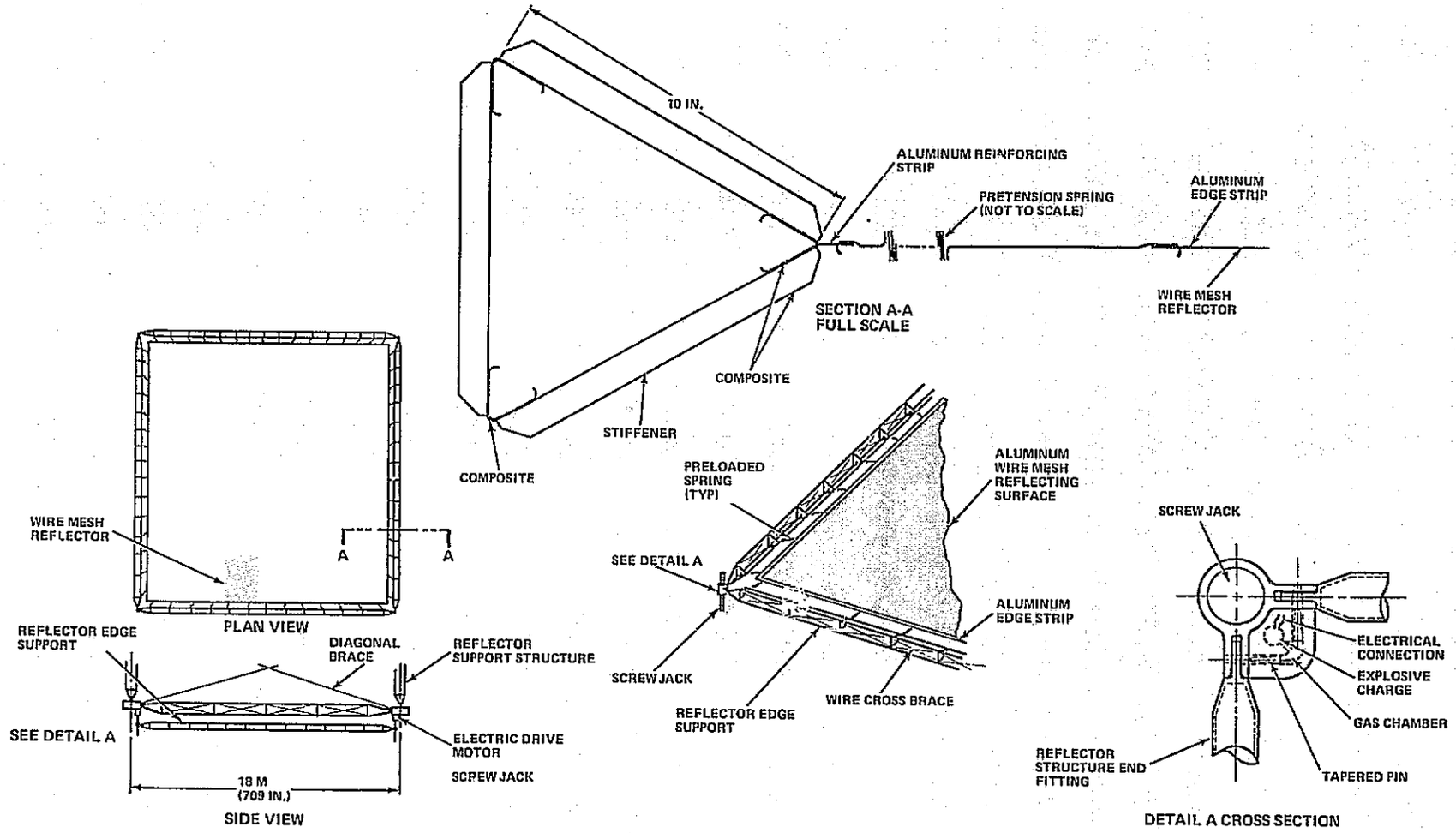

Figure 3.1-3 Reflector Module 18m x 18m Power Relay Satellite

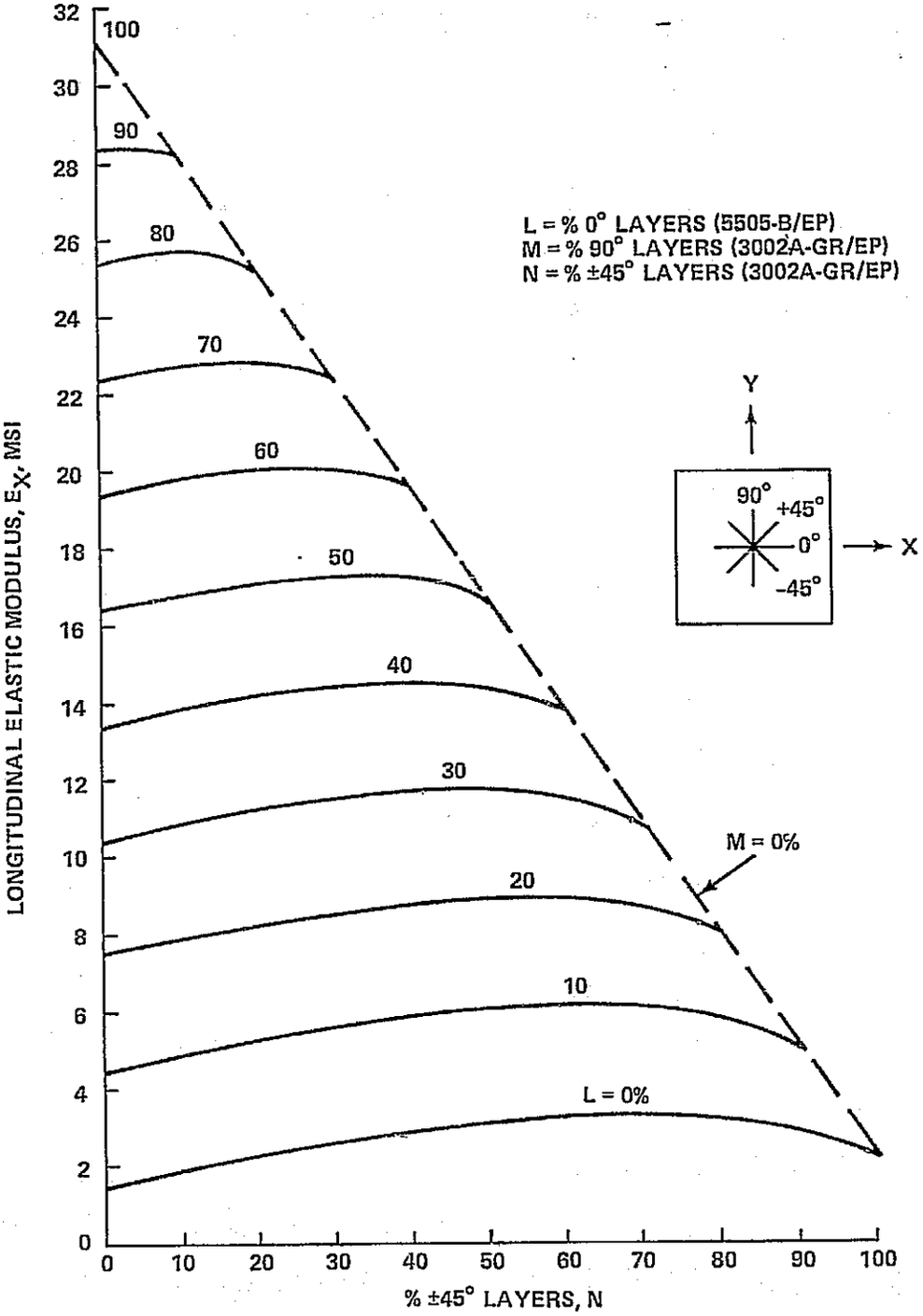

Figure 3.1-4 Longitudinal Elastic Modules of Hybrid Laminates at R.T.

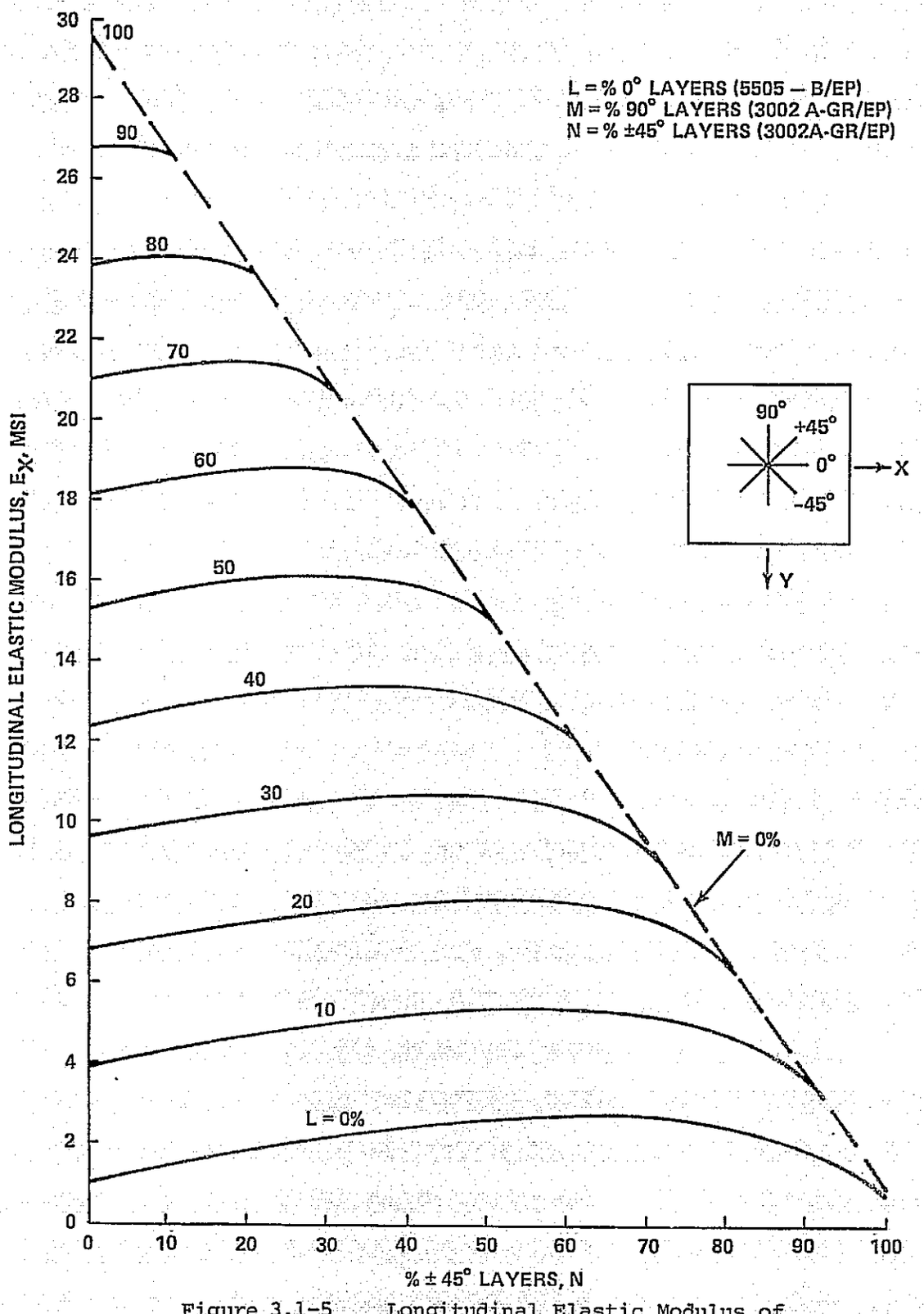

Figure 3.1-5 Longitudinal Elastic Modulus of Hybrid Laminates at 350°F

			Room Temp.	450°K
F_{tu}	ultimate tensile strength N/m^2	10^8	4.62	3.93
E_x	longitudinal N/m^2 modulus	10^{10}	8.27	7.17

Material density 2.076×10^3 Kg/m^3

Coefficient of thermal expansion

$$\alpha = 2 \times 10^{-6} \text{ m/m/}^\circ_F \qquad \text{(estimated for the hybrid)}$$

3.1.2.4 Analysis-Wire Mesh Reflector - The 18m x 18m refector module consists of a framework support by four screw-jacks at the corners and a wire mesh reflector surface attached by springs to the framework. The frame is fabricated using graphite epoxy composite; the wire mesh reflector consists of an aluminum wire 0.15 mm (0.0059 in) diameter with a spacing between wires of 2 mm (0.079 in.). As discussed in paragraph 3.1 the initial requirement for surface smoothness was taken as 1/80 of the wavelength which corresponds to a deflection of 1 mm; later data indicated that approximately 5 mm is permissible. For purposes of this analysis the permissible deflection of 1 mm was used. Figure 3.1-6 shows the loading system and deflections for member ACB. The initial assumption is made that the member is inextensible since the estimated elastic deformation is very low. The applied load q is supported by the deflected tension member ACD with the indicated internal loads. The deflection at the center is given by f. Using the condition for moment equilibrium about point A:

$$H = \frac{ql^2}{8f}$$

From the properties of a right triangle

$$S = H \left[1 + \left(\frac{4f}{\ell}\right)^2\right]^{\frac{1}{2}}$$

If f is prescribed, H and S can be calculated. It is evident that for the given conditions the value of $4f/\ell$ is very small and therefore S is approximately equal to H.

The aluminum wire mesh 0.15mm diameter at a spacing of 2mm in each direction has an equivalent uniaxial thickness of 0.0088mm.

The design load for assessing the preload requirements on the reflector for the permissible deflection is caused by the microwave radiate on pressure condition. The microwave radiation pressure is equal to p_r = 5.65 kp/km2 where kp is equal to 2.2 lb. Using a factor of safety of 1.50 for ultimate the value of p_r in pounds per square inch is 1.203×10^{-8} ultimate. Assuming the allowable deflection for the 18m (709 in) panel is 1mm (.03937 inches),

$$H = \frac{g\ell^2}{8f} = 3.362 \text{ N/m } (.0192 \text{ lbs/in})$$

also $S \simeq H$

The average stress in the wire is $\sigma = 3.81 \times .10^5$ N/m^2 (55.2 psi) which is very low for the selected material.

Analysis of the Reflector Support Frame - Figure 3.1-7 shows the loads applied to the 18m x 18m support frame by the were mesh as calculated above. The cross section of the 18 meter square frame is a triangular structure fabricated from graphite epoxy composite; the cap areas are 3.355×10^{-5} m . The ultimate bending moment in the 18 meter member is 136.3 N-m; the bending stress is 2.13×10^7 N/m^2. The Euler column load for the 18 meter member is significantly larger than the applied compression load of 30.3 N.

Evaluation of Reflector Support Frame Deflection Caused by Thermal Gradient - In addition to the deflection induced in the wire mesh by the microwave radiation pressure, thermal gradients through the reflector support frame as shown in Figure 3.1-8(a) also cause deflections which effect the reflector efficiency. The equivalent thermal moment M_T shown in Figure 3.1-8(b) is used to estimate the deflection, δ. The value of M_T is derived from the following:

$$\frac{M_T}{EI} = \frac{1}{R} = \frac{\alpha(T_1 - T_2)}{h}, \text{ for } \Delta T = (T_1 - T_2)$$

$$M_T = \frac{\alpha \Delta T \, EI}{h}$$

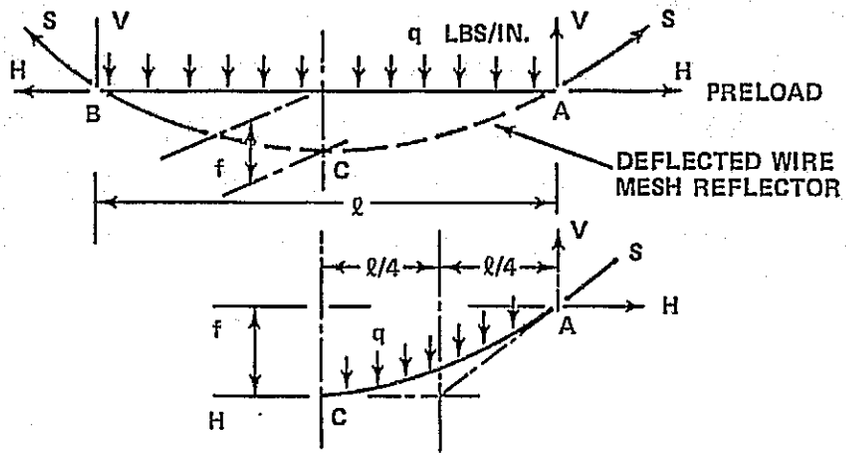

Figure 3.1-6 Reflector Load System

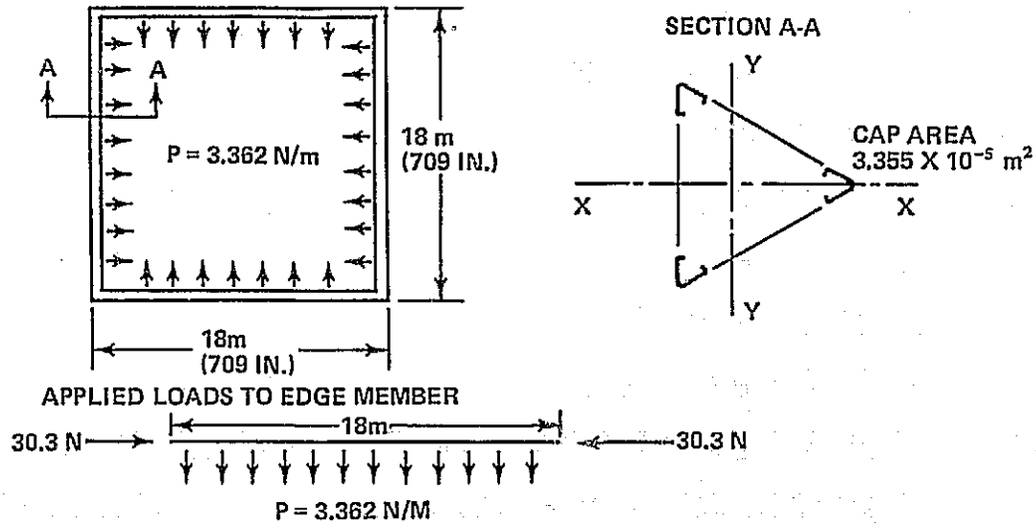

Figure 3.1-7 Reflector Support Frame

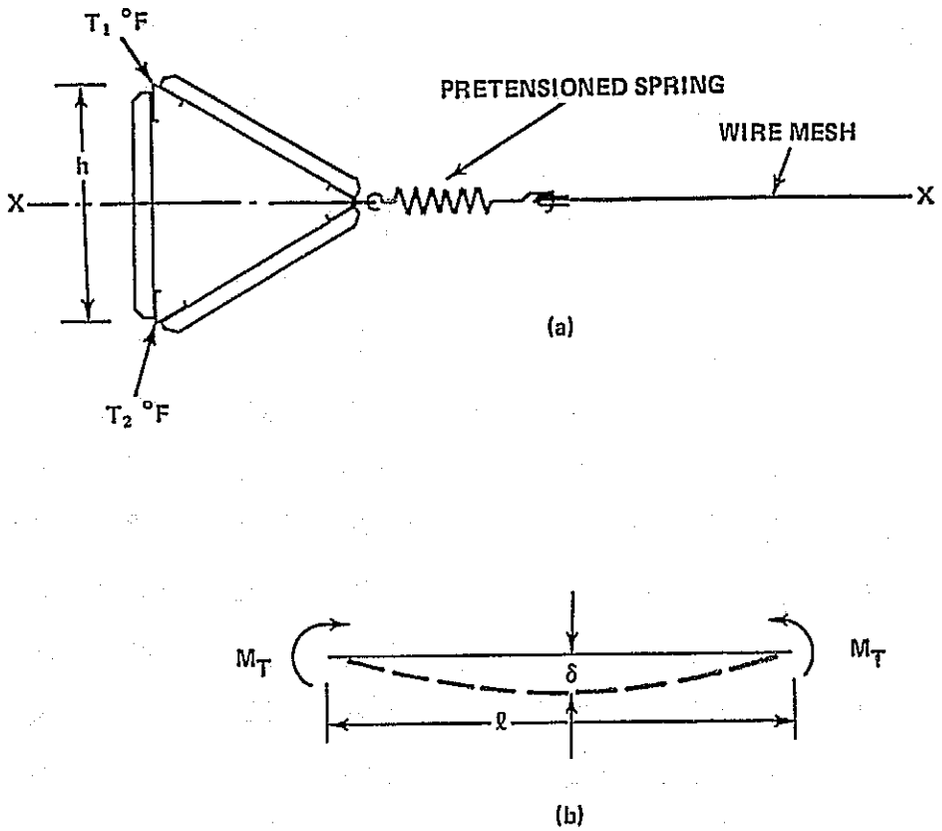

Figure 3.1-8 Reflector Support Frame - Deflection Under Thermal Gradient

This moment is applied to the end attachments of a simply supported beam as shown in the figure. The solution for the maximum deflection at the center of the beam is given by:

$$\delta = \frac{M\ell^2}{8EI} \text{ substituting}$$

$$M_T = \frac{\alpha \Delta T\ EI}{h} \text{ for M gives,}$$

$$\delta_\Gamma = \frac{\alpha \Delta T \ell^2}{8h} \text{ where h = .254 m (10 in)}$$

$$\delta_\Gamma = 0.01256\ \Delta T \text{ where } \Delta T \text{ is in } {}^\circ F \text{ and } \delta_\Gamma \text{ is in inches.}$$

For a maximum deflection of 5mm (.20 inches) the thermal gradient $\Delta\Gamma$ cannot exceed 29°K (16°F). The limitations on the temperature differences can be maintained by the proper selection of coatings and/or insulation.

The wire mesh used in the reflector is sandwiched between a bent strip of 2.54×10^{-4} m thick aluminum alloy and welded. Since there are temperature differences between the wire mesh and its supporting frame on entr into and emergence from an eclipse, springs having the pr er preload for all thermal conditions are used to keep the reflector deflection within limits.

3.1.3 Weight Data

The following weights data are for the 1 km diameter PRS; these data are subsequently corrected to reflect a 1 km by 1.km satellite.

	lb	kg
Primary Structure	206873	93820
Secondary Structure	65452	29683
Coatings & Insulation	49000	22222
Reflector module frame structure	175111	79415
Wire mesh	99786	45354
	596220	270494

Unit weight = 0.074 psf based on Reference (a) study

Corrected Weight for 1 km^2 Structure = 796536 lb

= 361241 kg

3.2 Flight Mechanics and Control

An assessment of PRS stationkeeping requirements indicate that yearly propellant requirements are modest, 812 kg/yr. using electric propulsion and 29,000 kg/yr using a cold gas system. Satellite orbit position should be maintained to within ± 10,000 km of the nominal location if transmitted beam steering is to be kept below 1 arc minute.

The dominant attitude disturbance torque is gravity gradient requiring 73 kg/yr (I_{sp} = 8000 sec) for correction. Unlike the SSPS which can be placed in a favorable orientation to minimize gravity gradient effects, the PRS must continually point in such a direction as to cause an offset of principle axes relative to the vertical.

A major PRS stationkeeping and control issue is the selection of a power source for electric propulsion control units. A trade-off is required to determine if it wouldn't be more cost effective to use a cold gas system (I_{sp} - 200 sec) which uses 31,940 kg per year of propellant. The cost of the power source, electric engines etc., could be more than the cost associated with the yearly resupply of propellants using the lower performing systems.

A dynamics analysis which couples the spacecraft attitude and stationkeeping control system with the structure and reflector contour control is needed to determine concept feasibility. Unlike the SSPS transmitting antenna where active electronic phase control can compensate for structural/mechanical control system errors, the PRS system must be maintained to extremely tight alignment through mechanical means only.

3.2.1 PRS Configuration

The mass of the PRS used in calculating preliminary stationkeeping requirements was taken from Ref. 3.2-1. The lowest weight aluminum design option presented in Ref. 3.2-1 was used. The overall spacecraft weight is 341,000 kg. which is approximately the weight estimated for the SSPS transmitting antenna structure, 350,000 kg (522,00 kg less support structure and mechanical systems required to interface the antenna with the spacecraft. This weight estimate is approximately 30% less than the PRS weight estimates in Section 3.1.

3.2.2 Stationkeeping Requirements

To establish the stationkeeping requirements for the PRS, the data generated for SSPS, Subsection 2.3, was used. The delta-V per year required for longitudinal and inclination control is independent of spacecraft geometry. The effects of solar pressure, however, is proportional to the spacecraft projected area normal to the sun vector. The projected area for PRS is approximately 1/60 of that of the SSPS including the effect that PRS does not continuously face its largest area toward the sun during its daily orbit. Microwave pressure was shown in Ref. 3.2-2 to be a significant orbit perturbation. This data was used to compile PRS propellant requirements for stationkeeping.

Table 3.2-1 summarizes the PRS stationkeeping requirements for two locations, 167°W and 113.5°W longitude. The first location is used for transmitting power from a source in the Southwest to a receiver in Japan. The second location transmits from the southwest for transmission to the CONUS Northeast.

The most severe perturbation is the microwave pressure. The 15 N force requires 118 mps delta-V for correction daily with an apogee/perigee maneuver. The next dominant perturbation is from sun/moon gravity, 46 mps/yr. Solar pressure perturbations require 0.24 mps for altitude control and 18 mps per year for eccentricity control. Four and 1/2 M/sec per year is required for longitudinal control at the mid Pacific location and 2.4 mps per year at the Southwest location, 113.5°W. longitude.

3.2.2.1 Propellant Requirements - Table 3.2-2 summarizes the PRS stationkeeping propellant requirements for two orbit positions (169°W and 113.5°W) and two propulsion system specific impulses (8000 sec and 200 sec). The difference in propellant requirement for the two orbit positions is small indicating that PRS will not be constrained from servicing any ground locations due to propellant factors. The difference in propellant for an ion propulsion system (8000 sec I_{sp}) is better than an order of magnitude lower than for a cold gas system. However, 29,000 kg for the cold gas system is not unreasonable and should be considered further.

3.2.2.2 Impact of Stationkeeping Accuracy on Microwave Performance:

The factors discussed in Subsection 2.3, covering the interrelationships between stationkeeping accuracy and MW transmission efficiency for SSPS, apply to the satellite-to-ground leg of the PRS mission. North-South drift (Inclination

Drift) was found to have a significant impact on system efficiency and, therefore, is controlled. On the other hand, the longitudinal cyclic motion resulting from uncontrolled eccentricity drift would not seriously effect MW performance. In analyzing PRS stationkeeping propellant requirements, Table 3.2-2, the quantity allocated to eccentricity control can be removed based on the down-leg MW performance sensitivities.

The impact of eccentricity drift on MW performance from the transmitting antenna on the ground to the satellite is not clear-cut. This assessment requires analysis of the MW performance degradation with increased electronic steering angles of the transmitted beam needed to track the satellite. We do know, however, from the Raytheon MPTS studies that MW performance drops off considerably beyond a steering angle of 1 arc minute. (Equivalent to an orbit position accuracy of 10,000 km). The PRS eccentricity drift caused by solar pressure would require at least 1 arc minute of transmitted beam steering. Therefore, it is recommended that eccentricity drift be controlled on the PRS.

Summary of Stationkeeping Requirements:

- The stationkeeping requirements for PRS are modest, 812 kg/Yr using electric propulsion and 29,000 kg/yr for a cold gas system. The lack of a substantial power source on PRS would tend to favor selection of the cold gas system.

- Better understanding of the relationships between microwave beam control and satellite position accuracy is needed to define stationkeeping requirements.

- The tight stationkeeping tolerances suggested in this preliminary study would lead to significant guidance and navigation design problems.

3.2.3 Attitude Control

The dominate disturbance torque which contributes to the PRS propellant requirements is gravity gradient (Table 3.2-3). Unlike the SSPS, the PRS must remain at a fixed attitude off-set from the local vertical causing a continuous torque bias on the system. This offset requires approximately 0.18 N (0.04 lb) of continuous thrust for attitude control. The effects of microwave and solar pressure on attitude control requirements are significantly lower than that of gravity gradients.

Table 3.2-1 Stationkeeping Delta - V, mps (FPS)

	LONGITUDE	
	167°W	113.5°W
LONGITUDINAL DRIFT	4.7 (15.5)	2.5 (8.2)
INCLINATION DRIFT	46.0 (151.5)	46.0 (151.5)
ALTITUDE DRIFT	0.3 (0.849)	0.3 (0.849)
ECCENTRICITY DRIFT	17.9 (58.7)	17.9 (58.7)
MW PRESSURE	117.8 (386.5)	117.8 (386.5)
TOTAL	186.8 (613)	184.6 (605.7)

Table 3.2-2 PRS Propellant Per Yr, kg (Lb)

DRIFT TERM	LONGITUDE			
	167°W		113.5°W	
	I_{SP} SEC		I_{SP} SEC	
	8000	200	8000	200
LONGITUDINAL	20.5 (45.3)	820 (1808)	10.8 (23.9)	434 (957)
INCLINATION	200.8 (442.3)	7940 (17490)	200.8 (442.3)	7940 (17490)
ALTITIDUE	1.1 (2.5)	45 (99)	1.1 (2.5)	45 (99)
ECCENTRICITY	77.8 (171.4)	310 (683)	77.8 (171.4)	310 (683)
MW PRESSURE	511.7 (1127)	19893 (43818)	511.7 (1127)	19893 (43818)
TOTAL	811.9 (1788.5)	29,009 (63,898)	802 (1767.1)	28623 (63,047)

Table 3.2-3 PRS Propellant Requirements, kg (Lb)

		I_{SP} = 8000 SEC	I_{SP} = 200 SEC
STATION KEEPING			
LONGITUDINAL DRIFT		20.5 (45.3)	820 (1808)
INCLINATION DRIFT		200.8 (442.3)	7940 (17490)
SOLAR PRESSURE			
– ALTITUDE		1.1 (2.5)	45 (99)
– ECCENTRICITY		77.8 (171.4)	310 (683)
MICRO WAVE PRESSURE		511.7 (1127)	19893 (43818)
ALTITUDE CONTROL	SUBTOTAL	811.9 (1788.5)	29009 (63,898)
GRAVITY GRADIENT		73 (161.4)	2932 (6457.6)
	TOTAL	885.3 (1949.9)	31941 (70,355.6)

Figure 3.2-1 is a schematic of the mechanical interaction of the attitude control system on the primary structures symetric and antisymetric bending modes. This system is idealized as a free-free beam with one reflector subarray mounted at the 1/4 span point. The relative vertical displacement of all reflector subarrays must be maintained to within 1/20 of a wavelength (approximately 5 inch or 12 cm) for efficient microwave performance. The structural deflection with the EI corresponding to the configuration discussed in Subsection 3.1 is given by relationship:

$$\delta u = .05F - 0.127F_1 \text{ (inches)}$$

where F = Attitude control system force at the support structure tips

F_1 = Contour control force for the reflector subarray

With an attitude control system force level of 0.18N (0.04 lb), the contour control actuator levels must be below 41 lb for primary structural deflections to be maintained below the $\lambda/20$ requirement. The need for 41 lb force actuators for the reflector subarrays appears to be far in excess of what will actually be used.

Based on this static assessment of the control system/structural interaction, it appears that the reflector subarrays could be maintained to within the required 1/20 of a wavelength provided the sensor information is accurate enough and the contour control system and attitude control system are detuned so as not to cause dynamic interactions. What is needed is a finite element and force response analysis coupled to the control system to determine the feasibility of maintaining the required flatness.

3.2.4 References

3.2-1 Rockwell Report E74-31, "Power Relay Satellite," March 1974.

3.2-2 GAC Report MPTS-R-002, "Microwave Power Transmission Systems Study - Task 2," December 1974.

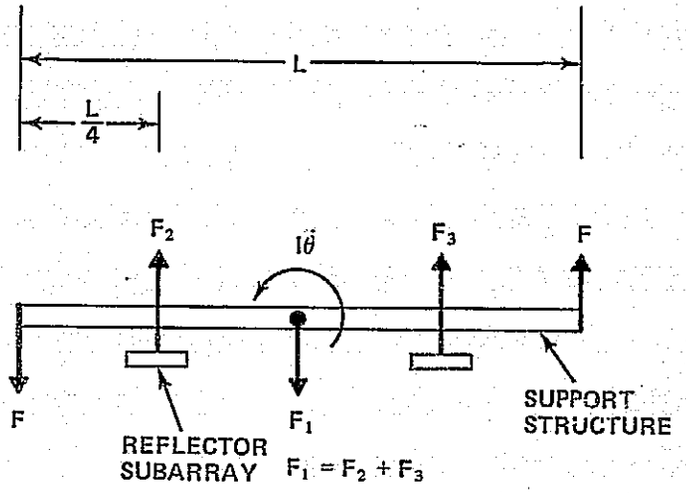

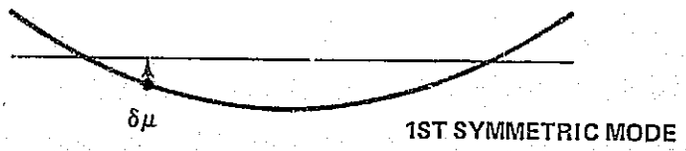

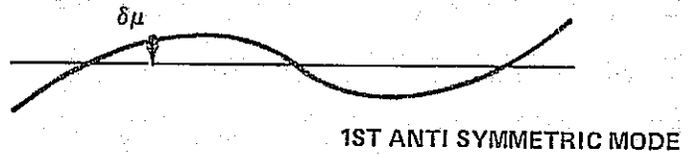

Figure 3.2-1 Simple Force-Moment Diagram of PRS Support Structure/Reflector Subarray Interaction

3.3 Transportation, Assembly and Maintenance

The economic and technical issues for transportation, assembly and maintenance are the same for the PRS as for the SSPS (See Subsection 2.4). The same array of transportation options should be considered in the assessment of PRS economics, though the use of a Heavy Lift Launch Vehicle (HLLV) may not be found to be cost effective. Simple derivatives of a Shuttle may be found to be adequate.

Figure 3.3-1 is a PRS development plan used as a strawman schedule for economic analysis. A geosynchronous demonstration satellite is scheduled for 1985. The transportation/assembly modes assumed available in this time frame are:

- Shuttle
- Full Capability Tug
- LEO Space Station
- SO Space Station.

Based on these major system elements the cost for transportation and assembly is approximately 4190 $/Kg. The 1990 system which is an improved version of the demonstration satellite was analyzed assuming the following transportation and assembly system elements:

- Deploy Only Launch Vehicle derivative of Shuttle
- Large Cryo Tugs which are derivatives of the Shuttle External Tanks
- LEO Space Station
- SO Space Station.

Based on these major elements the transportation and assembly costs are $1080/Kg, (see also Subsection 2.4 for transportation and assembly costs for the SSPS 1990 pilot plant).

Table 3.3-1 summarizes the maintenance costs for the PRS. The major maintenance cost drivers for PRS are similar to the SSPS, namely, the contour control actuators and the electric propulsion units used for attitude control and station-keeping.

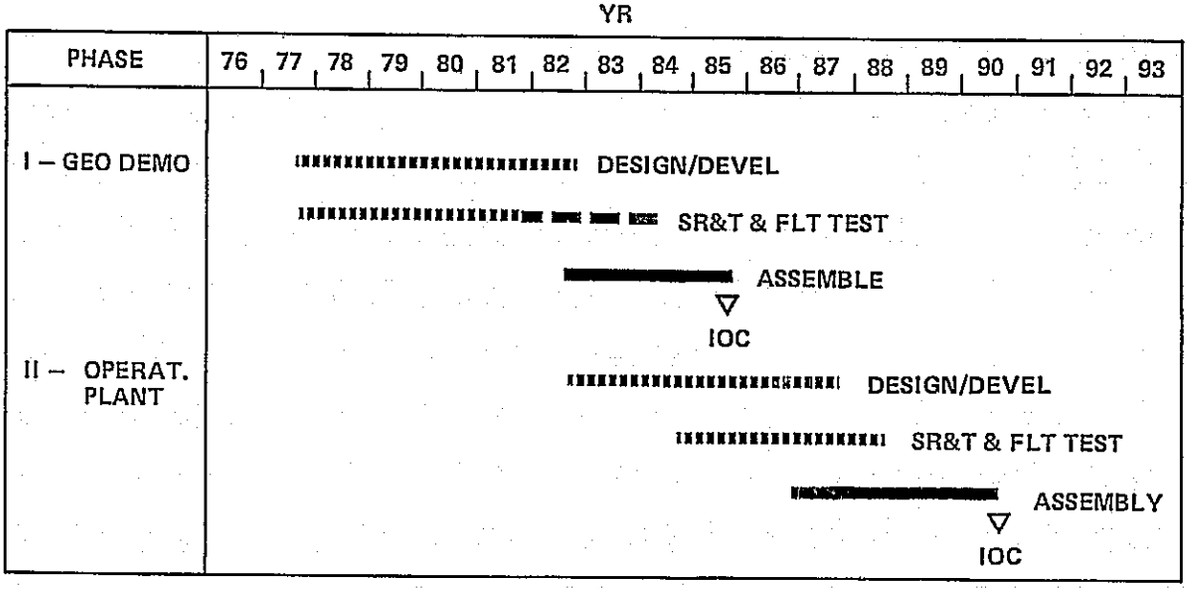

	1985 SYSTEM	1990 SYSTEM
WGT	.581 X 10^6 kg	0.505 X 10^6 kg
DDT & E	$1696M	$264M
UNIT COST	$2491M	$567M
MAINTENANCE	–	$90 M/YR

TOTAL PROGRAM THRU 1ST OPER. UNIT = $5.1B

Figure 3.3-1 PRS Orbital System Program Schedule and Cost

Table 3.3-1 PRS Maintenance Cost

ELEMENT	LRU DESCRIPTION	LRU WT, Kg	LRU FAILURES OVER 30 YRS	COST OVER 30 YRS, $M	AVG PER YR, $M
1 – STRUCTURE	TO DESIGN	–	–	–	–
2 – REFLECTORS	18 x 18m SURARRAY		1		
3 – CONTOUR CONTROL ACTUATORS	6680 UNITS	22	1404	0.35	0.01
4 – CONTROL SYSTEM – ACTUATORS	64 ELECTRIC ENGINES	203	640	1010	3.3
– PROPELLANT	885 Kg/YR	–	–	–	0.21
				TOTAL	3.52

The attitude control system electric propulsion units can be replaced by a cold gas system increasing propellant/year expenditure to 31,941 kg. The lower cost and lower weight of this lower performing propulsion system (I_{sp} = 200 sec.) would permit design of a highly redundant system with sufficient reliability to last 30 years.

The contour control system and associated electronics are the only elements in the PRS that appears to require any significant amounts of maintenance. Perhaps with sufficient design analysis, redundancy schemes could be introduced that would eliminate maintenance requirements for this subsystem.

Maintenance support costs for PRS are similar to those required for SSPS, namely costs associated with resupply and recycling crews of $86M/yr. The cost of equipments replaced each year is small, approximately $4M/yr. Subsection 2.4 discusses in detail the assumptions used to establish maintenance support costs.

4 - IMPLICATIONS FOR TECHNOLOGY DEVELOPMENT

This section summarizes the technology issues that must be funded to insure development of the space-based power generation options in the post 1990 time frame. Included are assessments of the technology risk, technology background and recommended technology programs in the following key areas:

- Point design development
- Systems and economic studies
- Microwave power technology
- Solar array technology
- Large structures including manufacturing, assembly, maintenance and control
- Environmental and other impacts.

The technology status and development risk of major technical areas have been assessed using the format adopted in the "Microwave Power Transmission System Studies (NAS3-17835)." This provides continuity of highly related efforts.

A risk rating, using the levels 1 through 5 shown in Table 4-1, provides a backdrop for delineating the status of technology. Each key area is addressed and technology programs and objectives suggested.

4.1 Point Design Development

The present (photovoltaic) baseline design--as well as others not included in this study--should be studied further. Special considerations should be given to satellite design as this will provide the basis for tradeoff studies and eventual subsystem optimization (from the technical and economic viewpoints).

Point design analysis of the solar array should project future states of technology, i.e., 1980, 1985 and 1990, as these are likely to be key decision points in the SSPS decision process.

A point design for the current "front-lit" concentration approach should be compared with a "back-lit" design to help identify the cost-effective configuration.

Point design studies of structural arrangements should compare the relatively standard approaches used in this study

Table 4-1 Technology and Hardware Development Risk Rating Definition

		RISK RATING				
		1	2	3	4	5
		IN USE	IN DEVELOPMENT	ON THE TECHNOLOGY FRONTIER	CONCEPTUAL	INVENTION
STATUS ANTICIPATED WITH: a) SPECIFIC MPTS-FUNDED PROGRAM b) OTHER KNOWN PROGRAMS	TECHNOLOGY	FULLY DEVELOPED	PARTLY DEVELOPED	KNOWN BUT NOT DEVELOPED	NOT KNOWN, CHANCE OF IT BECOMING KNOWN IN TIME FOR MPTS IS GOOD	NOT KNOWN, CHANCE OF IT BECOMING KNOWN IN TIME FOR MPTS IS POOR
	HARDWARE	OFF-THE-SHELF ITEM OR PROTOTYPE AVAILABLE HAVING REQUIRED FUNCTION, PERFORMANCE & PACKAGING	FUNCTIONALLY EQUIVALENT HARDWARE IN USE (OPERATIONAL)	FUNCTIONALLY EQUIVALENT HARDWARE IN DEVELOPMENT	NO HARDWARE IN USE OR DEVELOPMENT BUT DEVELOP-MENT IS PROBABLE	HARDWARE WILL NOT BE AVAILABLE UNLESS A BREAKTHROUGH OR INVENTION IS DEVELOPED
PROBABILITY OF DEVELOPMENT COMPLETION WITHIN SCHEDULE AND COST		CERTAIN (ALREADY EXIST)	VERY HIGH	HIGH	LOW	VERY LOW

with approaches that make maximum use of tension supports. An integral part of these structural studies should be the point design development of the power distribution system, including selection of ac or dc transmission and the system power level.

Point design options of the control system should consider both centrally located actuators and distributed actuators. These point designs should be used in detailed structural dynamics assessments.

4.2 Systems and Economic Studies

Systems and economic studies should be directed to two major areas, (1) the potential national (and world) economic benefits that may accrue from satellite power stations (SPS) and (2) the selection of the cost-effective SPS system.

Studies that would provide information in the first area include:

- Analysis of the market (demand) for SPS-provided electric power. Because the major proportion of SPS generation costs are capital-related (88 percent), and because the SPS plants are expected to operate at very high plant factors (95 percent), electric power cost (to the busbar) may be forecasted with relatively high accuracy over a 20- to 30-year period. The possibility raises the potential for the offering of long-term power contracts to power-intensive users. The consequences of this are only speculative at this point, but may include, the restructuring of production to capture cost advantages that may accrue from long-term power contracts, location of industry near ground station sites, and favorable environmental effects which may accrue from higher proportions of electrical sources of power.

- The 95 percent plant factor of SSPS (and presumably other forms of satellite power generation), which may allow for a restructuring of the supply elements of electric power generation. Currently there exist baseload plants, peaking plants, reserve peaking plants and standby reserve plants. Certainly, this is largely explained by the diurnal demand for power, but to some extent it is a requirement imposed by the system's reliability. The very high reliability of SPS plants coupled with the possibility that through pricing policies the diurnal demand might be altered (i.e., distributed more evenly throughout the day), the power supply structure might be altered in a cost-saving way.

Studies that are required to determine the most cost-effective variant of SPS include:

- The development of a cost model that includes the total SPS work breakdown structure and allows for the specification and estimation of probabilities of costs, performance and schedules.

- Risk analysis to estimate the distribution of total program costs and potential revenues. This includes the analysis of development, production and operational aspects of the PRS program alternatives.

- Potential constraints imposed by the social and environmental risks that may be involved in alternative PRS approaches.

- Separate programmatic and risk analysis of solar cell development, since future solar cell costs and technical characteristics are among the key uncertainties for SSPS.

4.3 Microwave Power Technology

The technical issues for the microwave power transmission systems (MPTS) were developed through a risk assessment of all elements of the concept as they impact the MPTS portions, and these were ranked in an estimated order of importance. For the 24 items in risk rating category 4 the issues presented in Table 4.3-1 specifically relate to the impact on the microwave portion.

Table 4.3-2 is a summary of cost estimates for the ground-based development program which would advance technology to a level suitable for the 1985 demonstration satellite. The technology issues have been broken down into four tasks. The first task encompasses those technologies associated with microwave transmission and conversion and is focused through a phased ground test program. The second task consists of the design, analysis, and test of a prototype rotary joint of sufficient size for proof of concept. The third task utilizes Arecibo to test high microwave power density impact on the lower altitude layers of the ionosphere. The fourth task is a detailed examination of radio frequency allocation issues and the selection of a frequency band for space-based power generation.

Table 4.3-1 Microwave Technology Requirements, Sheet 1 of 4

ITEM	TECHNOLOGY RISK ASSESSMENT		COMMENTS
	RATING	RANKING	
DC-RF Converters & Filters	4	1	BACKGROUND: Pre-amplifier amplifier & filters convert the high voltage DC power to RF power having low noise and harmonic content. There are at 0.1 to 1.5 million identical devices in one system. This is the highest single contributor to dissipation loss (15 to 19%) with the amplifier contributing 90% of that dissipation. The simplest design concept still results in the most complex mechanical, electrical and thermal set of technology development problems in the system. This combines with requirements for the development of a high production rate at low cost, resulting in reliable operation over a long life. What the noise & harmonic characteristics for the converters are and how they will act in cascade are not known. Filter requirements are to be determined. Ability to develop all the parts, interface them with each other and with the slotted array and operate them with full control and stability constitutes a high development risk and requires the longest lead time in an ambitious development program. TECHNICAL OBJECTIVES: Provide substantial data relating to technical feasibility, efficiency, safety and radio frequency interference.
Materials	4	2	BACKGROUND: Most critical and unusual requirements for materials in this application relate to the presence of the exposed cathodes for the RF generators. In addition, it is desirable that structural thermal strain be small so that distortions over the large dimensions are manageable. The waveguide distortions must be small to permit efficient phase front formation. The waveguide deployed configuration result in low packaging density so that it is desirable to form the low density configuration on orbit out of material packaged for high density launch. Before meaningful technology development can begin relating to fabrication, manufacture and assembly. It is necessary to determine the applicability of the non-metallic materials in particular as they relate to potential contamination of the open cathodes of the RF generators. Due to the critical interaction of materials with structures, waveguides and RF generators, the materials development risk rating should be a strong 4. TECHNICAL OBJECTIVES: Demonstrate cost effective use of non-metallic in terms of meeting distortion free waveguide and minimum impact on open cathodes performance.
Phase Control Subsystems	4	3	BACKGROUND: Phase front control subsystems projected scatter losses (2 to 6%) are second only to the microwave array losses (19 to 25%) in the microwave power transmission efficiency chain. The uncertainty associated with limiting losses to this value is significant. Phase control, being essential to beam pointing as well as focusing, must be shown to be reliable for power user and safety purposes. Risk rating should then be a strong 4. TECHNICAL OBJECTIVES: Demonstrate phase control steady state accuracy subject to error contributions of DC-RF converters and high power radio frequency environment.

Table 4.3-1 Microwave Technology Requirements, Sheet 2 of 4

ITEM	TECHNOLOGY RISK ASSESSMENT		COMMENTS
	RATING	RANKING	
Waveguide	4+	4	BACKGROUND: Slotted waveguides interface with the RF generators in a high temperature environment. They must distribute the power and emit it uniformly with low losses. They represent a large % of the weight and are conceived to be of .020" wall thickness in aluminum of possibly non-metallic composite layups with metallic coating. The ability to manufacture, fabricate and assemble such waveguides is not certain. To provide proper interfacing with RF generators, to limit distortion so as to operate satisfactorily as a subarray of slotted waveguides, and to do so within estimated cost and schedule constitutes high development risk. Risk rating should therefore be a strong 4+; however, significant materials technology development and selection must precede in depth technology investigations. TECHNICAL OBJECTIVES: Demonstrate capability of mass producing light weight, distortion free waveguides that can efficiently operate in a harsh thermal environment.
Biological	4	5	BACKGROUND: The CW microwave frequency and power densities to be investigated are rather well established. Effects to be anticipated in the sites yet to be selected are functions of ambient condition and the life forms peculiar to the region and those that are in transit. Most certainly areas like the desert southwest of the U.S. would be leading contenders so that effects on plants and animals should be investigated. Detailed investigations building on these conducted for more general purposes must be conducted to assure complete understanding of long-term and transient effects and to provide the basis for securing national and international agreement on frequency allocations, intensities and exposure limits. Development risk rating should be 4. TECHNICAL OBJECTIVES: Demonstrate safety of microwave frequency and power densities being considered for SSPS use.
Attitude Control	4	6	BACKGROUND: Control of antenna pointing conceived to be accomplished by mechanical action between the antenna and main mast as well as between the ends of the main mast and the solar array primary structure in the vicinity of the slip rings. These are very large members, of light weight construction, having to transmit unprecedented power across the relative motion interfaces, to operate in the space environment, with high reliability and safety, at low cost, packaged for high density earth launch, deployed or assembled in space, for a very long time with limited operations and maintenance attention. The actuators to establish the motion, the moving joints and the moving or flexing conductors are the largest and most complex machinery employed in the photovoltaic powered station and will be the subject of most critical operations and maintenance analyses in order to design the machinery to be essentially maintenance-free. Nevertheless it must be designed to permit maintenance under most adverse conditions of damage and environment. Development risk rating should be 4. TECHNICAL OBJECTIVES: Demonstrate the accuracy and life potential of the microwave mechanical pointing system.

Table 4.3-1 Microwave Technology Requirements, Sheet 3 of 4

ITEM	TECHNOLOGY RISK ASSESSMENT		COMMENTS
	RATING	RANKING	
Ionosphere	4	7	BACKGROUND: Effects of the ionosphere on the phase control link are not known definitively, however existing data and analysis indicate that they are probably insignificantly small at the frequencies and power densities being considered. The effects on the ionosphere induced by the microwave power beam are believed to be small. However, from the point of view of other users of the ionosphere and its participation in natural processes there may yet be limits imposed on the power density. The theoretical approaches to doing this are known but the limits that may yet be imposed are unknown. Development risk rating should be 4. TECHNICAL OBJECTIVES: Measure effects of microwave radiation on the ionosphere and determine social impact.
Power Transfer	4	8	BACKGROUND: The electrical power transfer function, at this large size and power level across flexing and rotating joints, cannot be separated from the mechanical and attitude control functions entirely. Although the technology for performing the functions is basically known, the large scale will present significant new problems. Development risk rating should be 4. TECHNICAL OBJECTIVES: Select power best power transfer design for SSPS and demonstrate performance.
Switch Gear	4	9	BACKGROUND: Switch gear had been conceived assuming multiple brushes from high voltage DC source transferred power to a single slip ring. Extraordinarily high currents in the switch gear resulted and would be the subject of a high risk (4+) technology development program. Decision has now been made to make the multiple brushes feed multiple sliprings, bringing the individual switch gear currents close to the region where the basic technology is known and the major advances would be in packaging for space operations. Risk rating should then be 4. Some aspects of the packaging technology having to do largely with size are not known, which leads to a risk rating of 4. TECHNICAL OBJECTIVES: Develop and demonstrate switch gear including protective elements for spaceborne applications.

Table 4.3-1 Microwave Technology Requirements, Sheet 4 of 4

ITEM	TECHNOLOGY RISK ASSESSMENT		COMMENTS
	RATING	RANKING	
Radio Frequency	4	10	BACKGROUND: Radio frequency and bandwidth allocation is normally a long process involving national and international technology and socio-economic considerations. It will take 2 to 4 years of DC-RF converters' and filters' technology development to mature the concept and make available meaningful data. Convincing the national and international community involved that gigawatts of power beamed from space at an allocated frequency with a specified narrow bandwidth will not in fact result in significant interference requires a positive approach that is yet to be defined. When it is shown convincingly that power from space would (a) be a significant answer to the national and international future power needs and (b) permit frequency allocation and bandwidth to be defined without significant interference outside the band; then securing high priority for frequency allocation will be a normal process. The appropriate risk rating is 4. TECHNICAL OBJECTIVES: Investigate radio frequency interference and allocate band to SSPS that would have minimum impact on other users, particularly Radio Astronomy.

Table 4.3-2 Microwave Technology Resource Requirements
($ Millions, 1975)

TASK	Calendar Year 76	77	78	79	80	81	82	83	84	85	COMMENTS
1 • DC-RF CONVERTERS & FILTERS	.5	.6	.4	.4	.4	.4					
• PHASE CONTROL	.4	.4	.3	.2	.2						
• WAVEGUIDE	.4	.4	.4	.4	.4	.2					
• SWITCH GEAR	.4	.4	.3	.2	.2						
• GROUND TEST (INCLUDE BIO TESTS)	2.4	2.5	2.2	3.3	5.3	7.0					
2 • ATTITUDE CONTROL	.3	1.0	2.0	2.0	.4	.4					
• POWER TRANSFER	.2	2.0	3.0	6.0	1.0	.4					
3 IONOSPHERE	←——— 11 ———→										REQUIRES MODIFICATION OF ARECIBO
4 RADIO FREQUENCY	.3	.3	.3								
TOTAL	6.3	9.4	10.7	14.3	9.7	10					

4.4 Solar Array Technology

Major system considerations are the cost, mass and efficiency of the solar cell blanket. Methods to achieve the goals needed for a cost-effective SSPS have been identified. Needed is an active solar cell development program that concentrates on a low cost fabrication and efficiency improvement for the single-crystal silicon cell for the prime program path, and an active research and proof of concept program for alternate photovoltaic devices for a backup program path.

Table 4.4-1 summarizes the key technical areas with their associated risk rating and ranking for developing a low-mass, low-cost, high efficient solar cell blanket for SSPS. The technology risks are rated in the categories outlined in Table 4-1. The rankings of the priority for the association technology programs are based on the status (risk) and the economic impact the technology improvement would have on the program.

Some of the technology issues identified in Table 4.4-1 are already being pursued by industry and ERDA. In ranking priorities, those technology programs that NASA might support are given higher rank. For example, cost improvements for processing raw materials to semi-conductor grade silicon is already being actively pursued by industry. Also, ERDA is supporting development of the EFG crystal growth process development. NASA might augment this program to insure that efficiency levels and quality control levels needed for a space-based array are met.

Table 4.4-2 is an overview of recommended technology development expenditures assuming that SSPS goals should be met in the mid-1980s for assurance of a 1995 operational plant IOC. These suggestions are in agreement with those recommended for terrestrial applications outlined in the "Workshop Proceedings for Photovoltaic Conversion of Solar Energy for Terrestrial Applications," held October 1973. NASA expenditures in Tasks 1 and 2 should be minimal. The unique requirements for space qualified solar cells warrants NASA expenditures in Tasks 3 through 5 at the same levels recommended for terrestrial applications.

The remainder of paragraph 4.4 describes issues requiring further systems study.

Solar concentration is shown to reduce SSPS cost. Lightweight mirror design concepts and their implementation are needed. New filter designs for concentrators will help improve solar cell life and performance. If high concentration is used, techniques for fabricating lightweight structure and contour control are needed.

Table 4.4-1 Large Solar Array Technology Requirements, Sheet 1 of 2

ITEM	TECHNOLOGY RISK ASSESSMENT		COMMENTS
	RATING	RANKING	
1. Raw Material Process	3	4	BACKGROUND: The initial process in fabricating solar blankets requires three energy intensive high temperature cycles. A single step process could result in savings of 3 to 5 over the $60/kg to $80/kg price paid today. Trichlorosilane used in the process is a large contributor to both energy use and cost. Alternates to this process should be pursued. Presently, Dow Corporation is researching more economical goals for producing semiconductor grade silicon. Dow is actively investigating 20 promising chemical reactions with the goal to reduce the cost to $10/kg. TECHNOLOGY OBJECTIVES: Achieve a 3 to 5 reduction in cost for bringing raw material to semiconductor grade silicon.
2. Crystal Growth	2	5	BACKGROUND: Three approaches to single-crystal growth being pursued today are: 1) Czochralski; 2) WEB and 3) EFG. The Czochralski method is characterized by large amounts of waste materials and is projected to achieve at most a factor of 2 savings in cost. WEB process could be sealed up in crystal growth speed and geometry with the potential of achieving a factor of 5 reduction in cost. The EFG process shows the promise for the most significant cost reductions (a factor of 10 to 100). The major problems are to find die materials that can withstand the temperatures of the process and you maintain the efficiency of the solar cell produced. The current process work being performed by TYCO fabricates a silicon ribbon 100 μ thick approaching the 50 μ SSPS requirement. TECHNOLOGY OBJECTIVES: Develop the EFG process to the point where 50 μ silicon ribbon can be produced with 100% crystal and cell yield. WEB process should be continued as a program backup.
3. Blanket Processes	4	2	BACKGROUND: Current methods for fabricating solar blankets is a slow, mostly hand-made process. A continuous process is indicated. An automated process that includes function formation, installs contacts, performs etching, etc. is basically an engineering problem. A pilot plant and verification program is needed. TECHNOLOGY OBJECTIVES: Formulate alternate concepts for blanket processing and demonstrate most promising techniques.
4. Packaging	3	5	BACKGROUND: The requirement for 30 year life in a space environment suggests that improvements in cell encapsulation would be required. Materials technology that improves the thermal and radiation resistance of the cell must be developed and included in the overall automated fabrication of the blanket. TECHNOLOGY OBJECTIVES: Develop new materials that improve cell efficiency and radiation resistance. Incorporate advanced encapsulation approach into the continuous cell fabrication process.

Table 4.4-1 Large Solar Array Technology Requirements, Sheet 2 of 2

ITEM	TECHNOLOGY RISK ASSESSMENT		COMMENTS
	RATING	RANKING	
5. Solar Cell Performance Improvement	4	1	BACKGROUND: Current industry space qualified solar cells can achieve beginning of life conversion efficiencies of 12 to 14%. A program that strives to improve these efficiency levels to 18 to 20% (AMO) is required. This goal can be achieved through increases in fill factor, short-circuit current, and open-circuit voltage. It would be desirable to decrease resistivity of the bulk silicon to 0.01 ohm-cm. Lower resistivity gives higher open-circuit voltage. Increased short-circuit current could be achieved by antireflective coatings that match across the cell spectrum. The major issue is to achieve these efficiency improvements in a mass produced light-weight solar cell blanket. TECHNOLOGY OBJECTIVES: Improve solar cell conversion efficiency to 19% (AMO) and maintain this efficiency in a mass produced light-weight solar cell blanket.
6. Alternate Photovoltaic Devices	4	3	BACKGROUND: Investigations into alternate photovoltaic conversion devices are showing a great deal of promise. Of particular interest is the Gallium Arsenside Al GaAs/GaAs heterojunction cell. These devices shown high performance at concentration (12% AMO at a concentration ratio of 300). An active research and proof of concept program on alternate devices to the silicon cell should be pursued. TECHNOLOGY OBJECTIVES: To identify and develop at least one new photovoltaic conversion device that can serve as an alternate to the silicon.

Table 4.4-2 - Large Solar Array Technology Resource Requirement, $M Terrestrial/$M Space

TASK	76	77	78	79	80	81	82	83	84	85	COMMENT
	TECHNOLOGY ←				→ PROOF OF CONCEPT						
1. REDUCE RAW MATERIAL PROCESS COST	0.8 (0.1)	1 (0.2)	1.5 (0.3)	2 (0.5)	←		50	→			AUGMENT INDUSTRY/ERDA EFFORT
					←	(1)	→				
2. REDUCE CRYSTAL GROWTH PROCESS	2.5 (0.5)	4 (1.0)	3.5 (1.0)	5 (2.0)	←		30	→			AUGMENT INDUSTRY/ERDA EFFORT
					←	(3)	→				
3. BLANKET PROCESS	2.5 (2.5)	2.5 (2.5)	3 (3)	4 (4)	5 (5)	←	80	→			NASA SUPPORT SPACE-BASED BLANKET PROCESS DEVELOPMENT
						←	(3)	→			
4. PERFORMANCE IMPROVEMENT	4 (4)	4.5 (4.5)	5 (5)	5 (5)	5 (5)	5 (5)	5 (5)	5 (5)	5	5	NASA SUPPORT SPACE-BASED BLANKET IMPROVEMENT
5. ALTERNATE PHOTOVOLTAIC DEVICES	3 (3)	3 (3)	3 (3)	4 (3)	5 (5)	5 (5)	5 (5)	5 (5)	5	5	NASA SUPPORT SPACE-BASED ALTERNATES
TOTAL	12.8 (10.1)	15 (11.2)	16 (12.3)	20 (14.5)	←		220	→			
					(←	(37)	→	)			

The SSPS will generate high-voltage power in a relatively stable thermal environment, but must maintain performance during a 30-year exposure to ultraviolet radiation as well as trapped particle radiation. The objective is 6 percent degradation over five years. Improvements in environment resistance can be achieved by improved material, spectral wavelength matching, high-voltage-plasma interaction protection, meteorite hardening and improved annealing techniques.

Multi-megawatt solar power generation requires switching protection at high voltage and current. Development of high-voltage switches and control devices are needed. Circuit design must consider induced magnetic moments to reduce effects on the overall spacecraft control. High voltage also leads to corona formation that reduces component life. The power distribution system design must address long transmission distances on SSPS. A key trade is to determine the extent to which the conducting buses can also be used as structure. A tradeoff between ease of assembly, cost, mass, reliability and electrical efficiency should be addressed.

A systems study summarized in Figure 4.4-1 should be performed to delineate a technology development program that establishes realistic goals in a phased program. The objective of this study would be to determine the primary and backup paths for the demonstration satellite's solar blanket.

The tasks in the systems study have the following outputs:

- Task 1: Configuration Concept Design/Selection
  - Candidate concept designs for the solar array using various levels of concentration and solar cell type
  - Structural thermal evaluation of the array including the solar blanket itself.
- Task 2: Programmatics
  - Evaluation of the costs of each candidate array
  - A ranking of program options with final selection of the primary and backup program path
  - Technology program schedule and performance goals.

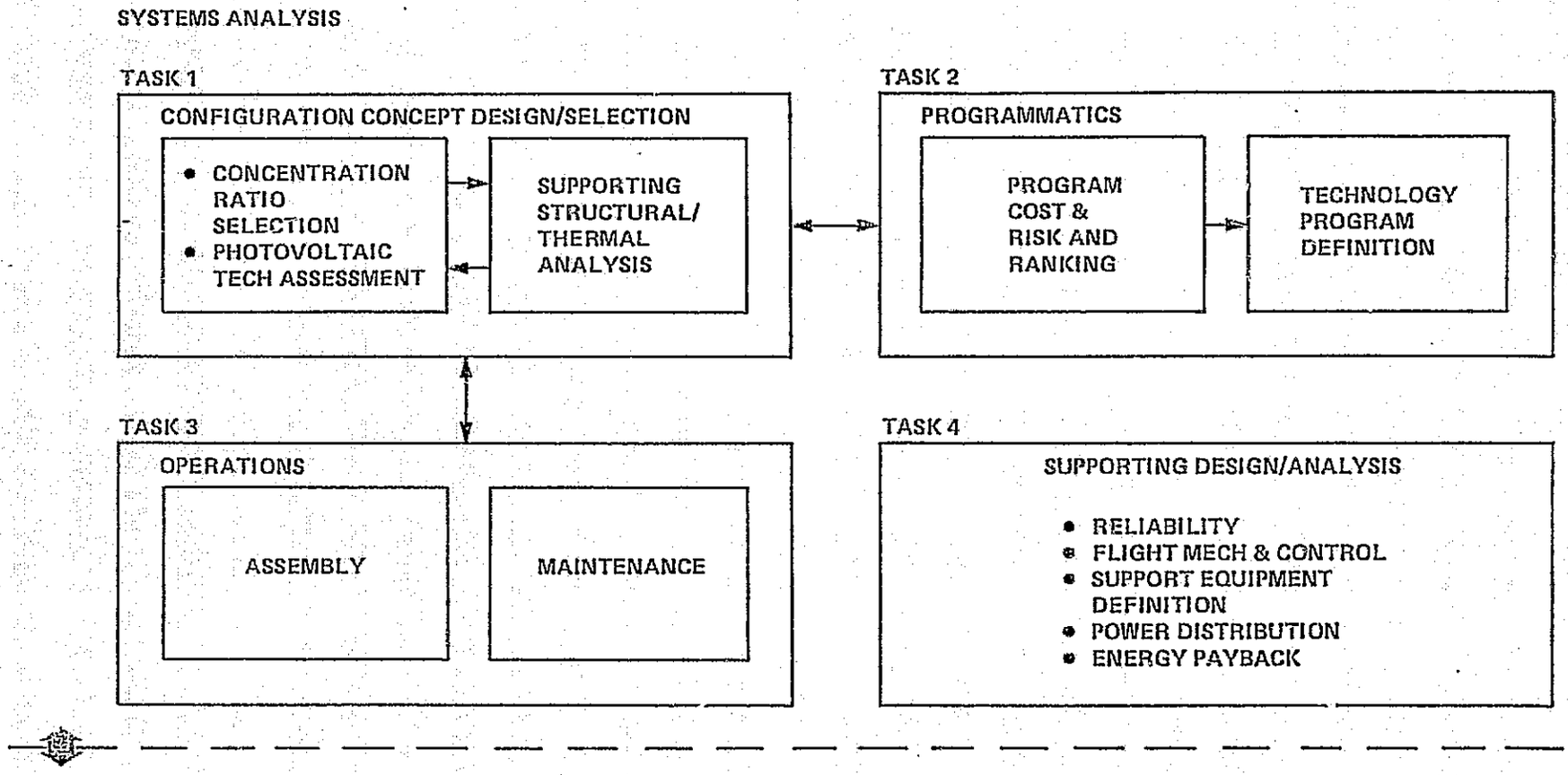

Figure 4.4-1 Large Solar Array Program Phase A Study

- Task 3: Operations
  - Identification and evaluation of solar blanket assembly and maintenance operations
  - Mission plan for Shuttle sortie demonstration flights.
- Task 4: Supporting Design/Analysis
  - Documentation of those efforts on assembly support equipment designs, power distribution interfaces, etc., needed to support the systems study.

4.5 Large Structures - Manufacturing, Assembly, Maintenance and Control

The development of necessary technologies for deployment of large structures in space requires a broad range of investigation including evaluation of materials characteristics, unique structural designs that are lightweight and capable of being tightly packaged for launch and development of low cost space assembly equipments and techniques. Table 4.5-1 is a top level summary of these issues.

Table 4.5-2 is an estimate of the near-term resource requirements needed to implement structural technology efforts. These technologies have been categorized under two broad tasks. The first is structural design and analysis which will provide the base upon which the design efforts for the demonstration satellite will build. The second task will design, build and test through simulation and verification programs, assembly/fabrication equipments and techniques.

The remainder of paragraph 4.5 describes issues requiring further systems study.

Static and Dynamic Structural Response to Thermal and Load Environments - The orbital load conditions which may design the structure are solar pressure, gravity gradient control torques and orbital station-keeping control torques and orbital station-keeping control forces. The dynamic responses of the large, flexible lightweight space structure to these disturbances require assessment to obtain a stress time history over the 30-year service life.

A significant contribution to the thermal stress/distortion is the induced thermal gradients resulting from the eclipse of the SSPS by the Earth's shadow. The SSPS experiences eclipse during a 45-day period at the vernal and autumnal equinoxes. The time in the Earth shadow varies from 0 to 72 minutes. As the satellite enters the shadow, the temperature decrease in the thin structural members will be rapid. Thus, the vehicle will experience significant thermal gradients. As the satellite exits the shadow, the thermal excitations will reverse. The entire thermal exposure cycle can induce low frequency oscillations in the entire flexible vehicle. The effects of these oscillations on the overall system require assessment.

Table 4.5-1 Structures Technology Requirements

ITEM	TECHNOLOGY RISK ASSESSMENT		COMMENTS
	RATING	RANKING	
Structure	4	1	BACKGROUND: Structure is characterized as being thin wall, low deployed density, high surface-to-mass ratio, metallic or possibly composite elements assembled into open space frame structural elements which in turn are assembled into yet larger space frames forming very large (approx. 1 km) antenna and even larger solar arrays. After materials technology development and selection, the new problems associated with low thermal inertia large dimension structures traversing the sunlight/shadow terminator at orbital velocities must be resolved. The resulting basic design, recognizing high launch packaging density limitations must be fabricated on orbit to achieve the final low density deployed configuration. How this should be done is not known and development risk rating should be considered as a firm four. TECHNICAL OBJECTIVES: Develop basic structural element with thickness of 0.02 inches (0.005 m) and less using aluminum and composites commensurate with required ground-based and/or space-based manufacturing and assembly techniques.
Manufacturing Modules	4	2	BACKGROUND: The specific technology for manufacturing modules is not known at this time, but should be relatively straightforward to develop once the basic design and materials have been established for the items to be manufactured in space. The major items are structural elements (open space frame structures) and slotted waveguides for the subarrays. Materials technology must be understood first and then engineering efforts for relatively automated manufacture must begin. Several iterations are probably required so the development must be paced to assure a reliable economic process. Development risk rating should be a firm 4. TECHNICAL OBJECTIVES: Develop modules for on-orbit manufacturing of waveguides and structure.
Remote Manipulators	4	3	BACKGROUND: The specific technology for remote manipulation modules is not known at this time. However, some investigations have been conducted in associated control systems. The development of these particular remote manipulators should begin after the hardware to be maneuvered and joined has been defined. The control links will probably be through TDRS so capabilities and limitations may begin earlier. Development risk rating should be a firm 4. TECHNICAL OBJECTIVES: Develop remote manipulator modules for the assembly, installation, removal, replacement, maintenance and operations in space.

Table 4.5-2 Structural Technology Resource Requirements

TASK	76	77	78	79	80	81	82	83	84	85
	PRELIMINARY DESIGN ⟷ DESIGN DEMO SATELLITE									
1. STRUCTURE										
• CONFIGURATION	.5	.5	1.0	1.0						
• STRUCTURAL & CONTROL ANALYSIS	.3	.7	1.0	1.6						
• THERMAL	.3	.7	1.0	1.0						
• STRUCTURAL ELEMENT DESIGN & FABRICATION	.7	1.0	2.0	3.5						
2. ASSEMBLY & OPERATIONS	2.0	3.5	7.0	10.0						
TOTAL	3.8	6.4	12	17.1						

To study the control of a flexible structure in a gravity-gradient field, it is necessary to accurately determine the difference between the gravity force and the orbital centrifugal force at each mass point. In many existing computer programs these effects are computed and then subtracted; however, the effects are nearly equal, and it is the small difference which is of consequence. This procedure is considered too inaccurate to be of value. To improve the procedure, the gravity and orbital centrifugal effects should be expanded in a series, analytically subtracted, and programmed in a general time-history structural program.

Required orientations and attitude control during build-up of the SSPS should be investigated. Concepts must be developed for efficient handling of changing configuration features such as inertias, moment arms, and disturbances.

Another area requiring further study is the interaction of the microwave antenna pointing system with the array control system. Elevation control of the antenna, including structural flexibility and the contour control system, should be evaluated.

Manufacturing and Assembly Techniques - The capability to fabricate and assemble large structures in space is a key issue. The design fabrication, assembly and transportation of the large space structure presents many significant problems requiring advances in the state-of-the-art of the related structural, materials, manufacturing and assembly technologies. The manufacturing and assembly techniques studied under this contract were based on the use of an automatic fabrication module; the module automatically fabricates and assembles the major structural components from raw stock in low earth orbit. These techniques now should be studied together with alternate methods of manufacture and assembly to establish the most effective and lightest configuration.

The manufacturing modules roll-form the basic structural elements which are assembled and welded into the progressively larger components. Investigations should be made to assess the use of other materials such as kevlar composites, graphite/epoxy composites, beryllium alloys, titanium alloys and various other aluminum alloys. These materials evaluations should be coupled with the use of other structural shapes and configurations to obtain a more realistic trade study of mass, cost and complexity.

Structural Verification Techniques - Investigations should be performed to evolve methods for verifying the structural integrity of the SSPS vehicle. The application of ground test techniques currently in use are obviously not suitable. It is proposed that ground test techniques for scale models which are structurally and dynamically similar be developed. This

procedure will provide verification of analysis methods. A second phase of this activity would be to design, fabricate and flight test an instrumented model of reasonable scale.

Maintenance - Additional system level studies are required to delineate technical issues and programs for maintenance operations. The failure rates assumed in the maintenance assessment in this study are soft at best. The failure rate for solar cells for example is based on OAO where careful selection of high quality components was the rule. On SSPS, mass production of solar blankets may preclude achieving as high a reliability. If the open-circuit failure rate for an individual solar cell increases an order of magnitude (2.63×10^{-3}/yr), 7.8 percent of the blanket LRU will fail in 30 years, requiring at least one replacement of the entire array ($112 M/yr) over the life of the satellite. A trend might also be demonstrated for the microwave components; however, the assumed redundancy and amplitron tolerance to malfunction may provide significant relief. An across-the-board reliability assessment of the SSPS is needed to more precisely determine maintenance cost.

The 5.6 percent power degradation level before lowest replaceable unit (LRU) replacement used to determine maintenance cost is driven by the assumed cost to repair (238 $/kg). If transportation and maintenance cost double, the point where cost of repair equals expected loss in revenue will also double. A study that more precisely evaluates the tradeoff between loss in revenue and the cost to repair is needed for each major satellite component. Amortization of support equipment costs for various approaches to maintenance should be included in the analysis.

The initial investment for maintenance support equipment, which assumes that one 6-man space station is allocated to each SSPS, appears to be excessive for the amount of maintenance predicted. Modifications to the maintenance scenario assumed should be reevaluated. Perhaps the space base and teleoperators assigned to each SSPS could be used to service several satellites, thus reducing considerably the cost to each unit. A second option would eliminate the use of multiple, manned space stations. An on-orbit maintenance "depot" facility would house spares and teleoperators and the manned transport vehicle would be of sufficient size to allow maintenance of support equipments and other functions requiring manned participation. In this manner, the costs for the man-rated equipments could be shared by many power stations. Additional study is needed to determine the most cost-effective approach.

4.6 Transportation

Transportation costs are potentially the most significant element in determining the costs of the SSPS. Transportation costs vary as a function of the lift capability of the launch system and the orbit inclination at which assembly is performed. The technology base for developing the launch vehicle is in-hand. Early SSPS development can be achieved with the Shuttle or derivatives of the Shuttle. Studies are already underway that are evaluating conceptual designs for heavy lift launch vehicles with payloads to low earth orbit of 182,000 kg (400,000 lb) or greater. The orbit transfer stage, which will transport the SSPS totally assembled or as large assembled modules to geosynchronous orbit, require more technology development if cost goals are to be met. Near-term system studies are required to delineate the requirements and cost impact of transportation options.

Figure 4.6-1 shows the relationship between orbit-to-orbit stage characteristics, launch system performance, and electric power incremental unit charge rate. A high performance gas core reactor or ion stage would be required for cost-effectiveness. The ion propulsion or other high performance propulsion systems appear to offer the lowest cost approach for orbit-to-orbit transport of material. The following list presents significant ion propulsion issues:

- Development of a large diameter thruster. Current engine development (LeRC) has concentrated on a 30 cm thruster. An extension of the ion thruster diameter to 1 meter seems within technical feasibility. The grid material of the engine will be the limit to the size of these devices. As the thruster operates, the grids distort thermally varying the spacing between the grids.

- Selection and development of the power source. The major concern is that the stage must transport materials through the Van Allen Belts. The silicon photovoltaic power source may not be the best approach when performance degradation of the cell due to radiation while in the belts is more precisely taken into account. Other power sources, such as nuclear or solar thermal, could readily get around the radiation problem but would introduce other technology problems. What is needed is an across-the-board system study of all options to better identify the more attractive approaches.

- Selection of the propellant. Most current technology development has concentrated on mercury propellants. Use of this material on a scale needed for the SSPS

may not be acceptable in terms of the potential contamination to SSPS sensitive devices as the microwave converters and solar cells. As in the case with selection of the power source, an across-the-board systems study of the propellant options is needed to clarify technology requirements.

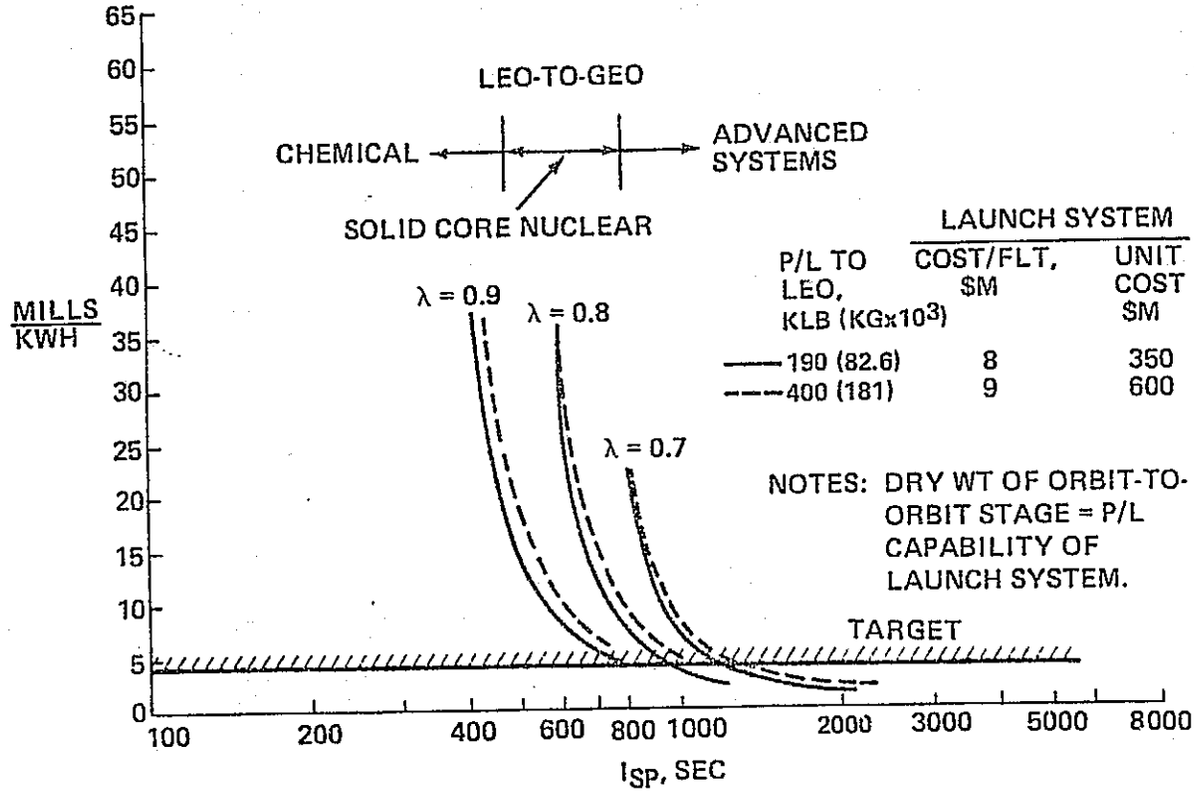

Figure 4.6-1 Orbit-To-Orbit Transport Costs

4.7 Environmental Impact Analysis

As in the case with any project that may significantly affect the human environment, all components of the SSPS and, more generally, SPS systems should be subjected to a thorough evaluation of the impact on the environment. In planning the SSPS (or SPS) program, this task should not be treated lightly, for it is the issue of environmental impact that has delayed construction of conventional nuclear reactors and liquefied natural gas storage projects, and was an emotional issue in the United States supersonic transport program.

Because of the magnitude of the SSPS (SPS) program, detailed environmental impact assessments (EIA) and environmental impact statements (EIS) must be prepared for the major components and subsystems of the SSPS (SPS). These assessments, in aggregate, will comprise the assessment of the SSPS (SPS) and will be used when comparing the impact of the SSPS (SPS) with the impact of alternative power systems.

APPENDIX A: WORK BREAKDOWN STRUCTURES-SSPS AND PRS SYSTEMS

A.1 Satellite Solar Power Station

A.1.1 Work Breakdown Structure and Program Schedule

A preliminary SSPS Work Breakdown Structure (WBS) and program schedule have been compiled to establish a "strawman" for programmatic analysis. The three-step program was based on the development of a small LEO Process Development and Test Facility, a geosynchronous-stationed 1 GW pilot plant, and a full capability plant (5 GW) scheduled for completion in 1995.

Figure A-1 is the WBS used as the roadmap for cost accounting and program planning. The 11 Level-2 elements of the WBS are identified as

- Project Management
- System Engineering and Integration
- Transportation
- Assembly
- On-Orbit Assembly Support Equipment
- Transportation and Assembly Ground Support Equipments
- LEO Development and Test Satellite Program
- Pilot Plant
- Operational Plant
- System Maintenance
- Facilities.

Project Management (-01) - This element of work accounts for the technical and administrative planning, organization, direction, coordination, control and approval mechanisms to accomplish overall program objectives.

System Engineering and Integration (-02) - This element includes all the necessary engineering and systems management efforts needed to achieve an integrated program. It includes engineering management, systems engineering, design engineering, support engineering, and the assurance technologies; namely,

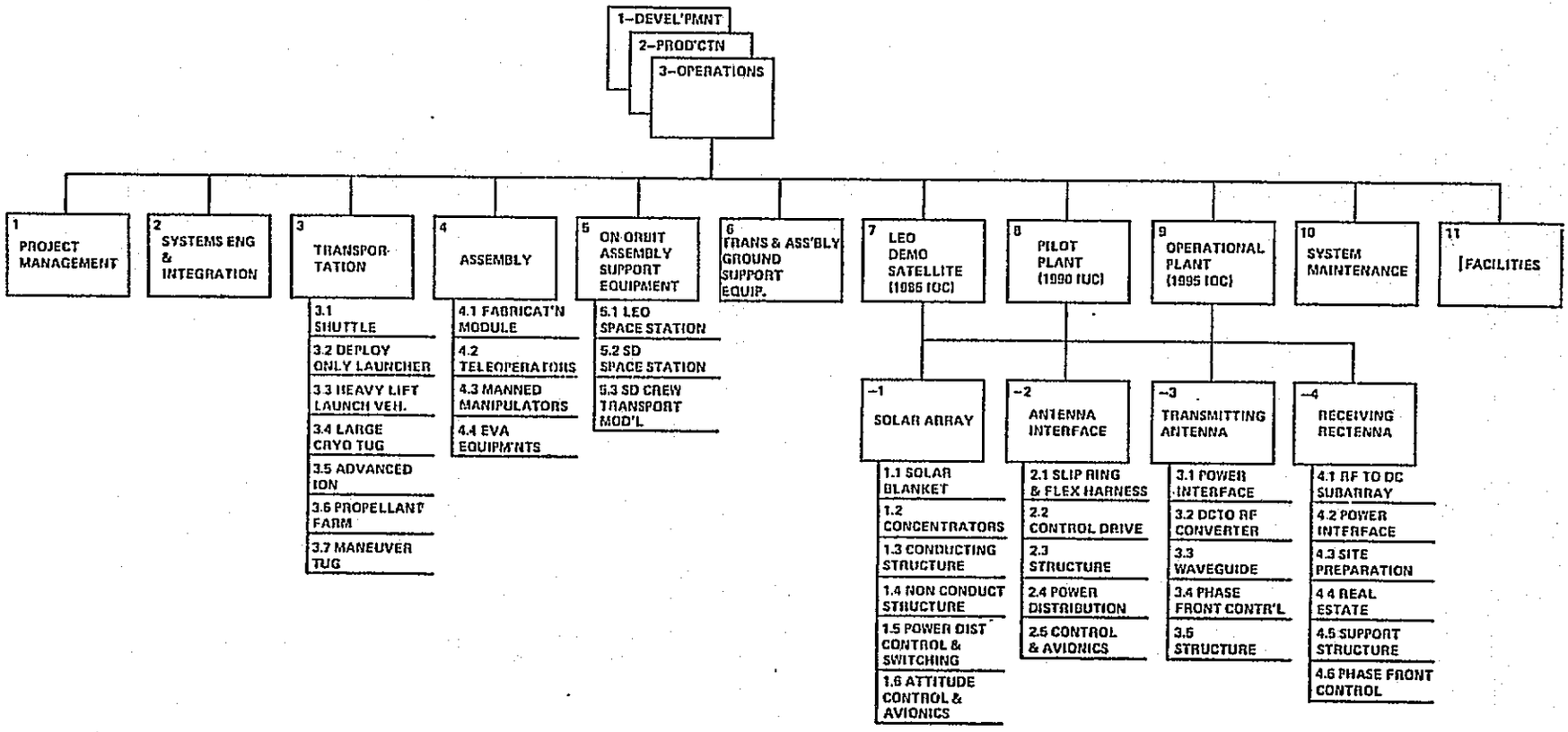

Figure A-1 Work Breakdown Structure

reliability, quality assurance maintainability, safety, environmental protection as well as impact and assessment.

Transportation (-03) - This element includes the development, production, and operation of all systems that transport materials, equipment, and personnel from launch through deployment at the designated mission orbit. The following elements are included:

- (-03-1) Shuttle (IOC 1981)
- (-03-2) Deploy Only Launcher (IOC 1987) - A derivative of shuttle using external tank, solid rockets, and a payload shroud which is integrated with a propulsion package of SSME's. This launch system is fully recoverable with a payload to low earth orbit of 72,640 kg (160,000 lb).
- (-03-3) HLLV (IOC 1992) - New heavy lift launch vehicle, fully recoverable with 181,600 kg (400,000 lb) payload to low earth orbit.
- (-03-4) Large Cryo Tug (IOC 1987) - An orbit transfer vehicle for transporting materials, equipments, and personnel between low and geosynchronous earth orbit. The vehicle baselined for this study is a derivative of the external tank and SSME, it requires in-orbit refueling.
- (-03-5) Advanced Ion (IOC 1992) - A large high performance stage with the capability to transport assembled SSPS from LEO to geosynchronous orbit.
- (-03-6) Propellant Farm (IOC 1987) - A set of propellant storage tanks and support equipment for storing and transferring propellants for the Large Cryo Tug and Advanced Ion stage.
- (-03-7) Maneuver Tug (IOC 1987) - A tug used to maneuver and transport large equipments, materials, propellants, etc in the vicinity of the assembly site and propellant farm.

Assembly (-04) - This WBS element includes all equipment required in the assembly operation for the fabrication, joining and integration of the SSPS.

- (-04-1) Fabrication Modules (IOC 1983) - A highly automated device that fabricates structural beams in orbit.

- (-04-2) Teleoperators (IOC 1983) - A remotely controlled module used to assemble structure, microwave components, solar blankets, etc.

- (-04-3) Manned Manipulators (IOC 1983) - A man-rated maneuvering vehicle with manipulator arms used in assembly.

- (-04-4) EVA Equipment (IOC 1983) - Space suits and equipment for an EVA mode of assembly.

- (-04-5) Logistics Equipments (IOC 1983) - A small tug used to move equipment, materials, and personnel in the vicinity of the assembly site.

On-Orbit Assembly Support Modules and Equipment (-05) - Equipment needed in support of assembly operations, this includes space stations, shuttle ancillary equipment, and crew transport modules. The following items comprise a summary of the Level-3 WBS elements:

- (-05-1) LEO Space Station (IOC 1987) - A modular, 6-man space station used to house the assembly crew, maintenance facilities, large elements work area (hangar), and assembly equipment in low earth orbit.

- (-05-2) SO Space Station (IOC 1987) - A modular, 6-man space station to perform functions similar to those for LEO Space Station but on geosynchronous orbit.

- (-05-3) SO Transfer Module (IOC 1987) - A crew transport module used to house crews for transport between LEO and synchronous orbit.

Transport and Assembly Ground Support Equipment (-06) - The ground equipment required to support launch and mission operations including development of communications centers and networks. This WBS element has not been included in the programmatic analyses because more depth of definition of the satellite, assembly equipment, and operations is required to define this WBS element to sufficient depth for costing. In the interim, this is considered to be included in the 20 percent task factor applied for cost uncertainty.

LEO Development and Test Satellite (-07) - Figure A-2 is a conceptual design for a 15 MW (transmitting antenna output power) demonstration and test satellite. The solar array is layed out at a concentration ratio of two. The silicon solar

15mw OUTPUT POWER

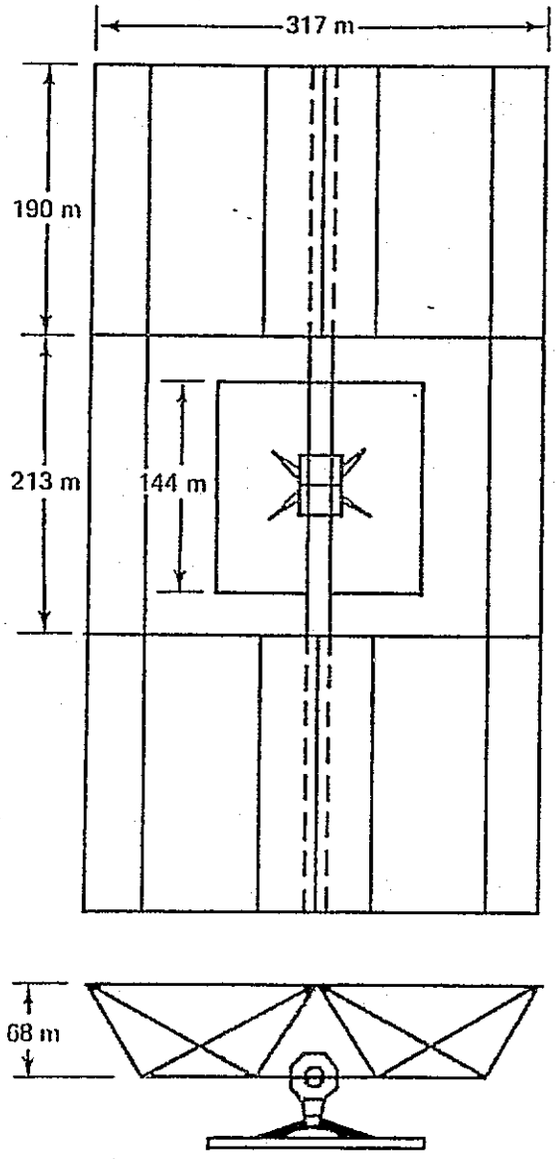

CHARACTERISTICS

- SOLAR BLANKET
  - CONCENTRATION RATIO = 2
  - CELL EFFICIENCY = 9.7%
  - POWER DISTRIBUTION EFFICIENCY = 92%
- MICROWAVE CONVERSION EFFICIENCY = 82%

WEIGHTS (228,343 KG)

ARRAY

• BLANKET	=	39,571 KG (0.525 KG/M^2)
• CONCENTRATOR	=	3,014 KG (0.02 KG/M^2)
• NONCONDUCT. STRUCT.	=	16,692 KG (2.76 KG/M LENGTH)
• CONDUCT. STRUCT.	=	2,633 KG (2.76 KG/M LENGTH)
• MAST	=	1,049 KG (2.76 KG/M LENGTH)
SUBTOTAL	=	62,959 KG

ROTARY JOINT = 12,670 KG (1/10 WT OPS SYST)

ANTENNA

• STRUCTURE	=	9,083 KG (.43 kg/m^2)
• CONTOUR CONTROL	=	3,648 KG (.38 kg/m^2)
• POWER DISTRIBUTION	=	10,648 KG (RAYTHEON EST)
• CONTROL ELECT	=	5,632 KG (RAYTHEON EST)
• TUBES	=	2,848 KG (RAYTHEON EST)
• WAVEGUIDE	=	95,296 KG (RAYTHEON EST)
SUBTOTAL	=	127,155 KG

Figure A-2 Demonstration and Test Satellite

cell blanket efficiency was established by using the projected efficiency for the SEPS array (12%) and then degrading efficiency for the operating temperature at a concentration ratio of two. A power distribution system efficiency of 82 percent was utilized to compute the array output power.

The array mass estimates used the projected SEPS solar blanket masses (0.525 kg/m^2) and the 0.5 mil aluminized Kapton masses projected for the 1995 mirror system. The mass per unit length of structure for the 1995 satellite was used to establish the non-conducting structural masses. The column lengths for this design are approximately the same as the 1995 system. The mass of the conducting structure and central mast are sized by electrical requirements in the 1995 system; but are sized by structural requirements in this system. The rotary joint is scaled down (1/10 size) from the 1995 system. The total mass of the satellite is 228,343 kg (503,148 lb).

Pilot Plant (-08) - Figure A-3 is a conceptual design of a 1 GW, ground-output pilot plant for operation at geosynchronous altitude. Whether this 1 GW plant should be built depends upon its economic merit. The assumptions used to size the configuration are included. The total system mass is 8.33 x 10^6 kg. The transmitting antenna on this configuration is the same size as that for the 1995 SSPS; however, it is assumed to transmit below the operational power level.

Operational Plant (IOC 1995) (-09) - The operational plant is a 5 GW facility which utilizes an advanced solar blanket and the same antenna size as the pilot plant with full complement of RF generators. The following items comprise a summary of the subdivision of work:

- (-09-01) Solar Array: A large photovoltaic array operated at 2:1 concentration with the following elements:
  - (-01.1) Solar Blankets
  - (-01.2) Concentrators
  - (-01.3) Conducting Structure
  - (-01.4) Non-Conducting Structure
  - (-01.5) Power Distribution, Control and Switching
  - (-01.6) Attitude Control and Avionics

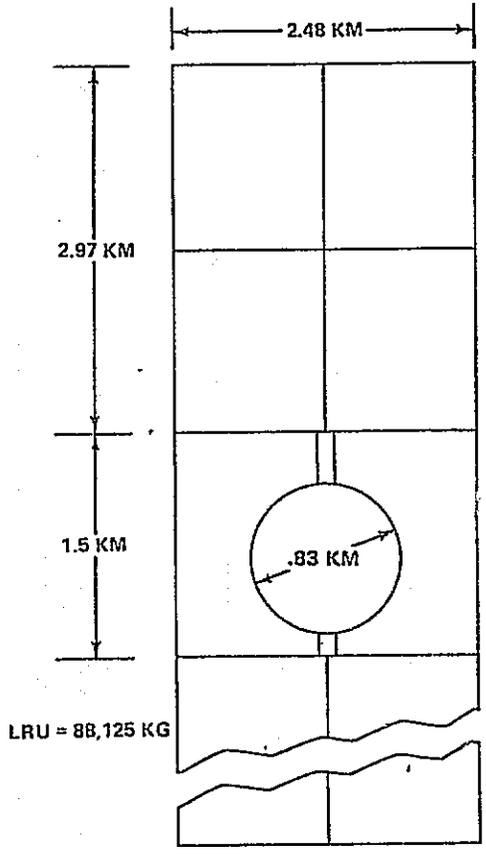

CHARACTERISTICS

- SOLAR BLANKET
  - CONCENTRATION RATIO = 2
  - CELL EFFICIENCY = 11%
  - POWER DISTRIBUTION EFFICIENCY = 92%
- MICROWAVE CONVERSION EFFICIENCY = 57% RECTIFIED AT GROUND

WEIGHTS

ARRAY	KG X 10^6	COMMENT
• BLANKET =	2.82	(7.04 KM^2) (0.4 KG/M^2)
• CONCENTRATOR =	0.31	(15.4 KM^2) (.02 KG/M^2)
• NONCONDUCT STRUCT =	0.61	(18.5 KM^2) (0.033 KG/M^2)
• CONDUCTING STRUCT =	0.07	(18.5 KM^2) (0.004 KG/M^2)
• MAST =	0.38	(7.4 KM) (0.052 KG/KM)
	4.19	
ROTARY JOINT	0.20	(SAME AS 1995 SYSTEM)
MW ANTENNA	3.94	(SAME AS 1995 SYSTEM WITH REDUCE # OF TUBES)
TOTAL	8.33	(18.3 X 10^6 LB)

Figure A-3 Pilot Plant - 1 GW Ground Power

- (-09-02) Antenna Interface: A large diameter rotary joint for fine pointing the antenna and transferring power with the following elements:
  - (-02.1) Slip Rings and Flex Harness
  - (-02.2) Control Drive
  - (-02.3) Structure
  - (-02.4) Power Distribution
  - (-02.5) Control and Avionics
- (-09-03) Transmitting Antenna: A large phased array that utilizes slotted waveguides and crossfield amplifiers. The following elements are included:
  - (-03.1) Power Interface
  - (-03.2) dc to rf Converter
  - (-03.3) Slotted Waveguide
  - (-03.4) Phase Front Control
  - (-03.5) Support Structure
- (-09-04) Rectenna: A large solid state receiving and rectifying antenna for conversion of rf power to dc electric. The following cost elements are included:
  - (-04.1) RF-DC Subarrays
  - (-04.2) Power Interface
  - (-04.3) Site Preparation
  - (-04.4) Real Estate
  - (-04.5) Support Structure
  - (-04.6) Phase Front Control.

Systems Maintenance (-10) - This includes those equipments for on-orbit maintenance of the satellite, and the cost of spares and the equipments necessary to maintain spares. The cost of the on-orbit equipments and spares have been included in the cost estimates.

Facilities (-11) - This WBS element includes the facilities required for support operations and the manufacture of the major hardware elements of the satellite. Cost estimates for facilities have not been included in the overall program assessment in this preliminary study. These are assumed to be covered in the 20 percent cost uncertainty allotment.

A.1.2 Cost Estimates

Cost estimates for the SSPS program have been made using existing cost estimating relationships (CER's). The Koelle model (presented at the International Academy of Astronautics, October 14, 1972) was used to establish development and unit production estimates for the transportation systems, and support equipments. The aerospace "Spacecraft System Cost Model," augmented with the Koelle model trends as a function of "new technology" required in the program, was used to estimate the SSPS subsystem development cost.

Table A-1 is a compilation of cost estimates for the SSPS program. Costs are listed by WBS element.

Estimates of the SSPS subsystem costs required an extensive extrapolation from the existing data base. Considerable "grass roots" estimating based on detailed engineering definition of the subsystem should be performed to refine the estimates presented here.

The major subsystem development cost is the solar array in which costs vary as a function of system power level and weight. Development costs for a 10 GW operational plant solar array could increase as much as $1 billion over that for a 5 GW system.

Cost sensitivity studies indicate that the SSPS rotary joint with its associated control system could be a major development cost driver. To limit maintenance cost, the design life of the rotary joint and control system is of major importance. These development cost estimates assumed a rotary joint and control system design life of five years. If the design life were increased to 30 years, development costs for the first full scale rotary joint (used in the pilot plant, if built) could run as high as $1 billion.

The cost estimates for structure are considered to be low. The CER's used to establish these estimates are based on a history of spacecraft launched as a single unit. The added complexity of space assembly on the design and development of the structure could impact the costs considerably.

Table A-1 System Cost Estimate, Sheet 1 of 3

WBS NO.	WBS IDENTIFICATION	IOC	LEVEL 1 WBS ELEMENTS 1–DEVELOPMENT	2–PRODUCTION	3–OPERATIONS	COMMENTS
–01 –02	PROJECT MANAGEMENT SYST ENG & INTEGRATION					40% OF TOTAL COST OF WBS ELEMENTS 02 THRU –11
–03	TRANSPORTATION					
–03–01	SHUTTLE DIRIV	1981	N/A	$ 200 M/UNIT	$12M/FLT	
–03–02	DEPLOY ONLY LAUNCHER	1987	$ 380 M	150 M/UNIT	$13M/FLT	
–03–03	HLLV	1992	6,540 M	400 M/UNIT	$9M/FLT	
–03–04	LARGE CRYO TUG	1987	166 M	15 M/UNIT	$1M/FLT	
–03–05	ADVANCED ION	1992	3,847 M	190 M/UNIT	$1M/FLT	
–03–06	PROPELLANT FARM	1987	223 M	16 M/UNIT		
–03–0	MANEUVER TUG	1987	215 M	2.6 M/UNIT		
–04	ASSEMBLY					
–04–01	FABRICATION MODULES	1983	$ 271 M	$ 12 M/UNIT		
–04–02	TELEOPERATORS	1983	19 M	2.5 M/UNIT		
–04–03	MANNED MANIPULATORS	1983	365 M	11 M/UNIT		
–04–04	EVA EQUIPMENT	1983	20 M	1.5 M/UNIT		
–04–05	LOGISTICS EQUIPMENT	1983	44 M	2.5 M/UNIT		
–05	ON-ORBIT ASSEMBLY SUPPORT EQUIPMENT					
–05–01	LEO SPACE STATION	1987	1,000 M	$ 16 M/YR/MAN		
–05–02	SO SPACE STATION	1987	57 M	16 M/YR/MAN		
–05–03	SO TRNASFER VEHICLE	1987	190 M	23 M/MAN		
–06	TRANSPORT & ASSEMBLY GROUND SUPPORT EQUIPMENT		TBD	TBD		INCLUDE IN UNCERTAINTY FACTOR
–07	LEO DEMO SATELLITE	1985			1376 $/KG(1)	(1) ASSEMBLY OPERATIONS
–07–01	SOLAR ARRAY		1,108 M	3,461 $/KW		
–07–02	ANTENNA INTERFACE		383 M	2,670 $/KW		
–07–03	TRANSMIT ANTENNA		610 M	386 $/KW		
–07–04	RECEIVING RECTENNA		59 M	1,099 $/KW		

Table A-1 System Cost Estimate, Sheet 2 of 3

WBS NO.	WBS IDENTIFICATION	IOC	LEVEL 1 WBS ELEMENTS 1—DEVELOPMENT	2—PRODUCTION	3—OPERATIONS	COMMENTS
—08	PILOT PLANT	1990			1086 $/KG(2)	(2) TRANSPORTATION & ASSEMBLY OPERATIONS
—08—01	SOLAR ARRAY		$2,453 M	765 $/KW		
—08—02	ANTENNA INTERFACE		446 M	105 $/KW		
—08—03	TRANSMIT ANTENNA		320 M	144 $/KW		
—08—04	RECEIVING ANTENNA		1,218 M	392 $/KW		
—09	OPERATIONAL PLANT	1995			180 $/KG(2)	(3) INCLUDED IN CONDUCTING STRUCTURE ESTIMATE
—09—01	SOLAR ARRAY	1995	$3,104 M			
—09—01.1	SOLAR BLANKET			55 $/M^2		
—09—01.2	CONCENTRATORS			1.1 $/M^2		
—09—01.3	CONDUCTING STRUCTURE			81 $/KG		
—09—01.4	NONCONDUCTING STRUCTURE			81 $/KG		
—09—01.5	PWR DIST CONT'L & SWITCH			(3)		
—09—01.6	ATT'D CONTR'L & AVIONICS			$2.1 M/THRUSTER		
—09—02	ANTENNA INTERFACE	1995	$ 149 M	18 $/KW		
—09—03	TRANSMIT ANTENNA	1995	$ 260 M			
—09—03.1	POWER INTERFACE			18 $/KW		
—09—03.2	DC TO RF CONVERTER			26 $/KW		
—09—03.3	WAVEGUIDE			14 $/KW		
—09—03.4	PHASE FRONT CONTROL			26 $/KW		
—09—03.5	SUPPORT STRUCTURE			15 $/KW		
—09—04	RECEIVING RECTENNA	1995	$ 403 M			
—09—04.1	RF TO DC SUBARRAY			76 $/KW		
—09—04.2	POWER INTERFACE			47 $/KW		
—09—04.3	SITE PREPARATION			8 $/KW		
—09—04.4	REAL ESTATE			19 $/KW		
—09—04.5	SUPPORT STRUCTURE			114 $/KW		
—09—04.6	PHASE FRONT CONTROL			5 $/KW		

Table A-1 System Cost Estimate, Sheet 3 of 3

WBS NO.	WBS IDENTIFICATION	IOC	LEVEL 1 WBS ELEMENTS			COMMENTS
			1–DEVELOPMENT	2–PRODUCTION	3–OPERATIONS	
–10	SYSTEM MAINTENANCE					(4) SEE SECTION 2.4
–10–01	LEO DEMO	1985	TBD	TBD	TBD	
–10–02	PILOT PLANT	1990	TBD	TBD	TDB	
–10–03	OPERATIONAL PLANT	1995		$919 M[4]/SSPS	$87.7 M/YR[4]	
–10–03.1	SOLAR ARRAY				42.7 /YR[4]	
–10–03.2	ANTENNA INTERFACE				0.4 M/YR[4]	
–10–03.3	TRANSMIT ANTENNA				1 M/YR[4]	
–10–03.4	RECEIVING RECTENNA				4.6 M/YR	
–11	FACILITIES		TBD	TBD	TBD	

Eighty-five percent of development costs for supporting systems is spent to develop three major systems. The major support system development cost is for the Heavy Lift Launch Vehicle with DDT&E of over $6 billion. The Advanced Ion propulsion stage is estimated to cost in excess of $3.5 billion while the Space Station is estimated at slightly above $2 billion.

A.2 Power Relay Satellite

A.2.1 Work Breakdown Structure and Program Schedule

A "strawman" PRS Work Breakdown Structure (WBS) and program schedule has been formulated to support programmatic studies. A two-step program was utilized. A geosynchronous demonstration satellite scheduled for 1985 required the development of a Low Earth Orbit and Synchronous Orbit space station over the next ten years. A refined version of the demonstration system was scheduled for 1990.

All elements of the WBS outlined for the SSPS in paragraph A.1, apply, with the exception of elements (-07) LEO Demonstration Satellite, (-08) Pilot Plant, and (-09) Operational Plant. Figure A-4 is a WBS replacement used for accounting PRS costs.

The 1 GW system scheduled for 1985 is assumed to be assembled and transported using the following major elements:

- Shuttle (IOC 1981)
- Full Capability Tug (IOC 1983)
- LEO Space Station (IOC 1983)
- SO Space Station (IOC 1983).

The 1990 system, rated at 10 GW, for purposes of the "strawman" plan is assumed to be assembled and transported using the following major elements:

- Deploy Only Launch (IOC 1987)
- Large Cryo Tugs (IOC 1987)
- LEO Space Station (IOC 1983)
- SO Space Station (IOC 1983)

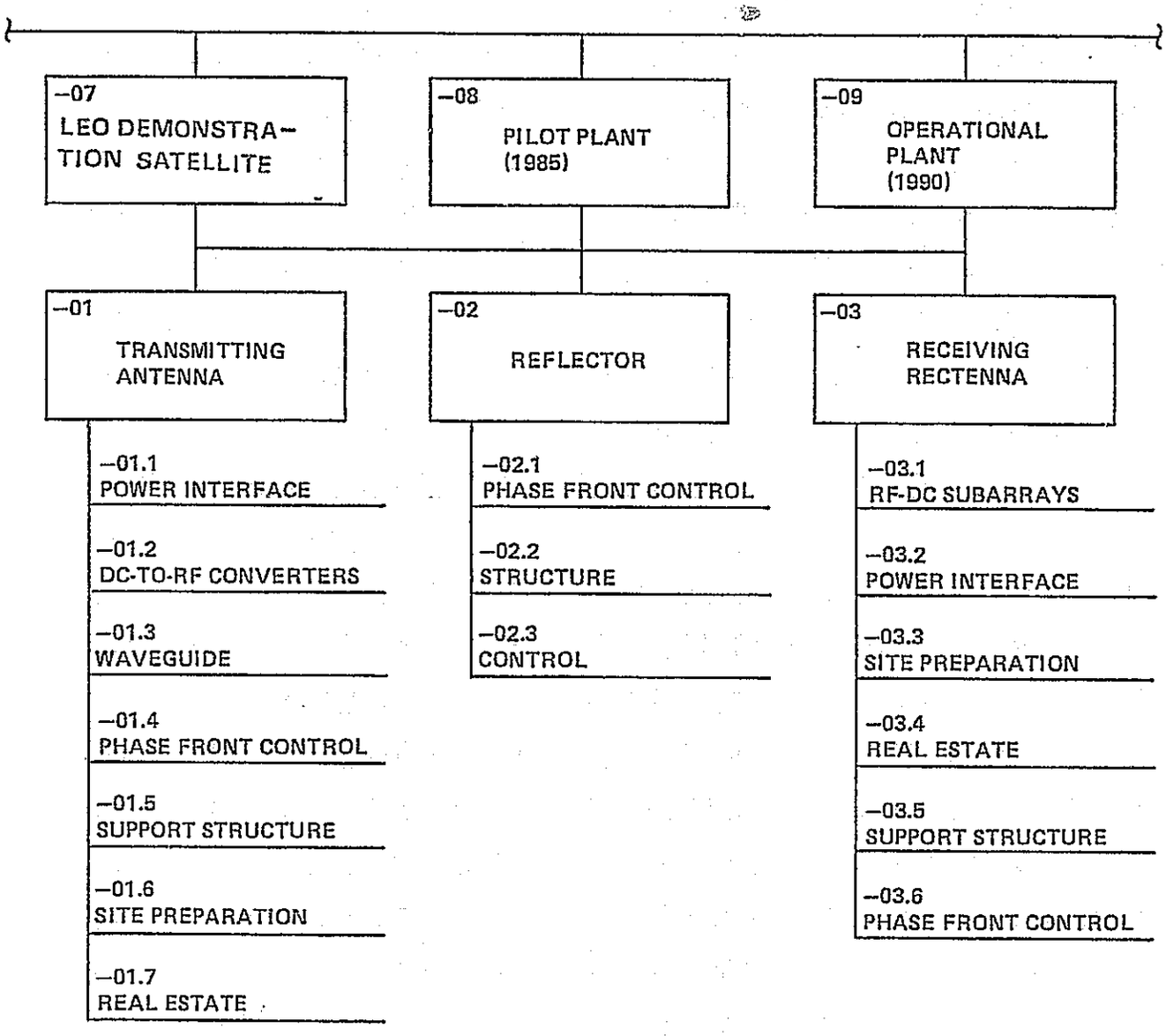

Figure A-4 Delta Work Breakdown Structure

A.2.2 PRS Cost Estimates

Table A-2 contains a compilation of costs based on the same relationships used in the SSPS estimates. The cost to develop a full scale (1 km) reflector and place it into geosynchronous orbit using a Full Capability Tug (P/L to SO $\leq$ 5000 kg) appears to be excessive. The development plan that solves the assembly technology problems with a small, low earth orbit demonstration satellite should be lower in cost. The use of Shuttle derivatives (i.e., DOL and Large Cryo Tug) significantly reduces transportation and assembly costs. The requirement for an HLLV and advanced ion stage still must be evaluated, though the relatively small mass-to-orbit for the PRS reflector may not justify the development of these advanced systems.

The dominant cost for the transmitter is the slotted waveguide, which must cover an area of almost 100 km^2 with a precisely dimensioned surface. The receiving antenna costs are the same as those used in the SSPS estimates.

The transmitter and receiving antenna maintenance costs are based on the assumption of 1 percent per year replacement of hardware and the following personnel (at each site):

- Control - Monitor Crew — 10/shift x 3 = 20
- Maintenance Crew — 8/shift x 3 = 24
- Support Personnel — 2/shift x 3 = 6

60

The important repairable items for the transmitting antenna are:

- Waveguides — \$ 35 x 10^6 (taken as 10% repairable)
- Phase Control — \$ 20 x 10^6
- DC-RF Converters — \$330 x 10^6
- Power Interface — \$410 x 10^6

For the receiving antenna, these are:

- Support Structure — \$ 23 x 10^6 (taken as 50% repairable)
- RF-DC Subarray — \$ 31 x 10^6

Table A-2 PRS System Cost Estimates

WBS NO.	WBS IDENTIFICATION	IOC	LEVEL 1 WBS ELEMENTS 1–DEVELOPMENT	2–PRODUCTION	3–OPERATIONS	COMMENTS
–08	PILOT PLANT	1985			3624 $/KG(1)	(1) TRANSPORTATION & ASSEMBLY – SHUTTLE – FULL CAPABILITY TUG – LEO & SO SPACE STATIONS
–08–01	TRANSMITTING ANTENNA		$1140 M	N/A		
–08–02	REFLECTOR		1521 M			
–08–03	RECEIVING RECTENNA		317 M			
–09	OPERATIONAL PLANT	1990			$11.6 M/YR	MAINTENANCE
–09–01	TRANSMITTING ANTENNA		$980 M			
–09–01.1	POWER INTERFACE			41 $/KW		
–09–01.2	DC-TO-RF CONVERTERS			33 $/KW		
–09–01.3	WAVEGUIDE			354 $/KW		
–09–01.4	PHASE FRONT CONTROL			2 $/KW		
–09–01.5	SUPPORT STRUCTURE			36 $/KW		
–09–01.6	SITE PREPARATION			14 $/KW		
–09–01.7	REAL ESTATE			8 $/KW		
–09–02	REFLECTOR		$30 M		1086 $/KG	TRANSPORTATION & ASSEMBLY MAINTENANCE
–09–02.1	PHASE FRONT CONTROL			16.3 $/KW	$90 M/YR	
–09–02.2	STRUCTURE			94 $/KG		
–09–02.3	CONTROL			$2.8 M/UNIT		
–09–03	RECEIVING RECTENNA		$280 M		$4.6 M/YR	MAINTENANCE
–09–03.1	RF-DC SUBARRAY			76 $/KW		
–09–03.2	POWER INTERFACE			47 $/KW		
–09–03.3	SITE PREPARATION			8 $/KW		
–09–03.4	REAL ESTATE			19 $/KW		
–09–03.5	SUPPORT STRUCTURE			114 $/KW		
–09–03.6	PHASE FRONT CONTROL			5 $/KW		

- Power Interface $ 47 x 10^6
- Phase Front Control $ 3 x 10^6

The yearly costs can thus be tabulated:

- PRS Transmitting Antenna O and M = \$11.5 x 10^6/year, total
  - Equipment \$795 x 10^6 x 0.01 = \$7.95 x 10^6/year
  - Personnel 60MY/yr x \$60K/yr = \$3.60 x 10^6/year
- PRS Receiving Antenna O&M = \$4.64 x 10^6/year, total
  - Equipment \$104 x 10^6 x 0.01 = \$1.04 x 10^6/year
  - Personnel 60MY/yr x \$60K/yr = \$3.60 x 10^6/year

APPENDIX B: BIBLIOGRAPHY

1. Spectrolab - 6011-03 Progress Report - "Feasibility Study of Satellite Solar Power Station," 1 October 1972.

2. Spectrolab - 6011-02 "Progress Report - Feasibility Study of Satellite Solar Power Station," 1 September 1972.

3. NAS, "Solar Cells - Outlook for Improved Efficiency," 1972.

4. NSS-MO-75-109, "SSPS Engineering Analysis of Special Requirements Transportation to Low Earth Orbit," 21 February 1975.

5. JPL, "Progress Report No. 2 - Comparative Assessment of Orbital and Terrestrial Central Power Station," August 1 to November 30, 1974.

6. NASA CR-2357, "Feasibility Study of a Satellite Solar Power Station," February 1975.

7. MPTS-R-002, "Task 2 Concept Definition, Microwave Power Transmission System Studies - Mechanical Systems & Flight Operations," 12 December 1974.

8. Spectrolab, "Satellite Solar Power Station" Technical Report, November 1971.

9. ECON, "Space Based Solar Power Conversion and Delivery Systems Study" - Interim Summary Report, March 31, 1976.

10. NASA CR-2357, "Feasibility Study of a Satellite Solar Power Station," February 1974.

11. NASA CR-134886, "Microwave Power Transmission System Studies," December 1975.

12. "Cost Prediction of Space Projects," Technical paper presented at 2nd Symposium on Cost Reduction in Space Operations, International Academy of Astronautics.

13. Grumman Report ASP-583-R-8, "Satellite Solar Power Station - Systems Engineering Report," November 1971.

14. Grumman Report ASP-583-R-11 "Satellite Solar Power Station - Technical Memoranda," June 1972.

15. Grumman Memo NSS-MO-75-111, "SSPS Engineering Analysis of Special Requirements - Orbit to Orbit Transportation," March 1975.

16. Grumman Memo ASP-611-M-1011 "Force Resulting From The Electromagnetic Radiation of Energy From the SSPS Antenna," September 1972.

17. Grumman Memo ASP-611-M-1004, "Sensitivity of Attitude Control Propellant Requirement to SSPS Deviation Angle Limits," August 1972.

18. Grumman Memo NSS-MO-75-118, "SSPS Engineering Analysis of Special Requirement - Large Solar Arrays," March 1975.

19. NASA CR-2357, "Feasibility Study of a Satellite Solar Power Station," February 1974.

20. Grumman/Raytheon, MPTS-R-002, "Microwave Power Transmission Systems Study - Task 2 Report," 12 December 1974.

21. Kaula, "Theory of Satellite Geodesy," 1966 Blarsdell Publishing Co., Waltham, Mass.

22. Rockwell Report E74-31, "Power Relay Satellite," March 1974.

23. GAC Report MPTS-R-002, "Microwave Power Transmission Systems Study - Task 2," December 1974.